Distribution Agreement

In presenting this thesis or dissertation as a partial fulfillment of the requirements for an advanced degree from Emory University, I hereby grant Emory University and its agents the non-exclusive license to archive, make accessible, and display my thesis or dissertation in whole or in part in all forms of media, now or hereafter known, including display on the world wide web. I understand that I may select some access restrictions as part of the online submission of this thesis or dissertation. I retain all ownership rights to the copyright of the thesis or dissertation. I also retain the right to use in future works (such as articles or books) all or part of this thesis or dissertation.

Signature:

Jiantao Fu Date

Development and Applications of a New Dirhodium(II) Tetracarboxylate Catalyst and Asymmetric Cyclopropanation of Heterocyclic Compounds

By

Jiantao Fu
Doctor of Philosophy

Chemistry

Huw M. L. Davies, Ph.D.
Advisor

Frank E. McDonald, Ph.D.
committee member

Dennis C. Liotta, Ph.D.
committee member

Accepted:

Lisa A. Tedesco, Ph.D.
Dean of the James T. Laney School of Graduate Studies

Date

Development and Applications of a New Dirhodium(II) Tetracarboxylate Catalyst and Asymmetric Cyclopropanation of Heterocyclic Compounds

By

Jiantao Fu
B.S., Dickinson College, 2015

Advisor: Huw M. L. Davies, Ph.D.

An abstract of
A dissertation submitted to the Faculty of the
James T. Laney School of Graduate Studies of Emory University
in partial fulfillment of the requirements for the degree of
Doctor of Philosophy
in Chemistry
2020

Abstract

Development and Applications of a New Dirhodium(II) Tetracarboxylate Catalyst and Asymmetric Cyclopropanation of Heterocyclic Compounds

By Jiantao Fu

Rhodium-stabilized carbene reactions have been extensively studied within the past decades, and one of the most promising applications is intermolecular C–H functionalization reactions. Even though once thought to be synthetically insignificant, these reactions have benefitted from the donor/acceptor carbenes that have tempered reactivity but enhanced selectivity. With the recent introduction of new chiral catalysts, rhodium-carbene chemistry has continued to evolve to become a powerful synthetic methodology for C–H functionalization and relied on in organic synthesis.

The first chapter of the dissertation discusses some general knowledge on dirhodium catalysis in C–H functionalization and recent progress on the development of new catalysts.

The second chapter focuses on the discussion of the development of new dirhodium catalysts for *N*-sulfonyl-1,2,3-triazoles as alternative precursors to donor/acceptor carbenes. These triazoles are capable of undergoing ring-opening to generate an α-imino diazo compound, which can then be trapped by a dirhodium catalyst. One interesting catalyst that stood out from the study was Rh_2(*S*-TPPTTL)$_4$, and although Rh_2(*S*-NTTL)$_4$ remained to be the chiral catalyst of choice for the triazoles, follow up studies on Rh_2(*S*-TPPTTL)$_4$ indicated that it was also capable of highly selective transformations using aryldiazoacetates.

The third chapter discusses further exploration of the selectivity profile of the Rh_2(*S*-TPPTTL)$_4$ in C–H functionalization of cyclohexanes, which are challenging substrates for C–H functionalization if they are unactivated or lack directing functionalities. Rh_2(*S*-TPPTTL)$_4$, however, can catalyze highly selective reactions at the C-3 equatorial C–H bond. The observed selectivities were explained via computational studies. The chapter will also discuss how Rh_2(*S*-TPPTTL)$_4$ contributed to the inception of a few other studies that aimed to explore other aspects of the new catalyst.

The last chapter covers a collaborative effort between the Davies and the Reiser group on asymmetric cyclopropanation of *N*-protected pyrroles. These nitrogen-containing heterocycles are ubiquitous in pharmaceutical research and can react with rhodium-carbenes in a number of pathways. Using Rh_2(*R*-*p*-PhTPCP)$_4$ as the chiral catalyst, *N*-protected pyrroles were found to undergo exceptionally clean monocyclopropanation with donor/acceptor carbenes. The synthetic potential was demonstrated via the synthesis of two biologically relevant compounds.

Development and Applications of a New Dirhodium(II) Tetracarboxylate Catalyst and Asymmetric Cyclopropanation of Heterocyclic Compounds

By

Jiantao Fu

B.S., Dickinson College, 2015

Advisor: Huw M. L. Davies, Ph.D.

A dissertation submitted to the Faculty of the
James T. Laney School of Graduate Studies of Emory University
in partial fulfillment of the requirements for the degree of
Doctor of Philosophy
in Chemistry
2020

Acknowledgements

One of the most precious and exciting experiences I have had and will ever have is getting my Ph.D. degree in the Davies group at Emory University. Being a foreign student in the U.S., I had my own challenges and difficulties, but I was so fortunate to be in a research group that has a very caring professor as my research advisor who guided me throughout my graduate career. I would first like to sincerely thank Professor Huw Davies for his time and willingness in mentoring me when I had little prior research experience in chemistry. I still remember the first few weeks in the lab when I didn't know how to run chromatography and spent almost an hour trying to analyze an NMR that only had solvent peaks. The feedback and instructions I received from Professor Davies have been indispensable for my personal and professional growth as a chemist. In many occasions, his comments and suggestions helped me navigate through projects and roadblocks that I would otherwise spend much more time on. I will also particularly thank the NSF Center for Selective C–H Functionalization, for which Professor Davies is the Director. His dedication in and enthusiasm for innovative research projects and collaborations with different groups were contagious and evident in Center meetings and many other occasions, which have also influenced how I would approach a research problem and interact with my collaborators. In addition, my trip to Germany and South Korea in 2019, which was sponsored by the Center, was one of the most valuable experiences I had in the past few years.

I would also like to thank my committee members, Professor Frank McDonald and Professor Dennis Liotta. Although I did not interact with them on a daily basis, their support and critique on my work and yearly milestone presentations were also instrumental for my professional development as a graduate student. I enjoyed my conversations with them on my research progress and receiving constructive feedback from different perspectives.

Working in the Davies group wouldn't be as productive and fun without all the group members that I have had the chance to meet and interact with for the past few years. They are not only co-workers but also close friends to me, and their inputs and comments in group meetings were very helpful to me. I learned a tremendous amount from them on how to present my work more effectively and confidently. In addition, throughout my graduate career I had the opportunity to work with a number of them on collaborative projects. I wish to thank them for their contribution and hard work. All of my publications in the Davies group wouldn't be possible without their inputs.

In my last two years of graduate school, I had the amazing opportunity to become the Service Instructor for the NMR Center. During this time I was able to provide training for new incoming students and scholars on proper use of our NMR spectrometers and on the user policies. I also had the chance to be the teaching assistant for a summer short course on NMR interpretation in 2018. These experiences are highly valuable to me and I wish to thank Dr. Bing Wang and Dr. Shaoxiong Wu in the NMR Center for their supervision. I enjoyed my technical and casual discussions with them.

And of course, my Ph.D. journey wouldn't be possible without support from my parents. They allowed and supported me to go to an international high school and then to the U.S. for my undergraduate study, both of which were the very foundation for my interest in science and decision to go to graduate school in chemistry. I wish to take this opportunity to thank them for their continued support and care.

Table of Contents

List of Figures

List of Schemes

List of tables

Chapter 1

Overview of Donor/Acceptor Dirhodium Carbene Chemistry

1.1 Introduction

One of the most heavily pursued goals within the chemical synthetic community continues to be the development of highly efficient and selective reactions that inspire new strategies and enhanced routes to complex targets and biologically important compounds. Even though known for decades, in recent years, transition metal-catalyzed carbene reactions have played an increasingly important role in organic synthetic chemistry and continue to stimulate the development of new catalytic systems.[1-22] In this regard, dirhodium tetracarboxylates have been shown to be particularly suitable for highly selective reactions using donor/acceptor carbenes,[21, 23-25] and some of the most notable examples include asymmetric C–H bond insertion,[17, 19, 24-28] olefin cyclopropanation,[29-37] and a number of cascade reactions, such as combined C–H insertion/Cope rearrangement,[38-46] among many other developments.[47]

The reactivity profile of a carbene largely depends on its electronic properties (Figure 1.1). Free carbenes generated under photolytic or thermolytic conditions from diazo compounds were previously thought to be not synthetically important because they tended to self-dimerize or undergo nonselective reactions and result in a mixture of products.[48-50] Acceptor carbenes (**1.1** and **1.2**) with one or two electron-withdrawing groups attached usually demonstrate limited selectivity as they are highly reactive and difficult to control. In contrast, donor/acceptor carbenes (**1.3**), developed by the Davies group, are capable of much more selective transformations, as the donor group serves to attenuate the carbene's electrophilicity by donating electron density into the empty

p-orbital of the carbene carbon.[51, 52] Therefore, even though these carbenes react more slowly, they exhibit a broad reactivity profile in some highly selective intermolecular reactions and are more amenable to various control elements by catalysts.[24, 26]

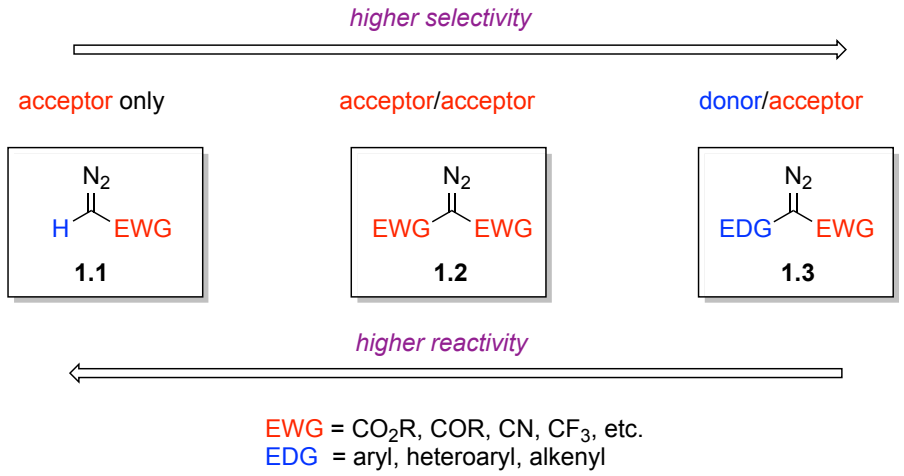

Figure 1.1 General classification of diazo compounds based on their flanking substituents

One of the earliest examples of carbene-induced C–H functionalization was achieved by Scott and co-workers, where he demonstrated that copper-catalyzed decomposition of ethyl diazoacetate was an effective way of functionalizing cyclohexane when it is reacted as the solvent, although substantial carbene self-dimerization was also observed as the side reaction.[50] It was later discovered that rhodium(II) carboxylates of perfluoroacids were more efficient for promoting carbene insertions.[53] Since then, numerous groups have worked on further developing and refining the structures of dirhodium catalysts that feature different ligand designs such as carboxylates (**1.4**), carboxamidates (**1.5**) and phosphonates (**1.6,** Figure 1.2).[54]

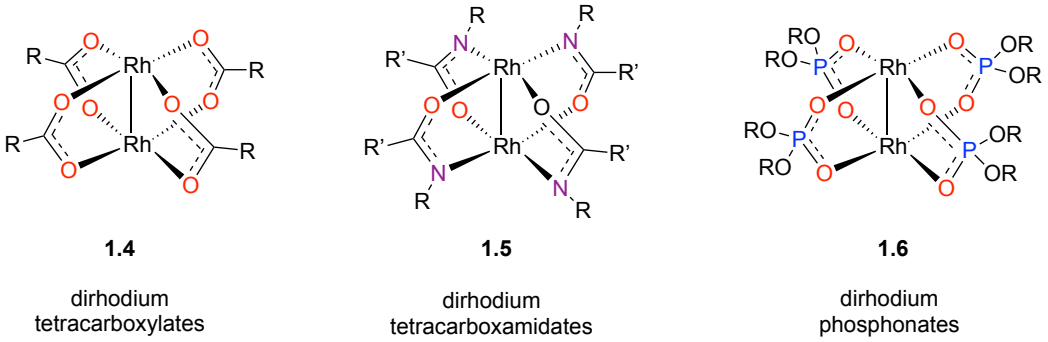

Figure 1.2 General structures of common dirhodium catalysts

Rhodium carboxylates are thought to be kinetically more active toward diazo decomposition and are the privileged catalysts for selective and intermolecular C–H functionalization reactions using donor/acceptor carbenes.[21, 26, 54] One of the earlier catalysts is dirhodium tetraacetate, $Rh_2(OAc)_4$ (**1.7**, Figure 1.3). It is very effective for carbene generation, and has four acetate ligands that are positioned around the dirhodium core to form a D_{4h}-symmetrical structure. These bridging carboxylate ligands effectively create a "paddlewheel" complex, where as axial ligands (usually H_2O or solvent molecules) are more labile and occupy the catalytically active sites.[9]

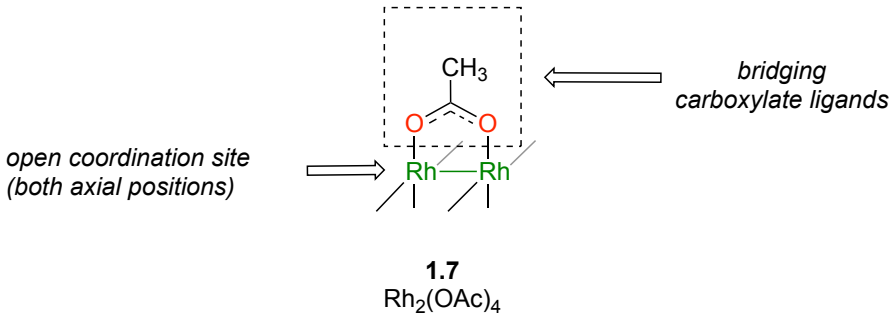

Figure 1.3 A dirhodium "paddlewheel" complex, rhodium tetraacetate

Rhodium carboxamidates are known to be effective catalysts for acceptor-only diazo compounds in some intramolecular reactions,[55] while rhodium phosphonates originally developed by McKervey and Pirrung have found limited utilizations.[56, 57] For these dirhodium complexes, it is suggested that only one of the rhodium atom can coordinate to the diazo compound to induce its decomposition, while the other one acts as an electron sink.[24] In recent years, some studies have been conducted to see if two rhodium atoms are required and if one of them can be replaced by another metal, although this topic falls outside the scope of the discussion herein.[58]

The outcome of C–H functionalization reactions by donor/acceptor carbene insertions is generally governed by several factors: 1) the nature of the carbene, 2) the electronic and steric properties of the substrate and 3) the identity and steric demand of the dirhodium catalyst. The transient metal carbene intermediate is generated *in situ* when the diazo compound reacts with the rhodium catalyst, which causes the extrusion of molecular nitrogen, and then the highly reactive rhodium-bound carbene inserts itself into a C–H bond via a hydride abstraction event.[26] Because of partial positive charge build-up during this process, the site on the substrate that better stabilizes the positive charge will be preferentially functionalized. However, because the rhodium carbene intermediate is sterically encumbered, sites that are highly substituted will react less efficiently, even though they may be electronically favorable. On both grounds, secondary sites are generally preferred by the rhodium carbene, particularly when a structurally flexible catalyst, such as $Rh_2(DOSP)_4$, is used, but the choice of a more crowded catalyst may override these generation considerations (Figure 1.4).[26, 54]

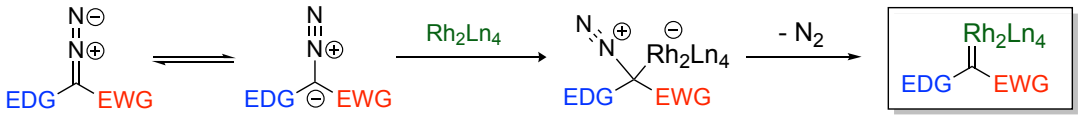

(a) Formation of rhodium-bound carbene upon nitrogen extrusion

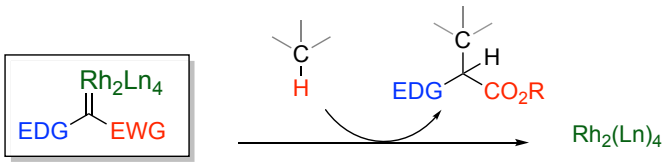

(b) C-H functionalization by a metal-stabilized donor/acceptor carbene

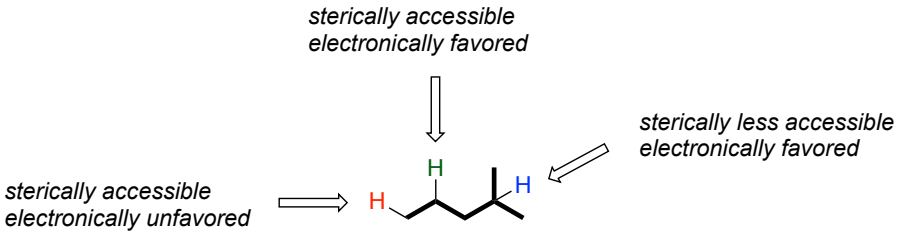

Figure 1.4 General scheme for the formation of carbene and rhodium(II)-catalyzed C–H bond functionalization, as well as the steric and electronic influences on site selectivity

Site-selective C–H functionalization reactions frequently leverage on intramolecular processes in which a particular C–H bond is placed in close proximity to the diazo functionality.[59-64] This was especially true when acceptor-only carbenes are involved because they would otherwise be more challenging to control (Scheme 1.1). This strategy is exemplified in the synthesis of (*R*)-(-)-baclofen (**1.10**) via a Rh_2(4*S*-MPPIM)$_4$ (**1.11**)-catalyzed intramolecular C–H functionalization.[65] The diazo compound (**1.8**), in this case, has only an acceptor group attached, and is therefore highly electrophilic. The C–H bond at the benzylic position is site-selectively functionalized due to electronic activation and the product (**1.9**) was obtained with high asymmetric induction (95% ee). Another example would be the synthesis of (+)-

isodeoxypodophyllotoxin (**1.13**), where a similar intramolecular cyclization event using **1.11** as the substrate was catalyzed by the same catalyst (**1.11**) with excellent level of regio- and stereocontrol, although in this case the benzylic position was not functionalized due to preferential formation of the 5-membered ring.

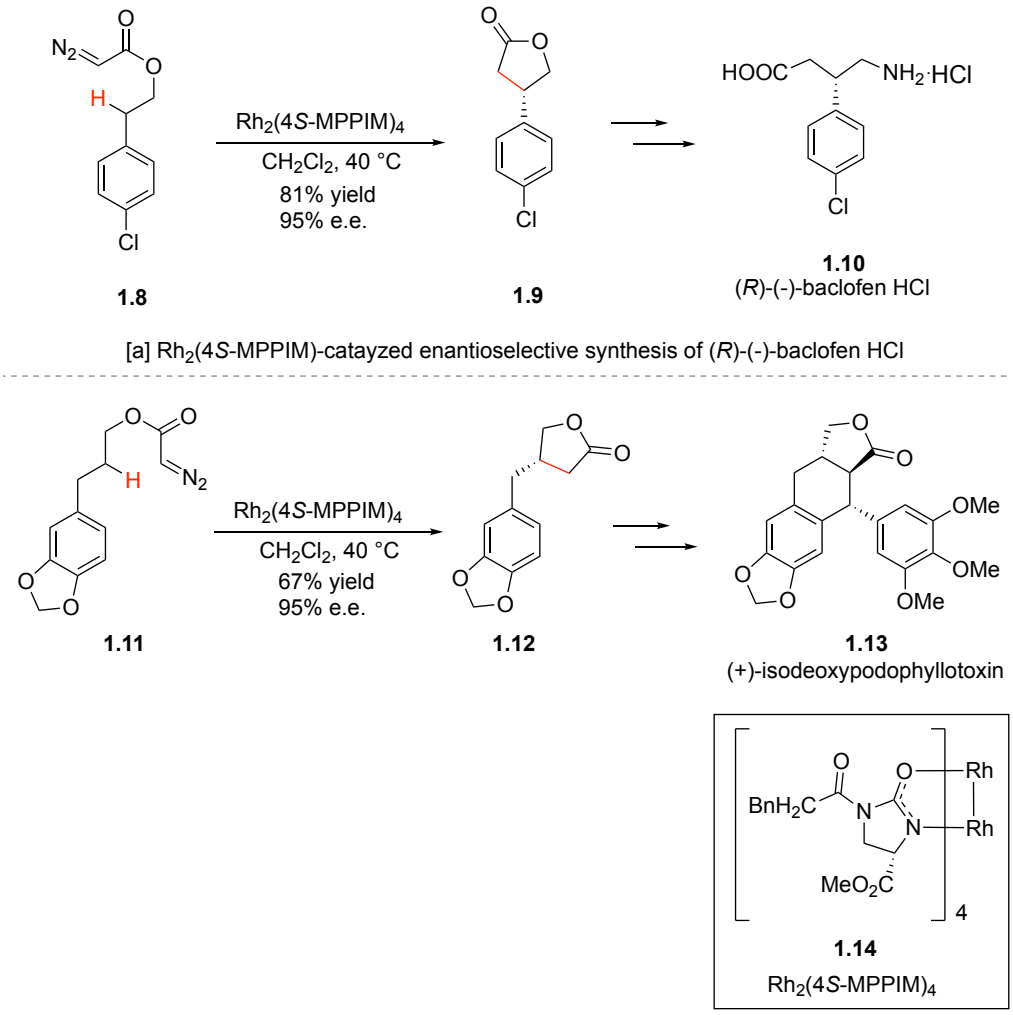

Scheme 1.1 Rhodium carboxamidates are used in a number of intramolecular C–H functionalization reactions using acceptor substituted carbenes

Nevertheless, intramolecular reactions can potentially limit the scope of the application because one would be required to go through multiple synthetic steps to prepare the substrate, which also happens to be the diazo compound in this case. Intermolecular reactions, on the other hand, would be a more powerful and generalizable strategy for C–H functionalization and would eliminate the requirement for the use of a "tether" that dictates regioselectivity, enabling much more modular syntheses.[26] However, some other controlling elements would be needed in order to achieve the desired regio- and stereoselectivity. In recent years, further optimization of the carbene precursors and extensive effort in rational design of dirhodium catalysts have allowed for many highly selective intermolecular C–H functionalization reactions to be realized, including unactivated substrates that contain multiple otherwise indistinguishable C–H bonds.[17-21, 25, 28, 47] In many cases, the selectivity is governed by the steric requirement of the catalyst and complementary site selectivities are achieved by simply choosing the appropriate catalyst. Some of the most relevant work from Davies and co-workers are discussed below.

One defining aspect of the C–H functionalization program in the Davies group is the strategic use of donor/acceptor carbenes and the appropriate rhodium catalyst. In 2014, it was discovered that 2,2,2-trichloroethyl aryldiazoacetates can act as even more robust source of donor/acceptor carbenes (Scheme 1.2).[66] Many challenging substrates, such as methyl ethers and electron-deficient anisoles, are readily functionalized with high yield and enantioselectivity when Rh_2(*R*-*p*Ph-TPCP)$_4$ (**1.18**) was used as the catalyst.[14] More importantly, it allowed a broad scope of heteroaryl donor groups (**1.17d-f**) to be incorporated into the design of the diazo compound that were ineffective when methyl esters were used (**1.17a-c**). In addition, fast addition (~5 seconds) of the diazo compound was possible due to suppressed carbene self-dimerization, adding to the

practicality of the new discovery. These more robust carbene precursors played an indispensable role in the functionalization of some unactivated substrates with unprecedented levels of site- and stereoselectivities that will be relevant throughout this thesis.

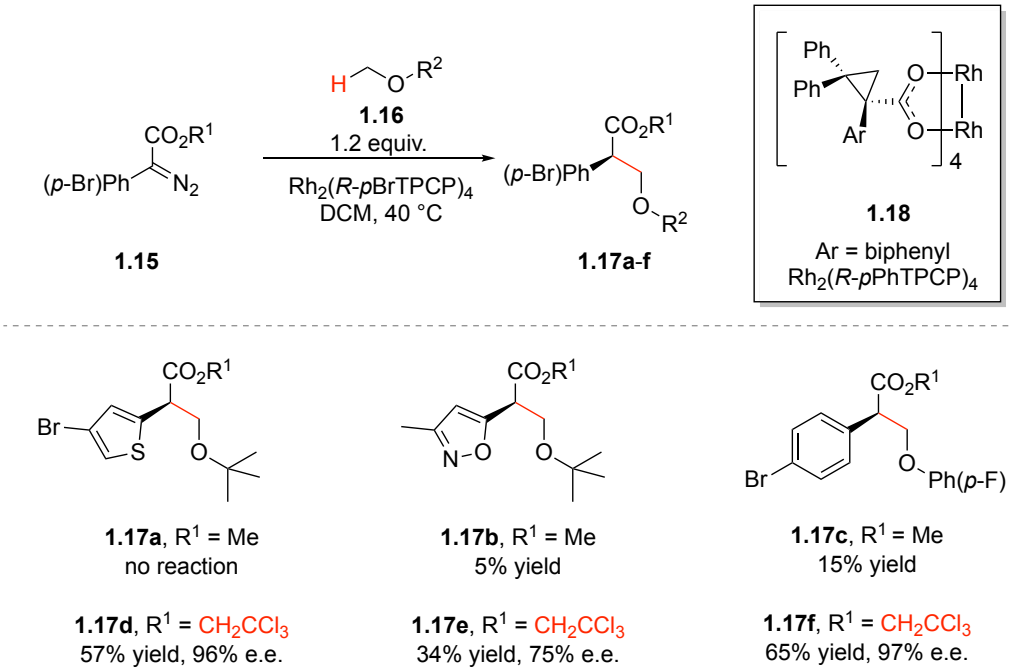

Scheme 1.2 The development of 2,2,2-trichloroethyl diazoacetates as a new class of donor/acceptor carbene precursor

It is equally important to realize that the development of new catalysts was essential in overcoming many synthetic challenges, even though rhodium tetracarboxylates were once considered to be unsuitable for high asymmetric induction.[24] In the Davies group, there are three main categories of chiral dirhodium catalysts that are utilized in a variety of contexts (Figure 1.5). The first generation catalysts have chiral sulfonyl proline ligands (**1.19-1.21**).[5, 7, 67] Rh_2(DOSP)$_4$ (**1.19**) is a broadly utilized catalyst that features a dodecyl sulfonyl proline ligand, and the long aliphatic chain allowed for its exceptional solubility in non-polar solvents, which enhances its

performance.[68] These dirhodium tetraprolinate catalysts were initially found to be exceptional for catalyzing cyclopropanation and C–H functionalization reactions at activated sites, such as those adjacent to heteroatoms or allylic positions.[54] Nonetheless, they have found limited applications in more recent studies as they are less effective for more challenging, unactivated substrates as compared to newer catalysts, and some chiral prolinate ligands are difficult to access. The second class of catalysts were originally developed by Hashimoto and have chiral phthalimide protected amino acid ligands (**1.22**-**1.24**).[5, 7, 67] These catalysts are very amenable to diversification as one can easily access a variety of chiral amino acids from commercial sources. These catalysts generally adopt a C_4-symmetrical "chiral crown" structure,[69] and their reactivities and structural features will be discussed in later chapters. The third class of catalysts are more recently discovered and feature chiral triarylcyclopropane ligands that are prepared via asymmetric cyclopropanation of 1,1-diphenylethylene using first or second generation catalysts (**1.25**-**1.27**).[11, 14, 17, 19, 20, 28] They also have highly modular synthetic routes and are capable of adopting a wide range of conformations that impart unique selectivities. Many of them are sterically highly congested, and are therefore capable of regioselectively functionalizing the most accessible primary[19] and secondary[28] C–H bonds. A limitation of synthesizing these cyclopropane ligands, however, is the need of screening a suitable catalyst for the asymmetric cyclopropanation step and extensive enantioenrichment after the cyclopropanation.

first generation catalysts: chiral prolinate ligands

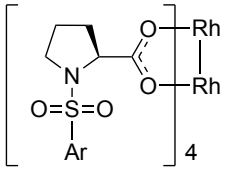

1.19
Ar = (p-$C_{12}H_{25}$)Ph
Rh_2(*S*-DOSP)$_4$

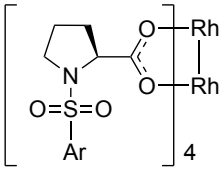

1.20
Ar = (p-tBu)Ph
Rh_2(*S*-TBSP)$_4$

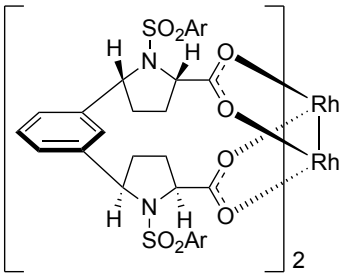

1.21
Ar = (p-$C_{12}H_{25}$)Ph
Rh_2(*S*-biDOSP)$_2$

second generation catalysts: phthalimide/naphthalimide-protected chiral amino acid ligands

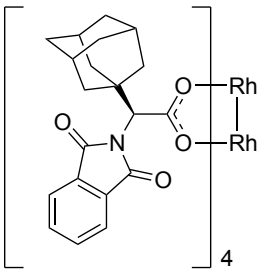

1.22
Rh_2(*S*-PTAD)$_4$

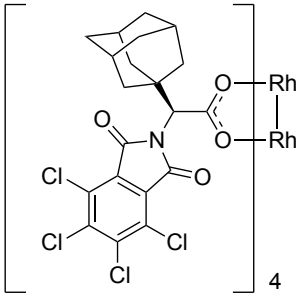

1.23
Rh_2(*S*-TCPTAD)$_4$

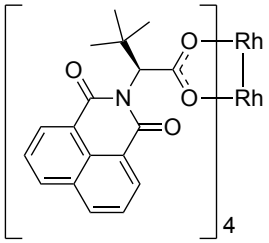

1.24
Rh_2(*S*-NTTL)$_4$

third generation catalysts: chiral TriPhenylCycloPropane (TPCP) ligands

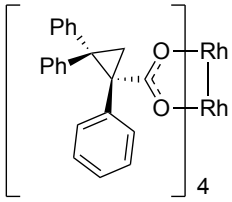

1.25
Rh_2(*R*-TPCP)$_4$

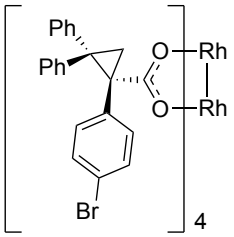

1.26
Rh_2(*R*-*p*BrTPCP)$_4$

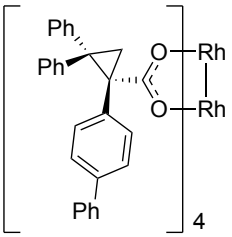

1.27
Rh_2(*R*-*p*PhTPCP)$_4$

Figure 1.5 Representative chiral dirhodium catalysts used in the Davies group

One of the research goals within the Davies group has been to develop a "toolbox" of catalysts that are capable of functionalizing C–H bonds that are difficult to control using other methods, such as when the C–H bond of interest is not electronically activated or adjacent to a directing group (Figure 1.6). This concept is nicely illustrated in the selective functionalization of pentane derivatives using donor/acceptor carbenes, where it was found that a new catalyst, Rh_2[*R*-3,5-di(*p*-^{t}BuPh)TPCP]$_4$ (**1.29**), is capable of functionalizing the most accessible secondary C–H bond in the substrates.[28] In this reaction, one of the biggest challenges is to achieve high diastereoselectivity, which typically requires there to be substantial steric difference between the two groups on the C–H bond. In this case, because the catalyst itself contains a sophisticated triphenylcyclopropane (TPCP) ligand, it is capable of achieving high diastereoselectivity even when the size difference is not sufficient. Since this discovery, other related efforts have allowed for site-selective functionalization of the most accessible primary by Rh_2[*R*-3,5-tris(*p*-^{t}BuPh)TPCP]$_4$ (**1.30**),[19] and tertiary C–H bonds by Rh_2(*R*-TCPTAD)$_4$ (**1.28**),[17] respectively, based on the steric demand of the catalysts, and the scope of substrates has evolved from hydrocarbons to more complex targets, such as cholesterol derivatives.

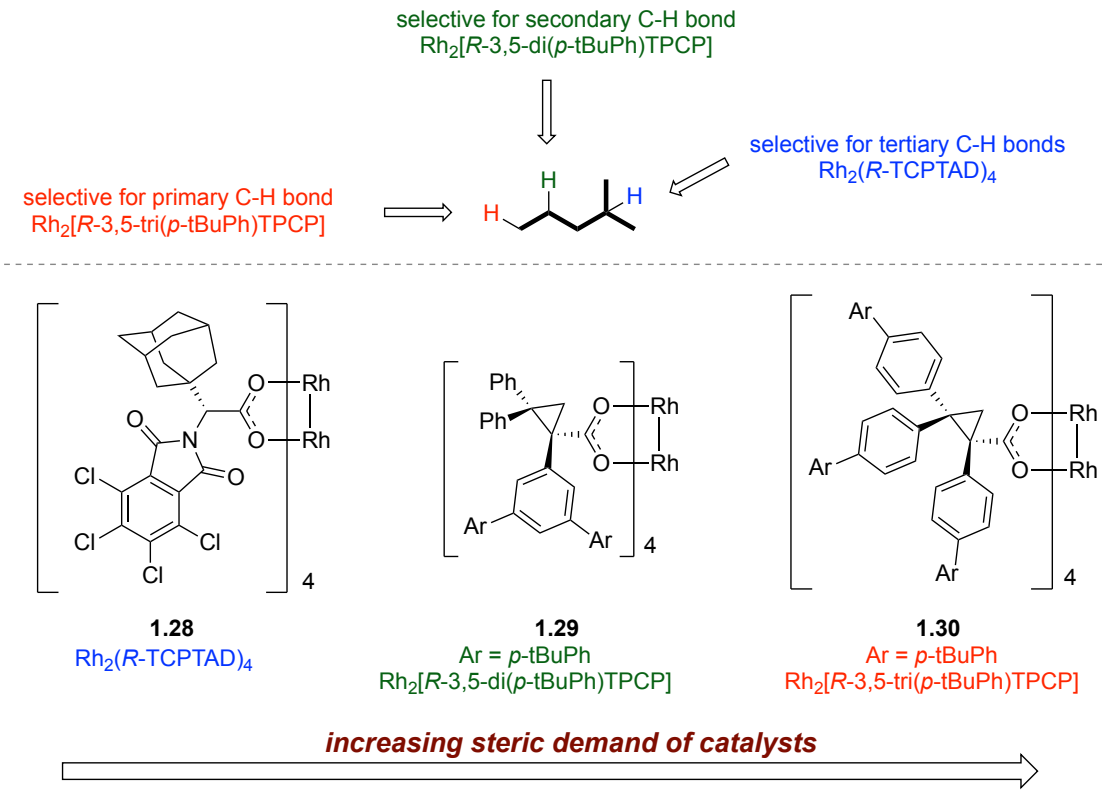

Figure 1.6 Highly regio- and stereoselective C–H functionalization of the most accessible primary, secondary and tertiary C–H bonds enabled by different catalysts

More recently, Davies and co-workers disclosed a new TPCP catalyst that has novel *o*-Cl substituent on one of the phenyl rings that has a substantial effect on the overall geometry of the dirhodium catalyst as well as its particularly interesting site selectivity (Figure 1.7).[20] This new catalyst, Rh_2(*S*-2-Cl-5-BrTPCP)$_4$ (**1.31**), is capable of overriding the normal preference of rhodium carbenes to favor electronically activated benzylic positions. Instead, it can functionalize the terminal C-2 position on the alkyl group with excellent regio- and stereoselectivity. More interestingly, complementary site-selectivity at the benzylic position could be achieved by simply switching the catalyst to Rh_2(*R*-TCPTAD)$_4$ (**1.28**), which is sterically much less hindered, and

therefore could accommodate the more crowded benzylic C–H bond. It was postulated that the *o*-Cl substituent was essential in constructing the overall C_4 symmetry of the complex, while other members of the TPCP family without *ortho*-substituents tend to adopt either D_2 or C_2 symmetry.[21] One challenge, however, for C_4-symmetric catalysts, is that the catalyst must only allow the carbene to bind only to the chiral face of the complex, while the other face is effectively blocked.[18, 20, 69] Ideally, there needs to be substantial steric differences between these two faces to provide for a substantial energetic cost if the carbene were to bind to the achiral face. For the Rh_2(*o*-ClTPCP)$_4$ family, the accessible chiral face is primarily controlled by the phenyl ring that contains the *o*-Cl substituent, while the other face is blocked by four unsubstituted phenyl rings. Because the original Rh_2(*o*-ClTPCP)$_4$ catalyst does not give excellent chiral induction in many cases and based on X-ray crystallography analysis, a 5-Br substituent was later introduced to limit the pathways for which the substrate can approach the rhodium carbene. This remote C–H functionalization strategy catalyzed by Rh_2(*S*-2-Cl-5-BrTPCP)$_4$ was applied toward the synthesis of the macrocyclic core of the cyclindrocyclophane natural products, where two key remote functionalization reactions allowed for rapid construction of the macrocyclic core structure (**1.32**).

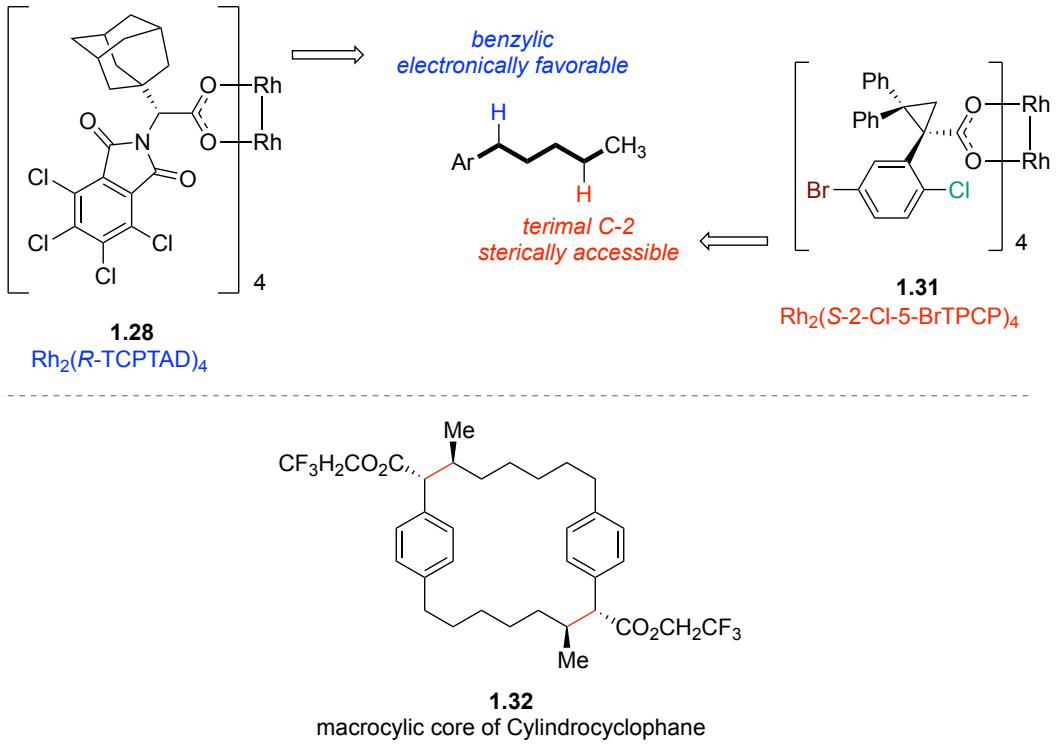

Figure 1.7 Rh_2(*S*-2-Cl-5-BrTPCP)$_4$ and Rh_2(*R*-TCPTAD)$_4$ can achieve complementary site selectivity

1.2 Conclusions

Even though rhodium carbene chemistry has been known for decades, it has continued to evolve to become a powerful strategy for selectively functionalizing small molecules and complex targets. One primary reason that accounts for its success is the advent of donor/acceptor carbenes, as continuous optimization of their structures has allowed for attenuation of its high reactivity that was previously challenging to control. In addition, rational design and development of a collection of chiral dirhodium catalysts has been indispensable for intermolecular C–H functionalization reactions, as a much wider range of substrates could now be envisioned and the reactions are frequently completed in a highly regio- and stereoselective manner.

This thesis will mainly focus on the discussion of a newly developed chiral dirhodium catalyst that has been used in variety of contexts and applications for selective C–H functionalization reactions. In many cases, high levels of regio- and stereocontrol are routinely observed. In addition, this thesis will also discuss a collaborative project on carbene chemistry using a TPCP catalyst with Dr. Oliver Reiser at University of Regensburg.

1.3 References

1. Callot, H. J.; Metz, F. *Tetrahedron Lett.* **1982,** *23*, 4321.
2. Callot, H. J.; Metz, F. *Tetrahedron* **1985,** *41*, 4495.
3. Doyle, M. P.; Dyatkin, A. B.; Roos, G. H. P.; Canas, F.; Pierson, D. A.; van Basten, A.; Mueller, P.; Polleux, P. *J. Am. Chem. Soc.* **1994,** *116*, 4507.
4. Doyle, M. P.; Kalinin, A. V.; Ene, D. G. *J. Am. Chem. Soc.* **1996,** *118*, 8837.
5. Yamawaki, M.; Tsutsui, H.; Kitagaki, S.; Anada, M.; Hashimoto, S. *Tetrahedron lett.* **2002,** *43*, 9561.
6. Caballero, A.; Diaz-Requejo, M. M.; Belderrain, T. R.; Nicasio, M. C.; Trofimenko, S.; Perez, P. J. *J. Am. Chem. Soc.* **2003,** *125*, 1446.
7. Tsutsui, H.; Abe, T.; Nakamura, S.; Anada, M.; Hashimoto, S. *Chem. Pharm. Bull.* **2005,** *53*, 1366.
8. Reddy, R. P.; Davies, H. M. L. *Org. lett.* **2006,** *8*, 5013.
9. Hansen, J.; Davies, H. M. L. *Coord. Chem. Rev.* **2008,** *252*, 545.
10. Caballero, A.; Despagnet-Ayoub, E.; Mar Díaz-Requejo, M.; Díaz-Rodríguez, A.; González-Núñez, M. E.; Mello, R.; Muñoz, B. K.; Ojo, W.-S.; Asensio, G.; Etienne, M.; Pérez, P. J. *Science* **2011,** *332*, 835.

11. Qin, C.; Boyarskikh, V.; Hansen, J. H.; Hardcastle, K. I.; Musaev, D. G.; Davies, H. M. L. *J. Am. Chem. Soc.* **2011,** *133*, 19198.

12. Boruta, D. T.; Dmitrenko, O.; Yap, G. P.; Fox, J. M. *Chem Sci* **2012,** *3*, 1589.

13. Adly, F. G.; Maddalena, J.; Ghanem, A. *Chirality* **2014,** *26*, 764.

14. Qin, C.; Davies, H. M. L. *J. Am. Chem. Soc.* **2014,** *136*, 9792.

15. Panish, R. A.; Chintala, S. R.; Fox, J. M. *Angew. Chem. Int. Ed.* **2016,** *55*, 4983.

16. Weldy, N. M.; Schafer, A. G.; Owens, C. P.; Herting, C. J.; Varela-Alvarez, A.; Chen, S.; Niemeyer, Z.; Musaev, D. G.; Sigman, M. S. *Chem Sci* **2016,** *7*, 3142.

17. Liao, K.; Pickel, T. C.; Boyarskikh, V.; Bacsa, J.; Musaev, D. G.; Davies, H. M. L. *Nature* **2017,** *551*, 609.

18. Fu, J.; Ren, Z.; Bacsa, J.; Musaev, D. G.; Davies, H. M. L. *Nature* **2018,** *564*, 395.

19. Liao, K.; Yang, Y. F.; Li, Y.; Sanders, J. N.; Houk, K. N.; Musaev, D. G.; Davies, H. M. L. *Nat. Chem.* **2018,** *10*, 1048.

20. Liu, W.; Ren, Z.; Bosse, A. T.; Liao, K.; Goldstein, E. L.; Bacsa, J.; Musaev, D. G.; Stoltz, B. M.; Davies, H. M. L. *J. Am. Chem. Soc.* **2018,** *140*, 12247.

21. Davies, H. M. L.; Liao, K. *Nat. Rev. Chem.* **2019,** *3*, 347.

22. Ferris, L.; Haigh, D.; Moody, C. J. *Tetrahedron lett.* **1996,** *37*, 107.

23. Davies, H. M. L. *Angew. Chem. Int. Ed.* **2006,** *45*, 6422.

24. Davies, H. M. L. *Chem. Soc. Rev.* **2011,** *40*, 1857.

25. Davies, H. M.; Morton, D. *J. Org. Chem.* **2016,** *81*, 343.

26. Davies, H. M.; Manning, J. R. *Nature* **2008,** *451*, 417.

27. Doyle, M. P.; Duffy, R.; Ratnikov, M.; Zhou, L. *Chem. Rev.* **2010,** *110*, 704.

28. Liao, K.; Negretti, S.; Musaev, D. G.; Bacsa, J.; Davies, H. M. L. *Nature* **2016,** *533*, 230.

29. Davies, H. M.; Townsend, R. J. *J. Org. Chem.* **2001,** *66*, 6595.

30. Negretti, S.; Cohen, C. M.; Chang, J. J.; Guptill, D. M.; Davies, H. M. L. *Tetrahedron* **2015,** *71*, 7415.

31. Chepiga, K. M.; Qin, C.; Alford, J. S.; Chennamadhavuni, S.; Gregg, T. M.; Olson, J. P.; Davies, H. M. L. *Tetrahedron* **2013**, *69*, 27.

32. Wu, W.; Lin, Z.; Jiang, H. *Org. Biomol. Chem.* **2018,** *16*, 7315.

33. Wang, H.; Guptill, D. M.; Alvarez, A. V.; Musaev, D. G.; Davies, H. M. L. *Chem. Sci.* **2013,** *4*, 2844.

34. Davies, H. M.; Lee, G. H. *Org. lett.* **2004,** *6*, 2117.

35. Denton, J. R.; Sukumaran, D.; Davies, H. M. L. *Org. lett.* **2007,** *9*, 2625.

36. Tinoco, A.; Steck, V.; Tyagi, V.; Fasan, R. *J. Am. Chem. Soc.* **2017,** *139*, 5293.

37. Lebel, H.; Marcoux, J. F.; Molinaro, C.; Charette, A. B. *Chem. Rev.* **2003,** *103*, 977.

38. Davies, H. M. L.; Beckwith, R. E. J. *J. Org. Chem.* **2004,** *69*, 9241.

39. Davies, H. M. L.; Lian, Y. *Acct. Chem. Res.* **2012,** *45*, 923.

40. Lian, Y.; Davies, H. M. L. *J. Am. Chem. Soc.* **2011,** *133*, 11940.

41. Davies, H. M. L.; Lian, Y. *Acct. Chem. Res.* **2012,** *45*, 923.

42. Davies, H. M. L.; Dai, X.; Long, M. S. *J. Am. Chem. Soc.* **2006,** *128*, 2485.

43. Lian, Y.; Hardcastle, K. I.; Davies, H. M. L. *Angew. Chem. Int. Ed.* **2011,** *50*, 9370.

44. Hansen, J. H.; Gregg, T. M.; Ovalles, S. R.; Lian, Y.; Autschbach, J.; Davies, H. M. L. *J. Am. Chem. Soc.* **2011,** *133*, 5076.

45. Hodgson, D. M.; Labande, A. H.; Pierard, F. Y. T. M.; Expósito Castro, M. Á. *J. Org. Chem.* **2003,** *68*, 6153.

46. Spangler, J. E.; Lian, Y.; Raikar, S. N.; Davies, H. M. L. *Org. lett.* **2014,** *16*, 4794.

47. Davies, H. M. L. *J. Org. Chem.* **2019,** *84*, 12722.

48. Moser, W. R. *J. Am. Chem. Soc.* **1969,** *91*, 1135.

49. Adams, J.; Spero, D. M. *Tetrahedron* **1991,** *47*, 1765.

50. Scott, L. T.; DeCicco, G. J. *J. Am. Chem. Soc.* **1974,** *96*, 322.

51. Davies, H. M. L.; Panaro, S. A. *Tetrahedron* **2000,** *56*, 4871.

52. Hansen, J.; Autschbach, J.; Davies, H. M. L. *J. Org. Chem.* **2009,** *74*, 6555.

53. Demonceau, A.; Noels, A. F.; Hubert, A. J.; Teyssié, P. *J. Chem. Soc., Chem. Commun.* **1981**, *14*, 688.

54. Davies, H. M.; Beckwith, R. E. *Chem. Rev.* **2003,** *103*, 2861.

55. Timmons, D. J.; Doyle, M. P. *J. Organomet. Chem.* **2001,** *617*, 98.

56. McCarthy, N.; McKervey, M. A.; Ye, T.; McCann, M.; Murphy, E.; Doyle, M. P. *Tetrahedron lett.* **1992,** *33*, 5983.

57. Pirrung, M. C.; Zhang, J. *Tetrahedron lett.* **1992,** *33*, 5987.

58. Ren, Z.; Sunderland, T. L.; Tortoreto, C.; Yang, T.; Berry, J. F.; Musaev, D. G.; Davies, H. M. L. *ACS Catal.* **2018,** *8*, 10676.

59. Taber, D. F.; Song, Y. *Tetrahedron lett.* **1995,** *36*, 2587.

60. Taber, D. F.; You, K. K. *J. Am. Chem. Soc.* **1995,** *117*, 5757.

61. Taber, D. F.; You, K. K.; Rheingold, A. L. *J. Am. Chem. Soc.* **1996,** *118*, 547.

62. Doyle, M. P.; Dyatkin, A. B. *J. Org. Chem.* **1995,** *60*, 3035.

63. Doyle, M. P.; Zhou, Q.-L.; Dyatkin, A. B.; Ruppar, D. A. *Tetrahedron lett.* **1995,** *36*, 7579.

64. Doyle, M. P.; Van Oeveren, A.; Westrum, L. J.; Protopopova, M. N.; Clayton, T. W. *J. Am. Chem. Soc.* **1991,** *113*, 8982.

65. Doyle, M. P.; Hu, W. *Chirality* **2002,** *14*, 169.

66. Guptill, D. M.; Davies, H. M. L. *J. Am. Chem. Soc.* **2014,** *136*, 17718.

67. Hashimoto, S.-i.; Watanabe, N.; Sato, T.; Shiro, M.; Ikegami, S. *Tetrahedron lett.* **1993,** *34*, 5109.

68. Davies, H. M. L.; Bruzinski, P. R.; Lake, D. H.; Kong, N.; Fall, M. J. *J. Am. Chem. Soc.* **1996,** *118*, 6897.

69. DeAngelis, A.; Dmitrenko, O.; Yap, G. P. A.; Fox, J. M. *J. Am. Chem. Soc.* **2009,** *131*, 7230.

Chapter 2

Asymmetric C–H Functionalization via *N*-Sulfonyl-1,2,3-Triazoles

---

2.1 Introduction

Recently, rhodium(II)-catalyzed intermolecular C–H Functionalization via *N*-sulfonyl triazoles has emerged as a novel, alternative methodology as compared to α-diazocarbonyl compounds that are traditionally used as carbene precursors.[1] Davies and co-workers have substantially advanced the field of selective intermolecular carbene reactions by developing the concept of donor/acceptor carbenes and a suite of chiral catalysts that feature different steric demands for various applications.[2-7] The hallmark of a donor/acceptor carbene is that the electron-donating group serves to enhance the selectivity by taming the reactivity. Because of its important role in modulating the overall reactivity, various donor groups have been studied in diazo chemistry (Figure 2.1). Aryldiazoacetates (**2.1**) and vinyldiazoacetates (**2.2**) are very well-established to date and easily accessed via base-promoted diazo transfer processes with an azide (Regitz diazo transfer)[2, 6], while diazo compounds bearing alkynes (**2.3**) as donor were found unstable even under regular conditions, and those bearing heteroatoms such as nitrogen (**2.4**) or oxygen (**2.5**) and are not isolable. Therefore, to access a wider range of donor/acceptor carbenes, a new class of precursor may be necessary. Most notably, having a heteroatom immediately adjacent to the diazo functionality should provide many exciting opportunities for the development of new carbene reactions and C–H functionalization reactions.

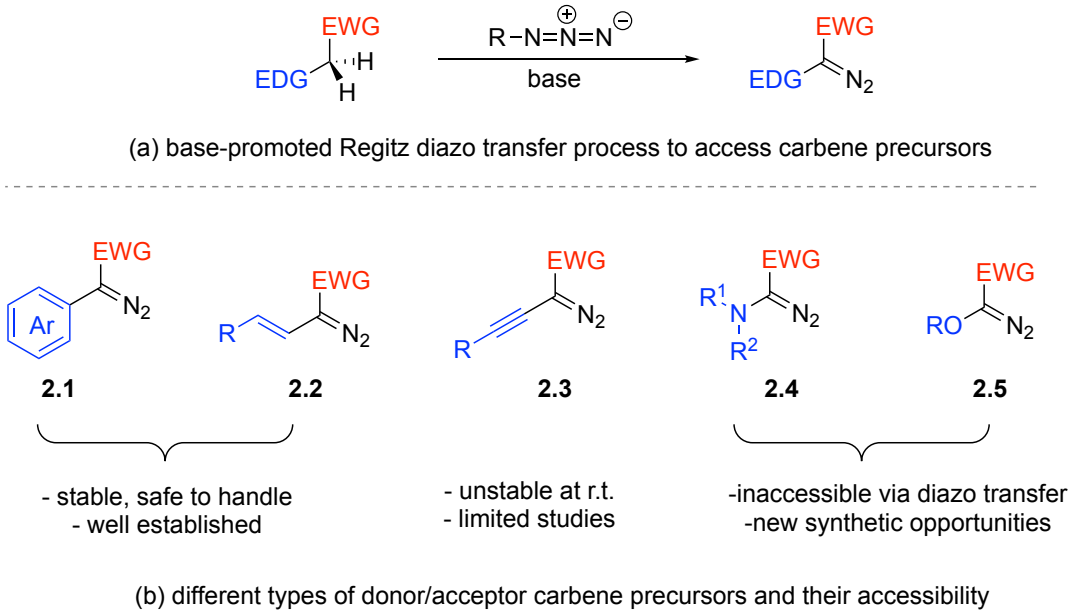

Figure 2.1 Different forms of donor/acceptor diazo compounds as carbene precursors

In 2002, Meldal and co-workers[8] described a 1,3-dipolar cycloaddition protocol to afford 1,4-disubstituted 1,2,3-triazoles that was later modified and popularized by Sharpless and co-workers,[9] where an organic azide (**2.6**) reacted with a terminal alkyne (**2.7**) under the catalysis of a Cu(I) catalyst in a regioselectively manner. Later work by Gevorgyan, Fokin and co-workers revealed that the 1,2,3-triazoles are capable of undergoing ring opening (via Dimroth rearrangement) to expose an α-imino diazo intermediate in equilibrium that can be quickly trapped by a $Rh_2(OAc)_4$ as an alternative entry into rhodium-stabilized donor/acceptor carbenes.[1, 10, 11] For example, they discovered that 7-chloro-substituted pyridotriazole **9** could undergo ring-opening to reveal a diazo intermediate **2.10** that can be trapped by $Rh_2(OAc)_4$ and react with triethylsilane to generate **2.11** via Si–H insertion and with benzonitrile to generate **2.12** via a transannulation reaction. In 2009, Fokin and co-workers reported that *N*-sulfonyl triazoles **2.13** tend to favor the

ring-opened form to a greater extent, and the resulting donor/acceptor diazo compound can then react with olefins to produce cyclopropanes **2.14** in a highly stereoselective manner using Rh_2(*S*-NTTL)$_4$.[12]

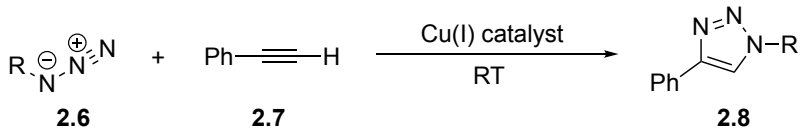

(a) Cu(I)-catalyzed regioselective synthesis of 1,2,3-triazoles

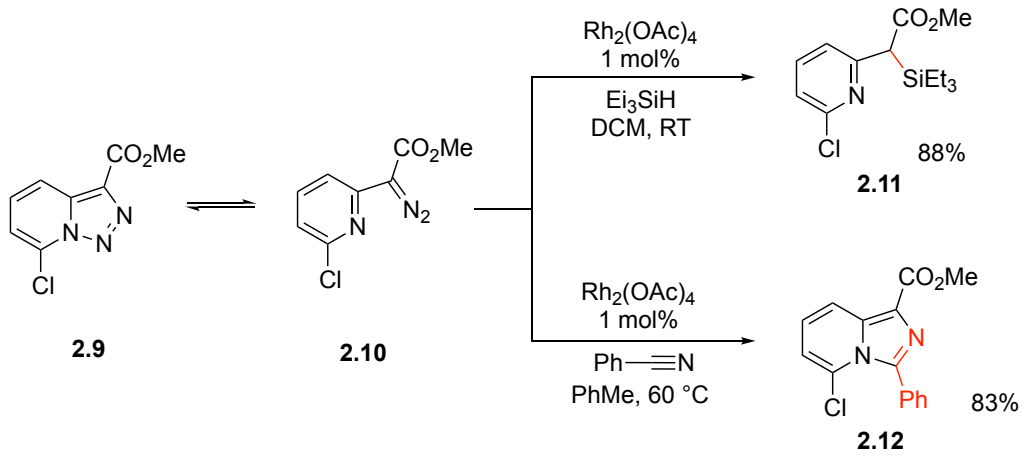

(b) 1,2,3-Triazoles can act as "masked" rhodium-carbene precursors

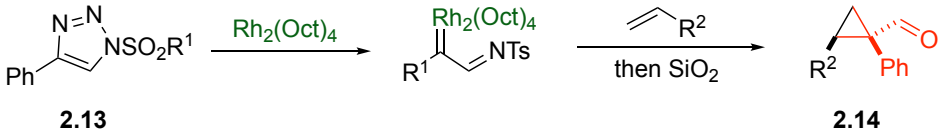

(c) cyclopropanation with styrene using *N*-sulfonyl triazole

Scheme 2.1 1,2,3-Triazoles can acted as a "masked" donor/acceptor diazo compound

Since these initial discoveries, *N*-sulfonyl 1,2,3-triazoles have quickly gained popularity within the synthetic community and a variety of new transformations have been developed. One particularly interesting feature of the *N*-sulfonyl triazoles is that after ring opening, the imine nitrogen displays stronger nucleophilicity than the oxygen in diazoesters. This distinct reactivity

was exploited in a number of contexts that involve zwitterionic intermediates to promote cyclization reactions that forms new heterocycles (Scheme 2.2). Some notable examples of reaction development have been reviewed.[13-19]

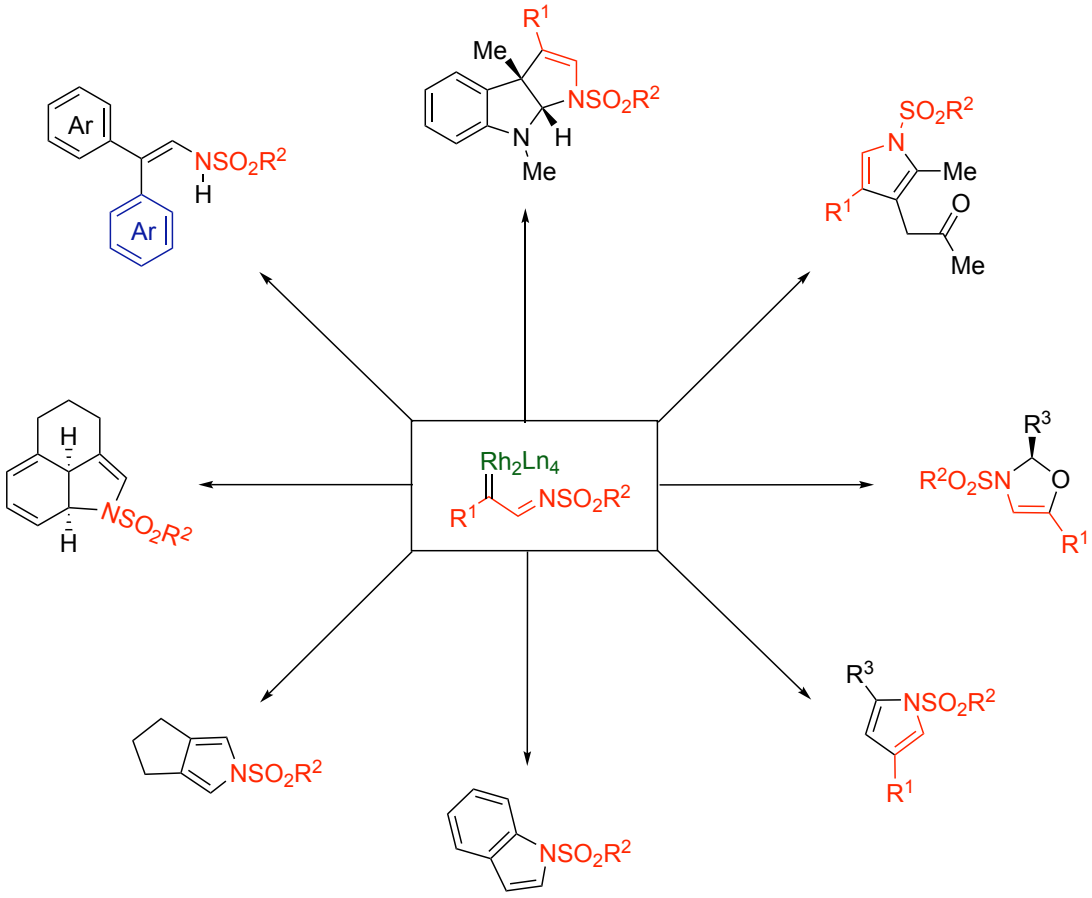

Scheme 2.2 Notable examples of reactions using *N*-sulfonyl triazoles

In addition, in 2011, Fokin and co-workers reported the first examples of enantioselective intermolecular C–H Functionalization reactions using these *N*-sulfonyl triazoles on unactivated C–H bonds (Table 2.1).[20] In this reaction, an aryl *N*-sulfonyl triazole (**2.15**) was found to undergo

facile ring-opening and C–H insertion reaction into a variety of unactivated C–H bonds to produce the functionalized products (**2.16a-d**). The resulting imine functionality in the product is unstable on silica gel but could be effectively reduced by treating the product with LAH at 0 °C to generate a secondary amine. The optimal dirhodium catalyst was found to be Rh_2(*S*-NTTL)$_4$ (**2.17**) for most substrates, which was originally developed by Müller and co-workers for cyclopropanation reactions using Meldrum's acid.[21] However, in a few cases where the *N*-sulfonyl group was more complex, it was found that Rh_2(*S*-PTAD)$_4$, developed by Davies,[22] had superior performance.

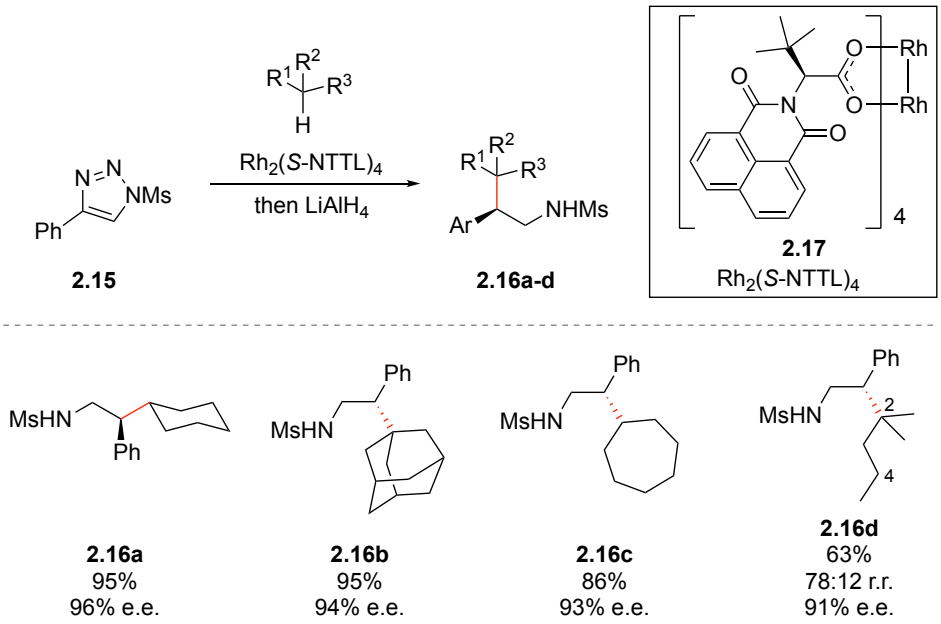

Table 2.1 Fokin's Rh_2(*S*-NTTL)$_4$-catalyzed asymmetric C–H Functionalization using *N*-sulfonyl triazole as carbene precursor

Recognizing the synthetic potential of these newer generation donor/acceptor carbenes, the Davies group became interested in further reaction and catalyst development. And as mentioned above, one of the primary objectives would be to incorporate oxygen and nitrogen as donors for

donor/acceptor carbenes. A significant advancement in the field was in 2012, Dr. Alford demonstrated that 4-phthalimido-*N*-methanesulfonyl-1,2,3-triazole (**2.19**), derived from Click reaction using precursor **2.18**, can decompose spontaneously at 55 °C to form a free carbene that can then undergo cyclopropanation in the presence of a variety of alkenes (Scheme 2.3).[23] The cyclopropanated product **2.20** could then be smoothly transformed to unmask a cyclopropyl α-amino acids **2.21**, which can have important biological properties. In this study, even though the reactions were highly diastereoselective, control experiments indicated that chiral dirhodium catalysts did not provide any asymmetric induction. Therefore, it was proposed that the thermal reaction predominated and the carbene did not engage with the rhodium because it was very short-lived.

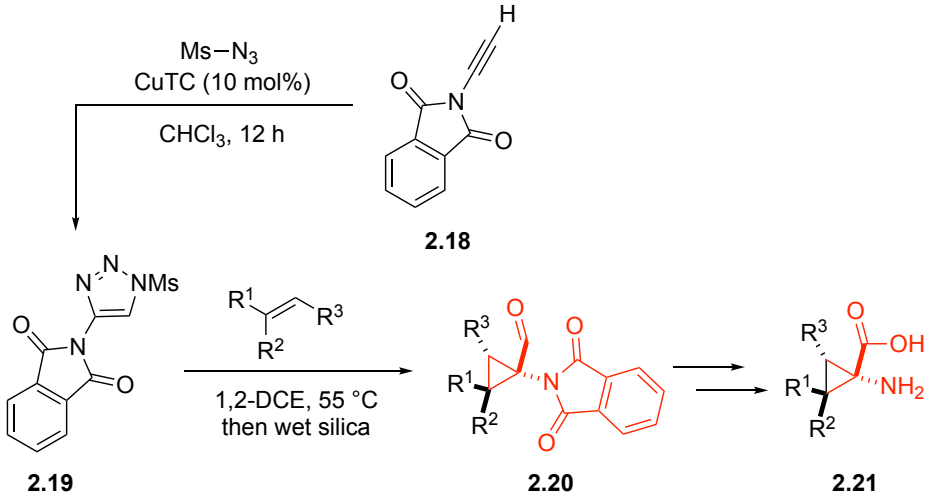

Scheme 2.3 α-Amino donor/acceptor carbenes can undergo thermal cyclopropanations

Nevertheless, C–H functionalization reactions using *N*-sulfonyl triazoles as carbene precursors have experienced quite limited development in the past decade. One primary reason that accounts for this is that to date, many dirhodium catalysts were designed for specifically for

aryl diazoacetates. In 2016, the Davies group demonstrated that, in addition to the study by Fokin and co-workers, it was possible to use *N*-sulfonyl triazoles to do selective intermolecular C–H functionalization reactions at activated benzylic and allylic sites, and the best catalyst was Rh_2(*S*-NTTL)$_4$ (Scheme 2.4).[23] When triazole **23** was used as the carbene precursor and *p*-cymene (**2.22**) was used as the substrate, where there is a competition between the activated primary and tertiary benzylic sites, the product **2.23** was obtained with moderate regioselectivity (4 : 1 rr) and enantioselectivity (74% ee), although the minor regioisomer had much higher enantioselectivity (95% ee). When the same substrate was functionalized with methyl phenyldiazoacetate (**2.24**), the enantioinduction was much lower (20% ee). In addition, when primary C–H functionalization was attempted using anisole **2.26** as the substrate, the product **2.27** was obtained with low yield (37% yield), even though the primary C–H bond was benzylic. Therefore, there could be new opportunities related to catalyst development that could enhance these results.

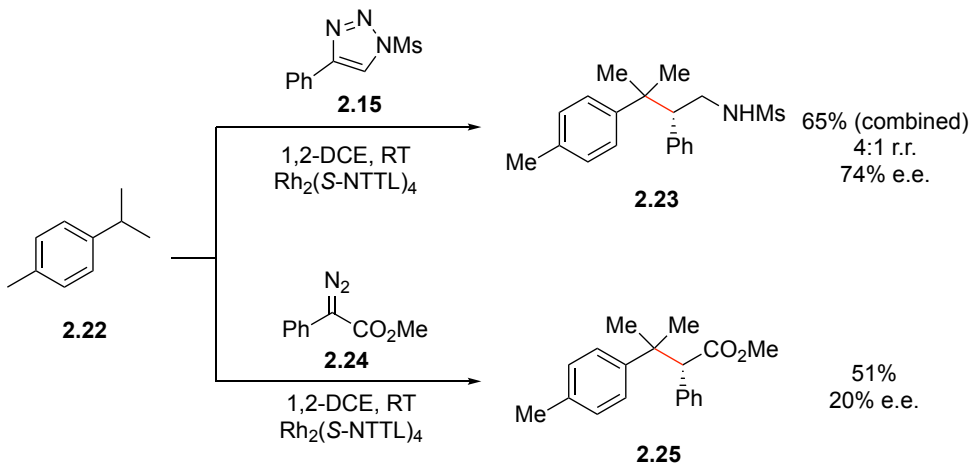

(a) When Rh_2(*S*-NTTL)$_4$ is used, *N*-sulfonyl triazole was a more effective carbene precursor

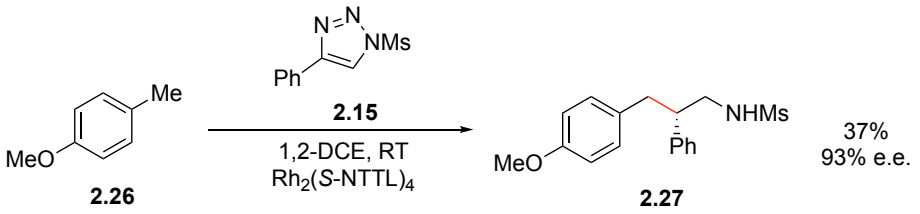

(b) Primary C-H functionalization using *N*-sulfonyl triazole gave low yield

Scheme 2.4 Benzylic C–H functionalization using *N*-sulfonyl triazole

Besides benzylic sites, rhodium-carbenes also react efficiently when the desired C–H bond is adjacent to a heteroatom. For example, when methyl phenyldiazoacetate **2.24** reacted with THF in the presence of Rh_2(*S*-DOSP)$_4$, the product **2.28** was obtained with high regio- and enantioselectivity (97% ee), although diastereoselectivity was lower (2:1 dr).[25] However, in 2014, Lacour and co-workers discovered that when the *N*-sulfonyl triazoles **2.29** were used as the carbene precursor, instead of carbene insertion, the THF oxygen interfered as a nucleophile and formed a oxonium rhodium-ylide (**2.31**) upon interacting with the carbene.[26] Then the imine nitrogen facilitates a cyclization event that provides a medium sized ring (**2.30**) as the product. Even though

this reaction still provides synthetic value, a general C–H functionalization reaction on these substrates using *N*-sulfonyl triazoles still remains to be desired.

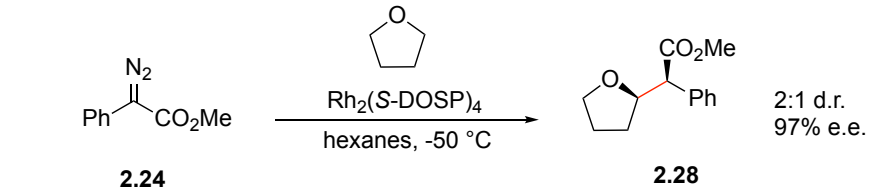

(a) Rh_2(*S*-DOSP)$_4$ is an effective catalyst for functionalizing THF

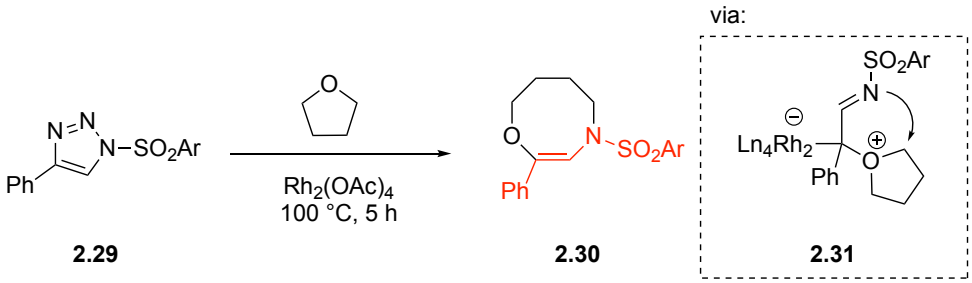

(b) Lacour synthesis of medium sized ring using *N*-sulfonyl triazole and THF

Scheme 2.5 Different reactivity of THF with an aryl diazoacetate and *N*-sulfonyl triazole

In summary, while *N*-sulfonyl triazoles are a new class of precursors to donor/acceptor carbenes that displays a promising reactivity profile and provides unique synthetic opportunities, their applications in C–H functionalization remain limited to only a handful of studies. The level of sophistication in catalyst-controlled site- and stereoselectivity for aryl diazoacetates is far superior than for *N*-sulfonyl triazoles, and the only few chiral catalysts that were applied in triazole chemistry, Rh_2(*S*-NTTL)$_4$ and Rh_2(*S*-PTAD)$_4$, are inherited from aryl diazoacetate chemistry. Ultimately we hoped to discover new reactivity with the development of catalysts and as well as new site selectivity that can be controlled by these catalysts when *N*-sulfonyl triazoles are used as the carbene precursors. This chapter will focus on the discussion of the design and synthesis of

several chiral dirhodium catalysts for triazole chemistry and the evaluation of their performance in cyclopropanation and C–H functionalization reactions.

2.2 Results and Discussion

2.2.1 Synthesis of dirhodium(II) tetracarboxylate catalysts

Guided by established results on the nature of the chiral crown cavity of C_4-symmetrical dirhodium complexes and their performance in *N*-sulfonyl triazole chemistry, we were initially interested in developing variations of such *N*-protected amino acid-based ligands, which were first discovered by Hashimoto and Müller (Figure 2.2).[21, 27, 28] Derivatives of both **2.32** and **2.33** have been shown to be effective ligands for dirhodium catalysts in triazole chemistry.[1, 20]

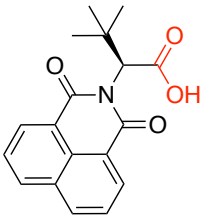

2.32
Müller's ligand, *S*-NTTL

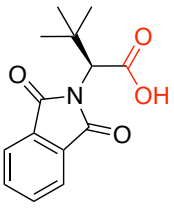

2.33
Hashimoto's ligand, *S*-PTTL

Figure 2.2 Müller and Hashimoto's chiral amino acid ligands

Based on these core structures, we planned to synthesize catalysts **2.34**-**2.41** (Figure 2.3). Because the halogenated derivatives of *S*-PTTL ligand are known be more structurally rigid,[29, 30] it would be interesting to see how different halogens affect the performance of the catalysts (**2.34**-**2.35**). However, both Rh_2(*S*-TCPTTL)$_4$[28] (**2.34**) and Rh_2(*S*-TFPTTL)$_4$[29] (**2.35**) are known catalysts

originally developed by Hashimoto and co-workers. In limited studies it has been shown that other variants with extended imido units and ligands with reduced local symmetry improved asymmetric induction,[32, 33] and therefore we wanted to incorporate **2.36**[34] and **2.37**[33] in the study to see the effects on *N*-sulfonyl triazole chemistry. Within the Davies group, we also heavily rely on manipulation of a catalyst's steric bulk to effect site and stereoselectivity,[35-38] and therefore **2.38**-**2.39** were synthesized to see the potential effect of added steric demand by the phenyl groups. Diels-alder reaction-derived ligands (**2.40**-**2.41**) are to date unknown in the literature, and it would be interesting to explore their reactivity and possibly obtain a crystal structure.

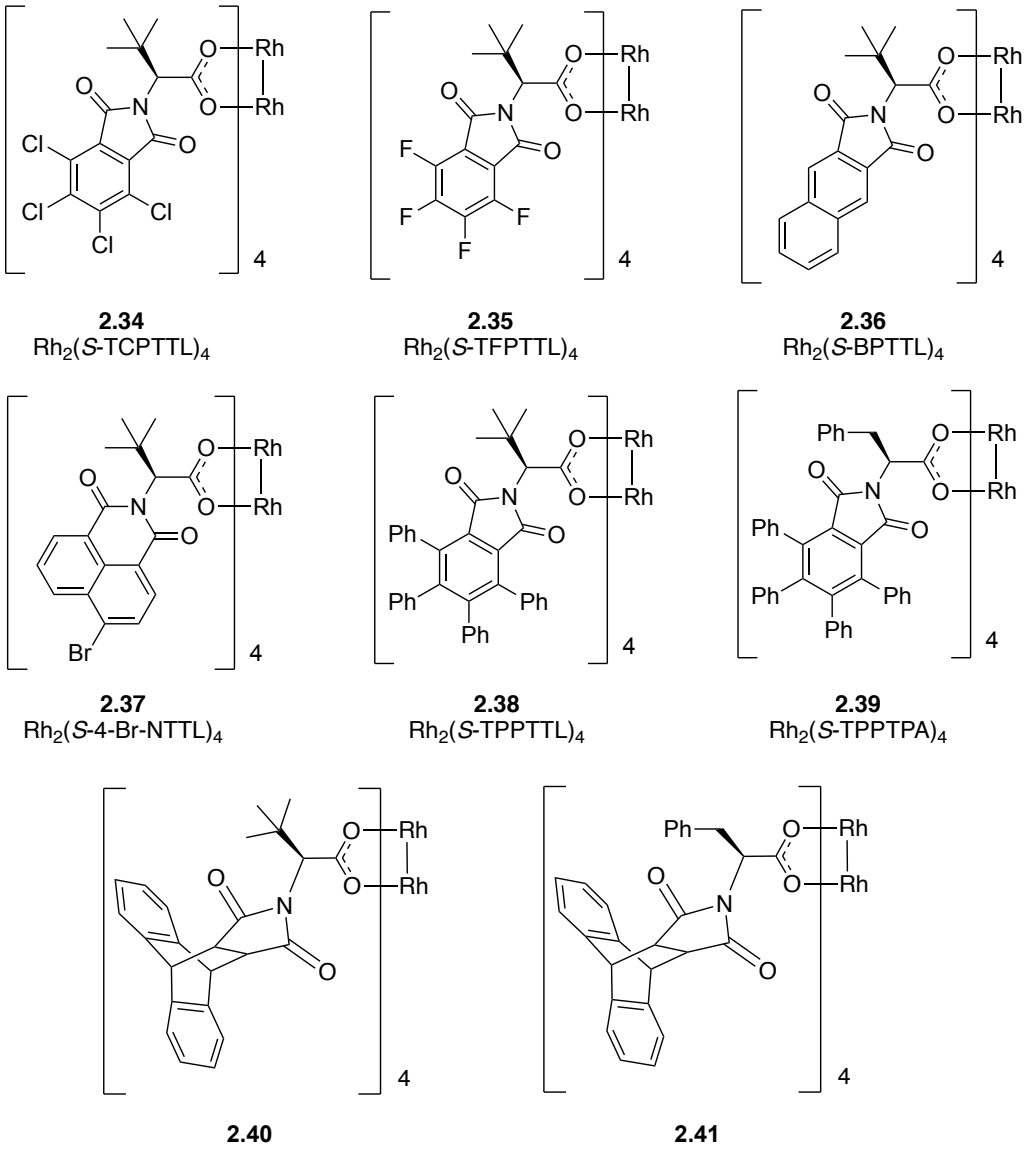

Figure 2.3 Dirhodium tetracarboxylate catalysts designed for *N*-sulfonyl triazole chemistry

The synthetic route toward the ligands of these catalysts involved condensation of the starting anhydrides **2.42** and the appropriate chiral amino acids **2.43**, both of which were commercially available except for catalysts **2.40** and **2.41**. Because the commercial amino acid was already enantiopure, the ligands did not require further recrystallization for enantioenrichment.

The catalysts were then synthesized by standard ligand exchange procedures using $Rh_2(OAc)_4$ with continuous removal of acetic acid byproduct through a Soxhlet extraction apparatus (Table 2.2). The reactions are mechanistically straightforward and have good literature precedence[21], although the first condensation reaction initially proved to be problematic, and solubility issues posed many challenges in terms of reaction efficiency and the workup procedures.

Table 2.2 Synthesis of different dirhodium catalysts for *N*-sulfonyl triazole chemistry

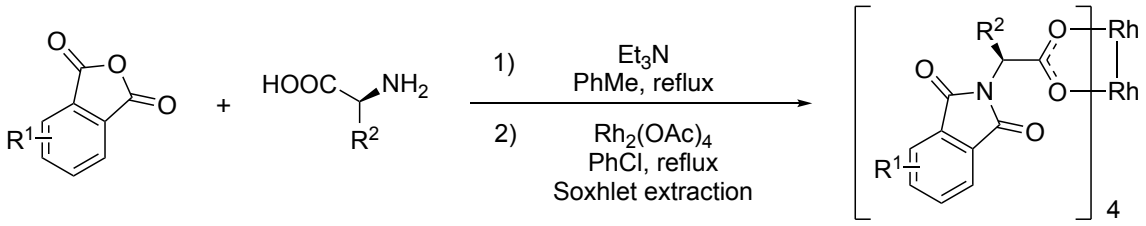

2.42 **2.43** **2.34-2.41**

entry	Rh(II) catalyst	additive	yield, (%) condensation	yield, (%) ligand exchange
1	**2.34** Rh_2(*S*-TCPTTL)$_4$	HFIP	82	63
2	**2.35** Rh_2(*S*-TFPTTL)$_4$	-	75	89
3	**2.36** Rh_2(*S*-BPTTL)$_4$	HFIP	95	93
4	**2.37** Rh_2(*S*-4-Br-NTTL)$_4$	HFIP	85	81
5	**2.38** Rh_2(*S*-TPPTTL)$_4$	-	86	84
6	**2.39** Rh_2(*S*-TPPTPA)$_4$	-	79	95
7	**2.40**	-	65	68
8	**2.41**	-	72	65

Because the synthesis of *S*-NTTL (**2.17**) has been reported,[21] it was initially chosen as the general procedure for the synthesis of all other ligands as they are structurally similar. However,

in the condensation reaction, the use of DMF as the solvent was found to be a poor choice. First, due to its high boiling point it was difficult to remove the solvent using various methods. The residual DMF resulted in a sticky crude residue that was difficult to purify by column chromatography. Furthermore, the miscibility of DMF with water made the acidic workup quite inefficient. Therefore, the solvent was then changed to toluene as a non-polar solvent, which mitigated the problem significantly. The new challenge, however, was that some starting anhydrides (Table 2.2, entries 1, 3 and 4) would not solubilize even under refluxing conditions and therefore the reaction did not proceed. The addition of a catalytic amount (0.1 equiv) of triethylamine only improved the reaction efficiency marginally, and the anhydride still had minimal solubility under this conditions and the reaction remained heterogeneous. In search of an appropriate co-solvent, Dr. Sidney Wilkerson-Hill discovered that a small amount (5 mL) of 1,1,1,3,3,3-hexafluoro-2-propanol (HFIP) as co-solvent can solubilize the anhydride within 5-15 min after the reaction reached its refluxing temperature. It was also discovered that a stoichiometric amount (1.1 equiv) of triethylamine was beneficial to ensure that the starting amino acid is not in its zwitterionic form, which is not nucleophilic toward the anhydride. As mentioned above, previous reports were cautious toward the use of triethylamine,[33] presumably due to concern about potential base-promoted epimerization of the chiral amino acid, but we found that this was not a problem. With these conditions in hand, we were able to fully access the desired ligands.

The ligand exchange reactions went smoothly when chlorobenzene was used as the solvent. In some literature examples toluene was the preferred solvent for TPCP ligands,[35, 38] presumably due to concern about prolonged heating would interfere with structural integrity of the fragile cyclopropane ligands, which would not be applicable for these phthalimide-protected amino acid

ligands. To push the reaction equilibrium forward and promote full conversion, acetic acid generated as the byproduct was effectively removed with the use of a Soxhlet extraction apparatus, which contained solid Na_2CO_3. The high temperature ligand exchange reactions proceeded with 55 – 88% yield, and homogenous ligation was achieved in all cases as indicated by HRMS studies.

2.2.2 Synthesis of 4-phenyl-1-(N-methanesulfonyl)-1,2,3-triazole

With the catalysts in hand, the next step was to synthesize 4-phenyl-1-(*N*-methanesulfonyl)-1,2,3-triazole for test reactions and evaluate the performance of the synthesized catalysts. The "click" reaction developed by Sharpless and co-workers allowed for highly regioselective synthesis of substituted heterocyclic compounds using copper catalysis.[9] This new methodology presented as a substantial improvement over past efforts due to its high selectivity and readily accessible starting materials.

The synthesis of the *N*-sulfonyl triazole was relatively straightforward (Scheme 2.6). The first step was to react methanesulfonyl chloride (**2.44**) with sodium azide (**2.45**), using an equal amounts of acetone and H_2O as solvents. This step was straightforward and the product, methanesulfonyl azide (**2.46**), was obtained in quantitative yield. Then, under the catalysis of copper(I) thiophene-2-carboxylate (CuTC, **2.49**),[39] **2.47** was reacted with phenylacetylene **2.48** to produce the final triazole product **2.15**, which was purified by recrystallization from a hot mixture of hexanes/ethyl acetate in 68% after two crops. It was later discovered that the triazole has decent, but limited shelf life if atmospheric moisture is not carefully excluded during storage or not stored

at low temperature, and the hydrolyzed product (*N*-H triazole, **2.50**) would impede Rh(II) catalysis[19] by irreversibly binding to the axial sites and shutting down the catalytic activity.

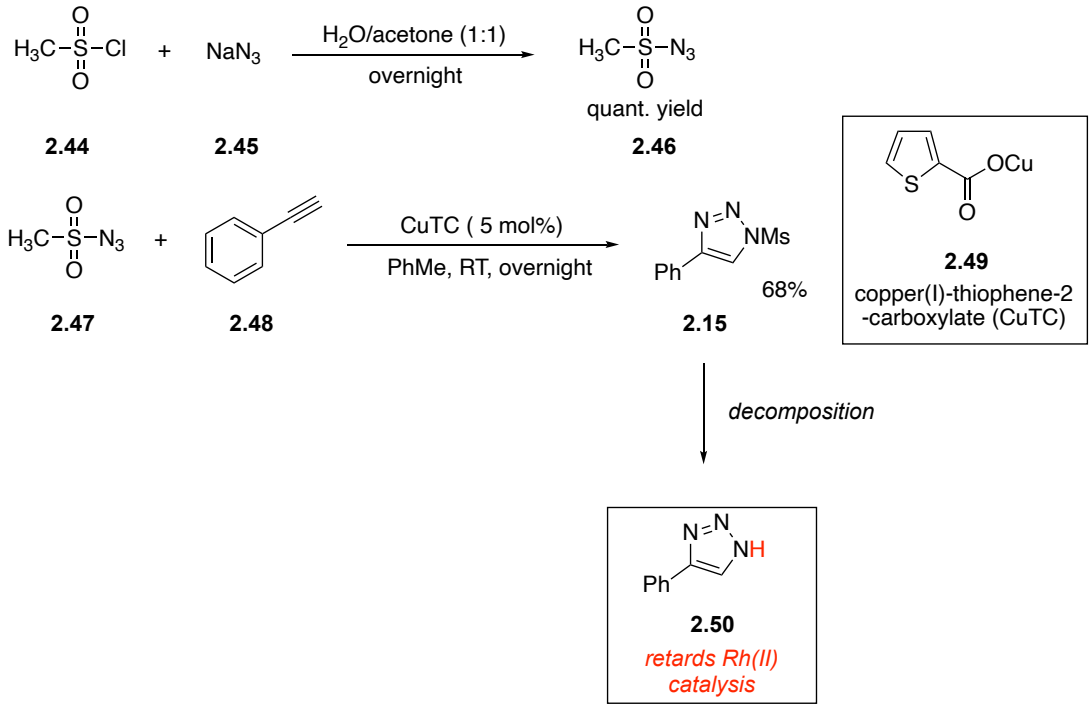

Scheme 2.6 CuTC-catalyzed regioselective synthesis of *N*-sulfonyl-1,2,3-triazole

2.2.3 Evaluation of new catalysts in styrene cyclopropanation reactions

In the Davies group, one of the benchmark reactions for evaluating catalysts is asymmetric cyclopropanation. To this end, we examined catalysts **2.34**-**2.41** as well as Rh_2(*S*-NTTL)$_4$ in a standard cyclopropanation reaction using *N*-sulfonyl triazole **2.15** and styrene as the substrate (Table 2.3). Based on previous experiences in the Davies group, trace amounts of impurities in catalysts and the triazole compound will inhibit Rh(II) catalysis, resulting in little to no desired product formation. Therefore, cyclopropanation serves as a good "quality control" experiment and

a means of providing some initial data. Unlike cyclopropanation with aryldiazoacetates, the intermediate imine **2.52** needs to be hydrolyzed to the corresponding aldehyde **2.51** to ensure product stability on silica gel and efficient purification. The procedures developed by Fokin and co-workers[11] allowed for low catalyst loading (0.5 mol %) and, interestingly, the reaction can be conducted without careful exclusion of atmospheric oxygen. In addition, unlike aryl diazoacetates that need to be added slowly using slow addition techniques for C–H functionalization, usually a syringe pump, triazoles can be added to the reactions in one portion at the beginning. After screening all catalysts, we were delighted to see that the initial results were promising.

Table 2.3 Evaluation of catalysts in asymmetric cyclopropanation reactions

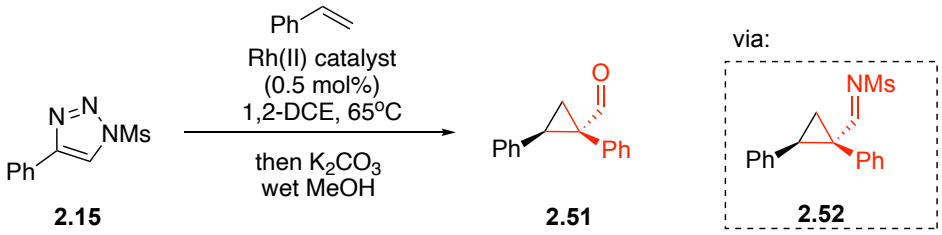

2.15 **2.51** **2.52**

entry	Rh(II) catalyst	yield[a] (%)	d.r.[b]	e.e.[c] (%)
1	**2.34** Rh_2(*S*-TCPTTL)$_4$	75	> 20:1	99
2	**2.35** Rh_2(*S*-TFPTTL)$_4$	95	> 20:1	91
3	**2.36** Rh_2(*S*-BPTTL)$_4$	88	> 20:1	95
4	**2.37** Rh_2(*S*-4-Br-NTTL)$_4$	78	> 20:1	96
5	**2.38** Rh_2(*S*-TPPTTL)$_4$	90	> 20:1	85
6	**2.39** Rh_2(*S*-TPPTPA)$_4$	90	> 20:1	78
7	**2.40**	91	> 20:1	53
8	**2.41**	88	> 20:1	47
9	Rh_2(*S*-NTTL)$_4$	86	> 20:1	96

[a] Yields refer to isolated yields.
[b] Diastereoselectivity was determined from the reaction crude 1H NMR spectra
[c] Enantiomeric excess data were obtained using HPLC on a chiral stationary phase

As shown in Table 2.3 above, all catalysts yielded the desired product with high level of diastereoselectivity, as no minor diastereomer was observed in crude ^{1}H NMR spectra. Rh_2(*S*-TCPTTL)$_4$ (**2.34**) provided the highest level of asymmetric induction (99% ee, entry 1), although the yield dropped slightly as compared to Rh_2(*S*-NTTL)$_4$ (86% yield, entry 9). Based on previous experience, it is reasonable to assume that these catalysts tend to adopt a C_4-symmetrical conformation due to their structural similarity,[28, 29] and the results further confirmed that this conformation is beneficial for asymmetric induction with *N*-sulfonyl triazole chemistry. It is also reasonable to conclude that the *tert*-butyl group of the ligands is sufficiently sterically demanding to block the "bottom" face of the dirhodium catalysts, while the "all-up" ligands provide a chiral environment for the rhodium-bound α-imino carbene to interact with the substrate (see crystal structure in supporting information). However, Diels-Alder reaction-derived catalysts **2.40** and **2.41** gave significantly inferior results (53% and 47% ee, entries 7 and 8), although the yield was satisfactory (91% and 81% yield). This suggests that there existed substantial competing thermal reaction or the chiral pocket has less limitation for the substrate to approach. From the X-ray crystallography study (Figure 2.4), it was observed that catalysts **2.40** and **2.41** do not have a obvious "chiral crown" structure, and both faces of the dirhodium core seem to be wide open for carbene and substrate binding. This could partially explain the substantially diminished enantioselectivity when this type of catalysts were used, and therefore they were excluded from further studies.

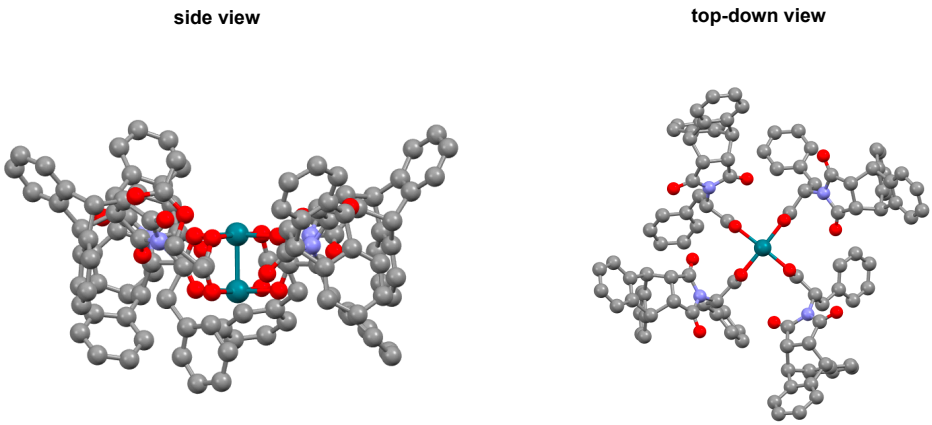

Figure 2.4 Crystal structure of catalyst **2.40** (both views)

2.2.4 Evaluation of new catalysts in site-selective C–H functionalization

In this study, *p*-cymene was chosen as the model substrate to examine the catalysts' site selectivity. This is a classic substrate used in the Davies group for initial evaluation of new dirhodium catalysts, as it contains an electronically activated primary and tertiary C–H bond, both of which are electronically favored toward C–H functionalization by carbene insertion.

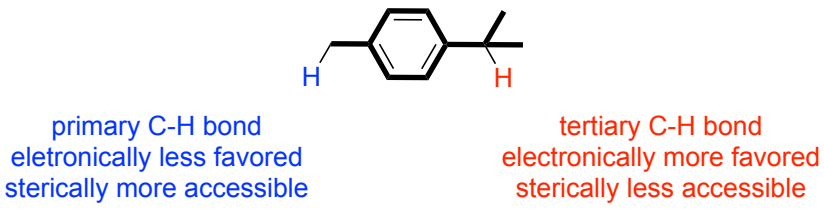

Figure 2.5 *p*-Cymene is a good substrate to evaluate site selectivity

The test reactions were run in 1,2-DCE at slightly elevated temperature (30 °C) to promote the ring opening rearrangement. Using Fokin's previous condition, the imine product then needed

to be reduced using lithium aluminum hydride at 0 °C after the C–H functionalization reaction to ensure product stability on silica gel. The C–H functionalization reaction and subsequent hydride reduction were done in a one-pot manner (Table 2.4).

It was surprising to see that while Rh_2(*S*-TCPTTL)$_4$ (**2.34**) gave superior results in cyclopropanation, it performed poorly in the C–H functionalization reaction, giving the desired tertiary insertion product only in low yield and mediocre enantioselectivity (28% yield, 43% ee, entry 1). Rh_2(*S*-TFPTTL)$_4$ (**2.35**) failed to decompose the starting triazole under the stated reaction conditions, even with prolonged stirring at elevated temperature (entry 2). Rh_2(*S*-BPTTL)$_4$ (**2.36**), similarly, was inefficient and only generated trace amount of product (15% yield, entry 3). Rh_2(*S*-4-Br-NTTL)$_4$ (**2.37**) performed comparably with the original catalyst, Rh_2(*S*-NTTL)$_4$, giving a higher regioselectivity (4.8 : 1 rr) but slightly diminished enantioselectivity (93% ee), but the overall similarity was consistent with our anticipation (entries 4 and 7).

It is important to note that so far (entries 1-4), all reactions in this study display a moderate to strong preference to tertiary C–H bonds. This could be presumably due to reduced steric hinderance of the rhodium-bound α-imino carbene, as compared to when an aryl diazoacetate was used as the carbene precursor. It is, therefore, very interesting to see that Rh_2(*S*-TPPTTL)$_4$ (**2.38**) was able to reverse this trend, showing the opposite site selectivity (1 : 1.25 rr, entry 5) and preferentially catalyzed the functionalization of the primary C–H bond to give product **2.54** with the use of *N*-sulfonyl triazole as the carbene precursor. Unfortunately, Rh_2(*S*-TPPTTL)$_4$ gave only moderate enantioselectivity (69% ee, entry 5) for the major regioisomer at the primary site. More impressively, Rh_2(*S*-TPPTPA)$_4$ (**2.39**) pushed the interesting site selectivity even further, giving

the highest observed 1 : 6 ratio, also favoring the formation of **2.54** over **2.23**, although the yield was low (40% yield) as well as the enantioselectivity (48% ee, entry 6). In comparison, Rh_2(*S*-NTTL)$_4$ gave the primary insertion product with excellent enantioselectivity (95% ee),[23] although it is not the major product in this transformation. At this point, we proposed that these catalysts that have the tetraphenyl-substituted phthalimides are more sterically demanding, which might explain the reversed site selectivity.

Table 2.4 Evaluation of catalysts in site selective C–H functionalization reaction using *p*-cymene as the substrate

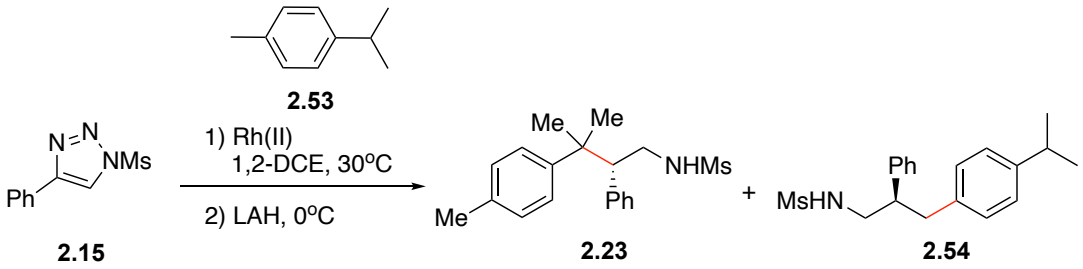

entry	Rh(II) catalyst	r.r.[a] (**2.23** : **2.54**)	yield[b] (%)	e.e.[c,d] (%)
1	**2.34** Rh_2(*S*-TCPTTL)$_4$	4 : 1	28	43
2[e]	**2.35** Rh_2(*S*-TFPTTL)$_4$	n.r.	n.r.	n.r.
3	**2.36** Rh_2(*S*-BPTTL)$_4$	1.7 : 1	15	n.d.
4	**2.37** Rh_2(*S*-4-Br-NTTL)$_4$	4.8 : 1	58	93
5	**2.38** Rh_2(*S*-TPPTTL)$_4$	1 : 2.5	62	69[d]
6	**2.39** Rh_2(*S*-TPPTPA)$_4$	1 : 6	40	48[d]
7	Rh_2(*S*-NTTL)$_4$	4 : 1	65	74

[a] Regioisomeric ratio was obtained from crude reaction ^{1}H NMR spectra
[b] Yields refer to combined yield of both regioisomer.
[c] Enantiomeric excess data were obtained using HPLC on a chiral stationary phase
[d] Enantiomeric excess data reported for major regioisomer
[e] The triazole did not decompose

Allylic C–H functionalization is also of significant interest to the Davies group, as these C–H bonds are also electronically activated toward carbene insertion. In this subsequent study,

trans-4-methyl-2-pentene (**2.55**) was chosen as the model substrate to screen the catalysts' efficacy in terms of site- and stereoselectivity (Table 2.5). Similar to *p*-cymene, **2.55** also contains competitive primary and tertiary sites that are both activated.

Again, despite good performance in cyclopropanation, Rh_2(*S*-TCPTTL)$_4$ (**2.34**) only gave the C–H functionalization product in a low 20% yield, and therefore the enantioselectivity was not determined (entry 1). In this reaction, Rh_2(*S*-TFPTTL)$_4$ (**2.35**) was again ineffective for decomposing the *N*-sulfonyl triazole (entry 2), and at this time it was presumed that **2.35** is an unsuitable catalyst for triazole chemistry and would need to be excluded from further studies. Rh_2(*S*-BPTTL)$_4$ (**2.36**) was only ineffective and low yielding. In terms of site selectivity, interestingly, all reactions showed strong preference for the tertiary allylic C–H bond, including Rh_2(*S*-TPPTTL)$_4$ (**2.38**) and Rh_2(*S*-TPPTPA)$_4$ (**2.39**) that were shown to prefer the primary C–H bond in *p*-cymene, even though they produced the tertiary functionalized products in decent yield (62% and 70% yield, entry 5 and 6). Presumably the tertiary C–H bond in *trans*-4-methyl-2-pentene (**2.55**) is much more accessible than that in *p*-cymene (**2.53**), where the approach of the rhodium carbene could be hampered by the phenyl ring. In other words, for the allylic system the tertiary C–H bond is preferred to a much higher extent than in benzylic system. Overall, the best catalyst for allylic functionalization remained to be Rh_2(*S*-NTTL)$_4$, although its derivative, Rh_2(*S*-4-Br-NTTL)$_4$ (**2.37**), also gave comparable results (entries 4 and 7).

Table 2.5 Evaluation of catalysts in site selective C–H functionalization reaction using *trans*-4-methyl-2-pentene as the substrate

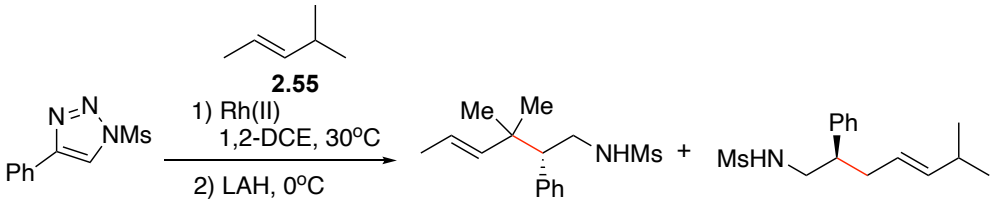

2.15 **2.56** **2.57**

entry	Rh(II) catalyst	r.r.[a] (**2.56** : **2.57**)	yield[b] (%)	e.e.[c,d] (%)
1	**2.34** Rh_2(*S*-TCPTTL)$_4$	> 30 : 1	20	n.d.
2[e]	**2.35** Rh_2(*S*-TFPTTL)$_4$	n.r.	n.r.	n.r.
3	**2.36** Rh_2(*S*-BPTTL)$_4$	> 30 : 1	15	n.d.
4	**2.37** Rh_2(*S*-4-Br-NTTL)$_4$	> 30 : 1	78	82
5	**2.38** Rh_2(*S*-TPPTTL)$_4$	> 30 : 1	62	30
6	**2.39** Rh_2(*S*-TPPTPA)$_4$	> 30 : 1	70	48
7	Rh_2(*S*-NTTL)$_4$	> 30 : 1	83	84

[a] Regioisomeric ratio was obtained from crude reaction ^{1}H NMR spectra
[b] Yields refer to combined yield of both regioisomer.
[c] Enantiomeric excess data were obtained using HPLC on a chiral stationary phase
[d] Enantiomeric excess data reported for major regioisomer
[e] The triazole did not decompose

2.2.5 Follow-up studies of Rh_2(S-TPPTTL)$_4$ and Rh_2(S-TPPTPA)$_4$ in aryl diazoacetate chemistry

From previous studies on *N*-sulfonyl triazoles, it was evident that Rh_2(*S*-NTTL)$_4$ remained to be the most effective chiral dirhodium catalyst for asymmetric cyclopropanation and C–H functionalization reactions. Even though Rh_2(*S*-TPPTTL)$_4$ and Rh_2(*S*-TPPTPA)$_4$ showed interesting site selectivity in the functionalization of *p*-cymene, they did not ultimately improve the reaction outcome as its stereoselectivity was poor. Therefore, reactions with the traditional aryl diazoacetates were also run in parallel in order to explore the maximum potential of the new catalysts.

Testing both catalysts in cyclopropanation reactions using styrene and aryl diazoacetates as the carbene precursor revealed some interesting results. We chose to initially test the cyclopropanation using methyl 2-(4-bromophenyl)-2-diazoacetate (**2.58**) as the carbene source and styrene as the substrate. The diazo compound **2.58** contains a methyl group in the ester functionality as the acceptor group, but Rh_2(*S*-TPPTTL)$_4$ and Rh_2(*S*-TPPTPA)$_4$ both gave poor asymmetric induction, as the cyclopropane **2.59** was generated in only 30% and 25% ee, respectively (Scheme 2.7).

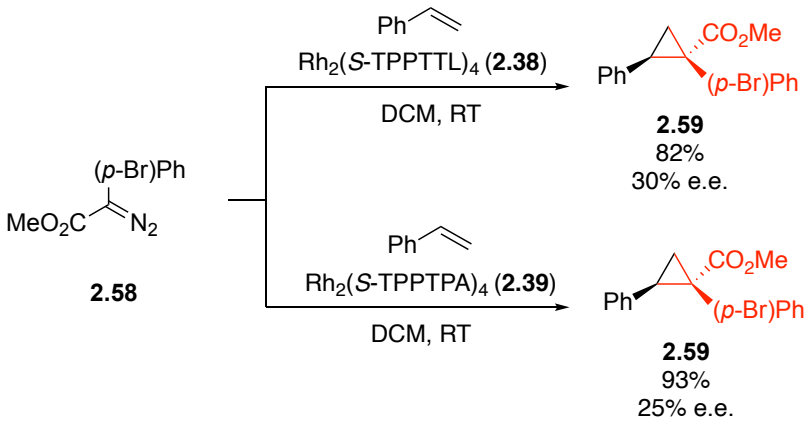

Scheme 2.7 Rh_2(*S*-TPPTTL)$_4$ and Rh_2(*S*-TPPTPA)$_4$-catalyzed cyclopropanation using methyl 2-(4-bromophenyl)-2-diazoacetate as the carbene precursor

As discussed previously, the Davies group has recently demonstrated that the discovery of 2,2,2-trichloroehtyl aryl diazoacetates has served as a key development in selective intermolecular carbene reactions catalyzed by dirhodium tetracarboxylate catalysts.[38] Therefore, we decided to further explore asymmetric cyclopropanations with these newer generation of carbene sources using Rh_2(*S*-TPPTTL)$_4$ and Rh_2(*S*-TPPTPA)$_4$ (Scheme 2.8). Surprisingly, we found that both catalysts were very sensitive to the identity of the ester group, and showed substantially improved enantioselectivity upon switching the carbene precursor to 2,2,2-trichloroethyl 2-(4-bromophenyl)-2-diazoacetate (**2.60**), as the desired cyclopropane product **2.61** was generated in 93% and 70% ee, respectively.

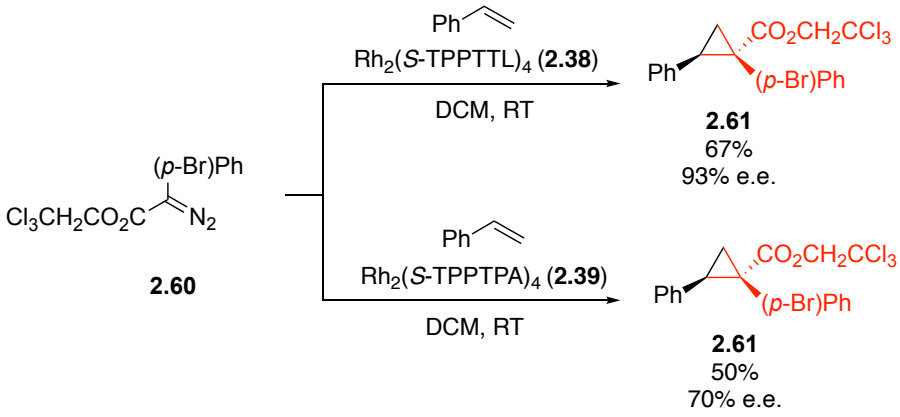

Scheme 2.8 Rh_2(*S*-TPPTTL)$_4$ and Rh_2(*S*-TPPTPA)$_4$-catalyzed cyclopropanation using 2,2,2-trichloroethyl 2-(4-bromophenyl)-2-diazoacetate as the carbene precursor

From this study, we concluded that the trichloroethyl ester was instrumental to the improved performance of these two catalysts. In particular, Rh_2(*S*-TPPTTL)$_4$ was able to give very high asymmetric induction for reaction, indicating that even though it did not exceed the performance of Rh_2(*S*-NTTL)$_4$ in *N*-sulfonyl triazole chemistry, it is indeed capable of highly stereoselective carbene reaction. Therefore, this catalyst was chosen to proceed to further studies, which was to explore how other halogenated ester groups would perform in the cyclopropanation reaction.

Because the reaction was facile, it was attempted at 0 °C to see if an even further enhancement in stereoselectivity could be obtained (Table 2.6). It was discovered that when the same carbene precursor **2.60** was used at 0 °C, the corresponding cyclopropanated product **2.61** was formed with marginally improved enantioselectivity (94% ee) and interestingly, the yield was improved to 91%. The use of trifluoroethyl derivative **2.62** produced the product **2.64** in less yield (75% yield), although the enantioselectivity was maintained (93% ee). The tribromoethyl

derivative **2.63** was found to easily crystallize on silica gel and complicated the chromatography. Nevertheless, the product **2.65** was still obtained with moderate yield (58% yield) and high enantioselectivity (92% ee).

Table 2.6 Scope of cyclopropanation catalyzed by Rh_2(*S*-TPPTTL)$_4$

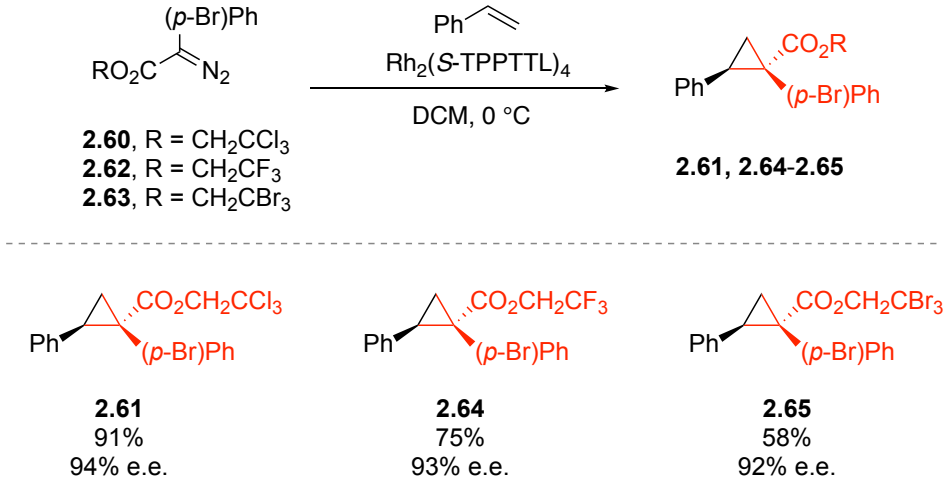

With positive results for cyclopropanation reactions in hand, we decided to further examine the catalyst's performance in benzylic functionalization (Table 2.7). Benzylic substrates such as *p*-cymene (**2.53**) and 4-ethyl toluene (**2.66**) are also commonly used substrates in the Davies group, because they provide essential information regarding the catalyst's selectivity profile even though they are highly electronically activated. To our surprise, when Rh_2(*S*-TPPTTL)$_4$ is used as the catalyst and *p*-cymene as the substrate, a highly regioselective transformation was observed (11 : 1 rr) that strongly favored the tertiary position of the substrate and generated product **2.69** with excellent enantiocontrol (90% ee, entry 1). When 4-ethyltoluene was used as the substrate, a competitive insertion could happen at the primary site, but we observed >30 : 1 regioisomeric ratio in favor of formation of the secondary insertion product **2.70** (entry 2). Generally speaking,

secondary insertion is favored by the rhodium carbene due to balance of steric and electronic factors, but the high level of regioselectivity is still very encouraging. The origin of this type of selectivity will be discussed in later chapters of the thesis. When 4-ethyl anisole (**2.67**) and 1-bromo-4-ethylbenzene (**2.68**) were used as the substrates, highly diastereoselective reactions at the secondary benzylic sites were observed and products **2.71** and **2.72** were obtained with good yield and high enantioselectivity (entries 3 and 4).

Table 2.7 Scope of Rh_2(*S*-TPPTTL)$_4$-catalyzed benzylic functionalization

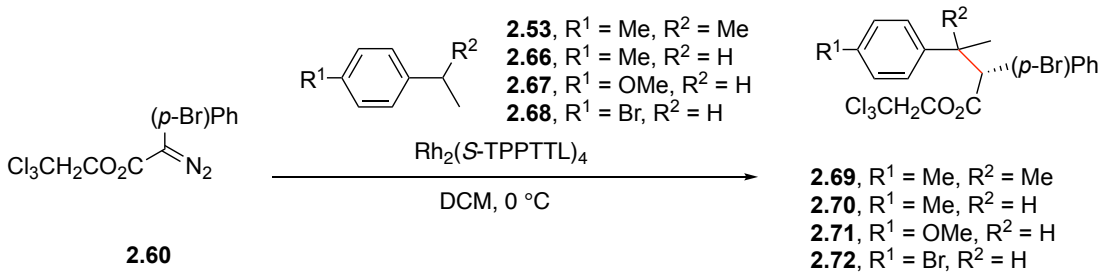

entry	substrate	product	yield[a] (%)	r.r.[b]	d.r.[b]	e.e.[c,d]
1	**2.53**	**2.69**	68	11 : 1	n/a	90
2	**2.66**	**2.70**	72	> 30 : 1	19.2 : 1	88
3	**2.67**	**2.71**	80	n/a	13.1 : 1	90
4	**2.68**	**2.72**	75	n/a	20 : 1	85

[a] Yield refers to combined yield.
[b] Regio- and diastereoselectivity were determined from the reaction crude ^{1}H NMR spectra
[c] Enantiomeric excess data were obtained using HPLC on a chiral stationary phase
[d] e.e. shown for the major isomer

2.3 Conclusions

In this study, a total of eight chiral dirhodium catalysts were prepared via the two-step procedure: (1) condensation reaction to synthesize the ligands using commercial anhydrides and chiral amino acid and then (2) followed by a high-temperature ligand exchange reaction to obtain the final catalysts. Improvement in the ligand synthesis step was achieved over literature method and the protocol is still operationally simple and the work up procedure as well as the purification process became trivial. A number of catalysts performed well in asymmetric cyclopropanation reaction using styrene as the standard substrate. However, for site selective C–H functionalization

reactions, Rh_2(*S*-NTTL)$_4$ remained to be the most capable and the catalyst of choice for *N*-sulfonyl triazole chemistry, giving the best yield and highest stereoselectivity, even though there was some room for further improvement. Unfortunately, other catalysts that were evaluated did not exceed the performance of Rh_2(*S*-NTTL)$_4$.

Nevertheless, parallel studies using aryl diazoacetates indicated that Rh_2(*S*-TPPTTL)$_4$ is also a very capable catalyst for asymmetric catalysis as indicated by the highly stereoselective cyclopropanation reactions. The catalyst also has a very interesting selectivity profile for C–H functionalization reactions. Even though the catalyst is somewhat sterically encumbered, particularly when compared to its parent compound, Rh_2(*S*-PTTL)$_4$, it showed a strong preference for the more hindered C–H bonds in benzylic substrates with high site selectivity. In addition, the reactions were highly diastereo- and enantioselective. Therefore, Rh_2(*S*-TPPTTL)$_4$ will be the catalyst of choice for further studies, which will be the focus of the following chapter of the thesis.

2.4 References

1. Davies, H. M. L.; Alford, J. S. *Chem. Soc. Rev.* **2014,** *43*, 5151.
2. Davies, H. M. L.; Manning, J. R. *Nature* **2008,** *451*, 417.
3. Hansen, J.; Davies, H. M. L. *Coord. Chem. Rev.* **2008,** *252*, 545.
4. Davies, H. M. L.; Liao, K. *Nat. Rev. Chem.* **2019,** *3*, 347.
5. Davies, H. M. L.; Morton, D. *J. Org. Chem.* **2016,** *81*, 343.
6. Davies, H. M. L.; Morton, D. *Chem. Soc. Rev.* **2011,** *40*, 1857.
7. Davies, H. M. L.; Beckwith, R. E. *Chem. Rev.* **2003,** *103*, 2861.
8. Tornøe, C. W.; Christensen, C.; Meldal, M. *J. Org. Chem.* **2002**, *67*, 3057

9. Rostovtsev, V. V.; Green, L. G.; Fokin, V. V.; Sharpless, K. B. *Angew. Chem. Int. Ed.* **2002,** *41*, 2596.

10. Horneff, T.; Chuprakov, S.; Chernyak, N.; Gevorgyan, V.; Fokin, V. V. *J. Am. Chem. Soc.* **2008,** *130*, 14972.

11. Chuprakov, S.; Hwang, F. W.; Gevorgyan, V. *Angew. Chem. Int. Ed.* **2007,** *46*, 4757.

12. Chuprakov, S.; Kwok, S. W.; Zhang, L.; Lercher, L.; Fokin, V. V. *J. Am. Chem. Soc.* **2009,** *131*, 18034.

13. Schultz, E. E.; Sarpong, R. *J. Am. Chem. Soc.* **2013,** *135*, 4696.

14. Alford, J. S.; Spangler, J. E.; Davies, H. M. L. *J. Am. Chem. Soc.* **2013,** *135*, 11712.

15. Parr, B. T.; Green, S. A.; Davies, H. M. L., *J. Am. Chem. Soc.* **2013,** *135*, 4716.

16. Miura, T.; Tanaka, T.; Hiraga, K.; Stewart, S. G.; Murakami, M. *J. Am. Chem. Soc.* **2013,** *135*, 13652.

17. Zibinsky, M.; Fokin, V. V. *Angew. Chem. Int. Ed.* **2013,** *52*, 1507.

18. Chuprakov, S.; Kwok, S. W.; Fokin, V. V. *J. Am. Chem. Soc.* **2013,** *135*, 4652.

19. Kubiak, R. W.; Davies, H. M. L. *Org. Lett.* **2018,** *20*, 3771.

20. Chuprakov, S.; Malik, J. A.; Zibinsky, M.; Fokin, V. V. *J. Am. Chem. Soc.* **2011,** *133*, 10352.

21. Müller, P.; Allenbach, Y.; Robert, E. *Tetrahedron: Asymmetry* **2003,** *14*, 779.

22. Reddy, R. P.; Davies, H. M. L. *Org. Lett.* **2006,** *8*, 5013.

23. Alford, J. S.; Davies, H. M. L. *Org. Lett.* **2012,** *14*, 6020.

24. Kubiak, R. W., 2nd; Mighion, J. D. *Org. Lett.* **2016,** *18*, 3118.

25. Davies, H. M. L.; Hansen, T.; Churchill, M. R. *J. Am. Chem. Soc.* **2000,** *122*, 3063.

26. Medina, F.; Besnard, C.; Lacour, J. *Org. Lett.* **2014,** *16*, 3232.

27. Tsutsui, H.; Abe, T.; Nakamura, S.; Anada, M.; Hashimoto, S. *Chem. Pharm. Bull.* **2005,** *53*, 1366.

28. Yamawaki, M.; Tsutsui, H.; Kitagaki, S.; Anada, M.; Hashimoto, S. *Tetrahedron Lett.* **2002,** *43*, 9561.

29. DeAngelis, A.; Boruta, D. T.; Lubin, J. B.; Plampin, J. N., 3rd; Yap, G. P.; Fox, J. M., *Chem. Commun.* **2010,** *46*, 4541.

30. DeAngelis, A.; Dmitrenko, O.; Yap, G. P. A.; Fox, J. M. *J. Am. Chem. Soc.* **2009,** *131*, 7230.

31. Adly, F. G.; Gardiner, M. G.; Ghanem, A. *Chem. Eur. J.* **2016,** *22*, 3447.

32. Adly, F. G.; Maddalena, J.; Ghanem, A. *Chirality* **2014,** *26*, 764.

33. Liao, K.; Negretti, S.; Musaev, D. G.; Bacsa, J.; Davies, H. M. L. *Nature* **2016,** *533*, 230.

34. Liao, K.; Pickel, T. C.; Boyarskikh, V.; Bacsa, J.; Musaev, D. G.; Davies, H. M. L., *Nature* **2017,** *551*, 609.

35. Liao, K.; Yang, Y. F.; Li, Y.; Sanders, J. N.; Houk, K. N.; Musaev, D. G.; Davies, H. M. L., *Nat. Chem.* **2018,** *10*, 1048.

36. Liu, W.; Ren, Z.; Bosse, A. T.; Liao, K.; Goldstein, E. L.; Bacsa, J.; Musaev, D. G.; Stoltz, B. M.; Davies, H. M. L. *J. Am. Chem. Soc.* **2018,** *140*, 12247.

37. Zhang, S.; Zhang, D.; Liebeskind, L. S. *J. Org. Chem.* **1997,** *62*, 2312.

38. Guptill, D. M.; Davies, H. M. L. *J. Am. Chem. Soc.* **2014,** *136*, 17718.

Chapter 3

Desymmetrization of Cyclohexanes by Site- and Stereoselective C–H Functionalization Using Donor/acceptor Carbenes

---

3.1 Introduction

Site-selective C–H functionalization has generated considerable interest within the synthetic community because it represents a new strategy for the synthesis and late stage modification of complex organic targets.[1-9] Traditionally, organic synthesis would rely on transformation of functional groups or structural features that display a higher level of reactivity. In this regard, C–H bonds are usually not considered as functional handles, but new methodologies and catalytic systems are continually being developed to carry out reactions on these bonds that are otherwise unreactive to general reagents. The challenge, however, is to achieve high level of control of which C–H bond is selectively functionalized, especially of it is not activated or not adjacent to a directing group.[10-12] In particular, methylene C–H bond functionalization has attracted wide scientific interest due to their ubiquitous presence in organic molecules. For example, while selective reactions on certain polycyclic molecules with appropriately positioned functional groups can be achieved,[13] in simple, unfunctionalized small molecules, more sophisticated control of site- and stereoselectivity remains to be very desirable.

The Davies group has been committed to solve these synthetic challenges by developing a "toolbox" of catalysts and reagents that would allow one to have catalyst-controlled site selectivity, whereby the natural tendencies of the substrates[14] may be overwhelmed by simply choosing an appropriate catalyst. Generally speaking, for a C–H bond in a more crowded environment to be

functionalized, one would need to choose a sterically less hindered and more flexible catalyst, and vice versa. For example, the group has already developed a collection of dirhodium catalysts that feature different triarylcyclopropane ligands with various steric environment, which would allow for site-selective functionalization of the most accessible primary, secondary and tertiary C–H bond in an unactivated system.[15-17] In addition, we could also achieve highly selective functionalization of the most accessible methylene C–H bond in the presence of more labile benzylic ones.[18] Key to these advancements is the rational design of the steric environments of these new catalysts so that they could target different C–H bonds with high specificity.[9]

Despite being some of the most classical structures in organic chemistry, cyclohexanes are difficult substrates for selective C–H functionalization. In general, equatorial C–H bonds are more sterically accessible than axial ones, but distinguishing between the different equatorial methylene C–H bonds is problematic. This challenge can be readily observed from a number of recent efforts directed toward selective cyclohexane functionalization using a variety of reagents (Scheme 3.1). For example, Baran and co-workers have shown that, when 1,1-dimethylcyclohexane is treated with methyl phenyldiazoacetate in the presence of catalytic $Rh_2(OAc)_4$, a 1 : 1 mixture of the C-3 and C-4 alkylated products were observed with little stereocontrol.[19] Because $Rh_2(OAc)_4$ is achiral and nonselective, this indicates that the cyclohexane system has little inherent bias that would cause any background selectivity without the influence from the rhodium catalyst. White and co-workers have developed an effective Fe catalyst for a C–H oxidation protocol, but applying this protocol to alkylcyclohexanes gave a mixture of products as essentially statistical mixture, while the starting material was not fully consumed.[13, 20] Radical-initiated C–H functionalization in cyclohexane substrates is also known, and a recent development from Alexanian and co-workers

demonstrated that even with a bulkier reagent, precise control of site selectivity is still a challenging process.[21, 22] Therefore, even though many C–H functionalization protocols for cyclohexanes are reported, the principal challenge of solving selectivity has not been satisfactorily achieved.

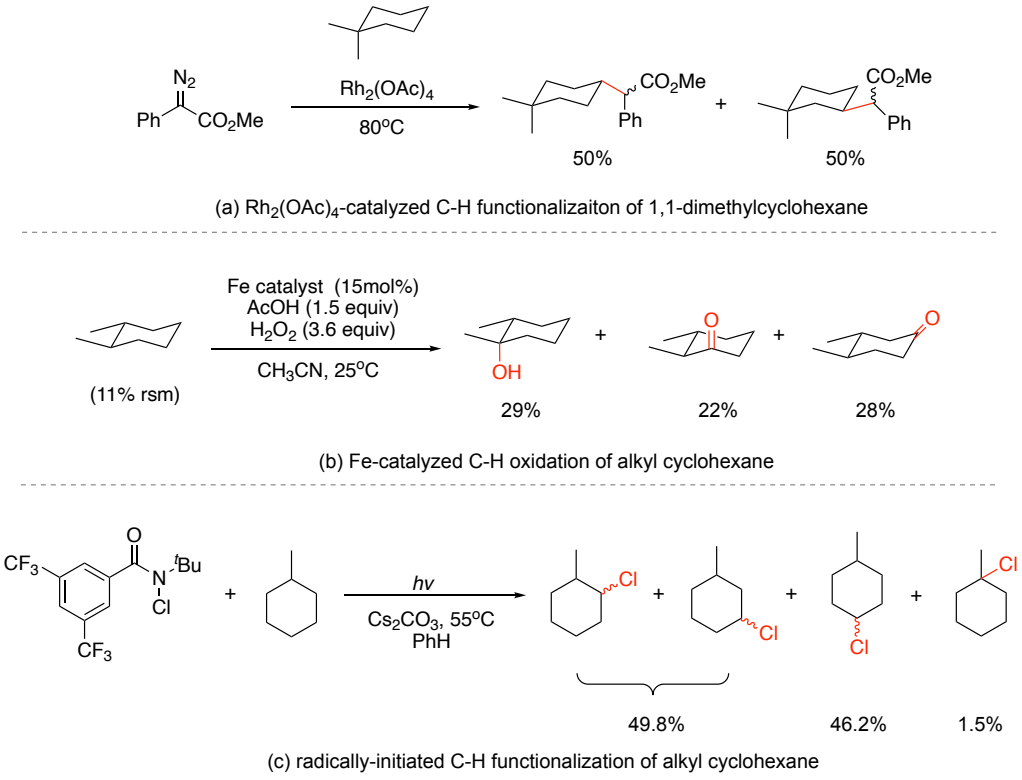

Scheme 3.1 Literature examples of C–H functionalization of unactivated cyclohexanes

The functionalization of unactivated substrates poses special challenges. Carbenes are very prone to self-dimerization. Therefore, in the absence of an effective trap, carbene dimerization would likely dominate and produce alkene byproducts. This is especially problematic when an acceptor diazo compound is used, but donor/acceptor carbenes generally tend to have better reactivity and selectivity profiles, although dimerization is still frequently seen. The Davies group

has reported stereoselective functionalization of a variety of cycloalkanes as well as tetrahydrofuran and *N*-protected pyrrolidine derivatives using Rh_2(*S*-DOSP)$_4$ as the catalyst (Scheme 3.2).[23, 24] When ethyl diazoacetate (**3.1**) or methyl diazoacetoacetate (**3.4**) was used, the desired functionalized product (**3.2** or **3.5**) was only produced in low to moderate yield with no stereocontrol, and the dimer (**3.3**) formation was substantial for ethyl diazoacetate. However, when methyl phenyldiazoacetate (**3.6**), a donor/acceptor diazo compound, was used, the reaction was much more selective, and gave the desired product **3.7** in 80% yield and 95% ee, although this result required meticulously degassed reaction environment and the use of cyclohexane as the solvent. In reactions with more valuable cyclohexane derivatives, the use of trapping agent as solvent would not be desirable.

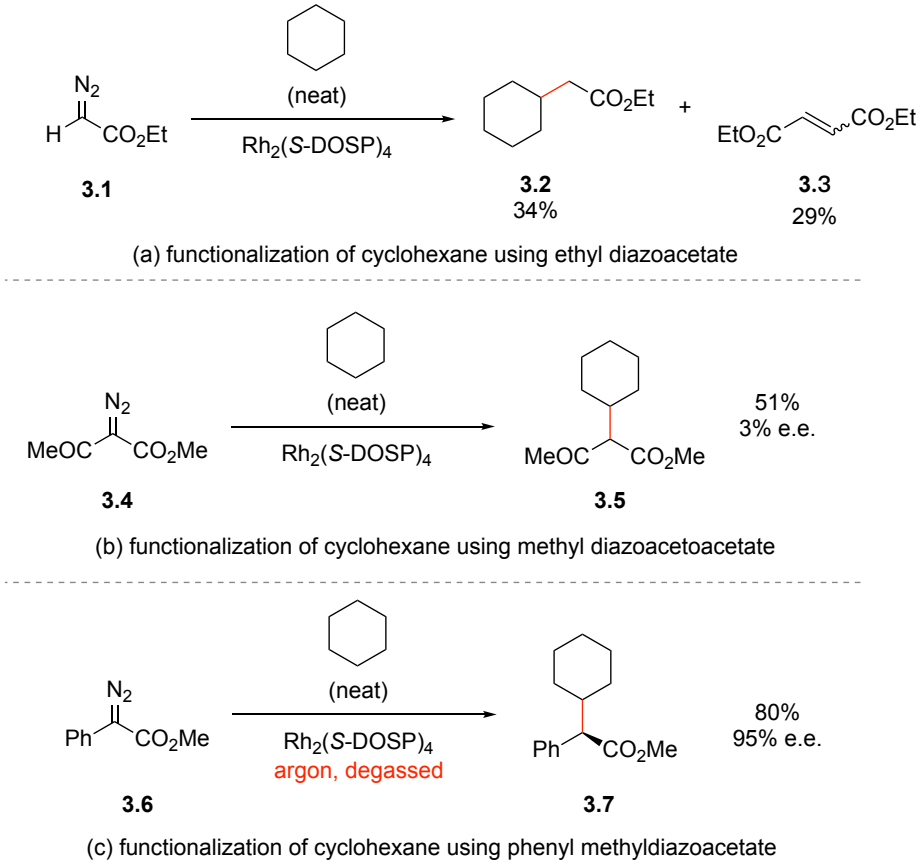

Scheme 3.2 Rh_2(*S*-DOSP)$_4$-catalyzed functionalization of cyclohexane

As the next challenge for our Rh(II)-catalyzed C–H functionalization program and with the recent development of 2,2,2-trichloroethyl aryldiazoacetates as more robust sources of donor/acceptor carbenes,[25] we became interested with the possibility of achieving site selective C–H functionalization of more elaborate systems, such as cyclohexanes bearing alkyl substituents. The alkyl group does not create significant electronic bias on the cyclohexane ring, but depending on its identity and size it may be able to effectively lock the cyclohexane chair conformation.

For the purpose of analysis, we choose *tert*-butylcyclohexane as the model substrate, as the bulky *tert*-butyl group should lock itself at the equatorial position (Figure 3.1).[26] Even with a stable chair conformation, there exist 11 different C–H bonds, excluding the primary ones (green) on the *tert*-butyl group, that are electronically favored toward carbene insertion. Considering the fact that an additional stereocenter is generated upon carbene insertion, 22 possible C–H functionalization products could in theory be formed. From an electronic point of view, functionalization at the C-1 axial position (light blue) may be feasible for a structurally flexible catalyst, such as Rh_2(*S*-DOSP)$_4$[27] or Rh_2(*S*-TCPTAD)$_4$[16], but still largely unfavored due to steric reasons. On similar steric grounds, the C–H bonds at C-2 and C-6 positions (purple) are also unlikely to be sites of functionalization, as the rhodium-carbene complex is sterically encumbered and these positions would be blocked by the alkyl substituent of the cyclohexane. This analysis allows for quick elimination of a lot of possibilities that could form from this reaction, and therefore the likely positions for functionalization would be C-3, C-4 and C-5 (blue and red).

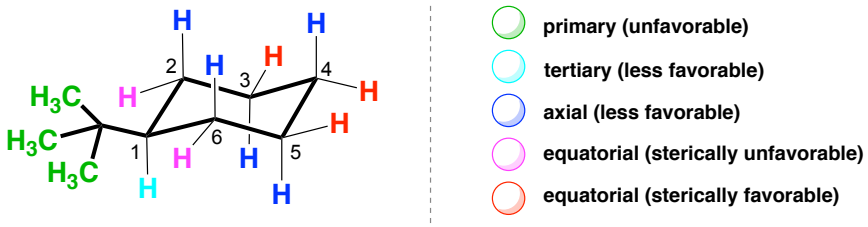

Figure 3.1 Analysis of regioselectivity in cyclohexane functionalization using *tert*-butylcyclohexane as the model substrate

3.2 Results and Discussions

3.2.1 Site- and stereoselective C–H functionalization of monosubstituted cyclohexanes

The first effort for the project was the identification of an appropriate dirhodium catalyst. In light of previous success,[9] screening of a number of catalysts that have chiral triphenylcyclopropane ligands was planned. In addition, catalysts bearing chiral phthalimide-protected chiral amino acid ligands were also explored, including Rh_2(*S*-TPPTTL)$_4$, which is a more recently discovered catalyst that had interesting site selectivity in carbene reactions involving *N*-sulfonyl triazoles and showed promising stereoselectivity in cyclopropanation reactions, as discussed in Chapter 2.

The initial exploratory study (Table 3.1) of the reaction involved using 2,2,2-trichloroethyl 2-(4-bromophenyl)-2-diazoacetate (**3.8**) as the donor/acceptor carbene precursor. This diazo compound has been shown to be highly selective in carbene insertion reactions and suppressed tendency to self-dimerize, and it also allowed for the incorporation of a variety of heteroaryl donor groups into the design of the diazo compound.[25] The model substrate we chose was *tert*-

butylcyclohexane (**3.9**), due to its inexpensive price, ease of analysis and a well-defined chair conformation. When Rh_2(*S*-DOSP)$_4$ (**3.14**) was used as the catalyst, a small but noticeable quantity of C-1 axial insertion product **3.13** was observed, along with other regioisomers and diastereomers at methylene sites (entry 1). This result was not surprising, because while Rh_2(*S*-DOSP)$_4$ has a flexible structure and while it is one of the classic catalysts available in the Davies group,[27] its performance in more recent studies are less effective than some of the newer catalysts. In addition, the reaction was conducted in refluxing dichloromethane, and this polar solvent is known to be detrimental to the performance of Rh_2(*S*-DOSP)$_4$. Rh_2(*R*-TCPTAD)$_4$ (**3.15**) has been known for highly selective C–H functionalization at tertiary positions,[16] but it performed relatively poorly in this reaction as it was not able to effectively distinguish between the C-3 and C-4 positions (entry 2). Rh_2[*R*-3,5-di(*p*-tBuPh)TPCP]$_4$[15] (**3.16**) and Rh_2[*R*-3,5-tris(*p*-tBuPh)TPCP]$_4$[17] (**3.17**) are sterically substantially more hindered catalysts, and they were also ineffective in terms of distinguishing between C-3 and C-4. Interestingly, however, Rh_2[*R*-3,5-di(*p*-tBuPh)TPCP]$_4$-catalyzed reaction favored the formation of C-4 insertion product to a slight extent, and this could be interesting for future studies as the C-4 position is statistically harder to functionalize (entry 3).

Rh_2(*S*-2-Cl-5-BrTPCP)$_4$[18] and Rh_2(*S*-2-Cl-4-BrTPCP)$_4$[28] are related catalysts and both have an interesting C_4-symmetrical, "all-up" conformation due to the presence of its *o*-Cl substituents, and have some unusual site selectivities.[18] However, they both gave poor selectivity in cyclohexane functionalization and some unidentified byproducts in the crude ^{1}H NMR spectra (see Supporting Information). Other C_4-symmetrical catalysts with chiral phthalimide-protected amino acid ligands that are all structurally related, such as Rh_2(*S*-PTTL)$_4$, Rh_2(*S*-TCPTTL)$_4$,

Rh_2(*S*-NTTL)$_4$ and Rh_2(*R*-PTAD)$_4$, and gave unsatisfactory results as well (see Supporting Information).

Rh_2(*S*-TPPTTL)$_4$ (**3.18**) is a previously unknown catalyst and is also a member of C_4-symmetrical catalysts with chiral phthalimide-protected amino acid ligands, which are based on Hashimoto's scaffold.[29, 30] This catalyst, surprisingly, gave a very good reaction outcome and strongly favored regioselective carbene insertion at the C-3 position. Because of the C-3 preference, the substrate, which does not contain any prior chiral information, is effectively desymmetrized upon carbene insertion and generates three new stereogenic centers. This result was particularly encouraging to us because of a number of reasons. First of all, we did not observe any C-4 insertion product from the crude ^{1}H NMR spectra (> 30 : 1 rr, entry 5), which is not the case for all other common catalysts. Regioselectivity is particularly important in this case, as more products can significantly obscure subsequent analysis by NMR and chiral HPLC. Even though C-4 is statistically more difficult to hit, it is essentially in the same electronic environment as C-3 and C-5, so theoretically it is still a favorable position. Therefore, there must exist certain properties of Rh_2(*S*-TPPTTL)$_4$ that allowed for a highly regioselective reaction, which will be discussed later in this chapter. Furthermore, in this reaction, the ratio between product **3.10** and **3.11** would give us information regarding the diastereoselectivity, as the catalyst should maintain the chirality at the carbene carbon. When the reaction was catalyzed by Rh_2(*S*-TPPTTL)$_4$, we observed moderate, but significant enhancement in diastereoselectivity (10.5 : 1 dr) over the other catalysts, meaning the chiral catalyst can differentiate between C-3 and C-5 equatorial hydrogens, which will also be discussed in later sections of this chapter. Overall, the selectivities of Rh_2(*S*-TPPTTL)$_4$ are remarkable if one considers how little steric or electronic bias there is among the C–H bonds at C-

3, C-4 and C-5. As will become apparent later, this catalyst is also generally very effective for a clean reaction at the C-3 position of a variety of other alkyl cyclohexanes.

Table 3.1 Evaluation of catalysts in site selective functionalization of *tert*-butylcyclohexane

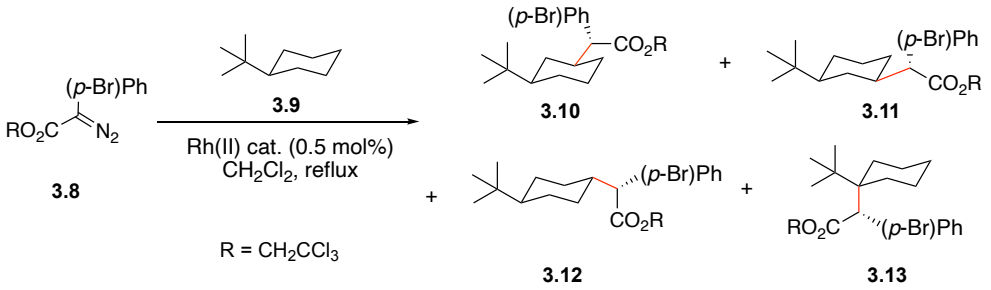

entry	Rh(II) catalyst	Product distribution[a]			
		3.10	**3.11**	**3.12**	**3.13**
1	**3.14**	60.8	9.7	24.1	5.3
2	**3.15**	49.6	9.3	40.6	n.d.
3	**3.16**	29.4	8.4	62.2	-
4	**3.17**	70.3	17.2	12.4	-
5	**3.18**	91.3	8.7	-	-

[a] Ratios determined from the crude ^{1}H NMR spectra

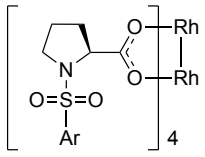

Ar = (p-$C_{12}H_{25}$)Ph
Rh_2(*S*-DOSP)$_4$ (**3.14**)

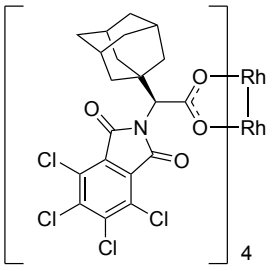

Rh_2(*S*-TCPTAD)$_4$ (**3.15**)

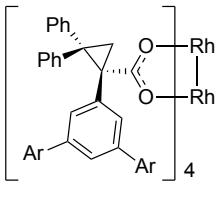

Ar = *p*-tBuPh
Rh_2[*R*-3,5-di(*p*-tBuPh)TPCP] (**3.16**)

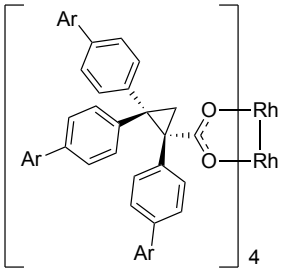

Ar = *p*-tBuPh
Rh_2[*R*-3,5-tri(*p*-tBuPh)TPCP] (**3.17**)

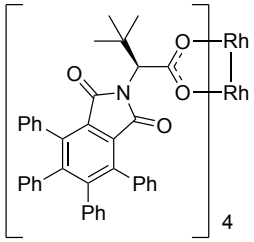

Rh_2(*S*-TPPTTL)$_4$ (**3.18**)

Having established that Rh_2(*S*-TPPTTL)$_4$ is the optimal catalyst for the selective functionalization of *tert*-butylcyclohexane, the next step was to further explore the reaction in other unactivated cycloalkane substrates (Table 3.2). Even though the project is focused on desymmetrization of alkyl cyclohexanes, we wanted to first see how this catalyst performs in more simple, unsubstituted cycloalkanes and adamantane (**3.19a-d**). These reactions only generate one stereogenic center, but we were happy to see that the catalyst has excellent stereocontrol and gave the desired C–H functionalization products (**3.20a-d**) in good yield and high enantioselectivity for all substrates. Adamantane (**3.19d**) is a relatively easy substrate. Even though it does not have an activating functionality, its tertiary C–H bonds are electronically favored and sterically very accessible. Importantly, only 2.5 equivalents of the substrates was required for high-yielding reactions, while previously Rh_2(*S*-DOSP)$_4$-catalyzed reactions could require the substrate to be used as co-solvent.[24]

Table 3.2[a-b] C–H functionalization of simple cycloalkanes using Rh_2(*S*-TPPTTL)$_4$

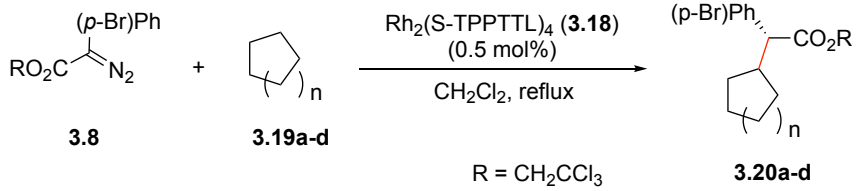

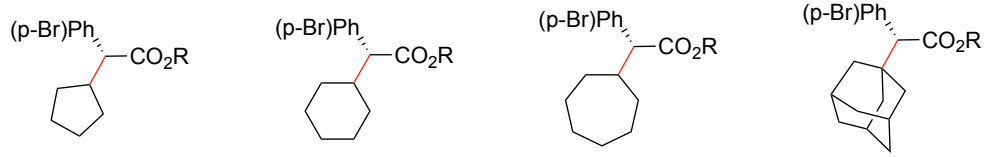

3.20a	**3.20b**	**3.20c**	**3.20d**
73%	79%	75%	72%
97% e.e.	99% e.e.	92% e.e.	90% e.e.

[a] Yield refers to isolated yields of purified products
[b] Enantiomeric excess data were determined from HPLC on a chiral stationary phase

Knowing that Rh_2(*S*-TPPTTL)$_4$ performs well in the C-H functionalization of simple cycloalkane substrates, we then examined the catalyst's performance in the reactions of more elaborate systems, such as when the cyclohexane substrate bears an alkyl substituent (Table 3.3). When methyl cyclohexane (**3.21a**) was used as the substrate, we observed high regioselectivity and enantioselectivity, but the diastereoselectivity was relatively poor (4 : 1 dr), indicating that the catalyst is not effectively differentiating between the C-3 and C-5 position during the desymmetrization event. Interestingly, we later discovered that the lower diastereoselectivity was generally the case when the alkyl substituents are small in size (substrates **3.21a-d**), such as methyl or even *n*-pentyl. Nevertheless, except for substrate **3.21a**, we were happy to observe generally excellent regiocontrol, all favoring highly selective carbene insertion at the C-3 equatorial position to generate products **3.22b-h**. When the substituent was a trimethylsilyl (TMS) group (**3.21h**), the reaction outcome was minimally affected, with marginal increase in diastereoselectivity and enantioselectivity. However, slight amount of side reaction on TMS functionalization by the carbene was observed and thus resulted in lower regioselectivity (19.0 : 1 rr).

A few substrates are worth special attention. For example, **3.21c** and **3.22d** both contain long aliphatic *n*-butyl or *n*-pentyl chains that were left intact by the rhodium carbene, and the corresponding products **3.22c** and **3.22d** were generated with high regioselectivity (>50 : 1 rr) despite the alkyl group residing in sterically open positions. Another notable example is the functionalization of isopropyl cyclohexane (**3.21e**), where the tertiary C–H bond is highly electronically activated toward carbene insertion and also not in a particularly crowded environment, but we still observed a clean C-3 insertion that produced **3.22e** and less than 5% of side products from isopropyl functionalization.

Table 3.3[a-c] C–H functionalization of alkyl cyclohexanes using Rh_2(*S*-TPPTTL)$_4$

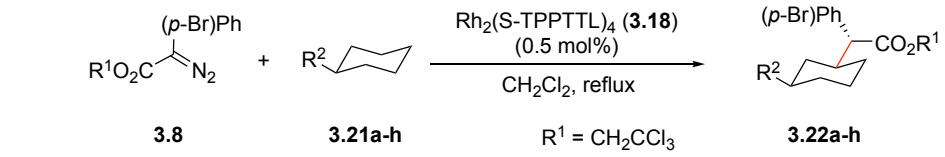

3.8 **3.21a-h** $R^1 = CH_2CCl_3$ **3.22a-h**

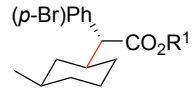

3.22a
85%
12.5:1 r.r.
4.0:1 d.r.
97% e.e.[d]

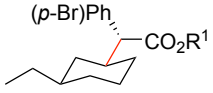

3.22b
81%
>50:1 r.r.
4.2:1 d.r.
96% e.e.

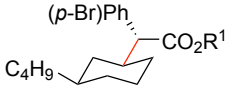

3.22c
77%
>50:1 r.r.
3.7:1 d.r.
90% e.e.

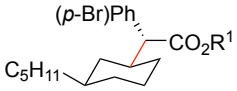

3.22d
80%
>50:1 r.r.
3.3:1 d.r.
91% e.e.

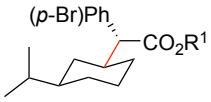

3.22e
82%
47.1:1 r.r.
10:1 d.r.
97% e.e.[d]

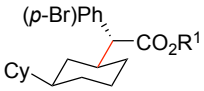

3.22f
85%
40:1 r.r.
12:1 d.r.
95% e.e.[d]

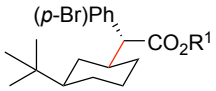

3.22g
80%
>50:1 r.r.
11:1 d.r.
95% e.e.[d]

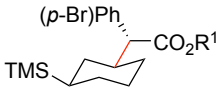

3.22h[d]
80%
19.0:1 r.r.[e]
14:1 d.r.
97% e.e.

[a] Yields refer to isolated yields of purified products
[b] Diastereoselectivity was determined from the crude reaction ^{1}H NMR spectrum
[c] Enantiomeric excess data were determined from HPLC on a chiral stationary phase
[d] Enantiomeric excess data were determined from the reduced primary alcohol
[e] Side reaction on the TMS functionality was observed

Even though the reaction outcomes have been excellent for alkyl or TMS cyclohexanes, with the introduction of a more polar substituent the selectivities could be affected due to electronic factors. Therefore, we decided to challenge this catalyst in a more diverse range of substrates by putting heteroatoms either directly on the cyclohexane as the substituent or in the side chain (substrates **3.23a-f**). When an ester functionality is placed directly on the cyclohexane (substrate **3.23a**), we observed substantially lowered regioselectivity (9.9 : 1 rr) and diastereoselectivity (7.7 : 1 dr). This is not surprising because the ester group would inductively deactivate across the

cyclohexane ring, and thereby disrupt the electronic properties at C-3. In this case, C-4 is the naturally preferred site for functionalization, and we did observe side reactions occurring at that position. This is also evident in substrates **3.23b** and **3.23c**, where the oxygen atom is one carbon further away from the cyclohexane ring, and we observed much improved site selectivity, as the electronic disruption is less direct. Interestingly, when the oxygen atom is directly attached to the cyclohexane ring (substrate **3.23d**), the regioselectivity was excellent (>50 : 1 rr), which is due to reasons that will be discussed in detail in later sections of this chapter. When the substrate bears a phthalimide-protected nitrogen atom or boronic ester as the substituent (**3.23e**-**f**), we also observed high level of regioselectivity for the transformations. Notably, for all substrates **3.23a-f**, excellent enantioselectivity was obtained. These results indicate that Rh_2(*S*-TPPTTL)$_4$ is capable of reactions not just on alkyl cyclohexanes but also more elaborate systems, and could serve as an interesting entry into building blocks such as chiral cyclohexyl amines, alcohols and boronic esters, *etc*. for subsequent transformations that leverage on these functionalities.

Table 3.4[a-c] C–H functionalization of functionalized cyclohexanes using Rh_2(*S*-TPPTTL)$_4$

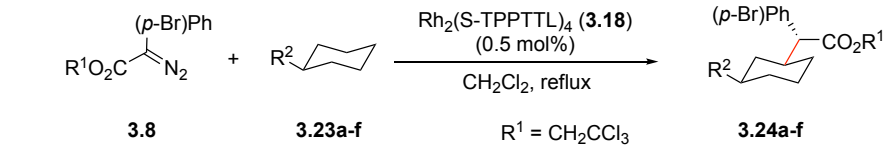

3.8 **3.23a-f** $R^1 = CH_2CCl_3$ **3.24a-f**

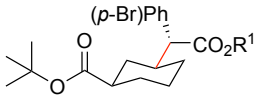

3.24a
58%
9.9:1 r.r.
7.7:1 d.r.
96% e.e.

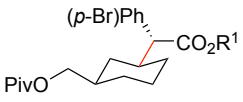

3.24b
68%
>50:1 r.r.
6.7:1 d.r.
95% e.e.

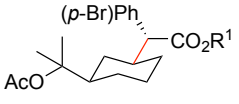

3.24c
75%
>50:1 r.r.
12.4:1 d.r.
97% e.e.

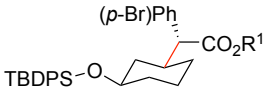

3.24d
70%
>50:1 r.r.
6:1 d.r.
97% e.e.

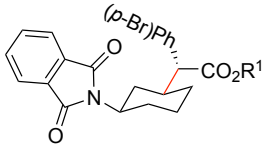

3.24e
42%
>50:1 r.r.
22:1 d.r.
96% e.e.

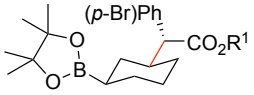

3.24f
81%
>50:1 r.r.
6:1 d.r.
96% e.e.

[a] Yields refer to isolated yields of purified products
[b] Diastereoselectivity was determined from the crude reaction ^{1}H NMR spectrum
[c] Enantiomeric excess data were determined from HPLC on a chiral stationary phase

With the optimal catalyst established and scope of substrates in hand, we then decided to explore the scope of aryldiazoacetates that would be compatible with this transformation and to further probe the catalyst's selectivity profile when the aryl ring is varied (Table 3.5). When *tert*-butylcyclohexane (**3.9**) was used to examine the scope, we were happy to see that **3.9** underwent clean functionalization to generate products **3.26a-l** when different types of aryldiazoacetates were used, including some heteroaryldiazoacetates. We were particularly encouraged to see that *ortho*-substituted aryldiazoacetates (**3.25a-b**) are fully compatible with the catalyst, as they are known to more easily undergo intramolecular cyclization when the diazoacetate contained an alkyl (e.g. methyl) ester,[31] although **3.26a** was obtained with slightly diminished regioselectivity. In addition,

meta- and *para*-substituted aryldiazoacetates (**3.25d-i**) were generally effective, but the catalyst seems to be sensitive to the steric bulk of the *para*-substituent on the aryl ring, as **3.26g** and **3.26h** were obtained with lowered enantioselectivity (47% and 79% ee, respectively). Lastly, naphthyl- (**3.26c**) and even heteroaryl donor groups, such as pyridine, benzothiazole and oxazole groups (**3.26j-l**), are found to be compatible for the C–H functionalization reactions, although with heteroaryl donor groups the yields tended to be lower.

Table 3.5[a-c] Scope of aryldiazoacetates in C–H functionalization of *tert*-butylcyclohexane using Rh_2(*S*-TPPTTL)$_4$

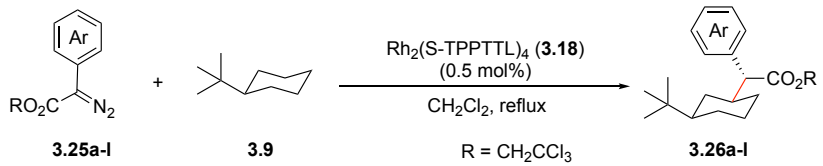

3.25a-l **3.9** **3.26a-l**

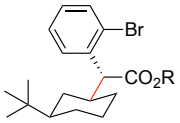

3.26a
62%
40:1 r.r.
19:1 d.r.
85% e.e.

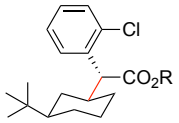

3.26b
64%
50:1 r.r.
15:1 d.r.
92% e.e.

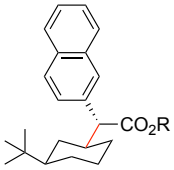

3.26c
81%
>50:1 r.r.
11:1 d.r.
98% e.e.

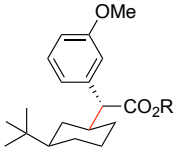

3.26d
61%
>50:1 r.r.
16:1 d.r.
96% e.e.

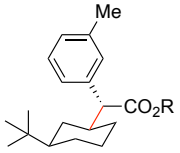

3.26e
88%
>50:1 r.r.
16:1 d.r.
94% e.e.

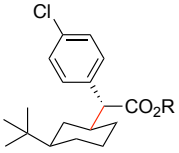

3.26f
89%
>50:1 r.r.
11:1 d.r.
97% e.e.

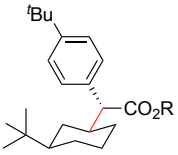

3.26g
81%
>50:1 r.r.
17:1 d.r.
47% e.e.

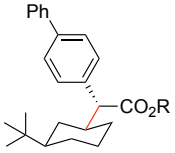

3.26h
81%
>50:1 r.r.
14:1 d.r.
79% e.e.

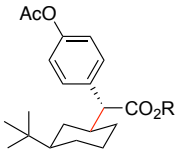

3.26i
72%
>50:1 r.r.
26:1 d.r.
84% e.e.

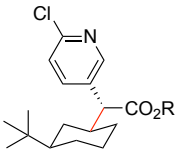

3.26j
58%
>50:1 r.r.
9.8:1 d.r.
98% e.e.

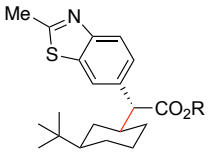

3.26k
71%
>50:1 r.r.
13:1 d.r.
98% e.e.

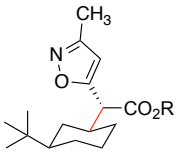

3.26l
41%
>50:1 r.r.
25:1 d.r.
83% e.e.

[a] Yields refer to isolated yields of purified products
[b] Diastereoselectivity was determined from the crude reaction ^{1}H NMR spectrum
[c] Enantiomeric excess data were determined from HPLC on a chiral stationary phase

3.2.2 Site- and stereoselective C–H functionalization of disubstituted cyclohexanes

The selectivity of C–H functionalization via rhodium-carbene insertion is generally considered to be government by a combination of steric and electronic influences from the substrate and the selection of the dirhodium catalyst.[9, 14, 24] The identity of aryldiazoacetate may also play a role, but to a less extent.[25] In the previous section, Rh_2(*S*-TPPTTL)$_4$ has been shown to be a highly competent catalyst for desymmetrizing alkyl cyclohexane substrates. We next decided to further evaluate the selectivity profile of the catalyst in more complex system, and to subject disubstituted cyclohexanes to the C–H functionalization reaction. This type of system poses even more challenge to the catalyst, as it now involves selectivity between the axial and equatorial C–H bonds, and kinetic resolution may occur if the substrate is racemic (Table 3.6).

For example, *cis*-1,2-dimethyl cyclohexane (**3.27a**) and *trans*-1,3-dimethyl cyclohexane (**3.27d**) are particularly interesting substrates because they exist as a 1:1 mixture of enantiomeric chair forms that could rapidly interconvert, especially at the elevated reaction temperature (40 °C). The C–H functionalization reaction catalyzed by Rh_2(*S*-TPPTTL)$_4$ worked smoothly for both substrates, generating products **3.28a** and **3.28d** in good yield and regioselectivity. However, the diastereoselectivity for both products was quite low (3.7 : 1 dr and 2 : 1 dr, respectively), which indicates that both enantiomeric chair forms of the substrates **3.27a** and **3.27d** could have reacted with the rhodium carbene. This would then maintain the same stereochemistry at the carbene carbon but also generate the low diastereoselectivity. Nevertheless, **3.28a** was produced in very high asymmetric induction (98% ee), although the enantioselectivity for **3.28c** was quite low (59% ee). *trans*-1,2-Dimethyl cyclohexane (**3.27b**) is a chiral molecule and was used as a racemic

mixture from the commercial sample. Even with this complication, **3.28b** was very effectively generated with high regioselectivity (>50 : 1 rr), yield (75% yield) and stereoselectivity (25 : 1 dr, 85% ee), indicating the occurrence of kinetic resolution during the reaction, where one of the enantiomers of **3.27b** was preferentially functionalized by the rhodium carbene, while the other enantiomer was left intact. Because the substrate was used in excess (2.5 equiv in relation to **3.8**), higher than 50% yield was possible. Moreover, *cis*- (**3.27e**) and *trans*-1,4-dimethyl cyclohexane (**3.27f**) are quite interesting substrates because they would allow one to assess the different reactivity between axial and equatorial C–H bonds. It is important to note that this assessment was only possible when Rh_2(*S*-TPPTTL)$_4$ was used as the catalyst, as other catalysts may not be selective and a mixture of product will complicate any analysis. When *cis*-1,4-dimethyl cyclohexane (**3.27e**) was used as the substrate, we observed a very clean (>50 : 1 rr) reaction at the tertiary equatorial position with excellent yield (80% yield) and stereoselectivity (>50 : 1 dr and 91% ee). The structure of this substrate is reminiscent of adamantane, both of which contains a highly reactive tertiary C–H bond at a sterically accessible position. *trans*-1,4-Dimethyl cyclohexane (**3.27f**) would be anticipated to exist primarily in the chair form where the two methyl groups exist in equatorial positions, even at the reaction temperature (40 °C). In this reaction, **3.27f** underwent effective functionalization to generate product **3.28f** with good yield (77% yield) and stereoselectivity (>50 : 1 rr, 94% ee). However, regioselectivity was substantially diminished (4.8 : 1 rr), presumably due to the highly unfavorable nature of the rhodium carbene reacting at the axial site. Because the rhodium carbene species is sterically encumbered, this result indicates that electronic preference at tertiary sites is a factor in determining site selectivity and may overcome the sterics in cyclohexane systems when Rh_2(*S*-TPPTTL)$_4$ is used as the catalyst. Lastly, *cis*- and *trans*-decahydronaphthalene (**3.27g** and **3.27h**) were also effective substrates for the C–H

functionalization reaction, generating the corresponding products (**3.28g** and **3.28h**) in good yield, regioselectivity and high enantioselectivity.

Table 3.6[a-c] C–H functionalization of disubstituted alkyl cyclohexanes using Rh_2(*S*-TPPTTL)$_4$

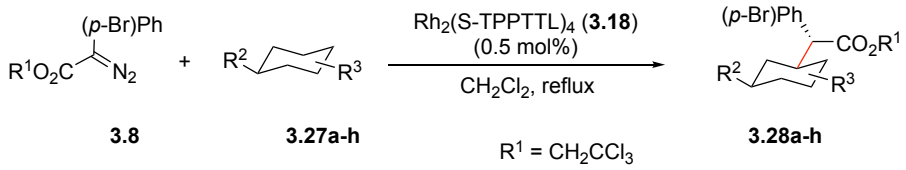

3.8 **3.27a-h** $R^1 = CH_2CCl_3$ **3.28a-h**

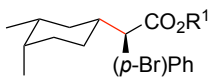

3.28a
70%
16:1 r.r.
3.7:1 d.r.
98% e.e.

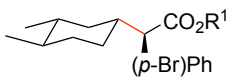

3.28b
75%
>50:1 r.r.
25:1 d.r.
85% e.e.

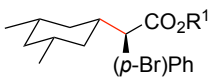

3.28c
62%
15:1 r.r.
>50:1 d.r.
59% e.e.

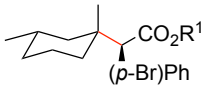

3.28d
70%
>50:1 r.r.
2:1 d.r.
94% e.e.

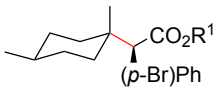

3.28e
80%
>50:1 r.r.
>50:1 d.r.
91% e.e.

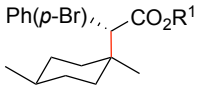

3.28f
77%
4.8:1 r.r.
>50:1 d.r.
94% e.e.

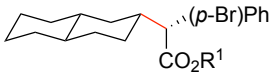

3.28g
72%
>50:1 r.r.
11:1 d.r.
90% e.e.

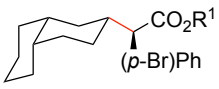

3.28h
68%
>50:1 r.r.
6.7:1 d.r.
98% e.e.

[a] Yields refer to isolated yields of purified products
[b] Diastereoselectivity was determined from the crude reaction ^{1}H NMR spectrum
[c] Enantiomeric excess data were determined from HPLC on a chiral stationary phase

At this point, we wondered if we could leverage on the interesting reactivity and selectivity profile of substrates **3.27e** and **3.27f** to conduct a substrate competition experiments. Our group has reported competition studies on various systems,[14] but one area that was somewhat overlooked is when axial versus equatorial selectivity is involved, presumably because a clean and reliable reaction system for studying such selectivity has been lacking. Because the ^{1}H NMR signals in the crude reaction mixture of **3.27e** and **3.27f** are very distinct, we considered them good candidates

for studying this selectivity. Therefore, a substrate competition experiment was carried out by subjecting a 1:1 mixture of both isomers to the reaction condition (Scheme 3.3). From the crude ^{1}H NMR analysis, only trace amount of **3.28f** was observed (**3.28e** : **3.28f** = 70 : 1), despite the presence of two identical axial C–H bonds in **3.27f**. After accounting for this, this study indicates that the equatorial C–H bond reacted 140 times faster than the axial one. However, one limitation of this study is that it relies on the assumption that **3.27e** and **3.28e** do not have non-zero quantity of their corresponding ring-flipped isomers in refluxing dichoromethane.

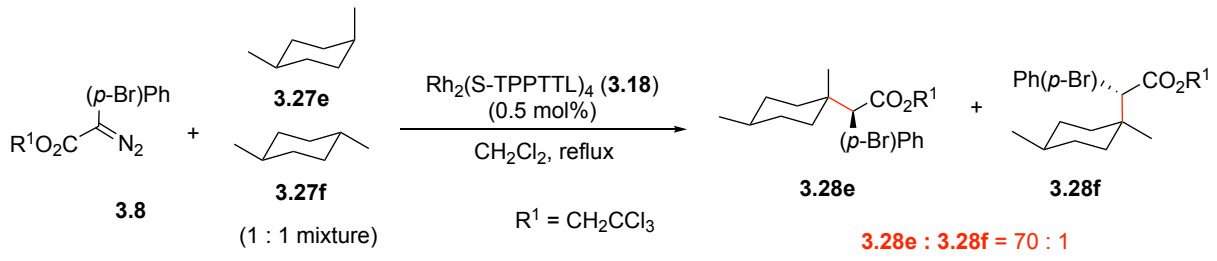

Scheme 3.3 Competition study between axial vs. equatorial functionalization

3.2.3 Analysis of regio- and stereochemistry

While X-ray crystallography remains one of the unambiguous ways of assigning the regio- and stereochemistry, for this study, it was necessary to use other spectroscopic and chromatographic methods to determine the structure of the products, as they were challenging to directly crystallize for X-ray crystallography.

For example, at the onset of the study, it was not immediately obvious whether the carbene insertion occurred at the C-3 or C-4 position. However, upon closer examination of the ^{1}H NMR spectrum of the purified product **3.22g**, the regiochemistry could indeed be unambiguously determined. Figure 3.2 shows the key aliphatic region of the ^{1}H NMR spectrum for purified **3.22g**, where a clear quartet at 0.5 ppm could be observed. Normally, this chemical shift is too low for a regular aliphatic proton, and therefore there needs to be certain electronic influence from adjacent functionalities that caused this particularly low chemical shift. We were able to attribute this signal to the axial proton at the C-2 position, in between the *tert*-butyl group and the site of functionalization (Figure 3.2). There are two main reasons for this proposed assignment. First of all, one would expect to observe a *quartet* only when the reaction occurred at the C-3 equatorial position, as the highlighted (light blue) proton would be split by two adjacent axial protons at the C-1 and C-3 position, as well as by its geminal C-2 proton at equatorial position. This would give two large *J* coupling due to axial coupling and one small geminal coupling, which is indeed what we observe in the spectrum. In addition, we propose that the adjacent phenyl ring can effectively "shield" the signal of the highlighted proton via the anistropic effect, which would explain its very low 0.5 ppm. Curiously, from the X-ray crystallographic study of the C–H functionalization

product, it seemed that the aryl group is not perfectly aligned with the axial C-2 proton. In fact, the crystal structure shows that the aryl group should shield the equatorial C-2 proton to a greater extent because of better alignment. Nevertheless, the very large coupling constants from the quartet at 0.5 ppm should serve as conclusive evidence that it corresponds to the equatorial C-2 proton.

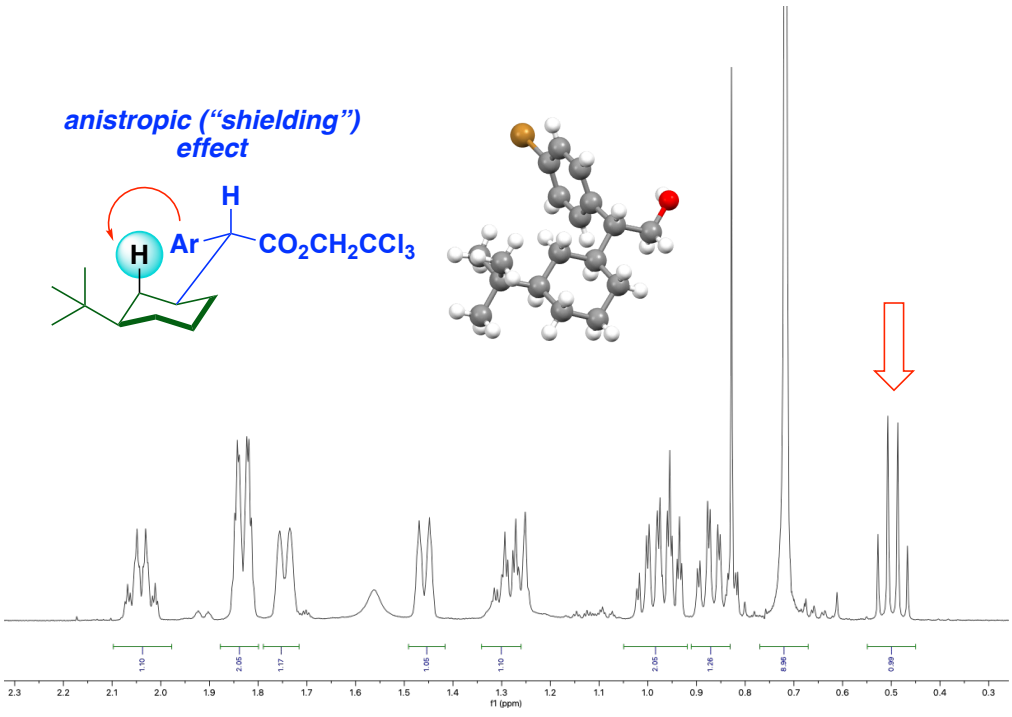

Figure 3.2 Assignment of regiochemistry using ^{1}H NMRs

Besides the remarkable asymmetric induction by Rh_2(*S*-TPPTTL)$_4$, one of the defining features of this catalyst is its ability to effectively desymmetrize the cyclohexane substrate with moderate to good level of diastereoselectivity. For example, the model reaction generated **3.22g** with 10.5 : 1 dr, and we became curious about the structure of the minor diastereomer. While the configuration of the major product could easily be identified from X-ray crystallographic analysis, the minor diastereomer was particularly challenging to be isolated using regular laboratory

methods. Therefore, we decided to resort on chiral HPLC to indirectly determine what was formed as the minor diastereomer, and there were a few possibilities.

Specifically, the same C–H functionalization reaction was repeated under identical conditions, but it was then allowed equilibrate by treating the crude reaction with stoichiometric quantity of 1,8-diazabicyclo[5.4.0]undec-7-ene (DBU) and stirred overnight (Figure 3.3). The base equilibration effectively epimerizes the benzylic stereogenic center and produce all compounds (**3.22g**, **3.27**-**3.29**), and we analyzed the purified sample along with (*rac*)-**3.22g** and **3.22g**. With the (*rac*)-**3.22g** sample in hand, it was clear that peak A corresponds to the major product **3.22g**, while peak B corresponds to its minor enantiomer **3.29**. When the sample was treated with DBU, it was reasonable to expect that **3.27** would be produced in significant quantity from epimerization of **3.22g**, as the enantioselectivity for **3.22g** was very high (95% ee). With this in mind, we were able to assign peak D to be **3.27**, because it was absent in the chiral sample. Therefore, peak C was deduced to be due to **3.28**. Overall, this indicates that the catalyst was indeed capable of maintaining the stereochemical integrity at the carbene carbon, but its ability to differentiate between C-3 and C-5 was only moderate, and thereby generating **3.22g** and **3.28** as a pair of diastereomers (10.5 : 1 dr) during the desymmetrization event.

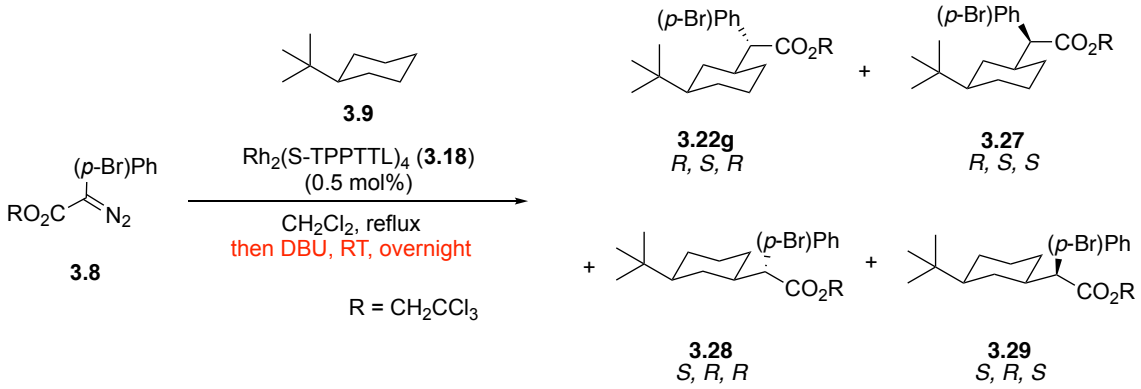

(a) C-H functionalization followed by epimerization using DBU

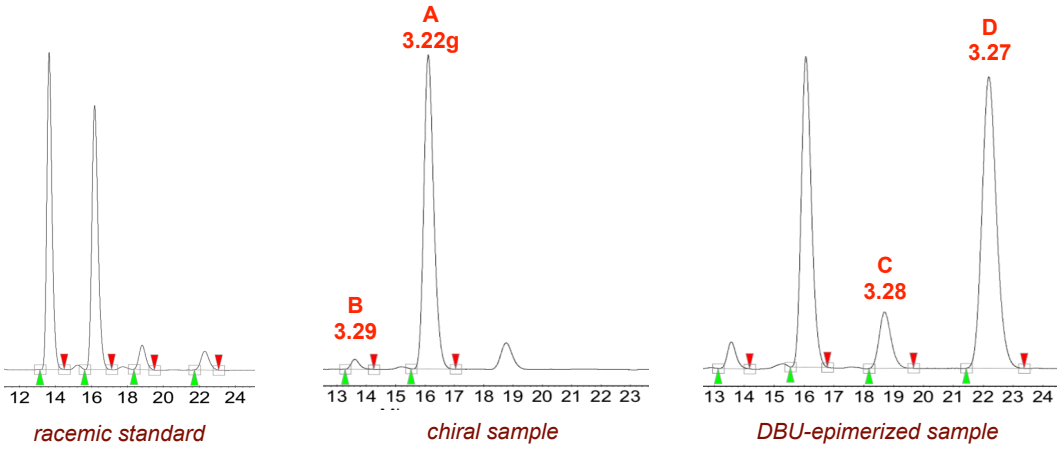

(b) Chiral HPLC spectra for racemic standard, chiral sample, and epimerized sample

Figure 3.3 Chiral HPLC analysis to determine the structure of the minor diastereomer

3.2.4 Rationale of selectivity through X-ray crystallographic analysis and computational studies (Note: computational studies in this section were conducted by Dr. Zhi (Zack) Ren and Dr. Jamal Musaev at Emory University, and X-ray crystallographic analysis was conducted by Dr. John Bacsa at Emory University.)

The strong C-3 preference of Rh_2(*S*-TPPTTL)$_4$ in the selective functionalization of alkyl cyclohexanes was very curious to us, as one would tend to think that the C-4 position is farthest away from the steric bulk of the cyclohexane substituent. Yet, in many substrates we observed essentially no evidence for the formation of the C-4 isomer. In order to understand what features of Rh_2(*S*-TPPTTL)$_4$ that can account for the exceptional selectivity, the structure of the catalyst was interrogated by X-ray crystallographic analysis and DFT calculations. As expected, X-ray crystallographic data indicate that Rh_2(*S*-TPPTTL)$_4$ adopts a "chiral crown" conformation[32, 33], even though it is slightly distorted from a perfect C_4-symmetrical structure (Figure 3.4). This is similar to what was previously seen with other catalysts has *N*-phthalimide-protected amino acid ligands, including Rh_2(*S*-TCPTAD)$_4$.[16] In this structure, all the chiral phthalimido groups are projected "upward" in relation to the dirhodium core, and the bulky *tert*-butyl group blocks the bottom achiral face of the catalyst, which is consistent with our observation that Rh_2(*S*-TPPTTL)$_4$ routinely gives high asymmetric induction in cyclopropanation and carbene insertion reactions.

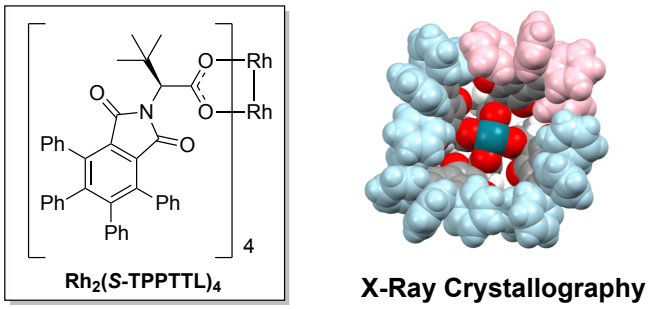

Figure 3.4 X-ray structure of Rh_2(*S*-TPPTTL)$_4$

While the overall structure of Rh_2(*S*-TPPTTL)$_4$ is similar to some other catalysts such as Rh_2(*S*-TCPTAD)$_4$, one unique feature of Rh_2(*S*-TPPTTL)$_4$ is the arrangement of the extremely congested tetraphenyl group on each ligand that effectively create a "wall" around the periphery of the catalyst. We hypothesize that this unique structural feature is the origin of the catalyst's exceptional site- and stereoselectivity.

We have previously used calculations to show that during the carbene insertion step, the angle between the C–H bond vector and the Rh-carbenoid plane is dependent on the nature of the substrate. When cyclopentane was used as the substrate, the angle was about 126.5°, with significantly more Rh-C bond breakage occurring.[34] During the C–H functionalization event, when the substrate approaches the rhodium carbene complex, the 16 phenyl groups of the catalyst can force the substrate to orient itself in a very specific way such that the alkyl substituent minimizes its unfavorable steric interaction with the catalyst and maintain the desired angle of attack. This orientation allows the C-3 equatorial C–H bond to be selectively functionalized in the presence of others with the hydride transfer transition state shown (Structures **3.30** and **3.31**, Figure 3.5). This mode of selectivity is more apparent when one considers the same reaction catalyzed by

structurally similar catalyst Rh_2(*S*-TCPTAD)$_4$ or Rh_2(*S*-TCPTTL)$_4$, where a marked drop in site-selectivity was observed in both cases, presumably due to the fact that the chlorine atoms are simply not able to create the same level of steric effect as the phenyl groups. In addition, even though the four tetraphenylphthalamido groups generate a deep pocket around the rhodium (structure **3.32**), computational studies indicate that the carbene binding to the top face (Structure **3.33**) is strongly preferred by 15.5 kcal/mol in energy as compared to the carbene binding to the bottom, achiral face of the catalyst (Structure **3.34**), presumably due to the steric bulk of the *tert*-butyl groups. Interestingly, we discovered that comparison between the free catalyst (**3.32**) and the carbene-bound catalyst (Structure **3.33**) show that the overall conformation of the ligand arrangement has changed in order to accommodate the approach of the carbene. Furthermore, the shape was changed once again upon the substrate (*tert*-butylcyclohexane) enters the "pocket" and interacts with the rhodium carbene (Structures **3.32**, **3.33** and **3.35**). This change is indicative of an induced fit model, suggesting that the catalyst, while possessing substantial steric demand, has some degree of flexibility to adjust its shape, which may be an important factor that explains why the reaction can accommodate disubstituted cyclohexanes and decalins. In addition, in Structure **3.36**, the C-3 equatorial hydrogen is placed closer to the rhodium carbene, giving the major product of the reaction. In Structure **3.37**, the C-5 equatorial hydrogen is placed closer to the rhodium carbene, giving the minor diastereomer. However, calculation shows that **3.37** is 5.4 kcal/mol higher in energy than **3.36**, which gives observed 10.5 dr in the desymmetrization event.

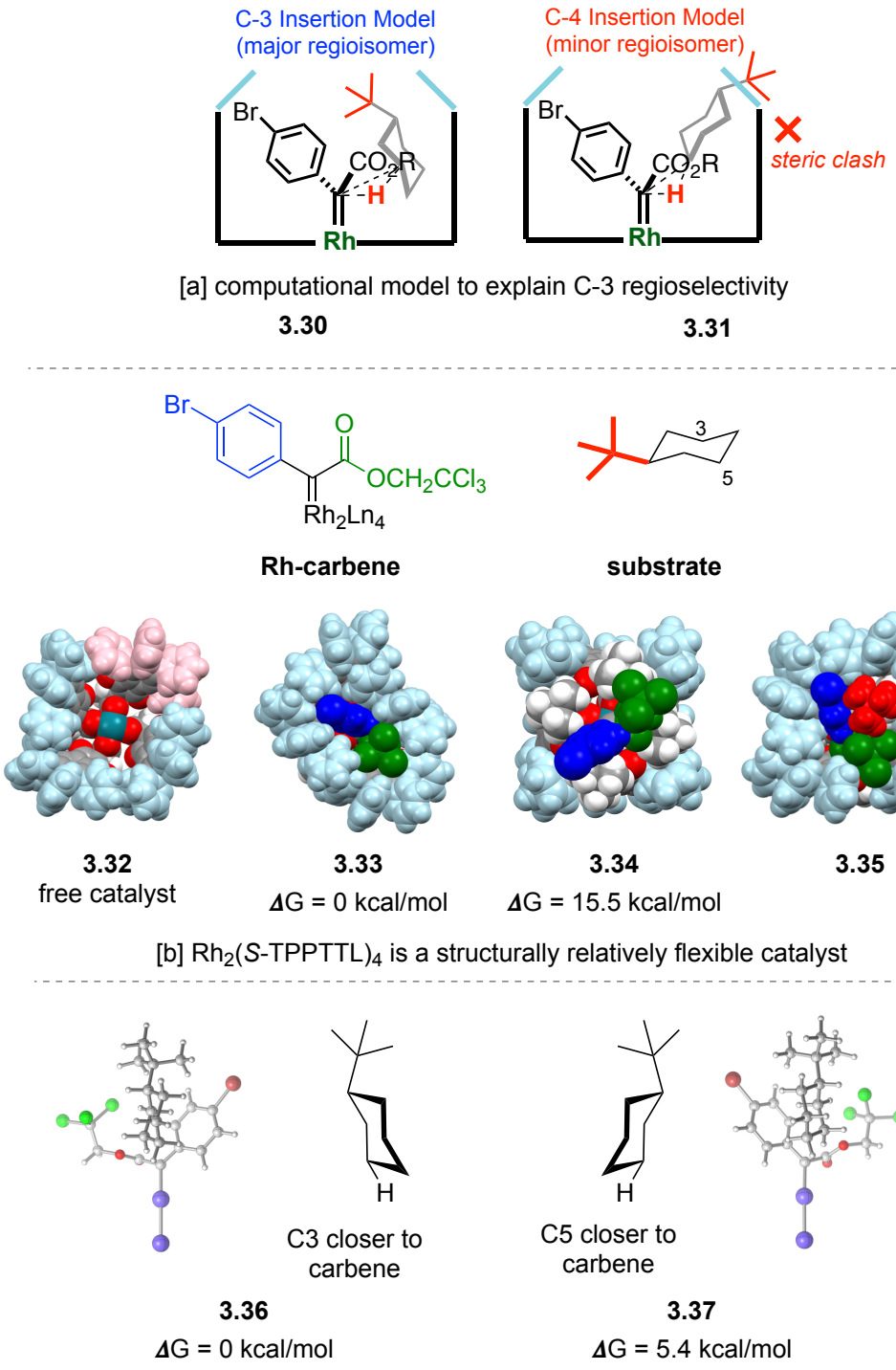

Figure 3.5 Rationalization of C-3 equatorial selectivities for Rh_2(*S*-TPPTTL)$_4$

The chemistries of dirhodium catalysis, donor/acceptor carbenes and selective C–H functionalization in general have provided many fascinating opportunities for new reaction development and continue to inspire new strategies toward complex organic synthesis. Key to the success of the C–H functionalization program in the Davies group is the continuous development of various new catalysts and donor/acceptor carbene precursors. The following sections will focus on the impact of the new tetraphenylphthalamido tert-leucine catalyst, Rh_2(S-TPPTTL)$_4$. As already discussed in this chapter, the catalyst was found to be capable of highly asymmetric C–H functionalization on cyclohexane substrates using donor/acceptor carbenes, but some more recent efforts from the group have led to exciting new discoveries that demonstrate the utility and practicality of this new catalyst beyond cyclohexane activation, which will be the focus of the following sections.

3.2.5 Regio- and Stereoselective functionalization of organosilanes

(Note: the project was initiated by Dr. Zachary Garlets and Elliot Hicks. My role in the included the exploration of heteroaryldiazoacetates in this chemistry)

The importance of organosilicon compounds is evident as they are widely represented in many chemical industries, such as agrochemical,[35, 36] material,[76, 38] and pharmaceutical applications.[39-44] While polar reactions and transition metal-mediated synthesis are frequently used to construct organosilanes,[45, 46] catalytic asymmetric C–H functionalization reactions would be an attractive entry into stereodefined organosilanes.

Recently, Dr. Zachary Garlets has developed an efficient method for the selective functionalization using *N*-sulfonyl triazoles as the carbene precursor and Rh_2(*S*-NTTL)$_4$ as the chiral catalyst of choice (Scheme 3.7).[47] For example, he discovered that triazole **3.38** could react effectively with silacyclobutanes **3.39** at room temperature to produce the functionalized product **3.40** in good yield (63% yield) and very high enantioselectivity (90% ee). Other silacyclobutanes also generally worked well as effective substrates, but the diastereoselectivity tend to be low when the substrate was a five-membered ring or unsymmetrical silanes. He showed that triazole **3.41** could react effectively with silacyclopentane **3.42** in high yield (89% yield) and enantioselectivity (88% ee), but the diastereoselectivity was only 3 : 1. In addition, examples where heteroaryl groups are incorporated into the triazole design were still lacking.

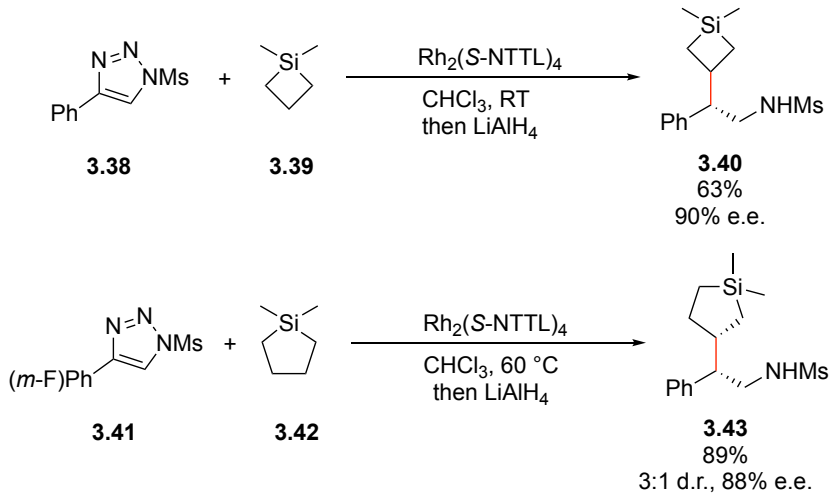

Scheme 3.4 Stereoselective C–H functionalization of organosilanes using *N*-sulfonyl triazoles

In light of previous success of Rh_2(*S*-TPPTTL)$_4$ in generating highly stereoselective reactions when cycloalkanes were used as substrates,[48] we also investigated its performance in the functionalization of organosilanes using aryldiazoacetates. We were delighted to see that the initial optimization studies indicated that Rh_2(*S*-TPPTTL)$_4$ was the optimal catalyst for functionalizing silacyclobutanes **3.39** when 2,2,2-trichloroethyl 2-(4-bromophenyl)-2-diazoacetate (**3.8**) was the donor/acceptor carbene precursor. Therefore, we decided then to challenge the new catalyst in the asymmetric functionalization of organosilanes where previous study showed unsatisfactory results. For example, while heteroaryl donor groups were incompatible with *N*-sulfonyl triazole chemistry, we observed that they can be effectively incorporated into aryldiazoacetate to functionalize silacyclobutane **3.39**. Pyridine, pyrimidine, thiophene and benzothiazole were all shown to be compatible functionalities with the chemistry, and the products (**3.45a-d**) were obtained with moderate to high yields and excellent enantioselectivity (Table 3.7).

Table 3.7[a-b] Rh_2(*S*-TPPTTL)$_4$-catalyzed stereoselective functionalization of silacyclobutane

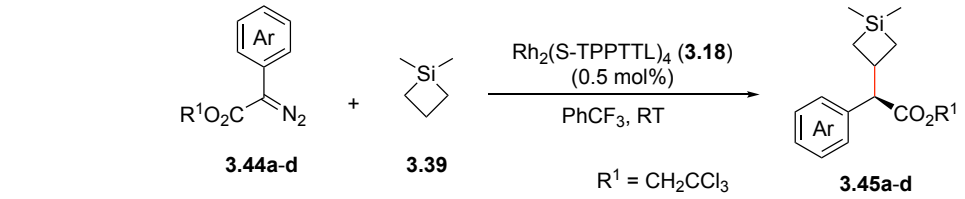

3.44a-d + **3.39** → **3.45a-d**

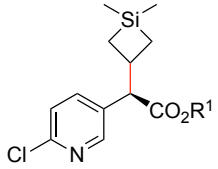

3.45a
67%
98% e.e.

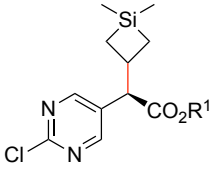

3.45b
41%
87% e.e.

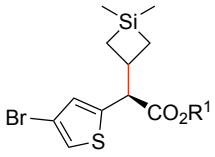

3.45c
54%
91% e.e.

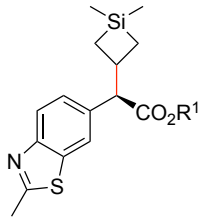

3.45d
65%
98% e.e.

[a] Yields refer to isolated yields of purified products
[b] Enantiomeric excess data were determined from HPLC on a chiral stationary phase

3.2.6 Development of catalysts that are related to Rh_2(S-TPPTTL)$_4$

(Note: the project was initiated by Dr. Zachary Garlets. He performed the experiments related to the synthesis of ligands and catalysts. My role included the C–H functionalization reactions)

The ability of Rh_2(*S*-TPPTTL)$_4$ to functionalize alkyl cyclohexanes with high levels of selectivities is astonishing if one considers the number of potential products that could be formed if the reaction was unselective.[48] Therefore, its success has led us to consider the possibility of exploration of even more extended ligand designs under the original tetraphenylphthalamido core scaffold (Figure 3.6). The Hashimoto-type ligands can be derivatized in two main ways. First of all, the identity of the amino phthalimido protecting group (shown in red, Figure 3.6) could be varied. Second, the side chain of the amino acid (blue, Figure 3.6) could also be varied. While changing the amino acid side chain is synthetically easier, we reasoned that this is unlikely to lead

to substantial change in the catalyst's reactivity and selectivity profile, as side chain resides in the achiral face of the catalyst (Figure 3.5) and does not directly interact with the carbene and substrate. The phthalamido group, on the other hand, is considered to create the chiral environment for the substrate approach, and therefore should play a more important role in determining the catalyst's overall performance and selectivity.

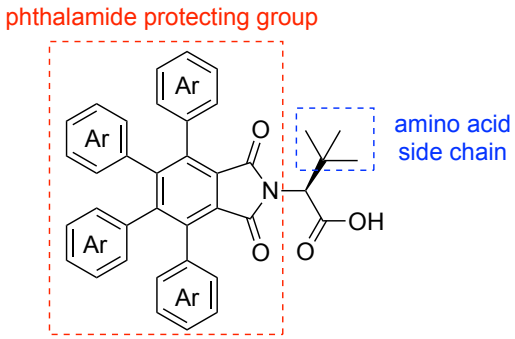

Figure 3.6 Structural features of Rh_2(*S*-TPPTTL)$_4$ derivatives

Therefore, to synthesize novel Rh_2(*S*-TPPTTL)$_4$ derivatives, the following synthetic route was designed and carried out to produce the new catalysts **3.51**-**3.53** (Scheme 3.5). First of all, the aryl acetic acid **3.46** undergoes self-condensation to produce a symmetrical ketone **3.47**, which then could condense with diketone **3.48** under base-mediated conditions. The resulting cyclopentadienone **3.49** would then react with maleic anhydride via a one-pot Diels-Alder/retro-Diels-Alder/bromine oxidation sequence to produce the key cyclic anhydride **3.50**. At this stage, the anhydride could then undergo condensation with a natural or unnatural chiral amino acid to produce the final ligand for the ligand exchange reaction. Even though the synthesis is overall ~ 5 steps, the reactions were found to be reproducible and scalable at multi-gram scale. In addition,

unlike dirhodium catalysts that have TPCP ligands, these Hashimoto-type ligands do not require enantioenrichment as an entiopure amino acid was used for the last condensation reaction.

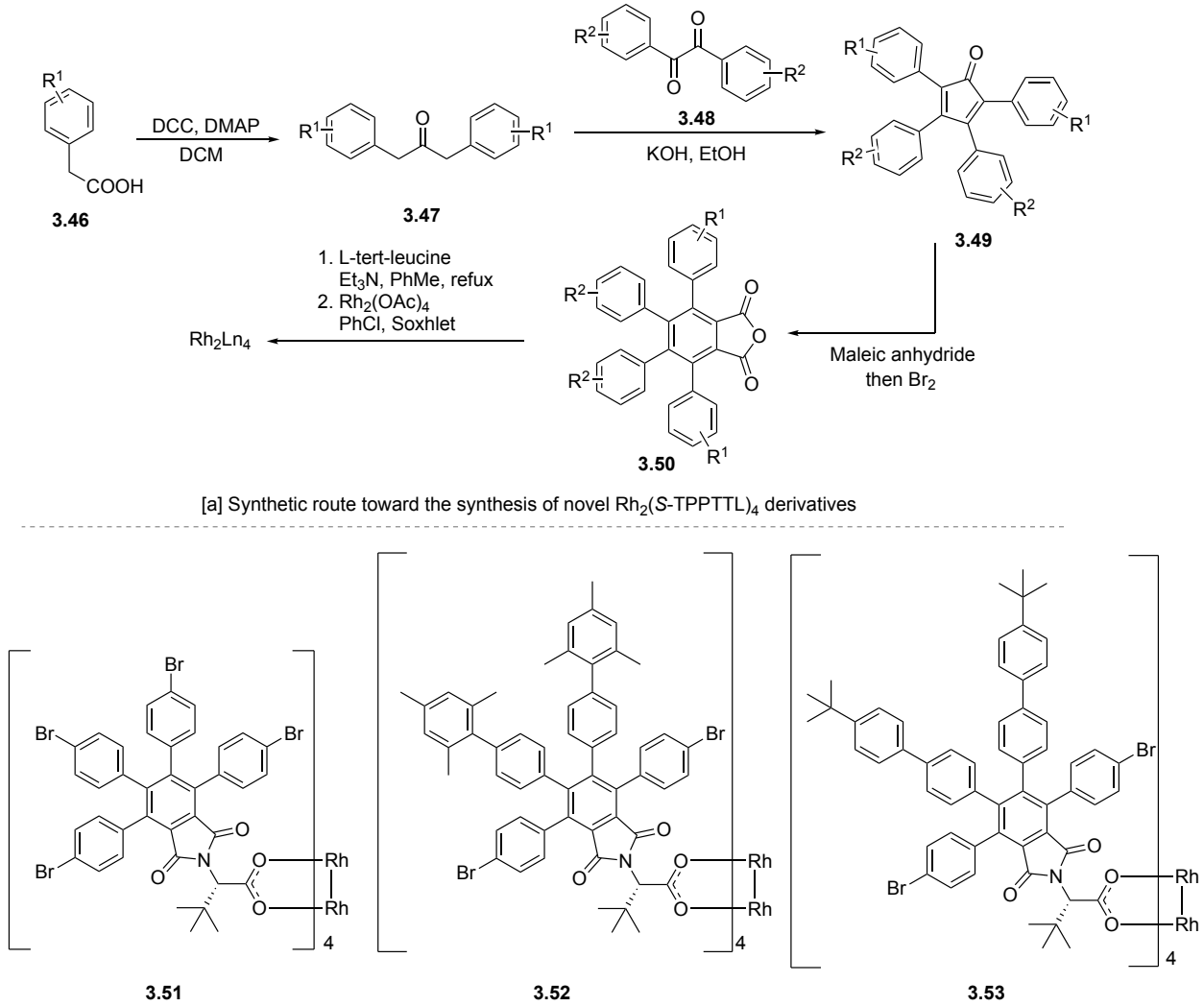

Scheme 3.5 Synthetic route and structures of novel Rh_2(*S*-TPPTTL)$_4$ derivatives

To evaluate the selectivity and synthetic potential of these new catalysts, a few standard C–H functionalization reactions were conducted using 2,2,2-trichloroethyl p-bromophenyldiazoacetate[25] (**3.8**) as the donor/acceptor carbene precursor (Table 3.8). For example, *p*-cymene (**3.55**) would be an optimal substrate for initial catalyst evaluation because it allows for comparison of selectivity at both a primary activated C–H bond and a tertiary activated C–H bond. The latter should be more favored on electronic grounds but less so for steric considerations. When the reaction was conducted under the catalysis of Rh_2(*S*-TPPTTL)$_4$ (**3.18**), a regioselective C–H insertion reaction was observed with strong preference for the more hindered tertiary benzylic C–H bond (11.3:1 rr, entry 1). This is a rather surprising result because our previous experience indicates that more hindered dirhodium catalysts, such as those bearing TPCP ligands, would preferentially attack a sterically more available position.[9, 14, 31] However, the level of regioselectivity was further enhanced when **3.51**-**3.53** were used as the catalysts, as competitive primary insertion was not observed in these cases (entries 2-4).

Another substrate we evaluated was 4-ethyltoluene. Although the benzylic C–H bonds are both electronically favored toward functionalization, they are also both in uncrowded environments. In addition, if the reaction occurs at the secondary site, diastereomers could be potentially generated, which could complicate the analysis. However, we were delighted to see that all catalysts gave clean (> 30 : 1 rr) reactions at the secondary site (entries 1-4). These results are in contrast to the reactions catalyzed by Rh_2[*R*-3,5-tris(*p*-tBuPh)TPCP]$_4$[17] and Rh_2(*R*-*p*-PhTPCP)$_4$,[48] where the primary C–H bond was preferentially functionalized with high selectivity. However, other catalysts gave improved diastereo- and enantioselectivity (entries 2-4).

Table 3.8[a-b] Evaluation of new Rh_2(*S*-TPPTTL)$_4$ derivatives in benzylic substrates

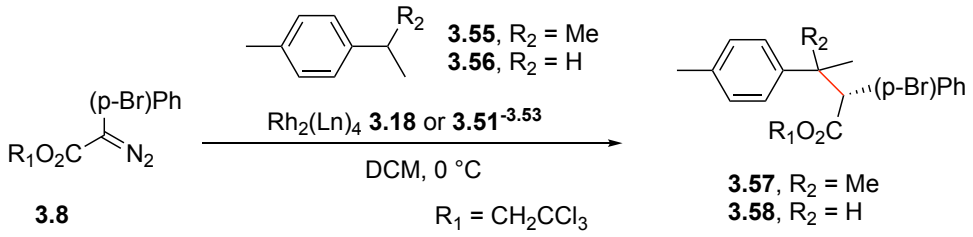

3.8

entry	Rh(II) catalyst	product	yield (%)	e.e.[c,d] (%)	product[e]	yield (%)	d.r.	e.e.[c,d] (%)
1	**3.18** Rh_2(*S*-TPPTTL)$_4$	**3.57**[f]	68	90	**3.58**	72	19.2:1	88
2	**3.51**	**3.57**	72	87	**3.58**	65	24.4:1	97
3	**3.52**	**3.57**	74	89	**3.58**	73	21.4	97
4	**3.53**	**3.57**	70	90	**3.58**	70	20.3:1	96

[a] Yields refer to combined, isolated yields.
[b] Regio- and diastereoselectivity were determined from the reaction crude 1H NMR spectra
[c] Enantiomeric excess data were obtained using HPLC on a chiral stationary phase
[d] e.e. shown for the major isomer
[e] No primary insertion was observed (> 30:1 r.r.)
[f] Primary insertion was observed, r.r. = 11.3:1

This pattern of selectivity, while astonishing, could be rationalized by carefully examining the structural features of the catalyst, in a very similar way as compared to the previous cyclohexane study (Figure 3.7).[48] As the catalysts (**3.51**-**3.53**) now have extended aryl rings with substantially more steric hinderance, the isopropyl group of *p*-cymene would have unfavorable interaction with the ligand (Structure **3.59**). As a result, it would preferentially be placed closer to the rhodium-carbene center and the tertiary position is functionalized (Structure **3.60**). This interesting selectivity profile is in contrast with our previous observations that a crowded, rigid catalyst would generally prefer sterically open sites.[9, 17, 49]

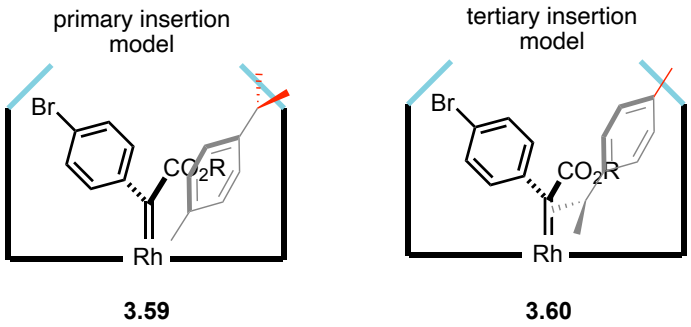

Figure 3.7 Rationalization of selectivity for the functionalization of *p*-cymene

3.2.7 Aryl diazoketones as new donor/acceptor carbene precursors for selective intermolecular C–H functionalization reactions

(Note: the project was in collaboration with Aaron Bosse.)

As discussed previously, donor/acceptor carbenes, developed and popularized by the Davies group, are known to undergo highly regio- and stereoselective transformations with an appropriate chiral dirhodium catalyst. The primary reason for the enhanced selectivity is due to attenuation of the carbene's electrophilicity from the electron-rich donor group.[7-9, 14] While heteroaryl donor groups are relatively established for aryldiazoacetates as the carbene precursor, the acceptor group was essentially limited to an ester functionality for intermolecular C–H functionalization reactions. While we have previously reported that aryl diazoketones are also competent donor/acceptor carbene precursors, the application was limited to cyclopropanation and the scope of alkene substrates was relatively narrow. The only example of C–H functionalization using aryl diazoketone used cyclohexadiene as the substrate, which is one of the easiest substrates due to double electronic activation from the diene functionality (Scheme 3.6). Therefore, one of

the primary goals for this project was to expand our donor/acceptor carbene reactions "toolbox" and demonstrate the synthetic utility of the newly incorporated ketone functionality as opposed to an ester group.

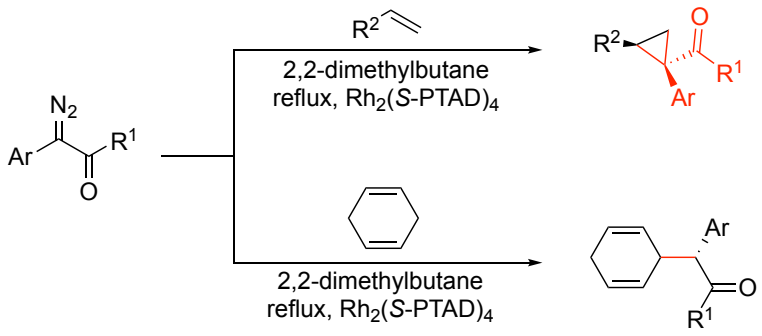

Scheme 3.6 Known chemistry on aryl diazoketones as donor/acceptor carbene precursors

Initial reaction optimization focused on the identification of an aryl diazoketone as an effective carbene precursor (Table 3.9). We chose 4-ethyltoluene (**3.56**) as the model substrate as it can evaluate the catalyst's regio-, diastereo- and enantioselectivity. We found that methyl (**3.61a**) and *tert*-butyl ketones (**3.61b**) were ineffective carbene precursors and resulted in no or little formation of the desired product (entries 1-2). We reasoned that the carbonyl on interfered as a nucleophile and led to unproductive reaction pathways. Therefore, we changed to aryl ketone (**3.61c**) and were delighted to find that we could now isolate the desired C–H functionalization products **3.62c** in moderate yield (55% yield) but excellent regio-, diastereo- and enantioselectivity (>30:1 rr, >30:1 dr, 99% ee, entry 3). Probing the electronics indicated that an electron-rich phenyl group was detrimental to the yield (30% yield) of the reaction, although the stereoselectivity remained high (entry 4). Therefore, we decided to incorporate an electron-deficient phenyl ring into the design of the diazoketone by attaching a halogen (entries 5-8). Testing Rh_2(*S*-PTAD)$_4$ in

the reaction, which was previously used for cyclopropanation reactions using aryl diazoketones, gave unsatisfactory results with poor yield and stereoselectivity, which helps to further confirm the importance of Rh_2(*S*-TPPTTL)$_4$ as the chiral catalyst of choice. Further screening of different aryl groups indicated that *p*-CF_3 group provided the product (**3.62g**) in highest yield and stereoselectivity (entry 8), which presumably resulted from a more electrophilic, and hence more reactive, donor/acceptor carbene. At this point, the yields remained to be only moderate, as the remaining mass balance of the reactions was found to be due to self-dimerization of the diazo compound, although further attempts of minimizing this side reactions were unsuccessful. Importantly, we did not observe any evidence for the formation of ketene byproducts, which could form via Wolff rearrangement under thermolytic or photolytic conditions with diazoketones.

Table 3.9 Optimization of C–H functionalization using aryl diazoketones as the carbene precursor

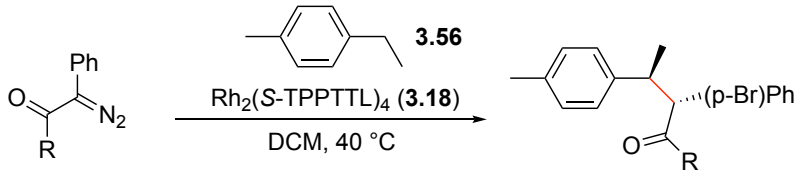

entry	R	yield[a] (%)	r.r.[b]	d.r.[b]	e.e.[c,d]
1	Me	n/a	n/a	n/a	n/a
2	*t*Bu	20	>30:1	n.d.	n.d.
3	Ph	55	>30:1	>30:1	99
4	(*p*-OMe)Ph	30	>30:1	20:1	>99
5[e]	(*p*-Br)Ph	15	4:1	12:1	77
6	(*p*-Br)Ph	55	>30:1	>30:1	99
7	(*p*-Cl)Ph	56	>30:1	>30:1	>99
8	(*p*-CF_3)Ph	57	>30:1	>30:1	>99

[a] Yields refer to combined, isolated yields.
[b] Regio- and diastereoselectivity were determined from the reaction crude 1H NMR spectra
[c] Enantiomeric excess data were obtained using HPLC on a chiral stationary phase
[d] e.e. shown for the major isomer
[e] Raction was catalyzed by Rh_2(*S*-PTAD)$_4$

With the optimized chiral catalyst, carbene precursor and reaction conditions in hand, the next step was to explore the scope of the reaction with a variety of activated and unactivated substrates (Table **3.10**). When activated benzylic compounds (**3.63a-c**) were used as the substrates, the C–H functionalization event occurred smoothly at the activated secondary benzylic position with high diastereoselectivity (>30 : 1 dr) and enantioselectivity (92% - >99% ee, **3.64a-c**). The regioselectivity for the formation of **3.64c** was also consistent with our previous observations that are discussed previously in this chapter. Allylic C–H functionalization was also successful in this transformation as **3.64d** was obtained with excellent regio- and stereoselectivity. In addition, the aryl diazoketone **3.61g** was also capable of functionalizing unactivated substrates to generate the corresponding products **3.64e-g**. Interestingly, we observed an even cleaner, diastereoselective desymmetrization on *tert*-butylcyclohexane using aryl diazoketone (**3.64g**) than 2,2,2-trichloroethyl aryldiazoacetate as previously reported.[48]

Table 3.10 Scope of substrates in of C–H functionalization using aryl diazoketones as the carbene precursor

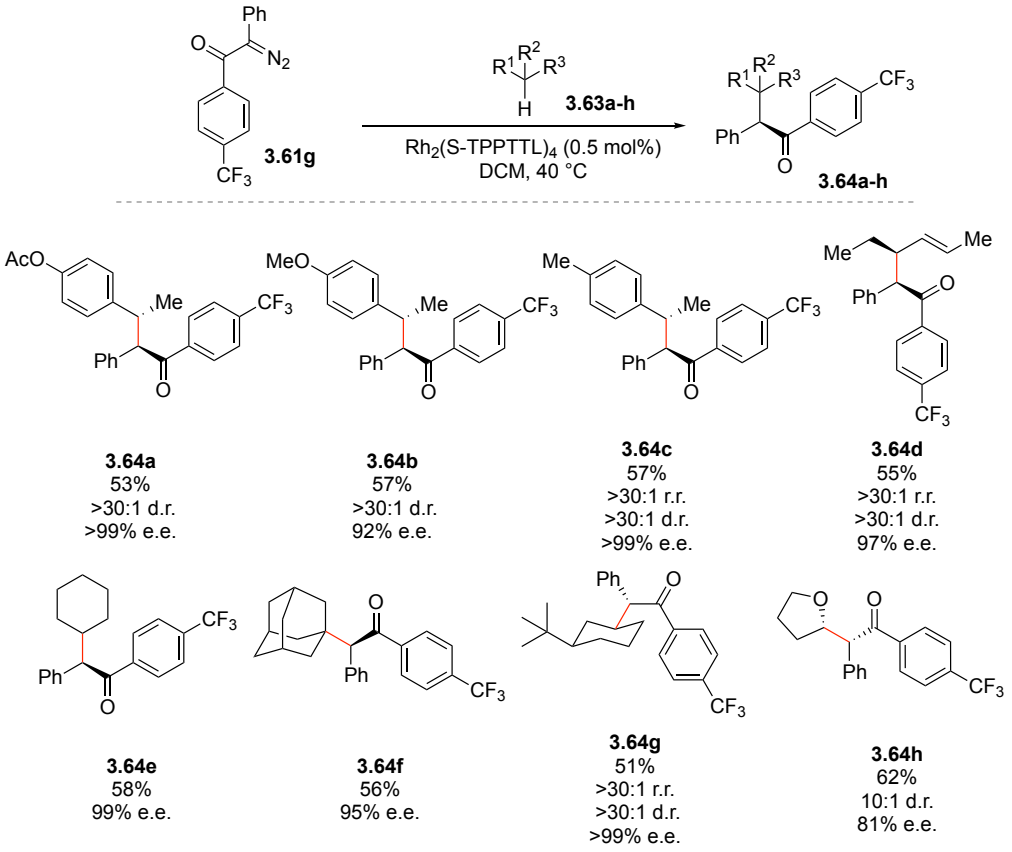

Knowing that aryldiazoketones are competent donor/acceptor carbene precursors for selective C–H functionalization reactions, we decided to explore the medicinal application and identified a drug candidate from AbbVie, a transient receptor potential vanilloid 3 (TRPV3) antagonist (**3.67**, Scheme 3.7) that had favorable preclinical profile in inflammation and neuropathic pain. The AbbVie synthesis relied on standard chemistry to construct the key cyclobutane core and the racemic alcohol **3.66** was resolved via chiral separation to afford enantiopure **3.67**. We reasoned that compound **3.67** contains a pyridinyl methanol moiety adjacent to an arylcyclobutane that may be accessed from a aryldiazoketone C–H functionalization

reaction/Baeyer-Villiger oxidation/reduction sequence, which would then allow us to obtain **3.67** in an asymmetric fashion. Therefore, a model study was conducted using the standard aryldiazoketone **3.61g** to first assess the feasibility of Rh_2(*S*-TPPTTL)$_4$ catalyzing reactions at a slightly hindered tertiary site. We were delighted to observe an effective C–H functionalization reaction at the desired benzylic position of the arylcyclobutane (**3.68**) with exceptional enantioselectivity (97% ee) but only moderate yield (47% yield) to give the desired product **3.69**. Nevertheless, competing reactions at the distal site on the cyclobutane[49] was not observed.

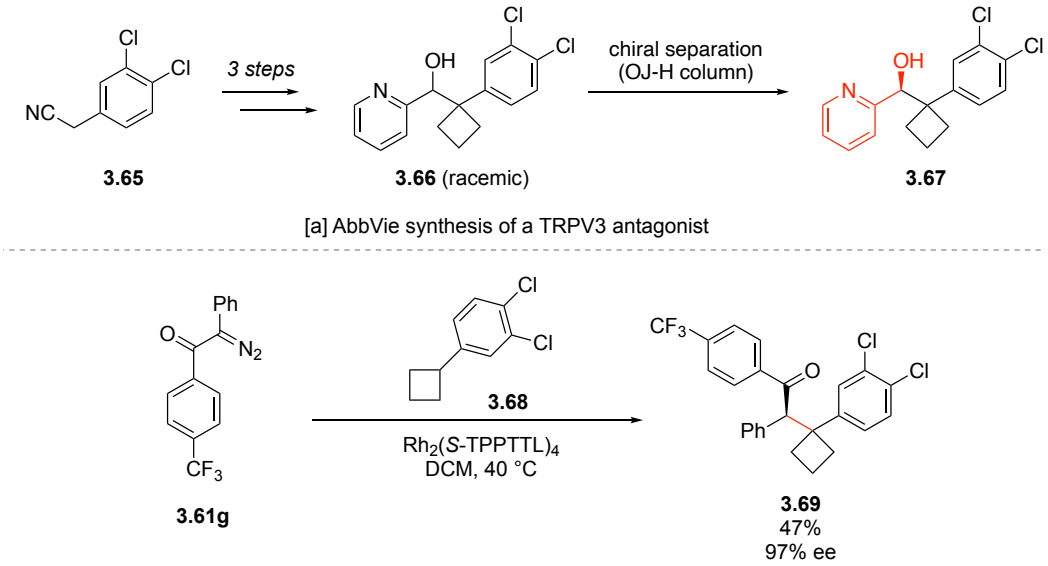

Scheme 3.7 Application of C–H functionalization of an arylcyclobutane

Overall, this study aims to demonstrate that there still exist opportunities for further diversifying our donor/acceptor carbene reaction toolbox, beyond developing new chiral catalysts. One of the ways of achieving this is to explore what other functionalities would be capable of mimicking the reactivity of the more established aryldiazoacetates, and we discovered that

aryldiazoketones can also undergo highly selective intermolecular C–H functionalization reactions with the use of the recently discovered chiral catalyst, Rh_2(*S*-TPPTTL)$_4$.

3.3 Conclusions

This study serves to demonstrate that C–H functionalization of substituted cyclohexanes in a site- and stereoselective manner is a viable process using a newly developed dirhodium catalyst, Rh_2(*S*-TPPTTL)$_4$. The catalyst can be easily accessed in two steps from commercial courses without the requirement for enantioenrichment of the ligand, adding to the practicality of the transformation. When an alkyl cyclohexane react with the rhodium-carbene, a desymmetrization reaction occurs at the C-3 equatorial position and generates three new stereogenic centers with the conversion of only one C–H bond. Different alkyl cyclohexanes, even a few functionalized ones, and wide range of aryl and heteroaryl diazoacetates are compatible with the reaction. X-Ray crystallographic analysis and computational studies indicate that the substituent of the cyclohexane is oriented toward the “opening” of the tetraphenylphthalamido group of the catalyst to minimize unfavorable steric interactions with the ligand.

In addition, the catalyst was applied in the functionalization of strained organosilicons, which are of pharmaceutical interests. We also demonstrated that aryl diazoketones are capable precursors to donor/acceptor carbenes for C–H functionalization reactions using Rh_2(*S*-TPPTTL)$_4$, and the newly introduced ketone functionality could be used as a handle for many subsequent transformations. Lastly, the novel site selectivity of Rh_2(*S*-TPPTTL)$_4$ continues to inspire the design and development of new ligands that originate from the tetraphenylphthalamido core scaffold.

3.4 References

1. Abrams, D. J.; Provencher, P. A.; Sorensen, E. J. *Chem. Soc. Rev.* **2018,** *47*, 8925.
2. Davies, H. M. L. *Angew. Chem. Int. Ed.* **2006,** *45*, 6422.
3. Davies, H. M. L.; Morton, D. *J. Org. Chem.* **2016,** *81*, 343.
4. Godula, K.; Sames, D. *Science* **2006,** *312*, 67.
5. He, J.; Hamann, L. G.; Davies, H. M. L.; Beckwith, R. E. *Nat. Commun.* **2015,** *6*, 5943.
6. Newhouse, T.; Baran, P. S. *Angew. Chem. Int. Ed.* **2011,** *50*, 3362.
7. Davies, H. M. L.; Manning, J. R. *Nature* **2008,** *451*, 417.
8. Davies, H. M. L. *J. Org. Chem.* **2019,** *84*, 12722.
9. Davies, H. M. L.; Liao, K. *Nat. Rev. Chem.* **2019,** *3*, 347.
10. Colby, D. A.; Bergman, R. G.; Ellman, J. A. *Chem. Rev.* **2010,** *110*, 624.
11. Hartwig, J. F.; Larsen, M. A. *ACS. Cent. Sci.* **2016,** *2*, 281.
12. He, J.; Wasa, M.; Chan, K. S. L.; Shao, Q.; Yu, J. Q. *Chem. Rev.* **2017,** *117*, 8754.
13. Chen, M. S.; White, M. C. *Science* **2010,** *327*, 566.
14. Davies, H. M. L.; Morton, D. *Chem. Soc. Rev.* **2011,** *40*, 1857.
15. Liao, K.; Negretti, S.; Musaev, D. G.; Bacsa, J.; Davies, H. M. L. *Nature* **2016,** *533*, 230.
16. Liao, K.; Pickel, T. C.; Boyarskikh, V.; Bacsa, J.; Musaev, D. G.; Davies, H. M. L. *Nature* **2017,** *551*, 609.
17. Liao, K.; Yang, Y. F.; Li, Y.; Sanders, J. N.; Houk, K. N.; Musaev, D. G.; Davies, H. M. L. *Nat. Chem.* **2018,** *10*, 1048.
18. Liu, W.; Ren, Z.; Bosse, A. T.; Liao, K.; Goldstein, E. L.; Bacsa, J.; Musaev, D. G.; Stoltz, B. M.; Davies, H. M. L. *J. Am. Chem. Soc.* **2018,** *140*, 12247.

19. Chen, K.; Eschenmoser, A.; Baran, P. S. *Angew. Chem. Int. Ed.* **2009,** *48*, 9705.

20. White, M. C.; Zhao, J. *J. Am. Chem. Soc.* **2018,** *140*, 13988.

21. Czaplyski, W. L.; Na, C. G.; Alexanian, E. J. *J. Am. Chem. Soc.* **2016,** *138*, 13854.

22. Schmidt, V. A.; Quinn, R. K.; Brusoe, A. T.; Alexanian, E. J. *J. Am. Chem. Soc.* **2014,** *136*, 14389.

23. Davies, H. M. L.; Hansen, T. *J. Am. Chem. Soc.* **1997,** *119*, 9075.

24. Davies, H. M. L.; Hansen, T.; Churchill, M. R. *J. Am. Chem. Soc.* **2000,** *122*, 3063.

25. Guptill, D. M.; Davies, H. M. L. *J. Am. Chem. Soc.* **2014,** *136*, 17718.

26. Antunez, S.; Juaristi, E. *J. Org. Chem.* **1996,** *61*, 6465.

27. Davies, H. M. L.; Bruzinski, P. R.; Lake, D. H.; Kong, N.; Fall, M. J. *J. Am. Chem. Soc.* **1996,** *118*, 6897.

28. Fu, L.; Hoang, K.; Tortoreto, C.; Liu, W.; Davies, H. M. L. *Org. Lett.* **2018,** *20*, 2399.

29. Yamawaki, M.; Tsutsui, H.; Kitagaki, S.; Anada, M.; Hashimoto, S. *Tetrahedron Lett.* **2002,** *43*, 9561.

30. Tsutsui, H.; Abe, T.; Nakamura, S.; Anada, M.; Hashimoto, S. *Chem. Pharm. Bull. (Tokyo)* **2005,** *53*, 1366.

31. Fu, L.; Wang, H.; Davies, H. M. L. *Org. Lett.* **2014,** *16*, 3036.

32. DeAngelis, A.; Boruta, D. T.; Lubin, J. B.; Plampin, J. N., 3rd; Yap, G. P.; Fox, J. M., *Chem. Commun. (Camb)* **2010,** *46*, 4541.

33. DeAngelis, A.; Dmitrenko, O.; Yap, G. P. A.; Fox, J. M. *J. Am. Chem. Soc.* **2009,** *131*, 7230.

34. Moberg, W. K.; Basarab, G. S.; Cuomo, J.; Liang, P. H., Biologically Active Organosilicon Compounds. In *Synthesis and Chemistry of Agrochemicals*, American Chemical Society: 1987; Vol. 355, pp 288-301.

35. Cash, G. G. *Pestic. Sci.* **1997,** *49*, 29.

36. Bai, D.; Han, S.; Lu, Z.-H.; Wang, S. *Can. J. Chem.* **2008,** *86*, 230.

37. Su, T. A.; Widawsky, J. R.; Li, H.; Klausen, R. S.; Leighton, J. L.; Steigerwald, M. L.; Venkataraman, L.; Nuckolls, C. *J. Am. Chem. Soc.* **2013,** *135*, 18331.

38. Seetharamsingh, B.; Ramesh, R.; Dange, S. S.; Khairnar, P. V.; Singhal, S.; Upadhyay, D.; Veeraraghavan, S.; Viswanadha, S.; Vakkalanka, S.; Reddy, D. S. *ACS Med. Chem. Lett.* **2015,** *6*, 1105.

39. Franz, A. K.; Wilson, S. O. *J. Med. Chem.* **2013,** *56*, 388.

40. Bertolini, A.; Ferrari, A.; Ottani, A.; Guerzoni, S.; Tacchi, R.; Leone, S. *CNS Drug Rev.* **2006,** *12*, 250.

41. Fujii, S.; Hashimoto, Y. *Future Med. Chem.* **2017,** *9*, 485.

42. Ramesh, R.; Reddy, D. S. *J. Med. Chem.* **2018,** *61*, 3779.

43. Tacke, R.; Handmann, V. I.; Bertermann, R.; Burschka, C.; Penka, M.; Seyfried, C. *Organometallics* **2003,** *22*, 916.

44. Cheng, C.; Hartwig, J. F. *Chem. Rev.* **2015,** *115*, 8946.

45. Komiyama, T.; Minami, Y.; Hiyama, T. *ACS Catal.* **2017,** *7*, 631.

46. Garlets, Z. J.; Davies, H. M. L. *Org. Lett.* **2018,** *20*, 2168.

47. Fu, J.; Ren, Z.; Bacsa, J.; Musaev, D. G.; Davies, H. M. L. *Nature* **2018,** *564*, 395.

48. Qin, C.; Davies, H. M. L. *J. Am. Chem. Soc.* **2014,** *136*, 9792.

49. Garlets, Z. J.; Wertz, B. D.; Liu, W.; Voight E. A.; Davies, H. M. L. *Chem*, **2020**, *6*, 304.

Chapter 4

Monocyclopropanation of Pyrroles by Rh(II)-donor/acceptor Carbenes

4.1 Introduction

Aromatic heterocycles such as pyrroles and furans are important structural motifs that are frequently encountered in biological and medicinal chemistry. In addition, drug development research often uses these heterocycles as pharmacophores for the design of new therapeutic agents.[1-7] Since a large number of natural and synthetic pharmaceuticals are constructed based on aromatic heterocyclic scaffolds, it is unsurprising that the development of new methodologies for the formation and functionalization of these compounds are of considerable scientific interest in synthetic chemistry.

In this regard, one of the effective ways to functionalize these electron-rich oxygen and nitrogen heterocycles is to react them with highly electrophilic carbene species under the catalysis of a copper or rhodium catalyst (Scheme 4.1). There are mainly two pathways that are possible between an electron-rich heterocycle (**4.1**) and a metal carbene (**4.2**). One of them is a concerted, asynchronous cyclopropanation reaction with partial positive charge build-up at either the 2- or 3-position. Alternatively, a zwitterionic pathway is also possible for particularly electron-rich heterocycles and carbenes that can effectively stabilize charges, which will lead to other types of products.[8, 9]

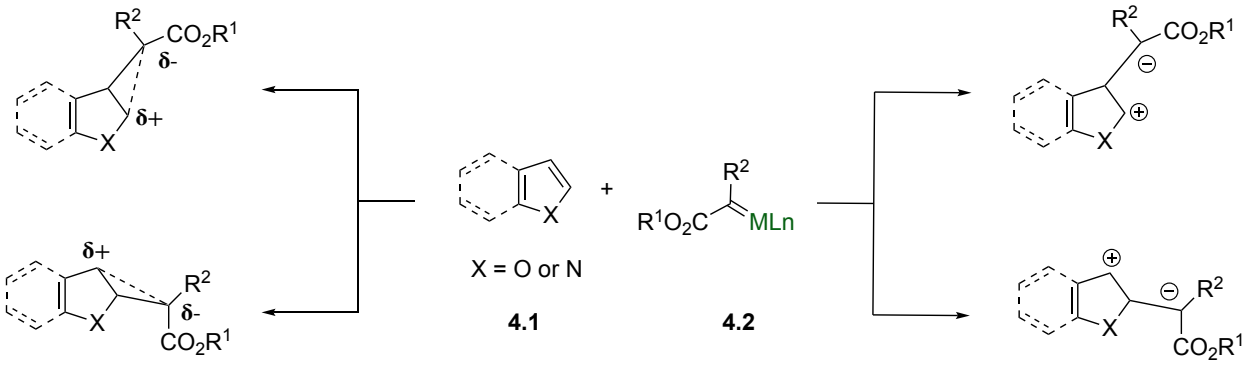

Scheme 4.1 Two possible pathways for metal carbene to react with heterocycles

Due to the powerful electron-donating nature of the lone pair of electrons on the nitrogen, pyrroles are particularly reactive substrates towards electrophilic metal carbene reactions, and even more so than furans.[3] However, in contrast to furans, the reactivity profile of pyrroles is influenced by the functionality on the nitrogen. For example, due to conjugation of the nitrogen lone pair with the carbonyl functionality, *N*-acyl or *N*-sulfonyl pyrroles are less electron-rich and tend to undergo predominantly cyclopropanation reactions. In contrast, *N*-H or *N*-alkyl pyrroles are more electron-rich and therefore usually undergo alkylation via the zwitterionic intermediates.

Recently, Reiser and co-workers have reported asymmetric cyclopropanation of furans and pyrroles using acceptor-only carbenes derived from alkyl diazoacetates and copper(II) catalyst that was activated by phenylhydrazine (Scheme 4.2).[10-14] For example, when *N*-Boc pyrrole (**4.4**) was treated with diazoacetate **4.3** in the presence of $Cu(OTf)_2$ and chiral ligand **4.5a**, monocyclopropane **4.6** was generated with high enantioselectivity (87% ee), although the yield was low (44% yield), and the undesired double cyclopropane was also isolated in 12% yield.

Similarly, furan **4.7** is also capable of cyclopropanation under similar conditions to generate product **4.8** in 38% yield but also quite high enantioselectivity (83% ee).

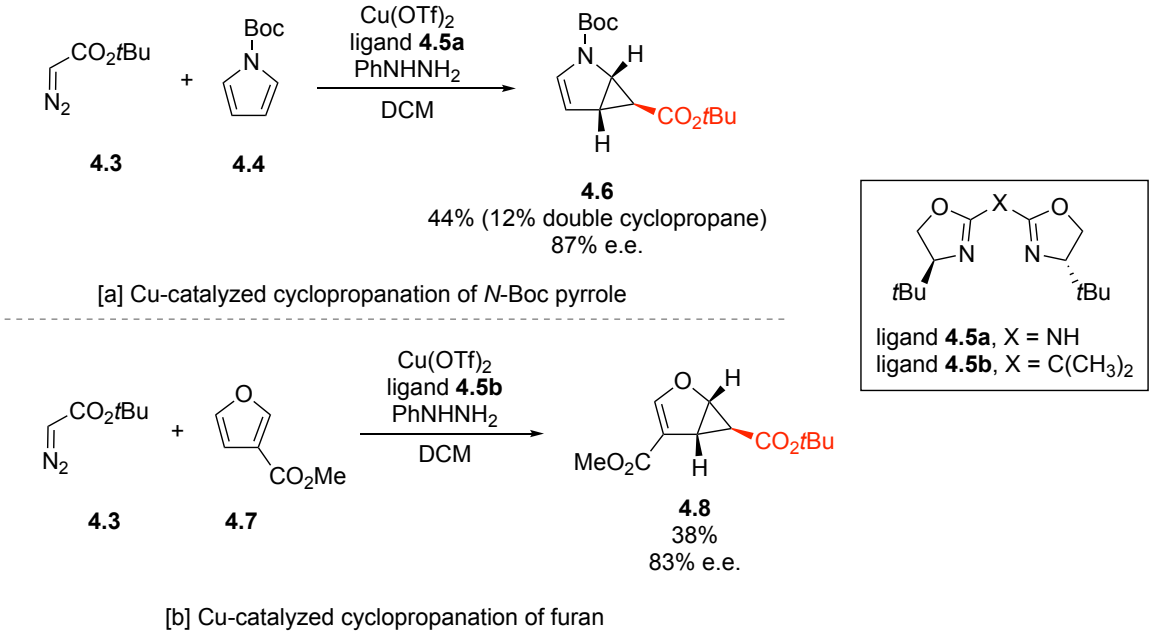

Scheme 4.2 Cu-catalyzed cyclopropanation using diazoacetates

On the other hand, reactions using donor/acceptor carbenes with *N*-acyl pyrroles are very different from those using diazoacetates, as the former usually show much better chemo- and stereoselectivity (Scheme 4.3).[3, 15] For example, Davies and co-workers have demonstrated that siloxy vinyl diazoacetate (**4.9**) can react with *N*-Boc pyrrole (**4.4**) to generate a functionalized tropane derivative (**4.10**) under the catalysis of a dirhodium catalyst, and it was possible to achieve high level of stereocontrol by using Rh_2(*S*-PTAD)$_4$.[16-19] In this reaction, even though the monocyclopropanated intermediate **4.11** was non-isolable, it was clearly implicated in the reaction mechanism. The formation of the tropane ring was proposed to go through this intermediate, which

contains a divinyl cyclopropane moiety, which would undergo facile Cope rearrangement at elevated temperature to give the final product **4.10**. However, when methyl 2-(4-bromophenyl)-2-diazoacetate (**4.12**) was used as the donor/acceptor carbene precursor, the reaction outcome was drastically different. In this case, a doubly cyclopropanated product (**4.13**) with six new stereogenic centers was formed as a single diastereomer with good enantioselectivity. While the formation of the monocyclopropanated intermediate, **4.14**, is also evident, the incorporation of the aryl group in place of vinyl functionality would effectively halt any further rearrangement. However, **4.14** contains a enamine functionality that was highly reactive and would then immediately undergo a second cyclopropanation to give **4.13**. Normally, carbene reactions in the Davies group tend to use an excess of the substrate to provide an effectively trap for the rhodium-carbene. In this case, it is important to note that the formation of **4.14** uses **4.13** as the substrate, but exclusive formation of the biscyclopropane (**4.13**) was still observed even when *N*-Boc pyrrole was used in vast excess, indicating that the enamine reactivity was challenging to overcome simply by manipulating reaction stoichiometry. Indeed, it was found the monocyclopropanated species (**4.14**) could be isolated in 54% yield only when *N*-Boc pyrrole was used as the reaction solvent. But even so a substantial amount (34% yield) of the biscyclopropane (**4.13**) was still observed. Therefore, a general method for the stereoselective formation of the monocyclopropanated pyrroles, which can be highly valuable chiral building blocks for biologically relevant applications,[12, 16, 19] remains to be very desirable.

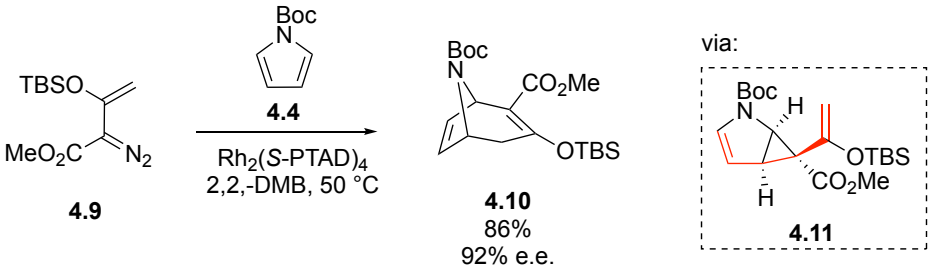

[a] Davies' synthesis of tropane using pyrrole and vinyl diazoacetate

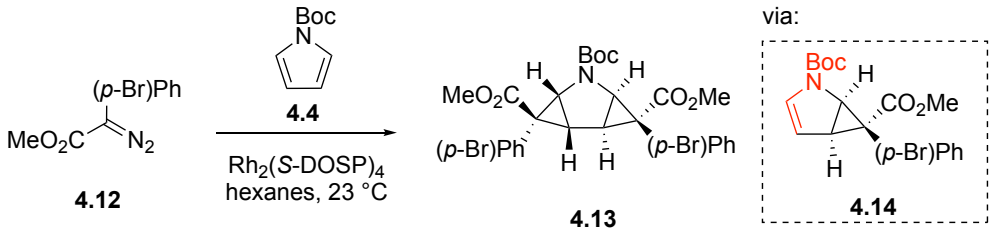

ratio **4.4**:**4.12** = 1:3, 93%, 83% e.e.
ratio **4.4**:**4.12** = 6:1, 77%, 77% e.e.

[b] Double cyclopropanation of pyrrole with donor/acceptor carbene

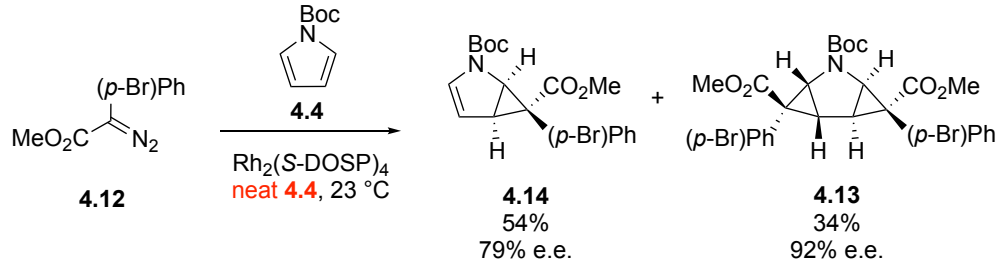

[c] Isolation of monocyclopropanated pyrrole under neat reaction condition

Scheme 4.3 Previous examples of asymmetric cyclopropanation reaction using pyrroles as substrates

More recently, work from Reiser and Davies has indicated that furans can be effectively cyclopropanated using a donor/acceptor carbene under the catalysis of Rh_2(*S*-TCPTTL)$_4$, which gave the desired product in very high yield and excellent enantioselectivity (86% yield, 96% ee), even when the catalyst loading was only 0.001 mol % (Scheme **4.4**). The methodology was applied toward the synthesis of (-)-roccellaric acid.[20] In light of this success, we decided to initiate the project by applying this catalyst to pyrrole systems and optimize toward a clean and stereoselective monocyclopropanation reaction.

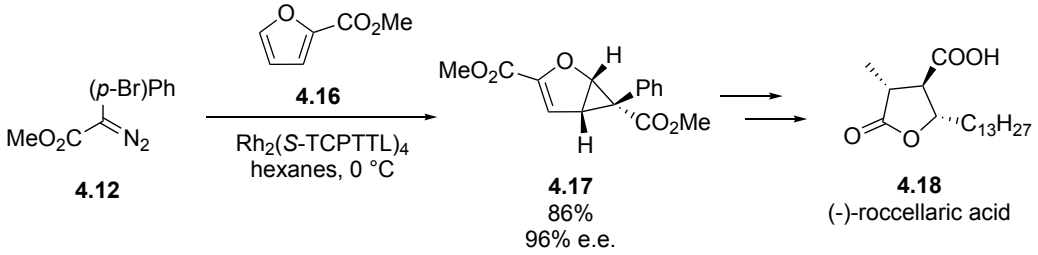

Scheme 4.4 Asymmetric cyclopropanation of furan derivatives

4.2 Results and Discussions

4.2.1 Optimization and scope of monocyclopropanation of N-protected pyrroles

(*Note: this project was a collaboration with Dr. Oliver Reiser's group at University of Regensburg, Germany. The initial optimization of protecting groups was completed by Dr. Verena Lehner, and the rest of the project was completed in collaboration with Nikolai Wurzer.)*

As discussed above, we initially aimed to find a suitable dirhodium catalyst that would give a highly selective monocyclopropanation on pyrrole substrates. Unfortunately, applying the previous reaction conditions using methyl 2-diazo-2-phenylacetate (**4.19**) and the catalyst, Rh_2(*S*-TCPTTL)$_4$, to *N*-Boc pyrrole (**4.4**) was not straightforward (Scheme 4.5), and only resulted in the exclusive formation of the biscyclopropane (**4.20**) in very low yield (< 20% yield).

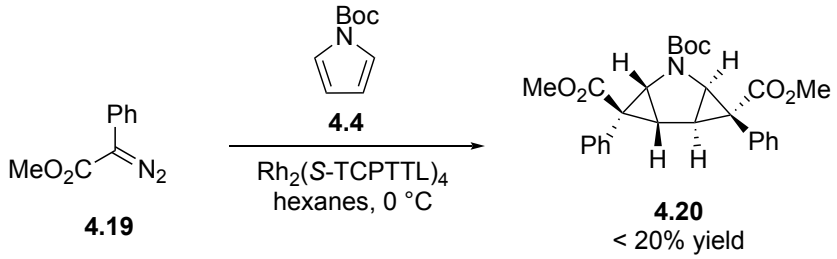

Scheme 4.5 Rh_2(*S*-TCPTTL)$_4$-catalyzed cyclopropanation of *N*-Boc pyrrole

Because the *tert*-butoxy carbonyl (Boc) group was not an effective protecting group for this reaction, a screening of other protecting groups seemed necessary at this stage. Therefore, a variety of different *N*-protected pyrroles (**4.21a**-**e**) were synthesized and evaluated in the asymmetric cyclopropanation reaction using Rh_2(*S*-TCPTTL)$_4$ as the catalyst and **4.19** as the carbene source (Table 4.1). Due to poor solubility of **4.21** in hexanes, the solvent was changed to toluene. The optimization study indicated that the nature of the protecting group had a substantial impact on the reaction outcomes. Specifically, *N*-sulfonyl pyrroles (**4.21c**-**e**, entries 3-5) performed much better than *N*-carboxyl pyrroles (**4.21a** and **b**, entries 1 and 2) in terms of yield of the desired product (**4.22**) and its enantioselectivity. Because of its highest yield (61% yield) and excellent enantioselectivity (93% ee), we decided to use *N*-tosyl (entry 5) as the protecting group of choice.

Table 4.1 Optimization of *N*-protecting group

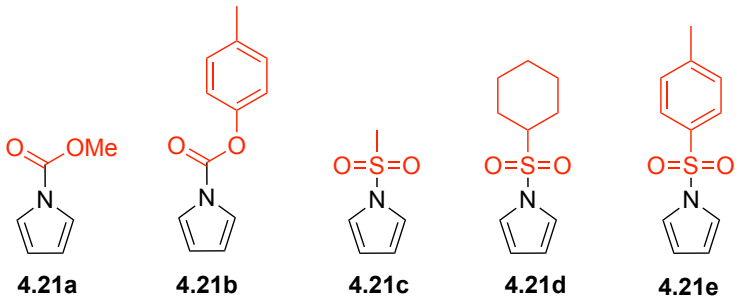

4.21a **4.21b** **4.21c** **4.21d** **4.21e**

[a] Different *N*-protected pyrroles

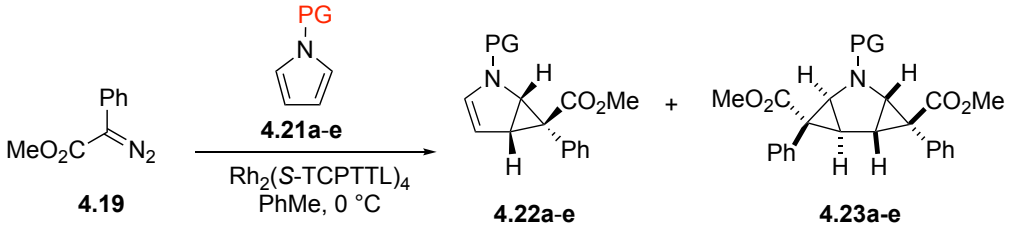

entry	substrate	product	yield[a] (%) **4.22**	e.e.[b] (%) **4.22**	yield[a] (%) **4.23**
1	**4.21a**	**4.22a**	8	7	26
2	**4.21b**	**4.22b**	40	57	27
3	**4.21c**	**4.22c**	n.d.	82	n.d.
4	**4.21d**	**4.22d**	40	94	21
5	**4.21e**	**4.22e**	61	93	15

[a] Isolated yield
[b] Enantimeric excess data obtained from HPLC on a chiral stationary phase

However, it is critical to note here that none of the protecting groups above was able to give a clean monocyclopropanation, as in all cases we observed substantial formation of the competing biscyclopropane (**4.23**). Therefore, a systematic catalyst optimization study using a wider range of chiral dirhodium catalysts was warranted at this point (Table 4.2). Rh_2(*S*-TCPTTL)$_4$ and its close derivative, Rh_2(*R*-TCPTAD)$_4$, both gave inferior result, producing the desired product

in low yield and selectivity, indicating that the tetrachloro scaffold on the catalyst may not be conducive to a clean monocyclopropanation reaction (entries 1 and 2). Rh_2(*R*-PTAD)$_4$ and Rh_2(*R*-PTTL)$_4$ are also closely related dirhodium catalysts, and while they were both capable of excellent asymmetric induction for the monocyclopropanation, the product ratios were less ideal and we still observed substantial competition from the double cyclopropanation (entries 3-5). The naphthalimido catalyst Rh_2(*S*-NTTL)$_4$ gave an exceptionally clean monocyclopropanation reaction, and the desired product **4.22e** was formed in 85% ee (entry 5). The more recently developed triarylcyclopropane carboxylate catalysts Rh_2(*R*-*p*-BrTPCP)$_4$ and Rh_2(*R*-*p*-PhTPCP)$_4$ are substantially sterically more demanding, and they also gave very clean monocyclopropanation with no competing formation of **4.23e** in the crude reaction mixture. However, Rh_2(*R*-*p*-PhTPCP)$_4$ was capable of much better asymmetric induction (91% ee, entry 7), and therefore it was selected to be the catalyst of choice for subsequent studies. The yield (56%) at this stage has room for improvement, but when we attempted the same reaction at reflux temperature (40 °C), a lower enantioselectivity (88% ee) was observed with only marginal improvement in yield (64%, entry 8).

Table 4.2 Catalyst optimization toward clean monocyclopropanation

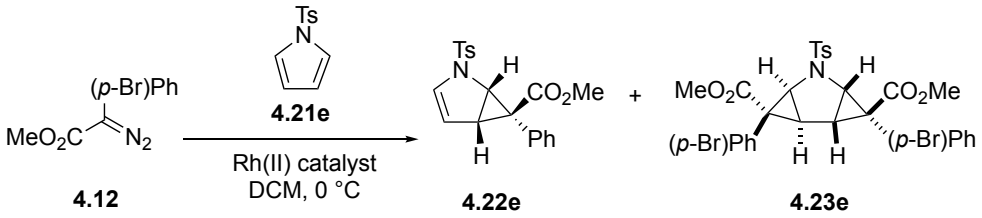

entry	Rh(II) catalyst	selectivity[a] (**4.22e**:**4.23e**)	yield[b] (%) **4.22e**	e.e.[c] (%) **4.22e**
1	Rh_2(*S*-TCPTTL)$_4$	1.4:1	33	66
2	Rh_2(*R*-TCPTAD)$_4$	3.1:1	39	-77
3	Rh_2(*R*-PTAD)$_4$	6.7:1	54	-97
4	Rh_2(*R*-PTTL)$_4$	22.7:1	59	-95
5	Rh_2(*S*-NTTL)$_4$	>30:1	60	85
6	Rh_2(*R*-*p*-BrTPCP)$_4$	>30:1	59	82
7	Rh_2(*R*-*p*-PhTPCP)$_4$	>30:1	56	91
8[d]	Rh_2(*R*-*p*-PhTPCP)$_4$	>30:1	64	88

[a] Ratios determined from the crude ^{1}H NMR spectra
[b] Yield refers to isolated yield
[c] Enantimeric excess data obtained from HPLC on a chiral stationary phase
[d] Reaction performed at 40 °C

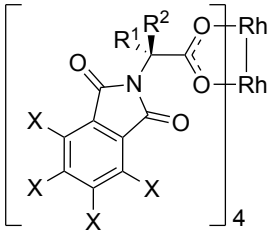

Rh_2(*S*-TCPTTL)$_4$: X = Cl, R^1 = H, R^2 = *t*Bu
Rh_2(*R*-TCPTAD)$_4$: X = Cl, R^1 = adamantyl, R^2 = H
Rh_2(*R*-PTAD)$_4$: X = H, R^1 = adamantyl, R^2 = H
Rh_2(*R*-PTTL)$_4$: X = H, R^1 = *t*Bu, R^2 = H

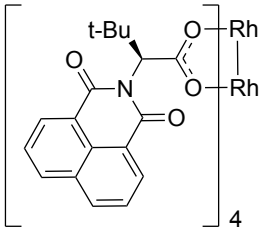

Rh_2(*S*-NTTL)$_4$

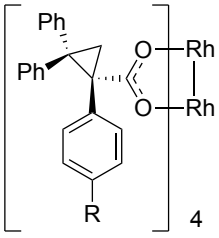

Rh_2(*R*-*p*-BrTPCP)$_4$: R = Br
Rh_2(*R*-*p*-PhTPCP)$_4$: R = Ph

With the optimized reaction condition and dirhodium catalyst in hand, we then sought to examine the scope of aryl diazoacetates that would be compatible with the transformation, using *N*-tosyl pyrrole as the substrate (Table 4.3). We were happy to see that a variety of aryl diazoacetates (**4.24a-i**) bearing different aryl rings are compatible with the cyclopropanation reaction, giving the corresponding products (**4.25a-i)** in good yield and high asymmetric induction, and variations in the electronics and substitution patterns on the aryl part did not have major impact on the reaction outcome. One exception is that the *o*-Bn diazoacetate (**4.24b**) gave the desired product in a lower 75% ee but satisfactory yield (60% yield). However, we discovered that when the aryl ring was a pyridine functionality (**4.24i**), a substantial drop in enantioselectivity (67% ee) was observed for the monocyclopropanated product (**4.25i**).

Table 4.3[a-b] Scope of aryl diazoacetates in pyrrole monocyclopropanation

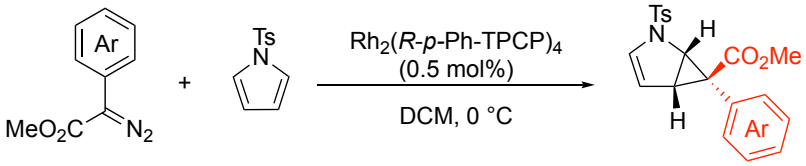

4.24a-i **4.21e** **4.25a-i**

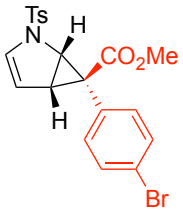

4.25a
56%
91% ee

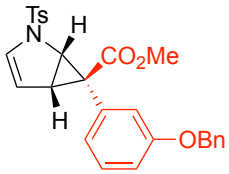

4.25b
60%
75% ee

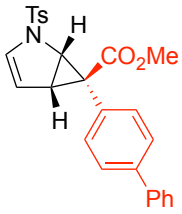

4.25c
78%
95% ee

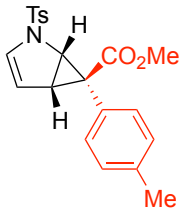

4.25d
69%
87% ee

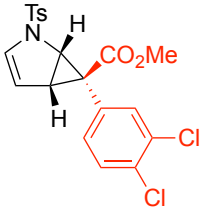

4.25e
60%
87% ee

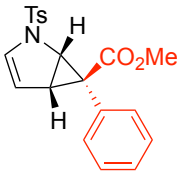

4.25f
72%
93% ee

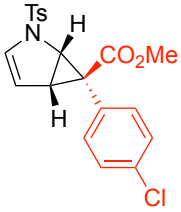

4.25g
70%
88% ee

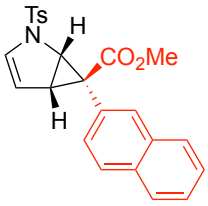

4.25h
62%
96% ee

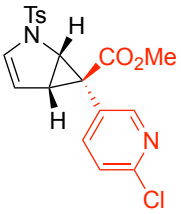

4.25i
65%
67% ee

[a] Yield refers to isolated yield
[b] Enantimeric excess data obtained from HPLC on a chiral stationary phase

Because we knew that 2-substituted furans are effective substrates for monocyclopropanation, we also attempted to expand the monocyclopropanation reaction of *N*-tosyl pyrrole to substituted pyrroles, such as methyl *N*-tosylpyrrole-2-carboxylate (**4.26**), to see if the transformation would be effective on functionalized pyrroles (Table 4.4). However, the direct application of the optimized reaction conditions did not initially lead to satisfactory results. We found that when the pyrrole contains a substituent at the 2-position, the reaction became very low yielding (34% yield) under the same condition, although enantioselectivity remained high (96% ee, entry 1). In the crude ^{1}H NMR spectrum, we saw substantial self-dimerization of the diazo compound (**4.12**). We reasoned that with the introduction of an electron-withdrawing substituent on the pyrrole ring and the sulfonyl protecting group, the aromatic heterocycle is now too electron-deficient to act as an effective trap for the rhodium-carbene. Therefore, we determined that a more robust source of donor/acceptor carbene may be necessary at this stage in order to expand the pyrrole scope.

We previously demonstrated that 2,2,2-trichloroethyl aryl diazoacetates are a more effective precursors to donor/acceptor carbenes for challenging reactions.[21] The trichloroethyl functionality was considered to make a more electrophilic carbene, which could then undergo many challenging C–H functionalization reactions in a selective manner.[22-27] Unfortunately, when we first attempted to apply this new carbene precursor to the monocyclopropanation of pyrrole **4.26**, an even lower yield of the desired product (**4.27**) was observed (15% yield, entry 2). However, when the reaction was conducted at reflux temperature (40 °C), the yield was significantly improved to 87% with essential no erosion in enantioselectivity (97% ee, entry 3). In addition, we found that the reaction was operable with the same enantioselectivity (97% ee) when the loading

of the catalyst was reduced to only 0.1 mol %, although the yield was reduced to 69% (entry 4). The possibility of doing the reaction at very low catalyst loading adds to the practicality of the methodology when one considers the cost of the rhodium catalyst if the reaction were to be performed on scale. Due to the electron-withdrawing nature of the methyl ester substituent and steric reason, no competitive double cyclopropanation was observed.

Table 4.4 Optimization of the reaction with methyl *N*-tosylpyrrole-2-carboxylate

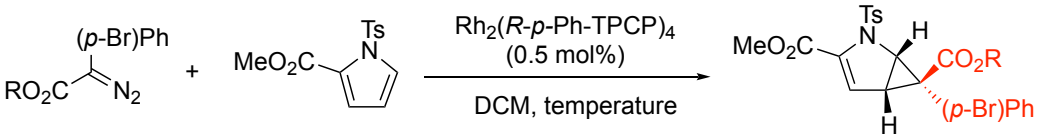

4.12 **4.26** **4.27**

entry	R	temperature (° C)	yield[a] (%)	e.e.[b] (%)
1	Me	0	34	96
2	CH_2CCl_3	0	15	98
3	CH_2CCl_3	40	87	97
4[c]	CH_2CCl_3	40	69	97

[a] Isolated yield
[b] Enantimeric excess data obtained from HPLC on a chiral stationary phase
[c] Reaction performed with 0.1 mol% catalyst loading

We next sought to evaluate the range of trichloroethyl aryl diazoacetates that would be compatible in the monocyclopropanation reaction (Table 4.5). We were happy to find that the reaction was tolerant to different substitution patterns on the aryl ring, as the monocyclopropanated products **4.29** were obtained with generally good yield and excellent enantioselectivity. However, we found that the cyclopropane was unstable even at room temperature when the aryl ring is a

thiophene (**4.29h**) and would quickly decompose in the same day, and therefore the yield was also diminished significantly (32% yield), although high enantioselectivity (96% ee) was still achieved. The only product that failed to give high enantioselectivity was the *o*-fluorophenyl derivative, which was obtained in 74% ee (**4.29j**).

Table 4.5 Scope of trichloroethyl aryl diazoacetates in monocyclopropanation of pyrrole

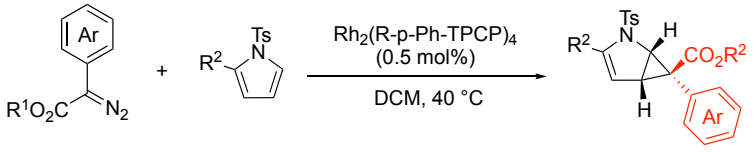

4.28a-j **4.26** **4.29a-j**

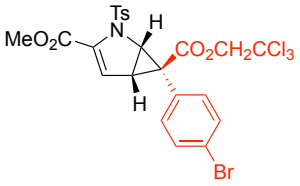

4.29a
87% (72%)
97% e.e. (96% e.e.)[c]

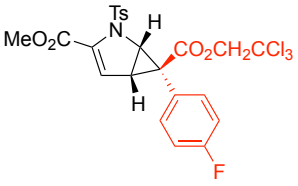

4.29b
72%
96% e.e.

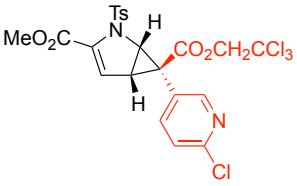

4.29c
66%
95% e.e.

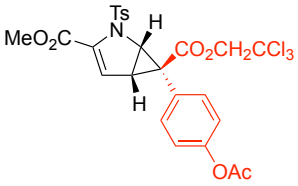

4.29d
62%
94% e.e.

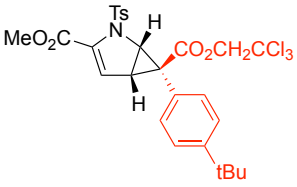

4.29e
70%
>99% e.e.

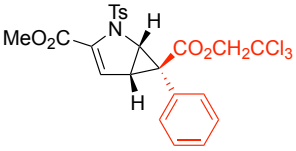

4.29f
60%
97% e.e.

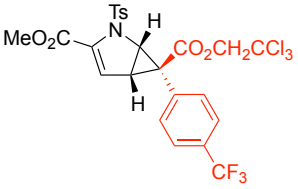

4.29g
68%
>99% e.e.

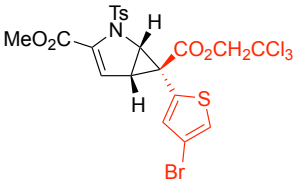

4.29h
32%[d]
96% e.e.

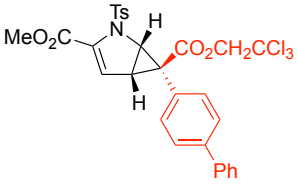

4.29i
63%
98% e.e.

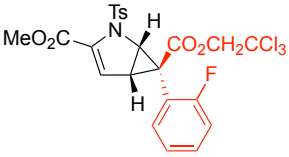

4.29j
75%
74% e.e.

[a] Yield refers to isolated yield
[b] Enantimeric excess data obtained from HPLC on a chiral stationary phase
[c] Scaled up to 3 mmol with a reduced catalyst loading of 0.25 mol%
[d] Product was unstable at room temperature

We also evaluated a number of other substituted pyrroles at either the 2- or 3-position in the monocyclopropanation reaction (Table 4.6). The reaction gave high asymmetric induction with other 2-substituted pyrroles to give **4.31a** and **4.31b** in 96% ee and 86% ee, respectively. However,

4.31b was formed in very low yield (24% yield), presumably because the trifluoroketone functionality made the pyrrole ring too electron-deficient to effectively react with the rhodium-carbene. When the pyrrole was unsubstituted, good yield (79% yield) and exceptional enantioselectivity (98% ee) was obtained for product **4.31c**. However, we also found that **4.31c** tend to decompose quickly at room temperature, while the methyl ester version **4.22e** was stable. Interestingly, while *N*-Boc pyrrole was a poor substrate for Rh_2(*S*-TCPTTL)$_4$-catalyzed reaction, its methyl ester derivative **4.30d** underwent very smooth monocyclopropanation to generate product **4.31d** in good yield (79% yield) and high enantioselectivity (96% ee) when Rh_2(*R*-*p*-PhTPCP)$_4$ was used as the catalyst. While 2-substituted pyrroles are well-tolerated in the reaction, we found that 3-substituted pyrrole **4.30e** gave no reaction and only observed dimerization of the diazo compound. This result is in contrast with our previous study with furans, where we found 3-methoxycaroxylfuran was an excellent candidate for cyclopropanation.[20]

Table 4.6 Scope of pyrrole in monocyclopropanation

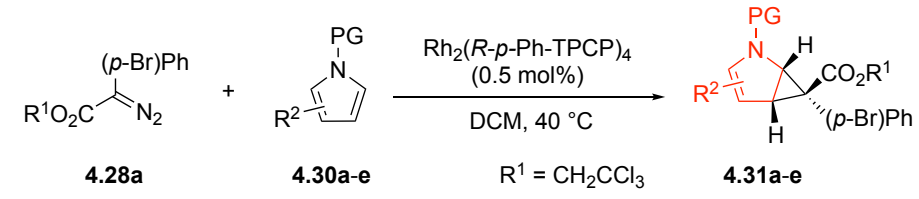

4.28a **4.30a-e** $R^1 = CH_2CCl_3$ **4.31a-e**

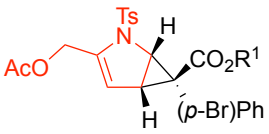

4.31a
75%
96% e.e.

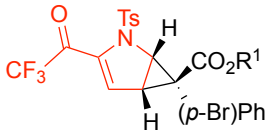

4.31b
24%
86% e.e.

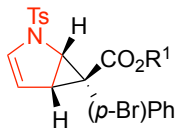

4.31c
79%
98% e.e.

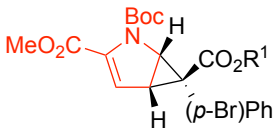

4.31d
79%
96% e.e.

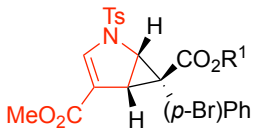

4.31e
no reaction

[a] Yield refers to isolated yield
[b] Enantimeric excess data obtained from HPLC on a chiral stationary phase

Unlike furans, we have observed that unsubstituted pyrroles tend to easily undergo double cyclopropanation when donor/acceptor carbenes are used. However, this can be controlled by the incorporation of the *N*-tosyl protecting group and the use of a sterically bulky catalyst, Rh_2(*R*-*p*-PhTPCP)$_4$. In addition, we have shown that while 2-substituted pyrroles are less reactive, substitution at the 3-postion would shut down any reactivity. This is, however, consistent with our previous hypotheses[15] for the mechanism by which these heterocycles approach the rhodium-carbene center.

One particularly interesting observation we have had in the past is that even when the heterocycle approach the same rhodium carbene from a single face, furans and pyrroles could give opposite asymmetric induction in product formation.[15] We hypothesized that furans would preferentially attack the rhodium-carbene center from its C-2 position during the asynchronous cyclopropanation step, due to better delocalization of positive charge build-up (**4.32**, Figure 4.1). For *N*-protected pyrroles, however, they tend to attack the rhodium-carbene center preferentially from its C-3 position, because the protecting group would have unfavorable steric interaction with the bulky rhodium catalyst if the C-2 position attacks the carbene (Structure **4.33**, Figure 4.1). This would explain why C-3 substitution would shut down the pyrrole's nucleophilicity toward the rhodium-carbene and therefore **4.30e** was an unreactive substrate.

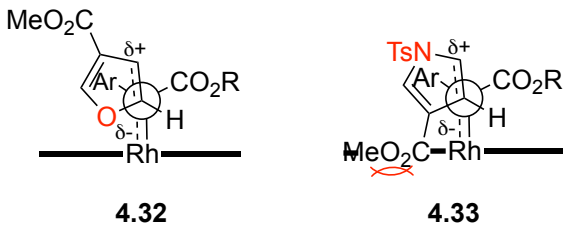

4.32 **4.33**

Figure 4.1 Different reactivity of furans and pyrroles toward rhodium-carbene

As discussed previously, pyrroles have a stronger tendency to undergo a second cyclopropanation, and this enhanced reactivity could be rationalized using a similar model (Figure 4.2). In Structure **4.34**, the pyrrole attacks the rhodium-carbene from the *Re* face. The product from the cyclopropanation reaction (**4.35**) would then become the "matched" enantiomer for a second cyclopropanation, since the new cyclopropane moiety is now pointing away from the carbene, as shown in **4.36**. We hypothesize that the use of the tosyl protecting group was instrumental in

effecting a clean monocyclopropanation. In Structure **4.36**, the tosyl group would make the pyrrole nitrogen effectively an sp^3-hybridized atom, with the lone pair of electrons pointing in the same face as the cyclopropane, while the tosyl group points to the opposite face toward the carbene. We believe that due to the steric bulk of the tosyl group *and* the catalyst, Rh_2(*R*-*p*-PhTPCP)$_4$, the formation of the biscyclopropane (**4.37**) would be prevented and only the monocyclopropane should be obtained.

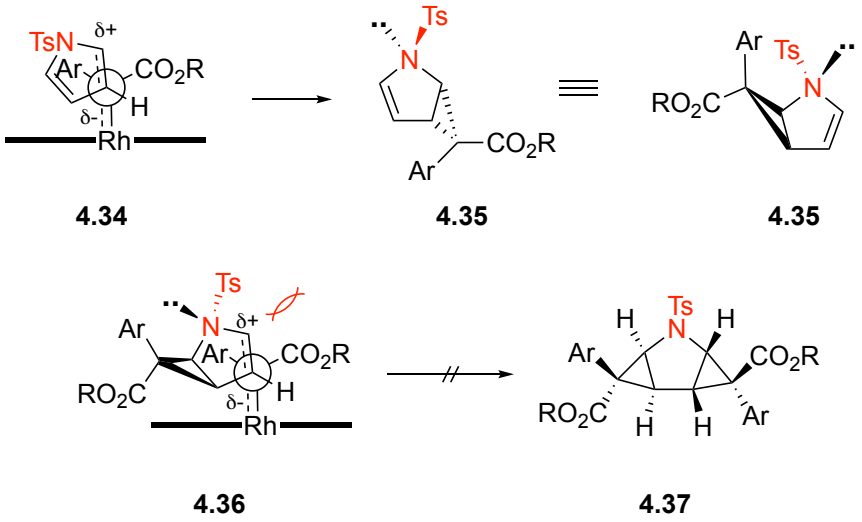

Figure 4.2 Tosyl protecting group prevents the second cyclopropanation

4.2.2 Synthetic applications

(Note: studies in this section were conducted by Dr. Verena Lehner and Nikolai Wurzer.)

Previous studies from Reiser and other groups have shown that monocyclopropanated pyrroles can be highly valuable chiral building blocks for biologically relevant targets. Specifically, they have been shown to be readily converted to β-aminocyclopropane carboxylic acids,[28-31]

pyrrolidones,[32, 33] or piperidines.[34-36] Therefore, the synthetic utility of monocyclopropanated pyrroles in this study was demonstrated with the synthesis of a homo-β-proline analog and a β-aminocyclopropane carboxylic acid (Scheme 4.6). The monocyclopropanated product **4.25f** could be easily enantioenriched to > 99% ee via recrystallization, which can then undergo a Pd-catalyzed hydrogenation and an acid-catalyzed reductive ring-opening to form **4.39**. Using conditions previously developed by Sharpless and co-workers,[37] global deprotection of **4.39** was achieved that gave the final homo-β-proline derivative **4.40** in quantitative yield. Alternatively, **4.25f** could also be converted to a β-aminocyclopropane carboxylic acid derivative **4.41** via a one-step ozonolysis reaction in 90% yield with retention of all stereochemistry.

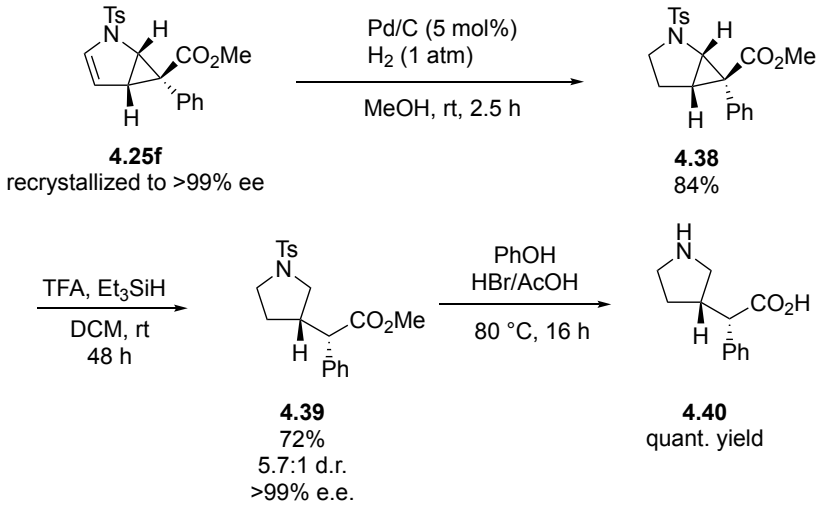

Scheme 4.6 Synthetic applications of a monocyclopropanated pyrrole

4.3 Conclusions

In this study, we have developed a highly enantioselective monocyclopropanation process for *N*-protected pyrroles using donor/acceptor carbenes and Rh_2(*R*-*p*-PhTPCP)$_4$ as the chiral catalyst. The products were generally obtained with good yields and exceptional enantioselectivity. We believe this study also represents an advancement in the field of dirhodium catalysis, as these monocyclopropanated species were considered highly reactive and non-isolable under previous conditions. The utility of the products was demonstrated via the synthesis of two biologically important compounds.

4.4 References

1. Sperry, J. B.; Wright, D. L. *Curr. Opin. Drug. Discov. Devel.* **2005,** *8*, 723.
2. Jampilek, J. *Molecules* **2019,** *24*, 3839.
3. Davies, H. M.; Hedley, S. J. *Chem. Soc. Rev.* **2007,** *36*, 1109.
4. Taylor, A. P.; Robinson, R. P.; Fobian, Y. M.; Blakemore, D. C.; Jones, L. H.; Fadeyi, O. *Org. Biomol. Chem.* **2016,** *14*, 6611.
5. Ahmad, S.; Alam, O.; Naim, M. J.; Shaquiquzzaman, M.; Alam, M. M.; Iqbal, M. *Eur. J. Med. Chem.* **2018,** *157*, 527.
6. Estevez, V.; Villacampa, M.; Menendez, J. C. *Chem. Soc. Rev.* **2014,** *43*, 4633.
7. Rassu, G.; Zanardi, F.; Battistini, L.; Casiraghi, G. *Chem. Soc. Rev.* **2000,** *29*, 109.
8. Lian, Y.; Davies, H. M. L. *Org. Lett.* **2012,** *14*, 1934.
9. Lian, Y.; Davies, H. M. L. *Org. Lett.***2010,** *12*, 924.
10. Harrar, K.; Reiser, O. *Chem. Commun.* **2012,** *48*, 3457.
11. Bohm, C.; Reiser, O. *Org. Lett.* **2001,** *3*, 1315.

12. Pilsl, L. K. A.; Ertl, T.; Reiser, O. *Org. Lett.* **2017,** *19*, 2754.

13. Schinnerl, M.; Böhm, C.; Seitz, M.; Reiser, O. *Tetrahedron: Asymmetry* **2003,** *14*, 765.

14. Beumer, R.; Bubert, C.; Cabrele, C.; Vielhauer, O.; Pietzsch, M.; Reiser, O. *J. Org. Chem.* **2000,** *65*, 8960.

15. Hedley, S. J.; Ventura, D. L.; Dominiak, P. M.; Nygren, C. L.; Davies, H. M. L. *J. Org. Chem.* **2006,** *71*, 5349.

16. Reddy, R. P.; Davies, H. M. L. *J. Am. Chem. Soc.* **2007,** *129*, 10312.

17. Davies, H. M. L.; Matasi, J. J.; Hodges, L. M.; Huby, N. J. S.; Thornley, C.; Kong, N.; Houser, J. H. *J. Org. Chem.***1997,** *62*, 1095.

18. Davies, H. M. L.; Young, W. B.; Smith, H. D. *Tetrahedron Lett.* **1989,** *30*, 4653.

19. Kende, A. S.; Smalley, T. L.; Huang, H. *J. Am. Chem. Soc.* **1999,** *121*, 7431.

20. Lehner, V.; Davies, H. M. L.; Reiser, O. *Org. Lett.* **2017,** *19*, 4722.

21. Guptill, D. M.; Davies, H. M. L. *J. Am. Chem. Soc.* **2014,** *136*, 17718.

22. Davies, H. M. L.; Liao, K. *Nat. Rev. Chem.* **2019,** *3*, 347.

23. Liao, K.; Negretti, S.; Musaev, D. G.; Bacsa, J.; Davies, H. M. *Nature* **2016,** *533*, 230.

24. Liao, K.; Pickel, T. C.; Boyarskikh, V.; Bacsa, J.; Musaev, D. G.; Davies, H. M. L. *Nature* **2017,** *551*, 609.

25. Liao, K.; Yang, Y. F.; Li, Y.; Sanders, J. N.; Houk, K. N.; Musaev, D. G.; Davies, H. M. L. *Nat. Chem.* **2018,** *10*, 1048.

26. Liu, W.; Ren, Z.; Bosse, A. T.; Liao, K.; Goldstein, E. L.; Bacsa, J.; Musaev, D. G.; Stoltz, B. M.; Davies, H. M. L. *J. Am. Chem. Soc.* **2018,** *140*, 12247.

27. Fu, J.; Ren, Z.; Bacsa, J.; Musaev, D. G.; Davies, H. M. L. *Nature* **2018,** *564*, 395.

28. D'Elia, V.; Zwicknagl, H.; Reiser, O. *J. Org. Chem.* **2008,** *73*, 3262.

29. De Pol, S.; Zorn, C.; Klein, C. D.; Zerbe, O.; Reiser, O. *Angew. Chem. Int. Ed.* **2004,** *43*, 511.

30. Schmid, M. B.; Fleischmann, M.; D'Elia, V.; Reiser, O.; Gronwald, W.; Gschwind, R. M. *Chembiochem* **2009,** *10*, 440.

31. Urman, S.; Gaus, K.; Yang, Y.; Strijowski, U.; Sewald, N.; De Pol, S.; Reiser, O. *Angew. Chem. Int. Ed.* **2007,** *46*, 3976.

32. Roy, S.; Reiser, O. *Angew. Chem. Int. Ed.* **2012,** *51*, 4722.

33. Gheorghe, A.; Schulte, M.; Reiser, O. *J. Org. Chem.* **2006,** *71*, 2173.

34. Watson, P. S.; Jiang, B.; Scott, B. *Org. Lett.* **2000,** *2*, 3679.

35. Yedoyan, J.; Wurzer, N.; Klimczak, U.; Ertl, T.; Reiser, O. *Angew. Chem. Int. Ed.* **2019,** *58*, 3594.

36. Zhou, Y.; Gregor, V. E.; Ayida, B. K.; Winters, G. C.; Sun, Z.; Murphy, D.; Haley, G.; Bailey, D.; Froelich, J. M.; Fish, S.; Webber, S. E.; Hermann, T.; Wall, D. *Bioorg. Med. Chem. Lett.* **2007,** *17*, 1206.

37. Li, G.; Sharpless, K. B. *Acta. Chem. Scand.* **1996,** *50*, 649.

Experimental Section

General Considerations

General starting materials were purchased from commercial sources (Sigma Aldrich, Thermo Fisher, TCI Chemicals, AK Scientific, Oakwood Chemical, Acros Organics, Combi-Blocks, and Santa Cruz Biotechnology) and used as received without purification. The G10 microwave reaction vials were purchased from Anton Paar. For any moisture sensitive and Rh-catalyzed cyclopropanation and C–H functionalization reactions, solvents were obtained from Glass Contour Solvent System, then refluxed over 4Å molecular sieves for an hour and stored under dry argon atmosphere; glassware were oven- and flame-dried prior to use. Otherwise, for regular applications, solvents were used directly from commercial sources. ^{1}H and ^{13}C NMR spectra were recorded on a Bruker 600, INOVA 600 or INOVA 500 or VNMR 400 MHz spectrometer. All NMR spectra were run in solutions of deuterated chloroform ($CDCl_3$) and processed by calibrating using residual $CHCl_3$ as the standard (7.26 ppm for ^{1}H, and 77.16 ppm for ^{13}C), and were reported in parts per million (ppm), unless otherwise specified. Abbreviations for signal multiplicity are as follow: s = singlet, d = doublet, t = triplet, q = quartet, m = multiplet, dd = doublet of doublet, etc. Coupling constants (*J* values) were calculated directly from the spectra. IR spectra were collected on a Nicolet iS10 FT-IR spectrometer. Mass spectra were taken on a Thermo Finnigan LTQ-HRMS spectrometer using APCI, ESI or NSI. Thin layer chromatographic (TLC) analysis was performed with aluminum-sheet silica gel plates, visualizing with UV light and/or staining with aqueous $KMnO_4$ stain. Melting points were measured in open capillary tubes with a Mel-Temp Electrothermal melting points apparatus and are uncorrected. Optical rotations were measured on Jasco P-2000 polarimeters. Enantiomeric excess (ee) data were

obtained on a Varian Prostar chiral HPLC instrument, eluting the purified products using a mixed solution of HPLC-grade 2-propanol and n-hexane.

Experimental Section for

Chapter 2: Asymmetric C–H Functionalization via *N*-Sulfonyl-1,2,3-Triazoles

General procedures for ligand synthesis

Procedure A. Direct synthesis of ligands from commercially available anhydrides

Into a 100 mL round bottom flask equipped with a star bar, the anhydride (1 equiv) and chiral amino acid were added, followed by 40 mL of toluene and triethylamine (1.1 equiv) under ambient atmosphere. The flask was fitted with a reflux condenser and heated to 120 °C. Upon reaching reflux, if the reaction remained heterogeneous and contained a lot of unreacted solids, approximately 5 mL of 1,1,1,3,3,3-hexafluoro-2-propanol was added via syringe from the top of the condenser. The solids immediately began to dissolve and the reaction mixture became completely homogenous after approximately 20 min. The reaction was allowed to stir for an additional 4 h. Then the reaction mixture was cooled down, diluted with 100 mL of EtOAc and thoroughly washed with dilute HCl solution (0.1 M, 50 mL x 3), followed by saturated NaCl solution (30 mL x 2). The combined organic layers were dried over anhydrous $MgSO_4$, filtered and concentrated under reduced pressure. Gradient flash chromatography (2% to 8% methanol in DCM) afforded to the pure ligands.

Procedure B. Synthesis of ligands derived from 9,10-dihydroanthracene-9,10-α,β-succinic acid anhydride

A 250 mL round bottom flask was charged with anthracene (10.0 g, 56.2 mmol) and 100 mL of DCM while placed in an ice/water bath. Aluminum chloride (7.47 g, 56.2 mmol) was added portion-wise. The resulting black suspension was briefly stirred for 10 min, and maleic anhydride (5.50 g, 56.2 mmol) was added. The mixture was stirred overnight at room temperature and poured onto ice water (200 mL). The organic layer was further washed with ice water (100 mL x 2), dried over anhydrous $MgSO_4$ and concentrated under reduced pressure. The dark red residue was purified by crystallization from EtOAc to afford a pale green solid as the pure product (12.5 g, 80% yield over two crops). This anhydride was then subjected to procedure A above with the appropriate chiral amino acids to synthesize the corresponding ligands.

N-Tetrachlorophthaloyl-(S)-tert-leucine

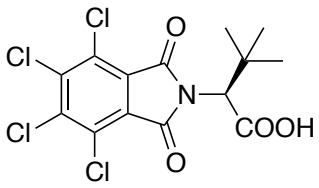

This compound was prepared according to the general procedure A for ligand synthesis using tetrachlorophthalic anhydride (1.00 g, 3.50 mmol) and L-tert-leucine (0.50 g, 3.85 mmol). The crude product was subjected to flash chromatography (2%, then 8% methanol in DCM) to afford the purified product as off-white solid (1.15 g, 82% yield).

^{1}H NMR and ^{13}C NMR spectral data are consistent with reported literature.[1]

^{1}H NMR (500 MHz, CDCl3) δ 4.70 (s, 1H), 1.17 (s, 9H);

^{13}C NMR (126 MHz, CDCl3) δ 173.3, 163.2, 140.5, 130.0, 127.1, 60.5, 35.7, 28.0.

N-Tetrafluorophthaloyl-(S)-tert-leucine

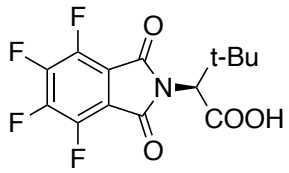

This compound was prepared according to the general procedure A for ligand synthesis using tetrafluorophthalic anhydride (1.50 g, 6.82 mmol) and L-tert-leucine (0.98 g, 7.50 mmol). The crude product was subjected to flash chromatography (2%, then 8% methanol in DCM) to afford the purified product as brown solid (1.70 g, 75% yield).

^{1}H NMR and ^{13}C NMR spectral data are consistent with reported literature.[2]

^{1}H NMR (500 MHz, $CDCl_3$) δ 4.68 (s, 1H), 1.17 (s, 9H).

^{13}C NMR (126 MHz, $CDCl_3$) δ 173.2, 162.1, 146.3, 144.2, 142.5, 60.5, 35.7, 28.0.

N-2,3-Naphthaloyl-(S)-tert-leucine

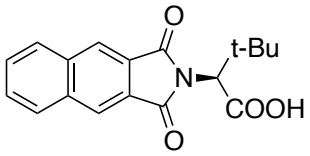

This compound was prepared according to the general procedure A for ligand synthesis using 2,3-naphthalic anhydride (1.20 g, 6.05 mmol) and L-tert-leucine(0.87 g, 6.66 mmol). The crude product was subjected to flash chromatography (2%, then 8% methanol in DCM) to afford the purified product as white solid (1.78 g, 95% yield).

^{1}H NMR and ^{13}C NMR spectral data are consistent with reported literature.[3]

^{1}H NMR (500 MHz, $CDCl_3$) δ 8.27 (s, 2H), 8.00 (dd, J = 6.2, 3.3 Hz, 2H), 7.66 (dt, J = 6.3, 3.4 Hz, 2H), 4.68 (s, 1H), 1.13 (s, 9H).

^{13}C NMR (126 MHz, $CDCl_3$) δ 173.0, 167.9, 135.5, 130.3, 129.2, 127.2, 125.1, 35.8, 28.0.

N-4-Br-1,8-naphthaloyl-(S)-tert-leucine

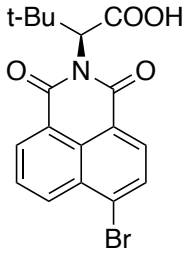

This compound was prepared according to the general procedure A for ligand synthesis using 4-bromo-1,8-naphthalic anhydride (1.50 g, 5.41 mmol) and L-tert-leucine (0.78 g, 5.95 mmol). The crude product was subjected to flash chromatography (2%, then 8% methanol in DCM) to afford the purified product as yellow/orange solid (1.79 g, 85% yield).

^{1}H NMR and ^{13}C NMR spectral data are consistent with reported literature.[4]

^{1}H NMR (500 MHz, $CDCl_3$) δ 8.63 (t, J = 8.2 Hz, 1H), 8.47 (dd, J = 8.5, 1.1 Hz, 1H), 8.39 (t, J = 8.1 Hz, 1H), 7.98 (d, J = 7.9 Hz, 1H), 7.84 – 7.77 (m, 1H), 5.56 (s, 1H), 1.17 (s, 9H).

^{13}C NMR (126 MHz, $CDCl_3$) δ 174.3, 163.7, 133.5, 132.8, 132.0, 131.9, 131.2, 130.6, 130.4, 128.8, 128.2, 122.6, 121.7, 59.9, 36.0, 28.4.

N-Tetraphenylphthaloyl-(S)-tert-leucine

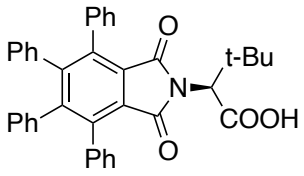

This compound was prepared according to the general procedure A for ligand synthesis using tetraphenylphthalic anhydride (2.00 g, 4.42 mmol) and L-tert-leucine (0.64 g, 4.86 mmol). The crude product was subjected to flash chromatography (2%, then 8% methanol in DCM) to afford the purified product as white solid (2.15 g, 86% yield).

Mp: > 255 °C

^{1}H NMR (500 MHz, $CDCl_3$) δ 7.23 – 7.06 (m, 10H), 6.92 – 6.87 (m, 6H), 6.76 – 6.71 (m, 4H), 4.66 (s, 1H), 1.13 (s, 9H).

^{13}C NMR (126 MHz, $CDCl_3$) δ 173.1, 166.9, 148.1, 139.6, 138.0, 135.5, 130.7, 130.7, 123.0, 127.8, 127.5, 127.3, 127.0, 126.3, 59.9, 59.8, 35.4, 28.2.

IR (neat): 3058, 2963, 1774, 1716, 1442, 1370, 1221, 1120, 1087, 781, 697 cm^{-1}

HRMS (+p NSI) calcd for $C_{38}H_{31}NO_4$ $(M+H)^+$ 565.2253 found 565. 2331

N-Tetraphenylphthaloyl-(S)-phenylalanine

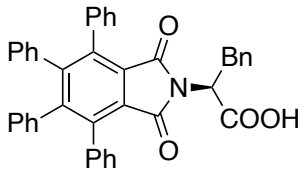

This compound was prepared according to the general procedure A for ligand synthesis using tetraphenylphthalic anhydride (2.00 g, 4.42 mmol), L-phenylalanine (0.80 g, 4.86 mmol). The crude product was subjected to flash chromatography (2%, then 8% methanol in DCM) to afford the purified product as white solid (2.09 g, 79% yield).

Mp: > 255 °C

^{1}H NMR (500 MHz, $CDCl_3$) δ 7.36 – 7.05 (coincidental with residual $CHCl_3$) (m, 15H), 6.94 (m, 6H), 6.81 – 6.75 (m, 4H), 5.18 (t, J = 8.2 Hz, 1H), 3.56 (d, J = 8.2 Hz, 2H).

^{13}C NMR (126 MHz, $CDCl_3$) δ 174.5, 166.4, 148.0, 139.6, 138.0, 136.9, 135.4, 130.7, 130.0, 129.0, 128.6, 127.7, 127.5, 127.3, 127.0, 126.7, 126.4, 52.9, 34.2.

IR (neat): 3085, 1771, 1714, 1603, 1496, 1386, 1372, 1265, 1118, 1073, 958, 696

HRMS (+p NSI) calcd for $C_{41}H_{29}NO_4$ $(M+H)^+$ 599.2097 found 599.2176

N-9,10-dihydroanthracene-9,10-α,β-succinic acid-(S)-tert-leucine

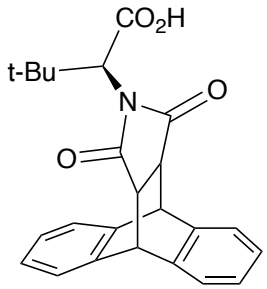

This compound was prepared according to the general procedure B for ligand synthesis using 9,10-dihydroanthracene-9,10-α,β-succinic acid anhydride (1.50 g, 5.43 mmol), L-tert-leucine (0.78 g, 5.97 mmol). The crude product was subjected to flash chromatography (2%, then 8% methanol in DCM) to afford the purified product as beige solid (1.37 g, 65% yield).

Mp: 130 – 135 °C

^{1}H NMR (600 MHz, $CDCl_3$) δ 7.37 (ddt, J = 5.8, 3.0, 1.3 Hz, 2H), 7.33 – 7.26 (m, 2H), 7.18 – 7.13 (m, 2H), 7.13 – 7.06 (m, 2H), 4.80 (dd, J = 5.2, 3.3 Hz, 2H), 4.19 (d, J = 2.9 Hz, 1H), 3.34 – 3.18 (m, 2H), 0.66 (s, 9H).

^{13}C NMR (126 MHz, $CDCl_3$) δ 176.9, 176.8, 171.8, 141.9, 139.1, 127.3, 126.7, 125.2, 124.2 60.4, 46.7, 45.2, 34.7, 27.4, 21.1, 14.2.

IR (neat): 2962, 1775, 1708, 1481, 1379, 1262, 1178, 974, 877, 760

HRMS (+p NSI) calcd for $C_{24}H_{23}NO_4$ 389.1627 found 389.1703

N-9,10-dihydroanthracene-9,10-α,β-succinic acid-(S)-phenylalanine

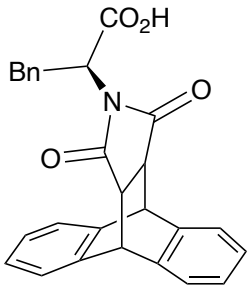

This compound was prepared according to the general procedure B for ligand synthesis using 9,10-dihydroanthracene-9,10-α,β-succinic acid anhydride (1.50 g, 5.43 mmol), L-phenylalanine (0.99 g, 5.97 mmol). The crude product was subjected to flash chromatography (2%, then 8% methanol in DCM) to afford the purified product as off-white solid (1.65 g, 72% yield).

Mp: 112 – 115 °C

^{1}H NMR (500 MHz, $CDCl_3$) δ 7.45 – 7.00 (coincidental with residual CH_3Cl) (m, 13H), 4.83 (d, J = 3.4 Hz, 1H), 4.76 (d, J = 3.4 Hz, 1H), 4.65 (dd, J = 8.3, 7.0 Hz, 1H), 3.27 (dd, J = 14.4, 7.0 Hz, 1H), 3.20 (dd, J = 8.6, 3.4 Hz, 1H), 3.08 (dd, J = 8.6, 3.4 Hz, 1H), 2.52 (dd, J = 14.4, 8.3 Hz, 1H).

^{13}C NMR (126 MHz, $CDCl_3$) δ 186.3, 175.6, 141.9, 141.8, 140.1, 138.1, 128.9, 128.3, 127.4, 126.9, 126.7, 126.3, 125.4, 124.3, 124.2, 60.5, 54.4, 46.5, 46.3, 45.5, 45.5, 45.4, 33.6, 21.1, 14.3.

IR (neat): 3059, 1770, 1715, 1386, 1373, 1264, 764, 733, 695

HRMS (+p NSI) calcd for $C_{27}H_{21}NO_4$ 423.1471 found 423.1463

General procedure for ligand exchange reactions

A 100 mL round bottom flask equipped with a stir bar was charged with the appropriate ligand (8 equiv), $Rh_2(OAc)_4$ and 50 mL of chlorobenzene under ambient atmosphere. The flask was then fitted with a Soxhlet extractor with a thimble filled with Na_2CO_3 and a thin layer of sand. On top of the Soxhlet extractor was fitted with a water condenser in the reverse direction. The reaction was briefly stirred at room temperature for 10 min and then heated to reflux at 170 °C (hot plate setting) for 24 h. A higher temperature (approximately 20-30 °C higher than the normal boiling point) was required for the solvent to effectively reflux into the Soxhlet extractor. Then the extractor and reflux condenser were removed and most of chlorobenzene was removed by short-path distillation into another round bottom flask. While still warm, the residual solvent was removed under vacuum. The green crude product was directly subjected to flash chromatography using dry loading onto silica gel.

Dirhodium(II) tetrakis[N-Tetrachlorophthaloyl-(S)-tert-leucine]

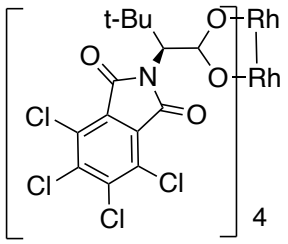

This compound was prepared by general ligand exchange procedure from *N*-Tetrachlorophthaloyl-(S)-tert-leucine (0.40 g, 1.0 mmol) and $Rh_2(OAc)_4$ (0.055g, 0.125 mmol). The crude product was subjected to flash chromatography (1-8% ether in hexanes) to afford the purified product as green solid (0.14 g, 63% yield).

^{1}H NMR spectral data are consistent with reported literature.[1]

^{1}H NMR (400 MHz, $CDCl_3$) δ 4.87 (d, J = 0.6 Hz, 1H), 1.11 (s, 9H).

^{13}C NMR (126 MHz, $CDCl_3$) δ 186.4, 163.4, 162.5, 140.3, 139.8, 130.9, 130.0, 129.4, 127.2, 68.2, 61.7, 61.6, 60.5, 38.7, 36.3, 30.4, 29.7, 27.8, 23.7, 23.0, 21.1, 14.2, 14.2, 14.1, 11.0.

HRMS (+p NSI) calcd for $C_{56}H_{40}Cl_{16}N_4O_{16}Rh_2$ 1789.5588 found 1789.5653

Dirhodium(II) tetrakis[N-Tetrafluorophthaloyl-(S)-tert-leucine]

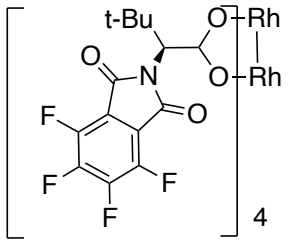

This compound was prepared by general ligand exchange procedure from *N*-tetrafluorophthaloyl-(S)-tert-leucine (1.00 g, 3 mmol) and $Rh_2(OAc)_4$ (0.17 g, 0.38 mmol). The crude product was subjected to flash chromatography (1-8% ether in hexanes) to afford the purified product as green solid (0.52 g, 89% yield).

^{1}H NMR and ^{13}C NMR spectral data are consistent with reported literature.[2]

^{1}H NMR (600 MHz, $CDCl_3$) δ 4.66 (s, 1H), 1.06 (s, 9H).

^{13}C NMR (126 MHz, $CDCl_3$) δ 186.3, 161.9, 146.2, 144.6, 141.9 113.4, 61.7, 35.8, 27.7.

HRMS (+p NSI) calcd for $C_{56}H_{40}F_{16}N_4O_{16}Rh_2$ 1534.0316 found 1534.0415

Dirhodium(II) tetrakis[N-2,3-Naphthaloyl-(S)-tert-leucine]

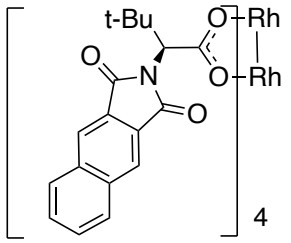

This compound was prepared by general ligand exchange procedure from N-2,3-naphthaloyl-(S)-tert-leucine (1.50 g, 4.82 mmol) and $Rh_2(OAc)_4$ (0.27 g, 0.60 mmol). The crude product was subjected to flash chromatography (1-8% ether in hexanes) to afford the purified product as green solid (0.82 g, 93% yield).

^1H NMR and ^{13}C NMR spectral data are consistent with reported literature.[3]

^{1}H NMR (400 MHz, $CDCl_3$) δ 8.25 (s, 2H), 7.98 (s, 2H), 7.61 (dd, J = 6.5, 3.2 Hz, 2H), 5.03 (d, J = 0.9 Hz, 1H), 1.18 (s, 9H).

^{13}C NMR (101 MHz, $CDCl_3$) δ 187.2, 135.4, 130.1, 127.7, 77.2, 61.6, 35.8, 28.1, 14.1.

HRMS (+p NSI) calcd for $C_{72}H_{64}N_4O_{16}Rh_2$ $(M+H)^+$ 1446.2449 found 1446.2442

Dirhodium(II) tetrakis[N-4-Br-1,8-naphthaloyl-(S)-tert-leucine]

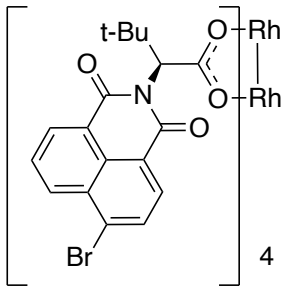

This compound was prepared by general ligand exchange procedure from N-4-Br-1,8-naphthaloyl-(S)-tert-leucine (1.20 g, 3.08 mmol) and $Rh_2(OAc)_4$ (0.17 g, 0.38 mmol). The crude product was subjected to flash chromatography (1-8% ether in hexanes) to afford the purified product as green solid (0.54 g, 81% yield).

^{1}H NMR and ^{13}C NMR spectral data are consistent with reported literature.[4]

^{1}H NMR (400 MHz, $CDCl_3$) δ 8.54 (m, 1H), 8.41 – 8.27 (m, 1H), 8.10 (m, 1H), 7.97 – 7.78 (m, 1H), 7.66 (m, 1H), 5.83 – 5.72 (m, 1H), 1.27 (s, 9H).

^{13}C NMR (101 MHz, $CDCl_3$) δ 174.3,163.6, 133.5, 132.8, 131.9, 131.2, 130.6, 130.4, 128.8, 128.2, 122.7,121.8, 59.9, 36.0, 28.4.

HRMS (+p NSI) calcd for $C_{72}H_{60}Br_4N_4O_{16}Rh_2$ $(M+H)^+$ 1757.8870 found 1757.8860.

Dirhodium(II) tetrakis[N-tetraphenylphthaloyl-(S)-tert-leucine]

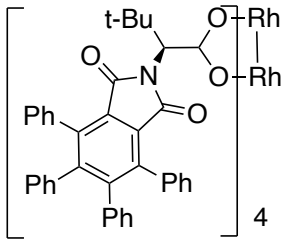

This compound was prepared by general ligand exchange procedure from N-tetraphenylphthaloyl-(S)-tert-leucine (1.70 g, 3 mmol) and $Rh_2(OAc)_4$ (0.166 g, 0.38 mmol). The crude product was subjected to flash chromatography (1-8% ether in hexanes) to afford the purified product as green solid (0.79 g, 84% yield).

^{1}H NMR (500 MHz, $CDCl_3$) δ 7.23 – 7.56 (m, 20H), 4.15 (s, 1H), 0.78 (s, 9H).

^{13}C NMR (126 MHz, $CDCl_3$) δ 187.2, 166.4, 165.6, 147.7, 146.8, 139.3, 138.7, 138.6, 138.5, 136.10, 135.7, 131.2, 131.1, 131.0, 130.8, 130.6, 130.5, 130.1, 129.6, 128.5, 127.9, 127.9, 127.1, 126.9, 126.9, 126.9, 126.8, 126.7, 126.6, 126.6, 126.5, 126.4, 126.1, 126.0, 60.0, 35.6, 28.1.

IR (neat): 3058, 2956, 2360, 1773, 1718, 1607, 1400, 1369, 696

HRMS (+p NSI) calcd for $C_{152}H_{120}N_4O_{16}Rh_2$ $(M+H)^+$ 2462.6831 found 2462.6809

Dirhodium(II) tetrakis[N-tetraphenylphthaloyl-(S)-phenylalanine]

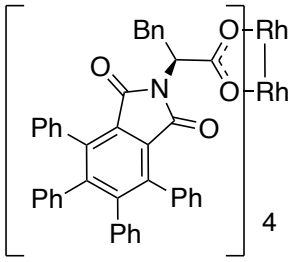

This compound was prepared by general ligand exchange procedure from N-tetraphenylphthaloyl-(S)-phenylalanine (1.50 g, 2.5 mmol) and $Rh_2(OAc)_4$ (0.14 g, 0.31 mmol). The crude product was subjected to flash chromatography (1-8% ether in hexanes) to afford the purified product as green solid (0.52 g, 95% yield).

^{1}H NMR (500 MHz, $CDCl_3$) δ 7.13 – 6.54 (m, 25H), 4.92 (dd, J = 10.1, 6.7 Hz, 1H), 3.26 – 3.15 (m, 2H).

^{13}C NMR (126 MHz, $CDCl_3$) δ 188.3, 165.7, 147.2, 139.0, 138.3, 137.9, 135.5, 130.9, 130.4, 129.7, 129.5, 128.4, 128.0, 127.2, 127.0, 126.9, 126.8, 126.1, 126.0, 54.1, 54.1, 34.6, 31.2.

IR (neat): 3059, 3027, 1773, 1717, 1608, 1410, 1371, 1375, 696.

HRMS (+p NSI) calcd for $C_{164}H_{112}N_4O_{16}Rh_2$ $(M+H)^+$ 2598.6205 found 2598.6231.

Dirhodium(II) tetrakis[N-9,10-dihydroanthracene-9,10-α,β-succinic acid-(S)-tert-leucine]

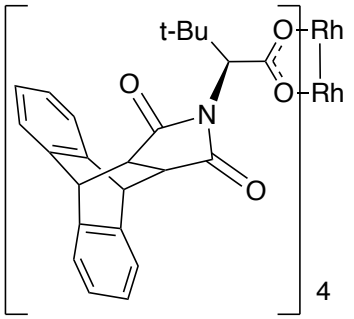

This compound was prepared by general ligand exchange procedure from N-9,10-dihydroanthracene-9,10-α,β-succinic acid-(*S*)-tert-leucine (1.00 g, 2.57 mmol) and $Rh_2(OAc)_4$ (0.14 g, 0.32 mmol). The crude product was subjected to flash chromatography (5-10% EtOAc in hexanes) to afford the purified product as green solid (0.38 g, 68% yield).

^{1}H NMR not determined due to substantial peak broadening in various solvents.

^{13}C NMR (126 MHz, $CDCl_3$) δ 186.6, 176.8, 176.0, 142.3, 142.1, 139.2, 127.1, 126.6, 125.2, 124.3, 124.1, 62.7, 60.7, 47.4, 46.3, 45.4, 34.2, 27.4.

IR (neat): 2959, 1776, 1705, 1605, 1465, 1376, 1177, 768, 734

HRMS (+p ESI) calcd for $C_{96}H_{88}N_4O_{16}Rh_2$ $(M+H)^+$ 1758.4327 found 1758.8784

Dirhodium(II) tetrakis[N-9,10-dihydroanthracene-9,10-α,β-succinic acid-(S)-phenylalanine]

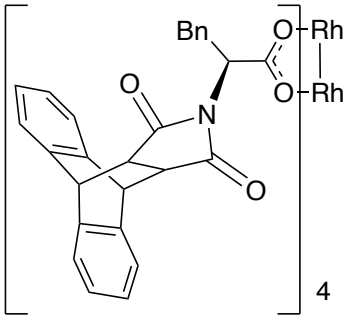

This compound was prepared by general ligand exchange procedure from N-9,10-dihydroanthracene-9,10-α,β-succinic acid-(S)-phenylalanine (1.20 g, 2.83 mmol) and $Rh_2(OAc)_4$ (0.16 g, 0.35 mmol). The crude product was subjected to flash chromatography (5-10% EtOAc in hexanes) to afford the purified product as green solid (0.43 g, 65% yield).

^{1}H NMR not determined due to substantial peak broadening in various solvents.

^{13}C NMR (126 MHz, $CDCl_3$) δ 186.3, 175.6, 141.9, 141.8, 140.1, 138.1, 128.9, 128.3, 127.4, 126.9, 126.7, 126.3, 125.4, 124.3, 124.2, 60.5, 54.4, 46.5, 46.3, 45.5, 45.5, 45.4, 33.6, 21.1, 14.3.

IR (neat): 3025, 1775, 1704, 1612, 1382, 1162, 756

HRMS (+p ESI) calcd for $C_{108}H_{80}N_4O_{16}Rh_2$ $(M+H)^+$ 1894.3701 found 1894. 3763

Generation procedure for cyclopropanation reaction

Into a 4 mL vial equipped with a stir bar, 4-phenyl-1-(*N*-sulfonyl)-1,2,3-triazole (0.112g, 0.5 mmol) and Rh(II) catalyst (0.5 mol %) were added under ambient atmosphere. Then 1.25 mL of distilled 1,2-DCE and styrene (0.06 g, 1.0 mmol) were added via syringe. The reaction mixture was capped and heated at 65 °C for 5 h. After cooling to room temperature, K_2CO_3 (0.138g, 1mmol) was added, followed by 1.25 mL of MeOH and a few drops of water. The mixture was then stirred vigorously for 1 h. Solvent was evaporated under reduced pressure and the residue was re-dissolved in DCM, dried with anhydrous $MgSO_4$, filtered and concentrated. The crude product was subjected to ^1H NMR to check diastereoselectivity and then flash chromatography using 5% EtOAc in hexanes as the eluent.

(1S,2R)-(+)-1,2-Diphenylcyclopropanecarbaldehyde

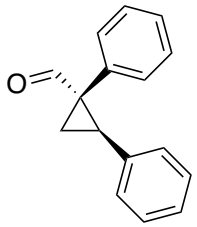

This compound was prepared by general cyclopropanation procedure using 4-phenyl-1-(N-sulfonyl)-1,2,3-triazole (0.112g, 0.5 mmol) and styrene (0.104g, 1.0 mmol) under Rh(II) catalysis. The crude product was subjected to flash chromatography (5-10% EtOAc in hexanes) to afford the purified product as a clear oil that solidified over long time.

^{1}H NMR and ^{13}C NMR spectra were consistent with literature data.[5]

^{1}H NMR (600 MHz, $CDCl_3$) δ 9.60 (s, 1H), 7.24 – 7.18 (m, 3H), 7.07 (td, J = 4.9, 2.0 Hz, 5H), 6.83 – 6.78 (m, 2H), 3.01 (dd, J = 9.2, 7.3 Hz, 1H), 2.20 (dd, J = 9.2, 5.1 Hz, 1H), 2.09 (dd, J = 7.4, 5.1 Hz, 1H).

^{13}C NMR (125 MHz, $CDCl_3$) δ 201.2, 135.9, 134.3, 131.8, 128.8, 128.4, 128.3, 128.0, 127.1, 46.9, 36.0, 20.2.

General procedure for C–H insertion reactions

The procedures for insertion into allylic and benzylic substrates are identical.

Into a 10 mL microwave vial equipped with a stir bar were added 4-phenyl-1-(*N*-sulfonyl)-1,2,3-triazole (0.116 g, 0.5 mmol) and Rh(II) (1 mol %) catalysts. The vial was then degassed and purged with argon. Then 4 mL of 1,2-DCE and appropriate substrate (1.5 mmol) were added via syringe. The cap of the vial was then thoroughly sealed with parafilm and then heated to 30 °C for 12 h. The reaction mixture was transferred to an ice bath and treated with lithium aluminum hydride solution (1.2 mL, 1 M in THF) and stirred for 40 min. Then the mixture was quenched with $Na_2SO_4 \cdot 10H_2O$ until bubbling stopped, filtered on Celite, eluted with DCM (50 mL) and concentrated under vacuum. The crude product was taken for ^1H NMR analysis for to check regioselectivity and then subjected to flash chromatography using a 30% EtOAc in hexanes as the eluent.

(S)-N-(3-methyl-2-phenyl-3-(p-tolyl)butyl)methanesulfonamide

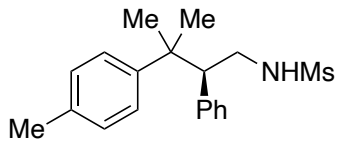

This compound was prepared by general C–H insertion reaction procedure using 4-phenyl-1-(N-sulfonyl)-1,2,3-triazole (0.116 g, 0.5 mmol) and *p*-cymene (0.201 g, 1.5 mmol) under Rh(II) catalysis. The crude product was subjected to flash chromatography (10-30% EtOAc in hexanes) to afford the purified product as clear oil.

^{1}H NMR and ^{13}C NMR spectra were consistent with literature data.[6]

^{1}H NMR (400 MHz, $CDCl_3$) δ 7.34 – 7.26 (m, 3H), 7.22 – 7.18 (m, 2H), 7.13 (d, J = 7.9 Hz, 2H), 7.11 – 7.04 (m, 2H), 3.67 (d, J = 8.0 Hz, 1H), 3.40 – 3.32 (m, 1H), 3.28 (ddt, J = 12.6, 8.4, 4.3 Hz, 1H), 3.05 (dd, J = 11.4, 4.2 Hz, 1H), 2.65 (s, 3H), 2.34 (s, 3H), 1.29 (s, 3H), 1.21 (s, 3H).

^{13}C NMR (125 MHz, $CDCl_3$): δ 144.3, 138.3, 135.9, 130.1, 129.1, 128.4, 127.6, 126.3, 57.5, 43.9, 40.4, 40.2, 29.3, 23.8, 21.0

Chiral HPLC: Chiralcel OD-H column, 3% isopropanol/hexanes, 1 mL/min, UV: 210 nm, t_R: 25.9 min (minor), t_R: 30.9 min (major).

(S)-N-(3-(4-isopropylphenyl)-2-phenylpropyl)methanesulfonamide

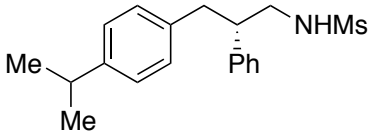

This compound was prepared by general C–H insertion reaction procedure using 4-phenyl-1-(N-sulfonyl)-1,2,3-triazole (0.116 g, 0.5 mmol) and *p*-cymene (0.201 g, 1.5 mmol) under Rh(II) catalysis. The crude product was subjected to flash chromatography (10-30% EtOAc in hexanes) to afford the purified product as clear oil.

^{1}H NMR and ^{13}C NMR spectra were consistent with literature data.[6]

^{1}H NMR (600 MHz, $CDCl_3$) δ 7.32 (t, J = 7.5 Hz, 2H), 7.27 – 7.23 (m, 2H), 7.20 – 7.17 (m, 2H), 7.09 (d, J = 8.1 Hz, 2H), 7.00 (d, J = 8.0 Hz, 2H), 3.93 (d, J = 7.0 Hz, 1H), 3.41 (ddd, J = 12.7, 7.8, 4.9 Hz, 1H), 3.28 (ddd, J = 12.8, 9.2, 4.9 Hz, 1H), 3.12 – 3.05 (m, 1H), 2.96 – 2.80 (m, 3H), 2.70 (s, 3H), 1.20 (dd, J = 7.0, 1.2 Hz, 6H).

^{13}C NMR (125 MHz, $CDCl_3$): δ 147.1, 141.4, 136.3, 129.1, 129.0, 128.0, 127.5, 126.7, 48.0, 47.8, 40.3, 39.9, 33.8, 24.1

Chiral HPLC: Chiralcel OD-H column, 5% isopropanol/hexanes, 1 mL/min, UV: 210 nm, t_R: 26.3 min (minor), t_R: 46.4 min (major)

(S,E)-N-(3,3-dimethyl-2-phenylhex-4-en-1-yl)methanesulfonamide

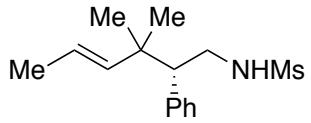

This compound was prepared by general C–H insertion reaction procedure using 4-phenyl-1-(N-sulfonyl)-1,2,3-triazole (0.116 g, 0.5 mmol) and trans-4-methyl-2-pentene (0.126 g, 1.5 mmol) under Rh(II) catalysis. The crude product was subjected to flash chromatography (10-30% EtOAc in hexanes) to afford the purified product as clear oil.

^{1}H NMR and ^{13}C NMR spectra were consistent with literature data.[6]

^{1}H NMR (600 MHz, $CDCl_3$) δ 7.39 – 7.28 (m, 3H), 7.28 – 7.22 (m, 2H), 7.17 – 7.11 (m, 2H), 5.43 (m, 1H), 5.35 (m, 1H), 3.79 (d, J = 7.8 Hz, 1H), 3.58 (ddd, J = 12.7, 8.7, 3.9 Hz, 1H), 3.35 (td, J = 12.2, 3.4 Hz, 1H), 2.76 (s, 3H), 2.64 (dd, J = 11.8, 4.0 Hz, 1H), 1.70 – 1.67 (m, 3H), 0.96 (s, 3H), 0.88 (s, 3H).

^{13}C NMR (125 MHz, $CDCl_3$): δ 138.7, 138.4, 129.8, 128.6, 128.5, 127.4, 123.3, 56.5, 44.2, 40.3, 38.7, 27.9, 24.3, 18.3

Chiral HPLC: Chiralcel OD column, 2% isopropanol/hexanes, 1.0 mL/min, UV: 230 nm, t_R: 51.0 min (major), 31.0 min (minor)

References

1. Hanari, T.; Shimada, N.; Kurosaki, Y.; Thrimurtulu, N.; Nambu, H.; Anada, M.; Hashimoto, S. *Chem. Eur. J.* **2015**, 21, 11671.

2. Tsutsui, H.; Yamagushi, Y.; Kitagaki, S.; Nakamura, S.; Anada, M.; Hashimoto, S. *Tetrahedron: Asymmetry*, **2003**, 14, 817.

3. Kitagaki, S.; Anada, M.; Kataoka, O.; Matsuno, K.; Umeda, C.; Watanabe, N.; Hashimoto, S. *J. Am. Chem. Soc.* **1999**, 121, 1417.

4. Müller, P.; Ghanen, A. *Org. Lett.* **2004**, 6, 4347.

5. Chuprakov, S.; Kwok, S.W.; Zhang, L.; Lercher L.; Fokin V.V. *J. Am. Chem. Soc.* **2009**, 131, 18034.

6. Kubiak, R. W.; Davies, H. M. L. *Org. Lett.* **2018,** 20, 3771.

Experimental Section for

Chapter 3: Desymmetrization of Cyclohexanes by Site- and Stereoselective C–H Functionalization Using Donor/acceptor Carbenes

Synthesis of Rh_2(S-TPPTTL)$_4$

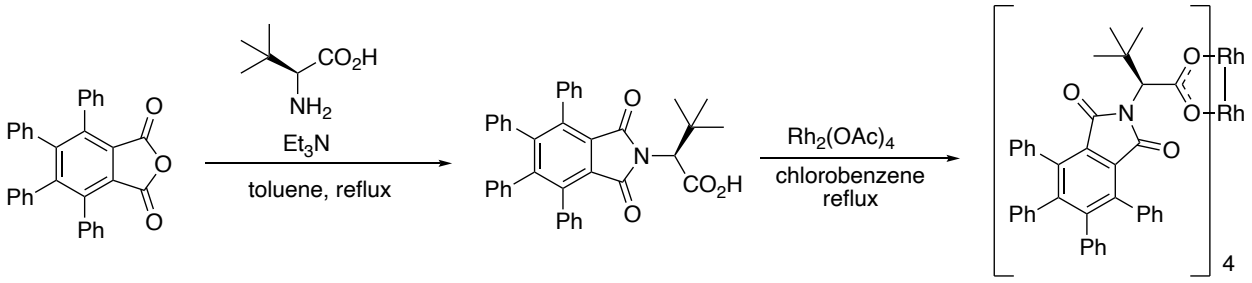

Ligand Synthesis. Into a 100 mL round bottom flask equipped with a stir bar was charged tetraphenylphthalic anhydride (1.50 g, 3.32 mmol, 1 equiv), L-tert-leucine (0.48 g, 3.65 mmol, 1.1 equiv). Then 30mL of toluene was added to the flask, and trimethylamine (0.37 g, 3.65 mmol, 1.1 equiv) was added via syringe. The flask was connected to a Findenser and the reaction mixture was brought to reflux temperature using a heating block (120 °C). The reaction turned homogenous approximately 30 min after reaching reflux temperature and was further allowed to react for 4 h. After cooling down to room temperature, the crude mixture was poured into a 250 mL separatory funnel, diluted with EtOAc, then washed with 0.5 M HCl until aqueous layer became clear and then brine. The organic layers were collected, dried with $MgSO_4$, filtered and concentrated to give a white solid. The crude material was subjected to flash chromatography using a solution of MeOH in DCM (1%, 5% and then 8%) as eluent. After evaporation of solvent under reduced pressure the purified product was obtained as a white solid (1.79 g, 95% yield). The characterization data were reported in previous sections.

Ligand exchange. Into a 100 mL round bottom flask equipped with a stir bar was charged the ligand (1.7 g, 3 mmol, 8 equiv) and $Rh_2(OAc)_4$ (0.16 g, 0.4 mmol, 1 equiv). Then 60 mL of anhydrous chlorobenzene was added, and the flask was fitted with a Soxhlet extractor with a thimble filled with K_2CO_3. A water condenser was connected onto the top of the Soxhlet extractor, and the reaction mixture was refluxed on a heating block at 170 °C (high temperature setting was necessary for efficient Soxhlet extraction) for 24 hrs. After the reaction was completed as indicated by TLC, chlorobenzene was removed by distillation and then vacuum while still hot, and the green crude residue was directly subjected to flash chromatography (dry loading for better separation) using a gradient of 50% - 80% DCM in hexanes as the eluent (only green fractions were collected). The product was obtained as a green solid after removal of solvent under reduced pressure (0.72 g, 77% yield). To further dry the catalyst the vial was placed under high vacuum overnight at 50 °C. The characterization data were reported in previous sections.

^{1}H NMR signals for determination of the selectivities and product stereochemistry

Asymmetric C–H functionalization reactions in this paper generate a mixture of isomers that are inseparable by standard laboratory chromatographic techniques. To determine site- and diastereoselectivity, a crude ^{1}H NMR spectrum was obtained for every reaction and are attached below in this section. Spectra were uniformly processed using MestReNova software (Version 12), applying standard auto-phase and baseline correction. Note that a frequency of 600MHz is recommended for crude ^{1}H NMR spectra for best separation of peaks and analysis. Unless otherwise specified, product ratios were determined from integration of the highlighted (red) benzylic proton as shown below. In a few cases the signals for benzylic protons of the major and minor products overlap and cannot be directly integrated in a reliable manner. Under this situation, diastereoselectivity was calculated by subtracting the integration of C-3 major product from the integration of the mixture that contain both diastereomers. See later this section for the structure and process of determining the minor diastereomer. Also note that the products indicated below are three pairs of enantiomers, therefore three sets of doublets that correspond to the benzylic proton are expected to be observed. Carbene insertion at the C-4 position does not produce diastereomers – only enantiomers. See spectra in this section for all product assignments (by analogy of the model substrate). Zoomed in regions for the highlighted benzylic protons are provided for each spectrum.

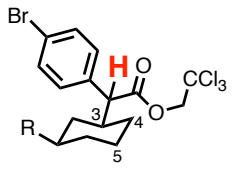

C-3 insertion

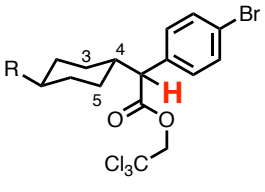

C-4 insertion

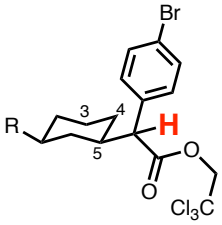

C-5 insertion

General procedure for C–H functionalization of cycloalkanes:

An oven-dried G10 microwave vial (Anton Paar) equipped with a stir bar was cooled under ambient atmosphere to slightly warmer than room temperature, then capped and further cooled under vacuum. Alternatively, regular reaction vials (16mL) with sealing capability may be used. While the vial was being cooled down, aryldiazoacetates (1 equiv) and Rh(II) catalyst (0.5 mol %) were weighed and added to two separate 20 mL scintillation vials. To the vial with Rh(II) catalyst the appropriate substrate (2.5 equiv) was added via syringe and then dissolved together in 2.5 mL of degassed dichloromethane (DCM). The aryldiazoacetate was dissolved in 2.5 mL of DCM. After both solutions are prepared, the reaction vial was purged with dry argon (vacuum/argon x5 times) and fitted with an argon balloon. Next, the solution containing the catalyst and substrate was transferred to the reaction vial via syringe, and then placed on a heating block that was pre-heated to 40^{o}C and stirred vigorously (approx. 1000 RPM). While this solution was being stirred at 40^{o}C, the aryldiazoacetate solution was added dropwise over 90 min via syringe using a syringe pump. After completing the addition any leftover aryldiazoacetate remaining in the syringe needles was manually injected into the reaction mixture slowly and the reaction was allowed to stir at 40^{o}C for another 30 min. The solution was then transferred to a 100 mL round bottom flask and solvent was evaporated under reduced pressure, and a crude ^{1}H NMR spectrum was taken to analyze selectivity (see previous section). Then the crude residue was directly subjected to flash chromatography using a mixture of diethyl ether in hexanes solution to obtain the pure product. The product was allowed to dry under vacuum overnight at 40^{o}C. Isomers were inseparable by standard laboratory techniques, and characterization data are reported only for the major diastereomer of the major regioisomer.

In a few cases the products needed to be converted to their corresponding alcohols for better chiral HPLC separation for ee analysis. Under this situation, after addition of aryldiazoacetate and cooling down to RT, the reaction mixture was directly treated with lithium aluminum hydride solution (1.2 equiv, 1 M solution in THF) and stirred at RT for 40 min. Then the reaction was quenched by slow addition of $Na_2SO_4 \cdot 10H_2O$ and then stirred until bubbling stopped (about 30 min), filtered over Celite and eluted with DCM. A crude ^1H NMR spectrum was taken to ensure product formation and the residue was directly purified by flash chromatography (eluent: 5%, then 25% EtOAc in hexanes).

2,2,2-trichloroethyl (R)-2-(4-bromophenyl)-2-cyclopentylacetate

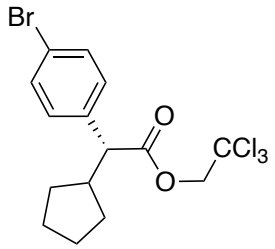

This compound was prepared according to the general procedure for C–H functionalization reaction, using cyclopentane (0.75 mmol, 53 mg, 2.5 equiv) as the substrate and 2,2,2-trichloroethyl 2-(4-bromophenyl)-2-diazoacetate (0.3 mmol, 112 mg, 1.0 equiv) under the catalysis of Rh_2(S-TPPTTL)$_4$ (0.0015 mmol, 3.7 mg, 0.5 mol %). After flash chromatography (0%, then 2% - 3% Et_2O in hexanes) the product was obtained as a clear oil that solidified slowly upon standing (93 mg, 73% yield). The product needed to be converted to the corresponding alcohol for ee determination via chiral HPLC (see general information of this section).

MP: 45^{o}C

$[\alpha]^{20}_D$ -15.1^o (c = 1.00, $CHCl_3$, 97% ee)

^{1}H NMR (600 MHz, $CDCl_3$) δ 7.47 – 7.43 (m, 2H), 7.29 – 7.24 (m, 2H, coincidental with residual $CHCl_3$), 4.76 (d, J = 12.0 Hz, 1H), 4.64 (d, J = 12.0 Hz, 1H), 3.39 (d, J = 11.2 Hz, 1H), 2.59 (m, 1H), 2.00 – 1.91 (m, 1H), 1.73 – 1.56 (m, 3H), 1.54 – 1.43 (m, 2H), 1.31 (m, 1H), 1.06 – 0.96 (m, 1H)

^{13}C NMR (150 MHz, $CDCl_3$) δ 171.8, 137.0, 131.7, 130.1, 121.5, 94.8, 74.1, 57.2, 43.1, 31.5, 30.7, 25.2, 24.9

IR (neat): 2953, 2868, 1749, 1488, 1210, 1160, 1073, 1011, 825, 760, 719 cm^{-1}

HR-MS (+p APCI): calcd for [$C_{15}H_{16}BrCl_3O_2$+H] 412.9478, found 412.9477

Chiral HPLC for the alcohol (Chiralcel ADH, 2% isopropanol in hexane, 1 mL/min, λ 230 nm) retention times of 19.06 min (major) and 24.64 min (minor), 97% ee

2,2,2-trichloroethyl (R)-2-(4-bromophenyl)-2-cyclohexylacetate

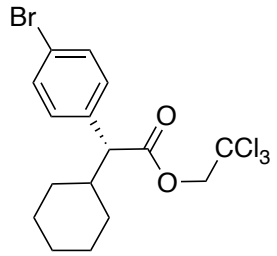

This compound was prepared according to the general procedure for C–H functionalization reaction, using cyclohexane (0.75 mmol, 63 mg, 2.5 equiv) as the substrate and 2,2,2-trichloroethyl 2-(4-bromophenyl)-2-diazoacetate (0.3 mmol, 112 mg, 1.0 equiv) under the catalysis of Rh_2(S-TPPTTL)$_4$ (0.0015 mmol, 3.7 mg, 0.5 mol %). After flash chromatography (0%, then 2% - 3% Et_2O in hexanes) the product was obtained as a clear oil (102 mg, 79% yield).

$[\alpha]^{20}_D$ -4.4° (c = 1.00, $CHCl_3$, 99% ee)

^{1}H NMR (600 MHz, $CDCl_3$) δ 7.47 – 7.42 (m, 2H), 7.26 – 7.22 (m, 2H), 4.76 (d, J = 12.0 Hz, 1H), 4.63 (d, J = 12.0 Hz, 1H), 3.35 (d, J = 10.6 Hz, 1H), 2.05 (qt, J = 11.1, 3.4 Hz, 1H), 1.86 (m, 1H), 1.75 (m, 1H), 1.70 – 1.58 (m, 2H), 1.43 – 1.25 (m, 2H), 1.22 – 1.04 (m, 3H), 0.82 – 0.72 (m, 1H)

^{13}C NMR (150 MHz, $CDCl_3$) δ 171.8, 136.1, 131.8, 130.6, 121.7, 94.9, 74.3, 58.2, 41.0, 32.0, 30.4, 26.3, 26.0, 25.9

IR (neat): 2926, 1748, 1448, 1142, 1122,1072, 1011, 827, 759, 720 cm^{-1}

HR-MS (+p NSI) calcd. for [$C_{16}H_{18}BrCl_3O_2$+H] 426.9634, found 426.9633

Chiral HPLC (Chiralcel S,S-Whelk, 0.5% isopropanol in hexane, 0.5 mL/min, λ 210-230 nm) retention times of 21.74 min (major) and 23.38 min (minor), 99% ee

2,2,2-trichloroethyl (R)-2-(4-bromophenyl)-2-cycloheptylacetate

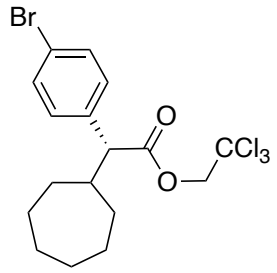

This compound was prepared according to the general procedure for C–H functionalization reaction, using cycloheptane (0.75 mmol, 74 mg, 2.5 equiv) as the substrate and 2,2,2-trichloroethyl 2-(4-bromophenyl)-2-diazoacetate (0.3 mmol, 112 mg, 1.0 equiv) under the catalysis of Rh_2(S-TPPTTL)$_4$ (0.0015 mmol, 3.7 mg, 0.5 mol %). After flash chromatography (0%, then 2% - 3% Et_2O in hexanes) the product was obtained as a clear oil that solidified slowly upon standing (100 mg, 75% yield).

MP: 65°C

$[\alpha]^{20}_D$ -2.3° (c = 1.00, $CHCl_3$, 92% ee)

^{1}H NMR (600 MHz, $CDCl_3$) δ 7.49 – 7.41 (m, 2H), 7.26 – 7.23 (m, 2H), 4.73 (d, J = 12.0, 1H), 4.64 (d, J = 12.0 Hz, 1H), 3.42 (d, J = 10.9 Hz, 1H), 2.30 (m, 1H), 1.83 (m, 1H), 1.69 (m, 1H), 1.65 – 1.28 (m, 9H), 1.01 (m, 1H)

^{13}C NMR (150 MHz, $CDCl_3$) δ 171.9, 136.5, 131.7, 130.5, 121.6, 94.8, 74.2, 58.3, 41.9, 33.1, 31.3, 28.2, 28.2, 26.3, 26.1

IR (neat): 2924, 2853, 1748, 1487, 1267, 1209, 1073, 1011, 828, 758, 721

HR-MS (+p APCI) calcd for [$C_{17}H_{20}BrCl_3O_2$+H] 440.9791, found 440.9785

Chiral HPLC (Chiralcel S,S-Whelk, 0.5% isopropanol in hexane, 0.5 mL/min, λ 210-230 nm) retention times of 21.53 min (major) and 25.17 min (minor), 92% ee

2,2,2-trichloroethyl (2R)-2-((1s,3S)-adamantan-1-yl)-2-(4-bromophenyl)acetate

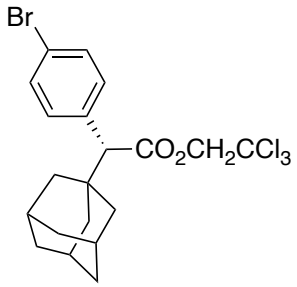

This compound was prepared according to the general procedure for C–H functionalization reaction, using adamantane (0.75 mmol, 102 mg, 2.5 equiv) as the substrate and 2,2,2-trichloroethyl 2-(4-bromophenyl)-2-diazoacetate (0.3 mmol, 112 mg, 1.0 equiv) under the catalysis of Rh_2(S-TPPTTL)$_4$ (0.0015 mmol, 3.7 mg, 0.5 mol %). After flash chromatography (0%, then 2% - 3% Et_2O in hexanes) the product was obtained as a clear oil that solidified slowly upon standing (108 mg, 72% yield)

MP: 105°C

$[\alpha]^{20}_D$ -2.3° (c = 1.00, $CHCl_3$, 90% ee)

^{1}H NMR (600 MHz, $CDCl_3$) δ 7.46 – 7.42 (m, 2H), 7.31 – 7.26 (m, 2H), 4.80 (d, J = 12.0 Hz, 1H), 4.62 (d, J = 12.0 Hz, 1H), 3.39 (s, 1H), 1.97 (m, 3H), 1.69 (m, 6H), 1.56 (m, 6H)

^{13}C NMR (150 MHz, $CDCl_3$) δ 170.6, 133.0, 131.9, 131.0, 121.6, 74.2, 62.5, 39.8, 36.6, 36.5, 28.5

IR (neat): 2904, 1746, 1486, 1123, 1045, 1028, 1011, 833, 757, 719 cm^{-1}

HR-MS (+p APCI) calcd for [$C_{20}H_{22}BrCl_3O_2$+H] 476.9785, found 476.9784

Chiral HPLC (Chiralcel R,R-Whelk, 0.5% isopropanol in hexane, 0.5 mL/min, λ 210-230 nm) retention times of 20.58 min (major), 17.38 min (minor), 90% ee

2,2,2-trichloroethyl (R)-2-(4-bromophenyl)-2-((1S,3R)-3-methylcyclohexyl)acetate

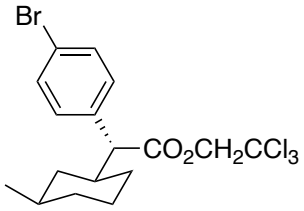

This compound was prepared according to the general procedure for C–H functionalization reaction, using methylcyclohexane (0.75 mmol, 74 mg, 2.5 equiv) as the substrate and 2,2,2-trichloroethyl 2-(4-bromophenyl)-2-diazoacetate (0.3 mmol, 112 mg, 1.0 equiv) under the catalysis of Rh_2(S-TPPTTL)$_4$ (0.0015 mmol, 3.7 mg, 0.5 mol %). After flash chromatography (0%, then 2% - 3% Et_2O in hexanes) the product was obtained as a clear oil (113 mg, 85% yield). The product needed to be converted to the corresponding alcohol for ee determination via chiral HPLC (see general information of this section).

$[\alpha]^{20}_D$ -13.7° (c = 1.00, $CHCl_3$, 97% ee)

^{1}H NMR (600 MHz, $CDCl_3$) δ 7.49 – 7.42 (m, 2H), 7.25 – 7.22 (m, 2H), 4.78 – 4.74 (d, J = 12.0 Hz 1H), 4.63 (d, J = 12.0 Hz, 1H), 3.31 (d, J = 10.6 Hz, 1H), 2.07 (m, 1H), 1.88 – 1.83 (m, 1H), 1.76 (m, 1H), 1.66 (m, 1H), 1.38 – 1.24 (m, 4H), 1.03 – 0.94 (m, 1H), 0.78 (d, J = 6.4 Hz, 3H), 0.49 – 0.38 (q, 1H)

^{13}C NMR (150 MHz, $CDCl_3$) δ 171.7, 135.9, 132.0, 130.4, 121.6, 94.8, 74.1, 58.4, 40.9, 38.9, 34.9, 32.4, 31.5, 25.9, 22.7

IR (neat): 2924, 1748, 1487, 1146, 1123, 1073, 1011, 824, 759, 719 cm^{-1}

HR-MS (+p NSI) calcd for [$C_{17}H_{20}BrCl_3O_2$+H] 440.9791 found 440.9791

Chiral HPLC for the alcohol (Chiralcel ADH, 0.5% isopropanol in hexane, 1 mL/min, λ 230 nm) retention times of 52.75 min (major), 48.46 min (minor), 97% ee

2,2,2-trichloroethyl (R)-2-(4-bromophenyl)-2-((1S,3R)-3-ethylcyclohexyl)acetate

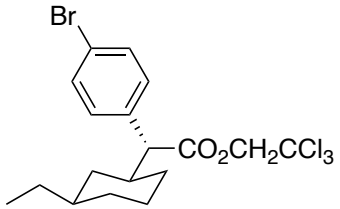

This compound was prepared according to the general procedure for C–H functionalization reaction, using ethylcyclohexane (0.75 mmol, 84.2 mg, 2.5 equiv) as the substrate and 2,2,2-trichloroethyl 2-(4-bromophenyl)-2-diazoacetate (0.3 mmol, 112 mg, 1.0 equiv) under the catalysis of Rh_2(S-TPPTTL)$_4$ (0.0015 mmol, 3.7 mg, 0.5 mol %). After flash chromatography (0%, then 2% - 3% Et_2O in hexanes) the product was obtained as a clear oil (111 mg, 81% yield).

$[\alpha]^{20}_D$ -11.8° (c = 1.00, $CHCl_3$, 96% ee)

^{1}H NMR (600 MHz, $CDCl_3$) δ 7.49 – 7.42 (m, 2H), 7.26 – 7.21 (m, 2H), 4.77 – 4.75 (d, J = 12.0 Hz, 1H), 4.63 (d, J = 12.0 Hz, 1H), 3.31 (d, J = 10.5, 1H), 2.06 (m, 1H), 1.89 – 1.83 (m, 1H), 1.82 – 1.71 (m, 2H), 1.43 – 0.91 (m, 6H), 0.76 (t, J = 7.1 Hz, 4H), 0.49 – 0.38 (m, 1H)

^{13}C NMR (150 MHz, $CDCl_3$) δ 171.7, 135.8, 131.7, 130.5, 121.6, 94.8, 74.1, 58.4, 40.9, 39.0, 36.8, 32.1, 31.9, 30.0, 25.8, 11.3

IR (neat): 2924, 1749, 1488, 1145, 1125, 1073, 1012, 825, 759, 719

HR-MS (+p APCI) calcd for [$C_{18}H_{22}BrCl_3O_2$+H] 454.9947, found 454.9948

Chiral HPLC (Chiralcel S,S-Whelk, 0% isopropanol in hexane, 0.5 mL/min, λ 230 nm) retention times of 41.34 min (major), 51.07 min (minor), 96% ee

2,2,2-trichloroethyl (R)-2-(4-bromophenyl)-2-((1S,3R)-3-isopropylcyclohexyl)acetate

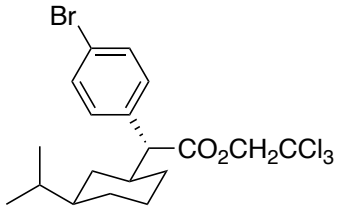

This compound was prepared according to the general procedure for C–H functionalization reaction, using isopropylcyclohexane (0.75 mmol, 95 mg, 2.5 equiv) as the substrate and 2,2,2-trichloroethyl 2-(4-bromophenyl)-2-diazoacetate (0.3 mmol, 112 mg, 1.0 equiv) under the catalysis of Rh_2(S-TPPTTL)$_4$ (0.0015 mmol, 3.7 mg, 0.5 mol %). After flash chromatography (0%, then 2% - 3% Et_2O in hexanes) the product was obtained as a clear oil (116 mg, 82% yield)

$[\alpha]^{20}_D$ -13.5° (c = 1.00, $CHCl_3$, 97% ee)

^{1}H NMR (600 MHz, $CDCl_3$) δ 7.49 – 7.42 (m, 2H), 7.26 – 7.22 (m, 2H), 4.76 (d, J = 12.0 Hz, 1H), 4.63 (d, J = 12.0 Hz, 1H), 3.34 (d, J = 10.5 Hz, 1H), 2.06 (m, 1H), 1.89 – 1.77 (m, 2H), 1.71 – 1.62 (m, 1H), 1.38 – 1.23 (m, 3H), 1.09 – 0.96 (m, 2H), 0.93 – 0.79 (m, 1H), 0.74 (d, J = 6.8, 1.8 Hz, 6H), 0.53 (q, J = 12.1 Hz, 1H)

^{13}C NMR (150 MHz, $CDCl_3$) δ 71.7, 135.8, 131.7, 130.5, 121.5, 94.8, 74.2, 58.5, 43.5, 41.1, 33.9, 32.8, 31.9, 28.6, 26.0, 19.9, 19.1.

IR (neat): 2926, 1749, 1487, 1146, 1123, 1074, 1011, 830, 759, 717 cm^{-1}

HR-MS (+p APCI) calcd for [$C_{19}H_{24}BrCl_3O_2$+H] 469.0104, found 469.0103

Chiral HPLC (Chiralcel R,R-Whelk, 0.3% isopropanol in hexane, 1 mL/min, λ 230 nm) retention times of 13.94 min (major), 11.54 min (minor), 97% ee

2,2,2-trichloroethyl (R)-2-(4-bromophenyl)-2-((1S,3R)-3-(tert-butyl)cyclohexyl)acetate

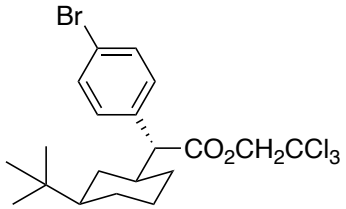

This compound was prepared according to the general procedure for C–H functionalization reaction, using tert-butylcyclohexane (0.75 mmol, 105 mg, 2.5 equiv) as the substrate and 2,2,2-trichloroethyl 2-(4-bromophenyl)-2-diazoacetate (0.3 mmol, 112 mg, 1.0 equiv) under the catalysis of Rh_2(S-TPPTTL)$_4$ (0.0015 mmol, 3.7 mg, 0.5 mol %). After flash chromatography (0%, then 2% - 3% Et_2O in hexanes) the product was obtained as a clear oil that solidified slowly upon standing (116 mg, 80% yield). The product needed to be converted to the corresponding alcohol for ee determination via chiral HPLC (see general information of this section). After reducing the ester functionality to the primary alcohol using lithium aluminum hydride (see General Information), the resulting compound could be crystallized by dissolving in minimal dichloromethane in a small vial and then stacking the solution with hexanes.

MP: 55^{o}C

$[\alpha]^{20}_D$ -9.2^o (c = 1.00, $CHCl_3$, 95% ee)

^{1}H NMR (600 MHz, $CDCl_3$) δ 7.48 – 7.43 (m, 2H), 7.26 – 7.22 (m, 2H), 4.76 (d, J = 12.0 Hz, 1H), 4.62 (d, J = 12.0 Hz, 1H), 3.35 (d, J = 10.3 Hz, 1H), 2.04 (m, 1H), 1.88 – 1.80 (m, 2H), 1.79 – 1.72 (m, 1H), 1.46 (m, 1H), 1.34 – 1.26 (m, 1H), 0.97 (m, 2H), 0.91 – 0.83 (m, 1H), 0.72 (s, 9H), 0.50 (q, J = 12.0 Hz, 1H)

^{13}C NMR (150 MHz, $CDCl_3$) δ 171.7, 135.8, 131.7, 130.4, 121.5, 94.8, 74.2, 58.5, 47.7, 41.3, 32.5, 31.7, 31.2, 27.4, 27.0, 26.2

IR (neat): 2491, 1750, 1488, 1366, 1112, 1073, 1012, 827, 761, 719 cm^{-1}

HR-MS (+p NSI) calcd for [$C_{20}H_{26}BrCl_3O_2$+H] 483.0260, found 483.0258

Chiral HPLC for the alcohol (Chiralcel ADH, 2% isopropanol in hexane, 1 mL/min, λ 230 nm) retention times of 16.11 min (major), 13.16 min (minor), 95% ee

2,2,2-trichloroethyl (R)-2-((1R,3S)-[1,1'-bi(cyclohexan)]-3-yl)-2-(4-bromophenyl)acetate

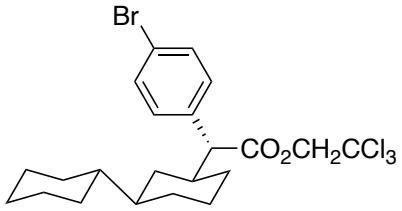

This compound was prepared according to the general procedure for C–H functionalization reaction, using dicyclohexyl (0.75 mmol, 125 mg, 2.5 equiv) as the substrate and 2,2,2-trichloroethyl 2-(4-bromophenyl)-2-diazoacetate (0.3 mmol, 112 mg, 1.0 equiv) under the catalysis of Rh_2(S-TPPTTL)$_4$ (0.0015 mmol, 3.7 mg, 0.5 mol %). After flash chromatography (0%, then 2% - 3% Et_2O in hexanes) the product was obtained as a clear oil (130 mg, 85% yield). The product needed to be converted to the corresponding alcohol for ee determination via chiral HPLC (see general information of this section).

$[\alpha]^{20}_D$ -20.6° (c = 1.00, $CHCl_3$, 95% ee)

^{1}H NMR (600 MHz, $CDCl_3$) δ 7.50 – 7.42 (m, 2H), 7.25 – 7.21 (m, 2H), 4.75 (d, J = 12.0 Hz, 1H), 4.62 (d, J = 12.0 Hz, 1H), 3.33 (d, J = 10.5 Hz, 1H), 2.05 (tdt, J = 11.7, 10.3, 3.3 Hz, 1H), 1.90 – 1.77 (m, 2H), 1.70 – 1.62 (m, 3H), 1.59 (m, 1H), 1.56 – 1.50 (m, 1H), 1.49 – 1.43 (m, 1H), 1.39 – 1.32 (m, 1H), 1.32 – 1.22 (m, 1H), 1.13 – 0.95 (m, 6H), 0.92 – 0.79 (m, 3H), 0.55 (q, J = 12.1 Hz, 1H)

^{13}C NMR (150 MHz, $CDCl_3$) δ 171.7, 135.8, 131.7, 130.5, 121.6, 94.8, 74.2, 74.2, 58.5, 43.3, 43.0, 41.1, 34.0, 32.0, 30.4, 29.5, 29.1, 26.8, 26.8, 26.1

IR (neat): 2922, 1749, 1488, 1125, 1011, 907, 826, 759, 730 cm^{-1}

HR-MS [$C_{22}H_{28}BrCl_3O_2$+H] 509.0417 found 509.0430

Chiral HPLC for the alcohol (Chiralcel S,S-Whelk, 3% isopropanol in hexane, 1 mL/min, λ 230 nm) retention times of 38.60 min (major), 26.62 min (minor), 95% ee

2,2,2-trichloroethyl (R)-2-(4-bromophenyl)-2-((1S,3R)-3-butylcyclohexyl)acetate

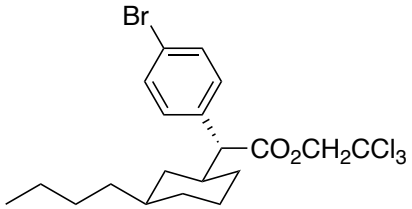

This compound was prepared according to the general procedure for C–H functionalization reaction, using n-butyl cyclohexane (0.75 mmol, 105 mg, 2.5 equiv) as the substrate and 2,2,2-trichloroethyl 2-(4-bromophenyl)-2-diazoacetate (0.3 mmol, 112 mg, 1.0 equiv) under the catalysis of Rh_2(S-TPPTTL)$_4$ (0.0015 mmol, 3.7 mg, 0.5 mol %). After flash chromatography (0%, then 2% - 3% Et_2O in hexanes) the product was obtained as a clear oil that solidified slowly upon standing (112 mg, 77% yield).

MP: 55^{o}C

$[\alpha]^{20}_D$ -13.2^o (c = 1.00, $CHCl_3$, 90% ee)

^{1}H NMR (600 MHz, $CDCl_3$) δ 7.45 (m, 2H), 7.25 – 7.22 (m, 2H), 4.76 (d, J = 12.0 Hz, 1H), 4.63 (d, J = 12.0, 1H), 3.31 (d, J = 10.5, 1H), 2.12 – 2.02 (m, 1H), 1.94 – 1.83 (m, 1H), 1.82 – 1.71 (m, 2H), 1.39 – 0.96 (m, 10H), 0.82 (t, J = 7.1 Hz, 3H), 0.76 (m, 1H), 0.44 (q, J = 12.1 Hz, 1H)

^{13}C NMR (150 MHz, $CDCl_3$) δ 171.7, 135.8, 131.7, 130.5, 121.6, 94.8, 74.2, 58.4, 40.9, 37.4, 37.23, 37.1, 32.6, 31.9, 28.9, 25.9, 22.9, 14.1

IR (neat): 2923, 1749, 1488, 1142, 1124, 1074, 1011, 825, 759, 718 cm^{-1}

HR-MS: (+p NSI) calcd for [$C_{20}H_{26}BrCl_3O_2$+H] 483.0260, found 483.0259

Chiral HPLC (Chiralcel R,R-Whelk, 0.1% isopropanol in hexane, 0.4 mL/min, λ 230 nm) retention times of 54.86 min (major), 49.14 min (minor), 90% ee

2,2,2-trichloroethyl (R)-2-(4-bromophenyl)-2-((1S,3R)-3-pentylcyclohexyl)acetate

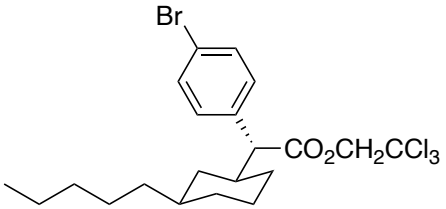

This compound was prepared according to the general procedure for C–H functionalization reaction, using n-pentyl cyclohexane (0.75 mmol, 116 mg, 2.5 equiv) as the substrate and 2,2,2-trichloroethyl 2-(4-bromophenyl)-2-diazoacetate (0.3 mmol, 112 mg, 1.0 equiv) under the catalysis of Rh_2(S-TPPTTL)$_4$ (0.0015 mmol, 3.7 mg, 0.5 mol %). After flash chromatography (0%, then 2% - 3% Et_2O in hexanes) the product was obtained as a clear oil (120 mg, 80% yield).

$[\alpha]^{20}_D$ -13.5° (c = 1.00, $CHCl_3$, 91% ee)

^{1}H NMR (600 MHz, $CDCl_3$) δ 7.45 (m, 2H), 7.25 – 7.20 (m, 2H), 4.78 – 4.73 (d, J = 12.0 Hz, 1H), 4.63 (d, J = 12.0, 1H), 3.31 (d, J = 10.5, 1H), 2.13 – 2.02 (m, 1H), 1.91 – 1.83 (m, 1H), 1.82 – 1.69 (m, 2H), 1.43 – 0.92 (m, 12H), 0.83 (t, J = 7.2 Hz, 3H), 0.81 – 0.70 (m, 1H), 0.44 (q, J = 11.8 Hz, 1H)

^{13}C NMR (150 MHz, $CDCl_3$) δ 171.7, 135.8, 131.7, 130.5, 121.6, 94.8, 74.2, 58.4, 40.9, 37.4, 37.4, 32.7, 32.6, 32.1, 31.9, 26.3, 25.9, 22.6, 14.1

IR (neat): 2923, 1750, 1488, 1142, 1124, 1074, 1011, 826, 759, 719 cm^{-1}

HR-MS (+p NSI) calcd for [$C_{21}H_{28}BrCl_3O_2$-C_5H_{10}+N] 439.9586, found 439.9587

Chiral HPLC (Chiralcel R,R-Whelk, 0% isopropanol in hexane, 1 mL/min, λ 230 nm) retention times of 21.84 min (major), 19.36 min (minor), 91% ee

2,2,2-trichloroethyl (R)-2-(4-bromophenyl)-2-((1S,3R)-3-(trimethylsilyl)cyclohexyl)acetate

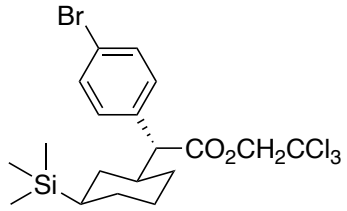

This compound was prepared according to the general procedure for C–H functionalization reaction, using trimethylsilyl cyclohexane (0.75 mmol, 117 mg, 2.5 equiv) as the substrate and 2,2,2-trichloroethyl 2-(4-bromophenyl)-2-diazoacetate (0.3 mmol, 112 mg, 1.0 equiv) under the catalysis of Rh_2(S-TPPTTL)$_4$ (0.0015 mmol, 3.7 mg, 0.5 mol %). After flash chromatography (0%, then 2% - 3% Et_2O in hexanes) the product was obtained as a clear oil (120 mg, 80% yield).

$[\alpha]^{20}_D$ -19.4° (c = 1.00, $CHCl_3$, 97% ee)

^{1}H NMR (600 MHz, $CDCl_3$) δ 7.47 – 7.42 (m, 2H), 7.26 – 7.21 (m, 2H), 4.76 (d, J = 12.0 Hz, 1H), 4.62 (d, J = 12.0 Hz, 1H), 3.33 (d, J = 10.3 Hz, 1H), 2.03 (m, 1H), 1.95 – 1.86 (m, 1H), 1.82 (m, 1H), 1.69 – 1.63 (m, 1H), 1.42 – 1.35 (m, 1H), 1.30 (qt, J = 13.1, 3.6 Hz, 1H), 1.07 (qd, J = 12.8, 3.6 Hz, 1H), 0.97 (qd, J = 13.0, 3.6 Hz, 1H), 0.62 (q, J = 11.5 Hz, 1H), 0.50 (tt, J = 12.9, 3.0 Hz, 1H), -0.17 (s, 9H)

^{13}C NMR (150 MHz, $CDCl_3$) δ 171.7, 135.8, 131.6, 130.4, 121.5, 94.8, 74.2, 58.5, 42.0, 31.9, 30.9, 27.6, 26.8, 25.4, -3.7

IR (neat): 2922, 1750, 1488, 1247, 1129, 1012, 861, 829, 760, 718 cm^{-1}

HR-MS (+p NSI): calcd for [$C_{19}H_{26}BrCl_3O_2Si$-TMS+N] 439.9586, found 439.9584

Chiral HPLC (Chiralcel S,S-Whelk, 0.5% isopropanol in hexane, 0.5 mL/min, λ 210-230 nm) retention times of 23.71 min (major), 20.01 min (minor), 97% ee

tert-butyl (1R,3S)-3-((R)-1-(4-bromophenyl)-2-oxo-2-(2,2,2-trichloroethoxy)ethyl)cyclohexane-1-carboxylate

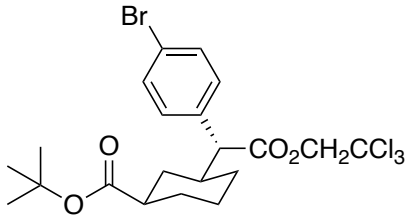

This compound was prepared according to the general procedure for C–H functionalization reaction, using tert-butyl cyclohexanecarboxylate (0.75 mmol, 138 mg, 2.5 equiv) as the substrate and 2,2,2-trichloroethyl 2-(4-bromophenyl)-2-diazoacetate (0.3 mmol, 112 mg, 1.0 equiv) under the catalysis of Rh_2(S-TPPTTL)$_4$ (0.0015 mmol, 3.7 mg, 0.5 mol %). After flash chromatography (3%, then 5% - 8% Et_2O in hexanes) the product was obtained as a clear oil (92 mg, 58% yield).

$[\alpha]^{20}_D$ -20.4° (c = 1.00, $CHCl_3$, 96% ee)

^{1}H NMR (500 MHz, $CDCl_3$) δ 7.45 (d, J = 8.5 Hz, 2H), 7.23 (d, J = 8.5 Hz, 2H), 4.76 (d, J = 11.9 Hz, 1H), 4.63 (d, J = 11.9 Hz, 1H), 3.35 (d, J = 10.5 Hz, 1H), 2.15 – 2.03 (m, 2H), 1.97 – 1.91 (m, 1H), 1.86 (dtd, J = 13.2, 8.1, 6.5, 3.1 Hz, 2H), 1.57 – 1.52 (m, 1H), 1.37 (s, 9H), 1.23 – 1.14 (m, 1H), 1.10 – 0.81 (m, 3H)

^{13}C NMR (125 MHz, $CDCl_3$) δ 174.9, 171.4, 135.3, 131.8, 130.4, 121.8, 94.7, 80.0, 74.1, 58.1, 43.9, 39.9, 32.0, 31.0, 29.1, 28.0, 25.2

IR (neat): 2934, 1751, 1724, 1489, 1367, 1138, 829, 761, 720 cm^{-1}

HR-MS (+p NSI): calcd for [$C_{21}H_{26}BrCl_3O_4$+Na] 548.9978, found 548.9986

Chiral HPLC (Chiralcel ODH, 0% isopropanol in hexane, 0.5 mL/min, λ 230 nm) retention times of 16.66 min (major), 15.05 min (minor), 96% ee

((1R,3S)-3-((R)-1-(4-bromophenyl)-2-oxo-2-(2,2,2-trichloroethoxy)ethyl)cyclohexyl)methyl pivalate

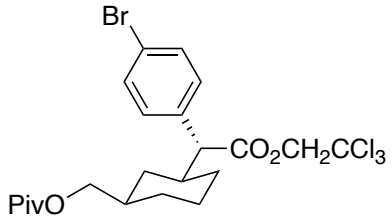

This compound was prepared according to the general procedure for C–H functionalization reaction, using cyclohexylmethyl pivalate (0.75 mmol, 149 mg, 2.5 equiv) as the substrate and 2,2,2-trichloroethyl 2-(4-bromophenyl)-2-diazoacetate (0.3 mmol, 112 mg, 1.0 equiv) under the catalysis of Rh_2(S-TPPTTL)$_4$ (0.0015 mmol, 3.7 mg, 0.5 mol %). After flash chromatography (1%, then 3% - 5% Et_2O in hexanes) the product was obtained as a clear oil (110 mg, 68% yield).

$[\alpha]^{20}_D$ -14.7° (c = 1.00, $CHCl_3$, 95% ee)

^{1}H NMR (600 MHz, $CDCl_3$) δ 7.44 (d, J = 8.5 Hz, 2H), 7.22 (d, J = 8.4 Hz, 2H), 4.76 (d, J = 12.0 Hz, 1H), 4.64 (d, J = 12.0 Hz, 1H), 3.76 (d, J = 6.6 Hz, 2H), 3.31 (d, J = 10.6 Hz, 1H), 2.11 – 2.02 (m, 1H), 1.91 (dt, J = 12.5, 3.3 Hz, 1H), 1.83 (dt, J = 13.5, 3.4 Hz, 1H), 1.72 (d, J = 13.1 Hz, 1H), 1.65 – 1.58 (m, 1H), 1.40 – 1.31 (m, 2H), 1.21 – 1.16 (m, 1H), 1.07 (s, 9H), 0.94 – 0.85 (m, 1H), 0.48 (q, J = 12.3 Hz, 1H)

^{13}C NMR (150 MHz, $CDCl_3$) δ 178.4, 171.5, 135.6, 131.8, 130.3, 121.7, 94.7, 74.2, 68.7, 58.1, 40.45, 38.7, 37.0, 33.2, 31.7, 29.0, 27.0, 25.2

IR (neat): 2930, 1750, 1727, 1488, 1283, 1154, 1125, 827, 761, 720 cm^{-1}

HR-MS (-p NSI): calcd for [$C_{22}H_{28}BrCl_3O_4$+Cl] 574.9925, found 574.9945

Chiral HPLC (Chiralcel OD, 0.5% isopropanol in hexane, 0.5 mL/min, λ 230 nm) retention times of 16.37 min (major), 15.24 min (minor), 95% ee

2,2,2-trichloroethyl (R)-2-((1S,3R)-3-(2-acetoxypropan-2-yl)cyclohexyl)-2-(4-bromophenyl)acetate

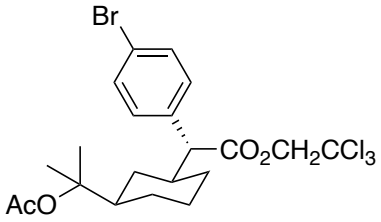

This compound was prepared according to the general procedure for C–H functionalization reaction, using 2-cyclohexylpropan-2-yl acetate (0.75 mmol, 138 mg, 2.5 equiv) as the substrate and 2,2,2-trichloroethyl 2-(4-bromophenyl)-2-diazoacetate (0.3 mmol, 112 mg, 1.0 equiv) under the catalysis of Rh_2(S-TPPTTL)$_4$ (0.0015 mmol, 3.7 mg, 0.5 mol %). After flash chromatography (1%, then 3% - 5% Et_2O in hexanes) the product was obtained as a clear oil (119 mg, 75% yield).

$[\alpha]^{20}_D$ -5.4° (c = 1.00, $CHCl_3$, 97% ee)

^{1}H NMR (600 MHz, $CDCl_3$) δ 7.46 (d, J = 8.5 Hz, 2H), 7.23 (d, J = 8.4 Hz, 2H), 4.75 (d, J = 12.0 Hz, 1H), 4.63 (d, J = 12.0 Hz, 1H), 3.35 (d, J = 10.5 Hz, 1H), 2.08 (m, 1H), 2.00 – 1.91 (m, 1H), 1.86 (ddt, J = 15.2, 10.1, 3.4 Hz, 2H), 1.79 (s, 3H), 1.73 – 1.68 (m, 1H), 1.34 (m, 2H), 1.32 (s, 3H), 1.22 (s, 3H), 1.08 – 0.91 (m, 2H), 0.57 (q, J = 12.2 Hz, 1H)

^{13}C NMR (150 MHz, $CDCl_3$) δ 171.4, 170.3, 135.7, 131.7, 130.4, 121.6, 94.7, 84.8, 74.2, 58.2, 45.3, 40.8, 31.6, 30.9, 26.9, 25.7, 23.7, 23.2, 22.2

IR (neat): 2934, 1750, 1727, 1488, 1368, 1257, 1132, 1012, 826, 760, 720 cm^{-1}

HR-MS (+APCI): calcd for [$C_{19}H_{23}BrCl_3O_2$-OAc] 466.9942, found 466.9941

Chiral HPLC (Chiralcel ADH, 0.5% isopropanol in hexane, 0.5 mL/min, λ 230 nm) retention times of 51.09 min (major), 39.12 min (minor), 97% ee

2,2,2-trichloroethyl (R)-2-(2-bromophenyl)-2-((1S,3R)-3-(tert-butyl)cyclohexyl)acetate

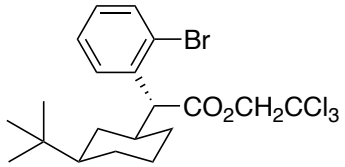

This compound was prepared according to the general procedure for C–H functionalization reaction, using tert-butylcyclohexane (0.75 mmol, 105 mg, 2.5 equiv) as the substrate and 2,2,2-trichloroethyl 2-(2-bromophenyl)-2-diazoacetate (0.3 mmol, 112 mg, 1.0 equiv) under the catalysis of Rh_2(S-TPPTTL)$_4$ (0.0015 mmol, 3.7 mg, 0.5 mol %). After flash chromatography (0%, then 2% - 3% Et_2O in hexanes) the product was obtained as a clear oil (90 mg, 62% yield).

$[\alpha]^{20}_D$ -20.0° (c = 1.00, $CHCl_3$, 85% ee)

^{1}H NMR (600 MHz, $CDCl_3$) δ 7.60 – 7.57 (dd, J = 8.0, 1.3 Hz, 1H), 7.54 (dd, J = 7.9, 1.7 Hz, 1H), 7.29 (td, J = 7.6, 1.3 Hz, 1H), 7.14 – 7.09 (m, 1H), 4.75 (d, J = 12.0 Hz, 1H), 4.67 (d, J = 12.0 Hz, 1H), 4.17 (d, J = 10.2 Hz, 1H), 2.09 (m, 1H), 1.94 – 1.88 (m, 1H), 1.85 (m, 1H), 1.78 – 1.72 (m, 1H), 1.44 (m, 1H), 1.34 – 1.26 (m, 1H), 1.09 (tdd, J = 12.8, 11.5, 3.7 Hz, 1H), 1.00 – 0.86 (m, 2H), 0.72 (s, 9H), 0.68 (q, J = 11.7 Hz, 1H)

^{13}C NMR (150 MHz, $CDCl_3$) δ 171.5, 136.5, 133.0, 129.2, 128.8, 127.7, 126.0, 94.8, 74.1, 56.2, 47.8, 41.9, 32.5, 31.5, 30.7, 27.4, 27.0, 26.3

IR (neat): 2941, 1750, 1470, 1137, 1109, 1022, 816, 747, 719 cm^{-1}

HRMS (+p NSI): calcd for [$C_{20}H_{26}BrCl_3O_2$+H] 483.0260, found 483.0260

Chiral HPLC (Chiralcel ADH, 0% isopropanol in hexane, 0.25 mL/min, λ 254 nm) retention times of 21.89 min (major), 20.54 min (minor), 85% ee

2,2,2-trichloroethyl (R)-2-((1S,3R)-3-(tert-butyl)cyclohexyl)-2-(2-chlorophenyl)acetate

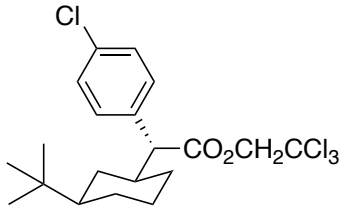

This compound was prepared according to the general procedure for C–H functionalization reaction, using tert-butylcyclohexane (0.75 mmol, 105 mg, 2.5 equiv) as the substrate and 2,2,2-trichloroethyl 2-(4-chlorophenyl)-2-diazoacetate (0.3 mmol, 98 mg, 1.0 equiv) under the catalysis of Rh_2(S-TPPTTL)$_4$ (0.0015 mmol, 3.7 mg, 0.5 mol %). After flash chromatography (0%, then 2% - 3% Et_2O in hexanes) the product was obtained as a clear oil (118 mg, 89% yield).

$[\alpha]^{20}_D$ -8.6° (c = 1.00, $CHCl_3$, 97% ee)

^{1}H NMR (600 MHz, $CDCl_3$) δ 7.30 (s, 4H), 4.76 (d, J = 12.0 Hz, 1H), 4.63 (d, J = 12.0 Hz, 1H), 3.37 (d, J = 10.3 Hz, 1H), 2.05 (m, 1H), 1.88 – 1.81 (m, 2H), 1.78 – 1.72 (m, 1H), 1.46 (m, 1H), 1.29 (m, 1H), 1.04 – 0.93 (m, 2H), 0.88 (td, J = 12.5, 3.3 Hz, 1H), 0.72 (s, 9H), 0.50 (q, J = 12.7, 1H)

^{13}C NMR (150 MHz, $CDCl_3$) δ 171.8, 135.3, 133.4, 130.1, 128.7, 94.8, 74.1, 58.4, 47.7, 41.3, 32.5, 31.7, 31.2, 27.4, 27.0, 26.3

IR (neat): 2959, 1750, 1491, 1366, 1261, 1217, 1093, 801, 741 cm^{-1}

HR-MS (+p APCI): calcd for [$C_{20}H_{26}Cl_4O_2$+H] 439.0765, found 439.0766

Chiral HPLC (Chiralcel S,S-Whelk, 0.5% isopropanol in hexane, 0.7 mL/min, λ 230 nm) retention times of 13.50 min (major), 15.12 min (minor), 97% ee

2,2,2-trichloroethyl (R)-2-((1S,3R)-3-(tert-butyl)cyclohexyl)-2-(2-chlorophenyl)acetate

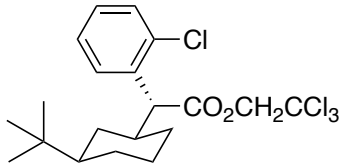

This compound was prepared according to the general procedure for C–H functionalization reaction, using tert-butylcyclohexane (0.75 mmol, 105 mg, 2.5 equiv) as the substrate and 2,2,2-trichloroethyl 2-(2-chlorophenyl)-2-diazoacetate (0.3 mmol, 98 mg, 1.0 equiv) under the catalysis of Rh_2(S-TPPTTL)$_4$ (0.0015 mmol, 3.7 mg, 0.5 mol %). After flash chromatography (0%, then 2% - 3% Et_2O in hexanes) the product was obtained as a clear oil (85 mg, 64% yield).

$[\alpha]^{20}_D$ -20.0° (c = 1.00, $CHCl_3$, 92% ee)

^{1}H NMR (600 MHz, $CDCl_3$) δ 7.55 (dd, J = 7.9, 1.7 Hz, 1H), 7.41 – 7.37 (dd, J = 8.0, 1.3 Hz 1H), 7.25 (td, J = 7.6, 1.4 Hz, 1H), 7.19 (ddd, J = 8.0, 7.3, 1.7 Hz, 1H), 4.75 (d, J = 12.0 Hz, 1H), 4.66 (d, J = 11.9 Hz, 1H), 4.17 (d, J = 10.2 Hz, 1H), 2.09 (m, 1H), 1.94 – 1.88 (m, 1H), 1.85 (m, 1H), 1.78 – 1.72 (m, 1H), 1.49 – 1.41 (m, 1H), 1.36 – 1.26 (m, 1H), 1.08 (tdd, J = 12.8, 11.5, 3.7 Hz, 1H), 1.00 – 0.93 (m, 1H), 0.93 – 0.86 (m, 1H), 0.72 (s, 9H), 0.66 (q, J = 12.7, 1H)

^{13}C NMR (150 MHz, $CDCl_3$) δ 171.5, 135.0, 134.7, 129.6, 129.1, 128.5, 127.0, 94.8, 74.1, 53.4, 47.8, 41.6, 32.5, 31.6, 30.8, 27.4, 27.0, 26.3

IR (neat): 2942, 1751, 1474, 1367, 1137, 1111, 749, 720 cm^{-1}

HR-MS (+p NSI): calcd for [$C_{20}H_{26}Cl_4O_2$+H] 439.0765, found 439.0766

Chiral HPLC (Chiralcel ADH, 0% isopropanol in hexane, 0.15 mL/min, λ 280 nm) retention times of 33.77 min (major), 32.06 min (minor), 92% ee

2,2,2-trichloroethyl (R)-2-((1S,3R)-3-(tert-butyl)cyclohexyl)-2-(3-methoxyphenyl)acetate

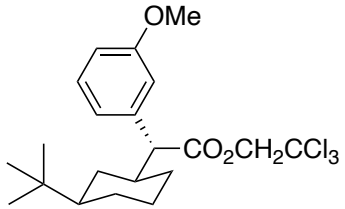

This compound was prepared according to the general procedure for C–H functionalization reaction, using tert-butylcyclohexane (0.75 mmol, 105 mg, 2.5 equiv) as the substrate and 2,2,2-trichloroethyl 2-diazo-2-(3-methoxyphenyl)acetate (0.3 mmol, 97 mg, 1.0 equiv) under the catalysis of Rh_2(S-TPPTTL)$_4$ (0.0015 mmol, 3.7 mg, 0.5 mol %). After flash chromatography (0%, then 2% - 3% Et_2O in hexanes) the product was obtained as a clear oil (80 mg, 61% yield).

$[\alpha]^{20}_D$ -18.2° (c = 1.00, $CHCl_3$, 96% ee)

^{1}H NMR (600 MHz, $CDCl_3$) δ 7.24 – 7.20 (m, 1H), 6.97 – 6.91 (m, 2H), 6.81 (ddd, J = 8.2, 2.6, 1.0 Hz, 1H), 4.78 (d, J = 12.0 Hz, 1H), 4.61 (d, J = 12.0 Hz, 1H), 3.80 (s, 3H), 3.36 (d, J = 10.4 Hz, 1H), 2.07 (tdt, J = 11.7, 10.3, 3.2 Hz, 1H), 1.88 – 1.80 (m, 2H), 1.75 (m, 1H), 1.51 (m, 1H), 1.35 – 1.21 (m, 1H), 1.05 – 0.93 (m, 2H), 0.88 (qd, J = 12.6, 3.5 Hz, 1H), 0.72 (s, 9H), 0.51 (q, 11.8 Hz, 1H)

^{13}C NMR (150 MHz, $CDCl_3$) δ 172.0, 159.7, 138.3, 129.4, 121.2, 114.3, 112.9, 94.9, 74.1, 59.1, 55.3, 47.7, 41.3, 32.5, 31.8, 31.3, 27.4, 27.1, 26.3

IR (neat): 2940, 1750, 1599, 1489, 1366, 1260, 1135, 1112, 1049, 747, 717 cm^{-1}

HR-MS (+p NSI) calcd for [$C_{21}H_{29}Cl_3O_3$+H] 435.1261, found 435.1264

Chiral HPLC (Chiralcel R,R-Whelk, 0.5% isopropanol in hexane, 0.5 mL/min, λ 230 nm) retention times of 36.40 min (major), 21.60 min (minor), 96% ee

2,2,2-trichloroethyl (R)-2-(4-acetoxyphenyl)-2-((1S,3R)-3-(tert-butyl)cyclohexyl)acetate

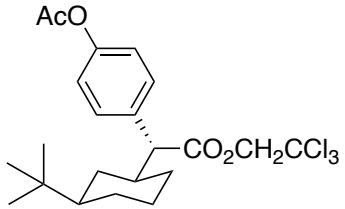

This compound was prepared according to the general procedure for C–H functionalization reaction, using tert-butylcyclohexane (0.75 mmol, 105 mg, 2.5 equiv) as the substrate and 2,2,2-trichloroethyl 2-(4-acetoxyphenyl)-2-diazoacetate (0.3 mmol, 105 mg, 1.0 equiv) under the catalysis of Rh_2(S-TPPTTL)$_4$ (0.0015 mmol, 3.7 mg, 0.5 mol %). After flash chromatography (0%, then 2% - 3% Et_2O in hexanes) the product was obtained as a clear oil (100 mg, 72% yield).

$[\alpha]^{20}_D$ -12.0° (c = 1.00, $CHCl_3$, 84% ee)

^{1}H NMR (600 MHz, $CDCl_3$) δ 7.41 – 7.33 (m, 2H), 7.11 – 7.01 (m, 2H), 4.78 (d, J = 12.0 Hz, 1H), 4.60 (d, J = 12.0 Hz, 1H), 3.40 (d, J = 10.3 Hz, 1H), 2.29 (s, 3H), 2.05 (m, 1H), 1.90 – 1.80 (m, 2H), 1.74 (m, 1H), 1.48 (m, 1H), 1.35 – 1.23 (m, 1H), 1.06 – 0.85 (m, 3H), 0.71 (s, 9H), 0.51 (q, 11.8 Hz, 1H)

^{13}C NMR (150 MHz, $CDCl_3$) δ 171.9, 169.3, 150.0, 134.3, 129.7, 121.6, 94.9, 74.2, 58.4, 47.7, 41.5, 32.5, 31.7, 31.3, 27.4, 27.0, 26.3, 21.2

IR (neat): 2940, 1750, 1506, 1367, 1198, 1135, 910, 719 cm^{-1}

HR-MS (+p APCI): calcd for [$C_{22}H_{29}Cl_3O_4$+H] 463.1210, found 463.1211

Chiral HPLC (Chiralcel ADH, 0.5% isopropanol in hexane, 0.8 mL/min, λ 230 nm) retention times of 16.16 min (major), 10.31 min (minor), 84% ee

2,2,2-trichloroethyl (R)-2-((1S,3R)-3-(tert-butyl)cyclohexyl)-2-(naphthalen-2-yl)acetate

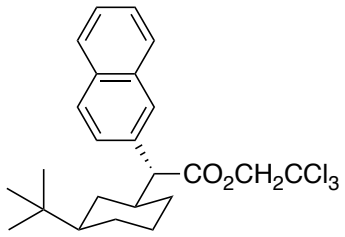

This compound was prepared according to the general procedure for C–H functionalization reaction, using tert-butylcyclohexane (0.75 mmol, 105 mg, 2.5 equiv) as the substrate and 2,2,2-trichloroethyl 2-diazo-2-(naphthalen-2-yl)acetate (0.3 mmol, 103 mg, 1.0 equiv) under the catalysis of Rh_2(S-TPPTTL)$_4$ (0.0015 mmol, 3.7 mg, 0.5 mol %). After flash chromatography (0%, then 2% - 3% Et_2O in hexanes) the product was obtained as a clear oil that solidified slowly upon standing (111 mg, 81% yield).

MP: 98°C

$[\alpha]^{20}_D$ -14.4° (c = 1.00, $CHCl_3$, 98% ee)

^{1}H NMR (600 MHz, $CDCl_3$) δ 7.86 – 7.80 (m, 4H), 7.57 – 7.51 (m, 1H), 7.51 – 7.45 (m, 2H), 4.80 (d, J = 12.0 Hz, 1H), 4.62 (d, J = 12.0 Hz, 1H), 3.59 (d, J = 10.3 Hz, 1H), 2.23 (tdt, J = 11.6, 10.2, 3.3 Hz, 1H), 1.93 (m, 1H), 1.87 (dp, J = 13.5, 3.4 Hz, 1H), 1.81 – 1.73 (m, 1H), 1.58 – 1.51 (m, 1H), 1.34 (qt, J = 13.1, 3.6 Hz, 1H), 1.08 (tdd, J = 12.8, 11.6, 3.7 Hz, 1H), 1.00 (tt, J = 11.8, 2.9 Hz, 1H), 0.96 – 0.87 (m, 1H), 0.69 (s, 9H), 0.59 (q, J = 12.8 Hz, 1H)

^{13}C NMR (150 MHz, $CDCl_3$) δ 172.1, 134.3, 133.4, 132.8, 128.2, 128.0, 127.9, 127.7, 126.4, 126.1, 125.9, 94.9, 74.2, 59.2, 47.7, 41.2, 32.5, 31.8, 31.4, 27.4, 27.1, 26.4

IR (neat): 2961, 1750, 1366, 1264, 803, 741 cm^{-1}

HR-MS (+p APCI): calcd for [$C_{24}H_{29}Cl_3O_2$+H] 454.1233, found 454.1228

Chiral HPLC (Chiralcel ADH, 0.3% isopropanol in hexane, 0.5 mL/min, λ 230 nm) retention times of 18.14 min (major), 15.50 min (minor), 98% ee

2,2,2-trichloroethyl (R)-2-((1S,3R)-3-(tert-butyl)cyclohexyl)-2-(4-(tert-butyl)phenyl)acetate

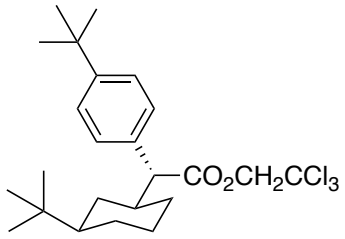

This compound was prepared according to the general procedure for C–H functionalization reaction, using tert-butylcyclohexane (0.75 mmol, 105 mg, 2.5 equiv) as the substrate and 2,2,2-trichloroethyl 2-(4-(tert-butyl)phenyl)-2-diazoacetate (0.3 mmol, 105 mg, 1.0 equiv) under the catalysis of Rh_2(S-TPPTTL)$_4$ (0.0015 mmol, 3.7 mg, 0.5 mol %). After flash chromatography (0%, then 2% - 3% Et_2O in hexanes) the product was obtained as a clear oil (112 mg, 81% yield).

$[\alpha]^{20}_D$ -6.3° (c = 1.00, $CHCl_3$, 47% ee)

^{1}H NMR (600 MHz, $CDCl_3$) δ 7.34 – 7.31 (m, 2H), 7.29 – 7.26 (m, 2H), 4.79 (d, J = 12.0 Hz, 1H), 4.59 (d, J = 12.0 Hz, 1H), 3.38 (d, J = 10.2 Hz, 1H), 2.06 (tdt, J = 11.6, 10.1, 3.1 Hz, 1H), 1.84 (m, 2H), 1.74 (m, 1H), 1.50 (m, 1H), 1.31 (m, 10H), 0.99 (m, 2H), 0.89 (m, 1H), 0.72 (s, 9H), 0.51 (q, J = 12.4, 1H)

^{13}C NMR (150 MHz, $CDCl_3$) δ 172.4, 150.3, 133.7, 128.3, 125.4, 95.0, 74.1, 58.5, 47.7, 41.3, 34.5, 32.5, 31.7, 31.4, 31.3, 27.4, 27.1, 26.4

IR (neat): 2959, 1751, 1366, 1135, 1126, 1110, 768, 722 cm^{-1}

HRMS (+p NSI): calcd for [$C_{24}H_{35}Cl_3O_2$+H] 461.1781, found 461.1778

Chiral HPLC (Chiralcel R,R-Whelk, 0.1% isopropanol in hexane, 0.6 mL/min, λ 230 nm) retention times of 28.89 min (major), 23.71 min (minor), 47% ee

2,2,2-trichloroethyl (R)-2-([1,1'-biphenyl]-4-yl)-2-((1S,3R)-3-(tert-butyl)cyclohexyl)acetate

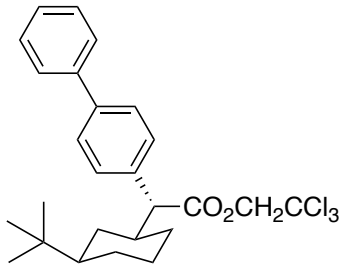

This compound was prepared according to the general procedure for C–H functionalization reaction, using tert-butylcyclohexane (0.75 mmol, 105 mg, 2.5 equiv) as the substrate and 2,2,2-trichloroethyl 2-([1,1'-biphenyl]-4-yl)-2-diazoacetate (0.3 mmol, 111 mg, 1.0 equiv) under the catalysis of Rh_2(S-TPPTTL)$_4$ (0.0015 mmol, 3.7 mg, 0.5 mol %). After flash chromatography (0%, then 2% - 3% Et_2O in hexanes) the product was obtained as a clear oil that solidified slowly upon standing (117 mg, 81% yield).

MP: 60°C

$[\alpha]^{20}_D$ -6.6° (c = 1.00, $CHCl_3$, 79% ee)

^{1}H NMR (600 MHz, $CDCl_3$) δ 7.63 – 7.56 (m, 4H), 7.44 (ddd, J = 8.1, 4.6, 2.1 Hz, 4H), 7.37 – 7.33 (m, 1H), 4.81 (d, J = 12.0 Hz, 1H), 4.64 (d, J = 12.0 Hz, 1H), 3.46 (d, J = 10.3 Hz, 1H), 2.18 – 2.09 (m, 1H), 1.87 (m, 2H), 1.77 (m, 1H), 1.60 – 1.53 (m, 1H), 1.32 (m, 1H), 1.03 (m, 2H), 0.95 – 0.87 (m, 1H), 0.73 (s, 9H), 0.56 (q, J = 12.1 Hz, 1H)

^{13}C NMR (150 MHz, $CDCl_3$) δ 172.1, 140.7, 140.3, 135.9, 129.2, 128.8, 127.3, 127.2, 127.0, 94.9, 74.2, 58.7, 47.7, 41.4, 32.5, 31.8, 31.4, 27.4, 27.1, 26.4

IR (neat): 2926, 1750, 1366, 1218, 1135, 1125, 742, 723, 697 cm-^{1}

HR-MS (+p NSI) calcd for [$C_{26}H_{31}Cl_3O_2$+H] 481.1468 found 481.1468

Chiral HPLC (Chiralcel S,S-Whelk, 0.5% isopropanol in hexane, 0.5 mL/min, λ 210-230 nm) retention times of 41.59 min (major), 49.89 min (minor), 79% ee

2,2,2-trichloroethyl (R)-2-((1S,3R)-3-(tert-butyl)cyclohexyl)-2-(m-tolyl)acetate

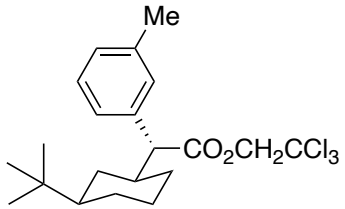

This compound was prepared according to the general procedure for C–H functionalization reaction, using tert-butylcyclohexane (0.75 mmol, 105 mg, 2.5 equiv) as the substrate and 2,2,2-trichloroethyl 2-diazo-2-(m-tolyl)acetate (0.3 mmol, 92 mg, 1.0 equiv) under the catalysis of Rh_2(S-TPPTTL)$_4$ (0.0015 mmol, 3.7 mg, 0.5 mol %). After flash chromatography (0%, then 2% - 3% Et_2O in hexanes) the product was obtained as a clear oil (111 mg, 88% yield).

$[\alpha]^{20}_D$ -13.3° (c = 1.00, $CHCl_3$, 94% ee)

^{1}H NMR (600 MHz, $CDCl_3$) δ 7.24 – 7.11 (m, 3H), 7.09 – 7.05 (m, 1H), 4.79 (d, J = 12.0 Hz, 1H), 4.60 (d, J = 12.0 Hz, 1H), 3.35 (d, J = 10.3 Hz, 1H), 2.35 – 2.31 (s, 3H), 2.07 (tdt, J = 11.7, 10.3, 3.2 Hz, 1H), 1.85 (m, 2H), 1.75 (m, 1H), 1.55 – 1.46 (m, 1H), 1.35 – 1.26 (m, 1H), 1.06 – 0.93 (m, 2H), 0.88 (qd, J = 12.6, 3.6 Hz, 1H), 0.72 (s, 9H), 0.51 (q, J = 12.7, 1H)

^{13}C NMR (150 MHz, $CDCl_3$) δ 172.2, 138.0, 136.7, 129.4, 128.3, 128.2, 125.8, 95.0, 74.1, 59.0, 47.7, 41.2, 32.5, 31.8, 31.3, 27.4, 27.1, 26.3, 21.5

IR (neat): 2951, 1751, 1366, 1261, 1217, 803, 742, 717 cm^{-1}

HR-MS (+p NSI): calcd for [$C_{21}H_{29}Cl_3O_2$+H] 419.1311, found 419.1314

Chiral HPLC (Chiralcel ADH, 0.5% isopropanol in hexane, 0.5 mL/min, λ 230 nm) retention times of 9.82 min (major), 9.23 min (minor), 94% ee

2,2,2-trichloroethyl (R)-2-((1S,3R)-3-(tert-butyl)cyclohexyl)-2-(6-chloropyridin-3-yl)acetate

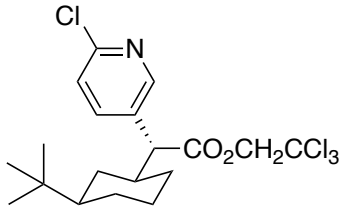

This compound was prepared according to the general procedure for C–H functionalization reaction, using tert-butylcyclohexane (0.75 mmol, 105 mg, 2.5 equiv) as the substrate and 2,2,2-trichloroethyl 2-(6-chloropyridin-3-yl)-2-diazoacetate (0.3 mmol, 99 mg, 1.0 equiv) under the catalysis of Rh_2(S-TPPTTL)$_4$ (0.0015 mmol, 3.7 mg, 0.5 mol %). After flash chromatography (0%, then 2% - 5% Et_2O in hexanes) the product was obtained as a white solid (77 mg, 58% yield).

$[\alpha]^{20}_D$ +1.7° (c = 1.00, $CHCl_3$, 98% ee)

^{1}H NMR (600 MHz, $CDCl_3$) δ 8.33 (m, 1H), 7.74 (dd, J = 8.2, 2.6 Hz, 1H), 7.34 – 7.30 (d, J = 8.4, 1H), 4.77 (d, J = 12.0 Hz, 1H), 4.66 (d, J = 12.0 Hz, 1H), 3.44 (d, J = 9.9 Hz, 1H), 2.05 (tdt, J = 11.7, 9.9, 3.3 Hz, 1H), 1.87 – 1.79 (m, 2H), 1.79 – 1.72 (m, 1H), 1.49 – 1.40 (m, 1H), 1.36 – 1.22 (m, 1H), 1.06 – 0.93 (m, 2H), 0.87 (tdd, J = 12.5, 8.9, 3.6 Hz, 1H), 0.73 (s, 9H), 0.55 (q, J = 12.1 Hz, 1H)

^{13}C NMR (150 MHz, $CDCl_3$) δ 171.0, 150.9, 150.1, 138.7, 131.5, 124.2, 94.6, 74.3, 55.6, 47.6, 41.4, 32.5, 31.6, 31.2, 27.4, 26.8, 26.1

IR (neat): 2931, 1750, 1461, 1366, 1138, 1106, 1022, 773, 721 cm^{-1}

HR-MS (+p NSI): calcd for [$C_{21}H_{25}Cl_4NO_2$+H] 440.0718, found 440.0715

Chiral HPLC (Chiralcel R,R-Whelk, 0.5% isopropanol in hexane, 1 mL/min, λ 230 nm) retention times of 36.01 min (major), 27.23 min (minor), 98% ee

2,2,2-trichloroethyl (R)-2-((1S,3R)-3-(tert-butyl)cyclohexyl)-2-(2-methylbenzo[d]thiazol-6-yl)acetate

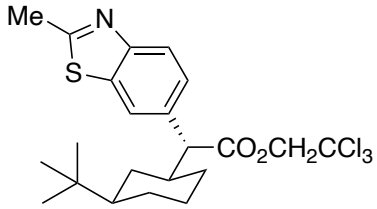

This compound was prepared according to the general procedure for C–H functionalization reaction, using tert-butylcyclohexane (0.75 mmol, 105 mg, 2.5 equiv) as the substrate and 2,2,2-trichloroethyl 2-diazo-2-(2-methylbenzo[d]thiazol-6-yl)acetate (0.3 mmol, 109 mg, 1.0 equiv) under the catalysis of Rh_2(S-TPPTTL)$_4$ (0.0015 mmol, 3.7 mg, 0.5 mol %). After flash chromatography (0%, then 2% - 5% Et_2O in hexanes) the product was obtained as a clear oil (102 mg, 71% yield).

$[\alpha]^{20}_D$ -10.2° (c = 1.00, $CHCl_3$, 98% ee)

^{1}H NMR (600 MHz, $CDCl_3$) δ 7.94 (s, 1H), 7.76 (d, J = 8.2 Hz, 1H), 7.38 (dd, J = 8.3, 1.8 Hz, 1H), 4.76 (d, J = 12.0 Hz, 1H), 4.62 (d, J = 12.0 Hz, 1H), 3.52 (d, J = 10.4 Hz, 1H), 2.83 (s, 3H), 2.15 (tdt, J = 11.6, 10.3, 3.3 Hz, 1H), 1.89 (m, 1H), 1.84 (m, 1H), 1.77 – 1.72 (m, 1H), 1.48 (dt, J = 12.6, 2.7 Hz, 1H), 1.36 – 1.23 (m, 1H), 1.08 – 0.99 (m, 1H), 0.95 (tt, J = 11.7, 2.9 Hz, 1H), 0.88 (td, J = 12.4, 3.6 Hz, 1H), 0.67 (s, 9H), 0.58 – 0.49 (q, J = 12.3, 1H)

^{13}C NMR (150 MHz, $CDCl_3$) δ 172.0, 167.6, 153.7, 135.0, 134.8, 125.3, 122.8, 121.4, 94.9, 74.1, 59.0, 47.7, 41.4, 32.5, 31.8, 31.3, 27.4, 27.0, 26.3, 20.2

IR (neat): 2940, 1748, 1366, 1172, 1110, 794, 737, 716 cm^{-1}

HR-MS (+p APCI): calcd for [$C_{22}H_{28}Cl_3NO_2S$+H] 476.0985 found 476.0981

Chiral HPLC (Chiralcel ODH, 2% isopropanol in hexane, 1 mL/min, λ 230 nm) retention times of 11.01 min (major), 7.13 min (minor), 98% ee

2,2,2-trichloroethyl (R)-2-((1S,3R)-3-(tert-butyl)cyclohexyl)-2-(3-methylisoxazol-5-yl)acetate

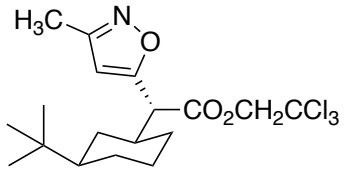

This compound was prepared according to the general procedure for C–H functionalization reaction, using tert-butylcyclohexane (0.75 mmol, 105 mg, 2.5 equiv) as the substrate and 2,2,2-trichloroethyl 2-diazo-2-(3-methylisoxazol-5-yl)acetate (0.3 mmol, 90 mg, 1.0 equiv) under the catalysis of Rh_2(S-TPPTTL)$_4$ (0.0015 mmol, 3.7 mg, 0.5 mol %). After flash chromatography (0%, then 2% - 5% Et_2O in hexanes) the product was obtained as a clear oil that solidified slowly upon standing (51 mg, 41% yield).

MP: 52°C

$[\alpha]^{20}_D$ +6.0° (c = 1.00, $CHCl_3$, 83% ee)

^{1}H NMR (600 MHz, $CDCl_3$) δ 6.15 (s, 1H), 4.84 (d, J = 11.9 Hz, 1H), 4.68 (d, J = 11.9 Hz, 1H), 3.83 (d, J = 8.1 Hz, 1H), 2.30 (s, 3H), 2.10 (tdt, J = 11.7, 8.1, 3.3 Hz, 1H), 1.82 (dp, J = 13.3, 3.4 Hz, 1H), 1.79 – 1.71 (m, 2H), 1.69 – 1.64 (m, 1H), 1.32 – 1.19 (m, 2H), 1.07 – 0.98 (m, 2H), 0.91 – 0.83 (m, 1H), 0.78 (s, 9H)

^{13}C NMR (150 MHz, $CDCl_3$) δ 168.7, 167.7, 159.9, 103.8, 94.5, 74.5, 50.9, 47.8, 41.3, 32.6, 31.3, 30.8, 27.5, 26.8, 26.2, 11.6

IR (neat): 2969, 1739, 1366, 1228, 1217, 802, 741 cm^{-1}

HR-MS (+p APCI): calcd for [$C_{18}H_{26}Cl_3NO_3$+H] 410.1057 found 410.1051

Chiral HPLC (Chiralcel R,R-Whelk, 0.5% isopropanol in hexane, 1 mL/min, λ 230 nm) retention times of 25.22 min (major), 27.94 min (minor), 83% ee

2,2,2-trichloroethyl (R)-2-(4-bromophenyl)-2-((1R,3R,4S)-3,4-dimethylcyclohexyl)acetate

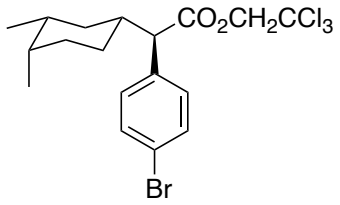

This compound was prepared according to the general procedure for C–H functionalization reaction, using cis-1,2-dimethyl cyclohexane (0.75 mmol, 84 mg, 2.5 equiv) as the substrate and 2,2,2-trichloroethyl 2-(4-bromophenyl)-2-diazoacetate (0.3 mmol, 112 mg, 1.0 equiv) under the catalysis of Rh_2(S-TPPTTL)$_4$ (0.0015 mmol, 3.7 mg, 0.5 mol %). After flash chromatography (0%, then 2% Et_2O in hexanes) the product was obtained as a clear oil (96 mg, 70% yield). The product needed to be converted to the corresponding alcohol for ee determination via chiral HPLC (see general information of this section).

$[\alpha]^{20}_D$ -20.4° (c = 1.00, $CHCl_3$, 98% ee)

^{1}H NMR (600 MHz, $CDCl_3$) δ 7.48 – 7.43 (m, 2H), 7.25 – 7.22 (m, 2H), 4.77 – 4.75 (d, J = 12.0 Hz ,1H), 4.62 (d, J = 12.0 Hz, 1H), 3.32 (d, J = 10.6 Hz, 1H), 2.05 (tdt, J = 11.9, 10.6, 3.4 Hz, 1H), 1.74 (m, 1H), 1.64 – 1.56 (m, 3H), 1.37 – 1.19 (m, 3H), 1.00 – 0.94 (m, 1H), 0.78 (d, J = 7.1 Hz, 3H), 0.73 (d, J = 6.9 Hz, 3H)

^{13}C NMR (150 MHz, $CDCl_3$) δ 171.7, 135.9, 131.7, 130.4, 121.6, 94.8, 74.2, 58.4, 41.3, 34.6, 33.0, 32.2, 32.1, 25.3, 20.0, 11.4

IR (neat): 2927, 1750, 1288, 1144, 1124, 1012, 826, 761, 721 cm^{-1}

HR-MS (+p APCI) calcd for [$C_{18}H_{22}BrCl_3O_2$+H] 454.9947 found 454.9942

Chiral HPLC for the alcohol (Chiralcel R,R-Whelk, 0.5% isopropanol in hexane, 0.8 mL/min, λ 210-230 nm) retention times of 64.22 min (major), 80.26 min (minor), 98% ee

2,2,2-trichloroethyl (R)-2-(4-bromophenyl)-2-((1R,3R,4R)-3,4-dimethylcyclohexyl)acetate

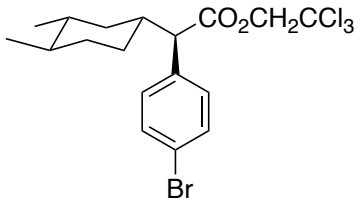

This compound was prepared according to the general procedure for C–H functionalization reaction, using trans-1,2-dimethyl cyclohexane (0.75 mmol, 84 mg, 2.5 equiv) as the substrate and 2,2,2-trichloroethyl 2-(4-bromophenyl)-2-diazoacetate (0.3 mmol, 112 mg, 1.0 equiv) under the catalysis of Rh_2(S-TPPTTL)$_4$ (0.0015 mmol, 3.7 mg, 0.5 mol %). After flash chromatography (0%, then 2% Et_2O in hexanes) the product was obtained as a clear oil (102 mg, 75% yield).

$[\alpha]^{20}_D$ -6.4° (c = 1.00, $CHCl_3$, 85% ee)

^{1}H NMR (600 MHz, $CDCl_3$) δ 7.45 (m, 2H), 7.25 – 7.21 (m, 2H), 4.75 (d, J = 12.0 Hz, 1H), 4.64 (d, J = 11.9 Hz, 1H), 3.30 (d, J = 10.6 Hz, 1H), 2.15 – 2.01 (m, 1H), 1.86 (m, 1H), 1.74 – 1.67 (m, 1H), 1.28 (m, 1H), 1.17 – 1.02 (m, 2H), 0.97 – 0.89 (m, 2H), 0.88 (d, J = 4.6 Hz, 3H), 0.78 (d, J = 5.9 Hz, 3H), 0.58 – 0.48 (m, 1H)

^{13}C NMR (150 MHz, $CDCl_3$) δ 171.7, 136.0, 131.7, 130.4, 121.6, 94.8, 74.2, 58.3, 41.0, 39.2, 38.8, 38.6, 35.0, 31.9, 20.1, 19.8

IR (neat) 2924, 1750, 1488, 1185, 1124, 1012, 825, 760, 719 cm^{-1}

HR-MS (+p APCI) calcd for [$C_{18}H_{22}BrCl_3O_2$+H] 454.9947 found 454.9940

Chiral HPLC (Chiralcel R,R-Whelk, 0% isopropanol in hexane, 0.5 mL/min, λ 230 nm) retention times of 49.19 min (major), 40.10 min (minor), 85% ee

2,2,2-trichloroethyl (R)-2-(4-bromophenyl)-2-((1s,3R,5S)-3,5-dimethylcyclohexyl)acetate

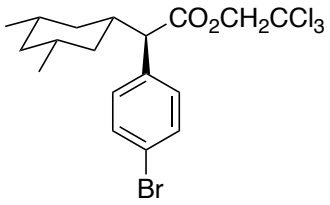

This compound was prepared according to the general procedure for C–H functionalization reaction, using cis-1,3-dimethyl cyclohexane (0.75 mmol, 84 mg, 2.5 equiv) as the substrate and 2,2,2-trichloroethyl 2-(4-bromophenyl)-2-diazoacetate (0.3 mmol, 112 mg, 1.0 equiv) under the catalysis of Rh_2(S-TPPTTL)$_4$ (0.0015 mmol, 3.7 mg, 0.5 mol %). After flash chromatography (0%, then 2% Et_2O in hexanes) the product was obtained as a clear oil (85 mg, 62% yield).

$[\alpha]^{20}_D$ -5.7° (c = 1.00, $CHCl_3$, 59% ee)

^{1}H NMR (600 MHz, $CDCl_3$) δ 7.48 – 7.44 (m, 2H), 7.25 – 7.22 (m, 2H), 4.75 (d, J = 12.0 Hz, 1H), 4.66 (d, J = 12.0 Hz, 1H), 3.30 (d, J = 10.6 Hz, 1H), 2.11 (tdt, J = 11.7, 10.5, 3.3 Hz, 1H), 1.80 (m, 1H), 1.64 (m, 1H), 1.54 – 1.41 (m, 1H), 1.40 – 1.32 (m, 1H), 1.08 – 0.98 (m, 1H), 0.89 (d, J = 6.6 Hz, 3H), 0.78 (d, J = 6.5 Hz, 3H), 0.68 (q, J = 11.9 Hz, 1H), 0.55 – 0.47 (q, J = 12.4, 1H), 0.36 (q, J = 12.1 Hz, 1H)

^{13}C NMR (150 MHz, $CDCl_3$) δ 171.7, 135.9, 131.7, 130.4, 121.6, 94.8, 74.1, 58.3, 43.7, 40.7, 40.1, 38.4, 32.1, 32.1, 22.5, 22.5

IR (neat): 2924, 1750, 1488, 1371, 1137, 1126, 1011, 826, 760, 719 cm^{-1}

HR-MS (+p APCI) calcd for [$C_{18}H_{22}BrCl_3O_2$+H] 454.9947 found 454.9940

Chiral HPLC (Chiralcel S,S-Whelk, 0.5% isopropanol in hexane, 0.5 mL/min, λ 210-230 nm) retention times of 21.78 min (major), 18.39 min (minor), 59% ee

2,2,2-trichloroethyl (R)-2-(4-bromophenyl)-2-((1R,3S)-1,3-dimethylcyclohexyl)acetate

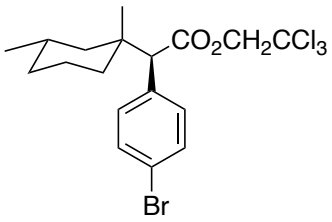

This compound was prepared according to the general procedure for C–H functionalization reaction, using trans-1,3-dimethyl cyclohexane (0.75 mmol, 84 mg, 2.5 equiv) as the substrate and 2,2,2-trichloroethyl 2-(4-bromophenyl)-2-diazoacetate (0.3 mmol, 112 mg, 1.0 equiv) under the catalysis of Rh_2(S-TPPTTL)$_4$ (0.0015 mmol, 3.7 mg, 0.5 mol %). After flash chromatography (0%, then 2% Et_2O in hexanes) the product was obtained as a clear oil (110 mg, 70% yield).

$[\alpha]^{20}_D$ -5.2° (c = 1.00, $CHCl_3$, 93% ee)

^{1}H NMR (500 MHz, $CDCl_3$) δ 7.44 (d, J = 8.6 Hz, 2H), 7.30 (d, J = 8.5 Hz, 2H), 4.83 (d, J = 12.0 Hz, 1H), 4.59 (d, J = 12.0 Hz, 1H), 3.49 (s, 1H), 1.67 – 1.60 (m, 1H), 1.58 – 1.19 (m, 6H), 1.17 – 1.07 (m, 1H), 1.04 (s, 3H), 0.82 (dd, J = 15.5, 6.4 Hz, 3H), 0.76 – 0.65 (m, 1H)

^{13}C NMR (125 MHz, $CDCl_3$) δ 171.0, 133.5, 132.0, 130.9, 121.6, 94.8, 74.1, 63.2, 44.2, 38.2, 35.4, 34.7, 27.8, 22.9, 21.6, 19.4

IR (neat): 2924, 1748, 1489, 1172, 1136, 1012, 827, 760, 721 cm^{-1}

HR-MS (+p APCI) calcd for [$C_{18}H_{22}BrCl_3O_2$+H] 454.9947 found 454.9940

Chiral HPLC (Chiralcel S,S-Whelk, 0.5% isopropanol in hexane, 0.5 mL/min, λ 210-230 nm) retention times of 11.94 min (major), 14.35 min (minor), 93% ee

2,2,2-trichloroethyl (R)-2-(4-bromophenyl)-2-((1r,4R)-1,4-dimethylcyclohexyl)acetate

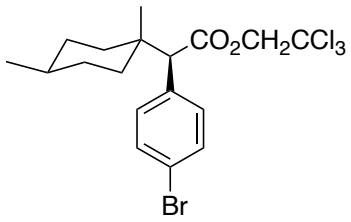

This compound was prepared according to the general procedure for C–H functionalization reaction, using cis-1,4-dimethyl cyclohexane (0.75 mmol, 84 mg, 2.5 equiv) as the substrate and 2,2,2-trichloroethyl 2-(4-bromophenyl)-2-diazoacetate (0.3 mmol, 112 mg, 1.0 equiv) under the catalysis of Rh_2(S-TPPTTL)$_4$ (0.0015 mmol, 3.7 mg, 0.5 mol %). After flash chromatography (0%, then 2% Et_2O in hexanes) the product was obtained as a clear oil (110 mg, 80% yield).

$[\alpha]^{20}_D$ -5.2° (c = 1.00, $CHCl_3$, 94% ee)

^{1}H NMR (600 MHz, $CDCl_3$) δ 7.47 – 7.41 (m, 2H), 7.32 – 7.28 (m, 2H), 4.81 (d, J = 12.0 Hz, 1H), 4.60 (d, J = 12.0 Hz, 1H), 3.50 (s, 1H), 1.58 – 1.43 (m, 4H), 1.39 (m, 1H), 1.31 – 1.22 (m, 2H), 1.15 – 1.04 (m, 2H), 1.03 (s, 3H), 0.87 (d, J = 6.5 Hz, 3H)

^{13}C NMR (150 MHz, $CDCl_3$) δ 167.0, 132.6, 130.9, 129.9, 120.6, 93.8, 73.1, 61.8, 36.1, 34.7, 34.1, 31.3, 29.5, 29.2, 21.3, 17.8

IR (neat): 2922, 1749, 1489, 1264, 1172, 1116, 1012, 828, 761, 743, 722 cm^{-1}

HR-MS (- ESI) calcd for [$C_{18}H_{22}BrCl_3O_2$-H] 452.9785 found 452.9793

Chiral HPLC (Chiralcel S,S-Whelk, 0.25% isopropanol in hexane, 0.25 mL/min, λ 230 nm) retention times of 20.65 min (major), 22.92 min (minor), 94% ee

2,2,2-trichloroethyl (R)-2-(4-bromophenyl)-2-((1s,4S)-1,4-dimethylcyclohexyl)acetate

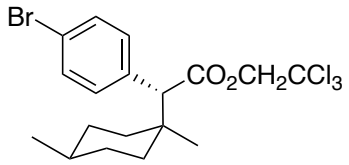

This compound was prepared according to the general procedure for C–H functionalization reaction, using trans-1,4-dimethyl cyclohexane (0.75 mmol, 84 mg, 2.5 equiv) as the substrate and 2,2,2-trichloroethyl 2-(4-bromophenyl)-2-diazoacetate (0.3 mmol, 112 mg, 1.0 equiv) under the catalysis of Rh_2(S-TPPTTL)$_4$ (0.0015 mmol, 3.7 mg, 0.5 mol %). After flash chromatography (0%, then 2% Et_2O in hexanes) the product was obtained as a clear oil that solidified slowly upon standing (105 mg, 77% yield).

MP: 84^{o}C

$[\alpha]^{20}_D$ -8.0^o (c = 1.00, $CHCl_3$, 95% ee)

^{1}H NMR (600 MHz, $CDCl_3$) δ 7.45 – 7.43 (m, 2H), 7.36 – 7.31 (m, 2H), 4.88 (d, J = 12.0 Hz, 1H), 4.55 (d, J = 12.0 Hz, 1H), 4.11 (s, 1H), 1.81 (m, 1H), 1.59 – 1.52 (m, 2H), 1.47 – 1.26 (m, 6H), 1.04 (s, 3H), 0.97 (d, J = 6.4 Hz, 3H)

^{13}C NMR (150 MHz, $CDCl_3$) δ 170.1, 133.1, 130.8, 130.0, 129.9, 120.6, 93.7, 73.3, 35.6, 34.0, 33.8, 30.8, 29.1, 29.0, 23.6, 20.9

IR (neat): 2922, 1750, 1489, 1135, 1109, 1012, 831, 761, 722 cm^{-1}

HR-MS (+p APCI) calcd for [$C_{18}H_{22}BrCl_3O_2$+H] 454.9947 found 454.9940

Chiral HPLC (Chiralcel S,S-Whelk, 0.5% isopropanol in hexane, 0.5 mL/min, λ 230 nm) retention times of 13.92 min (major), 11.74 min (minor), 95% ee

2,2,2-trichloroethyl (R)-2-(4-bromophenyl)-2-((2R,4aR,8aR)-decahydronaphthalen-2-yl)acetate

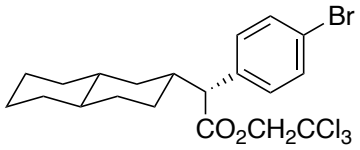

This compound was prepared according to the general procedure for C–H functionalization reaction, using trans-decahydronaphthalene (0.75 mmol, 103.5 mg, 2.5 equiv) as the substrate and 2,2,2-trichloroethyl 2-(4-bromophenyl)-2-diazoacetate (0.3 mmol, 112 mg, 1.0 equiv) under the catalysis of Rh_2(S-TPPTTL)$_4$ (0.0015 mmol, 3.7 mg, 0.5 mol %). After flash chromatography (0%, then 2% - 3% Et_2O in hexanes) the product was obtained as a white solid (104 mg, 72% yield).

MP: 85°C

$[\alpha]^{20}_D$ -10.8° (c = 1.00, $CHCl_3$, 90% ee)

^{1}H NMR (600 MHz, $CDCl_3$) δ 7.48 – 7.43 (m, 2H), 7.25 – 7.21 (m, 2H), 4.74 (d, J = 11.9 Hz, 1H), 4.63 (d, J = 12.0 Hz, 1H), 3.30 (d, J = 10.6 Hz, 1H), 2.10 (m, 1H), 1.87 (m, 1H), 1.71 – 1.53 (m, 5H), 1.40 (d, J = 10.4 Hz, 1H), 1.28 – 1.02 (m, 5H), 0.94 – 0.75 (m, 4H), 0.52 (q, J = 12.4 Hz, 1H)

^{13}C NMR (150 MHz, $CDCl_3$) δ 171.7, 136.0, 131.7, 130.4, 121.5, 94.8, 74.2, 58.3, 43.0, 42.6, 41.0, 37.6, 33.8, 33.6, 33.3, 31.8, 26.5, 26.4

IR (neat): 2918, 2849, 1750, 1488, 1126, 1012, 827, 761, 720 cm^{-1}

HR-MS (+p APCI) calcd for [$C_{20}H_{24}BrCl_3O_2$+H] 481.0104 found 481.0102

Chiral HPLC (Chiralcel S,S-Whelk, 0% isopropanol in hexane, 0.5 mL/min, λ 210-230 nm) retention times of 43.54 min (major),54.74 min (minor), 90% ee

2,2,2-trichloroethyl (R)-2-(4-bromophenyl)-2-((2R,4aS,8aR)-decahydronaphthalen-2-yl)acetate

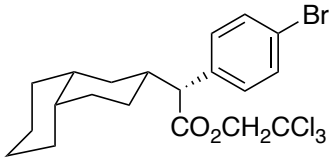

This compound was prepared according to the general procedure for C–H functionalization reaction, using cis-decahydronaphthalene (0.75 mmol, 103.5 mg, 2.5 equiv) as the substrate and 2,2,2-trichloroethyl 2-(4-bromophenyl)-2-diazoacetate (0.3 mmol, 112 mg, 1.0 equiv) under the catalysis of Rh_2(S-TPPTTL)$_4$ (0.0015 mmol, 3.7 mg, 0.5 mol %). After flash chromatography (0%, then 2% - 3% Et_2O in hexanes) the product was obtained as a clear oil (98 mg, 68% yield).

$[\alpha]^{20}_D$ -34.2° (c = 1.00, $CHCl_3$, 98% ee)

^{1}H NMR (600 MHz, $CDCl_3$) δ 7.50 – 7.43 (m, 2H), 7.29 – 7.21 (m, 2H), 4.78 (d, J = 12.0 Hz, 1H), 4.64 (d, J = 12.0, 1H), 3.39 (d, J = 10.6 Hz, 1H), 2.14 – 2.05 (m, 1H), 1.66 – 1.00 (m, 15H), 0.94 – 0.87 (m, 1H)

^{13}C NMR (150 MHz, $CDCl_3$) δ 171.8, 135.9, 131.7, 130.5,121.6, 94.8, 74.1, 58.4, 41.6, 35.7, 35.4, 32.1, 31.9, 29.2, 26.9, 26.3, 25.7, 20.8

IR (neat): 2922, 1748, 1488, 1122, 1011, 908, 760, 719 cm^{-1}

HR-MS (+p APCI) calcd for [$C_{20}H_{24}BrCl_3O_2$+H] 481.0104 found 481.0101

Chiral HPLC (Chiralcel R,R-Whelk, 0.5% isopropanol in hexane, 1 mL/min, λ 230 nm) retention times of 12.88 min (major), 9.46 min (minor), 98% ee

Chiral HPLC study for determining the stereoconfiguration of the minor diastereomer

Because the desymmetrization reaction of monosubstituted cyclohexanes produces the C–H functionalization products that contain three stereocenters, we sought to determine the structure of the minor diastereomer that are indicated in the above crude ^{1}H NMR spectra. Because the stereoisomers are not separable using standard laboratory chromatographic techniques, a detailed chiral HPLC study was carried out to determine the stereoconfiguration of the minor diastereomer by racemizing the chiral center at the carbene carbon and then carefully compare the resulting HPLC spectra and the retention times of the peaks.

In the following scheme, **A** is determined by X-ray crystallography to be the major enantiomer of the major diastereomer. Consequently, **B** is determined to be the minor enantiomer. Another reaction was run under the same condition except that a racemization is conducted with the addition of DBU (2 equiv), so that **C** is produced from **A**, and a trace amount of **D** is produced from **B**. It is important to note that without this racemization, **C** is not observed in the reaction, as the catalyst has excellent control of stereochemistry at the carbene carbon (as shown in the C–H functionalization of cyclohexane, where the product was obtained with 99% ee). It was concluded from this study that the minor diastereomer is due to competition between C-3 and C-5 insertion (enantiotopic hydrogens), rather than to inverse stereochemistry at the carbene carbon. See following annotated chiral HPLC spectra for detailed comparison.

racemic standard

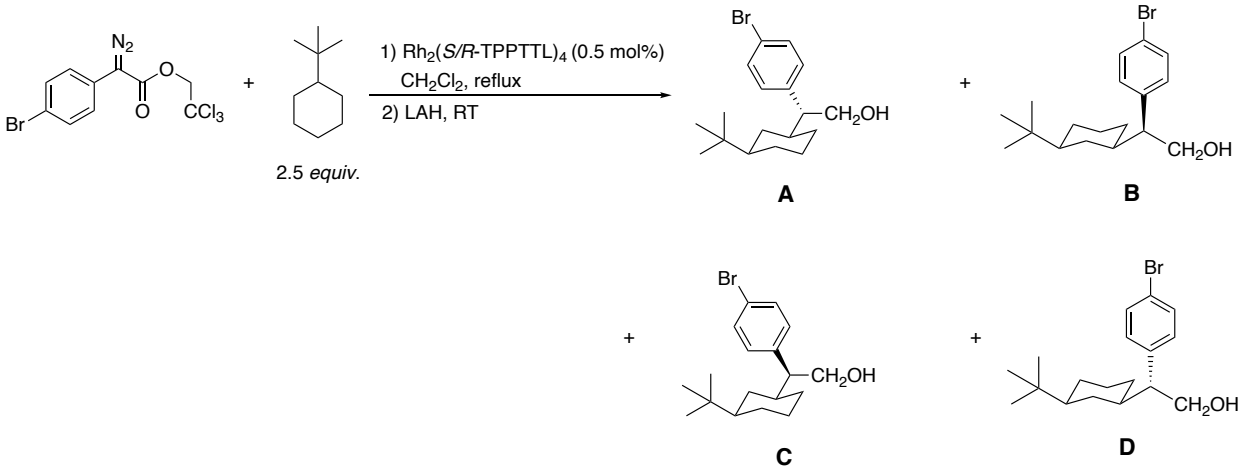

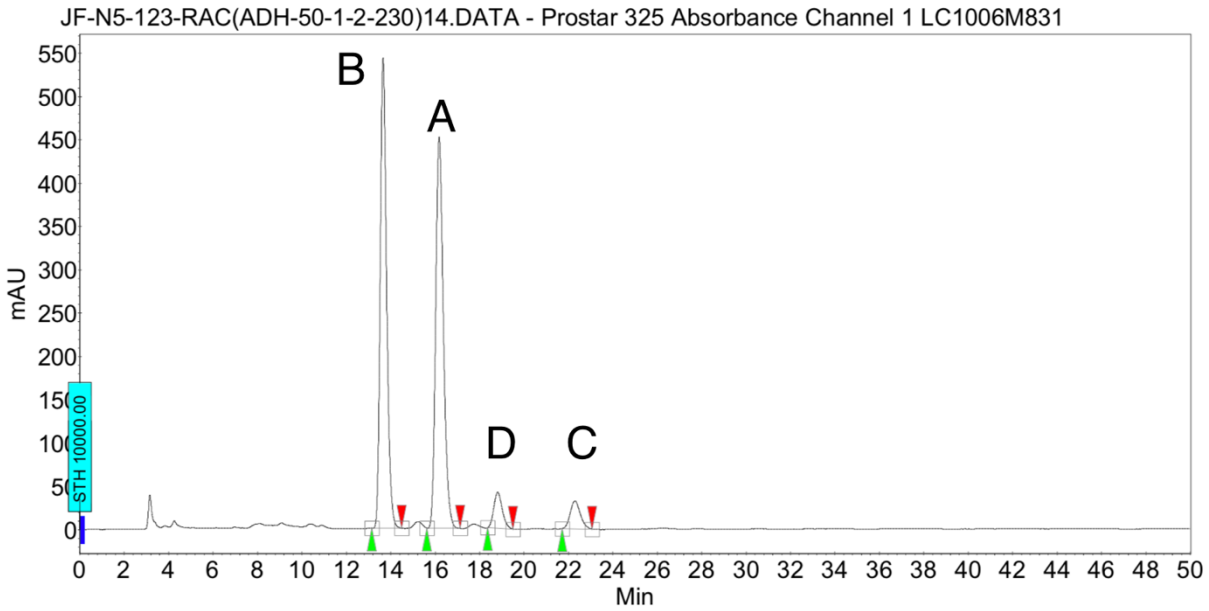

Peak results :

Index	Name	Time [Min]	Quantity [% Area]	Height [mAU]	Area [mAU.Min]	Area % [%]
1	UNKNOWN	13.65	45.52	543.1	180.9	45.521
2	UNKNOWN	16.18	45.59	451.8	181.2	45.590
3	UNKNOWN	18.82	4.61	41.6	18.3	4.610
4	UNKNOWN	22.29	4.28	32.1	17.0	4.278
Total			100.00	1068.6	397.4	100.000

Chiral reaction for e.e. determination

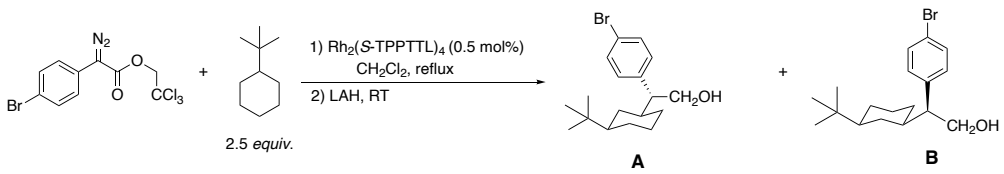

major enantiomer
as defined by X-ray
95% e.e.

minor enantiomer

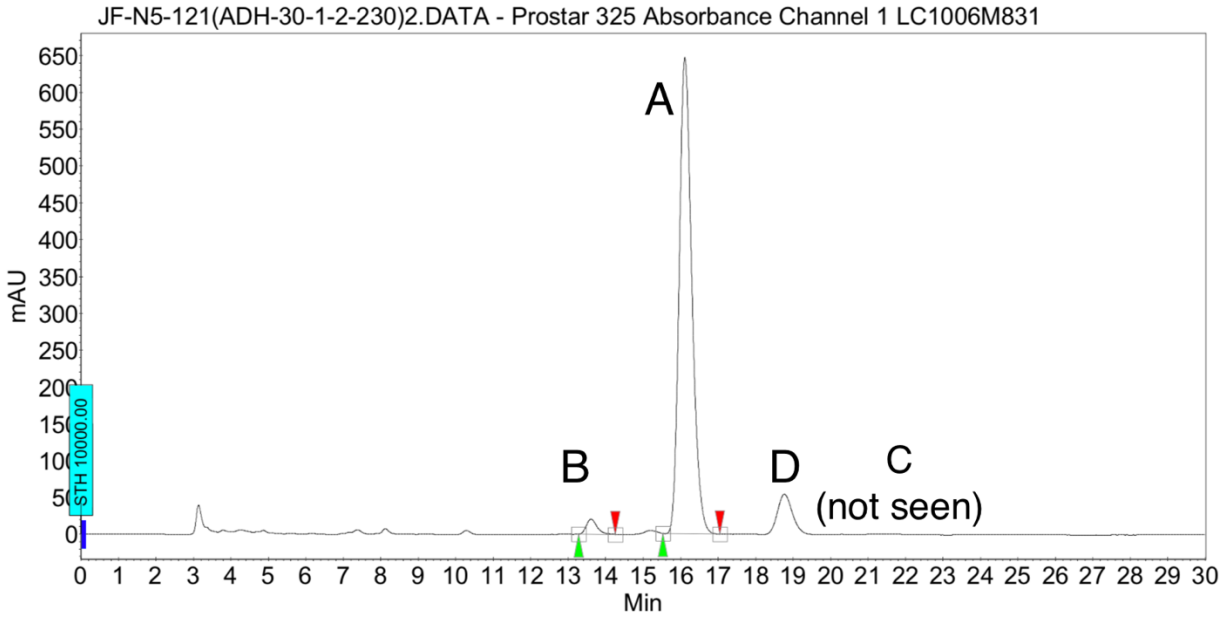

Peak results :

Index	Name	Time [Min]	Quantity [% Area]	Height [mAU]	Area [mAU.Min]	Area % [%]
1	UNKNOWN	13.61	2.63	20.6	6.8	2.628
2	UNKNOWN	16.11	97.37	647.1	253.5	97.372
Total			100.00	667.6	260.3	100.000

Chiral reaction, then racemization by DBU

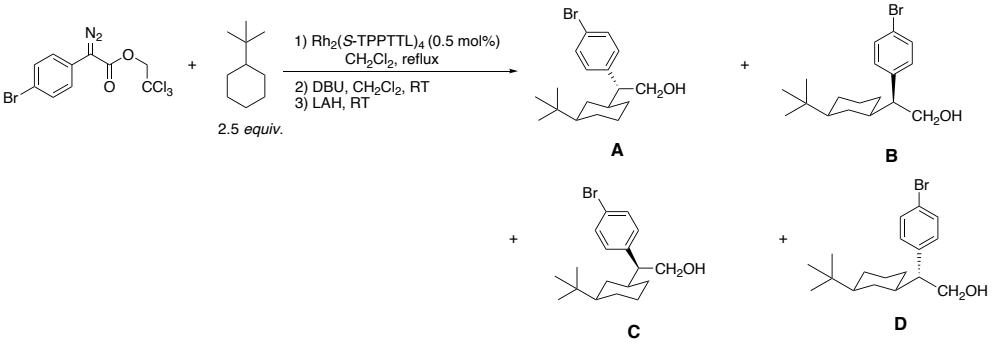

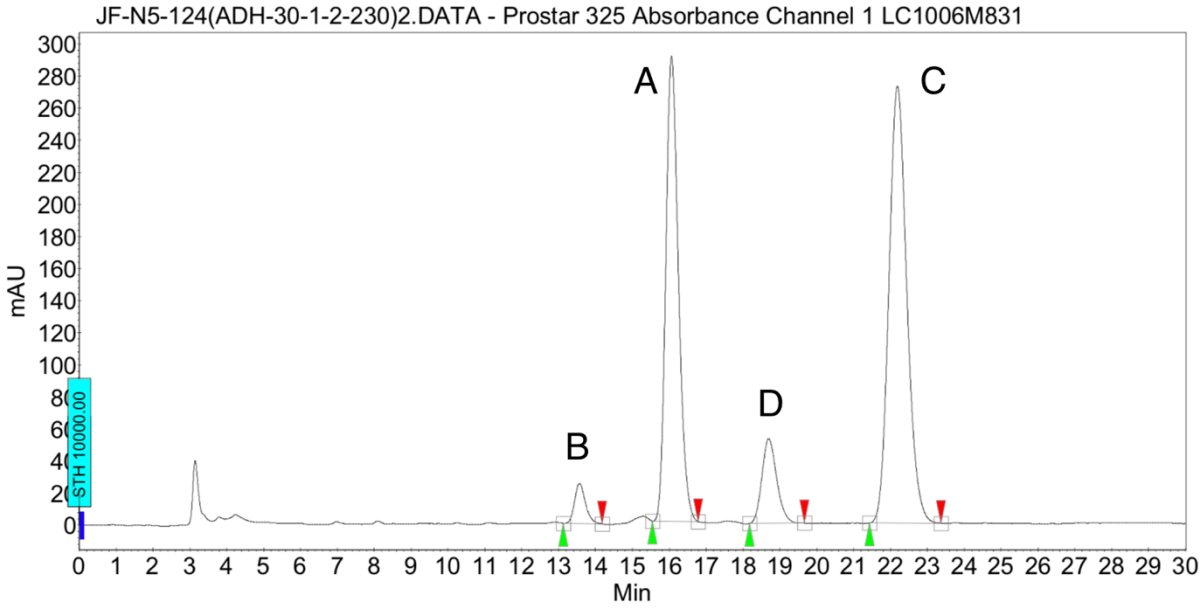

Peak results :

Index	Name	Time [Min]	Quantity [% Area]	Height [mAU]	Area [mAU.Min]	Area % [%]
3	UNKNOWN	13.57	2.84	25.0	8.6	2.844
1	UNKNOWN	16.06	38.12	289.9	114.7	38.119
4	UNKNOWN	18.70	8.15	52.8	24.5	8.154
2	UNKNOWN	22.19	50.88	272.3	153.2	50.883
Total			100.00	640.1	301.0	100.000

Substrate competition study to determine axial/equatorial selectivity

Within the area of Rh(II)-catalyzed carbene insertion reactions, substrate competition studies have been performed on various systems, such as among olefin cyclopropanation, insertion into activated (by heteroatoms) and unactivated alkanes. However, one area that has not been looked at is the selectivity between axial and equatorial functionalization in cyclohexanes, presumably due to a clean and appropriate system for this study was not established. Here, we demonstrate, using Rh_2(S-TPPTTL)$_4$ and a substrate competition experiment, that equatorial C–H bond functionalization is preferred to a very large extent as compared to axial C–H bond. In the following reaction, product **41** was formed only in trace amount (**40**:**41**=70:1). Note that trans-1,2-dimethylcyclohexane has two identical axial C–H bonds available, and this was considered when calculating the product ratio.

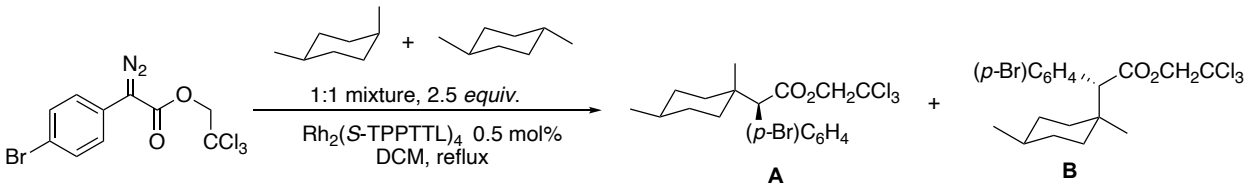
N2
O
O
CCl3
Br
+
1:1 mixture, 2.5 equiv.
Rh2(S-TPPTTL)4 0.5 mol%
DCM, reflux
CO2CH2CCl3
(p-Br)C6H4
A
+
(p-Br)C6H4
CO2CH2CCl3
B

A:**B** = 70:1

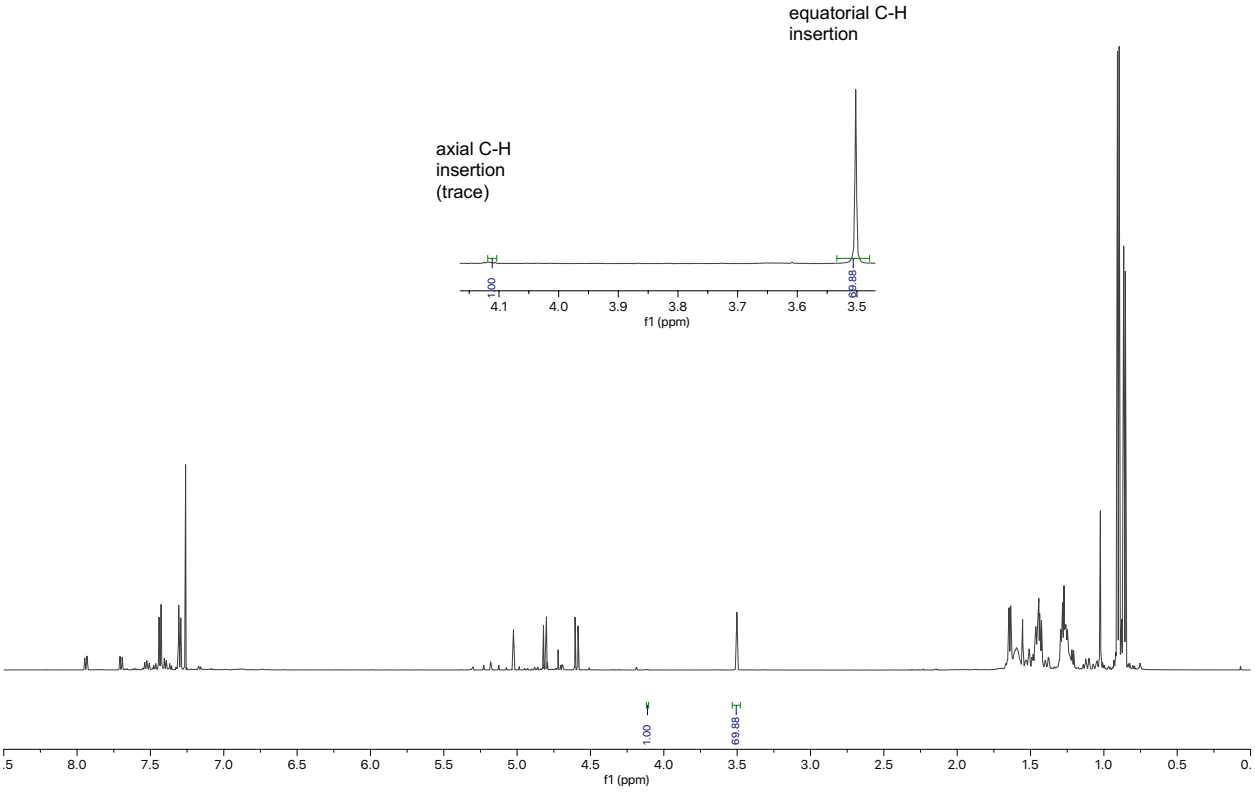
equatorial C-H
insertion
axial C-H
insertion
(trace)
1.00
69.88
4.1
4.0
3.9
3.8
3.7
3.6
3.5
f1 (ppm)
1.00
69.88
8.0
7.5
7.0
6.5
6.0
5.5
5.0
4.5
4.0
3.5
3.0
2.5
2.0
1.5
1.0
0.5
f1 (ppm)

Experimental Section for

Chapter 3.2.5: Regio- and Stereoselective Functionalization of Organosilanes

Substrates and reagents

The following compounds were purchased from commercial sources and used without further purification:

Sigma-Aldrich: 1-chloro-1-methylsiletane

Gelest: cyclotrimethylenedimethylsilane

The following diazo compounds were prepared according to published procedures

2,2,2-trichloroethyl 2-(6-chloropyridin-3-yl)-2-diazoacetate[1]

2,2,2-trichloroethyl 2-(2-chloropyrimidin-5-yl)-2-diazoacetate[1]

2,2,2-trichloroethyl 2-diazo-2-(4-(N-methylacetamido)phenyl)acetate[1]

2,2,2-trichloroethyl 2-diazo-2-(2-methylbenzo[d]thiazol-5-yl)acetate[1]

2,2,2-trichloroethyl 2-(4-bromothiophen-2-yl)-2-diazoacetate[2]

General procedure for C–H functionalization of organosilanes

An oven-dried round bottom flask was equipped with stir bar and cooled under vacuum. A second oven-dried round bottom flask was cooled under vacuum. After cooling both flasks to room temperature, the flask with the stir bar was loaded with Rh catalyst (0.5 mol %), silane (3 equiv) and trifluorotoluene as solvent (1 mL per mmol silane). Diazo compound (1 equiv) was added to the second flask and dissolved in solvent (6 mL per mmol diazo compound). The solution of diazo compound was added to the first solution of catalyst and silane dropwise via syringe pump over 3

hours. The reaction mixture was allowed to stir at least 2h after the addition was complete, but could be left overnight without product decomposition or ee erosion. Then the solvent was removed under reduced pressure. The crude residue was then directly subjected to silica gel chromatography for purification.

2,2,2-Trichloroethyl (*R*)-2-(6-chloropyridin-3-yl)-2-(1,1-dimethylsiletan-3-yl)acetate

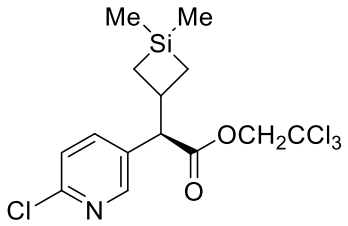

This compound was prepared according to the general procedure for C–H functionalization reaction, using 1,1-dimethylsiletane (150.0 mg, 1.50 mmol, 3 equiv) as the substrate and 2,2,2-trichloroethyl 2-(6-chloropyridin-3-yl)-2-diazoacetate (164.5 mg, 0.5 mmol) under the catalysis of Rh_2(S-TPPTTL)$_4$ (6.2 mg, 0.5 mol %). After flash chromatography (0%, then 2% - 15% Et_2O in hexanes) the product was obtained as a colorless oil (133.4 mg, 67% yield).

[α]$^{23}_{D}$ -8.9 (*c* = 1.0, CH_2Cl_2)

^{1}H NMR (500 MHz, $CDCl_3$) δ 8.34 (d, *J* = 2.3 Hz, 1H), 7.73 (dd, *J* = 8.3, 2.5 Hz, 1H), 7.30 (d, *J* = 8.3 Hz, 1H), 4.78 (d, *J* = 12.0 Hz, 1H), 4.66 (d, *J* = 12.0 Hz, 1H), 3.52 (d, *J* = 10.5 Hz, 1H), 2.86–2.75 (m, 1H), 1.37–1.29 (m, 1H), 0.90–0.82 (m, 2H), 0.53 (dd, *J* = 14.0, 10.9 Hz, 1H), 0.28 (s, 3H), 0.28 (s, 3H)

^{13}C NMR (126 MHz, $CDCl_3$) δ 170.9, 150.8, 149.9, 138.5, 132.1, 124.3, 94.8, 74.4, 59.1, 36.0, 20.7, 19.9, 1.4, -2.0

IR (neat) 2959, 1749, 1584, 1565, 1457, 1390, 1249, 1122, 1105, 832, 807 cm^{-1}

HRMS (NSI+) calcd for [$C_{14}H_{18}O_2NCl_4Si$+ H] 399.98554 found 399.98572

Chiral HPLC (Chiralcel R,R-Whelk, 1% isopropanol in hexane, 1 mL/min, λ 230 nm) retention times of 10.5 min and 12.8 min, 98% ee

(*R*)-2-chloro-5-(1-(1,1-dimethylsiletan-3-yl)-2-((2,2,2-trichloroethyl)peroxy)ethyl)pyrimidine

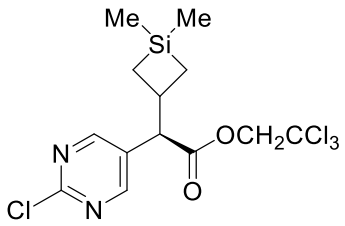

This compound was prepared according to the general procedure for C–H functionalization reaction, using 1,1-dimethylsiletane (150.0 mg, 1.50 mmol, 3 equiv) as the substrate and 2,2,2-trichloroethyl 2-(2-chloropyrimidin-5-yl)-2-diazoacetate (165.0 mg, 0.5 mmol) under the catalysis of Rh_2(S-TPPTTL)$_4$ (6.2 mg, 0.5 mol %). After flash chromatography (10%, then 0% EtOAc in hexanes) the product was obtained as a slightly brown oil (82.0 mg, 41% yield).

[α]$^{23}_{D}$ -2.9 (*c* = 1.0, CH_2Cl_2)

^{1}H NMR (500 MHz, $CDCl_3$) δ 8.64 (s, 2H), 4.79 (d, *J* = 11.9 Hz, 1H), 4.69 (d, *J* = 12.0 Hz, 1H), 3.52 (d, *J* = 10.3 Hz, 1H), 2.80 (m, 1H), 1.39–1.28 (m, 1H), 0.96–0.84 (m, 2H), 0.59–0.48 (m, 1H), 0.29 (s, 3H), 0.28 (s, 3H)

^{13}C NMR (126 MHz, $CDCl_3$) δ 170.0, 160.6, 159.3, 129.5, 94.4, 74.5, 56.8, 36.0, 20.6, 19.9, 1.2, 1.2, -2.2

IR (neat) 2960, 1750, 1577, 1547, 1398, 1153, 1124, 807, 718, 574 cm^{-1}

HRMS (APCI+) calcd for [$C_{14}H_{18}O_2NCl_4Si$+ H] 400.98079 found 400.98114

Chiral HPLC (Chiralpak IA-U, 3% isopropanol in hexane, 0.5 mL/min, λ 280 nm) retention times of 3.0 min and 3.2 min, 87% ee

2,2,2-Trichloroethyl (*S*)-2-(4-bromothiophen-2-yl)-2-(1,1-dimethylsiletan-3-yl)acetate

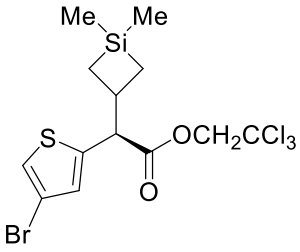

This compound was prepared according to the general procedure for C–H functionalization reaction, using 1,1-dimethylsiletane (150.0 mg, 1.50 mmol, 3 equiv) as the substrate and 2,2,2-trichloroethyl 2-(4-bromothiophen-2-yl)-2-diazoacetate (189.2 mg, 0.5 mmol) under the catalysis of Rh_2(S-TPPTTL)$_4$ (6.2 mg, 0.5 mol %). After flash chromatography (1%, then 2% - 15% Et_2O in hexanes) the product was obtained as a colorless oil (121.7 mg, 54% yield).

[α]$^{23}_{D}$ -13.1 (*c* = 1.0, CH_2Cl_2)

^{1}H NMR (500 MHz, $CDCl_3$) δ 7.12 (d, *J* = 1.5 Hz, 1H), 6.93 (d, *J* = 1.5 Hz, 1H), 4.80 (d, *J* = 12.0 Hz, 1H), 4.68 (d, *J* = 11.9 Hz, 1H), 3.74 (d, *J* = 10.2 Hz, 1H), 2.78 (tdd, *J* = 10.5, 8.1, 2.4 Hz, 1H), 1.32–1.22 (m, 1H), 1.11–1.01 (m, 1H), 0.85 (dd, *J* = 13.9, 10.7 Hz, 1H), 0.67 (dd, *J* = 14.1, 10.9 Hz, 1H), 0.29 (s, 3H), 0.28 (s, 3H)

^{13}C NMR (126 MHz, $CDCl_3$) δ 170.6, 140.9, 128.8, 122.3, 109.2, 94.8, 74.5, 57.4, 37.1, 20.4, 20.2, 1.4, -1.9

IR (neat) 2958, 1751, 1522, 1249, 1213, 1122, 829, 807, 741, 719 cm^{-1}

HRMS (APCI+) calcd for [$C_{14}H_{18}O_2NCl_4Si$+ H] 448.89620 found 448.89665

Chiral HPLC (Chiralcel R,R-Whelk, 0.5% isopropanol in hexane, 0.5 mL/min, λ 210 nm) retention times of 10.4 min and 11.7 min, 91% ee

(*R*)-*N*-(4-(1-(1,1-dimethylsiletan-3-yl)-2-((2,2,2-trichloroethyl)peroxy)ethyl)phenyl)-*N*-methylacetamide

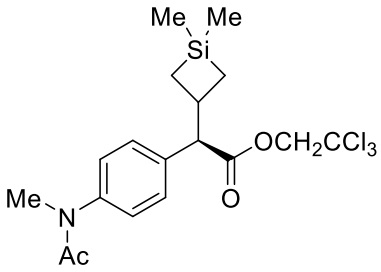

This compound was prepared according to the general procedure for C–H functionalization reaction, using 1,1-dimethylsiletane (150.0 mg, 1.50 mmol, 3 equiv) as the substrate and 2,2,2-trichloroethyl 2-diazo-2-(4-(N-methylacetamido)phenyl)acetate (182.3 mg, 0.5 mmol) under the catalysis of Rh_2(S-TPPTTL)$_4$ (6.2 mg, 0.5 mol %). After flash chromatography (10%, then 15% EtOAc in hexanes) the product was obtained as a colorless oil (141.9 mg, 65% yield).

[α]$^{23}_{D}$ -26.3 (*c* = 1.0, CH_2Cl_2)

^{1}H NMR (500 MHz, $CDCl_3$) δ 7.95 (s, 1H), 7.76 (d, *J* = 8.3 Hz, 1H), 7.39 (d, *J* = 6.9 Hz, 1H), 4.78 (d, *J* = 12.0 Hz, 1H), 4.64 (d, *J* = 12.0 Hz, 1H), 3.64 (d, *J* = 10.6 Hz, 1H), 3.03–2.90 (m, 1H), 2.83 (s, 3H), 1.37 (m, 1H), 0.91–0.83 (m, 2H), 0.57 (dd, *J* = 14.2, 10.8 Hz, 1H), 0.28 (s, 3H), 0.28 (s, 3H)

^{13}C NMR (126 MHz, $CDCl_3$) δ 171.8, 167.5, 153.7, 135.5, 134.7, 125.1, 122.3, 121.2, 94.9, 74.0, 62.3, 35.7, 20.6, 20.2, 19.7, -2.0

IR (neat) 2858, 1750, 1526, 1249, 1120, 832, 807, 760, 718 cm^{-1}

HRMS (APCI+) calcd for [$C_{14}H_{18}O_2NCl_4Si$+ H] 436.06628 found 436.06682

Chiral HPLC (Chiralpak IA-U, 2% isopropanol in hexane, 0.5 mL/min, λ 280 nm) retention times of 6.6 min and 6.8 min, 95% ee

2,2,2-trichloroethyl (*R*)-2-(1,1-dimethylsiletan-3-yl)-2-(2-methylbenzo[*d*]thiazol-5-yl)acetate

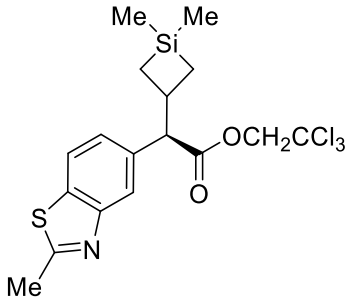

This compound was prepared according to the general procedure for C–H functionalization reaction, using 1,1-dimethylsiletane (150.0 mg, 1.50 mmol, 3 equiv) as the substrate and 2,2,2-trichloroethyl 2-diazo-2-(2-methylbenzo[d]thiazol-5-yl)acetate (182.3 mg, 0.5 mmol) under the catalysis of Rh_2(S-TPPTTL)$_4$ (6.2 mg, 0.5 mol %). After flash chromatography (10%, then 20% - 40% EtOAc in hexanes) the product was obtained as a colorless oil (159.4 mg, 73% yield).

[α]$^{23}_{D}$ -22.5 (*c* = 1.0, CH_2Cl_2)

^{1}H NMR (500 MHz, $CDCl_3$) δ 7.39 (d, *J* = 8.0 Hz, 2H), 7.11 (d, *J* = 8.0 Hz, 2H), 4.77 (d, *J* = 11.9 Hz, 1H), 4.64 (d, *J* = 12.0 Hz, 1H), 3.52 (d, *J* = 10.6 Hz, 1H), 3.22 (s, 3H), 2.93–2.80 (m, 1H), 1.82 (s, 3H), 1.33 (ddd, *J* = 13.5, 7.9, 5.0 Hz, 1H), 0.92–0.79 (m, 2H), 0.54 (dd, *J* = 14.3, 10.8 Hz, 1H), 0.27 (s, 3H), 0.26 (s, 3H)

^{13}C NMR (126 MHz, $CDCl_3$) δ 171.5, 170.5, 143.7, 136.9, 129.7, 127.1, 94.9, 74.0, 62.0, 37.1, 35.6, 22.4, 20.5, 19.8, 1.3, -2.0

IR (film) 2858, 1750, 1526, 1249, 1120, 832, 807, 760, 718 cm^{-1}

HRMS (APCI+) calcd for [$C_{14}H_{18}O_2NCl_4Si$+ H] 436.01224 found 436.01288

Chiral HPLC (Chiralpak IA-U, 10% isopropanol in hexane, 0.5 mL/min, λ 280 nm) retention times of 1.5 min and 61.8 min, 98% ee

Experimental Section for

Chapter 3.2.6: Development of Catalysts that Are Related to Rh_2(*S*-TPPTTL)$_4$

General procedure for C–H functionalization of benzylic substrates:

An oven-dried 10-mL reaction vial equipped with a stir bar was cooled to ambient atmosphere under vacuum. While the vial was being cooled down, aryldiazoacetate (1 equiv) and Rh(II) catalyst (0.5 mol %) were weighed and added to two separate 20 mL scintillation vials. To the vial with Rh(II) catalyst the appropriate substrate (2.5 equiv) was added via syringe and then dissolved together in 2.5 mL of degassed dichloromethane (DCM). The aryldiazoacetate was also dissolved in 2.5 mL of DCM. After both solutions were prepared, the reaction vial was purged with dry argon (vacuum/argon x5 times) and fitted with an argon balloon. Next, the solution containing the catalyst and substrate was transferred to the reaction vial via syringe, and then placed in an ice/water bath. The aryldiazoacetate solution was added dropwise over 90 min via syringe using a syringe pump. The reactions were allowed to stir for at least 1 h after addition. Solvent was then removed under reduced pressure and the crude residue was analyzed using ^{1}H NMR to determine regio- and diastereoselectivity and then purified by silica gel chromatography.

2,2,2-trichloroethyl (2*R*,3*S*)-2-(4-bromophenyl)-3-(*p*-tolyl)butanoate

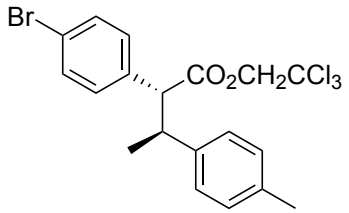

This compound was prepared according to the general procedure for C–H functionalization reaction, using 4-ethyltoluene (90.1 mg, 0.75 mmol, 2.5 equiv) as the substrate and 2,2,2-trichloroethyl 2-(4-bromophenyl)-2-diazoacetate (111.7 mg, 0.3 mmol) under the catalysis of the corresponding Rh catalyst (0.5 mol %). After flash chromatography (0% - 2% Et_2O in hexanes) the product was obtained as a colorless oil.

This compound is known in the literature, and the spectral data are consistent.[3]

^{1}H NMR (500 MHz, $CDCl_3$) δ 7.51-7.47 (m, 2H), 7.38-7.35 (m, 2H), 7.19 (d, 2H, J = 8.0 Hz), 7.09 (d, 2H, J = 7.7 Hz), 4.49 (d, 1H, J = 12.0 Hz), 4.32 (d, 1H, J = 12.0 Hz), 3.80 (s, 1H), 3.45 (s, 1H), 2.29 (s, 3H), 1.02 (d, 3H, J = 7.0 Hz)

^{13}C NMR (126 MHz, $CDCl_3$) δ 171.8, 141.0, 136.7, 136.0, 132.1, 130.6, 129.5, 127.5, 122.1, 94.9, 74.5, 59.0, 43.2, 21.2, 20.3

Chiral HPLC (Chiralpak AD-H, 1% isopropanol in hexane, 0.5 mL/min, λ 210 nm) retention times of 17.1 min and 21.3 min

2,2,2-trichloroethyl (*R*)-2-(4-bromophenyl)-3-methyl-3-(*p*-tolyl)butanoate

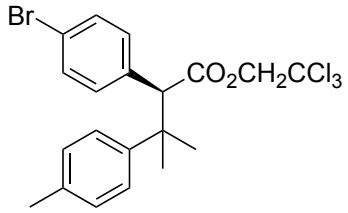

This compound was prepared according to the general procedure for C–H functionalization reaction, using *p*-cymene (90.1 mg, 0.75 mmol, 2.5 equiv) as the substrate and 2,2,2-trichloroethyl 2-(4-bromophenyl)-2-diazoacetate (100.7 mg, 0.3 mmol) under the catalysis of the corresponding Rh catalyst (0.5 mol %). After flash chromatography (0% - 2% Et_2O in hexanes) the product was obtained as a colorless oil.

This compound is known in the literature, and the spectral data are consistent.[3]

^{1}H NMR (500 MHz, $CDCl_3$) δ 7.27 (d, 2H, J = 8.4 Hz), 7.18 (d, 2H, J = 8.2 Hz), 7.11-7.06 (m, 4H), 4.59 (d, 1H, J = 12.0 Hz), 4.45 (d, 1H, J = 12.0 Hz), 3.98 (s, 1H), 2.30 (s, 3H), 1.51 (s, 3H), 1.33 (s, 3H)

^{13}C NMR (126 MHz, $CDCl_3$) δ 170.7, 143.4, 136.2, 133.9, 132.0, 131.1, 129.0, 126.5, 122.0, 94.8, 74.3, 61.9, 41.3, 26.7, 25.1, 21.1

Chiral HPLC (Chiralpak AD-H, 0.5% isopropanol in hexane, 0.5 mL/min, λ 210 nm) retention times of 11.8 min and 13.0 min

Experimental Section for

Chapter 3.2.7: Aryldiazoketones as New Donor/acceptor Carbene Precursors for Selective Intermolecular C–H Functionalization Reactions

General procedure for C–H functionalization reactions using aryldiazoketones:

Ambient light was avoided as much as possible during the reaction setup to prevent auto-decomposition of the aryldiazoketone via Wolff rearrangement.

An oven-dried 10-mL reaction vial equipped with a stir bar was cooled to ambient atmosphere under vacuum. While the vial was being cooled down, aryldiazoketone (1 equiv) and Rh(II) catalyst (0.5 mol %) were weighed and added to two separate 20 mL scintillation vials. To the vial with Rh(II) catalyst the appropriate substrate (5.0 equiv) was added via syringe and then dissolved together in 2.5 mL of degassed dichloromethane (DCM). The aryldiazoketone was also dissolved in 2.5 mL of DCM. After both solutions were prepared, the reaction vial was purged with dry argon (vacuum/argon x5 times) and fitted with an argon balloon. Next, the solution containing the catalyst and substrate was transferred to the reaction vial via syringe, and then placed on a hot plate preset to 40 °C. The aryldiazoketone solution was added dropwise over 90 min via syringe using a syringe pump. The reactions were allowed to stir for at least 1 h after addition. Solvent was then removed under reduced pressure and the crude residue was analyzed using ^{1}H NMR to determine regio- and diastereoselectivity and then purified by silica gel chromatography.

4-((2*R*,3*R*)-4-oxo-3-phenyl-4-(4-(trifluoromethyl)phenyl)butan-2-yl)phenyl acetate

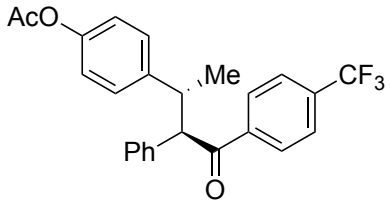

This compound was prepared according to the general procedure for C–H functionalization reaction, using 4-ethylphenyl acetate (264.3 mg, 1.5 mmol, 5 equiv) as the substrate and 2-diazo-2-phenyl-1-(4-(trifluoromethyl)phenyl)ethan-1-one (87.1 mg, 0.3 mmol) under the catalysis of the Rh_2(*S*-TPPTTL)$_4$ (3.7 mg, 0.5 mol %). After flash chromatography (3%-5%, then 10%-15% Et_2O in hexanes) the product was obtained as a colorless oil (67.8 mg, 53% yield).

^{1}H NMR (400 MHz, $CDCl_3$) δ 8.08 (d, *J* = 8.1 Hz, 2H), 7.66 (d, *J* = 8.2 Hz, 2H), 7.16 – 6.95 (m, 7H), 6.85 (d, *J* = 8.6 Hz, 2H), 4.62 (d, *J* = 10.5 Hz, 1H), 3.70 (dq, *J* = 10.5, 6.7 Hz, 1H), 2.24 (s, 3H), 1.39 (d, *J* = 6.8 Hz, 3H)

^{13}C NMR (100 MHz, $CDCl_3$) δ 198.8, 169.4, 148.9, 141.4, 140.1 (d, *J* = 1.3 Hz), 136.9, 134.2 (q, *J* = 32.7 Hz), 128.9, 128.7, 128.7 (d, *J* = 2.2 Hz), 127.2, 125.7(q, *J* = 3.7 Hz), 124.9, 122.2, 121.0, 61.8, 43.3, 21.1, 20.6

IR (film) 2923, 2360, 2342, 1742, 1323, 1217, 1205, 1067, 669, 438, 418, cm^{-1}

HRMS (–APCI) calcd for [$C_{25}H_{21}F_3O$–H] 425.1359 found 425.1365

Chiral HPLC (Chiralpak RRW, 1% isopropanol in hexane, 2 mL/min, λ 230 nm) retention times of 27.6 min and 33.9 min, 99% ee

(2*R*,3*S*)-2-phenyl-3-(*p*-tolyl)-1-(4-(trifluoromethyl)phenyl)butan-1-one

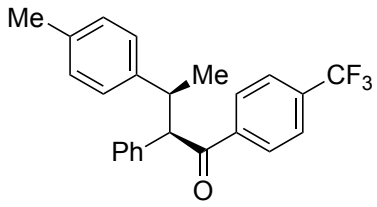

This compound was prepared according to the general procedure for C–H functionalization reaction, using 4-ethyltoluene (180.3 mg, 1.5 mmol, 5 equiv) as the substrate and 2-diazo-2-phenyl-1-(4-(trifluoromethyl)phenyl)ethan-1-one (87.1 mg, 0.3 mmol) under the catalysis of the Rh_2(*S*-TPPTTL)$_4$ (3.7 mg, 0.5 mol %). After flash chromatography (0% - 3% Et_2O in hexanes) the product was obtained as a colorless oil (65.4 mg, 57% yield).

^{1}H NMR (400 MHz, $CDCl_3$) δ 8.09 (d, *J* = 8.1 Hz, 2H), 7.67 (d, *J* = 8.0 Hz, 2H), 7.13 – 7.01 (m, 5H), 6.97 – 6.86 (m, 4H), 4.66 (d, *J* = 10.6 Hz, 1H), 3.66 (dq, *J* = 10.6, 6.7 Hz, 1H), 2.22 (s, 3H), 1.36 (d, *J* = 6.7 Hz, 3H)

^{13}C NMR (100 MHz, $CDCl_3$) δ 199.2, 140.8, 140.2, 137.1, 135.6, 134.2 (q, *J* = 32.6 Hz), 129.0 – 128.8 (d, *J* = 5.8), 128.5, 127.6, 127.0, 125.7 (q, *J* = 3.8 Hz), 124.9, 122.2, 61.6, 43.5, 21.0, 20.9

IR (film) 2924, 2362, 1679, 1325, 1168, 1133, 1067, 824, 429, cm^{-1}

HRMS (–APCI) calcd for [$C_{24}H_{21}F_3O$–H] 381.1461 found 381.1467

Chiral HPLC (Chiralpak RRW, 0.5% isopropanol in hexane, 0.5 mL/min, λ 230 nm) retention times of 13.6 min and 18.5 min, 99% ee

(2*R*,3*R*,*E*)-3-ethyl-2-phenyl-1-(4-(trifluoromethyl)phenyl)hex-4-en-1-one

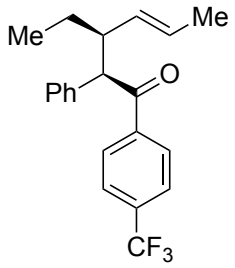

This compound was prepared according to the general procedure for C–H functionalization reaction, using *trans*-2-hexene (126.2 mg, 1.5 mmol, 5 equiv) as the substrate and 2-diazo-2-phenyl-1-(4-(trifluoromethyl)phenyl)ethan-1-one (87.1 mg, 0.3 mmol) under the catalysis of the Rh_2(*S*-TPPTTL)$_4$ (3.7 mg, 0.5 mol %). After flash chromatography (0% - 3% Et_2O in hexanes) the product was obtained as a colorless oil (57.2 mg, 55% yield).

^{1}H NMR (400 MHz, $CDCl_3$) δ 8.05 (d, *J* = 8.1 Hz, 2H), 7.66 (d, *J* = 8.1 Hz, 2H), 7.30 – 7.13 (m, 5H), 5.22 – 5.10 (m, 1H), 4.98 (ddq, *J* = 15.1, 9.3, 1.5 Hz, 1H), 4.44 (d, *J* = 9.9 Hz, 1H), 2.85 (qd, *J* = 9.7, 3.1 Hz, 1H), 1.55 – 1.47 (m, 1H), 1.44 (dd, *J* = 6.3, 1.6 Hz, 3H), 1.25 (ddq, *J* = 13.1, 9.8, 7.3 Hz, 1H), 0.87 (t, *J* = 7.3 Hz, 3H)

^{13}C NMR (100 MHz, $CDCl_3$) δ 199.3, 140.3, 137.5, 134.0 (q, *J* = 32.7 Hz), 131.4, 129.1, 128.7 (d, *J* = 21.4 Hz), 127.6, 127.1, 125.6 (q, *J* = 3.8 Hz), 124.9, 122.2, 59.1, 48.1, 26.9, 17.8, 12.0

IR (film) 2964, 2933, 2360, 2342, 1686, 1322, 1170, 1132, 1067, 747, 410, cm^{-1}

HRMS (+APCI) calcd for [$C_{21}H_{21}F_3O$+H] 347.1623 found 347.1609

Chiral HPLC (Chiralpak SSW, 0.5% isopropanol in hexane, 0.5 mL/min, λ 230 nm) retention times of 11.5 min and 13.9 min, 96% ee

(*R*)-2-cyclohexyl-2-phenyl-1-(4-(trifluoromethyl)phenyl)ethan-1-one

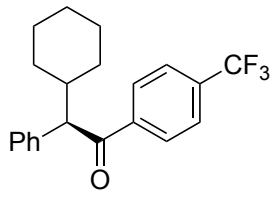

This compound was prepared according to the general procedure for C–H functionalization reaction, using cyclohexane (126.2 mg, 1.5 mmol, 5 equiv) as the substrate and 2-diazo-2-phenyl-1-(4-(trifluoromethyl)phenyl)ethan-1-one (87.1 mg, 0.3 mmol) under the catalysis of the Rh_2(*S*-TPPTTL)$_4$ (3.7 mg, 0.5 mol %). After flash chromatography (0% - 3% Et_2O in hexanes) the product was obtained as a colorless oil (60.3 mg, 58% yield).

^{1}H NMR (400 MHz, $CDCl_3$) δ 8.01 (d, *J* = 8.1 Hz, 2H), 7.61 (d, *J* = 8.1 Hz, 2H), 7.34 – 7.10 (m, 5H), 4.23 (d, *J* = 10.1 Hz, 1H), 2.26 (tdt, *J* = 11.3, 10.1, 3.3 Hz, 1H), 1.83 – 1.74 (m, 1H), 1.63 (m, 3H), 1.36 – 1.04 (m, 4H), 1.00 – 0.73 (m, 2H)

^{13}C NMR (100 MHz, $CDCl_3$) δ199.7, 140.5, 137.3, 134.0 (q, *J* = 32.8 Hz), 128.9 (d, *J* = 0.9 Hz), 128.8, 127.3, 125.6 (q, *J* = 3.8 Hz), 124.9, 122.2, 60.7, 41.1, 32.7, 30.7, 26.5, 26.16, 26.12

IR (film) 2926, 2854, 2360, 2342, 1686, 1323, 1260, 1169, 1132, 1066, 802, 429, cm^{-1}

HRMS (+APCI) calcd for [$C_{21}H_{21}F_3O$+H] 347.1623 found 347.1610

Chiral HPLC (Chiralpak SSW, 0.5% isopropanol in hexane, 0.5 mL/min, λ 230 nm) retention times of 13.4 min and 17.4 min, 99% ee

(*R*)-2-((1*S*,3*R*)-3-(*tert*-butyl)cyclohexyl)-2-phenyl-1-(4-(trifluoromethyl)phenyl)ethan-1-one

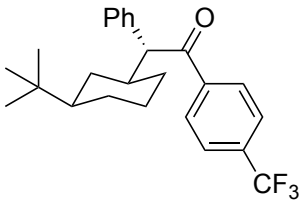

This compound was prepared according to the general procedure for C–H functionalization reaction, using *tert*-butylcyclohexane (210.4 mg, 1.5 mmol, 5 equiv) as the substrate and 2-diazo-2-phenyl-1-(4-(trifluoromethyl)phenyl)ethan-1-one (87.1 mg, 0.3 mmol) under the catalysis of the Rh_2(*S*-TPPTTL)$_4$ (3.7 mg, 0.5 mol %). After flash chromatography (0% - 3% Et_2O in hexanes) the product was obtained as a colorless oil (61.6 mg, 51% yield).

^{1}H NMR (400 MHz, $CDCl_3$) δ 7.98 (d, *J* = 8.1 Hz, 1H), 7.58 (d, *J* = 8.2 Hz, 1H), 7.30 – 7.15 (m, 4H), 7.19 – 7.09 (m, 1H), 4.20 (d, *J* = 9.9 Hz, 1H), 2.19 (tdt, *J* = 11.7, 9.8, 3.2 Hz, 1H), 1.78 – 1.62 (m, 3H), 1.32 (dt, *J* = 12.6, 2.7 Hz, 1H), 1.31 – 1.16 (m, 1H), 0.96 – 0.66 (m, 4H), 0.64 (s, 9H), 0.49 (q, *J* = 12.0 Hz, 1H)

^{13}C NMR (100 MHz, $CDCl_3$) δ 199.8, 140.5, 137.2, 134.0 (q, *J* = 32.6 Hz), 128.82, 128.76, 127.3, 125.6 (q, *J* = 3.8 Hz), 125.0, 122.2, 61.0, 47.7, 41.5, 32.5, 32.53, 31.48, 27.4, 27.2, 26.4

IR (film) 2925, 2854, 2360, 2342, 1688, 1322, 1170, 1133, 1067, 748, 702, 418, cm^{-1}

HRMS (+APCI) calcd for [$C_{25}H_{29}F_3O$+H] 403.2249 found 403.2237

Chiral HPLC (Chiralpak SSW, 0.5% isopropanol in hexane, 0.35 mL/min, λ 230 nm) retention times of 21.5 min and 35.8 min, 99% ee

(*R*)-2-phenyl-2-((*S*)-tetrahydrofuran-2-yl)-1-(4-(trifluoromethyl)phenyl)ethan-1-one

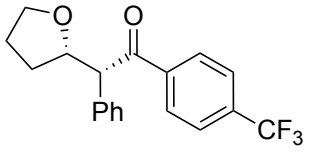

This compound was prepared according to the general procedure for C–H functionalization reaction, using tetrahydrofuran (108.2 mg, 1.5 mmol, 5 equiv) as the substrate and 2-diazo-2-phenyl-1-(4-(trifluoromethyl)phenyl)ethan-1-one (87.1 mg, 0.3 mmol) under the catalysis of the Rh_2(*S*-TPPTTL)$_4$ (3.7 mg, 0.5 mol %). After flash chromatography (0% - 8% Et_2O in hexanes) the product was obtained as a colorless oil (62.2 mg, 62% yield).

^{1}H NMR (400 MHz, $CDCl_3$) δ 7.93 (d, *J* = 8.1 Hz, 2H), 7.54 (d, *J* = 8.1 Hz, 2H), 7.30 – 7.19 (m, 4H), 7.17 – 7.11 (m, 1H), 4.50 – 4.40 (m, 2H), 3.74 (dtd, *J* = 9.5, 6.7, 2.8 Hz, 1H), 3.65 – 3.55 (m, 1H), 2.23 – 2.08 (m, 1H), 1.89 – 1.69 (m, 2H), 1.54 – 1.37 (m, 1H)

^{13}C NMR (100 MHz, $CDCl_3$) δ 198.0, 139.4, 136.6, 134.2 (q, *J* = 32.9 Hz), 129.0 (d, *J* = 7.0 Hz), 128.7, 127.7, 125.7 (q, *J* = 3.8 Hz), 124.9, 122.2, 81.1, 68.1, 59.7, 30.9, 25.7

IR (film) 2923, 2854, 2360, 2342, 1687, 1325, 1170, 1129, 1066, 701, 417, cm^{-1}

HRMS (–APCI) calcd for [$C_{19}H_{17}F_3O$–H] 333.1097 found 333.1106

Chiral HPLC (Chiralpak OD-H, 1% isopropanol in hexane, 1 mL/min, λ 210 nm) retention times of 8.24 min and 8.93 min, 78% ee

(*R*)-2-((3*R*,5*R*,7*R*)-adamantan-1-yl)-2-phenyl-1-(4-(trifluoromethyl)phenyl)ethan-1-one

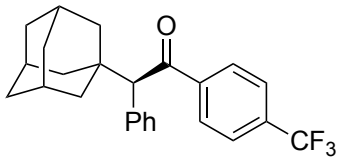

This compound was prepared according to the general procedure for C–H functionalization reaction, using adamantane (204.4 mg, 1.5 mmol, 5 equiv) as the substrate and 2-diazo-2-phenyl-1-(4-(trifluoromethyl)phenyl)ethan-1-one (87.1 mg, 0.3 mmol) under the catalysis of the Rh_2(*S*-TPPTTL)$_4$ (3.7 mg, 0.5 mol %). After flash chromatography (0% - 3% Et_2O in hexanes) the product was obtained as a colorless oil (66.0 mg, 56% yield).

^{1}H NMR (400 MHz, $CDCl_3$) δ 7.94 (d, *J* = 8.2 Hz, 2H), 7.59 (d, *J* = 8.2 Hz, 2H), 7.35 – 7.30 (m, 2H), 7.29 – 7.18 (m, 3H), 4.28 (s, 1H), 1.91 (m, 3H), 1.78 (m, 3H), 1.65 – 1.47 (m, 9H)

^{13}C NMR (100 MHz, $CDCl_3$) δ 199.9, 141.8, 134.2, 133.8 (q, *J* = 32.8 Hz), 130.5, 128.34 (d, *J* = 35.9 Hz), 127.3, 125.5 (q, *J* = 3.8 Hz), 125.0, 122.26, 64.2, 40.3, 37.7, 36.8, 28.7

IR (film) 2906, 2849, 2360, 2342, 1738, 1323, 1132, 1067, 668, 418, cm^{-1}

HRMS (–APCI) calcd for [$C_{25}H_{25}F_3O$–H] 397.1774 found 397.1778

Chiral HPLC (Chiralpak SSW, 0.5% isopropanol in hexane, 0.5 mL/min, λ 230 nm) retention times of 14.2 min and 16.2 min, 95% ee

References

1. Fu, L.; Mighion J. D.; Voight, E. A.; Davies, H. M. L. *Chem. Eur. J.* **2017**, *23*, 3272

2. Guptill, D. M.; Davies, H. M. L. *J. Am. Chem. Soc.* **2014**, *136*, 17718

3. Bess, E. N.; Guptill, D. M.; Davies, H. M. L.; Sigman, M. S. *Chem. Sci.* **2015**, *6*, 3057

4. Garlets, Z. J.; Wertz, B. D.; Liu, W.; Voight E. A.; Davies, H. M. L. *Chem*, **2020**, *6*, 304.

Experimental Section for

Chapter 4: Monocyclopropanation of Pyrroles by Rh(II)-donor/acceptor Carbenes

Procedures for the synthesis of starting materials

1-tosyl-1H-pyrrole

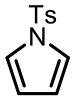

Pyrrole (6.92 mL, 100.0 mmol, 1.0 equiv) was added to suspension of sodium hydroxide (16.0 g, 400 mmol, 4.0 equiv) in dichloroethane (66 mL) and stirred for 10 min at 0 °C. A solution of tosylchloride (23.4 g, 123.0 mmol, 1.23 equiv) in dichloroethane (40 mL) was then added dropwise. After the addition was complete, the reaction was stirred for 30 min at 0 °C and further 18 h at room temperature. The reaction mixture was subsequently poured into a separation funnel containing water (240 mL) and the organic layer was separated. The remaining aqueous phase was extracted with DCM (3 x 50 mL) and the combined organic layers were washed with water (6 x 50 mL) to neutrality and dried over Na_2SO_4. Removal of the solvent in vacuo gave the product (18.2 g, 82.1 mmol, 82%) as a colorless solid.

^{1}H NMR and ^{13}C NMR spectral data are consistent with reported literature.[1]

^{1}H-NMR (500 MHz, $CDCl_3$) δ = 7.79 – 7.71 (m, 2H), 7.30 – 7.27 (m, 2H), 7.18 – 7.13 (m, 2H), 6.37 – 6.00 (m, 2H), 2.40 (s, 3H).

^{13}C-NMR (126 MHz, $CDCl_3$) δ = 145.0, 136.1, 130.0, 126.8, 120.7, 113.5, 21.6.

methyl 1-tosyl-1H-pyrrole-2-carboxylate

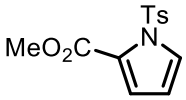

A flame dried 100 mL round bottomed flask equipped with a magnetic stir bar and a rubber septum was purged with argon and charged with 2-methyl-1H-pyrrolecarboxylate (2.0 g, 15.98 mmol, 1.0 equiv) and anhydrous THF (30 mL). Sodium hydride (0,96 g, 24.0 mmol, 1.5 equiv) was cautiously added as a 60% suspension in mineral oil at 0 °C and the mixture was stirred for 30 min. Next, tosylchloride (4,57 g, 24.0 mmol, 1.5 equiv) was added in one portion and the reaction was stirred for 48 h at room temperature. Another portion of NaH (0.28 g, 8.0 mmol, 0.5 equiv) was added and the mixture was stirred for further 24 h. After TLC analysis (DCM) confirmed full consumption of starting the starting material the mixture was slowly poured into a separation funnel containing a concentrated ammonium chloride solution (50 mL). The organic was separated, and the remaining aqueous phase was extracted with DCM (3 x 50 mL). The combined organic layers were dried over Na_2SO_4 and after the solvent was removed in vacuo the product was purified by column chromatography on silica gel (5% to 20% ethyl acetate in hexanes) to give the product (3.69 g,13.2 mmol, 83%) as a colorless solid.

^{1}H NMR and ^{13}C NMR spectral data are consistent with reported literature.[2]

^{1}H-NMR (600 MHz, $CDCl_3$) = δ 7.95 – 7.80 (m, 2H), 7.71 (dd, J = 3.2, 1.9, 1H), 7.31 (m, 2H), 7.03 (dd, J = 3.7, 1.9, 1H), 6.29 (dd, J = 3.7, 3.3, 1H), 3.72 (s, 3H), 2.41 (s, 3H).

^{13}C-NMR (126 MHz, $CDCl_3$) δ = 159.1, 144.9, 135.8, 129.4, 129.2, 128.2, 124.8, 123.3, 110.3, 51.8, 21.69.

1-(tert-butyl) 2-methyl 1H-pyrrole-1,2-dicarboxylate

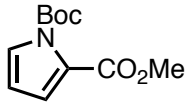

A 100 mL round bottomed flask equipped with a magnetic stir bar was charged with 2-methyl-1H-pyrrolecarboxylate (500.0 mg, 4.0 mmol, 1.0 equiv) and di-tert-butylcarbonate (1.05 g, 4.8 mmol, 1.2 equiv) and acetonitrile (30 mL). After 4-dimetylaminopyridine (48.0 mg, 0.4 mmol, 0.1 equiv) was added to the solution, the reaction as stirred for 2 h at room temperature. The mixture was then poured into a separation funnel containing water (50 mL) and the organic layer was separated. The aqueous phase was extracted with ethyl acetate (3 x 50 mL) and the combined organic layers were dried over Na_2SO_4. After the solvent was removed in vacuo the pure product (881.0 mg, 3.92 mmol, 98%) was obtained as a colorless oil.

^{1}H NMR and ^{13}C NMR spectral data are consistent with reported literature.[3]

^{1}H-NMR (600 MHz, $CDCl_3$) δ = 7.30 (dd, J = 3.2, 1.7 Hz, 1H), 6.82 (dd, J = 3.5, 1.7 Hz, 1H), 6.15 (t, J = 3.4 Hz, 1H), 3.83 (s, 3H), 1.57 (s, 9H).

^{13}C-NMR (126 MHz, $CDCl_3$) δ = 161.2, 148.4, 126.6, 125.1, 120.8, 110.1, 84.7, 51.8, 27.6.

methyl 1-tosyl-1H-pyrrole-3-carboxylate

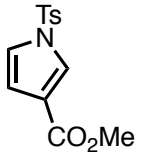

A flame dried 100 mL round bottomed flask equipped with a magnetic stir bar and a rubber septum was purged with argon and charged with 3-methyl-1H-pyrrolecarboxylate (1.50 g, 12.0 mmol, 1.0 equiv), sodium hydroxide (1.92 g, 48.0 mmol, 4.0 equiv), tetrabutylammonium hydrogen sulfate (0.47 g, 1.2 mmol, 0.1 equiv) and anhydrous DCM (30 mL). After the mixture was stirred for 10 min at room temperature, a solution of tosylchloride (3.43 g, 18.0 mmol. 1.5 equiv) in DCM (10mL) was added and the reaction was stirred for 2 days at room temperature. The reaction was then quenched with water (50mL) and the organic layer was separated. The aqueous phase was extracted with ethyl acetate (3 x 50 mL) and the combined organic layers were dried over Na_2SO_4. After the solvent was removed in vacuo the product was purified by column chromatography on silica gel (5% to 10% ethyl acetate in hexanes) to obtain the product (3.35 g, 12.0 mmol, quant.) as a colorless solid.

^{1}H NMR and ^{13}C NMR spectral data are consistent with reported literature.[4]

^{1}H-NMR (600 MHz, $CDCl_3$) δ = 7.82 – 7.75 (m, 2H), 7.73 (dd, J = 2.3, 1.6 Hz, 1H), 7.33 – 7.29 (m, 2H), 7.10 (dd, J = 3.3, 2.3 Hz, 1H), 6.64 (dd, J = 3.4, 1.6 Hz, 1H), 3.78 (s, 3H), 2.40 (s, 3H).

^{13}C-NMR (126 MHz, $CDCl_3$) δ = 163.8, 145.9, 145.8, 135.2, 130.3, 127.2, 127.2, 125.0, 121.1, 120.5, 113.3, 51.6, 21.7.

1-tosyl-1H-pyrrole-2-carbaldehyde

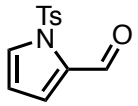

A flame dried 100 mL round bottomed flask equipped with a magnetic stir bar and a rubber septum was purged with argon and charged with pyrrole-2-carboxaldehyd (1.50 g, 15.8 mmol, 1.0 equiv) and anhydrous THF (30 mL). Sodium hydride (0,95 g, 23.7 mmol, 1.5 equiv) was cautiously added as a 60% suspension in mineral oil at 0 °C and the mixture was stirred for 30 min. Next, a solution of tosylchloride (3.61 g, 18.9 mmol, 1.2 equiv) in anhydrous THF (10 mL) was added and the reaction was stirred for 18 h at room temperature. After the starting material was consumed, water (30 mL) was added dropwise at 0 °C and the organic layer was subsequently separated. The aqueous phase was extracted with DCM (3 x 50 mL) and the combined organic layers were dried over Na_2SO_4. After the solvent was removed in vacuo the product was purified by column chromatography on silica gel (5% to 20% ethyl acetate in hexanes) to obtain the product (2.09 g, 8.36 mmol, 53%) as a colorless solid.

^{1}H NMR and ^{13}C NMR spectral data are consistent with reported literature.[5]

^{1}H-NMR (500 MHz, $CDCl_3$) δ = 9.96 (s, 1H), 7.79 (d, J = 8.4 Hz, 2H) 7.61 (m, 1H), 7.31 (d, J = 8.1 Hz, 2H), 7.14 (m, 1H), 6.40 (m, 1H), 2.40 (s, 3H).

^{13}C-NMR (126 MHz, $CDCl_3$) δ = 178.9, 145.9, 135.2, 133.5, 130.1, 129.4, 127.5, 124.4, 112.4, 21.7.

(1-tosyl-1H-pyrrol-2-yl)methyl acetate

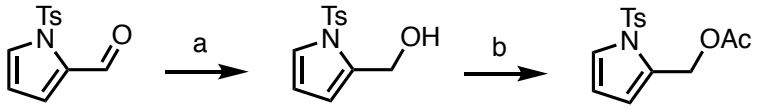

step (a)

A flame dried 50 mL round bottomed flask equipped with a magnetic stir bar and a rubber septum was purged with argon and charged with a solution of sodium borohydride (113.0 mg, 3.0 mmol, 1.5 equiv) in anhydrous methanol (15 mL). A solution of 1-tosyl-1H-pyrrole-2-carbaldehyde (498.0 mg, 2.0 mmol, 1.0 equiv) in anhydrous methanol (15 ml) was then added and the resulting mixture was stirred for 2 h at room temperature. The reaction mixture was subsequently poured into a separation funnel containing water (100 mL) and the organic layer was separated. The remaining aqueous phase was extracted with DCM (3 x 50 mL) and the combined organic layers were dried over Na_2SO_4. After the solvent was removed in vacuo (503 mg, 2.0 mmol, quant.) the product was obtained as a colorless solid.

^{1}H-NMR (400 MHz, $CDCl_3$) δ = 7.69 7.73 (m, 2H), 7.29 7.32 (m, 2H), 7.26 – 7.23 (m, 1H), 6.29 – 6.15 (m, 2H), 4.58 (d, J = 7.2 Hz, 2H), 2.71 (t, J = 7.2 Hz, 1H), 2.39 (s, 3H).

The analytical data matched with the literature[6] and the crude material was clean enough to be used without further purification.

step (b)

A flame dried 25 mL round bottomed flask equipped with a magnetic stir bar and a rubber septum was purged with argon and charged with pyrrole (503 mg, 2.0 mmol, 1.0 equiv) and pyridine (5 mL). Acetic anhydride (0.95 mL, 1.02 g, 10.0 mmol, 5.0 equiv) was then added at 0 °C and the reaction was stirred for 10 min and another 2 h at room temperature. The reaction was quenched

with water (50 mL) and the organic layer was separated. The remaining aqueous phase was extracted with ethyl acetate (3 x 50 mL) and the combined organic layers were washed with water (50 mL) and brine (50 mL). After drying over Na_2SO_4 and removal of the solvent under reduced pressure, pure product (518 mg, 1.8 mmol, 88%) was obtained after filtration through a short silica plug (20% ethyl acetate in hexanes).

R_f (20% ethyl acetate in hexanes) = 0.39

mp. = 94-95 °C

^{1}H-NMR (600 MHz, $CDCl_3$) δ = 7.72 – 7.68 (m, 2H), 7.33 (dd, J = 3.4, 1.7 Hz, 1H), 7.29 – 7.26 (m, 2H), 6.33 (dd, J = 3.4, 1.7 Hz, 1H), 6.23 (t, J = 3.4 Hz, 1H), 5.19 (s, 2H), 2.38 (s, 3H), 1.88 (d, J = 0.7 Hz, 3H).

^{13}C-NMR (126 MHz, $CDCl_3$) δ = 170.3, 145.0, 136.4, 129.9, 128.8, 127.0, 124.4, 117.6, 111.5, 57.5, 21.6, 20.8.

IR (neat): 3122, 2969, 1732, 1595, 1499, 1475, 1451, 1400, 1361, 1316, 1305, 1292, 1234, 1192, 1172, 1150, 1089, 1058, 1017, 965, 920, 889, 854, 828, 818, 802, 759, 736, 707, 667, 615, 586, 543 cm^{-1}.

HRMS (+NSI): calcd. for $C_{14}H_{15}O_4NNaS$ $(M+Na)^+$ 316.0614 found 316.0618.

2,2,2-trifluoro-1-(1-tosyl-1H-pyrrol-2-yl)ethan-1-one

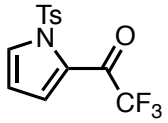

A flame dried 100 mL round bottomed flask equipped with a magnetic stir bar and a rubber septum was purged with argon and charged with 2,2,2-trifluoro-1-(1H-pyrrol-2-yl)ethan-1-one (3.26 g, 20.0 mmol, 1.0 equiv), potassium hydroxide (1.68 g, 30.0 mmol, 1.5 equiv), tetrabutylammonium hydrogensulfate (0.67 g, 2.0 mmol, 0.1 equiv) and anhydrous DCM (30 mL). After the mixture was stirred for 10 min at room temperature, a solution of tosylchloride (4.58 g, 24.0 mmol. 1.2 equiv) in anhydrous DCM (10mL) was added and the reaction was stirred for 2 days at room temperature. The reaction was then quenched with water (50mL) and the organic layer was separated. The aqueous phase was extracted with ethyl acetate (3 x 50 mL) and the combined organic layers were dried over Na_2SO_4. After the solvent was removed in vacuo the product was purified by column chromatography on silica gel (5% to 10% ethyl acetate in hexanes) to obtain the product (0.95 g, 3.0 mmol, 15%) as a colorless solid.

R_f (20% ethyl acetate in hexanes) = 0.5

mp. = 91-92 °C

^{1}H-NMR (600 MHz, $CDCl_3$) δ = 8.01 (ddd, J = 3.1, 1.7, 0.6 Hz, 0H), 7.95 – 7.89 (m, 1H), 7.37 – 7.35 (m, 0H), 7.36 – 7.31 (m, 1H), 6.47 (ddd, J = 3.9, 3.1, 0.6 Hz, 0H), 2.42 (s, 1H).

^{13}C-NMR (126 MHz, $CDCl_3$) δ = 168.2 (d, *J* = 36.5 Hz), 145.8, 134.5, 133.7, 129.6, 128.72, 128.68, 126.1, 116.3 (q, *J* = 291.2 Hz), 111.5, 21.7.

^{19}F-NMR (282 MHz, $CDCl_3$) δ = -71.5

IR (neat): 3143, 1697, 1596, 1536, 1494, 1426, 1412, 1373, 1287, 1242, 1204, 1191, 1171, 1137, 1189, 1072, 1026, 902, 869, 811, 751, 735, 702, 664, 635, 578, 540 cm^{-1}.

HRMS (+NSI): calcd. for $C_{13}H_{11}O_3NF_3S$ $(M+H)^+$ 318.0406 found 318.0411.

2,2,2-trichloro-1-(1-tosyl-1H-pyrrol-2-yl)ethan-1-one

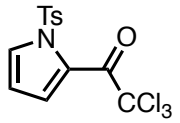

A flame dried 100 mL round bottomed flask equipped with a magnetic stir bar and a rubber septum was purged with argon and charged with 2,2,2-trichloro-1-(1H-pyrrol-2-yl)ethan-1-one (1.00 g, 4.7 mmol, 1.0 equiv) and anhydrous THF (30 mL). Sodium hydride (0,30 g, 7.5 mmol, 1.6 equiv) was cautiously added as a 60% suspension in mineral oil at 0 °C and the mixture was stirred for 30 min. Next, a solution of tosylchloride (1.35 g, 7.1 mmol, 1.5 equiv) in anhydrous THF (5 mL) was added and the reaction was stirred for 18 h at room temperature. After the starting material was consumed, water (30 mL) was added dropwise at 0 °C and the organic layer was subsequently separated. The aqueous phase was extracted with ethyl acetate (3 x 50 mL) and the combined organic layers were washed with water (50 mL) and brine (50 mL) and dried over Na_2SO_4. After the solvent was removed in vacuo the product was purified by flash column chromatography on silica gel (5% to 7% ethyl acetate in hexanes) to obtain the product (0.99 g, 2.7 mmol, 57%) as a colorless solid.

R_f (20% ethyl acetate in hexanes) = 0.5

mp. = 72–73 °C

^{1}H-NMR (500 MHz, $CDCl_3$) δ = 7.98 – 7.90 (m, 3H), 7.60 (dd, J = 4.0, 1.6 Hz, 1H), 7.39 – 7.33 (m, 2H), 6.43 (t, 4.0 Hz, 1H), 2.44 (s, 3H).

^{13}C-NMR (126 MHz, $CDCl_3$) δ = 171.4, 145.4, 135.2, 132.3, 129.6, 128.4, 127.5, 124.4, 110.7, 95.1, 21.7.

IR (neat): 3157, 1689, 1595, 1537, 1420, 1404, 1366, 1315, 1260, 1193, 1174, 1137, 1087, 1067, 1037, 1018, 862, 846, 801, 753, 739, 700, 681, 664, 611, 592, 574, 551, 537 cm^{-1}.

HRMS (+NSI): calcd. for $C_{13}H_{10}O_3NCl_3NaS$ $(M+Na)^+$ 387.9339 found 387.9348.

Procedure for the enantioselective cyclopropanation of pyrroles and product characterization

General procedure A for cyclopropanation of unsubstituted Ts-pyrrole

A flame dried 10 mL reaction vessel with rubber septum was equipped with a magnetic stir bar and purged with argon. The vial was charged with a solution of 1-tosyl-1H-pyrrole (135.2 mg, 0.6 mmol, 2.0 equiv) and Rh_2(R-p-PhTPCP)$_4$ (2.6 mg, 1.5 μmol, 0.5 mol %) in anhydrous DCM (2.5 mL), and then fitted with an argon balloon. Then a solution of the aryldiazoacetate in anhydrous DCM (2.5 mL) was added over a period of 90 min with the aid of a syringe pump at 0 °C while the reaction was stirred on an ice/water bath. After the addition was complete, the reaction was stirred for another 30 min at 0 °C. The solvent was then removed in vacuo and a crude ^{1}H NMR was taken to ensure product formation and to examine the ratio of monocyclopropanation to double cyclopropanation. The crude residue was then directly purified by flash column chromatography on silica gel (10%, then 15-20% ethyl acetate in hexanes with the addition of 1% triethylamine) to obtain the pure product. A substantial amount of the ring-opened/hydrolyzed aldehyde by-product was observed when the silica gel was not neutralized with 1% triethylamine.

General procedure B for cyclopropanation of Ts-pyrrole bearing substituents at the 2-position

A flame dried 10 mL reaction vessel with rubber septum was equipped with a magnetic stir bar and purged with argon. The vial was charged with a solution of the appropriate pyrrole substrate (0.6 mmol, 2.0 equiv) and Rh_2(R-p-PhTPCP)$_4$ (2.6 mg, 1.5 μmol, 0.5 mol %) in anhydrous DCM (2.5 mL), and then fitted with an argon balloon. Then a solution of the aryldiazoacetate in anhydrous DCM (2.5 mL) was added over a period of 90 min with the aid of a syringe pump at 40 °C while the reaction was stirred on an aluminum heating block. After the addition was complete, the reaction was stirred for another 30 min at 40 °C. The solvent was then removed in vacuo and a crude ^{1}H NMR was taken to ensure product formation and to examine the ratio of monocyclopropanation to double cyclopropanation. The crude residue was then directly purified by flash column chromatography on silica gel (using a mixed solution of ethyl acetate and hexanes with added 1% triethylamine) to obtain the pure product.

methyl (1S,5S,6R)-6-(4-bromophenyl)-2-tosyl-2-azabicyclo[3.1.0]hex-3-ene-6-carboxylate

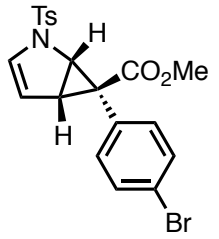

This compound was prepared according to the general procedure A, using 1-tosyl-1H-pyrrole (132.8 mg, 0.6 mmol, 2.0 equiv) as the substrate and methyl 2-(4-bromophenyl)-2-diazoacetate (76.5 mg, 0.3 mmol, 1.0 equiv), under the catalysis of Rh_2(R-p-PhTPCP)$_4$ (2.6 mg, 1.5 μmol, 0.5 mol %). The crude residue was subjected to flash chromatography (10%, then 15% ethyl acetate in hexanes with 1% triethylamine) to obtain the pure product as an off-white solid (104.8 mg, 0.23 mmol, 78%).

R_f (30% ethyl acetate in hexanes) = 0.5

$[\alpha]_D^{20}$ = -374.5° ($CHCl_3$, c = 1)

mp. 130°C

^{1}H-NMR (500 MHz, $CDCl_3$) δ = 7.70 (d, J = 8.4 Hz, 2H), 7.39 (d, J = 8.7 Hz, 2H), 7.36 – 7.32 (m, 2H), 7.07 (d, J = 7.9 Hz, 2H), 5.98 (dd, J = 3.9, 1.5 Hz, 1H), 5.26 (dd, J = 3.9, 2.6 Hz, 1H), 4.52 (dd, J = 6.6, 1.5 Hz, 1H), 3.61 (s, 3H), 3.14 (dd, J = 6.6, 2.5 Hz, 1H), 2.45 (s, 3H).

^{13}C-NMR (126 MHz, $CDCl_3$) δ = 173.0, 144.5, 134.8, 134.2, 131.1, 131.1, 130.0, 129.5, 127.2, 121.7, 110.9, 52.9, 52.2, 38.8, 27.4, 21.6.

IR (neat): 2952, 1715, 1490, 1360, 1262, 1167, 1137, 753, 668, 592 cm^{-1}.

HRMS (+APCI): calcd. for $C_{20}H_{19}BrNO_4S$ $(M+H)^+$ 448.0218 found 448.0217.

HPLC analysis: ADH column, 1 mL/min, 3% iPrOH in hexanes, 70 min, λ = 230 nm, t_R: Major: 30.34 min, Minor: 27.01 min, 91% ee.

methyl (1S,5S,6R)-6-(p-tolyl)-2-tosyl-2-azabicyclo[3.1.0]hex-3-ene-6-carboxylate

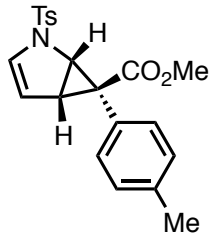

This compound was prepared according to the general procedure A, using 1-tosyl-1H-pyrrole (132.8 mg, 0.6 mmol, 2.0 equiv) as the substrate and methyl 2-diazo-2-(p-tolyl)acetate (57.1 mg, 0.3 mmol, 1.0 equiv), under the catalysis of Rh_2(R-p-PhTPCP)$_4$ (2.6 mg, 1.5 μmol, 0.5 mol %). The crude residue was subjected to flash chromatography (10%, then 15% ethyl acetate in hexanes with 1% triethylamine) to obtain the pure product as a slightly pink oil (79.4 mg, 0.21 mmol, 69%).

$\mathbf{R_f}$ (30% ethyl acetate in hexanes) = 0.4

$[\boldsymbol{\alpha}]_{\mathbf{D}}^{\mathbf{20}}$ = -340.5° ($CHCl_3$, c = 1)

^{1}H NMR (500 MHz, $CDCl_3$) δ = 7.70 (d, J = 8.3 Hz, 2H), 7.33 (d, J = 8.5 Hz, 2H), 7.08 (d, J = 2.3 Hz, 4H), 5.97 (dd, J = 3.9, 1.5 Hz, 1H), 5.27 (dd, J = 3.9, 2.5 Hz, 1H), 4.50 (dd, J = 6.5, 1.5 Hz, 1H), 3.60 (s, 3H), 3.12 (dd, J = 6.6, 2.5 Hz, 1H), 2.45 (s, 3H), 2.32 (s, 3H).

^{13}C NMR (126 MHz, $CDCl_3$) δ = 173.8, 144.3, 137.1, 134.9, 132.3, 130.9, 130.9, 130.0, 128.6, 127.2, 111.3, 111.3, 52.8, 52.2, 38.7, 21.6, 21.3.

IR (neat): 2952, 1712, 1582, 1435, 1361, 1263, 1217, 1168, 698, 667, 595 cm^{-1}.

HRMS (+APCI): calcd. for $C_{21}H_{22}NO_4S$ $(M+H)^+$ 384.1270 found 383.1266.

HPLC analysis: ADH column, 1 mL/min, 3% iPrOH in hexanes, 70 min, λ = 230 nm, t_R: Major: 62.18 min, Minor: 45.34 min, 87% ee.

methyl (1S,5S,6R)-6-(3-(benzyloxy)phenyl)-2-tosyl-2-azabicyclo[3.1.0]hex-3-ene-6-carboxylate

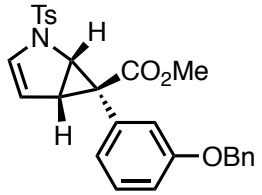

This compound was prepared according to the general procedure A, using 1-tosyl-1H-pyrrole (132.8 mg, 0.6 mmol, 2.0 equiv) as the substrate and methyl 2-(3-(benzyloxy)phenyl)-2-diazoacetate (84.7 mg, 0.3 mmol, 1.0 equiv), under the catalysis of Rh_2(R-p-PhTPCP)$_4$ (2.6 mg, 1.5 μmol, 0.5 mol %). The crude residue was subjected to flash chromatography (10%, then 15% ethyl acetate in hexanes with 1% triethylamine) to obtain the pure product as a slightly yellow solid (85.6mg, 0.18 mmol, 60%).

R_f (30% ethyl acetate in hexanes) = 0.6

$[\alpha]_D^{20}$ = -395.9° ($CHCl_3$, c = 1)

mp. 142-145°C

^{1}H-NMR (500 MHz, $CDCl_3$) δ = 7.73 – 7.67 (m, 2H), 7.48 – 7.42 (m, 2H), 7.38 (ddd, J = 7.7, 6.3, 1.2 Hz, 2H), 7.35 – 7.31 (m, 3H), 7.19 (t, J = 7.9 Hz, 1H), 6.89 (ddd, J = 8.3, 2.6, 1.0 Hz, 1H), 5.98 (dd, J = 3.9, 1.5 Hz, 1H), 5.22 – 5.15 (m, 1H), 5.06 (d, J = 4.1 Hz, 2H), 4.50 (dd, J = 6.6, 1.5 Hz, 1H), 3.61 (s, 3H), 3.12 (dd, J = 6.5, 2.5 Hz, 1H), 2.43 (s, 3H).

^{13}C-NMR (126 MHz, $CDCl_3$) δ = 158.2, 144.4, 137.2, 134.9, 131.8, 130.8, 130.8, 130.0, 128.8, 128.5, 127.9, 127.7, 127.2, 125.2, 118.8, 114.3, 111.2, 70.0, 52.8, 52.2, 38.8, 28.0, 21.6.

IR (neat): 2952, 1712, 1435, 1361, 1262, 1168, 761, 669, 595 cm^{-1}.

HRMS (+APCI): calcd. for $C_{27}H_{26}NO_5S$ $(M+H)^+$ 476.1532 found 476.1529.

HPLC analysis: ADH column, 1 mL/min, 1% iPrOH in hexanes, 70 min, λ = 230 nm, t_R: Major: 46.23 min, Minor: 41.85 min, 75% ee.

methyl (1S,5S,6R)-6-(3,4-dichlorophenyl)-2-tosyl-2-azabicyclo[3.1.0]hex-3-ene-6-carboxylate

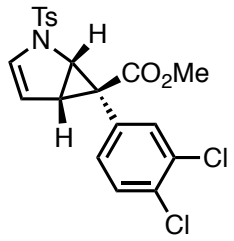

This compound was prepared according to the general procedure A, using 1-tosyl-1H-pyrrole (132.8 mg, 0.6 mmol, 2.0 equiv) as the substrate and methyl 2-diazo-2-(3,4-dichlorophenyl)acetate (73.5 mg, 0.3 mmol, 1.0 equiv), under the catalysis of Rh_2(R-p-PhTPCP)$_4$ (2.6 mg, 1.5 μmol, 0.5 mol %). The crude residue was subjected to flash chromatography (10%, then 15% ethyl acetate in hexanes with 1% triethylamine) to obtain the pure product as a dark brown oil (94.7 mg, 0.22 mmol, 60%).

R_f (30% ethyl acetate in hexanes) = 0.45

$[\alpha]_D^{20}$ = -305.9° ($CHCl_3$, c = 1)

^{1}H-NMR (500 MHz, $CDCl_3$) δ = 7.74 – 7.68 (m, 2H), 7.37 – 7.32 (m, 3H), 7.23 (s, 1H), 7.09 (d, J = 8.2 Hz, 1H), 6.02 (dd, J = 3.9, 1.5 Hz, 1H), 5.30 (dd, J = 3.9, 2.5 Hz, 1H), 4.53 (dd, J = 6.6, 1.5 Hz, 1H), 3.62 (d, J = 0.9 Hz, 3H), 3.16 (dd, J = 6.6, 2.5 Hz, 1H), 2.45 (s, 3H).

^{13}C-NMR (126 MHz, $CDCl_3$) δ = 172.6, 144.7, 134.7, 134.3, 131.9, 131.8, 131.3, 131.3, 130.7, 130.1, 130.0, 127.2, 110.6, 52.9, 52.3, 38.9, 27.1, 21.6.

IR (neat): 2953, 1717, 1361, 1263, 1168, 1134, 763, 668, 594, 544 cm^{-1}.

HRMS (+APCI): calcd. for $C_{20}H_{18}Cl_2NO_4S$ $(M+H)^+$ 438.0334 found 438.0329.

HPLC analysis: ADH column, 1 mL/min, 2% iPrOH in hexanes, 70 min, λ = 230 nm, t_R: Major: 26.72 min, Minor: 25.01 min, 87% ee.

methyl (1S,5S,6R)-6-(6-chloropyridin-3-yl)-2-tosyl-2-azabicyclo[3.1.0]hex-3-ene-6-carboxylate

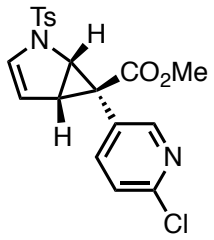

This compound was prepared according to the general procedure A, using 1-tosyl-1H-pyrrole (132.8 mg, 0.6 mmol, 2.0 equiv) as the substrate and methyl 2-(6-chloropyridin-3-yl)-2-diazoacetate (63.5 mg, 0.3 mmol, 1.0 equiv), under the catalysis of Rh_2(R-p-PhTPCP)$_4$ (2.6 mg, 1.5 μmol, 0.5 mol %). The crude residue was subjected to flash chromatography (10%, then 15%-30% ethyl acetate in hexanes with 1% triethylamine) to obtain the pure product as a slightly pink solid (78.9 mg, 0.19 mmol, 65%).

R_f (30% ethyl acetate in hexanes) = 0.25

$[\alpha]_D^{20}$ = -465.9° ($CHCl_3$, c = 1)

mp. 155°C

^{1}H-NMR (500 MHz, $CDCl_3$) δ 8.13 (d, J = 2.5 Hz, 1H), 7.70 (d, J = 6.5 Hz, 2H), 7.66 – 7.59 (m, 1H), 7.39 – 7.31 (m, 2H), 7.24 (dt, J = 8.1, 0.7 Hz, 1H), 6.00 (dd, J = 3.9, 1.4 Hz, 1H), 5.31 (dd, J = 3.9, 2.5 Hz, 1H), 4.53 (dd, J = 6.6, 1.4 Hz, 1H), 3.62 (s, 3H), 3.20 (dd, J = 6.6, 2.6 Hz, 1H), 2.45 (s, 3H).

^{13}C-NMR ^{13}C NMR (126 MHz, $CDCl_3$) δ 172.3, 153.5, 150.3, 144.8, 142.8, 134.5, 131.6, 130.1, 127.2, 125.6, 123.7, 110.3, 53.0, 51.9, 38.8, 24.7, 21.7.

IR (neat): 2954, 1720, 1460, 1363, 1264, 1168, 759, 669, 593 cm^{-1}.

HRMS (+APCI): calcd. for $C_{19}H_{18}ClN_2O_4S$ $(M+H)^+$ 405.0676 found 405.0673.

HPLC analysis: ADH column, 1 mL/min, 5% iPrOH in hexanes, 70 min, λ = 230 nm, t_R: Major: 46.54 min, Minor: 26.87 min, 67% ee.

methyl (1S,5S,6R)-6-(4-chlorophenyl)-2-tosyl-2-azabicyclo[3.1.0]hex-3-ene-6-carboxylate

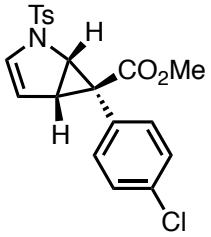

This compound was prepared according to the general procedure A, using 1-tosyl-1H-pyrrole (132.8 mg, 0.6 mmol, 2.0 equiv) as the substrate and methyl 2-(4-chlorophenyl)-2-diazoacetate (63.2 mg, 0.3 mmol, 1.0 equiv), under the catalysis of Rh_2(R-p-PhTPCP)$_4$ (2.6 mg, 1.5 µmol, 0.5 mol %). The crude residue was subjected to flash chromatography (10%, then 15% ethyl acetate in hexanes with 1% triethylamine) to obtain the pure product as an off-white solid (78.9 mg, 0.19 mmol, 65%).

$\mathbf{R_f}$ (30% ethyl acetate in hexanes) = 0.5

$[\boldsymbol{\alpha}]_{\mathbf{D}}^{\mathbf{20}}$ = -453.0° ($CHCl_3$, c = 1)

mp. 120°C

^{1}H-NMR (500 MHz, $CDCl_3$) δ = 7.73 – 7.66 (m, 2H), 7.38 – 7.31 (m, 2H), 7.25 – 7.20 (m, 2H), 7.13 (d, J = 8.0 Hz, 2H), 5.98 (dd, J = 3.9, 1.5 Hz, 1H), 5.27 (dd, J = 3.9, 2.5 Hz, 1H), 4.52 (dd, J = 6.5, 1.5 Hz, 1H), 3.61 (s, 3H), 3.14 (dd, J = 6.5, 2.5 Hz, 1H), 2.45 (s, 3H).

^{13}C-NMR (126 MHz, $CDCl_3$) δ = 173.1, 144.5, 134.8, 133.8, 133.4, 131.1, 130.0, 128.9, 128.2, 127.2, 110.9, 52.9, 52.2, 38.8, 27.3, 21.6.

IR (neat): 2953, 1714, 1495, 1359, 1261, 1166, 752, 668, 592, 544 cm^{-1}.

HRMS (+APCI): calcd. for $C_{20}H_{19}ClNO_4S$ $(M+H)^+$ 404.0723 found 404.0718.

HPLC analysis: ADH column, 1 mL/min, 1% iPrOH in hexanes, 70 min, λ = 230 nm, t_R: Major: 28.71 min, Minor: 25.94 min, 88% ee.

methyl (1S,5S,6R)-6-([1,1'-biphenyl]-4-yl)-2-tosyl-2-azabicyclo[3.1.0]hex-3-ene-6-carboxylate

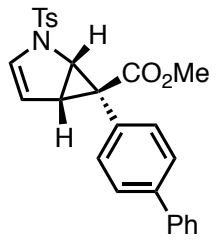

This compound was prepared according to the general procedure A, using 1-tosyl-1H-pyrrole (132.8 mg, 0.6 mmol, 2.0 equiv) as the substrate and methyl 2-([1,1'-biphenyl]-4-yl)-2-diazoacetate (75.7 mg, 0.3 mmol, 1.0 equiv), under the catalysis of Rh_2(R-p-PhTPCP)$_4$ (2.6 mg, 1.5 μmol, 0.5 mol %). The crude residue was subjected to flash chromatography (10%, then 15% ethyl acetate in hexanes with 1% triethylamine) to obtain the pure product as a yellow thick oil (104 mg, 0.23 mmol, 78%).

R_f (30% ethyl acetate in hexanes) = 0.4

$[\alpha]_D^{20}$ = -406.8° ($CHCl_3$, c = 1)

^{1}H-NMR (500 MHz, $CDCl_3$) δ = 7.72 (d, J = 8.2 Hz, 2H), 7.62 – 7.58 (m, 2H), 7.50 (dt, J = 8.3, 1.0 Hz, 2H), 7.46 – 7.41 (m, 2H), 7.35 (dt, J = 8.7, 1.5 Hz, 3H), 7.26 (m, J = 3.9 Hz, 2H), 6.00 (dt, J = 3.8, 1.2 Hz, 1H), 5.32 (ddd, J = 3.6, 2.5, 0.9 Hz, 1H), 4.56 (dt, J = 6.5, 1.1 Hz, 1H), 3.64 (d, J = 0.9 Hz, 3H), 3.17 (ddd, J = 6.6, 2.5, 0.9 Hz, 1H), 2.46 (s, 3H).

^{13}C-NMR (126 MHz, $CDCl_3$) δ = 173.6, 144.4, 140.1, 134.9, 132.8, 131.0, 130.0, 129.4, 128.8, 128.7, 127.5, 127.2, 127.1, 126.5, 111.3, 52.9, 52.3, 38.8, 27.7, 21.6.

IR (neat): 3039, 2952, 1709, 1360, 1261, 1167, 752, 668, 594, 540 cm^{-1}.

HRMS (+APCI): calcd. for $C_{26}H_{24}NO_4S$ $(M+H)^+$ 446.1426 found 446.1424.

HPLC analysis: ADH column, 1 mL/min, 2% iPrOH in hexanes, 70 min, λ = 230 nm, t_R: Major: 48.22 min, Minor: 43.91 min, 95% ee.

methyl (1S,5S,6R)-6-phenyl-2-tosyl-2-azabicyclo[3.1.0]hex-3-ene-6-carboxylate

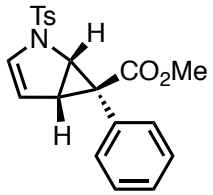

This compound was prepared according to the general procedure A, using 1-tosyl-1H-pyrrole (132.8 mg, 0.6 mmol, 2.0 equiv) as the substrate and methyl 2-diazo-2-phenylacetate (52.9 mg, 0.3 mmol, 1.0 equiv), under the catalysis of Rh_2(R-p-PhTPCP)$_4$ (2.6 mg, 1.5 μmol, 0.5 mol %). The crude residue was subjected to flash chromatography (10%, then 15% ethyl acetate in hexanes with 1% triethylamine) to obtain the pure product as a white solid (79.8 mg, 0.22 mmol, 72%).

R_f (30% ethyl acetate in hexanes) = 0.5

$[\alpha]_D^{20}$ = -519.9° ($CHCl_3$, c = 1)

mp. 130°C

^{1}H-NMR (500 MHz, $CDCl_3$) δ = 7.73 – 7.69 (m, 2H), 7.35 – 7.32 (m, 2H), 7.26 (dq, J = 4.1, 1.8 Hz, 3H), 7.20 (t, J = 4.2 Hz, 2H), 5.96 (dd, J = 3.9, 1.4 Hz, 1H), 5.28 (dd, J = 3.9, 2.5 Hz, 1H), 4.53 (dd, J = 6.5, 1.5 Hz, 1H), 3.61 (s, 3H), 3.14 (dd, J = 6.5, 2.5 Hz, 1H), 2.45 (s, 3H).

^{13}C-NMR (126 MHz, $CDCl_3$) δ = 173.6, 144.4, 134.9, 132.5, 130.8, 130.4, 130.0, 127.8, 127.4, 127.2, 111.3, 52.8, 52.2, 38.7, 28.0, 21.6

IR (neat): 3029, 2952, 1711, 1361, 1263, 1168, 702, 667, 594 cm^{-1}.

HRMS (+APCI): calcd. for $C_{20}H_{20}NO_4S$ $(M+H)^+$ 370.1113 found 370.1109.

HPLC analysis: ADH column, 1 mL/min, 2% iPrOH in hexanes, 70 min, λ = 230 nm, t_R: Major: 41.40 min, Minor: 30.27 min, 93% ee.

methyl (1S,5S,6R)-6-(naphthalen-2-yl)-2-tosyl-2-azabicyclo[3.1.0]hex-3-ene-6-carboxylate

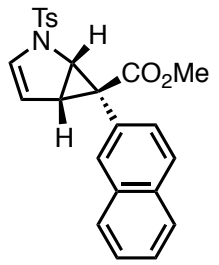

This compound was prepared according to the general procedure A, using 1-tosyl-1H-pyrrole (132.8 mg, 0.6 mmol, 2.0 equiv) as the substrate and methyl 2-diazo-2-(naphthalen-2-yl)acetate (67.9 mg, 0.3 mmol, 1.0 equiv), under the catalysis of Rh_2(R-p-PhTPCP)$_4$ (2.6 mg, 1.5 μmol, 0.5 mol %). The crude residue was subjected to flash chromatography (10%, then 15% ethyl acetate in hexanes with 1% triethylamine) to obtain the pure product as a bright yellow solid (78 mg, 0.19 mmol, 62%).

R_f (30% ethyl acetate in hexanes) = 0.5

$[\alpha]_D^{20}$ = -400.0° ($CHCl_3$, c = 1)

mp. 120°C

^{1}H-NMR (500 MHz, $CDCl_3$) δ = 7.94 – 7.75 (m, 4H), 7.72 (d, J = 8.0 Hz, 2H), 7.68 (m, 1H), 7.47 – 7.43 (m, 2H), 7.36 – 7.32 (m, 2H), 5.90 (dt, J = 3.9, 1.3 Hz, 1H), 5.32 (t, J = 3.3 Hz, 1H), 4.62 (d, J = 6.5 Hz, 1H), 3.60 (t, J = 0.7 Hz, 3H), 3.25 – 3.18 (m, 1H), 2.46 (s, 3H).

^{13}C-NMR (126 MHz, $CDCl_3$) δ = 173.7, 144.4, 134.9, 133.0, 132.6, 132.0, 131.0, 130.0, 129.9, 128.0, 127.8, 127.6, 127.4, 127.2, 126.0, 125.7, 111.2, 52.8, 52.4, 38.9, 28.1, 21.6.

IR (neat): 3054, 2952, 1711, 1359, 1263, 1168, 762, 669, 594 cm^{-1}.

HRMS (+APCI): calcd. for $C_{24}H_{22}NO_4S$ $(M+H)^+$ 420.1270 found 420.1267.

HPLC analysis: ADH column, 1 mL/min, 1% iPrOH in hexanes, 70 min, λ = 230 nm, t_R: Major: 91.69 min, Minor: 81.36 min, 96% ee.

dimethyl (1S,5S,6R)-6-(4-bromophenyl)-2-tosyl-2-azabicyclo[3.1.0]hex-3-ene-3,6-dicarboxylate

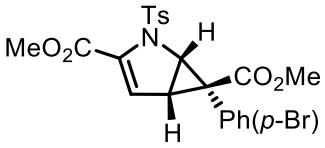

This compound was prepared according to the general procedure B, using methyl 1-tosyl-1H-pyrrole-2-carboxylate (167.6 mg, 0.6 mmol, 2.0 equiv) as the substrate and methyl 2-(4-bromophenyl)-2-diazoacetate (76.5 mg, 0.3 mmol, 1.0 equiv), under the catalysis of Rh_2(R-p-PhTPCP)$_4$ (2.6 mg, 1.5 μmol, 0.5 mol %). The crude residue was subjected to flash chromatography (1% to 15% ethyl acetate in hexanes) to obtain the pure product as an off-white solid (51.9 mg, 0.102 mmol, 34%).

R_f (20% ethyl acetate in hexanes) = 0.2

$[\alpha]_D^{20}$ = -262.1 ° ($CHCl_3$, c = 1)

mp. 170-171 °C

^{1}H-NMR (600 MHz, $CDCl_3$) δ = 7.83 – 7.77 (m, 2H), 7.39 – 7.34 (m, 2H), 7.30 – 7.27 (m, 2H), 6.89 – 6.83 (m, 2H), 6.01 (d, J = 2.5 Hz, 1H), 4.77 (d, J = 5.8 Hz, 1H), 3.62 (s, 3H), 3.59 (s, 3H), 3.11 (dd, J = 5.8, 2.5 Hz, 1H), 2.47 (s, 3H).

^{13}C-NMR (126 MHz, $CDCl_3$) δ = 172.1, 161.0, 144.9, 135.8, 134.2, 133.7, 131.0, 129.7, 128.6, 128.0, 122.7, 121.8, 53.0, 52.2, 51.6, 36.3, 29.2, 21.7.

IR (neat): 3109, 2958, 1733, 1717, 1594, 1485, 1369, 1323, 1257, 1226, 1167, 1059, 999, 958, 897, 842, 800, 750, 689, 649, 589, 541 cm^{-1}.

HRMS (+NSI): calcd. for $C_{22}H_{21}O_6NBrS$ $(M+H)^+$ 506.0268 found 506.0279.

HPLC analysis: ADH column, 0.5 mL/min, 10% iPrOH in hexanes, 60 min, λ = 230 nm, t_R: Major: 25.70 min, Minor: 34.80 min, 96% ee.

3-methyl 6-(2,2,2-trichloroethyl) (1S,5S,6R)-6-(4-bromophenyl)-2-tosyl-2-azabicyclo[3.1.0]hex-3-ene-3,6-dicarboxylate

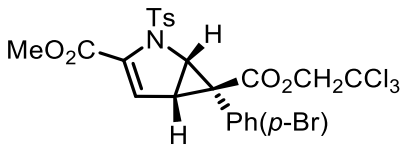

This compound was prepared according to the general procedure B, using methyl 1-tosyl-1H-pyrrole-2-carboxylate (167.6 mg, 0.6 mmol, 2.0 equiv) as the substrate and 2,2,2-trichloroethyl 2-(4-bromophenyl)-2-diazoacetate (112 mg, 0.3 mmol, 1.0 equiv), under the catalysis of Rh_2(R-p-PhTPCP)$_4$ (2.6 mg, 1.5 μmol, 0.5 mol %). The crude residue was subjected to flash chromatography (1% to 15% ethyl acetate in hexanes) to obtain the pure product as an off-white solid (82.0 mg, 0.16 mmol, 54%). The compound was crystallized by dissolving in $CHCl_3$ and then placing in a vessel containing Et_2O, which diffused into solution to give colorless blocks.

R_f (20% ethyl acetate in hexanes) = 0.35.

$[\alpha]_D^{20}$ = -135.8 ° ($CHCl_3$, c = 1)

mp. = 130-132 °C

^{1}H-NMR (600 MHz, $CDCl_3$) δ = 7.86 – 7.74 (m, 2H), 7.36 (m, 2H), 7.28 – 7.25 (m, 2H), 6.91 – 6.81 (m, 2H), 6.01 (dd, J = 2.5, 0.6 Hz, 1H), 4.90 (dd, J = 5.8, 0.5 Hz, 1H), 4.71 (d, J = 11.9 Hz, 1H), 4.61 (dd, J = 11.9, 0.5 Hz, 1H), 3.59 (s, 3H), 3.23 (ddd, J = 5.9, 2.5, 1H), 2.46 (s, 3H).

^{13}C-NMR (126 MHz, $CDCl_3$) δ = 170.1, 160.8, 145.0, 136.3, 134.2, 133.7, 131.1, 129.8, 128.1, 127.7, 122.1, 122.0, 94.5, 74.4, 52.3, 51.9, 36.8, 29.1, 21.7.

IR (neat): 2954, 1736, 1596, 1491, 1436, 1397, 1368, 1285, 1221, 1188, 1169, 1120, 1100, 1086, 1013, 978, 813, 763, 734, 717, 670 cm^{-1}.

HRMS (+APCI): calcd. for $C_{23}H_{20}O_6NBrCl_3S$ $(M+H)^+$ 621.9255 found 621.9258.

HPLC analysis: OD column, 1.0 mL/min, 3% iPrOH in hexanes, 50 min, λ = 230 nm, t_R: Major: 20.53 min, Minor: 32.62 min, 97% ee.

2-(tert-butyl) 3-methyl 6-(2,2,2-trichloroethyl) (1S,5S,6R)-6-(4-bromophenyl)-2-azabicyclo[3.1.0]hex-3-ene-2,3,6-tricarboxylate

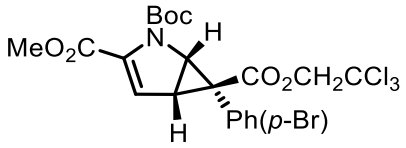

This compound was prepared according to the general procedure B, using methyl 1-Boc-1H-pyrrole-2-carboxylate (167.6 mg, 0.6 mmol, 2.0 equiv) as the substrate and 2,2,2-trichloroethyl 2-(4-bromophenyl)-2-diazoacetate (112 mg, 0.3 mmol, 1.0 equiv), under the catalysis of Rh_2(R-p-PhTPCP)$_4$ (2.6 mg, 1.5 μmol, 0.5 mol %). The crude residue was subjected to flash chromatography (1% to 15% ethyl acetate in hexanes) to obtain the pure product as a colorless solid (128.0 mg, 0.20 mmol, 68%).

R_f (20% ethyl acetate in hexanes) = 0.45

$[\alpha]_D^{20}$ = -191.8 ° ($CHCl_3$, c = 1)

mp. = 137-138 °C

^{1}H-NMR (600 MHz, $CDCl_3$) δ = 7.41 – 7.35 (m, 2H), 7.03 (m, 2H), 5.77 (d, J = 2.6 Hz, 1H), 4.86 (d, J = 6.2 Hz, 1H), 4.69 (s, 2H), 3.52 (s, 3H), 3.42 (dd, J = 6.2, 2.6 Hz, 1H), 1.46 (s, 9H).

^{13}C-NMR (75 MHz, $CDCl_3$) δ = 170.8, 161.2, 151.1, 135.7, 134.0, 131.2, 128.3, 121.9, 116.1, 94.7, 83.3, 74.3, 51.9, 49.8, 36.6, 28.5, 28.0.

IR (neat): 2925, 1728, 1456, 1436, 1389, 1369, 1218, 1149, 1070, 952, 792, 768, 716 cm^{-1}.

HRMS (+NSI): calcd. for $C_{21}H_{22}O_6NBrCl_3S$ $(M+H)^+$ 567.9691 found 567.9698.

HPLC analysis: ADH column, 1.0 mL/min, 3% iPrOH in hexanes, 30 min, λ = 230 nm, t_R: Major: 8.77 min, Minor: 16.02 min, 96% ee.

3-methyl 6-(2,2,2-trichloroethyl) (1S,5S,6R)-6-(4-fluorophenyl)-2-tosyl-2-azabicyclo[3.1.0]hex-3-ene-3,6-dicarboxylate

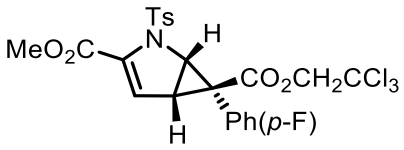

This compound was prepared according to the general procedure B, using methyl 1-tosyl-1H-pyrrole-2-carboxylate (167.6 mg, 0.6 mmol, 2.0 equiv) as the substrate and 2,2,2-trichloroethyl 2-(4-fluorophenyl)-2-diazoacetate (93.5 mg, 0.3 mmol, 1.0 equiv), under the catalysis of Rh_2(R-p-PhTPCP)$_4$ (2.6 mg, 1.5 μmol, 0.5 mol %). The crude residue was subjected to flash chromatography (1% to 15% ethyl acetate in hexanes) to obtain the pure product as a colorless solid (122.1 mg, 0.22 mmol, 72%).

R_f (20% ethyl acetate in hexanes) = 0.3

$[\alpha]_D^{20}$ = -208.7 ° ($CHCl_3$, c = 1)

mp. = 126-127 °C

^{1}H-NMR (500 MHz, $CDCl_3$) δ = 7.84 – 7.76 (m, 2H), 7.40 – 7.36 (m, 2H), 6.97 (dd, J = 8.5, 5.2 Hz, 2H), 6.84 (t, J = 8.5 Hz, 2H), 6.04 (d, J = 2.5 Hz, 1H), 4.91 (d, J = 5.9 Hz, 1H), 4.76 – 4.67 (m, 1H), 4.66 – 4.60 (m, 1H), 3.60 (s, 3H), 3.28 – 3.21 (m, 1H), 2.48 (s, 3H).

^{13}C-NMR (126 MHz, $CDCl_3$) δ = 170.4, 163.2, 161.0 (d, *J* = 47.5 Hz), 145.0, 136.3, 134.2, 133.8 (d, *J* = 8.5 Hz), 129.7, 128.1, 124.3 (d, *J* = 3.3 Hz), 122.1, 114.9 (d, *J* = 21.9 Hz), 94.5, 74.5, 52.3, 52.0, 36.9, 28.9, 21.7.

^{19}F-NMR (282 MHz, $CDCl_3$) δ = -113.4.

IR (neat): 2954, 2360, 2342, 1732, 1598, 1514, 1437, 1367, 1279, 1220, 1169, 1120, 1096, 1060, 1016, 978, 948, 910, 840, 814, 761, 738, 719, 705, 670 cm^{-1}.

HRMS (+APCI): calcd. for $C_{23}H_{20}O_6NCl_3FS$ $(M+H)^+$ 562.0056 found 562.0056.

HPLC analysis: OD column, 1.0 mL/min, 3% iPrOH in hexanes, 50 min, λ = 230 nm, t_R: Major: 19.29 min, Minor: 24.20 min, 96% ee.

3-methyl 6-(2,2,2-trichloroethyl) (1S,5S,6R)-2-tosyl-6-(4-(trifluoromethyl)phenyl)-2-azabicyclo[3.1.0]hex-3-ene-3,6-dicarboxylate

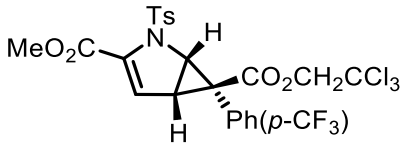

This compound was prepared according to the general procedure B, using methyl 1-tosyl-1H-pyrrole-2-carboxylate (167.6 mg, 0.6 mmol, 2.0 equiv) as the substrate and 2,2,2-trichloroethyl 2-(4-(trifluoromethyl)phenyl)-2-diazoacetate (108.5 mg, 0.30 mmol, 1.0 equiv), under the catalysis of Rh_2(R-p-PhTPCP)$_4$ (2.6 mg, 1.5 μmol, 0.5 mol %). The crude residue was subjected to flash chromatography (1% to 15% ethyl acetate in hexanes) to obtain the pure product as a colorless solid (125.2 mg, 0.20 mmol, 68%).

R_f (20% ethyl acetate in hexanes) = 0.3

$[\alpha]_D^{20}$ = -300.0 ° ($CHCl_3$, c = 1)

mp. = 102-103 °C

^{1}H-NMR (600 MHz, $CDCl_3$) δ = 7.77 (d, J = 8.3 Hz, 2H), 7.41 (d, J = 8.0 Hz, 2H), 7.36 (d, J = 8.0 Hz, 2H), 7.14 (d, J = 8.0 Hz, 2H), 6.01 (d, J = 2.5 Hz, 1H), 4.90 (d, J = 5.8 Hz, 1H), 4.71 (d, J = 11.8 Hz, 1H), 4.61 (d, J = 11.9 Hz, 1H), 3.52 (s, 3H), 3.26 (dd, J = 5.8, 2.4 Hz, 1H), 2.46 (s, 3H).

^{13}C-NMR (151 MHz, $CDCl_3$) δ = 169.8, 160.9, 145.2, 136.2, 133.9, 132.8, 130.0 (q, J = 32.8 Hz) 129.8, 128.1, 124.9, 124.8 (q, J = 3.7 Hz), 123.8 (q, J = 270.1 Hz), 121.9, 94.5, 74.5, 52.2, 51.8, 36.8, 29.21, 21.7.

^{19}F-NMR (282 MHz, $CDCl_3$) δ = -62.7.

IR (neat): 2924, 2361, 1733, 1620, 1597, 1323,1220, 1188, 1166, 1123, 1108, 1066, 1018, 977, 949, 912, 843, 806, 770, 761, 736, 704, 669, 590, 540 cm^{-1}.

HRMS (+NSI): calcd. for $C_{24}H_{20}O_6NCl_3F_3S$ $(M+H)^+$ 612.0026 found 612.0030.

HPLC analysis: ADH column, 1.0 mL/min, 2% iPrOH in hexanes, 80 min, $\lambda = 230$ nm, t_R: Major: 26.04 min, Minor: 66.23 min, >99% ee.

3-methyl 6-(2,2,2-trichloroethyl) (1S,5S,6R)-6-phenyl-2-tosyl-2-azabicyclo[3.1.0]hex-3-ene-3,6-dicarboxylate

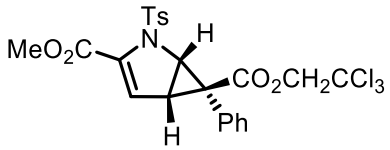

This compound was prepared according to the general procedure B, using methyl 1-tosyl-1H-pyrrole-2-carboxylate (167.6 mg, 0.6 mmol, 2.0 equiv) as the substrate and 2,2,2-trichloroethyl 2-phenyl-2-diazoacetate (88.1 mg, 0.3 mmol, 1.0 equiv), under the catalysis of Rh_2(R-p-PhTPCP)$_4$ (2.6 mg, 1.5 μmol, 0.5 mol %). The crude residue was subjected to flash chromatography (1% to 15% ethyl acetate in hexanes) to obtain the pure product as a colorless solid (97.5 mg, 0.18 mmol, 60%).

R_f (20% ethyl acetate in hexanes) = 0.3

$[\alpha]_D^{20}$ = -241.1 ° ($CHCl_3$, c = 1)

mp. = 119-120 °C

^{1}H-NMR (600 MHz, $CDCl_3$) δ = 7.80 (d, J = 8.3 Hz, 2H), 7.35 (d, J = 8.4 Hz, 2H), 7.18 – 7.14 (m, 1H), 7.13 – 7.10 (m, 2H), 6.97 – 6.95 (m, 2H), 6.05 (d, J = 2.5 Hz, 1H), 4.92 (d, J = 5.8 Hz, 1H), 4.70 (d, J = 12.0 Hz, 1H), 4.61 (d, J = 12.0 Hz, 1H), 3.55 (s,1H), 3.23 (dd, J = 5.8, 2.5 Hz, 1H), 2.46 (s, 3H).

^{13}C-NMR (151 MHz, $CDCl_3$) δ = 170.6, 160.9, 144.8, 136.1, 134.3, 132.1, 129.7, 128.5, 128.1, 127.9, 127.8, 122.7, 94.6, 74.4, 52.2, 51.9, 36.7, 29.9, 21.7.

IR (neat): 3030, 2954, 1731, 1597, 1497, 1436, 1368, 1289, 1219, 1168, 1120, 1084, 1060, 977, 947, 907, 806, 784, 758, 702, 668 cm^{-1}.

HRMS (+APCI): calcd. for $C_{23}H_{20}O_6NBrCl_3S$ $(M+H)^+$ 544.0150 found 544.0154.

HPLC analysis: OD column, 1.0 mL/min, 3% iPrOH in hexanes, 60 min, λ = 230 nm, t_R: Major: 18.99 min, Minor: 32.17 min, 97% ee.

3-methyl 6-(2,2,2-trichloroethyl) (1S,5S,6R)-6-(4-(tert-butyl)phenyl)-2-tosyl-2-azabicyclo[3.1.0]hex-3-ene-3,6-dicarboxylate

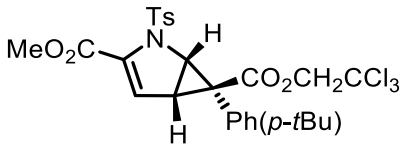

This compound was prepared according to the general procedure B, using methyl 1-tosyl-1H-pyrrole-2-carboxylate (167.6 mg, 0.6 mmol, 2.0 equiv) as the substrate and 2,2,2-trichloroethyl 2-(4-(tert-butyl)phenyl)-2-diazoacetate (104.9 mg, 0.3 mmol, 1.0 equiv), under the catalysis of Rh_2(R-p-PhTPCP)$_4$ (2.6 mg, 1.5 μmol, 0.5 mol %). The crude residue was subjected to flash chromatography (1% to 15% ethyl acetate in hexanes) to obtain the pure product as a colorless solid (125.9 mg, 0.21 mmol, 70%).

R_f (20% ethyl acetate in hexanes) = 0.35

$[\alpha]_D^{20}$ = -237.0 ° ($CHCl_3$, c = 1)

mp. = 114-115 °C.

^{1}H-NMR (600 MHz, $CDCl_3$) δ = 7.76 – 7.73 (m, 2H), 7.36 – 7.32 (m, 2H), 7.17 – 7.12 (m, 2H), 6.97 – 6.88 (m, 2H), 6.05 (d, J = 2.4 Hz, 1H), 4.84 (dd, J = 5.7, 1.7 Hz, 1H), 4.75 – 4.67 (m, 1H), 4.65 – 4.51 (m, 1H), 3.50 (s, 3H), 3.16 (dd, J = 5.7, 2.5 Hz, 1H), 2.46 (s, 3H), 1.23 (s, 9H).

^{13}C-NMR (126 MHz, $CDCl_3$) δ 170.6, 161.3, 150.6, 144.8, 135.8, 133.8, 131.8, 129.7, 128.1, 125.2, 124.7, 123.6, 94.7, 74.3, 52.0, 51.6, 36.4, 34.5, 31.2, 29.5, 21.7.

IR (neat): 2958, 2360, 1731, 1597, 1514, 1436, 1366, 1289, 1220, 1170, 1106, 1060, 979, 949, 841, 807, 762, 737, 706, 690, 670 cm^{-1}.

HRMS (+APCI): calcd. for $C_{27}H_{29}O_6NCl_3S$ $(M+H)^+$ 600.0776 found 600.0779.

HPLC analysis: OD column, 1.0 mL/min, 3% iPrOH in hexanes, 30 min, λ = 230 nm, t_R: Major: 11.93 min, Minor: 18.18 min, >99% ee.

3-methyl 6-(2,2,2-trichloroethyl) (1S,5S,6R)-6-(4-acetoxyphenyl)-2-tosyl-2-azabicyclo[3.1.0]hex-3-ene-3,6-dicarboxylate

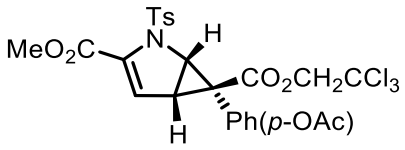

This compound was prepared according to the general procedure B, using methyl 1-tosyl-1H-pyrrole-2-carboxylate (167.6 mg, 0.6 mmol, 2.0 equiv) as the substrate and 2,2,2-trichloroethyl 2-(4-acetoxyphenyl)-2-diazoacetate (105.5 mg, 0.3 mmol, 1.0 equiv), under the catalysis of Rh_2(R-p-PhTPCP)$_4$ (2.6 mg, 1.5 μmol, 0.5 mol %). The crude residue was subjected to flash chromatography (1% to 20% ethyl acetate in hexanes) to obtain the pure product as a colorless solid (112.6 mg, 0.19 mmol, 62%).

R_f (20% ethyl acetate in hexanes) = 0.1

$[\alpha]_D^{20}$ = -261.6 ° ($CHCl_3$, c = 1)

mp. = 148-149 °C.

^{1}H-NMR (400 MHz, $CDCl_3$) δ = 7.84 – 7.74 (m, 2H), 7.39 – 7.32 (m, 2H), 7.03 – 6.95 (m, 2H), 6.92 – 6.81 (m, 2H), 6.02 (dd, J = 2.5, 0.5 Hz, 1H), 4.87 (dd, J = 5.8, 0.5 Hz, 1H), 4.70 (d, J = 11.9 Hz, 1H), 4.59 (d, J = 11.9 Hz, 1H), 3.56 (s, 3H), 3.21 (dd, J = 5.8, 2.5 Hz, 1H), 2.44 (s, 3H), 2.22 (s, 3H).

^{13}C-NMR (151 MHz, $CDCl_3$) δ = 170.3, 168.9, 161.0, 150.2, 144.9, 136.2, 134.1, 133.2, 129.8, 128.1, 126.0, 122.4, 121.0, 94.6, 74.4, 52.3, 51.7, 36.8, 29.1, 21.7, 21.1.

IR (neat): 2955, 1729, 1597, 1510, 1437, 1368, 1281, 1216, 1169, 1167, 1120, 1083, 1059, 1017, 978, 947, 912, 850, 808, 757, 724, 705, 6609 cm^{-1}.

HRMS (+APCI): calcd. for $C_{25}H_{23}O_8NCl_3S$ $(M+H)^+$ 602.0205 found 602.0205.

HPLC analysis: OD column, 1.0 mL/min, 30% iPrOH in hexanes, 30 min, λ = 230 nm, t_R: Major: 7.31 min, Minor: 18.20 min, 94% ee.

3-methyl 6-(2,2,2-trichloroethyl) (1S,5S,6R)-6-([1,1'-biphenyl]-4-yl)-2-tosyl-2-azabicyclo[3.1.0]hex-3-ene-3,6-dicarboxylate

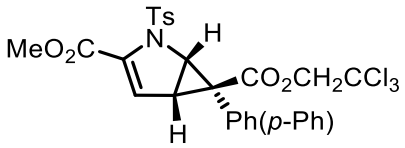

This compound was prepared according to the general procedure B, using methyl 1-tosyl-1H-pyrrole-2-carboxylate (167.6 mg, 0.6 mmol, 2.0 equiv) as the substrate and 2,2,2-trichloroethyl 2-(-([1,1'-biphenyl]-4-yl)-2-diazoacetate (111.7 mg, 0.30 mmol, 1.0 equiv), under the catalysis of Rh_2(R-p-PhTPCP)$_4$ (2.6 mg, 1.5 μmol, 0.5 mol %). The crude residue was subjected to flash chromatography (1% to 10% ethyl acetate in hexanes) to obtain the pure product as a colorless solid (117.7 mg, 0.19 mmol, 63%).

R_f (20% ethyl acetate in hexanes) = 0.29

$[\alpha]_D^{20}$ = -325.6 ° ($CHCl_3$, c = 1)

mp. = 145 °C

^{1}H-NMR (600 MHz, $CDCl_3$) δ = 7.81 (d, J = 8.3 Hz, 2H), 7.39 (dt, J = 20.9, 7.6 Hz, 6H), 7.35 – 7.30 (m, 1H), 7.13 – 7.03 (m, 2H), 6.10 (d, J = 2.5 Hz, 1H), 4.95 (d, J = 5.8 Hz, 1H), 4.74 (d, J = 11.9 Hz, 1H), 4.64 (d, J = 11.9 Hz, 1H), 3.52 (s, 3H), 3.26 (dd, J = 5.8, 2.5 Hz, 1H), 2.47 (s, 3H).

^{13}C-NMR (126 MHz, $CDCl_3$) δ = 170.5, 161.0, 144.9, 140.7, 140.6, 136.1, 134.2, 132.5, 129.7, 128.7, 128.1, 127.6, 127.3, 127.0, 126.5, 122.9, 94.7, 74.4, 52.1, 51.9, 36.7, 29.6, 21.7.

IR (neat): 2925, 1732, 1597, 1489, 1436, 1369, 1287, 1220, 1169, 1120, 1086, 1059, 1009, 978, 947, 842, 778, 758, 728, 700, 670, 655, 590, 543 cm^{-1}.

HRMS (+NSI): calcd. for $C_{29}H_{25}O_6NCl_3S$ $(M+H)^+$ 620.0463 found 620.0468.

HPLC analysis: OD column, 1.0 mL/min, 20% iPrOH in hexanes, 30 min, λ = 230 nm, t_R: Major: 8.26 min, Minor: 12.11 min, 98% ee.

3-methyl 6-(2,2,2-trichloroethyl) (1S,5S,6R)-6-(6-chloropyridin-3-yl)-2-tosyl-2-azabicyclo[3.1.0]hex-3-ene-3,6-dicarboxylate

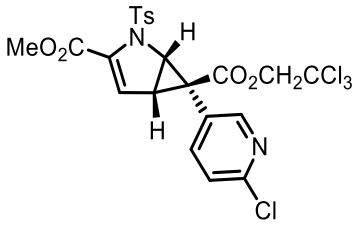

This compound was prepared according to the general procedure B, using methyl 1-tosyl-1H-pyrrole-2-carboxylate (167.6 mg, 0.6 mmol, 2.0 equiv) as the substrate and 2,2,2-trichloroethyl 2-(6-chloropyridin-3-yl)-2-diazoacetate (98.7 mg, 0.3 mmol, 1.0 equiv), under the catalysis of Rh_2(R-p-PhTPCP)$_4$ (2.6 mg, 1.5 μmol, 0.5 mol %). The crude residue was subjected to flash chromatography (1% to 30% ethyl acetate in hexanes) to obtain the pure product as a colorless solid (115 mg, 0.20 mmol, 66%).

R_f (20% ethyl acetate in hexanes) = 0.13

$[\alpha]_D^{20}$ = -249.7 ° ($CHCl_3$, c = 1)

mp. = 146-148 °C.

^{1}H-NMR (600 MHz, $CDCl_3$) δ = 8.02 (d, J = 2.5 Hz, 1H), 7.83 – 7.75 (m, 2H), 7.36 (d, J = 8.1 Hz, 2H), 7.33 – 7.30 (m, 1H), 7.10 (d, J = 8.2 Hz, 1H), 6.01 (d, J = 2.5 Hz, 1H), 4.90 (d, J = 5.9 Hz, 1H), 4.69 (d, J = 11.9 Hz, 1H), 4.61 (d, J = 11.8 Hz, 1H), 3.59 (s, 3H), 3.30 (dd, J = 5.9, 2.5 Hz, 1H), 2.45 (s, 4H).

^{13}C-NMR (126 MHz, $CDCl_3$) δ = 169.4, 160.5, 153.0, 150.8, 145.3, 142.4, 136.8, 134.0, 129.9, 128.0, 124.0, 123.5, 120.6, 94.3, 74.6, 52.5, 51.7, 37.0, 26.4, 21.7.

IR (neat): 2955, 1736, 1590, 1561, 1462, 1436, 1368, 1283, 1223, 1189, 1170, 1126, 1106, 1020, 977, 947, 806, 760, 737, 706, 670 cm^{-1}.

HRMS (+APCI): calcd. for $C_{22}H_{19}O_6N_2Cl_4S$ $(M+H)^+$ 578.9712 found 578.9712.

HPLC analysis: OD column, 1.0 mL/min, 3% iPrOH in hexanes, 80 min, λ = 230 nm, t_R: Major: 43.78 min, Minor: 66.51 min, 95% ee.

3-methyl 6-(2,2,2-trichloroethyl) (1S,5S,6R)-6-(4-bromothiophen-2-yl)-2-tosyl-2-azabicyclo[3.1.0]hex-3-ene-3,6-dicarboxylate

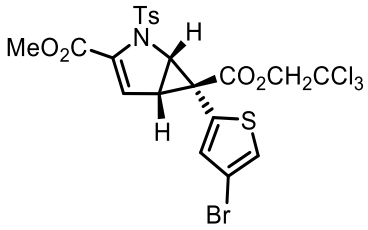

This compound was prepared according to the general procedure B, using methyl 1-tosyl-1H-pyrrole-2-carboxylate (167.6 mg, 0.6 mmol, 2.0 equiv) as the substrate and 2,2,2-trichloroethyl 2-(4-bromothiophen-2-yl)-2-diazoacetate (113.5 mg, 0.3 mmol, 1.0 equiv), under the catalysis of Rh_2(R-p-PhTPCP)$_4$ (2.6 mg, 1.5 μmol, 0.5 mol %). The crude residue was subjected to flash chromatography (1% to 10% ethyl acetate in hexanes) to obtain the pure product as a brownish, viscous oil (60 mg, 0.10 mmol, 32%).

$\mathbf{R_f}$ (20% ethyl acetate in hexanes) = 0.35

$[\alpha]_D^{20}$ = -142.9 ° ($CHCl_3$, c = 1)

^{1}H-NMR (600 MHz, $CDCl_3$) δ = 7.77 (d, J=8.2, 2H), 7.32 (d, J = 8.0, 2H), 6.99 (s, 1H), 6.41 (s, 1H), 5.94 (d, J = 2.5, 1H), 4.99 (d, J = 5.8, 1H), 4.73 (d, J = 11.9, 1H), 4.58 (d, J = 11.9, 1H), 3.65 (s, 3H), 3.30 (dd, J = 5.9, 2.6, 1H), 2.41 (s, 3H).

^{13}C-NMR (151 MHz, $CDCl_3$) δ = 169.5, 161.0, 145.3, 137.1, 134.9, 134.5, 131.6, 130.0, 128.2, 124.2, 121.2, 108.2, 94.6, 74.8, 53.3, 52.7, 39.6, 24.0, 21.9.

IR (neat): 2953, 2159, 2029, 1736, 1597, 1436, 1366, 1283, 1219, 1169, 1108, 1056, 974, 813, 760, 705, 667 cm^{-1}.

HRMS (+APCI): calcd. for $C_{21}H_{18}O_6NBrCl_3FS_2$ $(M+H)^+$ 627.8819 found 562.8823.

HPLC analysis: OD column, 1.0 mL/min, 3% iPrOH in hexanes, 40 min, λ = 230 nm, t_R: Major: 19.66 min, Minor: 29.18 min, 96% ee.

3-methyl 6-(2,2,2-trichloroethyl) (1S,5S,6R)-6-(2-fluorophenyl)-2-tosyl-2-azabicyclo[3.1.0]hex-3-ene-3,6-dicarboxylate

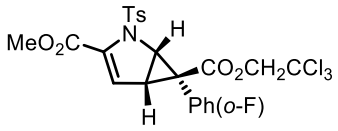

This compound was prepared according to the general procedure B, using methyl 1-tosyl-1H-pyrrole-2-carboxylate (167.6 mg, 0.6 mmol, 2.0 equiv) as the substrate and 2,2,2-trichloroethyl 2-(2-fluorophenyl)-2-diazoacetate (93.5 mg, 0.3 mmol, 1.0 equiv), under the catalysis of Rh_2(R-p-PhTPCP)$_4$ (2.6 mg, 1.5 μmol, 0.5 mol %). The crude residue was subjected to flash chromatography (1% to 20% ethyl acetate in hexanes) to obtain the pure product as a colorless solid (126.0 mg, 0.23 mmol, 75%).

R_f (20% ethyl acetate in hexanes) = 0.3

$[\alpha]_D^{20}$ = -158.4 ° ($CHCl_3$, c = 1)

mp. = 111-112°C.

^{1}H-NMR (600 MHz, $CDCl_3$) (rotamers) δ = 7.81 (d, J = 7.9 Hz, 2H), 7.47 – 7.27 (m, 2H), 7.23 – 7.16 (m, 1H), 7.12 – 6.77 (m, 3H), 6.22 – 6.01 (m, 1H), 5.21 – 4.84 (m, 1H), 4.80 – 4.54 (m, 1H), 3.57 (s, 3H), 3.34 – 3.24 (m, 1H), 2.47 (s, 3H).

^{13}C-NMR (151 MHz, $CDCl_3$) δ = 169.9, 161.0, 145.1, 136.4, 134.0, 134.0, 130.35 (d, *J* = 7.6 Hz), 129.9, 128.2, 123.6, 122.3, 121.5, 116.32 (d, *J* = 14.0 Hz), 115.10 (d, *J* = 20.9 Hz), 94.6, 74.7, 52.3, 51.1, 37.4, 24.6, 21.8.

^{19}F-NMR (282 MHz, $CDCl_3$) δ = (-114.1), -114.8.

IR (neat): 2954, 2159, 1732, 1597, 1497, 1370, 1284, 1265, 1218, 1169, 1128, 1096, 1059, 977, 951, 812, 756, 724, 705, 669 cm^{-1}.

HRMS (+APCI): calcd. for $C_{23}H_{20}O_6NCl_3FS$ $(M+H)^+$ 562.0056 found 562.0060.

HPLC analysis: OD column, 1.0 mL/min, 3% iPrOH in hexanes, 40 min, λ = 230 nm, t_R: Major: 17.07 min, Minor: 24.96 min, 74% ee.

2,2,2-trichloroethyl (1S,5S,6R)-6-(4-bromophenyl)-2-tosyl-2-azabicyclo[3.1.0]hex-3-ene-6-carboxylate

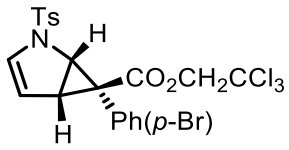

This compound was prepared according to the general procedure B, using methyl 1-tosyl-1H-pyrrole (132.8 mg, 0.6 mmol, 2.0 equiv) as the substrate and 2,2,2-trichloroethyl 2-(4-bromophenyl)-2-diazoacetate (111.7 mg, 0.3 mmol, 1.0 equiv), under the catalysis of Rh_2(R-p-PhTPCP)$_4$ (2.6 mg, 1.5 μmol, 0.5 mol %). The crude residue was subjected to flash chromatography on Florisil® (1% to 5% ethyl acetate in hexanes) to obtain the pure product as a colorless solid (134.0 mg, 0.24 mmol, 79%).

R_f (20% ethyl acetate in hexanes) = 0.4

$[\alpha]_D^{20}$ = -288.2 ° ($CHCl_3$, c = 1)

^{1}H-NMR (500 MHz, $CDCl_3$) δ = 7.71 (d, J = 8.5 Hz, 2H), 7.42 – 7.37 (m, 2H), 7.35 (d, 2H), 7.09 (d, J = 8.5 Hz, 2H), 6.04 (dd, J = 3.9, 1.4 Hz, 1H), 5.30 (dd, J = 3.9, 2.5 Hz, 1H), 4.71 (d, J = 11.9 Hz, 1H), 4.65 (dd, J = 6.6, 1.5 Hz, 1H), 4.61 (d, J = 11.9 Hz, 1H), 3.27 (dd, J = 6.6, 2.5 Hz, 1H), 2.46 (s, 3H).

^{13}C-NMR (126 MHz, $CDCl_3$) δ = 171.0, 144.7, 134.7, 134.2, 131.5, 131.2, 130.0, 128.5, 127.2, 121.9, 110.5, 94.6, 74.3, 52.5, 39.4, 27.4, 21.6.

IR (neat): 1728, 1596, 1489, 1360, 1318, 1220, 1166,1135, 1089, 1071, 1011, 981, 945, 810, 780, 764, 746, 715, 667, 591, 543 cm^{-1}.

HRMS (+NSI): calcd. for $C_{21}H_{18}O_4NBrCl_3S$ $(M+H)^+$ 563.9200 found 563.9206.

HPLC analysis: OD column, 1.0 mL/min, 3% iPrOH in hexanes, 40 min, λ = 230 nm, t_R: Major: 41.91 min, Minor: 54.62 min, 98% ee.

2,2,2-trichloroethyl (1S,5S,6R)-3-(acetoxymethyl)-6-(4-bromophenyl)-2-tosyl-2-azabicyclo[3.1.0]hex-3-ene-6-carboxylate

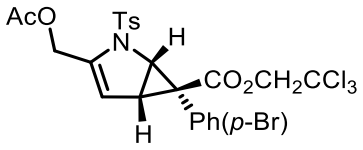

This compound was prepared according to the general procedure B, using (1-tosyl-1H-pyrrol-2-yl)methyl acetate (176.0 mg, 0.6 mmol, 2.0 equiv) as the substrate and 2,2,2-trichloroethyl 2-(4-bromophenyl)-2-diazoacetate (111.7 mg, 0.3 mmol, 1.0 equiv), under the catalysis of Rh_2(R-p-PhTPCP)$_4$ (2.6 mg, 1.5 μmol, 0.5 mol %). The crude residue was subjected to flash chromatography (1% to 15% ethyl acetate in hexanes) to obtain the pure product as a colorless solid (142.4 mg, 0.23 mmol, 75%).

R_f (20% ethyl acetate in hexanes) = 0.3

$[\alpha]_D^{20}$ = -132.3 ° ($CHCl_3$, c = 1)

^{1}H-NMR (600 MHz, $CDCl_3$) δ = 7.73 (d, J = 8.4 Hz, 2H), 7.40 – 7.37 (m, 2H), 7.35 – 7.32 (m, 2H), 7.10 (d, J = 7.9 Hz, 2H), 5.38 (d, J = 2.5, 0.7 Hz, 1H), 4.83 (d, J = 6.5 Hz, 1H), 4.70 (d, J = 11.9 Hz, 1H), 4.62 – 4.59 (m, 2H), 4.39 (d, J = 13.7 Hz, 1H), 3.17 (dd, J = 6.5, 2.4 Hz, 1H), 2.44 (s, 3H), 1.84 (s, 3H).

^{13}C-NMR (126 MHz, $CDCl_3$) δ = 170.6, 170.0, 144.8, 139.9, 135.0, 134.3, 131.1, 130.1, 128.3, 127.2, 122.0, 114.2, 94.6, 74.4, 57.6, 53.9, 36.3, 28.0, 21.6, 20.6.

IR (neat): 2956, 1736, 1628, 1596, 1490, 1445, 1361, 1213, 1187, 1167, 1101, 1069, 1036, 1011, 987, 929, 833, 811, 768, 735, 715, 665, 589, 542 cm^{-1}.

HRMS (+NSI): calcd. for $C_{24}H_{22}O_6NBrCl_3S$ $(M+H)^+$ 635.9411 found 635.9426.

HPLC analysis: ADH column, 1.0 mL/min, 10% iPrOH in hexanes, 30 min, λ = 230 nm, t_R: Major: 11.56 min, Minor: 20.98 min, 96% ee.

2,2,2-trichloroethyl (1R,1aS,6bS)-1-(4-bromophenyl)-2-tosyl-1,1a,2,6b-tetrahydrocyclopropa[b]indole-1-carboxylate

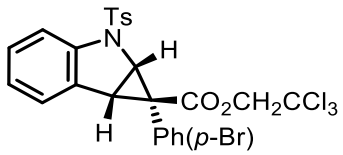

This compound was prepared according to the general procedure B, using 1-tosyl-1H-indole (163.0 mg, 0.6 mmol, 2.0 equiv) as the substrate and 2,2,2-trichloroethyl 2-(4-bromophenyl)-2-diazoacetate (111.7 mg, 0.3 mmol, 1.0 equiv), under the catalysis of Rh_2(S-TCPTTL)$_4$ (2.7 mg, 1.5 μmol, 0.5 mol %). The crude residue was subjected to flash chromatography (1% to 10% ethyl acetate in hexanes) to obtain the pure product as a colorless solid (67.3 mg, 0.11 mmol, 36%).

R_f (20% ethyl acetate in hexanes) = 0.48

$[\alpha]_D^{20}$ = -48.8 ° ($CHCl_3$, c = 1)

mp. = 67 °C

^{1}H-NMR (600 MHz, $CDCl_3$) δ = 7.68 – 7.65 (m, 2H), 7.32 (dd, J = 7.5, 1.2 Hz, 1H), 7.24 – 7.18 (m, 5H), 7.06 – 6.90 (m, 4H), 5.01 (d, J = 6.7 Hz, 1H), 4.72 (d, J = 11.8 Hz, 1H), 4.68 (d, J = 11.9 Hz, 1H), 3.70 (d, J = 6.6 Hz, 1H), 2.36 (s, 3H).

^{13}C-NMR (151 MHz, $CDCl_3$) δ = 170.6, 144.7, 141.2, 135.2, 134.0, 131.0, 129.9, 128.5, 128.4, 127.8, 126.9, 125.7, 123.9, 121.9, 114.5, 94.6, 74.5, 53.4, 35.6, 30.2, 21.6.

IR (neat): 2955, 1729, 1596, 1490, 1464, 1396, 1362, 1307, 1237, 1209, 1168, 1116, 1089, 1059, 1025, 1012, 970, 933, 831, 811 cm^{-1}

HRMS (+NSI): calcd. for $C_{25}H_{20}O_4NBrCl_3S$ $(M+H)^+$ 613.9357 found 613.9360.

HPLC analysis: ADH column, 1.0 mL/min, 3% iPrOH in hexanes, 45 min, λ = 230 nm, t_R: Major: 23.50 min, Minor: 35.83 min, 93% ee.

2,2,2-trichloroethyl (1S,5S,6R)-6-(4-bromophenyl)-2-tosyl-3-(2,2,2-trifluoroacetyl)-2-azabicyclo[3.1.0]hex-3-ene-6-carboxylate

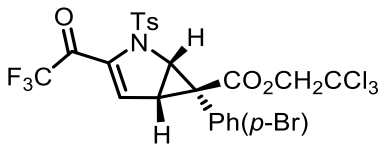

This compound was prepared according to the general procedure B, using 2,2,2-trifluoro-1-(1-tosyl-1H-pyrrol-2-yl)ethan-1-one (190.4 mg, 0.6 mmol, 2.0 equiv) as the substrate and 2,2,2-trichloroethyl 2-(4-bromophenyl)-2-diazoacetate (111.7 mg, 0.3 mmol, 1.0 equiv), under the catalysis of Rh_2(R-p-PhTPCP)$_4$ (2.6 mg, 1.5 μmol, 0.5 mol %). The crude residue was subjected to flash chromatography (1% to 15% ethyl acetate in hexanes) to obtain the pure product as a colorless solid (45.6 mg, 0.07 mmol, 24%).

R_f (20% ethyl acetate in hexanes) = 0.3

$\boldsymbol{[\alpha]_D^{20}}$ = -4.6 ° ($CHCl_3$, c = 1)

mp. = 70 °C

^{1}H-NMR (600 MHz, $CDCl_3$) δ = 7.84 – 7.71 (m, 2H), 7.40 (d, J = 8.0 Hz, 2H), 7.25 (d, J = 6.4 Hz, 2H), 6.87 – 6.74 (m, 2H), 6.39 (d, J = 2.7 Hz, 1H), 5.00 (d, J = 5.7 Hz, 1H), 4.70 (d, J = 11.9 Hz, 1H), 4.64 (d, J = 11.9 Hz, 1H), 3.38 (dd, J = 5.7, 2.8 Hz, 1H), 2.48 (s, 3H).

^{13}C-NMR (151 MHz, $CDCl_3$) δ = 174.07 (q, *J* = 38.6 Hz), 169.5, 145.6, 137.5, 133.9, 133.4, 131.4, 130.0, 128.2, 127.8, 126.9, 122.6, 115.04 (q, *J* = 290.2 Hz), 94.4, 74.6, 52.4, 37.3, 30.3, 21.8.

^{19}F-NMR (282 MHz, $CDCl_3$) δ = -73.8.

IR (neat): 2925, 2361, 2338, 1728, 1596, 1491, 1457,1397, 1368, 1202, 1168, 1095, 1070, 1012, 878, 813,767, 716, 704, 672, 590 cm^{-1}.

HRMS (+NSI): calcd. for $C_{23}H_{17}O_5NBrCl_3F_3S$ $(M+H)^+$ 659.9023 found 659.9029.

HPLC analysis: ADH column, 1.0 mL/min, 8% iPrOH in hexanes, 30 min, $\lambda = 230$ nm, t_R: Major: 7.99 min, Minor: 13.04 min, 86% ee.

2-(tert-butyl) 3-methyl 6-(2,2,2-trichloroethyl) (1S,5S,6R)-6-(4-bromophenyl)-2-azabicyclo[3.1.0]hex-3-ene-2,3,6-tricarboxylate

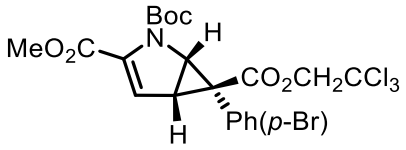

This compound was prepared according to the general procedure B, using methyl 1-Boc-1*H*-pyrrole-2-carboxylate (167.6 mg, 0.6 mmol, 2.0 equiv) as the substrate and 2,2,2-trichloroethyl 2-(4-bromophenyl)-2-diazoacetate (112 mg, 0.3 mmol, 1.0 equiv), under the catalysis of Rh_2(*R*-*p*-PhTPCP)$_4$ (2.6 mg, 1.5 μmol, 0.5 mol%). The crude residue was subjected to flash chromatography (1% to 15% ethyl acetate in hexanes) to obtain the pure product as a colorless solid (134.0 mg, 0.28 mmol, 79%).

R_f (20% ethyl acetate in hexanes) = 0.45

$[\alpha]_D^{20}$ = -191.8 ° ($CHCl_3$, *c* = 1)

mp. = 137-138 °C

^{1}H-NMR (600 MHz, $CDCl_3$) δ = 7.41 – 7.35 (m, 2H), 7.03 (m, 2H), 5.77 (d, *J* = 2.6 Hz, 1H), 4.86 (d, *J* = 6.2 Hz, 1H), 4.69 (s, 2H), 3.52 (s, 3H), 3.42 (dd, *J* = 6.2, 2.6 Hz, 1H), 1.46 (s, 9H).

^{13}C-NMR (75 MHz, $CDCl_3$) δ = 170.8, 161.2, 151.1, 135.7, 134.0, 131.2, 128.3, 121.9, 116.1, 94.7, 83.3, 74.3, 51.9, 49.8, 36.6, 28.5, 28.0.

IR (neat): 2925, 1728, 1456, 1436, 1389, 1369, 1218, 1149, 1070, 952, 792, 768, 716 cm^{-1}.

HRMS (+NSI): calcd. for $C_{21}H_{22}O_6NBrCl_3S$ $(M+H)^+$ 567.9691 found 567.9698.

HPLC analysis: ADH column, 1.0 mL/min, 3% *i*PrOH in hexanes, 30 min, λ = 230 nm, t_R: Major: 8.77 min, Minor: 16.02 min, 96% ee.

Synthetic Applications

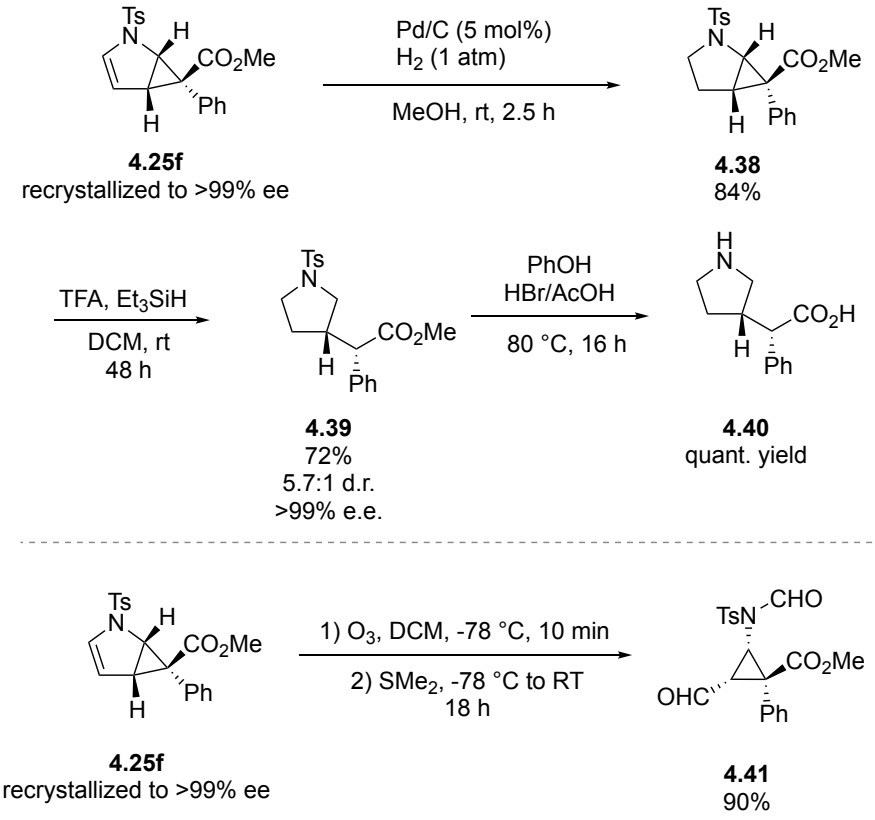

methyl (1*S*,5*S*,6*R*)-6-phenyl-2-tosyl-2-azabicyclo[3.1.0]hexane-6-carboxylate

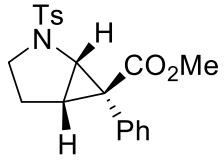

A Schlenk flask was charged with enantiopure cyclopropane **4.25f** (211 mg, 0.571 mol, 1.0 equiv), methanol (8 mL) and Pd/C (10 wt%, 30 mg Pd/C, 29 µmol Pd, 5 mol% Pd). The resulting solution was flushed with hydrogen gas for ten times (balloon, 1 atm) and stirred under hydrogen atmosphere at room temperature for 2.5 h. After completion the crude mixture was filtered through two consecutive folded filter and washed with methanol. The solvent was removed under vacuum and the product (177 mg, 84%) was obtained as a white solid.

R_f = 0.28 (hexanes: ethyl acetate = 4: 1, vanillin)

$[\alpha]_D^{20}$ -58.8° (c = 0.54, $CHCl_3$)

m.p. 140 °C

^{1}H-NMR (300 MHz, $CDCl_3$) δ = 7.73 (d, *J* = 8.3 Hz, 2H), 7.37 – 7.27 (m, 7H), 4.25 (d, *J* = 6.7 Hz, 1H), 3.57 (s, 3H), 3.29 – 3.11 (m, 1H), 2.48 – 2.46 (m, 1H), 2.44 (s, 3H), 1.98 – 1.69 (m, 3H).

^{13}C-NMR (75 MHz, $CDCl_3$): δ 171.8, 143.6, 136.4, 131.5, 131.2, 129.9, 128.6, 127.8, 127.0, 52.7, 51.8, 48.0, 37.1, 30.6, 25.0, 21.6

IR (neat): 3060, 3030, 2952, 2363, 2121, 1715, 1599, 1495, 1435, 1346, 1252, 1159, 1103, 1014, 982, 872, 813, 731, 701, 664 cm^{-1}

HRMS (+ESI) calcd. for $C_{20}H_{22}NO_4S$ $(M+H)^+$ 372.1264 found 372.1266.

methyl (*S*)-2-phenyl-2-((*S*)-1-tosylpyrrolidin-3-yl)acetate

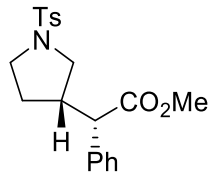

In a round-bottom flask, hydrogenated cyclopropane **4.38** (131 mg, 0.35 mmol, 1.0 equiv) was dissolved in DCM (7 mL). Triethylsilane (0.17 mL, 1.1 mmol, 3.0 equiv) and trifluoroacetic acid (54 μL, 0.70 mmol, 2.0 equiv) were added, and the solution was stirred at room temperature for 2 days. The solvent was evaporated under reduced pressure and the crude product (*dr* = 5.7:1, crude ^{1}H-NMR) was purified by flash chromatography (SiO_2, hexanes/EtOAc, 4:1) to give the main diastereomer (95 mg, 72%) as a white solid.

R_f = 0.30 (hexanes: ethyl acetate = 4: 1, Vanillin)

$[\alpha]_D^{20}$ 46,3 (c = 1.01, $CHCl_3$, 99% ee)

m.p. 140 °C

^{1}H-NMR (400 MHz, $CDCl_3$): δ 7.62 (d, *J* = 8.2 Hz, 2H), 7.35 – 7.27 (m, 5H), 7.21 – 7.16 (m, 2H), 3.61 (s, 3H), 3.42 (ddd, *J* = 9.8, 8.4, 3.9 Hz, 1H), 3.29 (d, *J* = 10.8 Hz, 1H), 3.22 (ddd, *J* = 9.8, 8.4, 7.5 Hz, 1H), 3.04 (dd, *J* = 9.7, 6.9 Hz, 1H), 2.84 – 2.68 (m, 2H), 2.44 (s, 3H), 2.10 (dtd, *J* = 10.9, 6.9, 3.9 Hz, 1H), 1.59 – 1.48 (m, 1H)

^{13}C-NMR (75 MHz, $CDCl_3$): δ 173.1, 143.5, 136.9, 133.5, 129.7, 129.0, 128.0, 127.9, 127.5, 54.9, 52.2, 51.1, 47.6, 41.7, 30.5, 21.6

IR (neat): 3064, 3030, 2952, 2878, 2363, 1733, 1599, 1495, 1454, 1342, 1215, 1122, 1092, 1033, 824, 745, 709 cm^{-1}

HRMS (+ESI) calcd. for $C_{20}H_{24}NO_4S$ $(M+H)^+$ 374.1421 found 374.1422

HPLC analysis: Phenomenex Lux Cellulose-2 column, 0.5 mL/min, 50% *i*PrOH in *n*-heptane, 60 min, λ = 215 nm, t_R: Major: 33.14 min, Minor: not observed, >99% ee

(*R*)-2-phenyl-2-((*S*)-pyrrolidin-3-yl)acetic acid

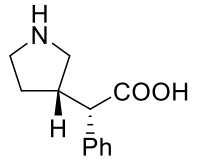

Under nitrogen atmosphere a flame dried heavy-wall Schlenk tube was charged with ester **4.39** (50 mg, 0.13 mmol, 1.0 equiv), phenol (39 mg) and HBr in acetic acid (0.75 mL). The resulting solution was stirred at 80 °C for 16 h. Afterwards, distilled water (0.75 mL) was added and the reaction mixture was stirred at 50 °C for 20 min. The solvent was evaporated under reduced pressure to yield **38** as acetate salt. To purify the crude product and remove the acetate, the residue was loaded onto a column with Dowex 50WX8-400 (preactivated with 0.1 M HCl). The resin washed with water (300 mL) and subsequently eluted with aqueous ammonia solution (15%) to afford **38** (27 mg, quant.) as a white solid.

R_f = 0.72 (methanol, ninhydrin)

$[\alpha]_D^{20}$ 40.0° (c = 1.02, H_2O)

m.p. >250 °C

^{1}H NMR (400 MHz, D_2O) δ = 7.30 – 7.16 (m, 5H), 3.35 – 3.13 (m, 3H), 3.01 – 2.81 (m, 2H), 2.62 (dd, *J* = 11.3, 8.7 Hz, 1H), 2.25 – 2.13 (m, 1H), 1.71 – 1.57 (m, 1H)

^{13}C NMR (101 MHz, D_2O) δ = 180.1, 139.5, 129.0, 127.8, 127.5, 58.5, 48.3, 45.4, 40.8, 29.3

IR (neat): 2952, 2714, 2617, 2363, 2113, 1644, 1566, 1491, 1457, 1375, 1245, 1171, 1111, 1074, 1006, 980, 910, 731, 700 cm^{-1}

HRMS (-ESI) calcd. for $C_{12}H_{14}NO_2$ $(M-H)^-$ 204.1030 found 204.1033.

methyl (1R,2S,3S)-2-formyl-1-phenyl-3-(N-tosylformamido)cyclopropane-1-carboxylate--

methyl (1S,5S,6R)-6-phenyl-2-tosyl-2-azabicyclo[3.1.0]hex-3-ene-6-carboxylate

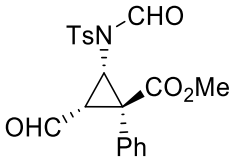

A flame dried Schlenk tube was charged with cyclopropane **4.25f** (185 mg, 0.5 mmol, 1.0 equiv) and anhydrous DCM (5 ml). The reaction was cooled to -78 °C (dry ice/acetone) and ozone was passed through the reaction mixture until a blue color appeared. 10 min after the color change, excess of ozone was expelled by passing a constant stream of oxygen through the solution until it turned colorless. The stream of oxygen was continued for further 5 min and dimethylsulfide (DMS) (0.185 mL, 2.5 mmol, 5.0 equiv) was added. The reaction mixture was allowed to warm up to room temperature and stirred overnight. The solution was then washed with sat. NaHCO3 (10 ml) and water (10 ml). After drying over $MgSO_4$ and filtration, the solvent was removed under reduced pressure to afford **39** (180 mg, 0.45 mmol, 90% yield) as a white solid. Further purification was not required.

$[\boldsymbol{\alpha}]_{\boldsymbol{D}}^{\boldsymbol{20}} =$ -10.8 ° ($CHCl_3$, c = 1)

R_f (33% ethyl acetate in hexanes) = 0.28

mp. = 125 – 126 °C

^{1}**H-NMR (**400 MHz, $CDCl_3$) δ = 9.22 (s, 1H), 8.86 (d, *J* = 6.9 Hz, 1H), 7.72 – 7.67 (m, 2H), 7.43 – 7.37 (m, 2H), 7.35 – 7.24 (m, 5H), 3.61 (s, 3H), 3.24 (d, *J* = 8.6 Hz, 1H), 2.87 (dd, *J* = 8.6, 6.9 Hz, 1H), 2.46 (s, 3H).

^{13}**C-NMR** (101 MHz, $CDCl_3$) δ = 193.7, 171.2, 165.8, 146.7, 133.6, 132.1, 130.9, 128.9, 128.8, 128.1, 127.5, 53.7, 41.6, 39.6, 37.5, 21.8.

IR (neat): 3060, 2956, 1707, 1595, 1498, 1312, 1435, 1384, 1312, 1252, 1170, 1088, 1029, 816, 705, 664 cm^{-1}.

HRMS (+ESI, 120 V): calcd. for $C_{20}H_{19}NNaO_6S$ $[M+Na]^+$424.0825 found 424.0826.

References

1. C. Zonta, F. Fabris, O. De Lucchi, *Org. Lett.* **2005**, *7*, 1003.

2. J. K. Laha, S. Sharma, R. A. Bhimpuria, N. Dayal, G. Dubey, P. V. Bharatam, *New. J. Chem.* **2017**, *41*, 8791.

3. I. Kholod, O. Vallat, A. M. Buciumas, A. Neels, R. Neier, *Eur. J. Org. Chem.* **2014**, *2014*, 7865.

4. D. J. Rivinoja, Y. S. Gee, M. G. Gardiner, J. H. Ryan, C. J. T. Hyland, *ACS Catal.* **2017**, *7*, 1053.

5. B. Wei, C. Chen, C. You, H. Lv, X. Zhang, *Org. Chem. Front.* **2017**, *4*, 288.

6. A. S. K. Hashmi, M. Rudolph, J. Huck, W. Frey, J. W. Bats, M. Hamzić, *Angew. Chemie. Int. Ed.* **2009**, *48*, 5848.

X-ray Crystallography Studies of Key Compounds

(Note: X-ray crystallography studies were completed by Dr. John Bacsa.)

Rh_2(*S*-TPPTTL)$_4$

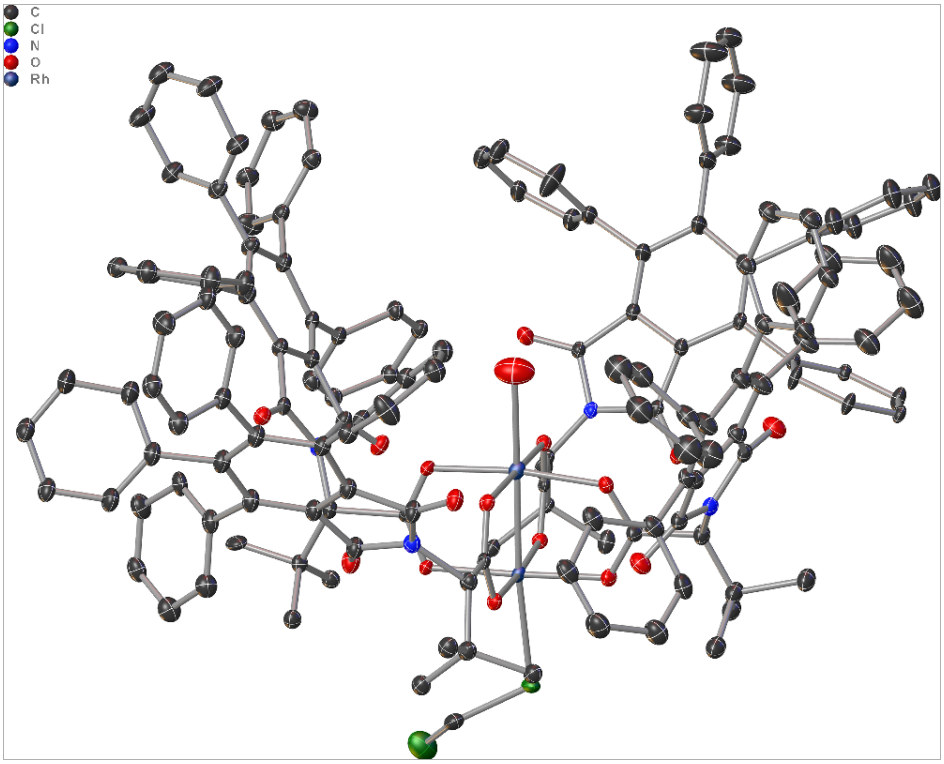

Identification code	rh2s-tppttl4_sq
Empirical formula	$C_{157}H_{0.25}Cl_2O_{17}Rh_2$
Formula weight	2434.54
Temperature/K	100(2)
Crystal system	orthorhombic
Space group	$P2_12_12_1$
a/Å	20.1022(4)

b/Å	20.7993(7)
c/Å	37.9099(9)
α/°	90.028(2)
β/°	89.9749(17)
γ/°	90.108(2)
Volume/Å^3	15850.6(7)
Z	4
ρ_{calc}g/cm^3	1.020
μ/mm^{-1}	2.432
F(000)	4809.0
Radiation	CuKα (λ = 1.54184)
2Θ range for data collection/°	4.662 to 124.408
Index ranges	-20 ≤ h ≤ 20, -21 ≤ k ≤ 20, -39 ≤ l ≤ 35
Reflections collected	65270
Independent reflections	18937 [R_{int} = 0.0866, R_{sigma} = 0.0806]
Data/restraints/parameters	18937/1279/1616
Goodness-of-fit on F^2	1.057
Final R indexes [I>=2σ (I)]	R_1 = 0.1207, wR_2 = 0.3055
Final R indexes [all data]	R_1 = 0.1297, wR_2 = 0.3122
Largest diff. peak/hole / e Å^{-3}	3.48/-1.13
Flack parameter	0.21(2)

(*R*)-2-(4-bromophenyl)-2-((1*S*,3*R*)-3-(*tert*-butyl)cyclohexyl)ethan-1-ol

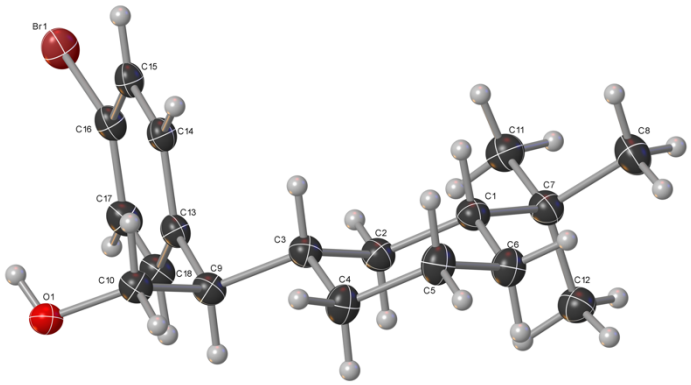

Experimental. Single colourless needle-shaped crystals were recrystallised from a mixture of water and ethanol by vapor diffusion. A suitable crystal 0.49×0.05×0.04 mm^3 was selected and mounted on a loop with paratone oil on a Synergy-S Dualflex diffractometer with a HyPix detector. The crystal was cooled to T = 101(2) K during data collection. The structure was solved with the **ShelXT** (Sheldrick, 2015) structure solution program using the Intrinsic Phasing solution method and by using **Olex2** (Dolomanov et al., 2009) as the graphical interface. The model was refined with version 2017/1 of **ShelXL** (Sheldrick, 2015) using Least Squares minimisation.

Crystal Data. $C_{18}H_{27}BrO$, M_r = 339.30, monoclinic, $P2_1$ (No. 4), a = 17.1203(2) Å, b = 5.94424(7) Å, c = 25.7524(3) Å, β = 92.8227(12)°, $\alpha = \gamma$ = 90°, V = 2617.57(6) Å^3, T = 101(2) K, Z = 6, Z' = 3, μ (CuK$_\alpha$) = 3.149 mm^{-1}, 20887 reflections measured, 8577 unique (R_{int} = 0.0472) which were used in all calculations. The final wR_2 was 0.1178 (all data) and R_1 was 0.0436 (I > 2σ(I)).

Formula	$C_{18}H_{27}BrO$
$D_{calc.}$/ g cm^{-3}	1.291
μ/mm^{-1}	3.149
Formula Weight	339.30
Colour	colourless
Shape	needle
Size/mm^3	0.49×0.05×0.04
T/K	101(2)
Crystal System	monoclinic
Flack Parameter	-0.06(2)
Hooft Parameter	-0.021(8)
Space Group	$P2_1$
a/Å	17.1203(2)
b/Å	5.94424(7)
c/Å	25.7524(3)
α/°	90
β/°	92.8227(12)
γ/°	90
V/Å^3	2617.57(6)
Z	6
Z'	3
Wavelength/Å	1.54184
Radiation type	CuKα

$\Theta_{min}/^{\circ}$	1.718
$\Theta_{max}/^{\circ}$	65.828
Measured Refl.	20887
Independent Refl.	8577
Reflections with I > 2σ(I)	8000
R_{int}	0.0472
Parameters	569
Restraints	515
Largest Peak	0.707
Deepest Hole	-0.430
GooF	1.029
wR_2 (all data)	0.1178
wR_2	0.1146
R_1 (all data)	0.0471
R_1	0.0436

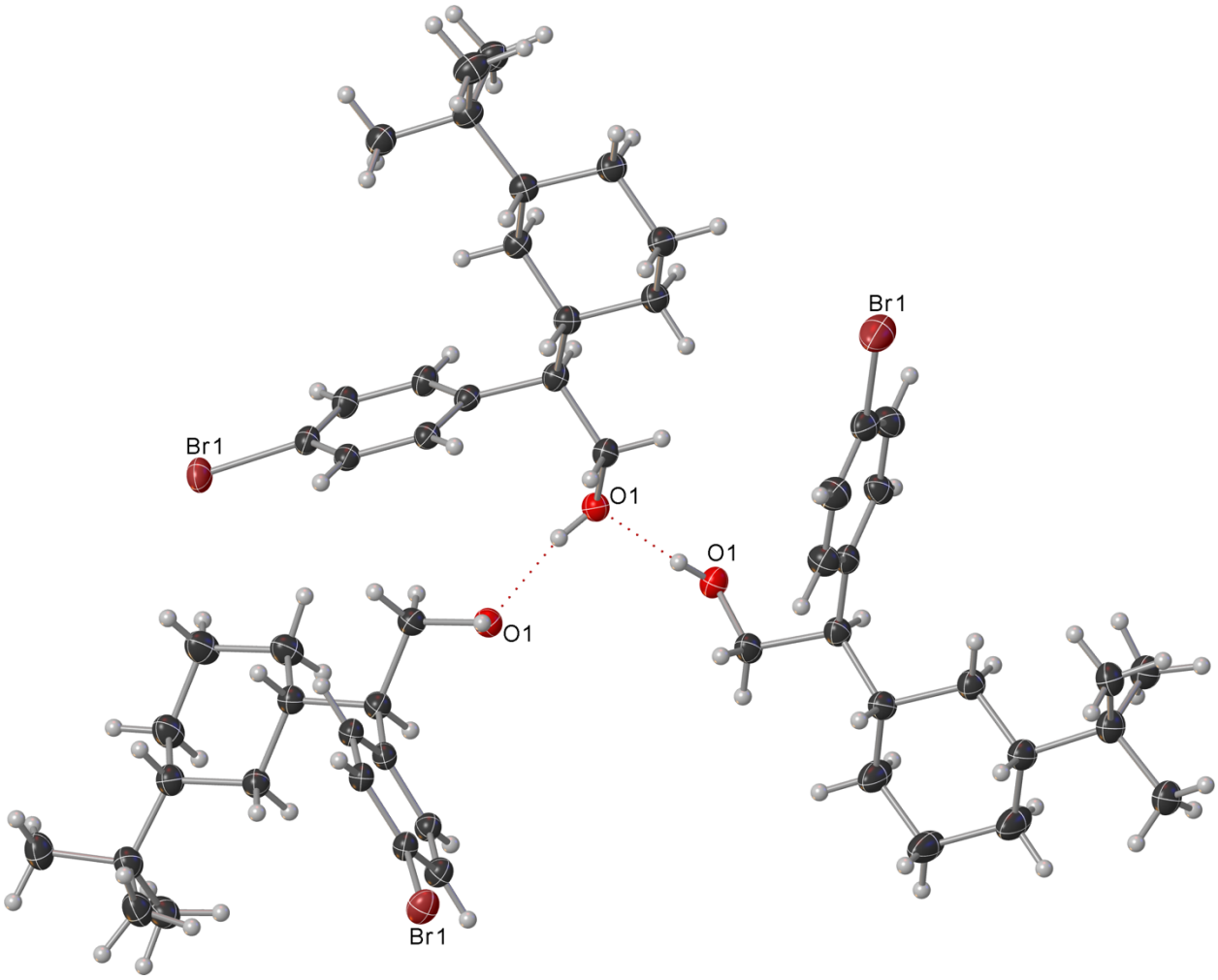
Br1
O1
O1
O1
Br1
Br1

2,2,2-trichloroethyl (*R*)-2-(4-bromophenyl)-2-((2*R*,4a*R*,8a*R*)-decahydronaphthalen-2-yl)acetate

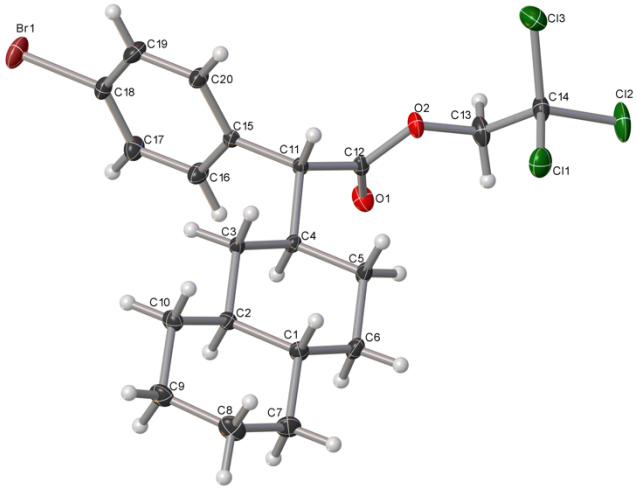

Experimental. Single colourless irregular-shaped crystals of **42** were recrystallised from a mixture of pentane and DCM by vapor diffusion. A suitable crystal 0.51×0.36×0.19 mm^3 was selected and mounted on a loop with paratone oil on an XtaLAB Synergy, Dualflex, HyPix diffractometer. The crystal was cooled to T = 100(2) K during data collection. The structure was solved with the **ShelXT** (Sheldrick, 2015) structure solution program using the Intrinsic Phasing solution method and by using **Olex2** (Dolomanov et al., 2009) as the graphical interface. The model was refined with version 2014/7 of **ShelXL-2014** (Sheldrick, 2015) using Least Squares minimisation.

Crystal Data. $C_{20}H_{24}BrCl_3O_2$, M_r = 482.65, triclinic, $P\bar{1}$ (No. 1), a = 5.5757(2) Å, b = 9.7138(3) Å, c = 10.9743(4) Å, α = 64.283(4)°, β = 82.117(3)°, γ = 86.555(2)°, V = 530.45(4) Å^3, T = 100(2) K, Z = 1, Z' = 1, μ (MoK$_\alpha$) = 2.327 mm^{-1}, 17106 reflections measured, 6464 unique (R_{int} = 0.0440) which were used in all calculations. The final wR_2 was 0.1530 (all data) and R_1 was 0.0582 (I > 2σ(I)).

Formula	$C_{20}H_{24}BrCl_3O_2$
$D_{calc.}$/ g cm^{-3}	1.511
μ/mm^{-1}	2.327
Formula Weight	482.65
Colour	colourless
Shape	irregular
Size/mm^3	0.51×0.36×0.19
T/K	100(2)
Crystal System	triclinic
Flack Parameter	0.010(10)
Hooft Parameter	0.020(2)
Space Group	P1
a/Å	5.5757(2)
b/Å	9.7138(3)
c/Å	10.9743(4)
α/°	64.283(4)
β/°	82.117(3)
γ/°	86.555(2)
V/Å^3	530.45(4)
Z	1
Z'	1
Wavelength/Å	0.71073
Radiation type	MoKα

$\Theta_{min}/^{\circ}$	2.076
$\Theta_{max}/^{\circ}$	30.506
Measured Refl.	17106
Independent Refl.	6464
Reflections with I > 2σ(I)	6149
R_{int}	0.0440
Parameters	235
Restraints	3
Largest Peak	1.015
Deepest Hole	-0.626
GooF	1.114
wR_2 (all data)	0.1530
wR_2	0.1516
R_1 (all data)	0.0604
R_1	0.0582

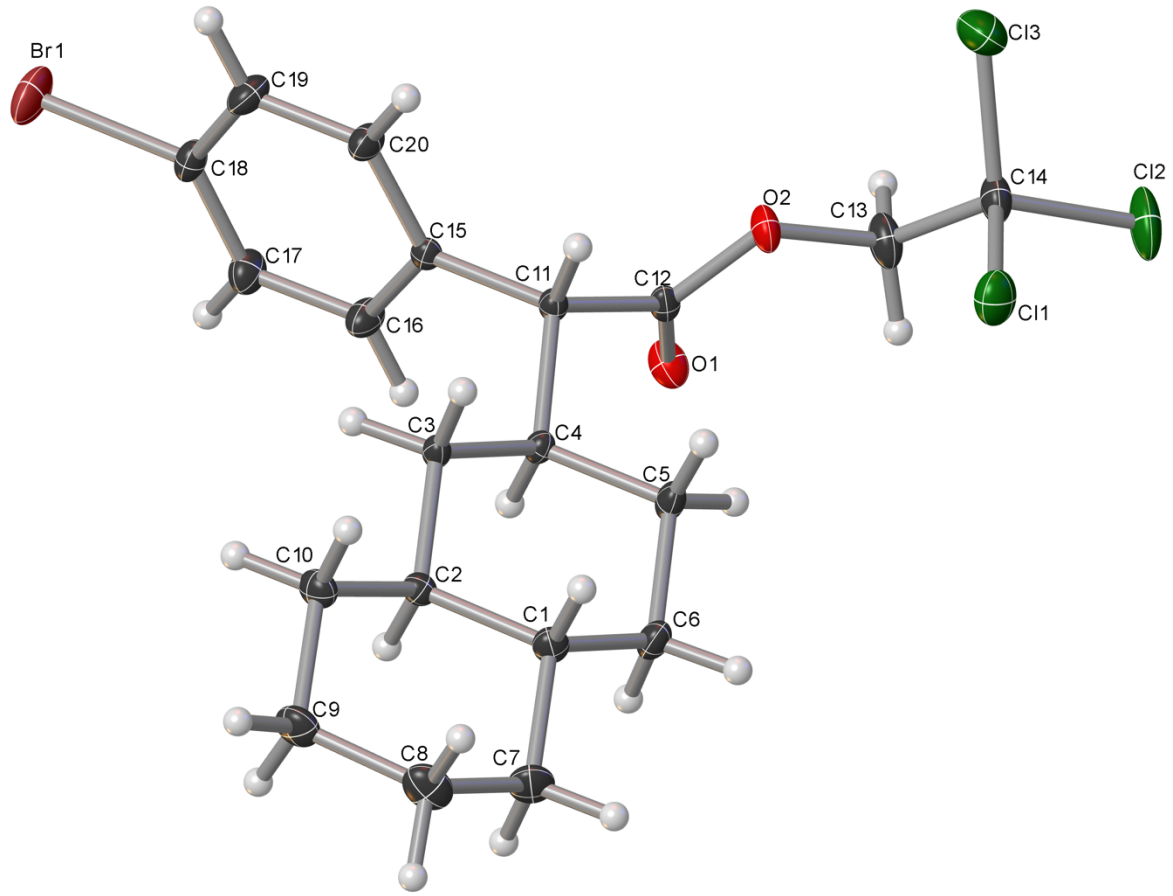
Br1
C19
C20
C18
C15
C17
C11
C12
O2
C13
C14
Cl2
Cl3
Cl1
C16
O1
C3
C4
C5
C10
C2
C1
C6
C9
C8
C7

3-methyl 6-(2,2,2-trichloroethyl) (1S,5S,6R)-6-(4-bromophenyl)-2-tosyl-2-azabicyclo[3.1.0]hex-3-ene-3,6-dicarboxylate

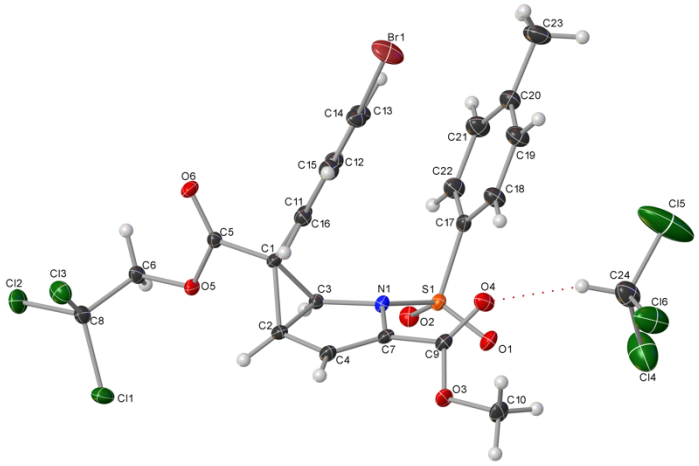

Experimental. Single colourless block-shaped crystals were recrystallised from a mixture of $CHCl_3$ and pentane by slow evaporation. A suitable crystal 0.40×0.36×0.21 mm^3 was selected and mounted on a loop with paratone oil on an XtaLAB Synergy, Dualflex, HyPix diffractometer. The crystal was kept at a steady T = 103(4) K during data collection. The structure was solved with the **ShelXT** (Sheldrick, 2015) structure solution program using the Intrinsic Phasing solution method and by using **Olex2** (Dolomanov et al., 2009) as the graphical interface. The model was refined with version 2018/3 of **ShelXL** (Sheldrick, 2015) using Least Squares minimisation.

Crystal Data. $C_{24}H_{20}BrCl_6NO_6S$, M_r = 743.08, monoclinic, $P2_1$ (No. 4), a = 10.2763(2) Å, b = 10.3939(2) Å, c = 14.2314(3) Å, β = 101.621(2)°, $\alpha = \gamma = 90°$, V = 1488.92(6) $Å^3$, T = 103(4) K, Z = 2, Z' = 1, μ (MoKα) = 2.029 mm^{-1}, 43885 reflections measured, 14981 unique (R_{int} = 0.0451) which were used in all calculations. The final wR_2 was 0.1019 (all data) and R_1 was 0.0417 (I > 2σ(I)).

Formula	$C_{24}H_{20}BrCl_6NO_6S$
$D_{calc.}$/ g cm^{-3}	1.657
μ/mm^{-1}	2.029
Formula Weight	743.08
Colour	colourless
Shape	block
Size/mm^3	0.40×0.36×0.21
T/K	103(4)
Crystal System	monoclinic
Flack Parameter	-0.003(3)
Hooft Parameter	0.020(2)
Space Group	$P2_1$
a/Å	10.2763(2)
b/Å	10.3939(2)
c/Å	14.2314(3)
α/°	90
β/°	101.621(2)
γ/°	90
V/Å^3	1488.92(6)
Z	2
Z'	1
Wavelength/Å	0.71073
Radiation type	MoKα

$\Theta_{min}/^{\circ}$	2.023
$\Theta_{max}/^{\circ}$	38.108
Measured Refl.	43885
Independent Refl.	14981
Reflections with I > 2σ(I)	12523
R_{int}	0.0451
Parameters	354
Restraints	1
Largest Peak	1.495
Deepest Hole	-1.062
GooF	1.041
wR_2 (all data)	0.1019
wR_2	0.0968
R_1 (all data)	0.0552
R_1	0.0417

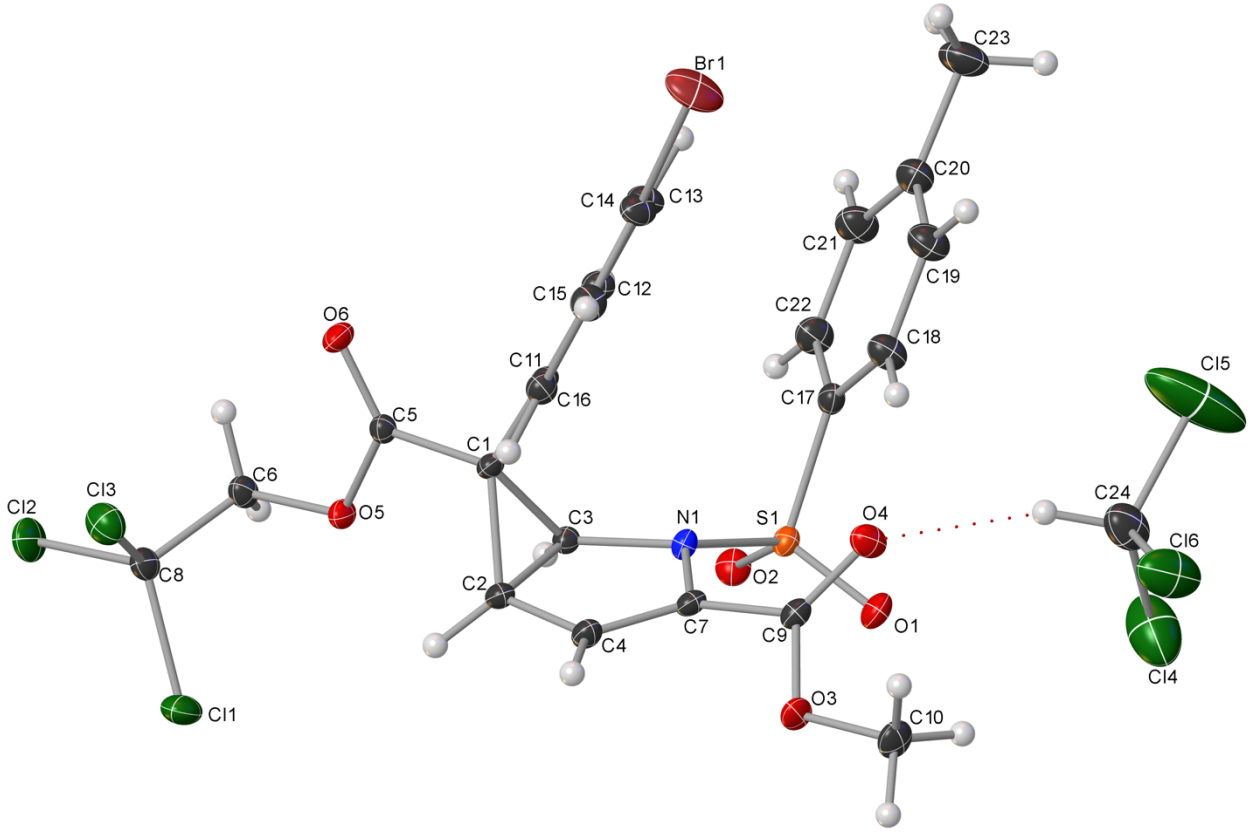
Br1
C23
C20
C14
C13
C21
C19
C15
C12
C22
C18
O6
C11
C16
C17
Cl5
C5
C1
C6
C24
Cl3
Cl2
O5
C3
N1
S1
O4
Cl6
C8
O2
C2
C7
C9
O1
C4
Cl4
O3
C10
Cl1

Appendix - Spectra

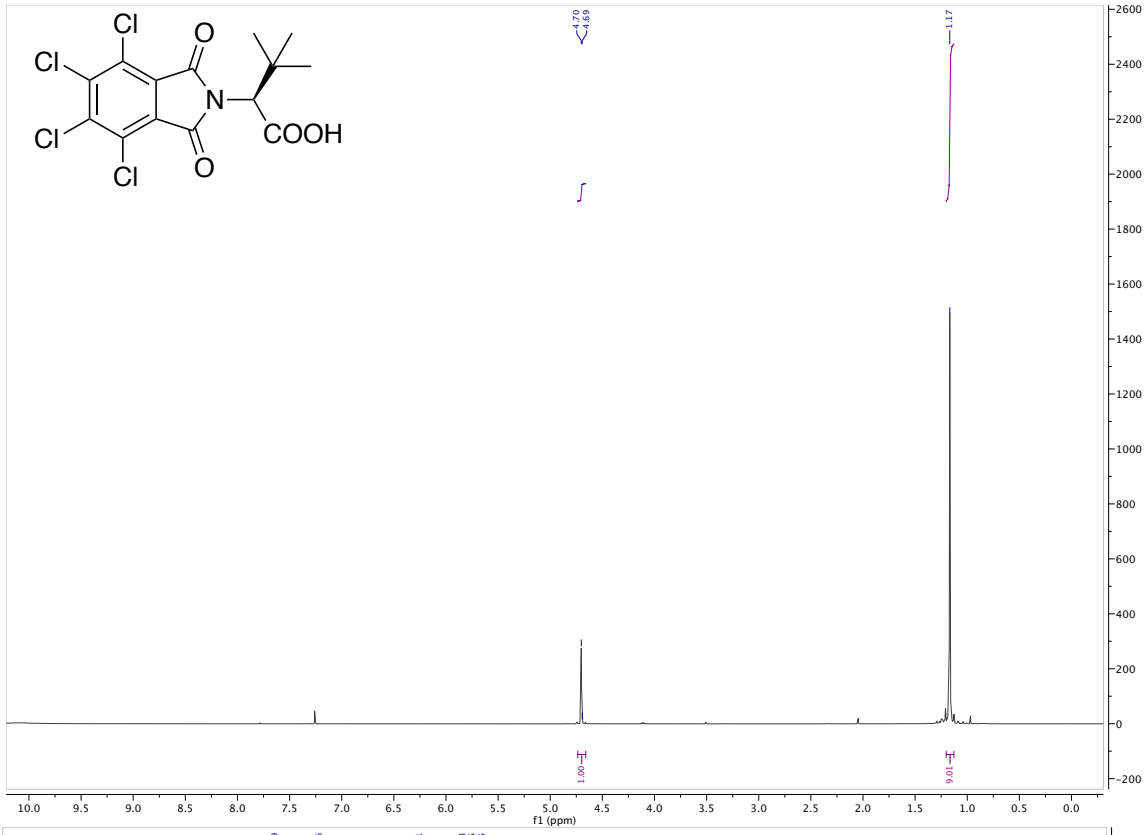
Cl
Cl
Cl
Cl
O
O
N
COOH
4.70
4.69
1.17
1.00
9.01
f1 (ppm)

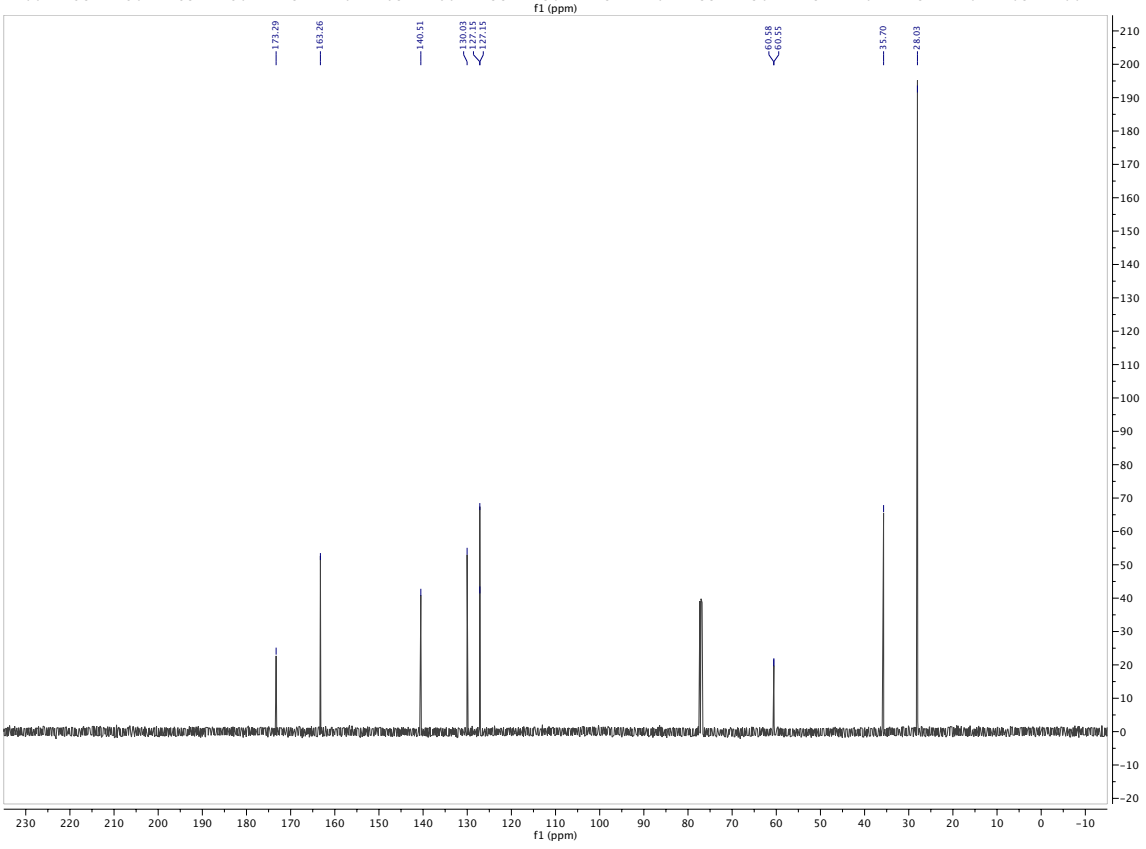
173.29
162.26
140.51
130.03
127.15
127.15
60.58
60.55
35.70
28.03
f1 (ppm)

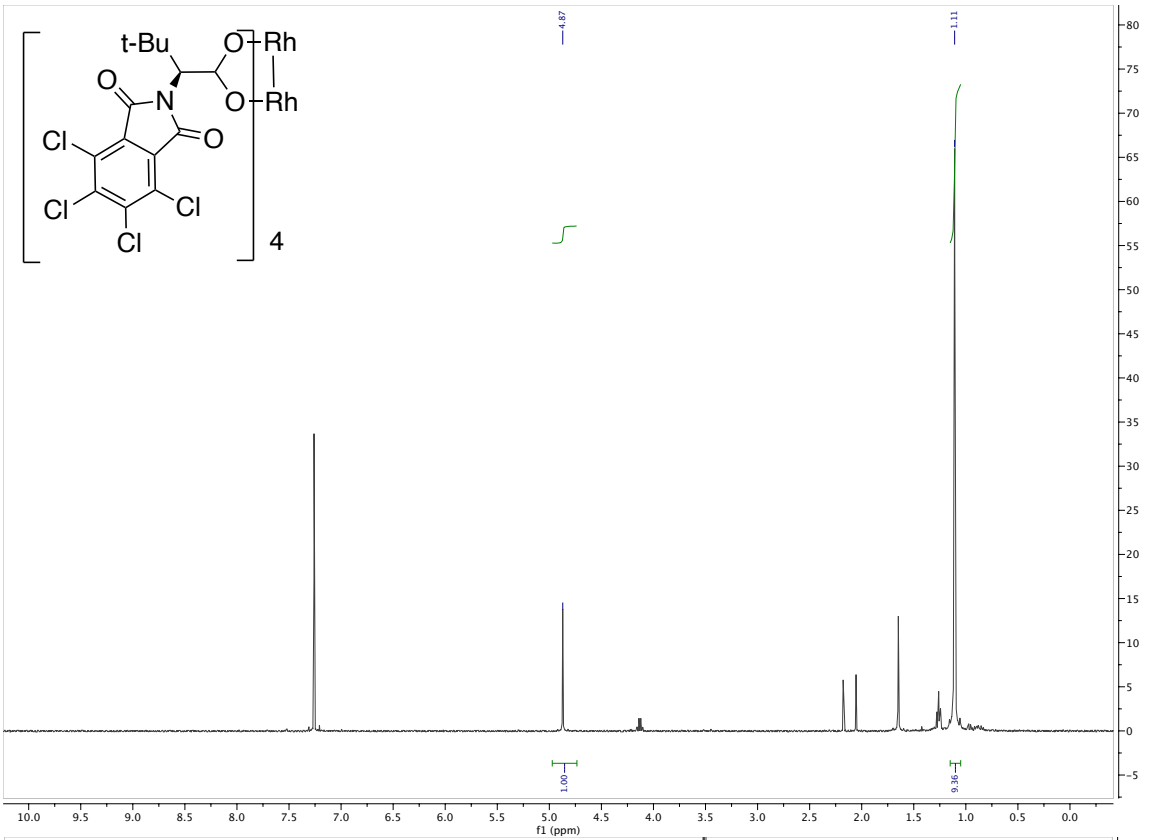
t-Bu
O
N
O
O
Rh
O
Rh
Cl
Cl
Cl
Cl
4
4.67
1.11
1.00
9.36
f1 (ppm)

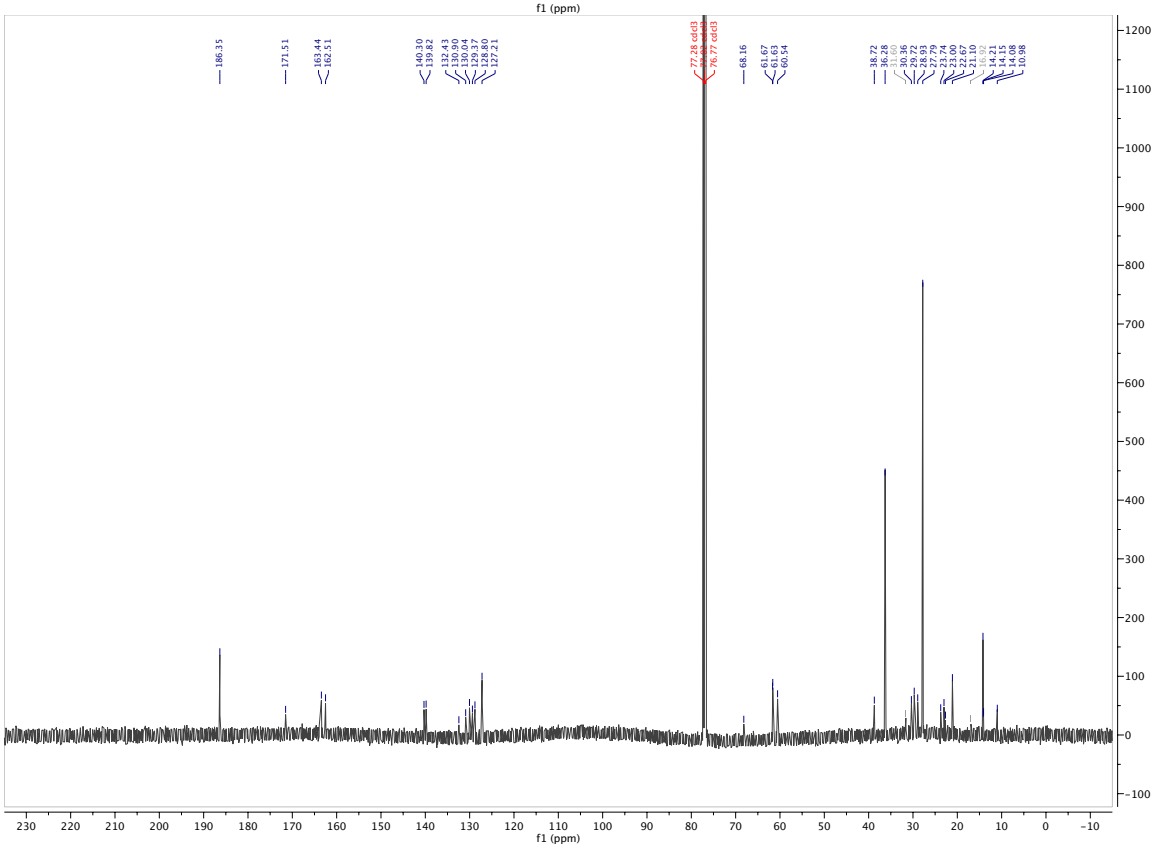
186.35
171.51
163.44
162.51
140.30
139.82
132.43
130.90
130.64
129.37
128.80
127.21
77.28 cdcl3
77.04
76.77 cdcl3
68.16
61.67
61.43
60.54
38.72
36.28
31.60
30.36
30.22
28.93
27.79
23.74
23.00
22.67
21.10
16.02
14.21
14.15
14.08
10.98
f1 (ppm)

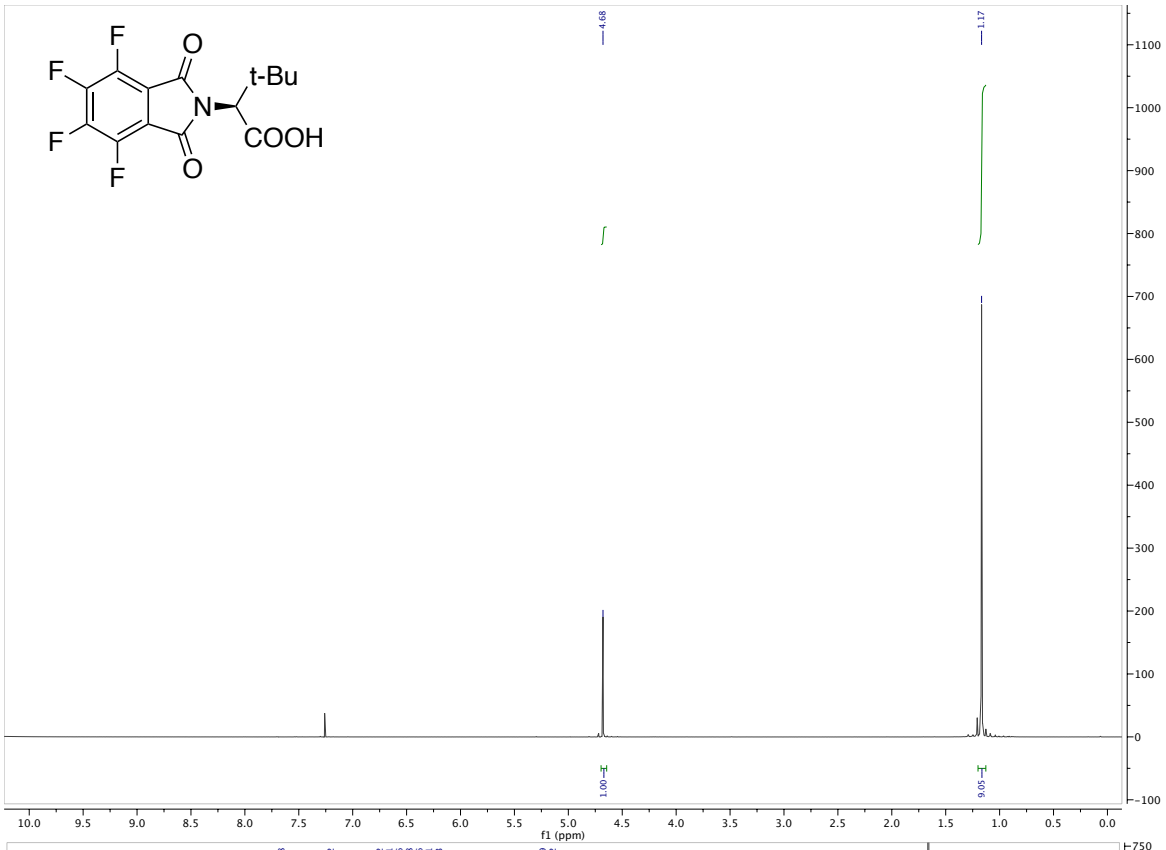
F
F
F
F
O
O
N
t-Bu
COOH
4.68
1.17
1.00
9.05
f1 (ppm)

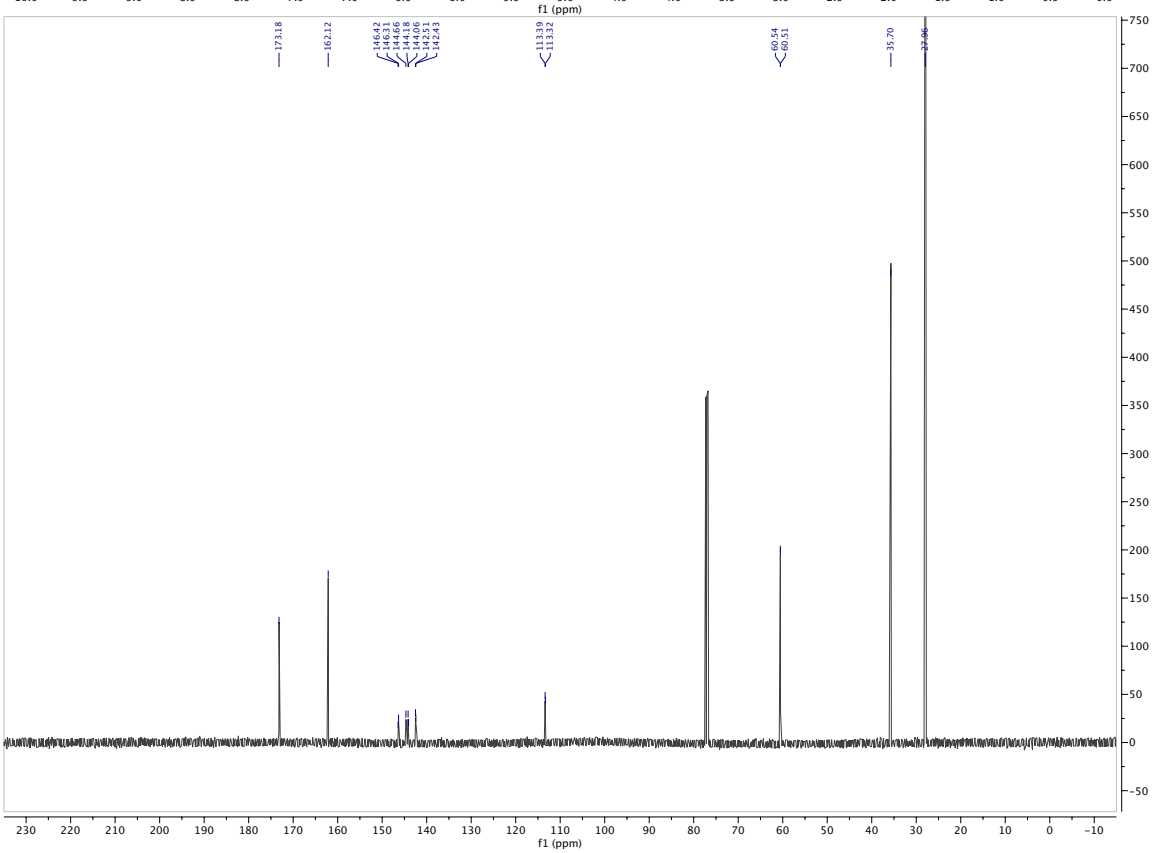
173.18
162.12
146.42
146.31
144.46
144.18
144.06
143.51
142.43
113.30
113.32
60.54
60.51
35.70
27.96
f1 (ppm)

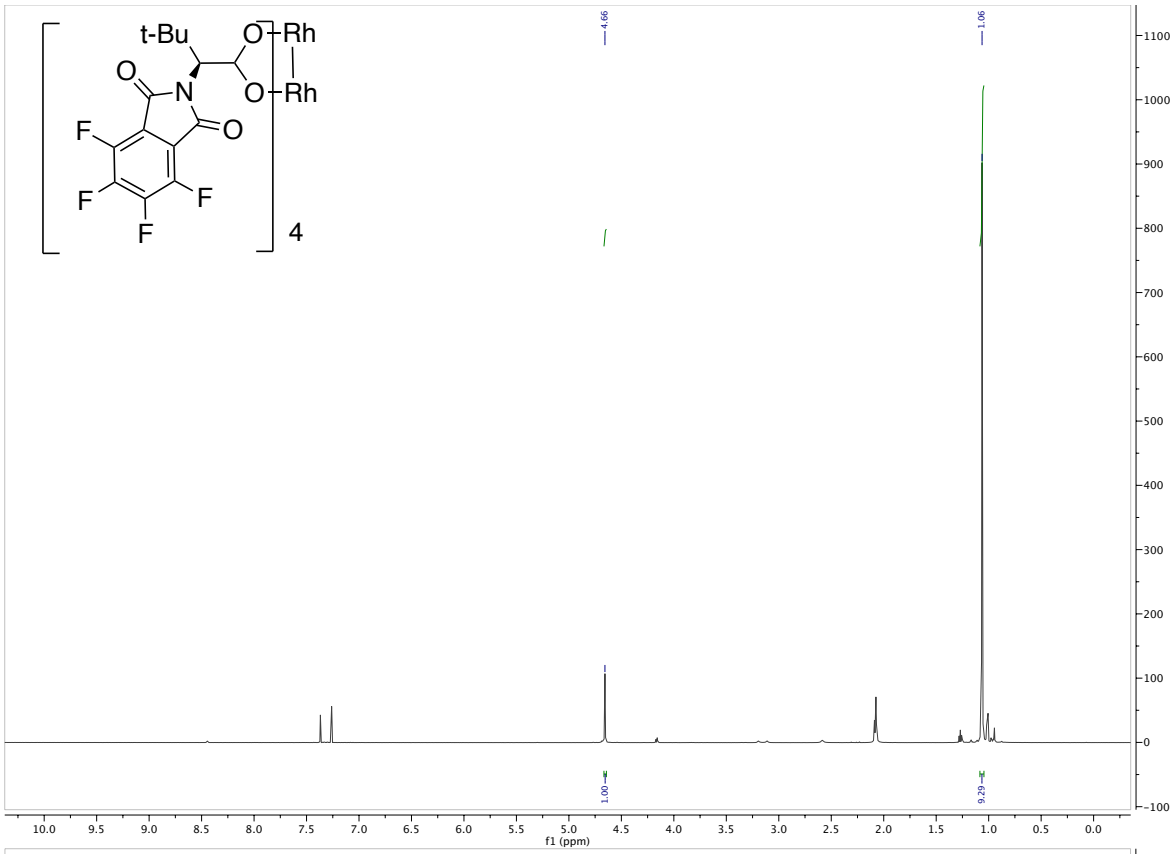
t-Bu
O
N
O
O
Rh
O
Rh
F
F
F
F
4
4.66
1.06
1.00
9.29
f1 (ppm)

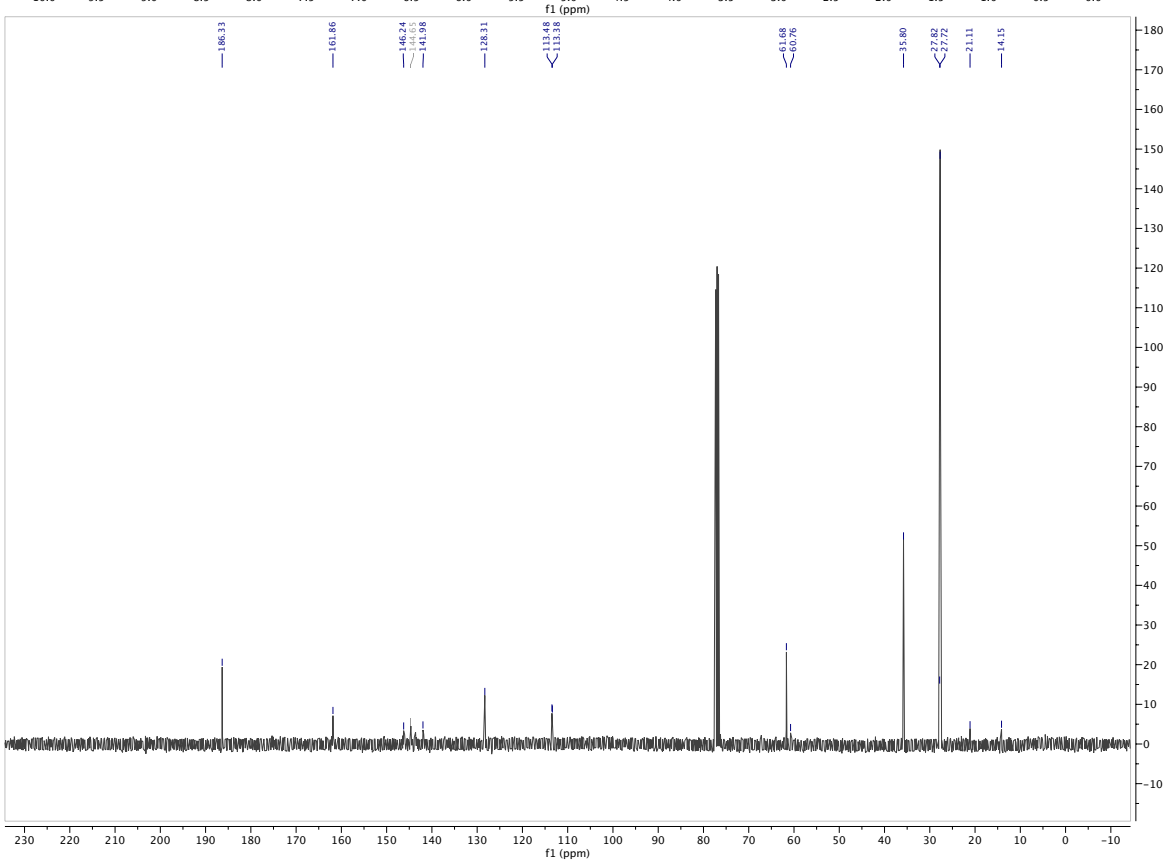
186.33
161.86
146.24
144.65
141.98
128.31
113.48
113.18
61.68
60.76
35.80
27.82
27.72
21.11
14.15
f1 (ppm)

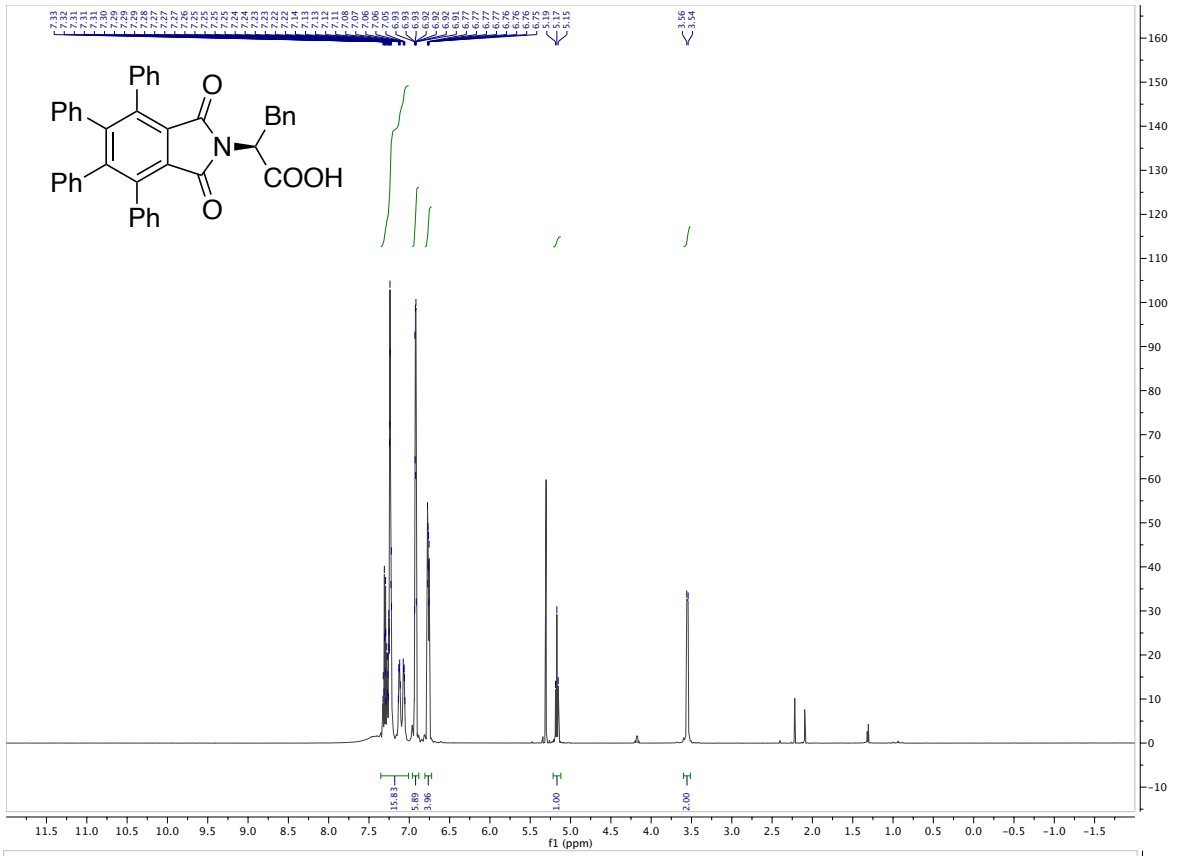
Ph
Ph
Ph
Ph
O
O
N
Bn
COOH
f1 (ppm)

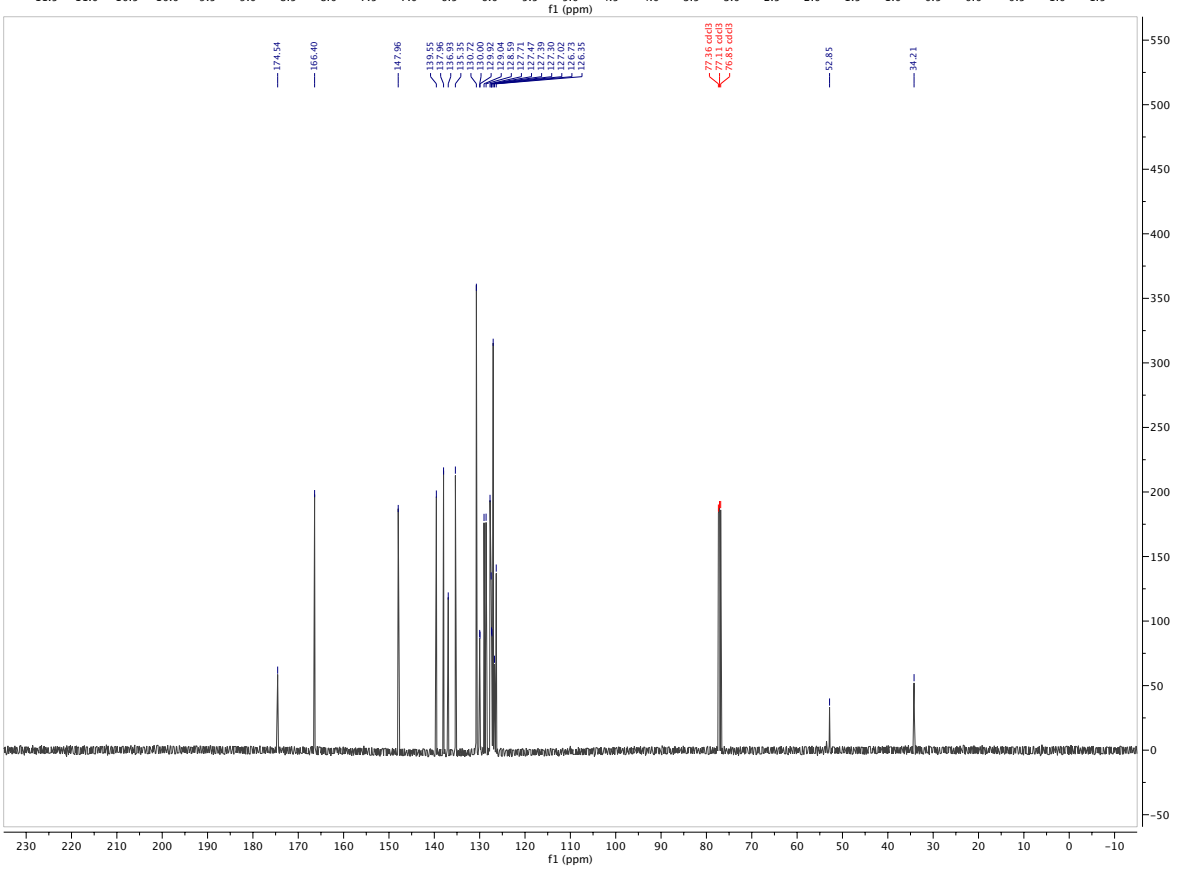
174.54
166.40
147.96
139.55
137.96
136.93
135.35
130.72
130.00
129.92
129.04
128.59
128.21
127.47
127.39
127.30
127.02
126.73
126.35
77.36 cdcl3
77.11 cdcl3
76.86 cdcl3
52.85
34.21
f1 (ppm)

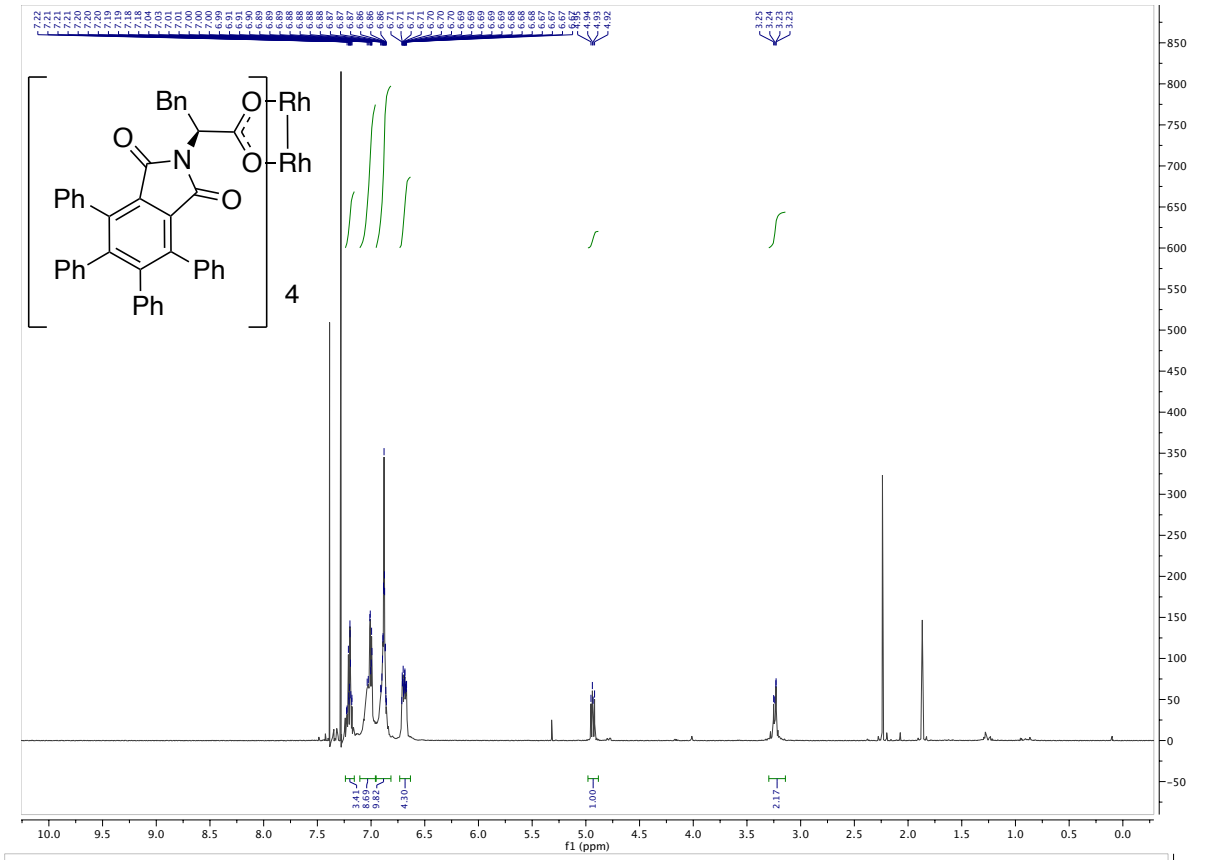
Bn
O
Rh
N
Ph
Ph
Ph
Ph
4
f1 (ppm)

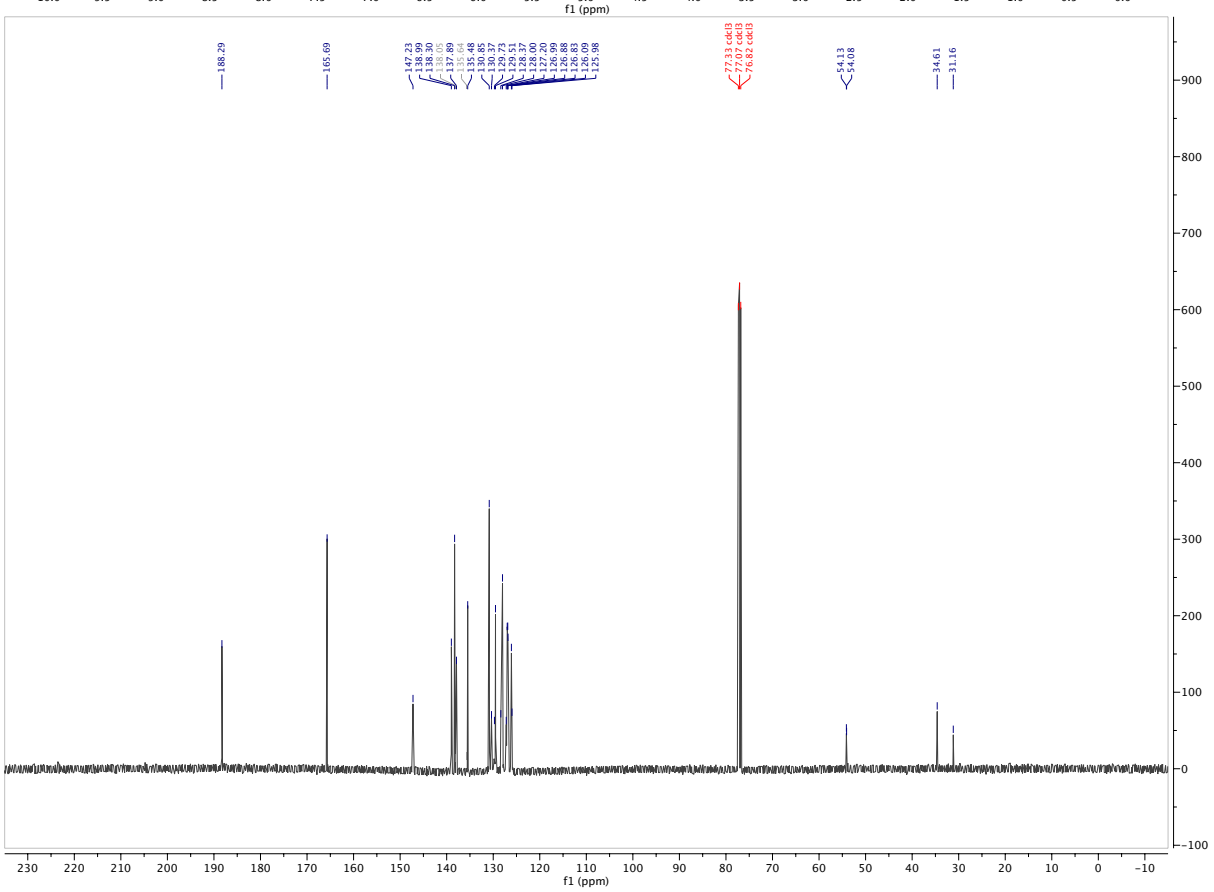
188.29
165.69
147.23
138.99
138.30
137.89
135.48
130.37
129.73
129.51
128.37
128.00
127.20
126.99
126.88
126.83
126.09
125.98
77.33 cdcl3
77.07 cdcl3
76.82 cdcl3
54.13
54.08
34.61
31.16
f1 (ppm)

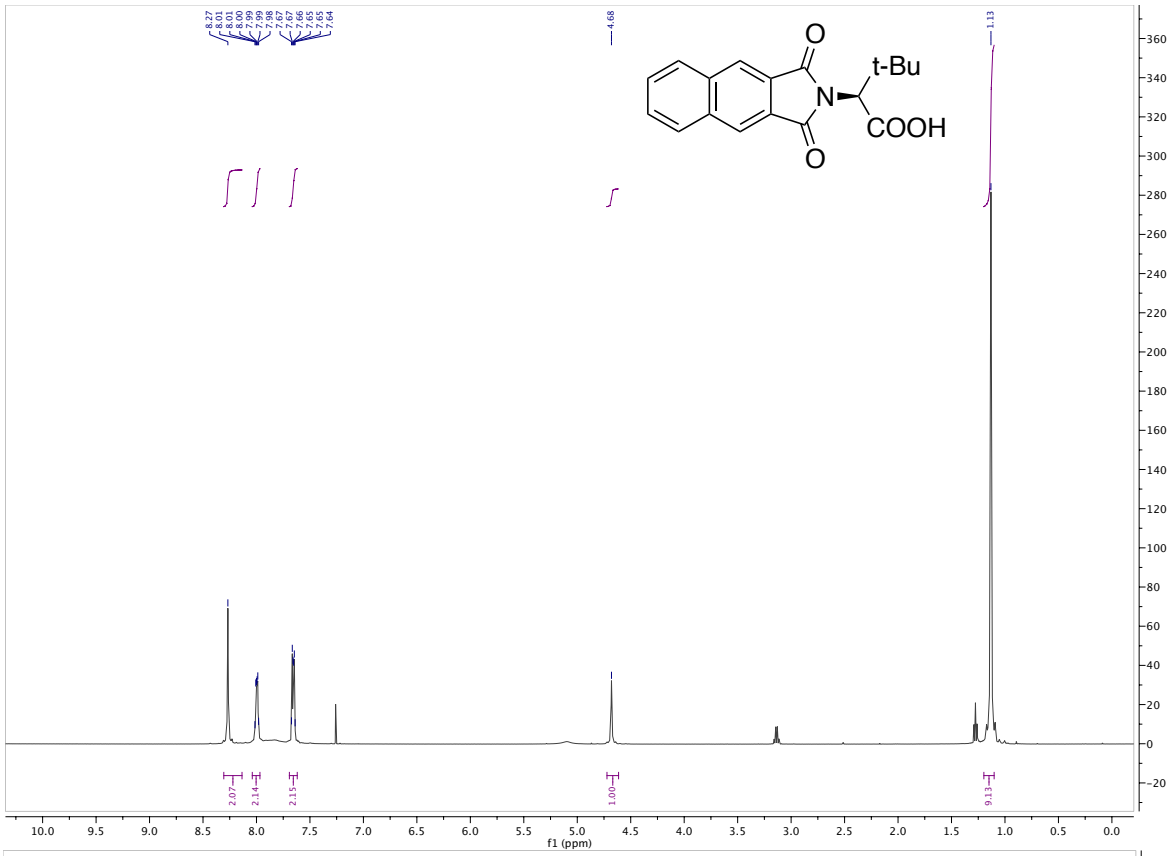
8.27
8.01
8.00
7.99
7.98
7.67
7.66
7.65
7.64
4.68
1.13
O
t-Bu
N
COOH
O
2.07
2.14
2.15
1.00
9.13
f1 (ppm)

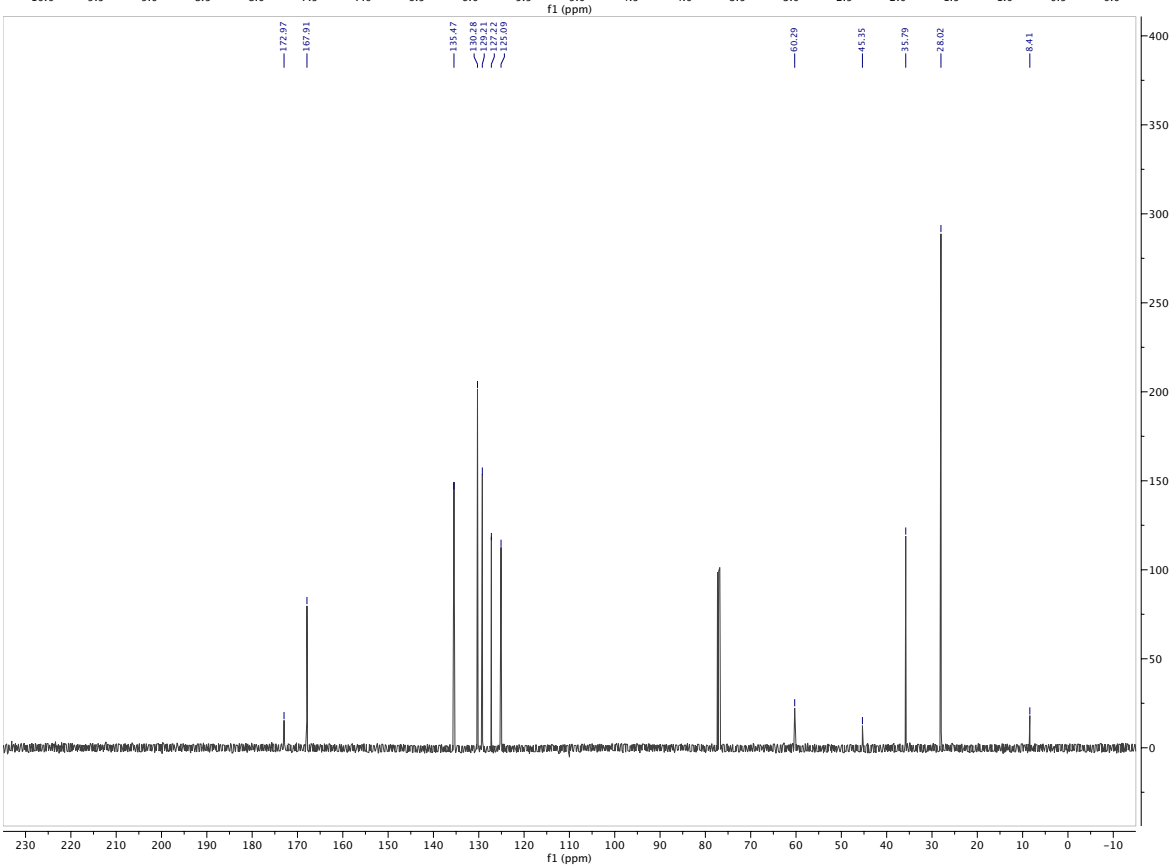
172.97
167.91
135.47
130.28
129.21
127.22
125.08
60.29
45.35
35.79
28.02
8.41
f1 (ppm)

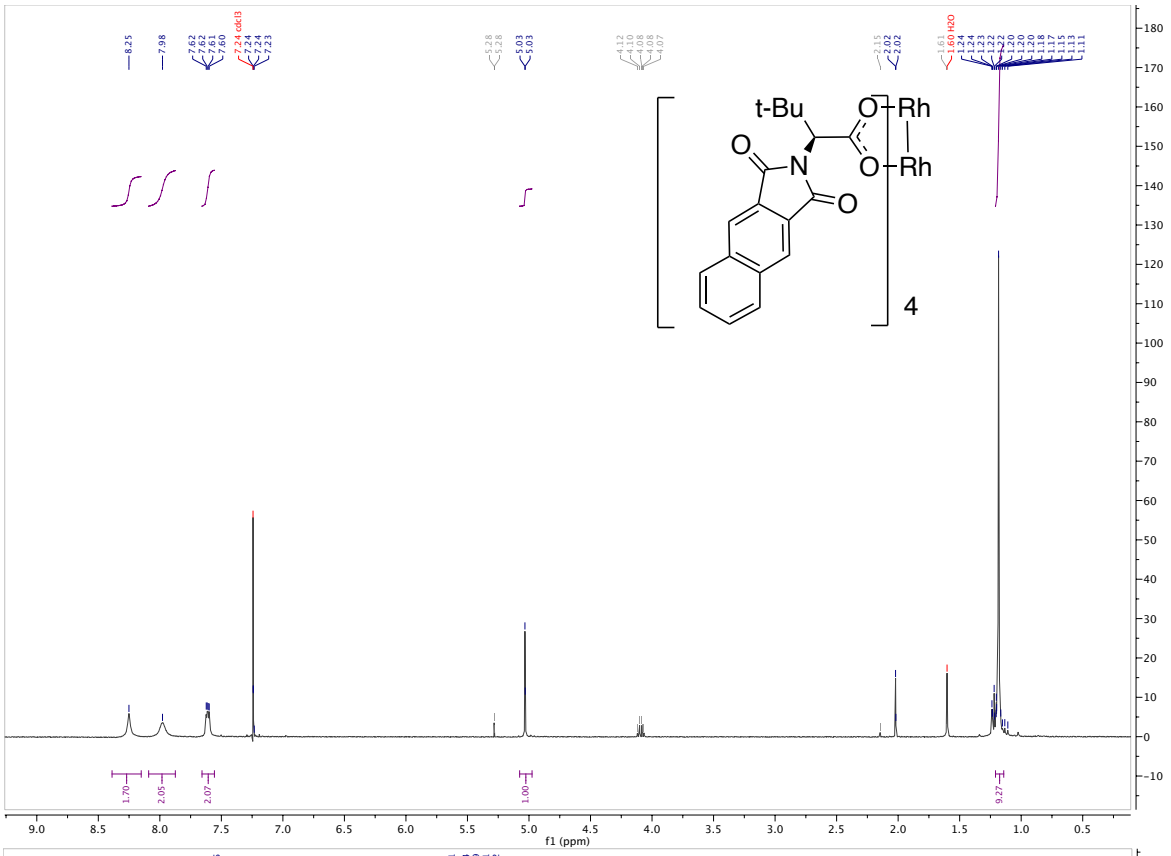
t-Bu
O
Rh
N
O
4
f1 (ppm)

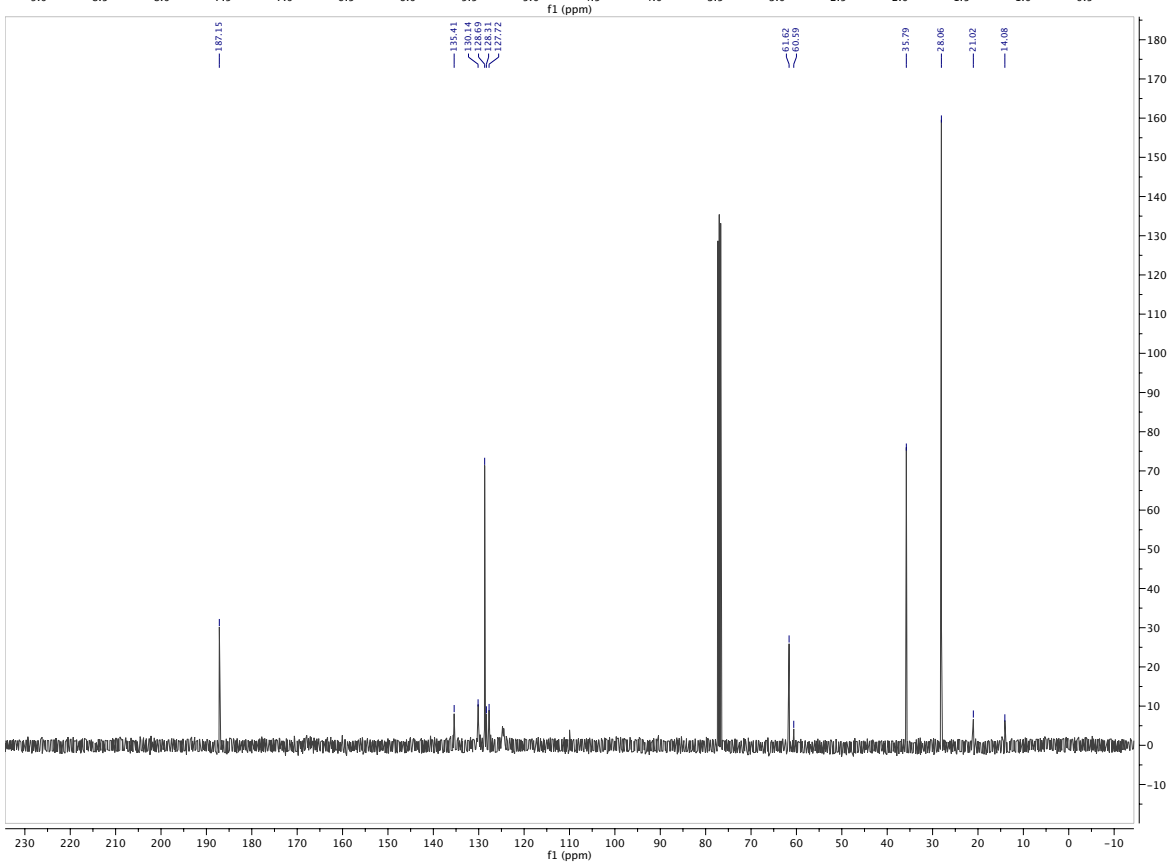
187.15
135.41
130.14
128.91
128.31
127.72
61.62
60.59
35.79
28.06
21.02
14.08
f1 (ppm)

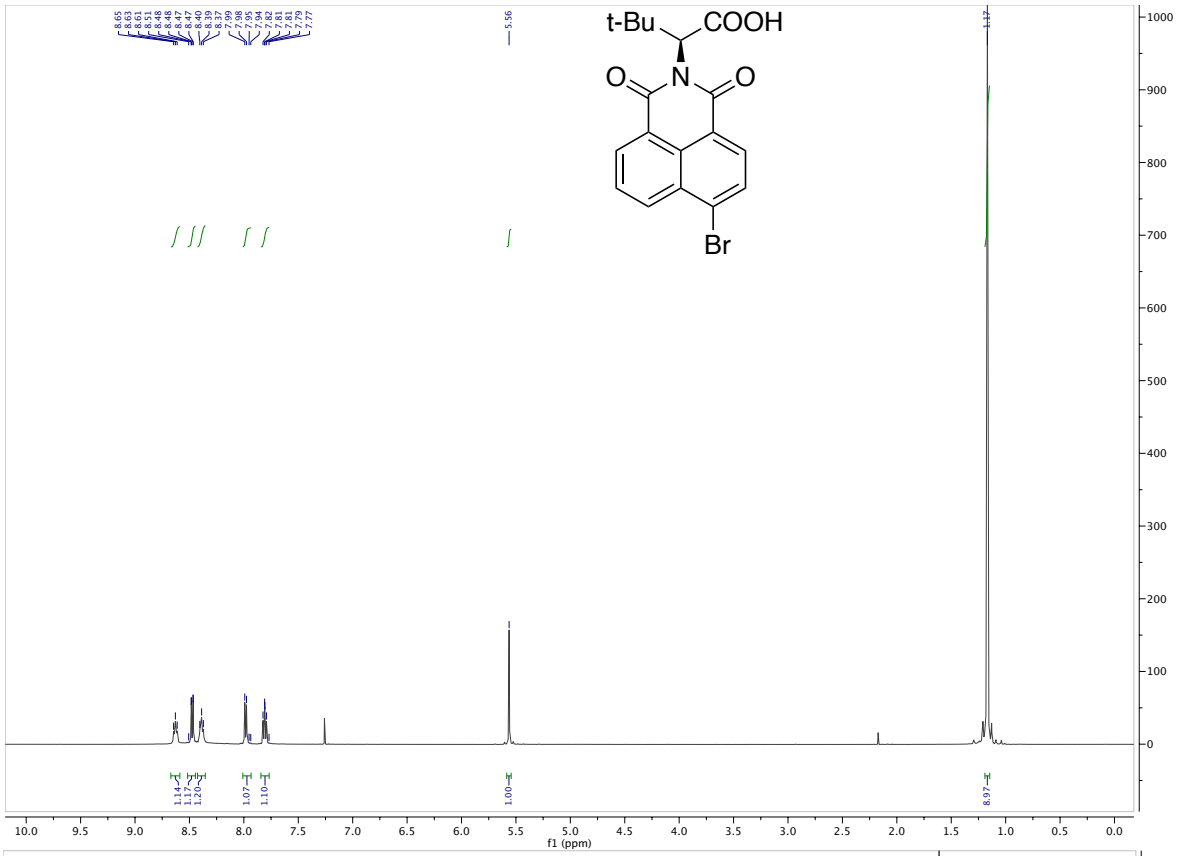
t-Bu
COOH
O
N
O
Br
f1 (ppm)

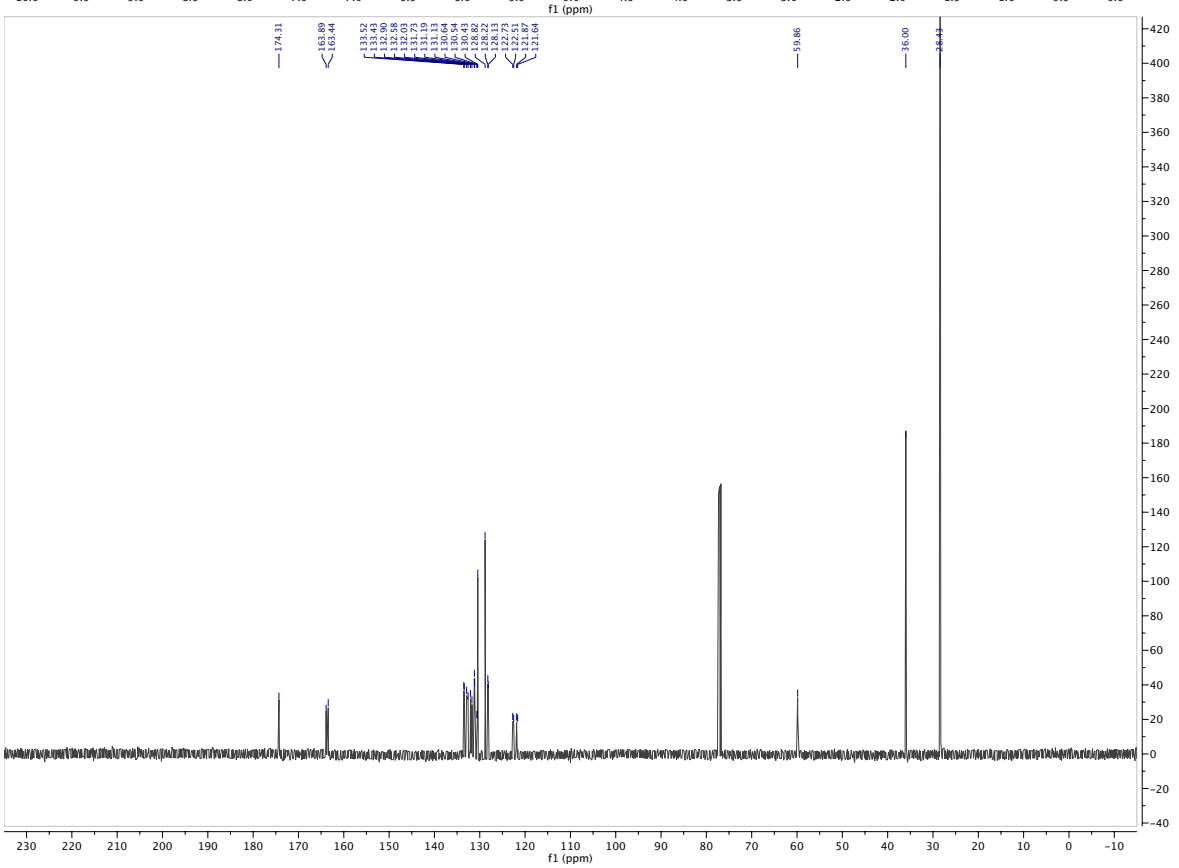
f1 (ppm)

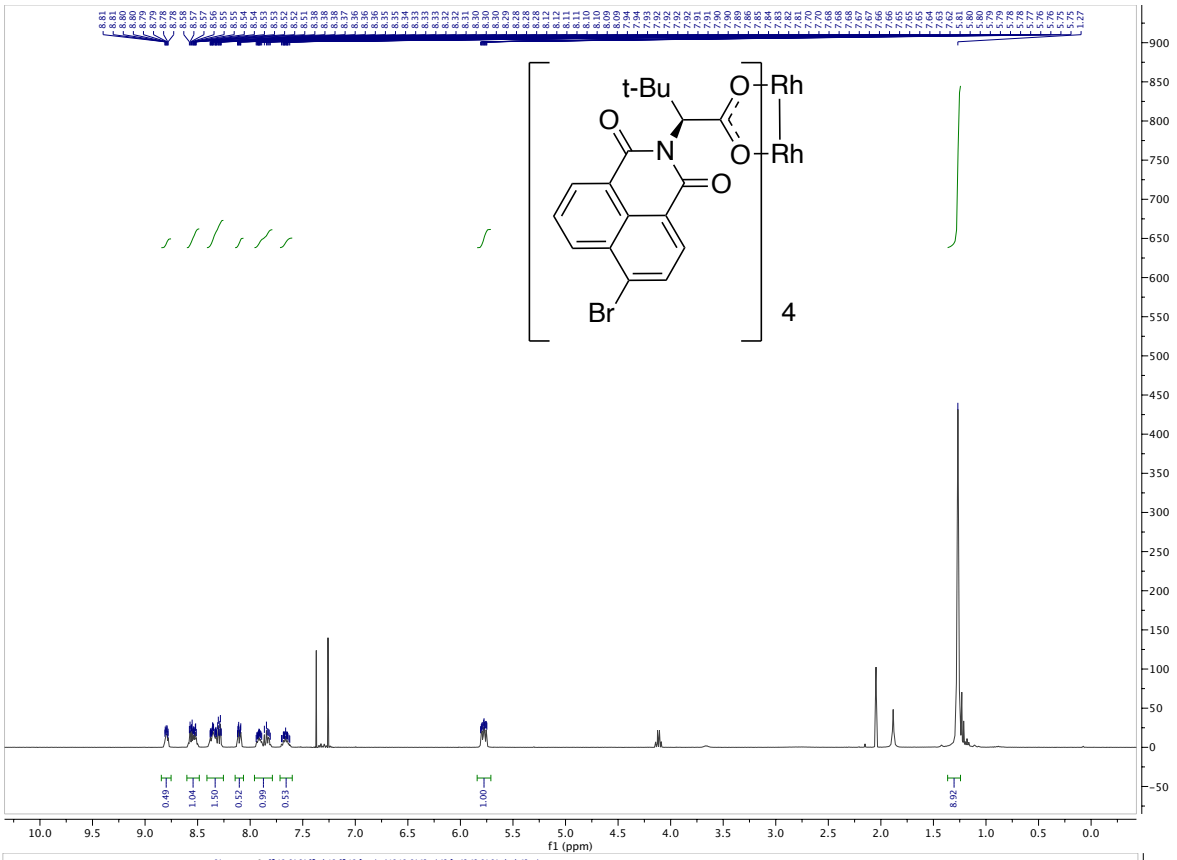
t-Bu
O
N
O
O
Rh
O
Rh
Br
4
0.49
1.04
1.50
0.52
0.99
0.53
1.00
8.92
f1 (ppm)

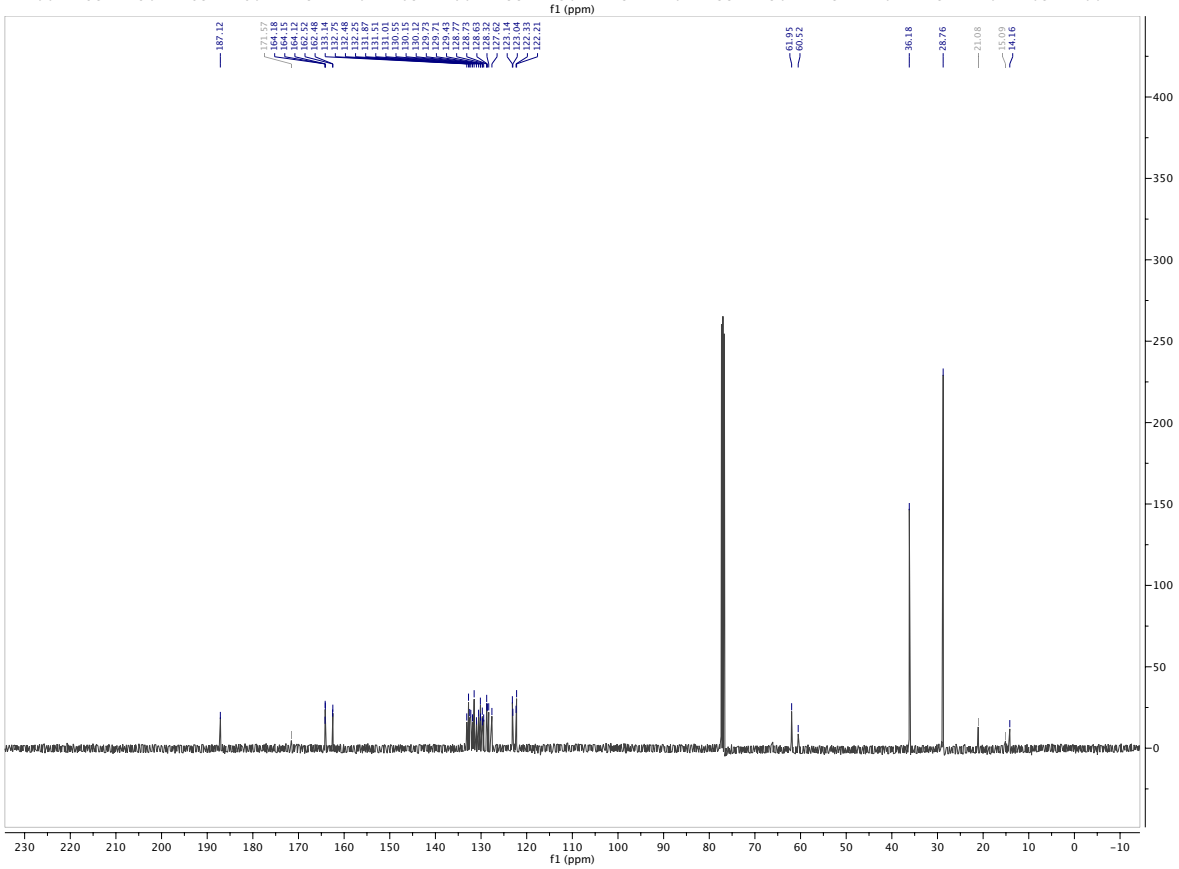
187.12
171.57
164.18
164.15
164.12
162.52
162.48
161.46
132.75
132.48
132.27
131.87
131.51
131.01
130.55
130.15
130.12
129.73
129.71
129.43
128.77
128.72
128.63
128.32
127.62
127.14
123.04
122.33
122.21
61.95
60.52
36.18
28.76
21.08
15.19
14.16
f1 (ppm)

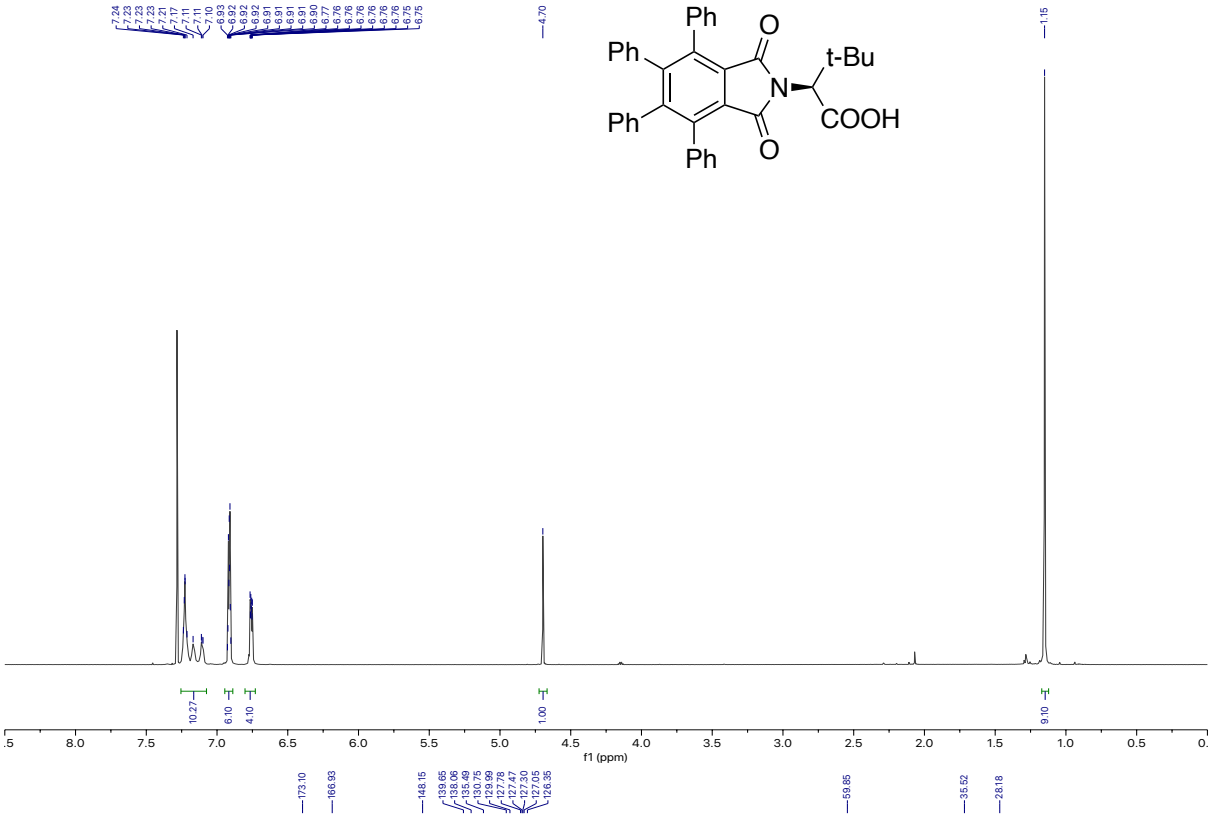
Ph
Ph
Ph
Ph
O
O
N
t-Bu
COOH
f1 (ppm)

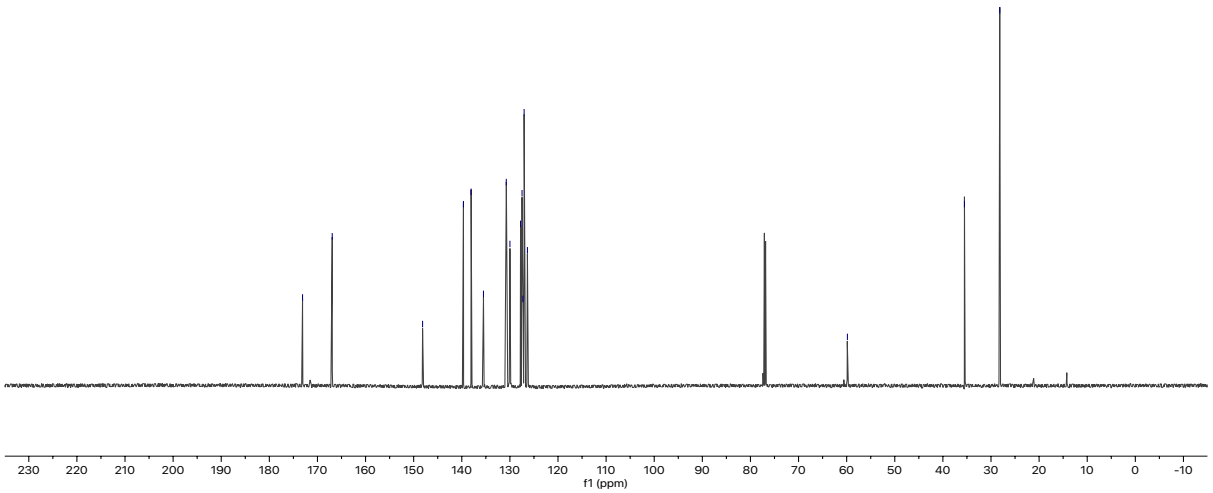
f1 (ppm)

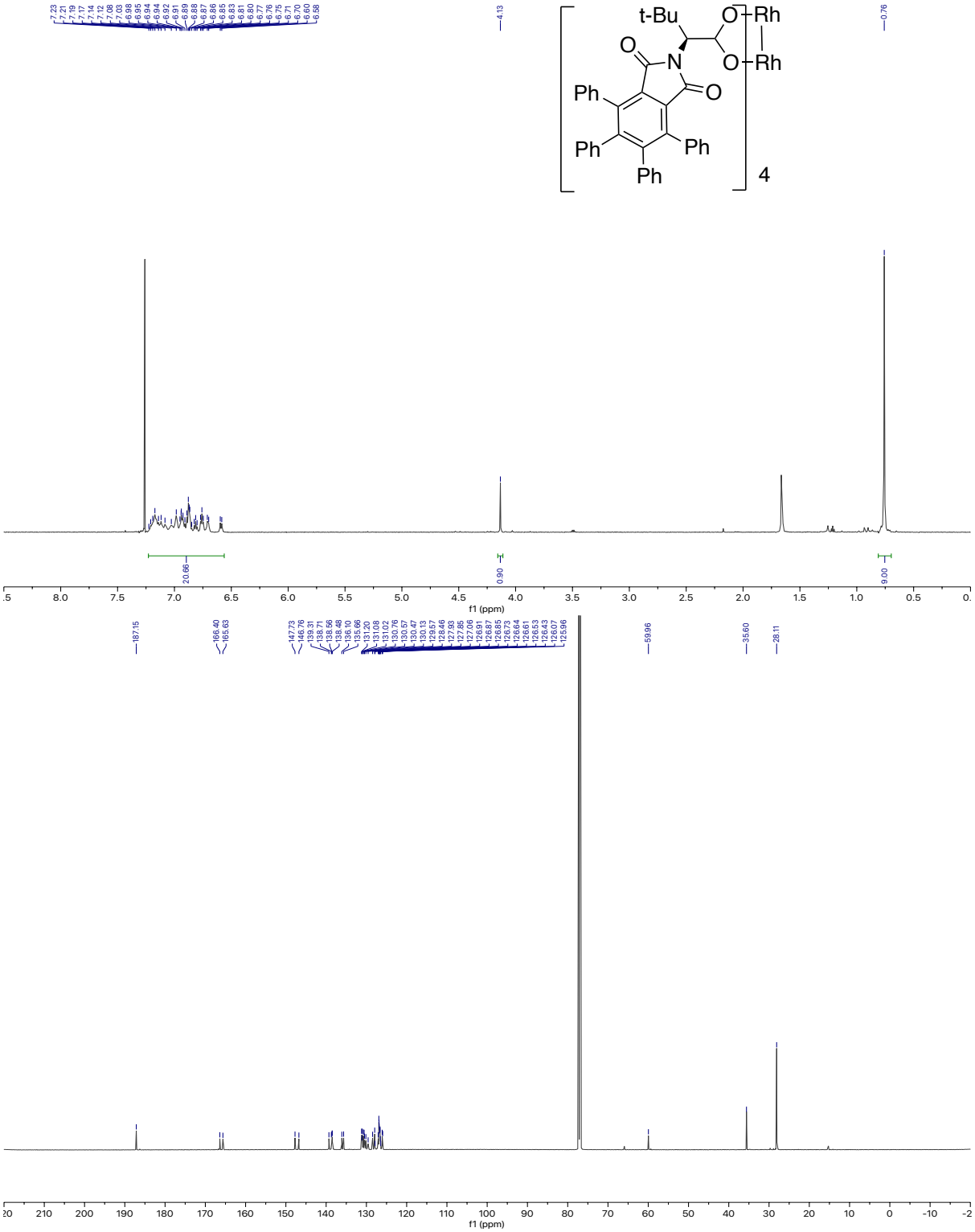
t-Bu
O
Rh
N
Ph
Ph
Ph
Ph
4
f1 (ppm)
f1 (ppm)

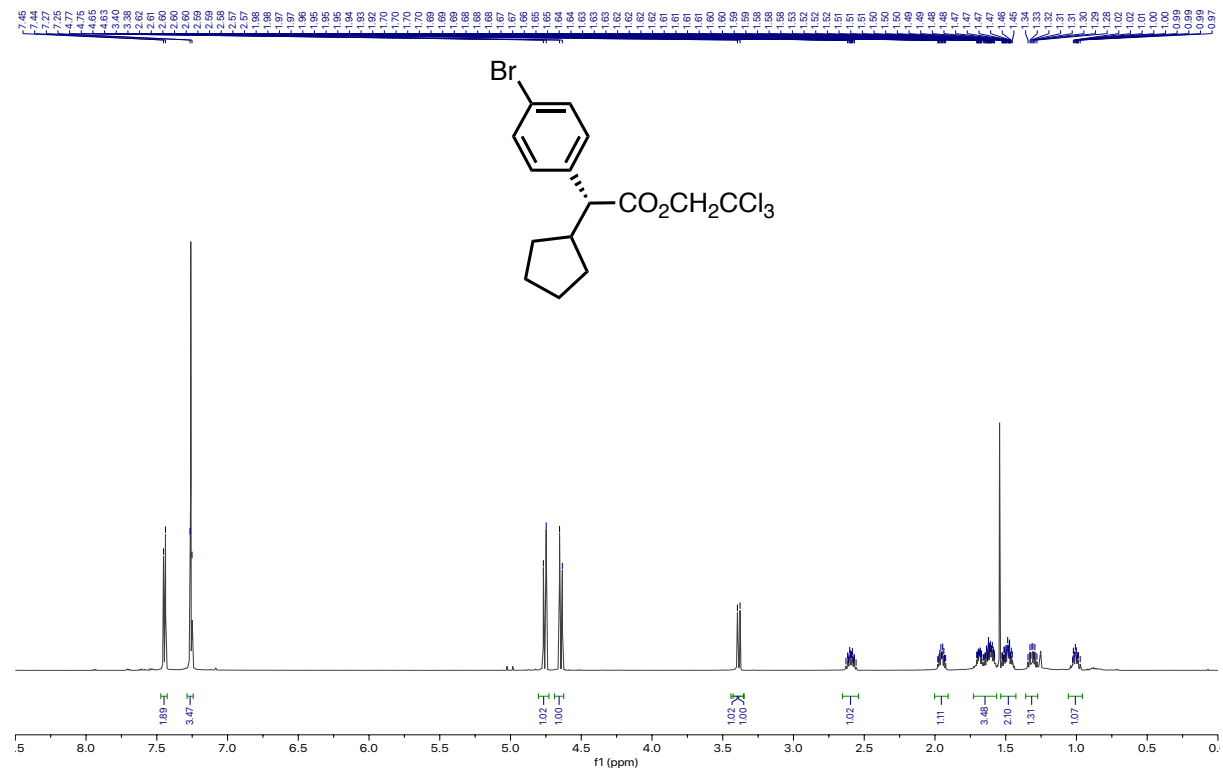
Br
CO2CH2CCl3
f1 (ppm)

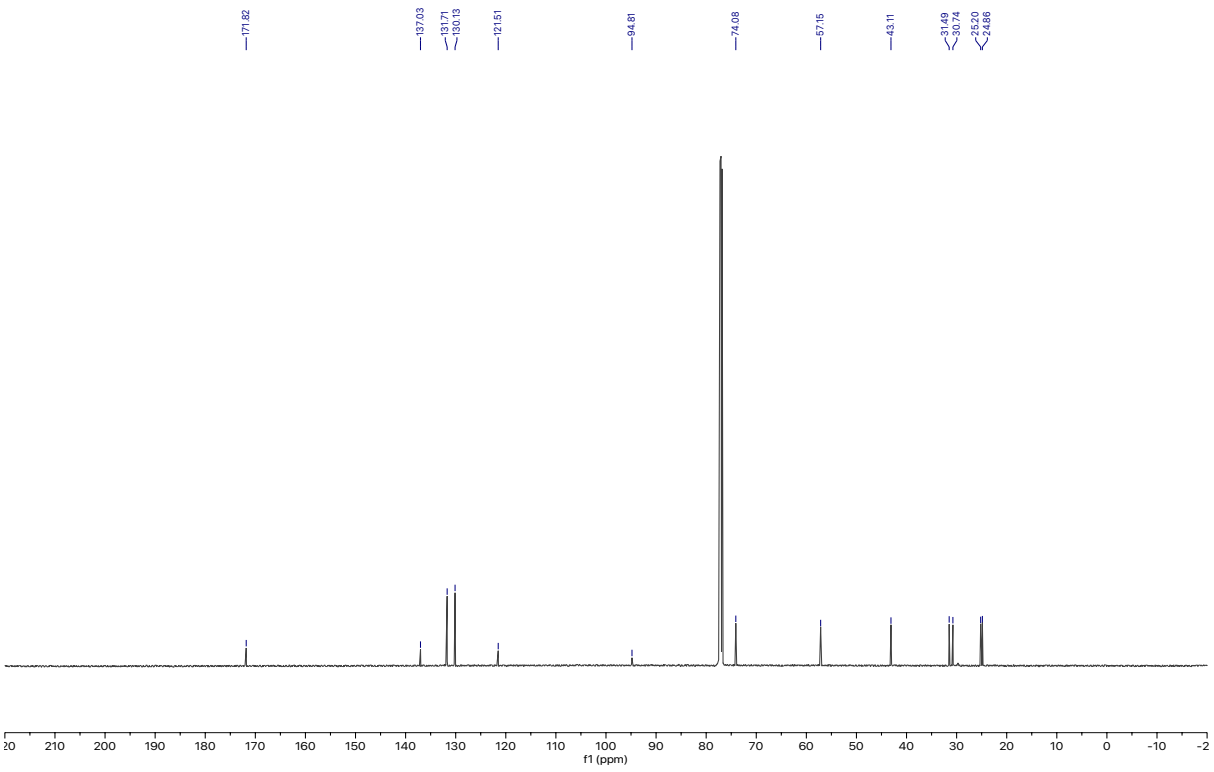
171.82
137.03
131.71
130.13
121.51
94.81
74.08
57.15
43.11
31.49
30.74
25.20
24.86
f1 (ppm)

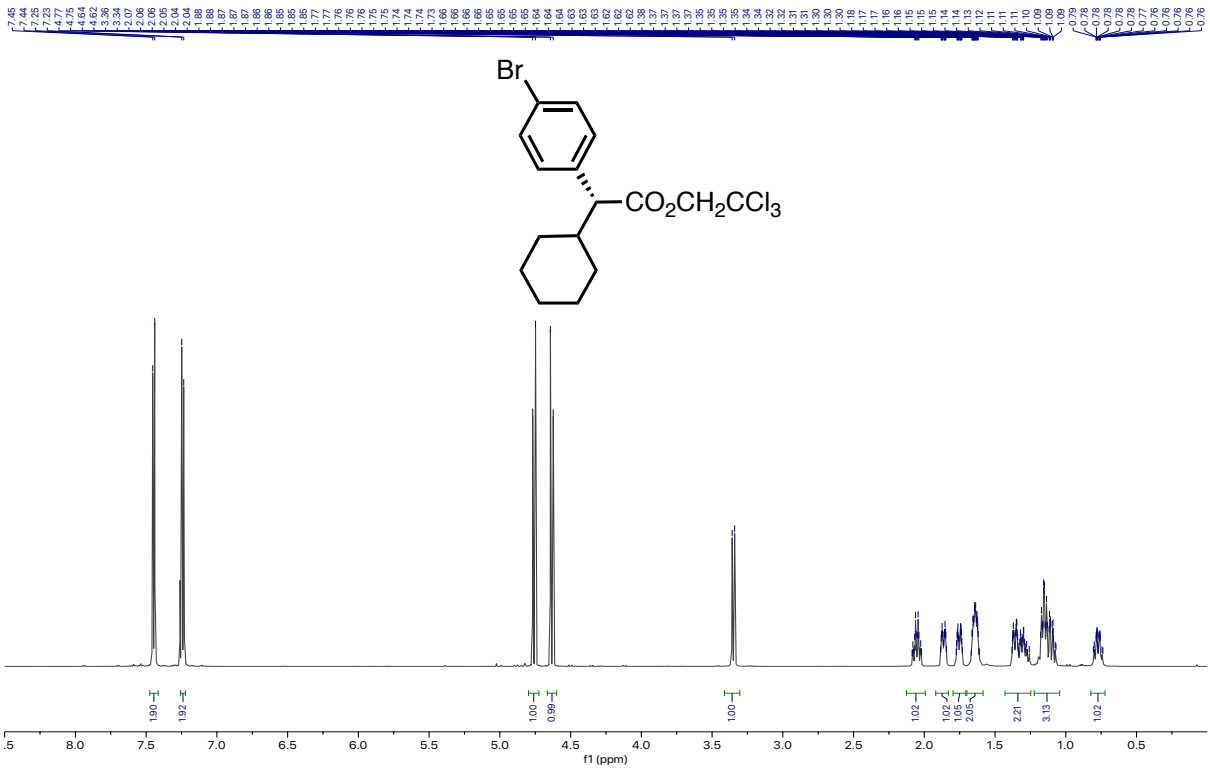
Br
CO2CH2CCl3
f1 (ppm)

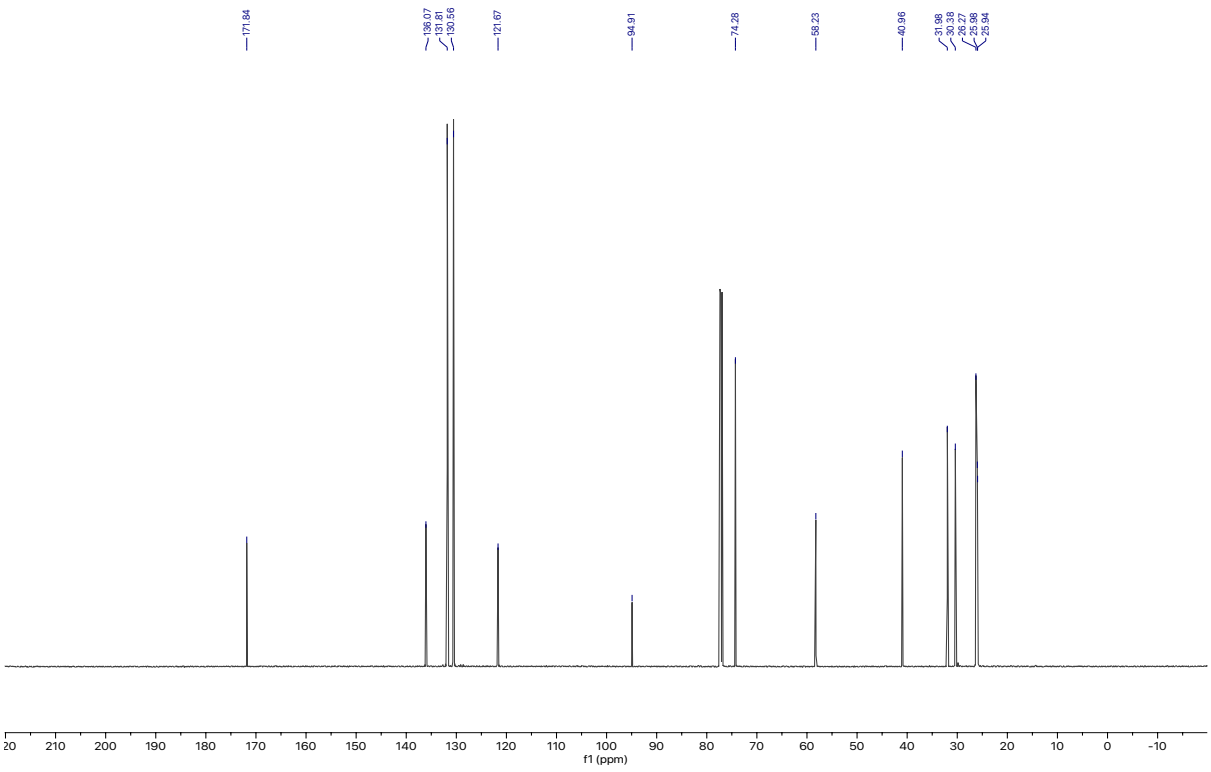
171.84
136.07
131.87
130.56
121.67
94.91
74.28
58.23
40.96
31.98
30.38
26.27
25.98
25.94
f1 (ppm)

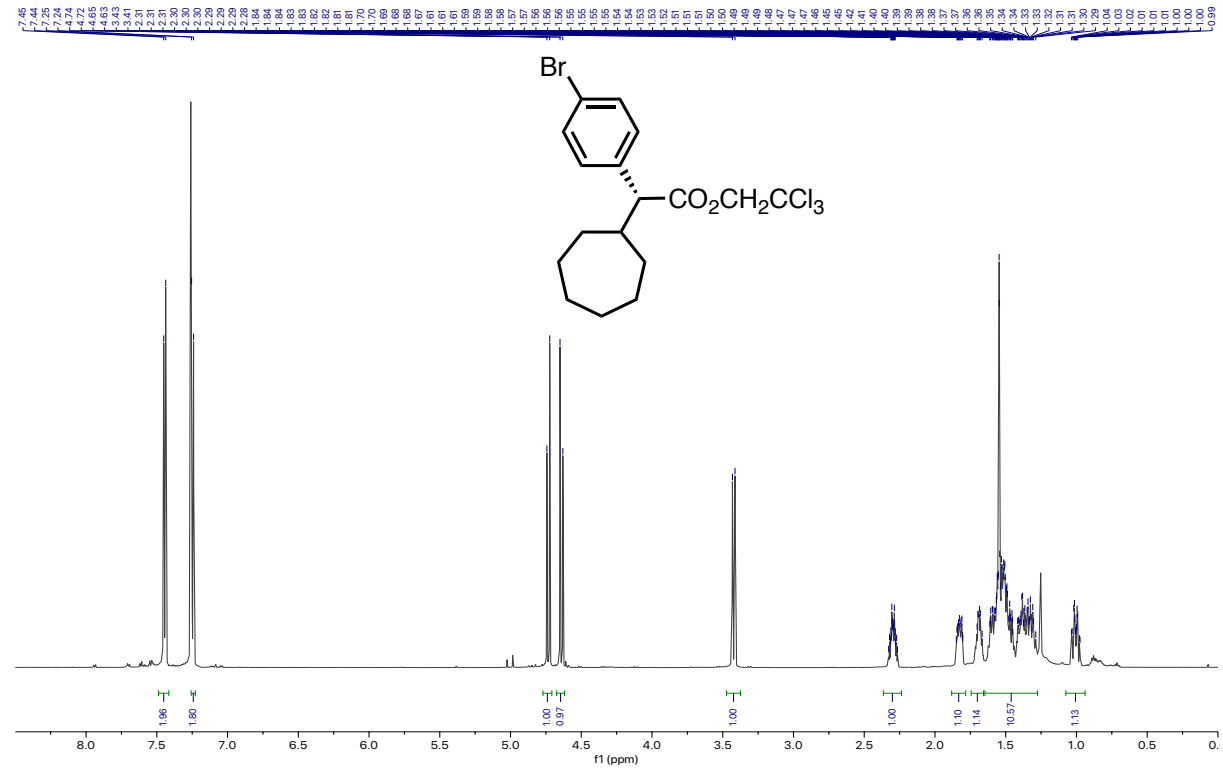
Br
CO2CH2CCl3
f1 (ppm)

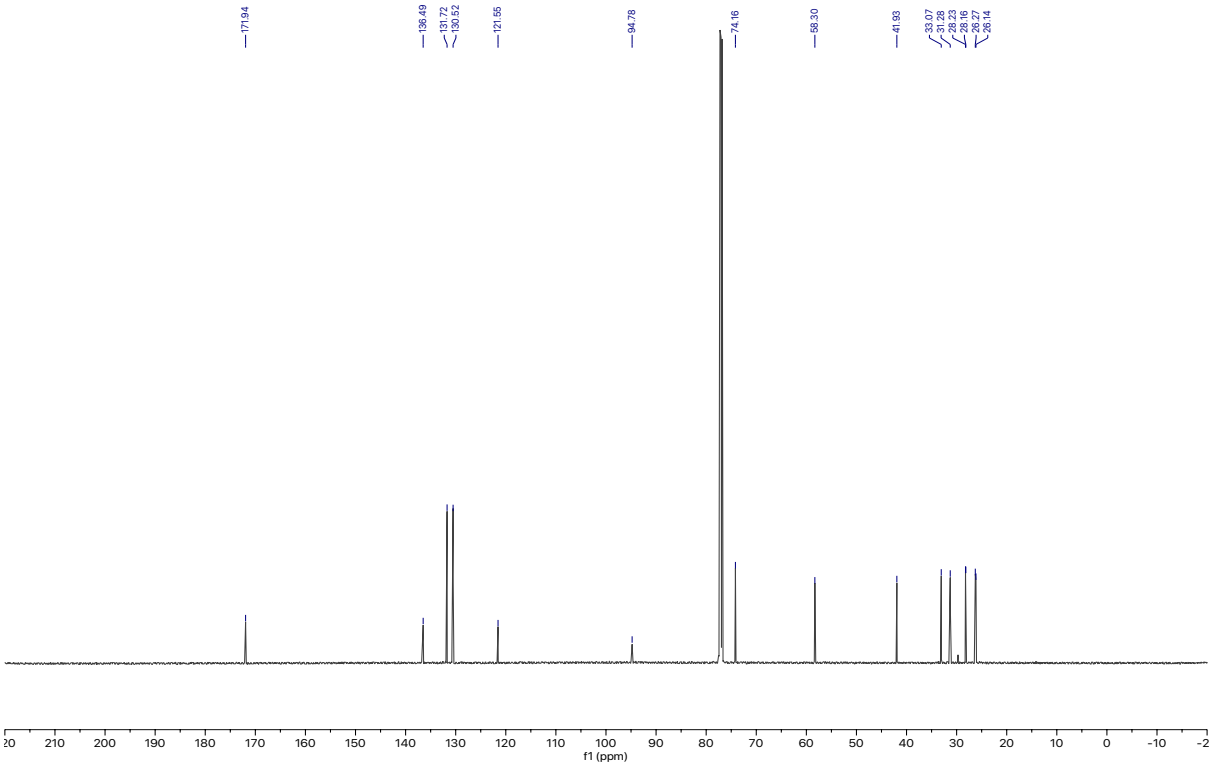
171.94
136.49
131.72
130.52
121.55
94.78
74.16
58.30
41.93
33.07
31.25
28.23
28.16
26.27
26.14
f1 (ppm)

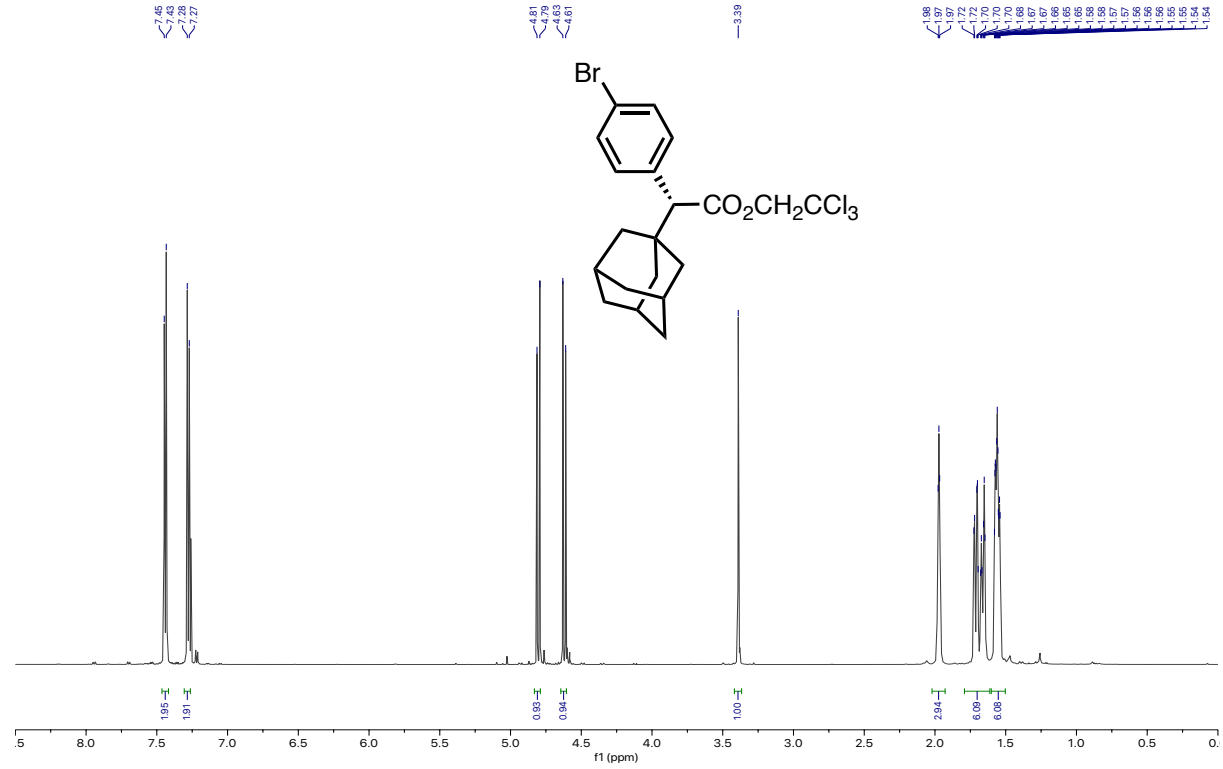
7.45
7.43
7.28
7.27
4.81
4.79
4.63
4.61
3.39
1.98
1.97
1.97
1.72
1.70
1.70
1.70
1.68
1.67
1.67
1.66
1.65
1.65
1.58
1.58
1.57
1.57
1.56
1.56
1.56
1.55
1.55
1.54
1.54
Br
CO2CH2CCl3
1.95
1.91
0.93
0.94
1.00
2.94
6.09
6.08
f1 (ppm)

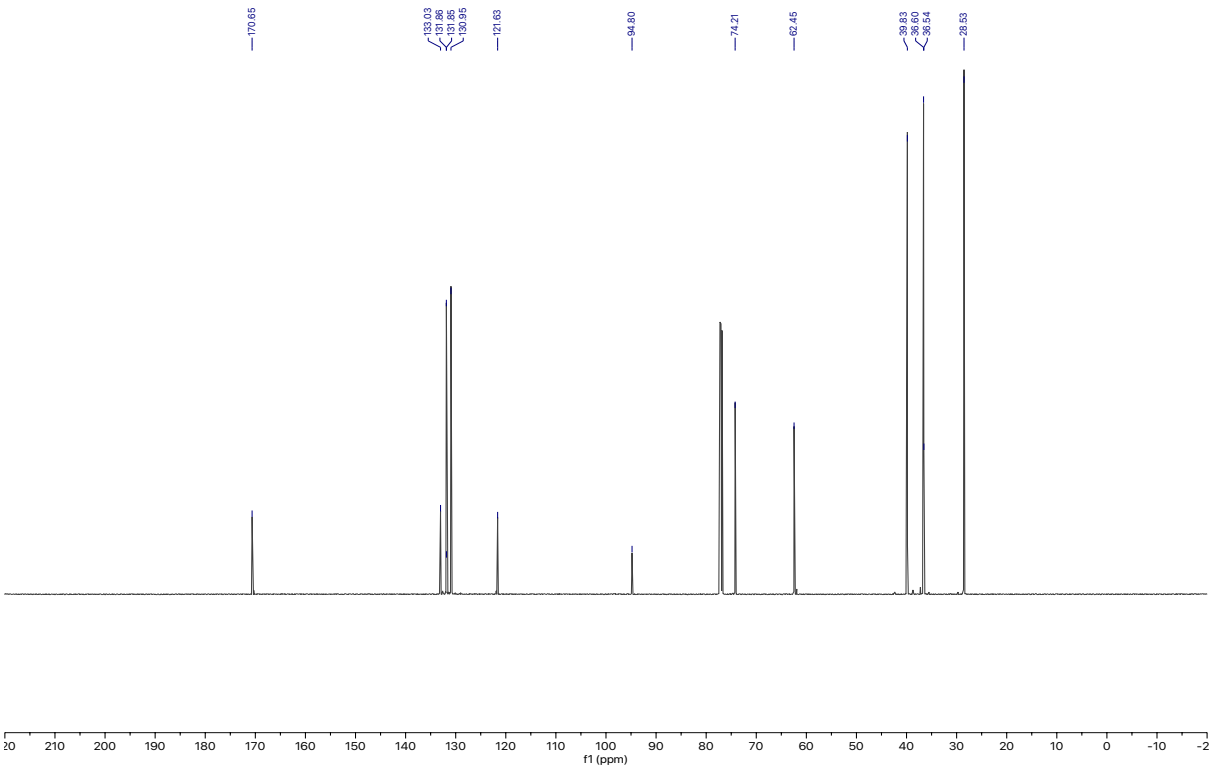
170.65
133.03
131.96
131.85
130.95
121.63
94.80
74.21
62.45
39.83
39.60
38.54
28.53
f1 (ppm)

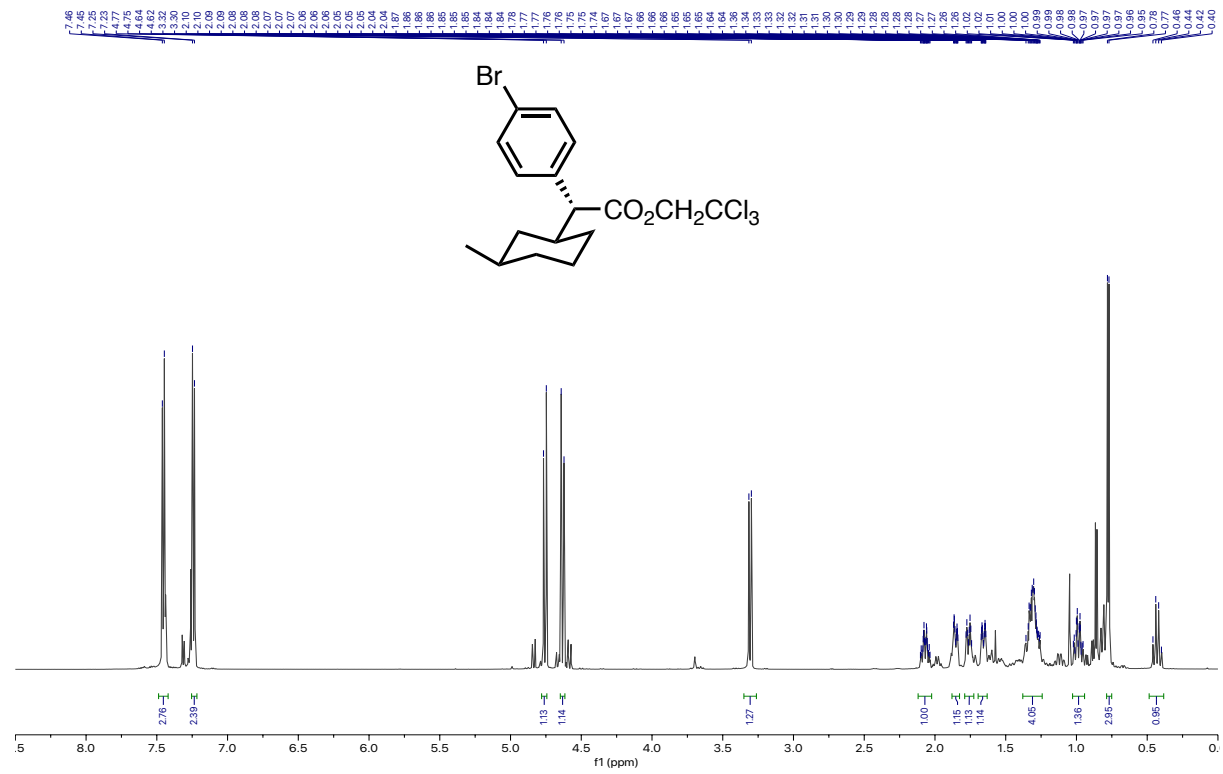
Br
CO2CH2CCl3
f1 (ppm)

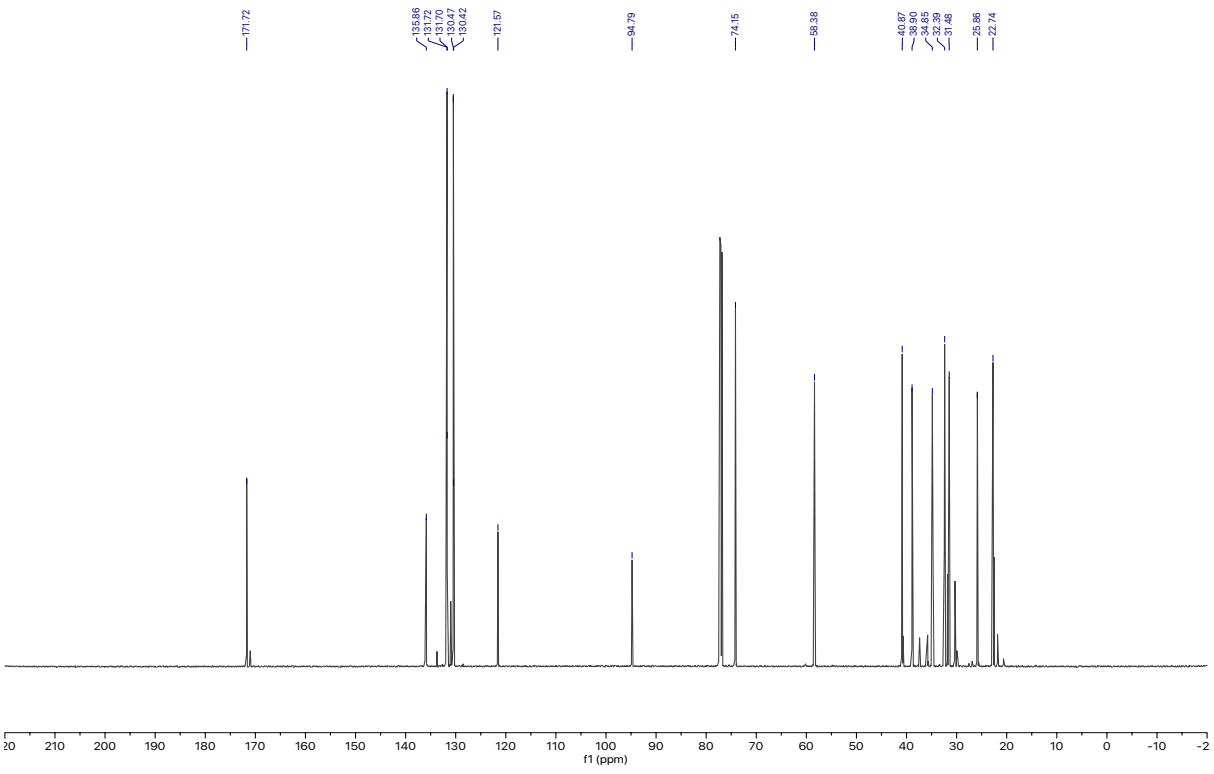
171.72
135.68
131.72
131.70
130.47
130.42
121.57
94.79
74.15
58.38
40.87
38.90
34.85
32.39
31.48
25.86
22.74
f1 (ppm)

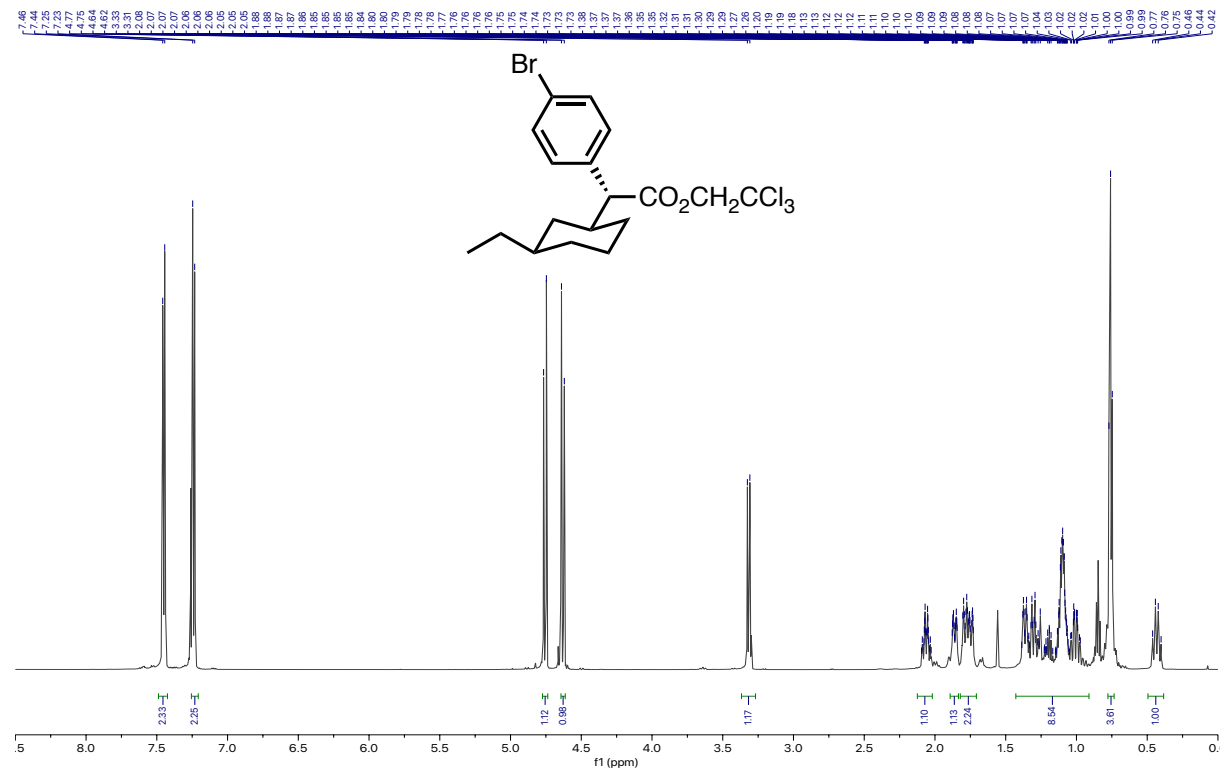
Br
CO2CH2CCl3
f1 (ppm)

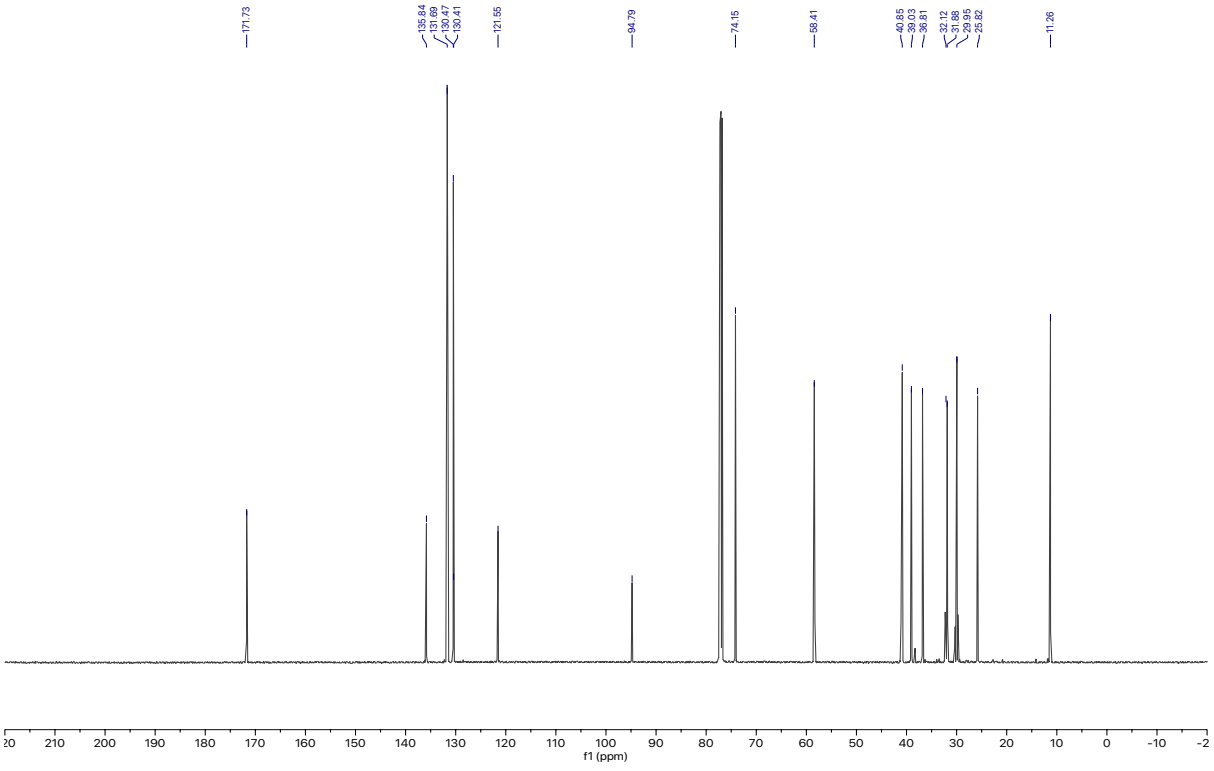
171.73
135.84
131.69
130.47
130.41
121.55
94.79
74.15
58.41
40.85
39.03
38.81
32.12
31.88
29.95
25.82
11.26
f1 (ppm)

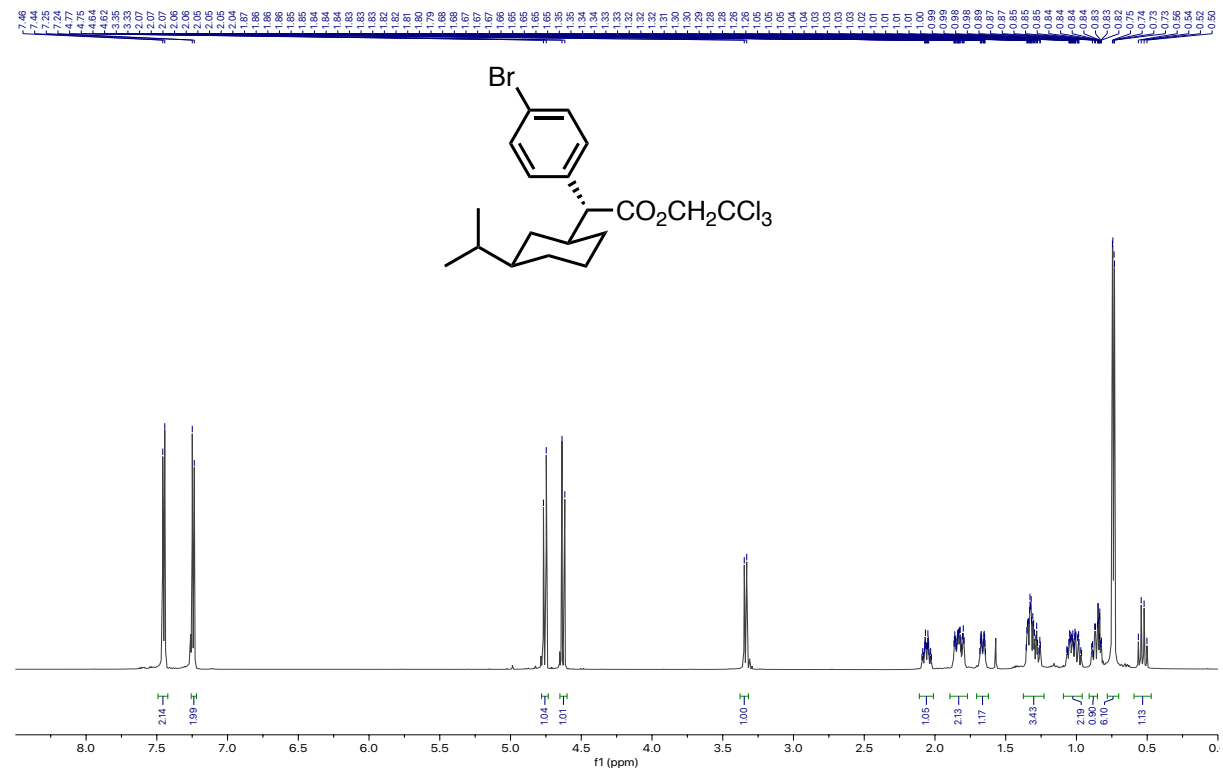
Br
CO2CH2CCl3
f1 (ppm)

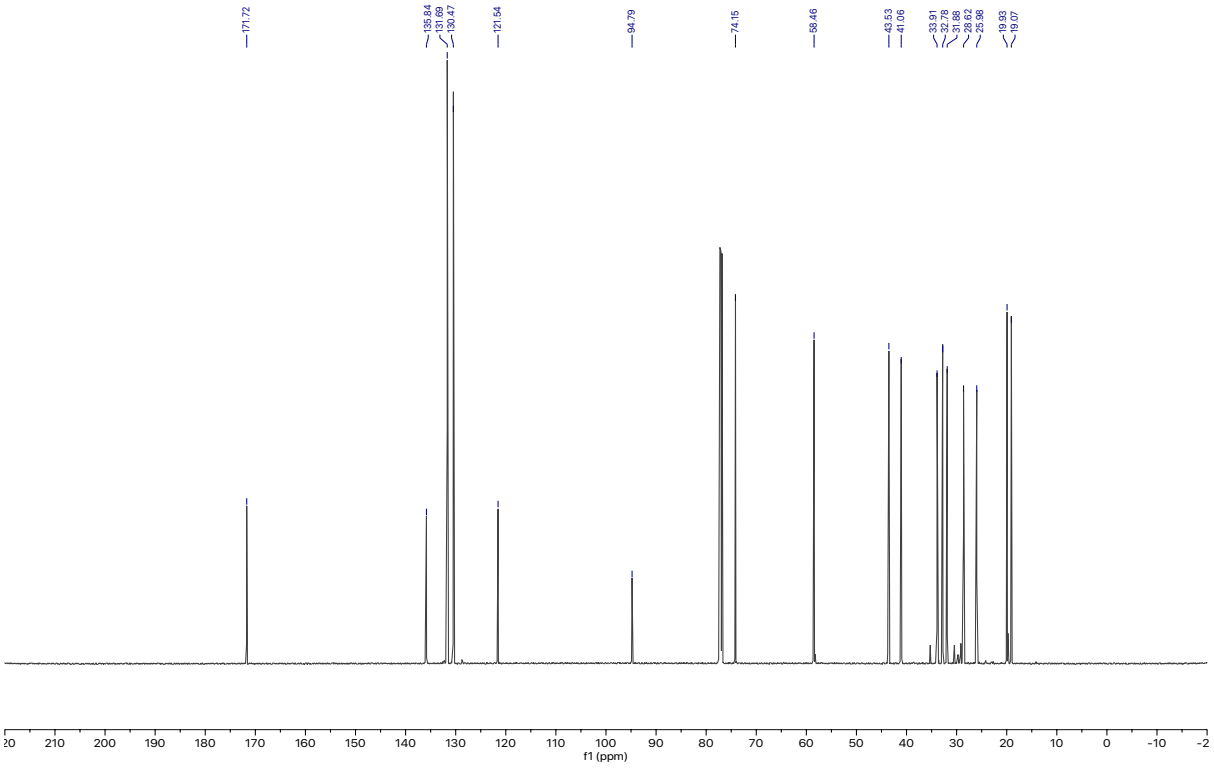
171.72
135.84
130.47
121.54
94.79
74.15
58.46
43.53
41.06
33.91
29.62
25.98
19.93
19.07
f1 (ppm)

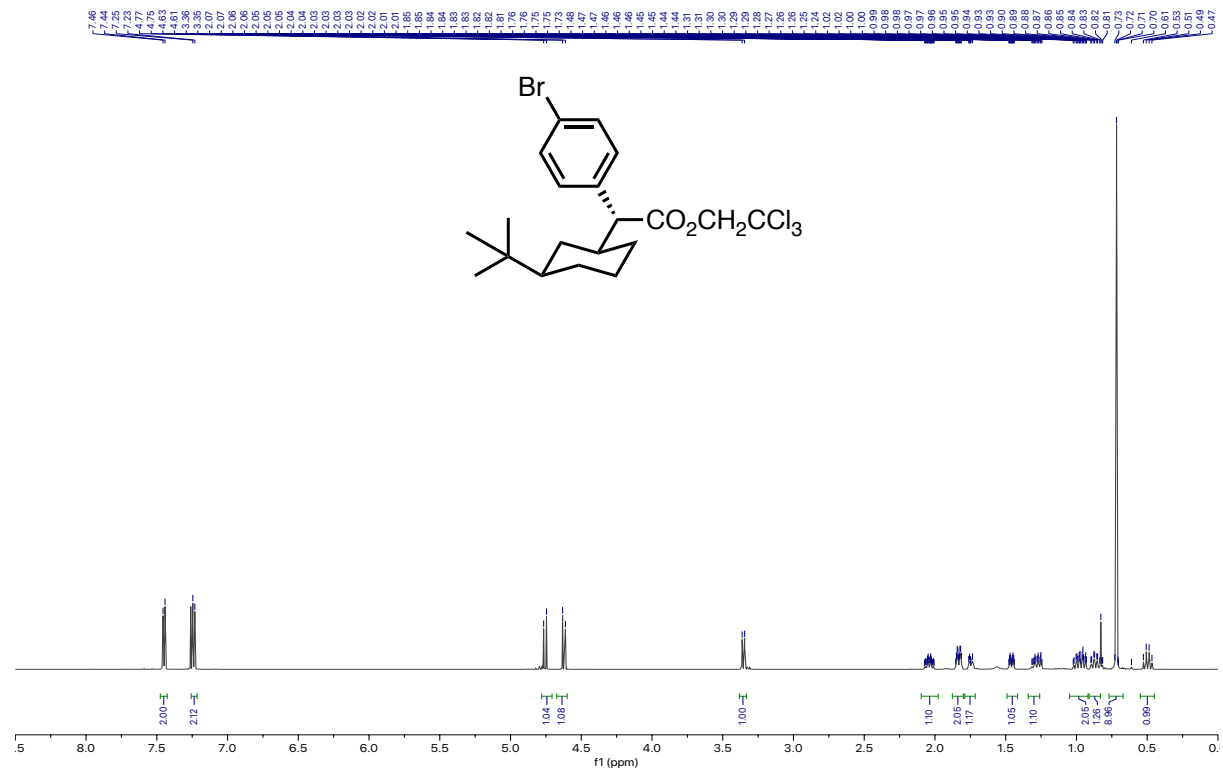
Br
CO2CH2CCl3
f1 (ppm)

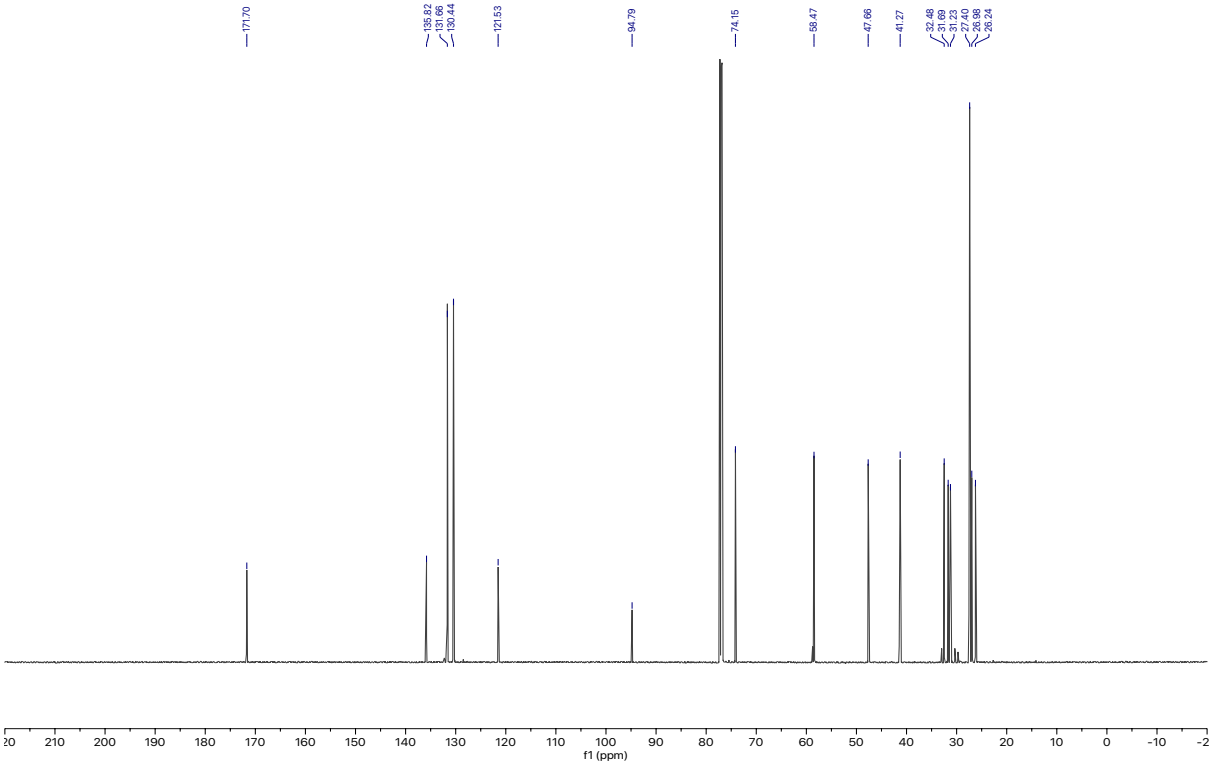
171.70
135.62
133.66
130.44
121.53
94.79
74.15
58.47
47.66
41.27
33.48
31.60
31.23
27.40
26.98
26.24
f1 (ppm)

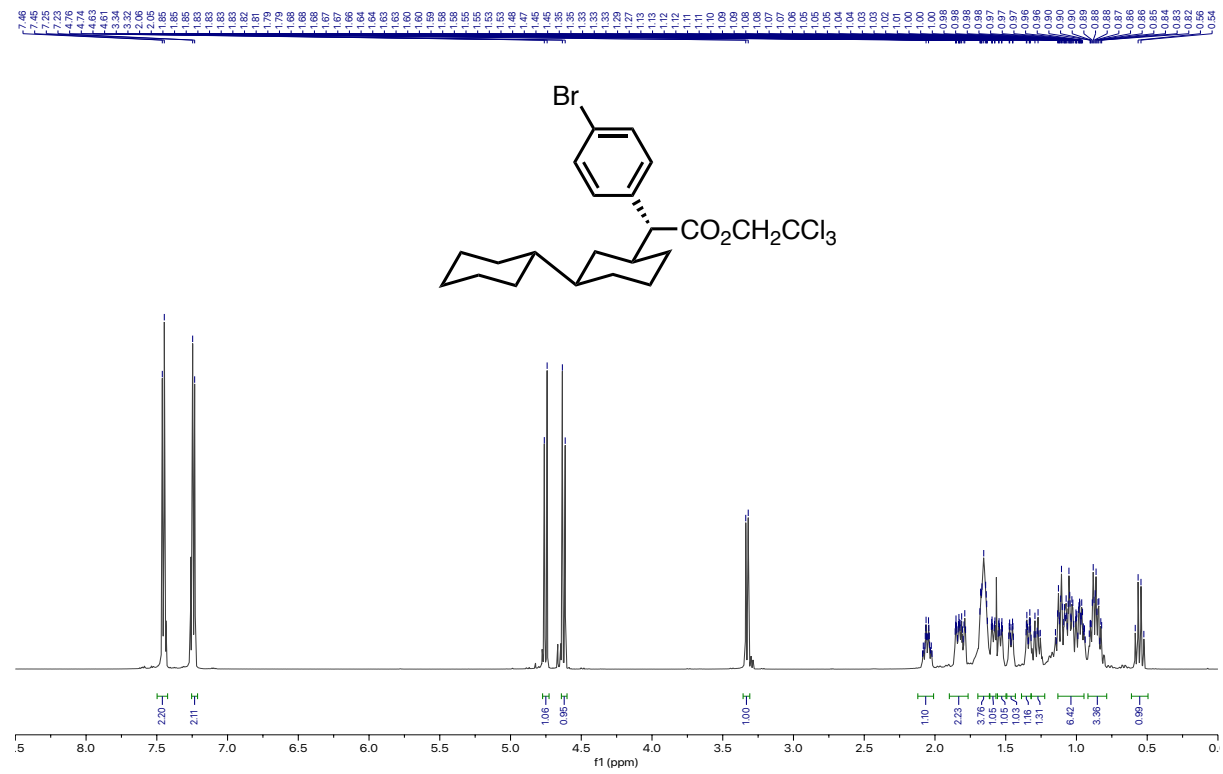
Br
CO2CH2CCl3
f1 (ppm)

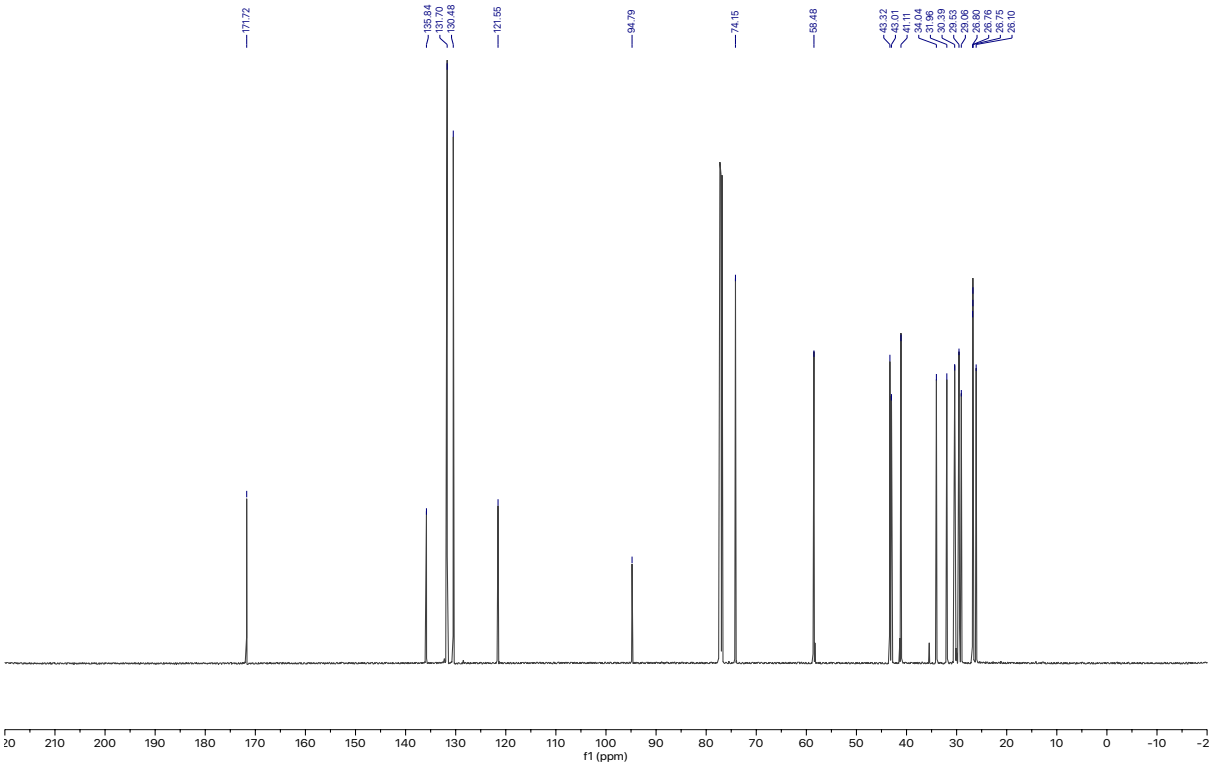
171.72
135.84
132.70
130.48
121.55
94.79
74.15
58.48
43.32
43.01
41.11
34.04
31.96
30.39
29.53
29.06
26.80
26.76
26.75
26.10
f1 (ppm)

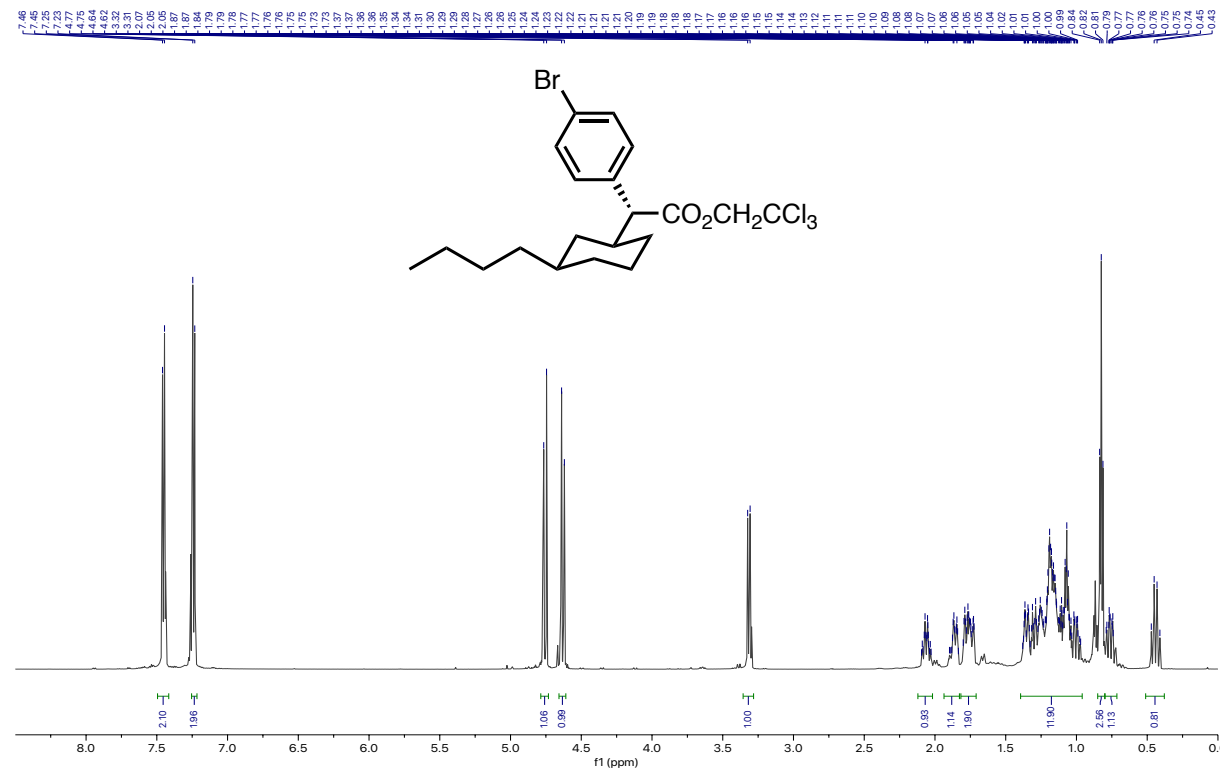
Br
CO2CH2CCl3
f1 (ppm)

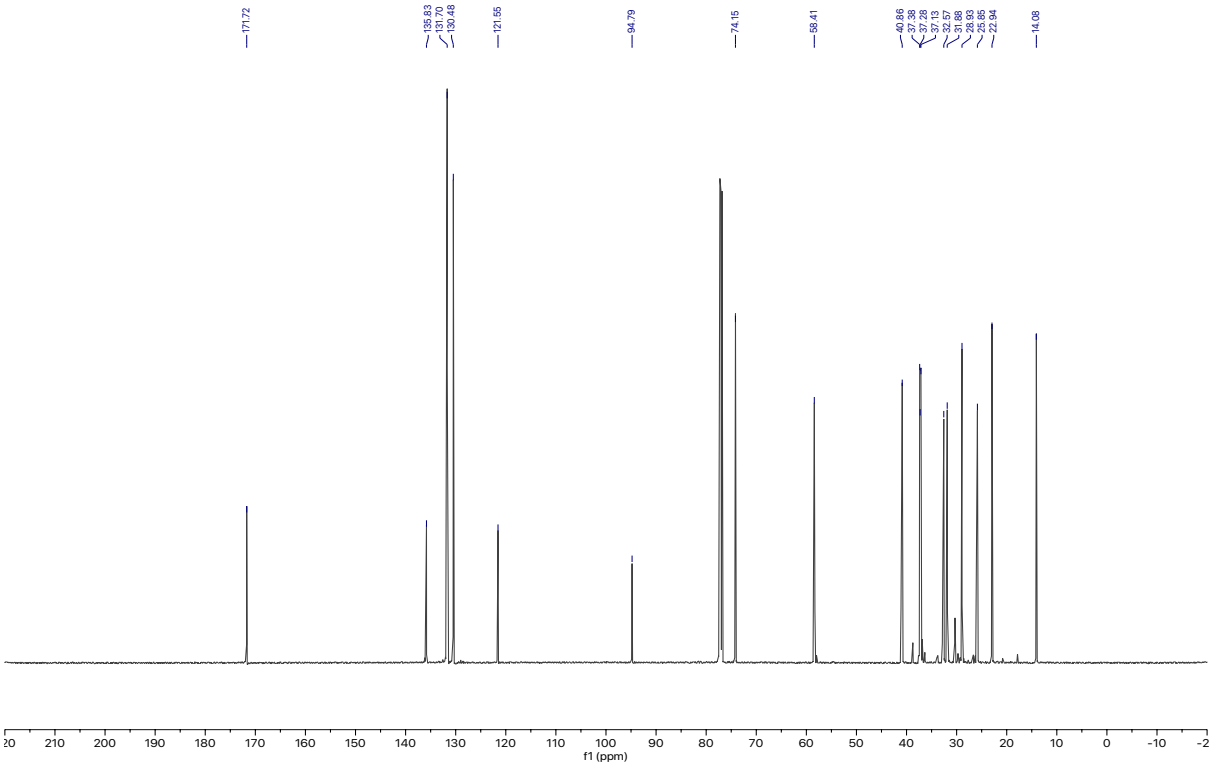
171.72
135.63
131.70
130.48
121.55
94.79
74.15
58.41
40.86
37.38
37.28
37.13
32.57
31.66
29.93
25.85
22.94
14.08
f1 (ppm)

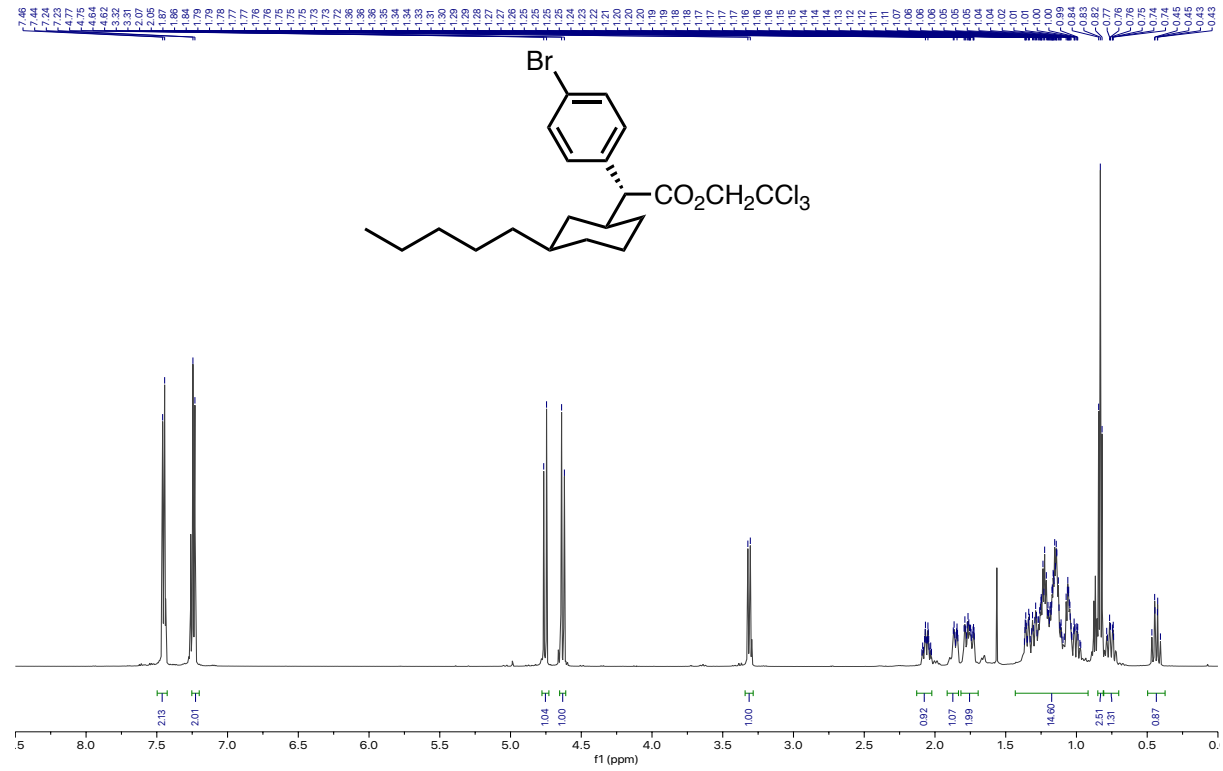
Br
CO2CH2CCl3
f1 (ppm)

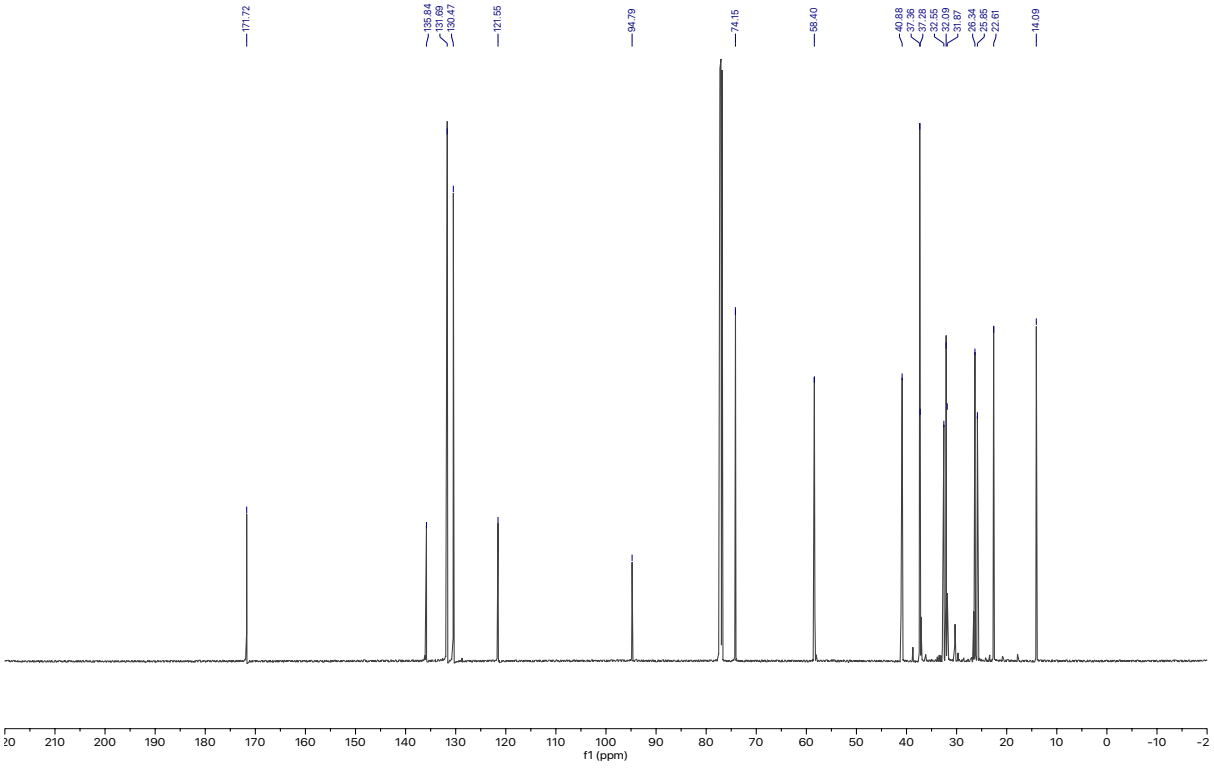
171.72
135.84
131.69
130.47
121.55
94.79
74.15
58.40
40.88
37.36
37.28
32.55
32.09
31.87
29.34
25.86
22.61
14.09
f1 (ppm)

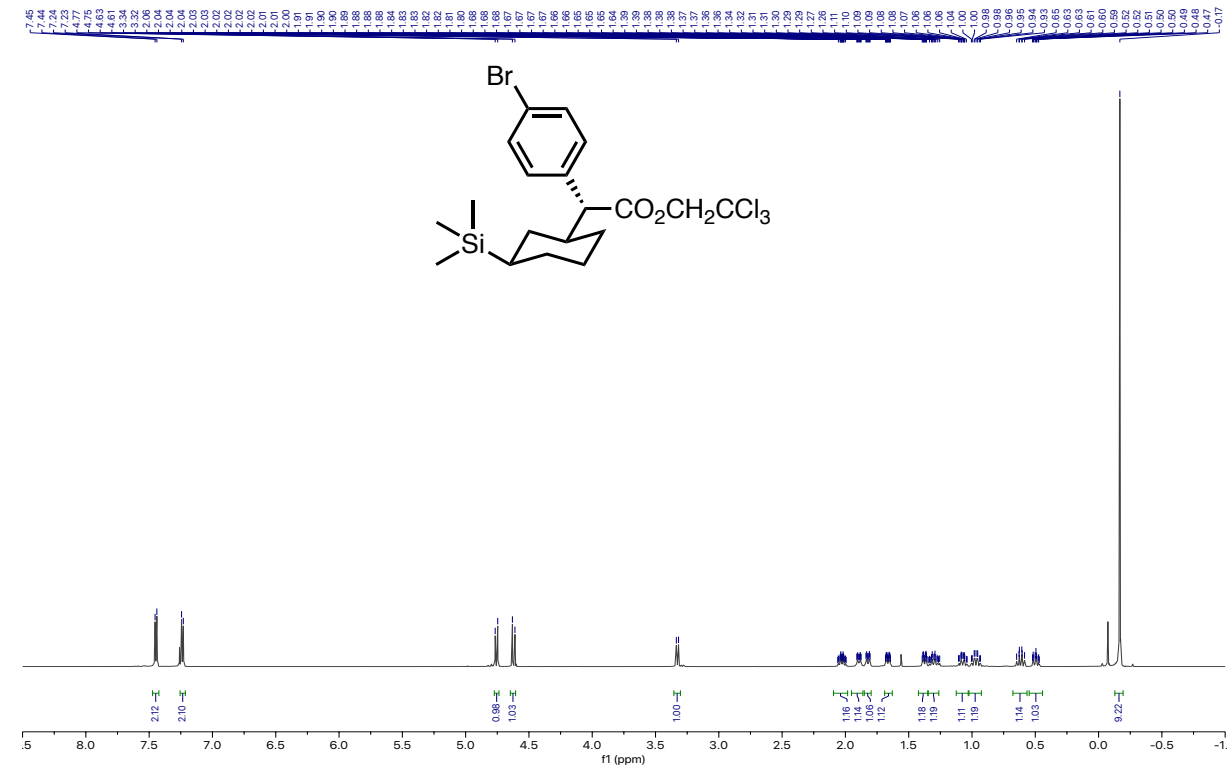
Br
CO2CH2CCl3
Si
f1 (ppm)

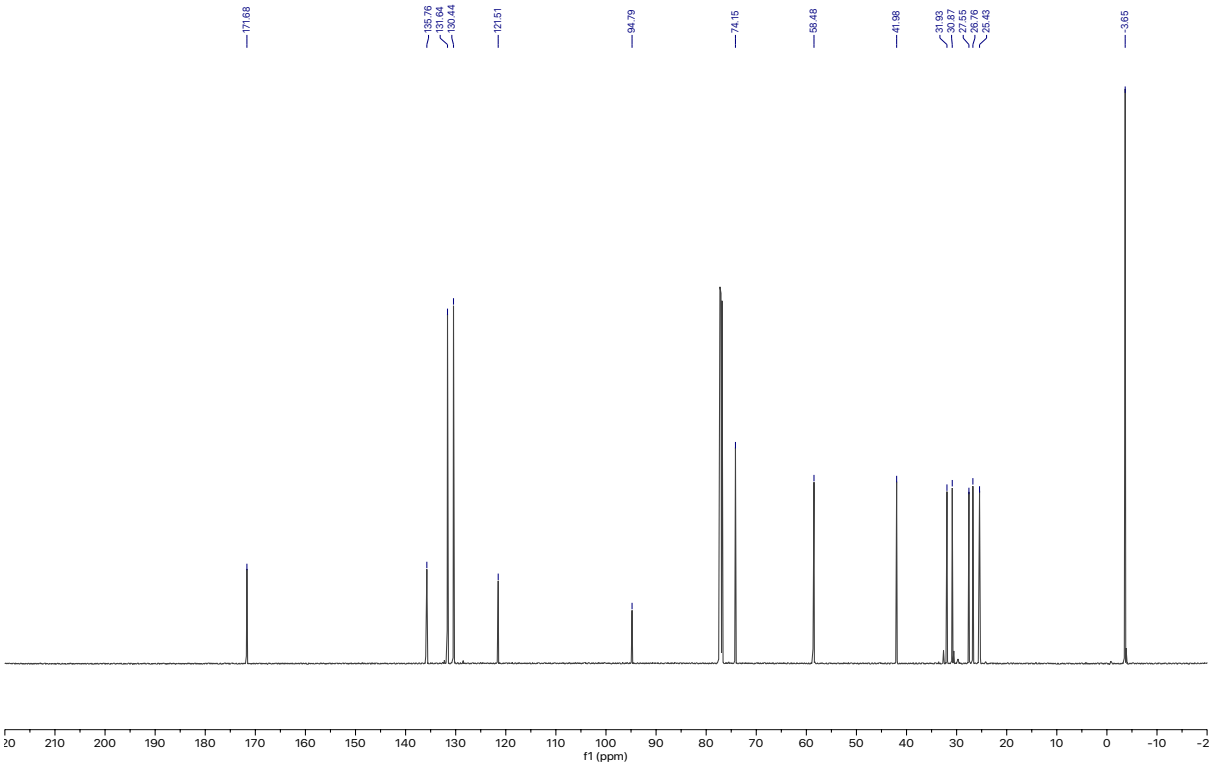
171.68
135.76
130.44
121.51
94.79
74.15
58.48
41.98
31.93
30.87
27.55
26.76
25.43
3.65
f1 (ppm)

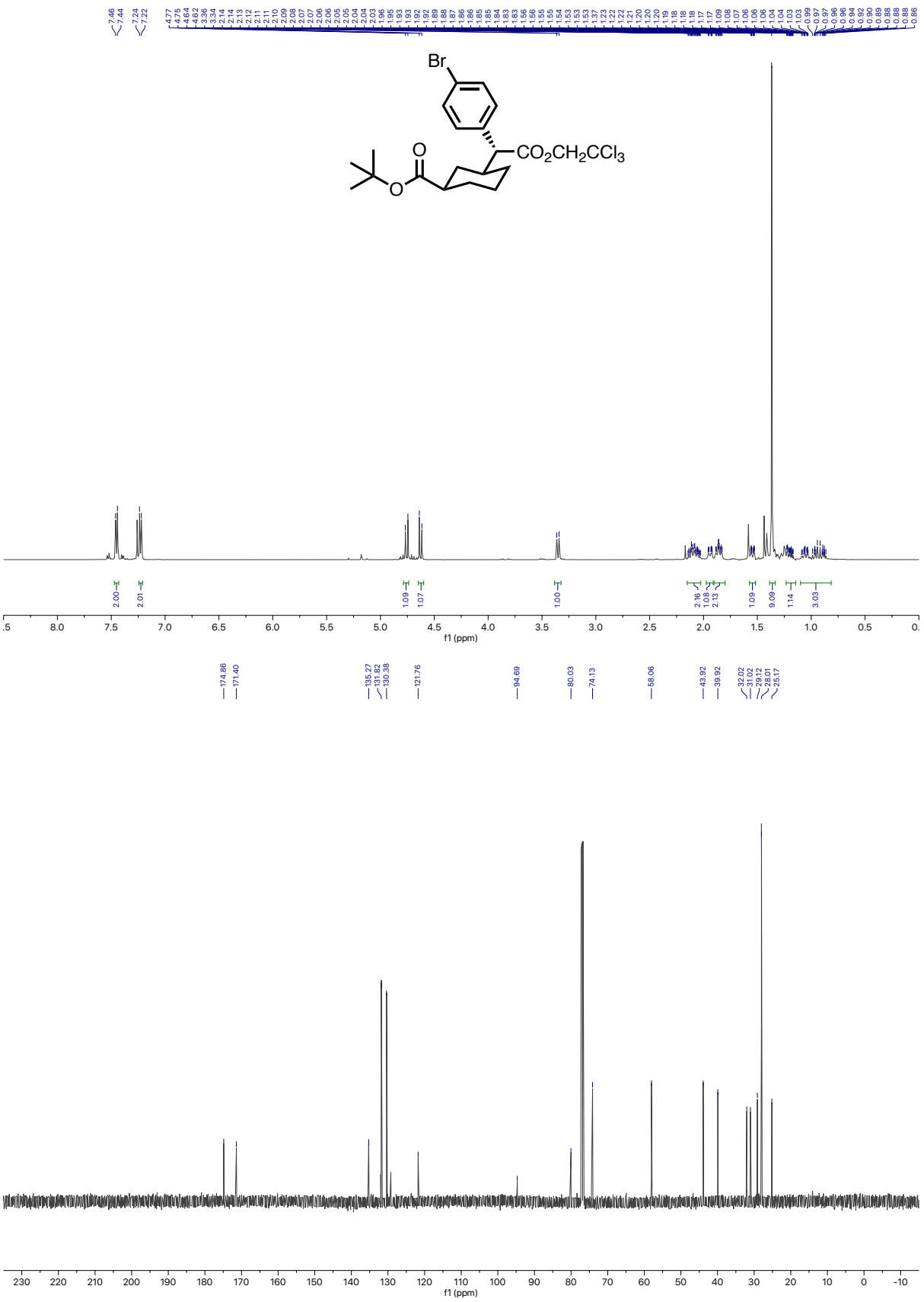
Br
O
O
CO2CH2CCl3
f1 (ppm)
f1 (ppm)

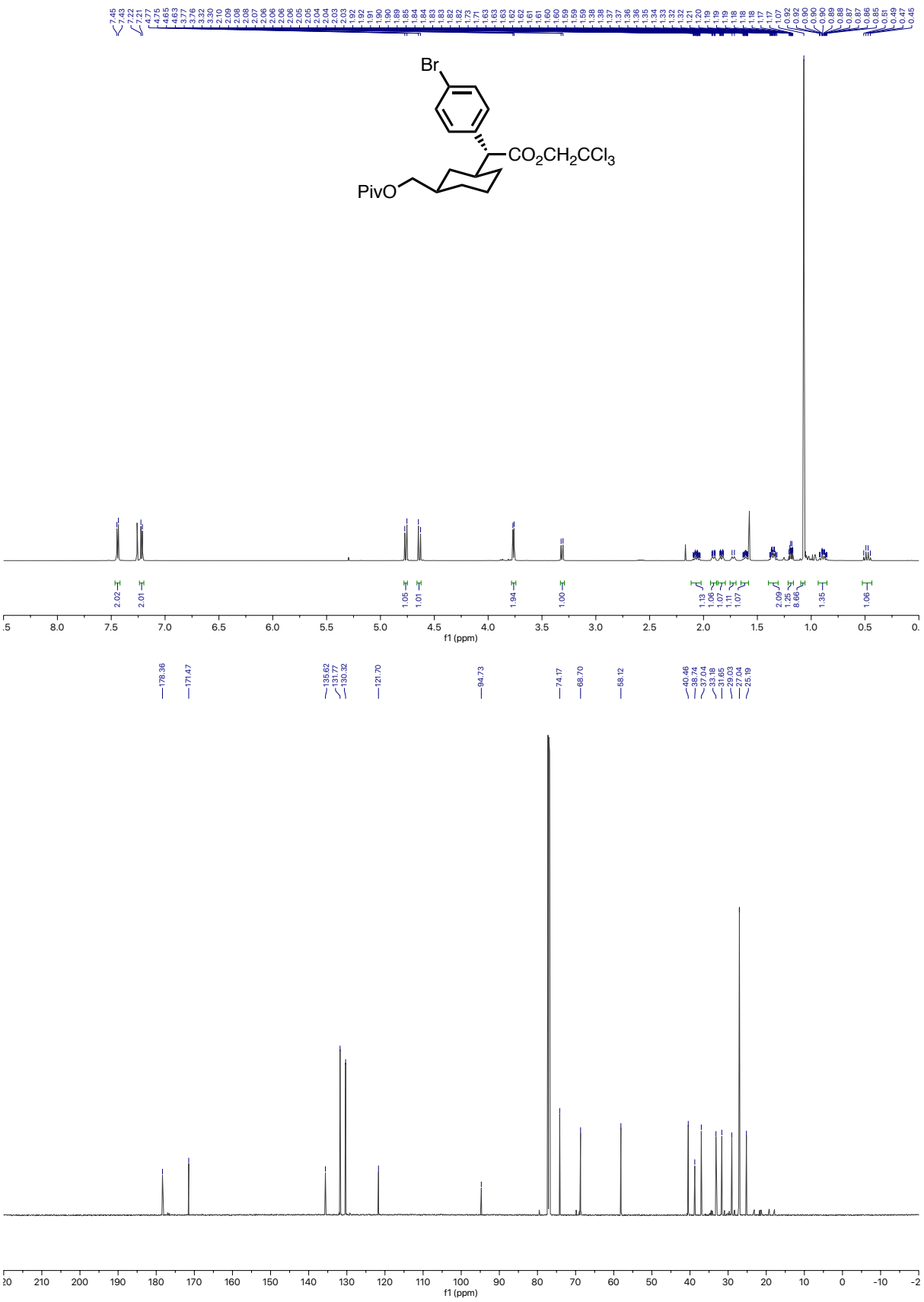
Br
CO2CH2CCl3
PivO
f1 (ppm)
f1 (ppm)

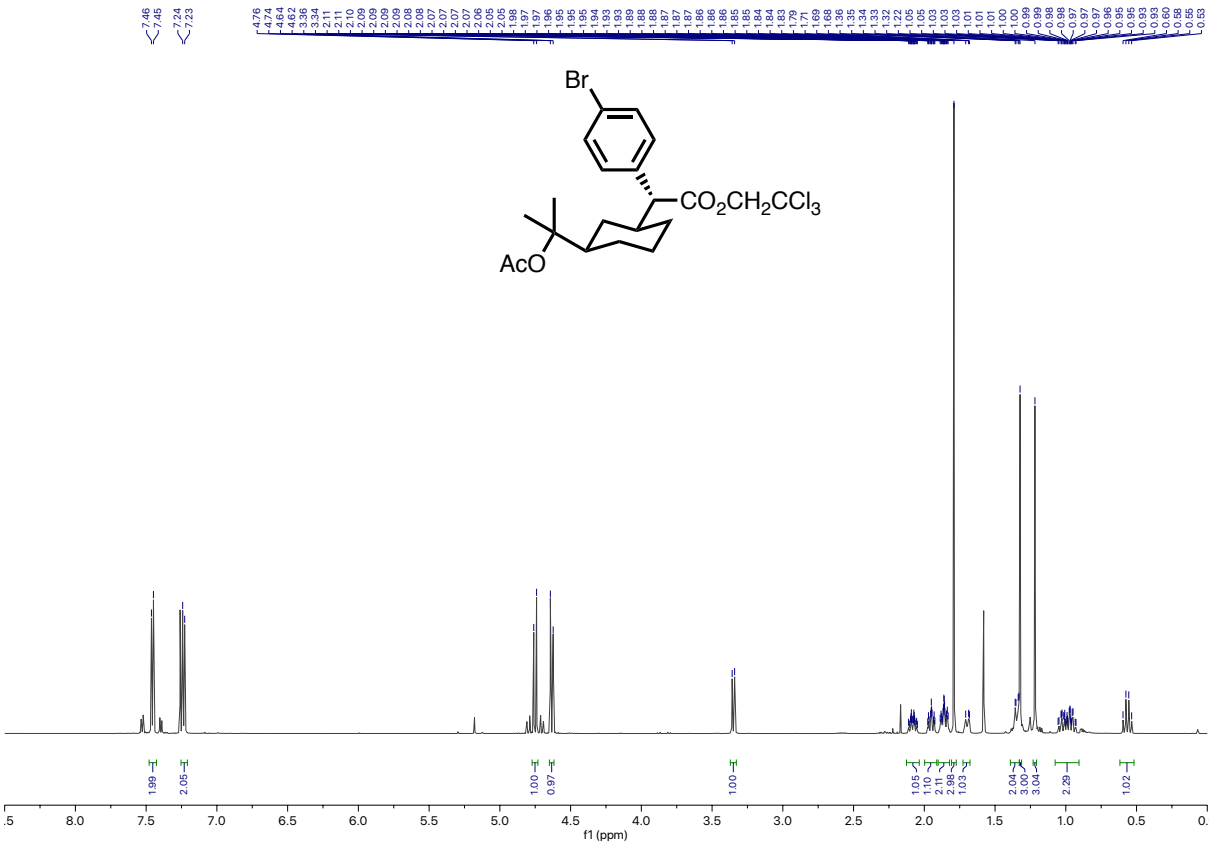
Br
CO2CH2CCl3
AcO
f1 (ppm)

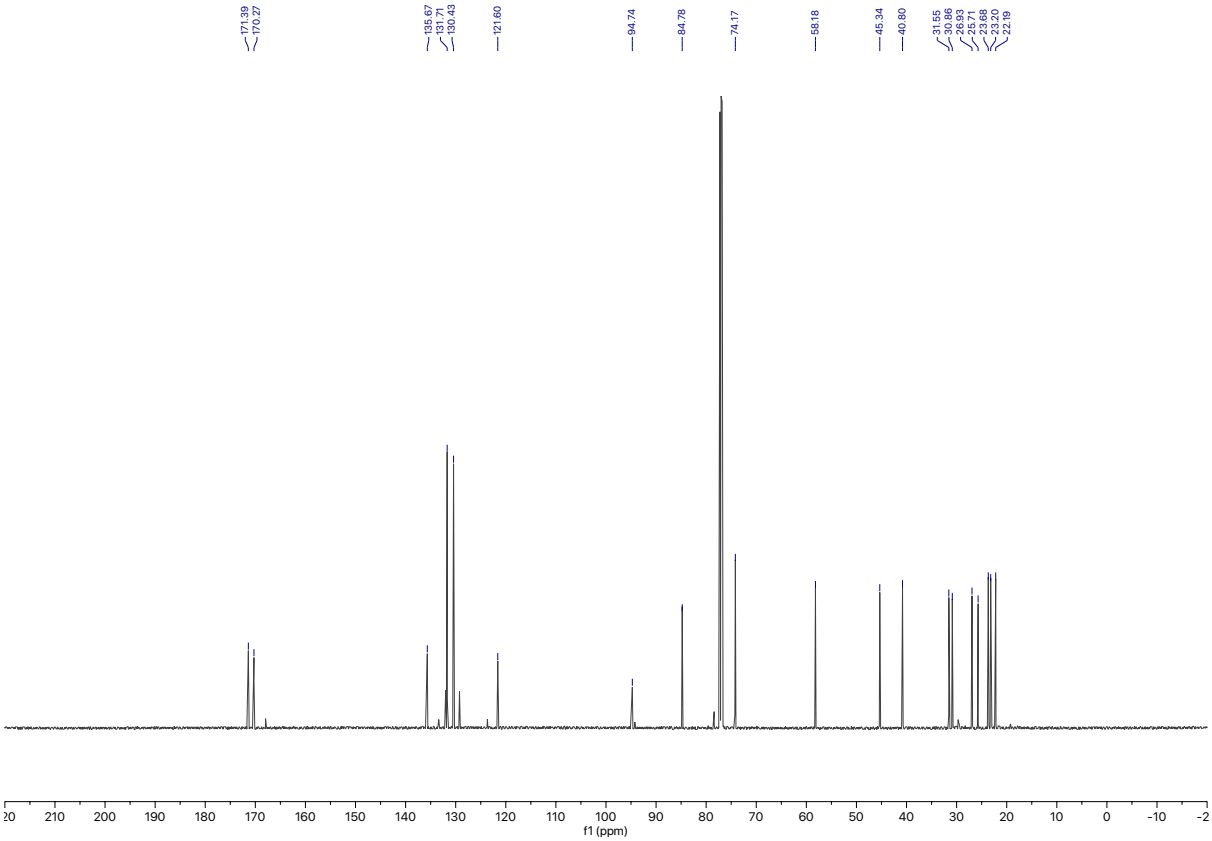
f1 (ppm)

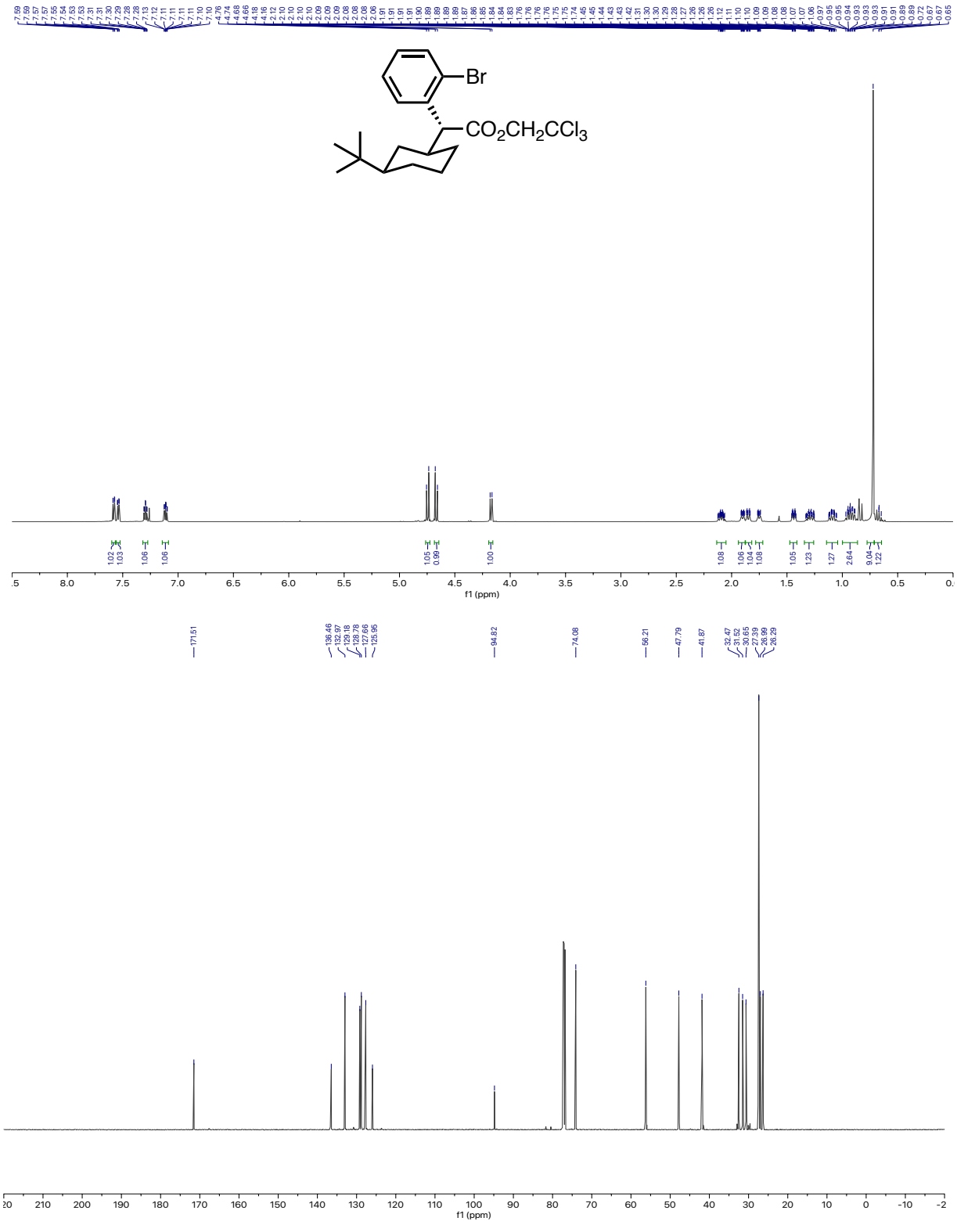
Br
CO2CH2CCl3
f1 (ppm)
f1 (ppm)

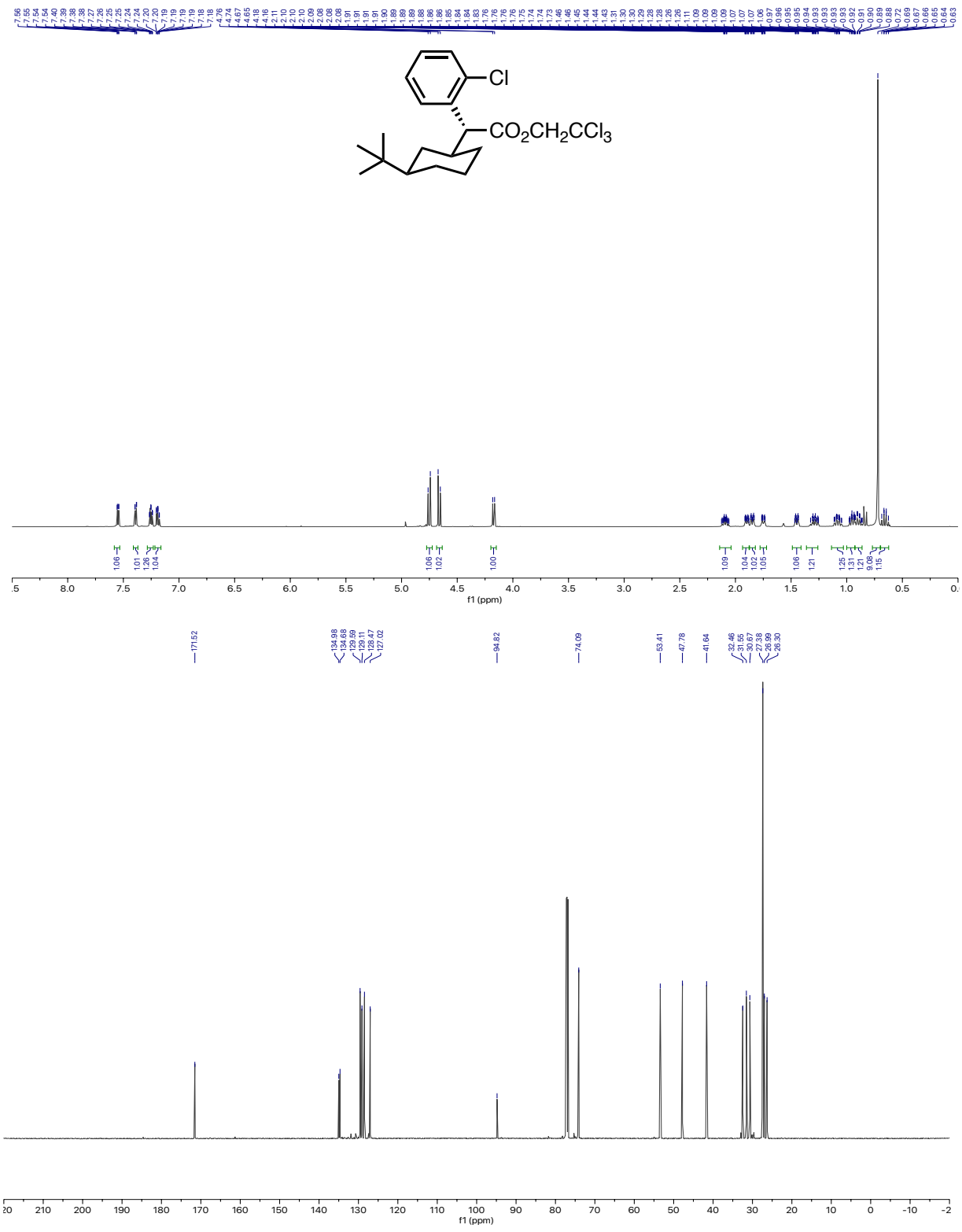
Cl
CO2CH2CCl3
f1 (ppm)
f1 (ppm)

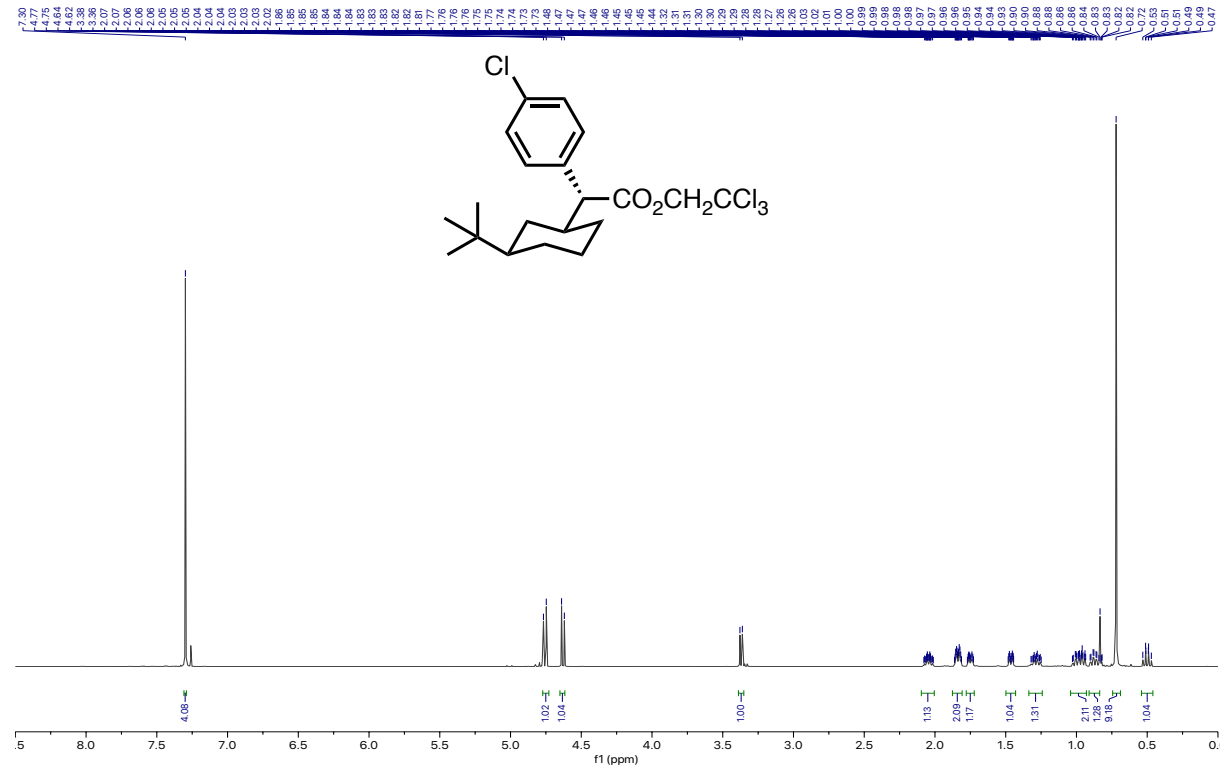
Cl
CO2CH2CCl3
f1 (ppm)

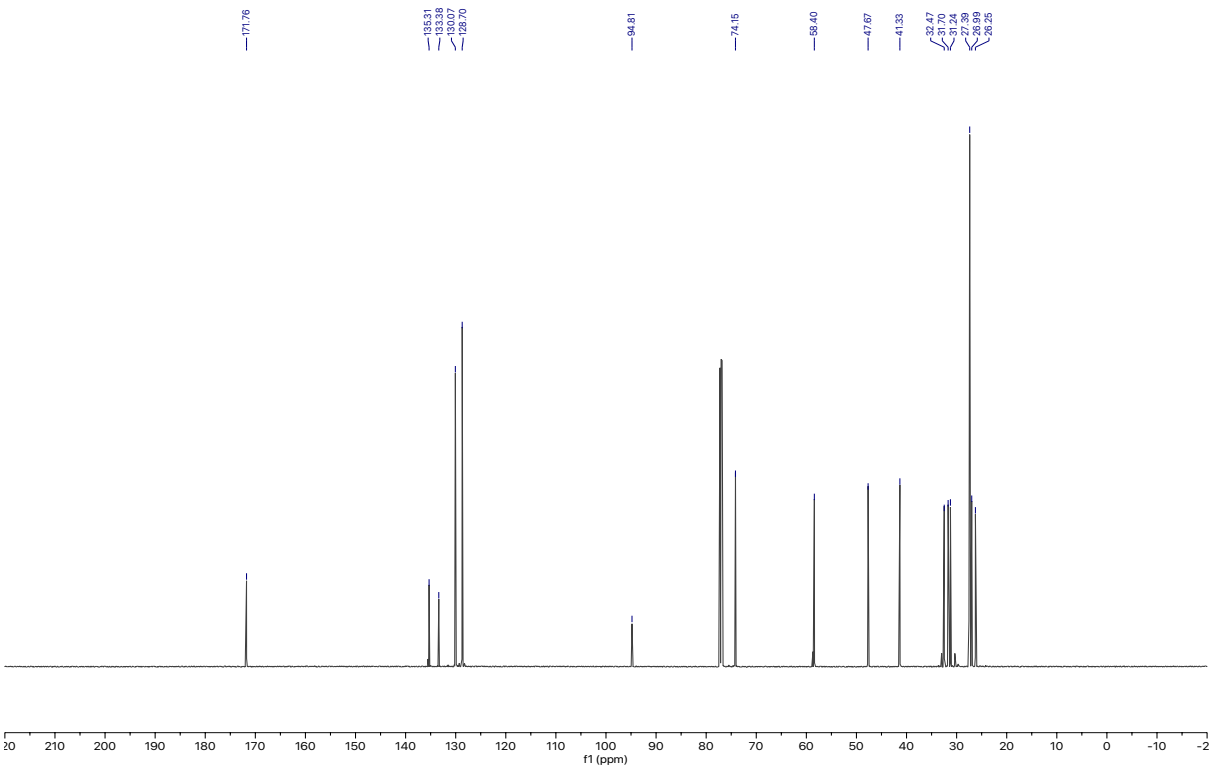
171.76
135.51
133.38
130.07
128.70
94.81
74.15
58.40
47.67
41.33
32.47
31.70
31.24
27.39
26.99
26.25
f1 (ppm)

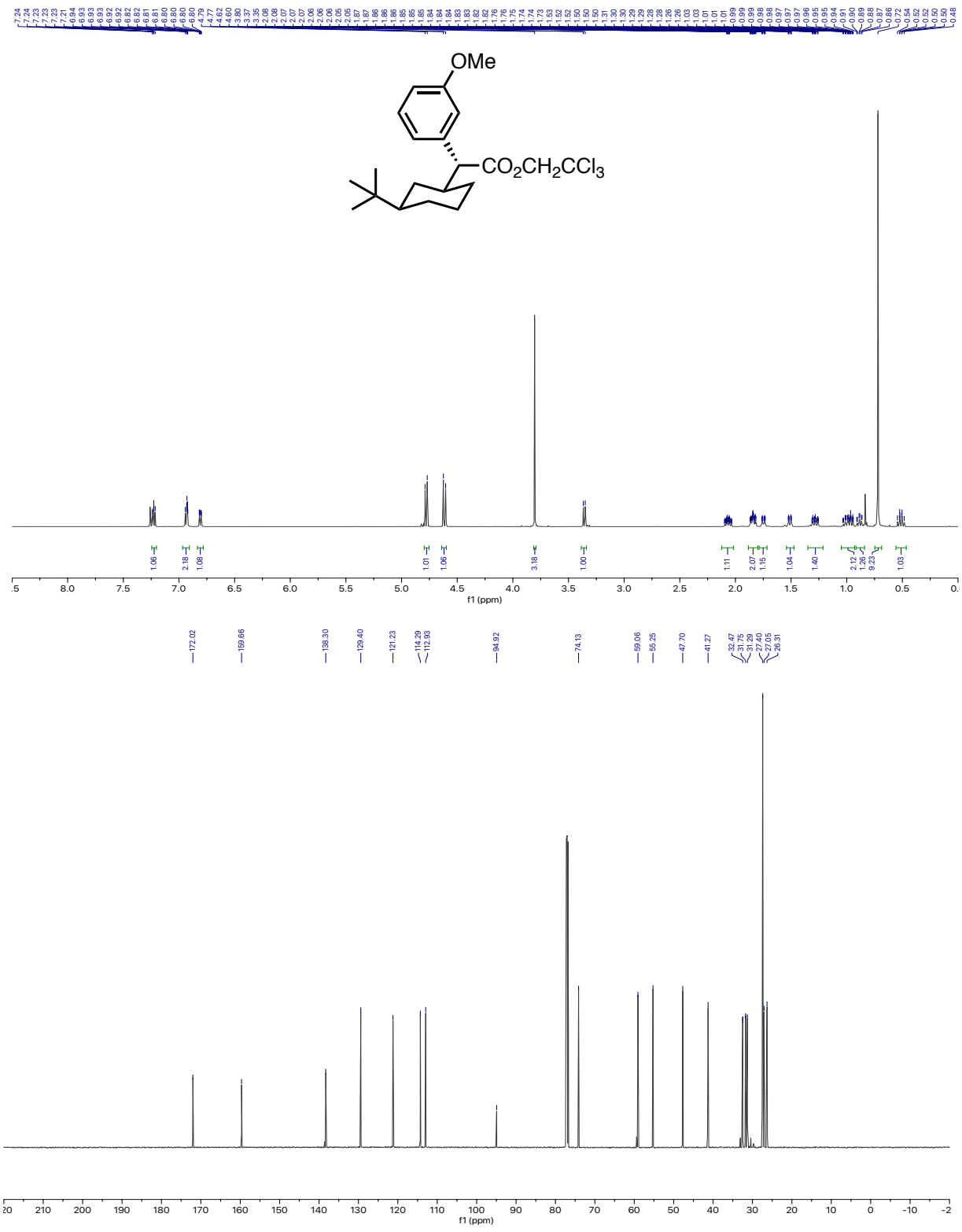
OMe
CO2CH2CCl3
f1 (ppm)
f1 (ppm)

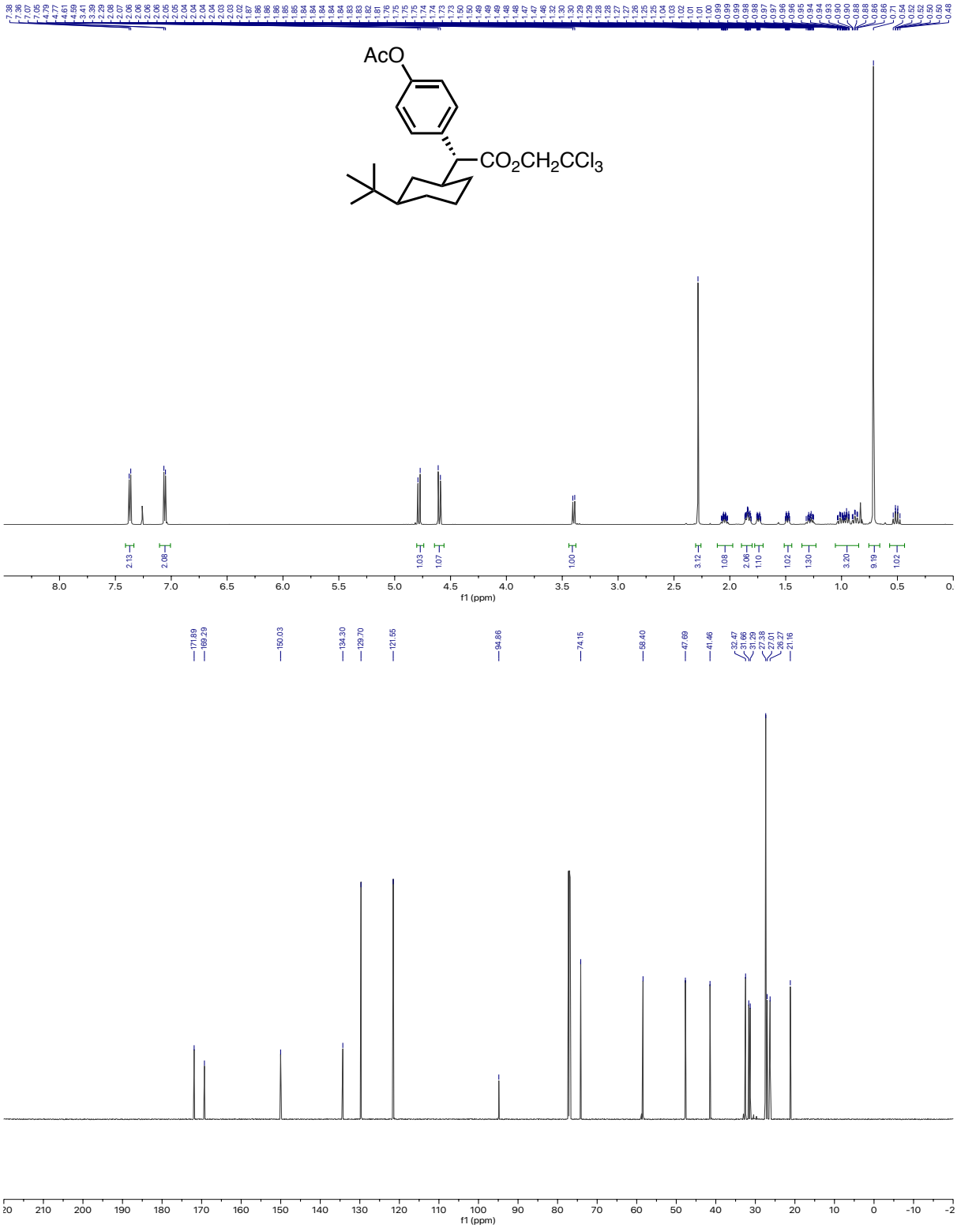
AcO
CO2CH2CCl3
f1 (ppm)
f1 (ppm)

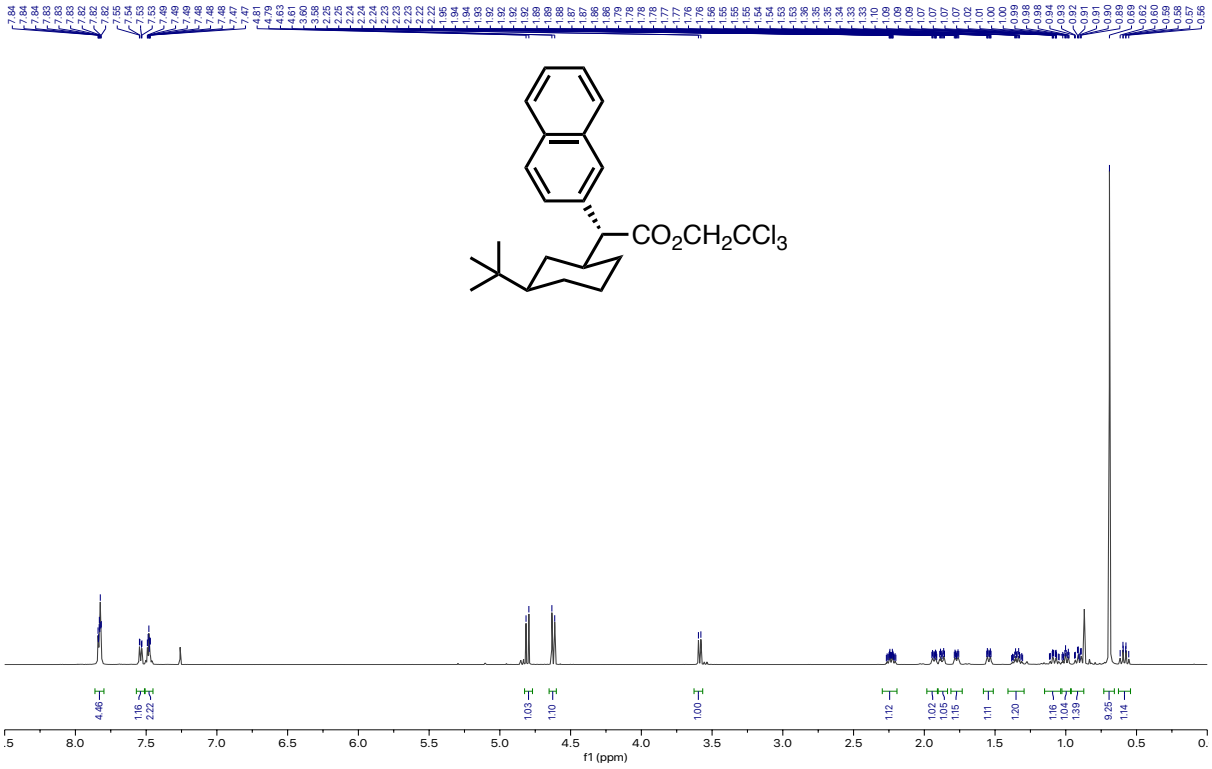
CO2CH2CCl3
f1 (ppm)

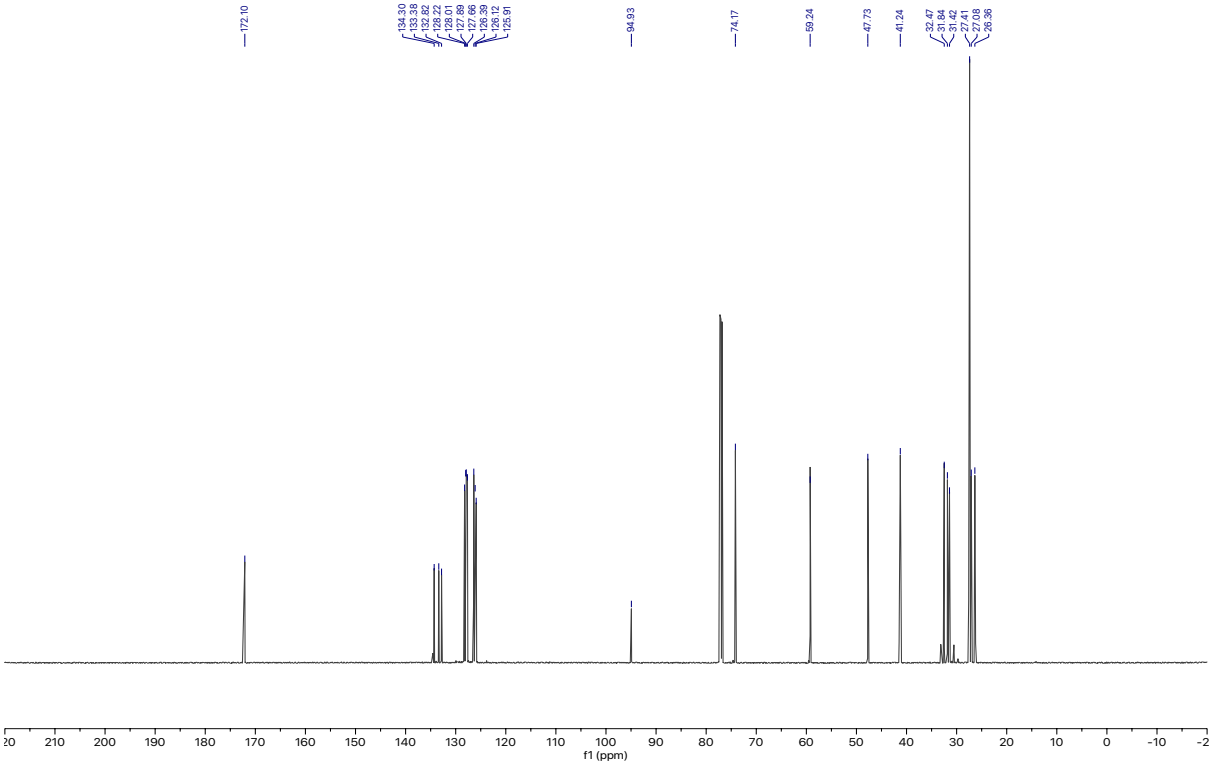
f1 (ppm)

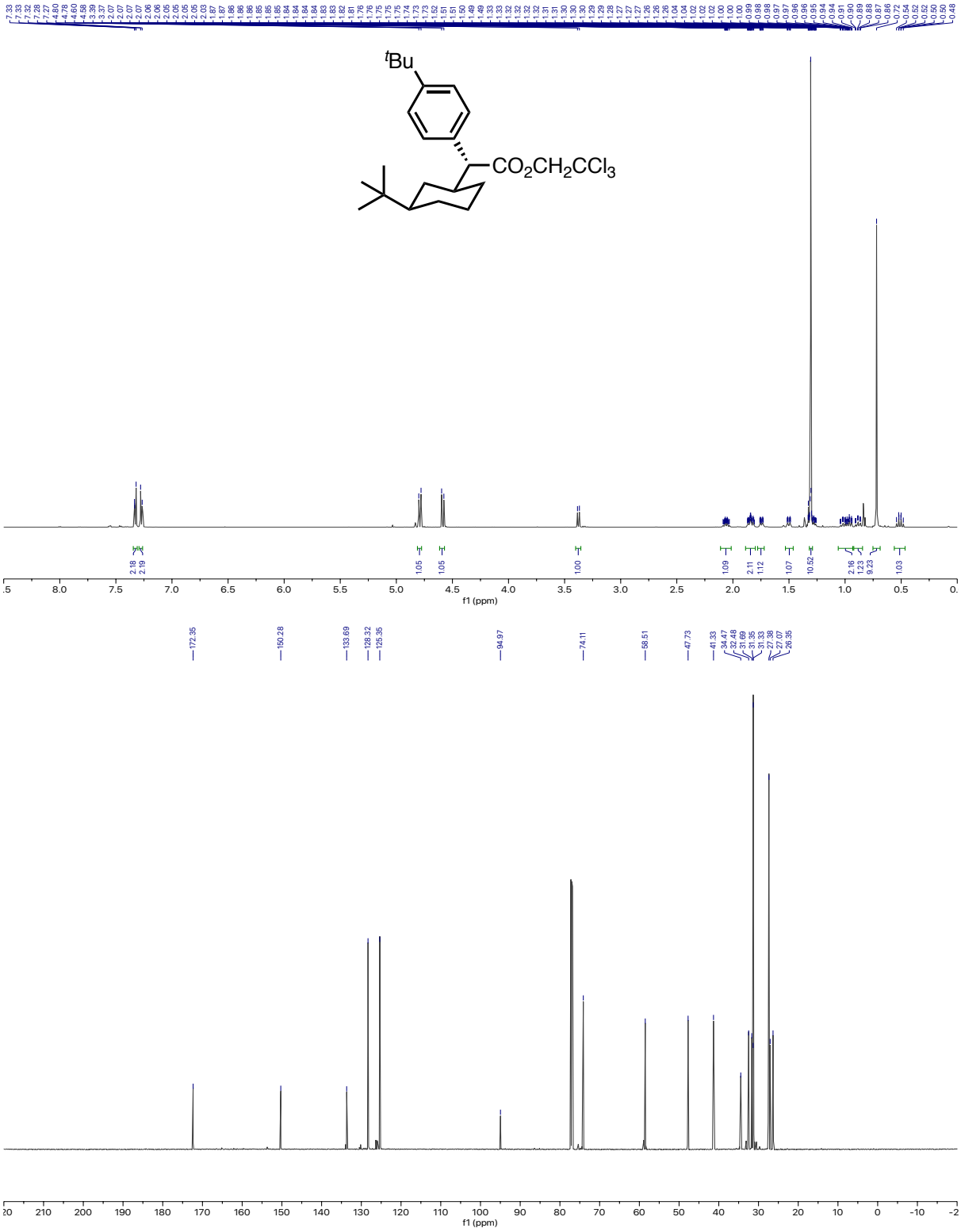
tBu
CO2CH2CCl3
f1 (ppm)
f1 (ppm)

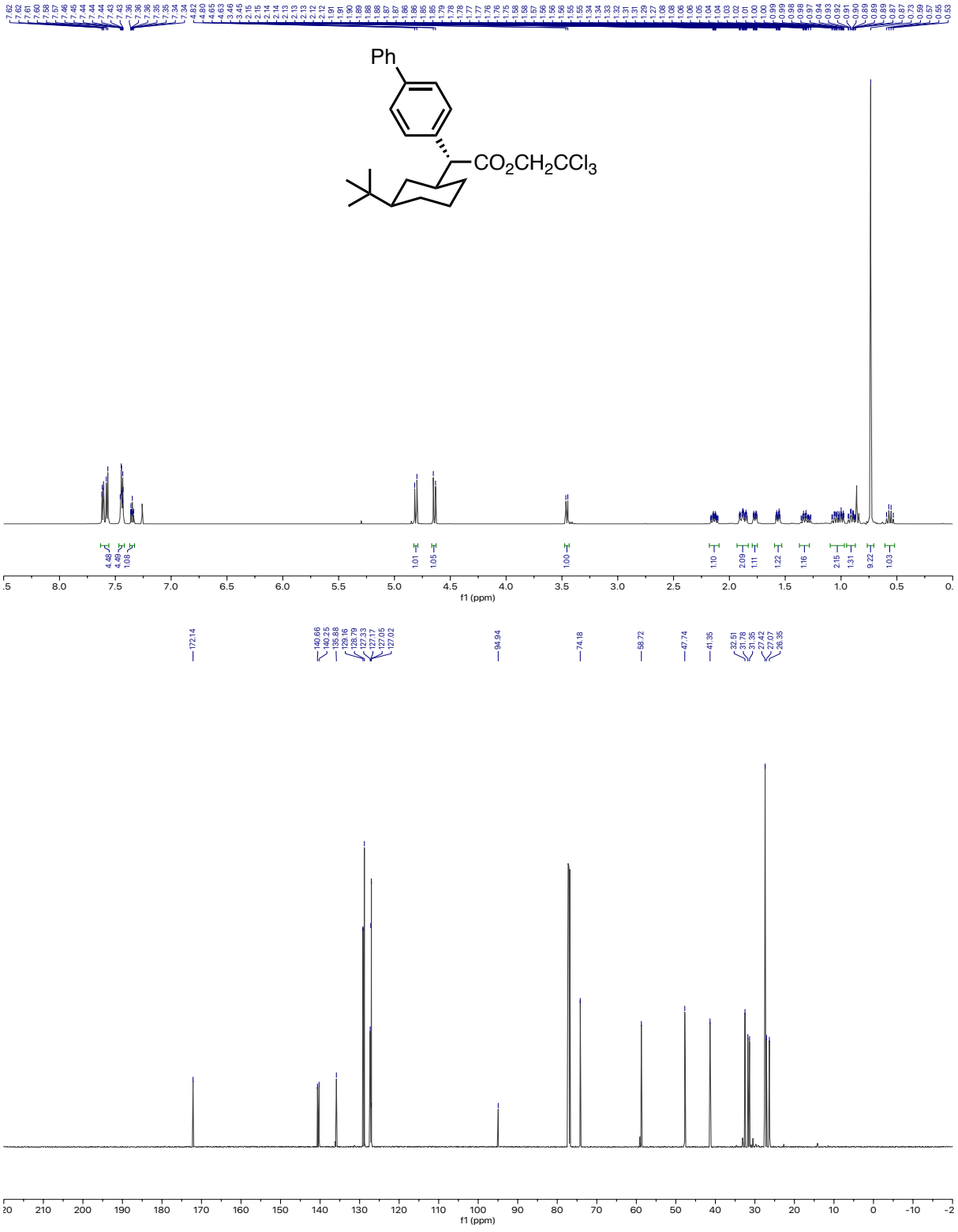
Ph
CO2CH2CCl3
f1 (ppm)
f1 (ppm)

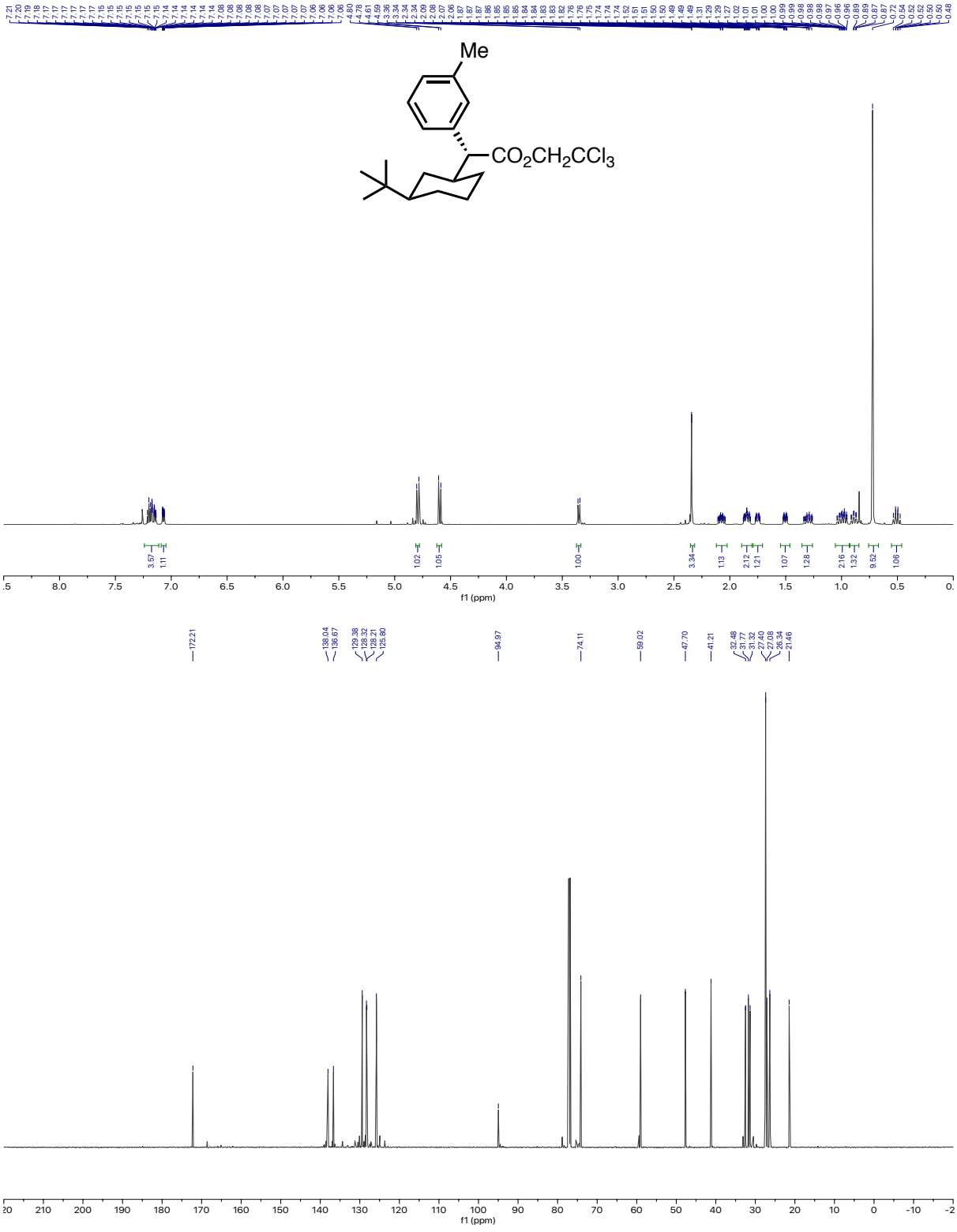
Me
CO2CH2CCl3
f1 (ppm)
f1 (ppm)

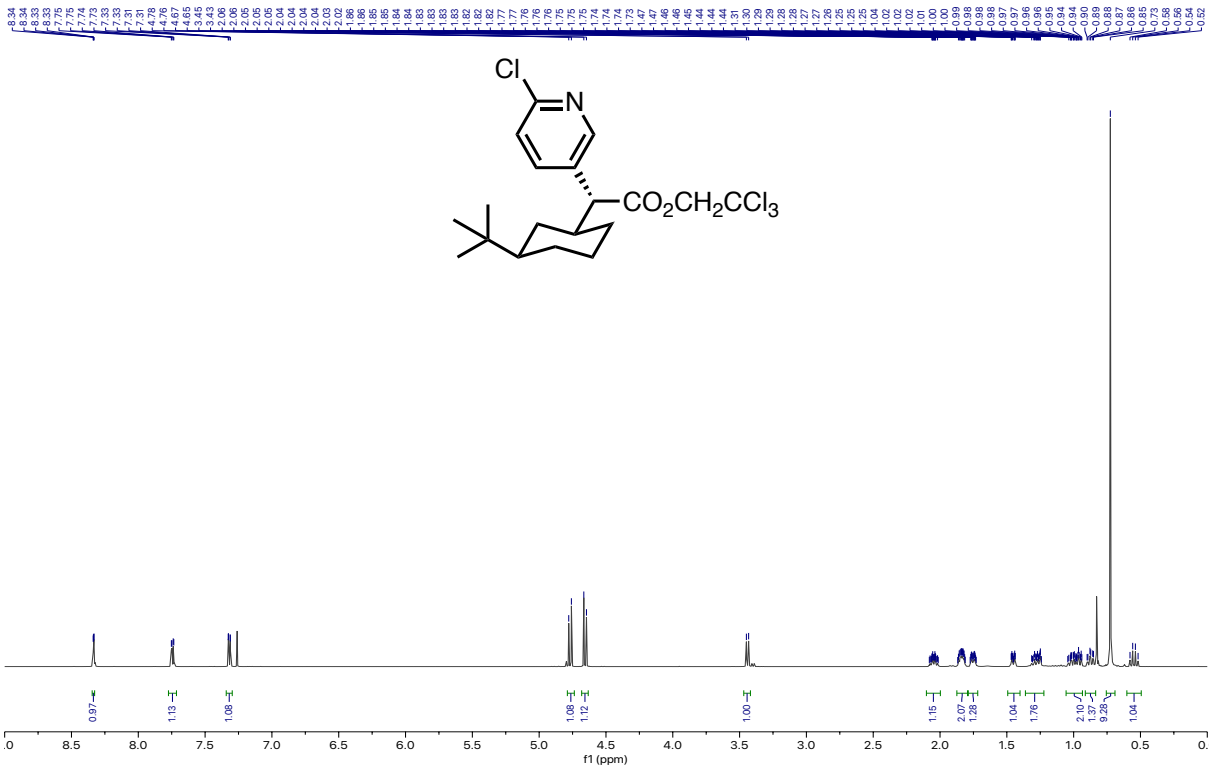
Cl
N
CO2CH2CCl3
f1 (ppm)

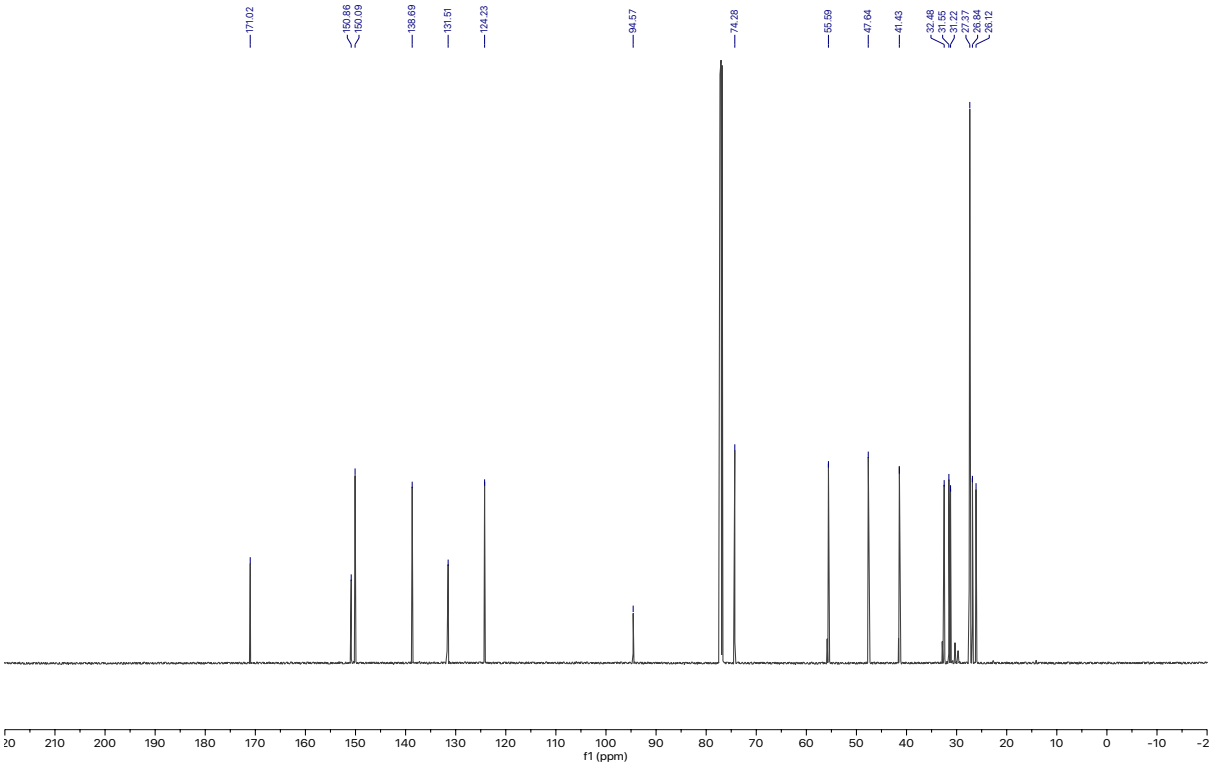
171.02
150.86
150.09
138.69
131.51
124.23
94.57
74.28
55.59
47.64
41.43
32.48
31.55
31.22
27.37
26.84
26.12
f1 (ppm)

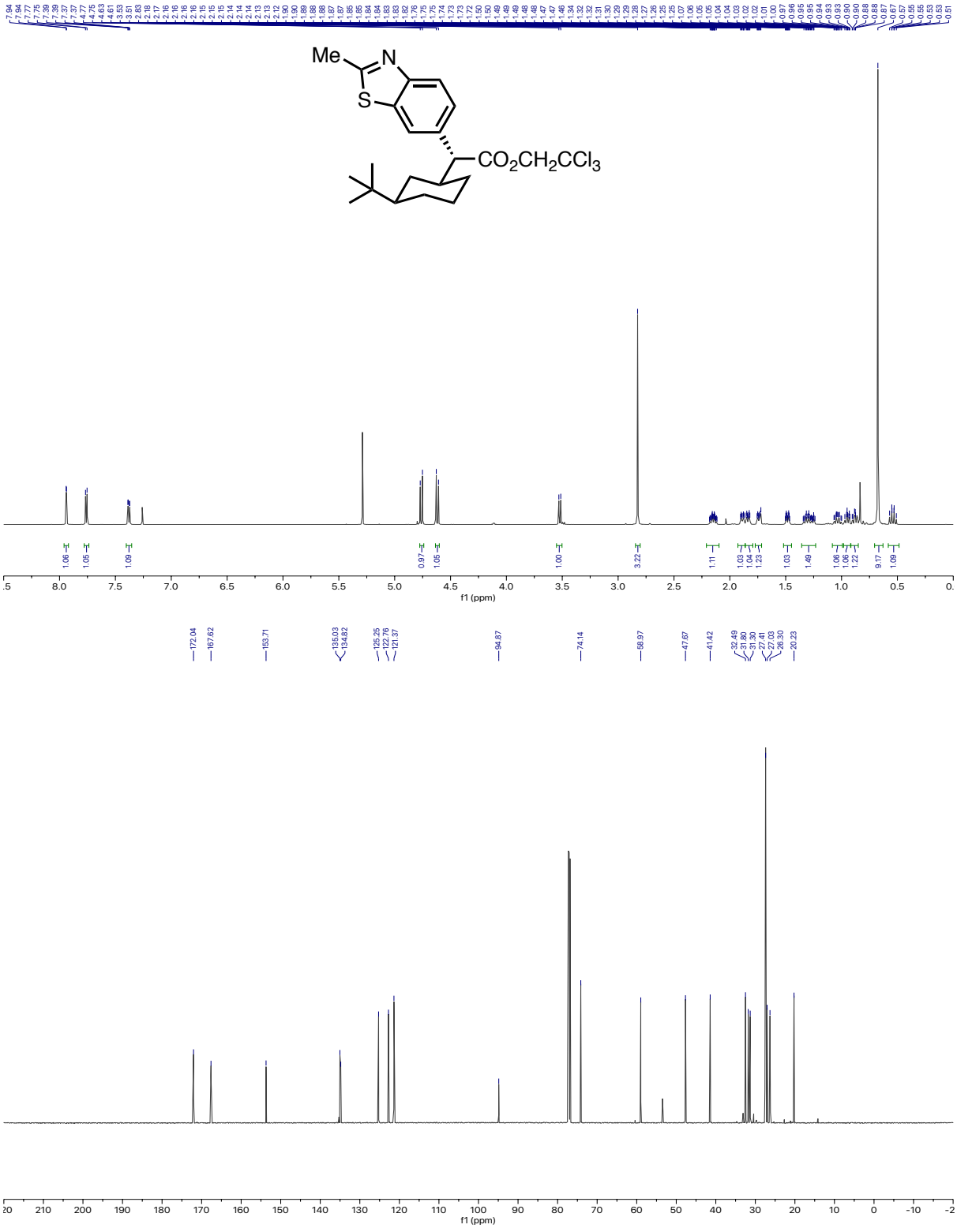
Me
N
S
CO2CH2CCl3
f1 (ppm)
f1 (ppm)

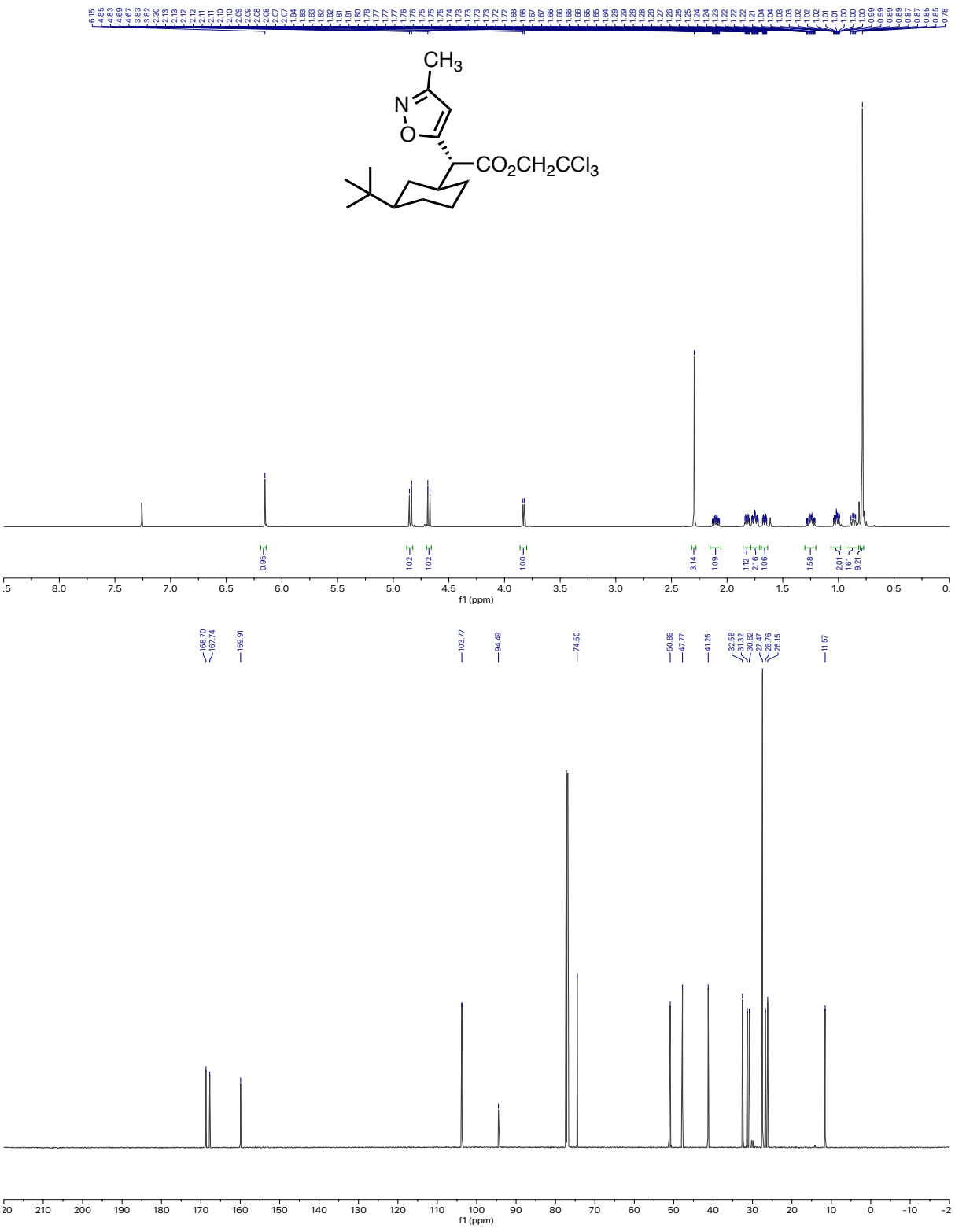
CH3
N
O
CO2CH2CCl3
f1 (ppm)
f1 (ppm)

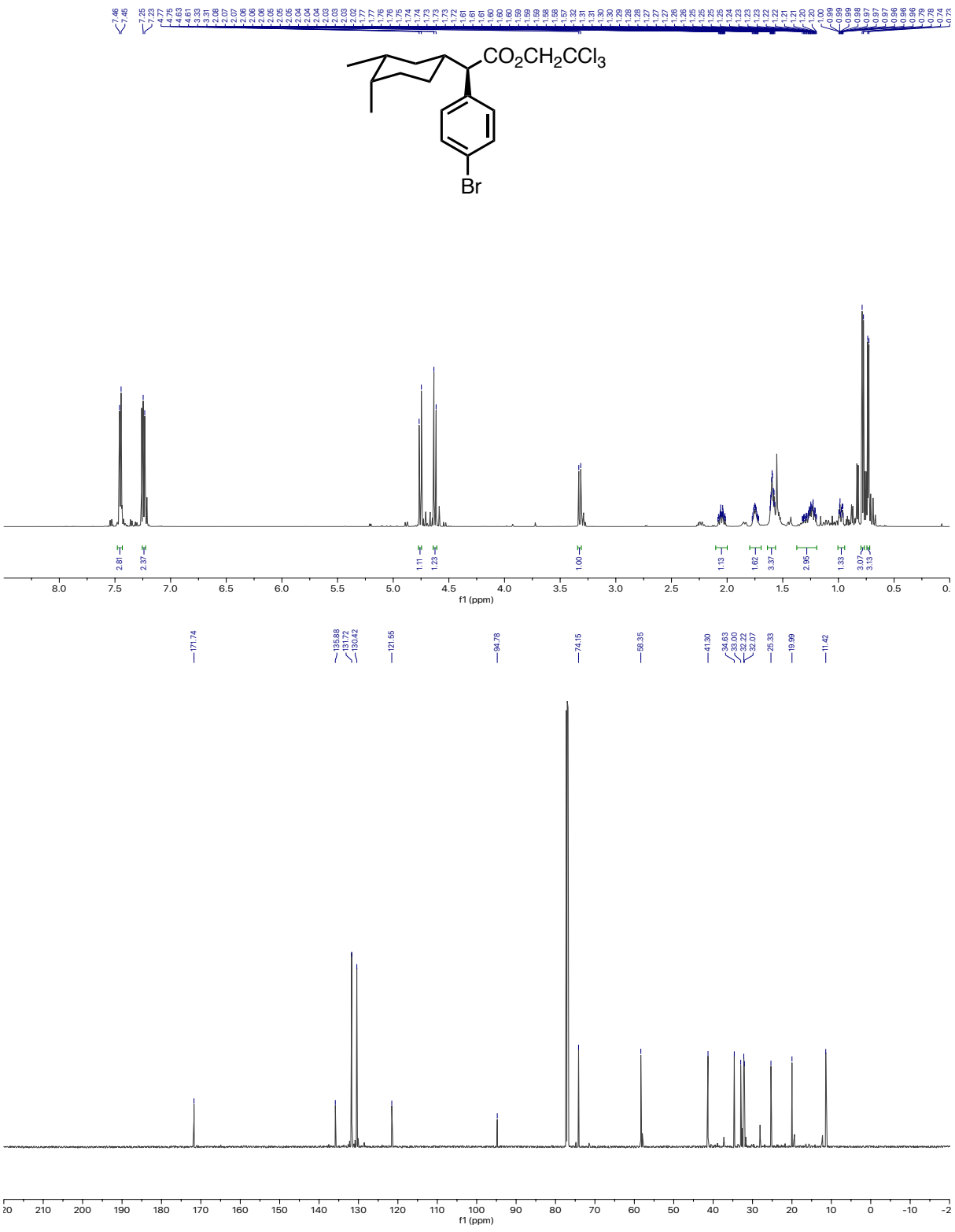
CO2CH2CCl3
Br
f1 (ppm)
f1 (ppm)

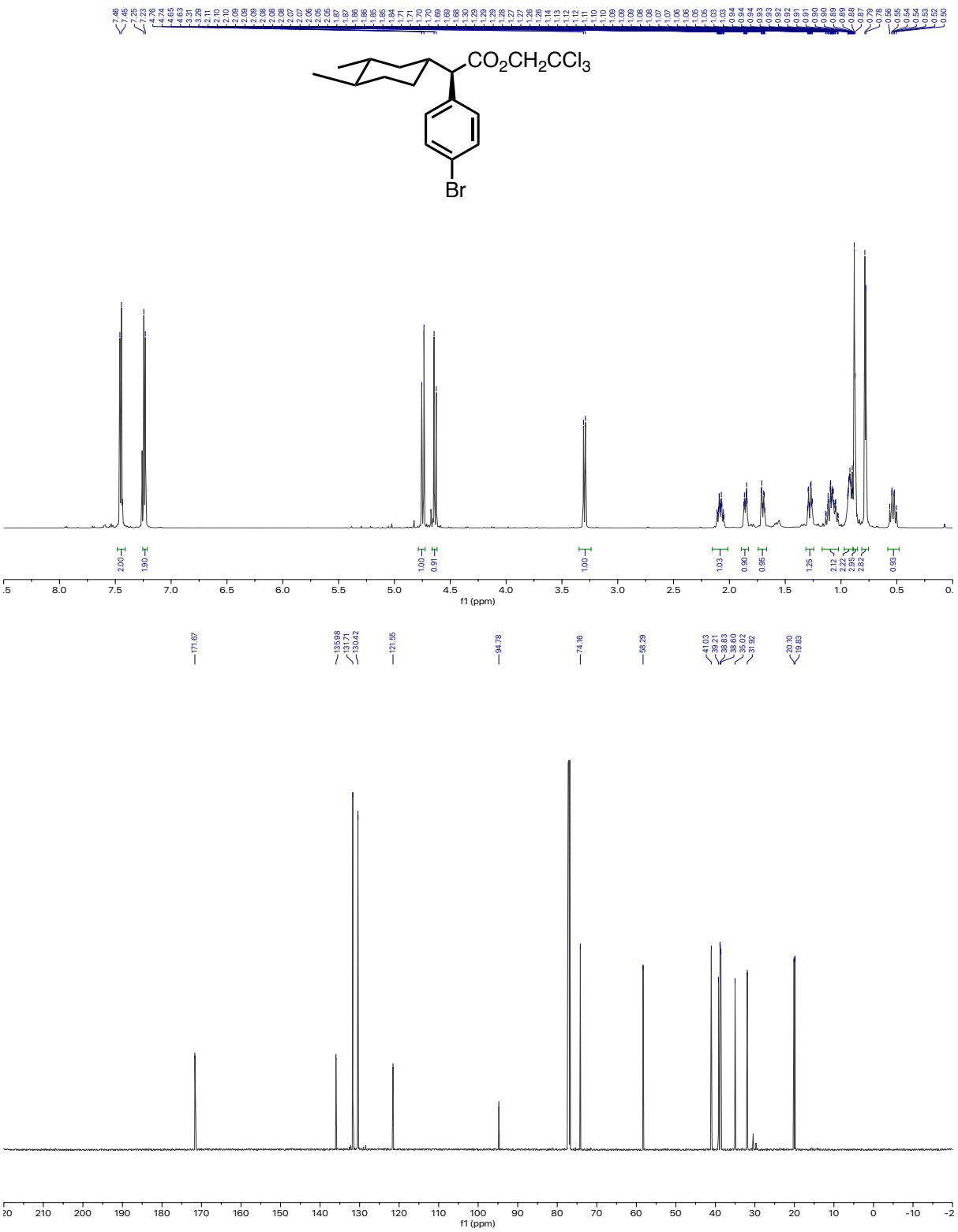
CO2CH2CCl3
Br
f1 (ppm)
f1 (ppm)

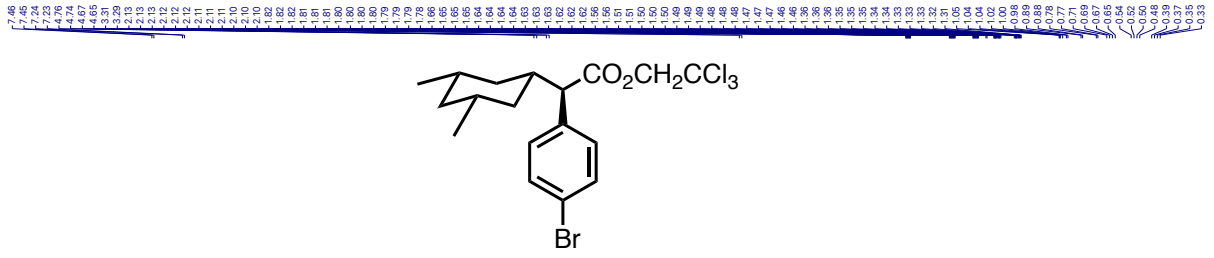

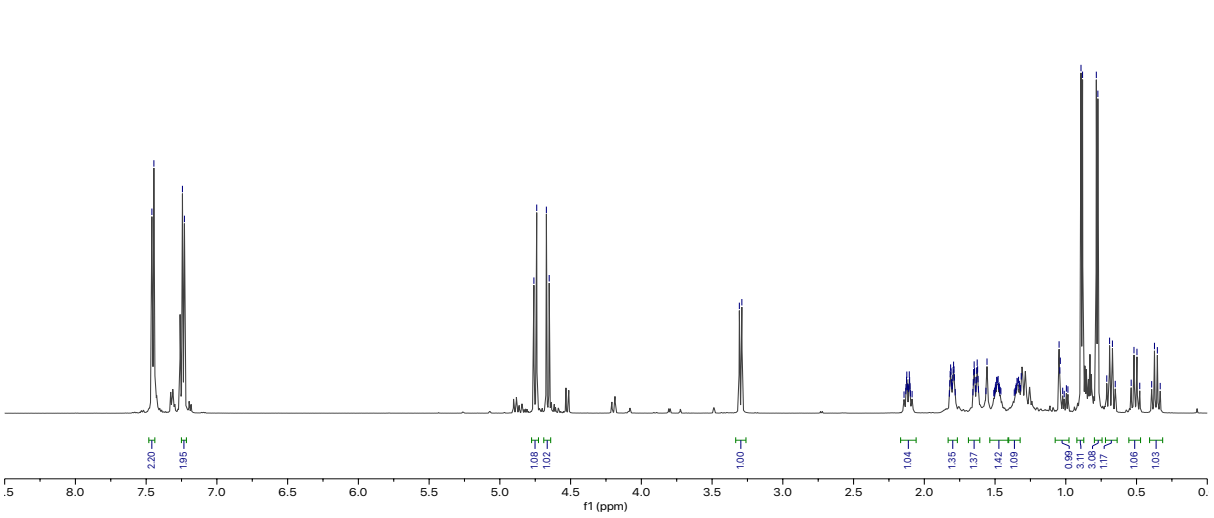
CO2CH2CCl3
Br
f1 (ppm)

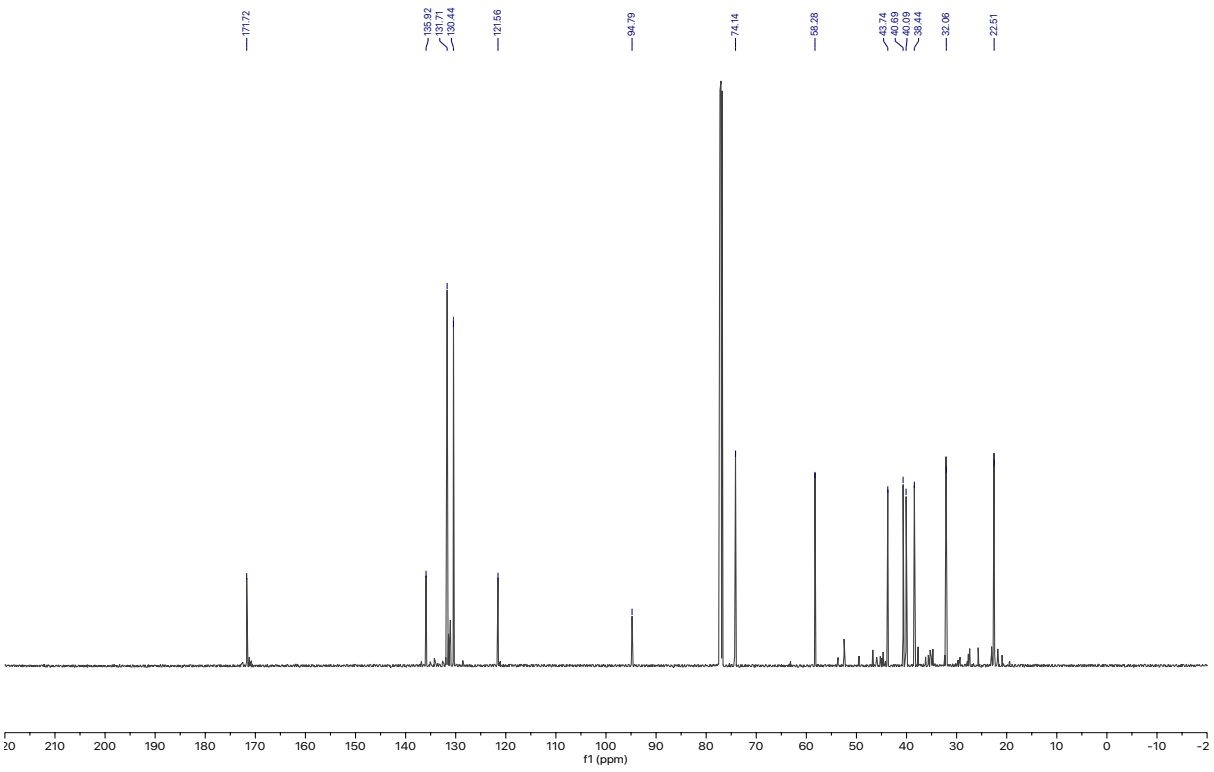
171.72
135.92
131.71
130.44
121.56
94.79
74.14
58.28
43.74
40.69
40.09
38.44
32.06
22.51
f1 (ppm)

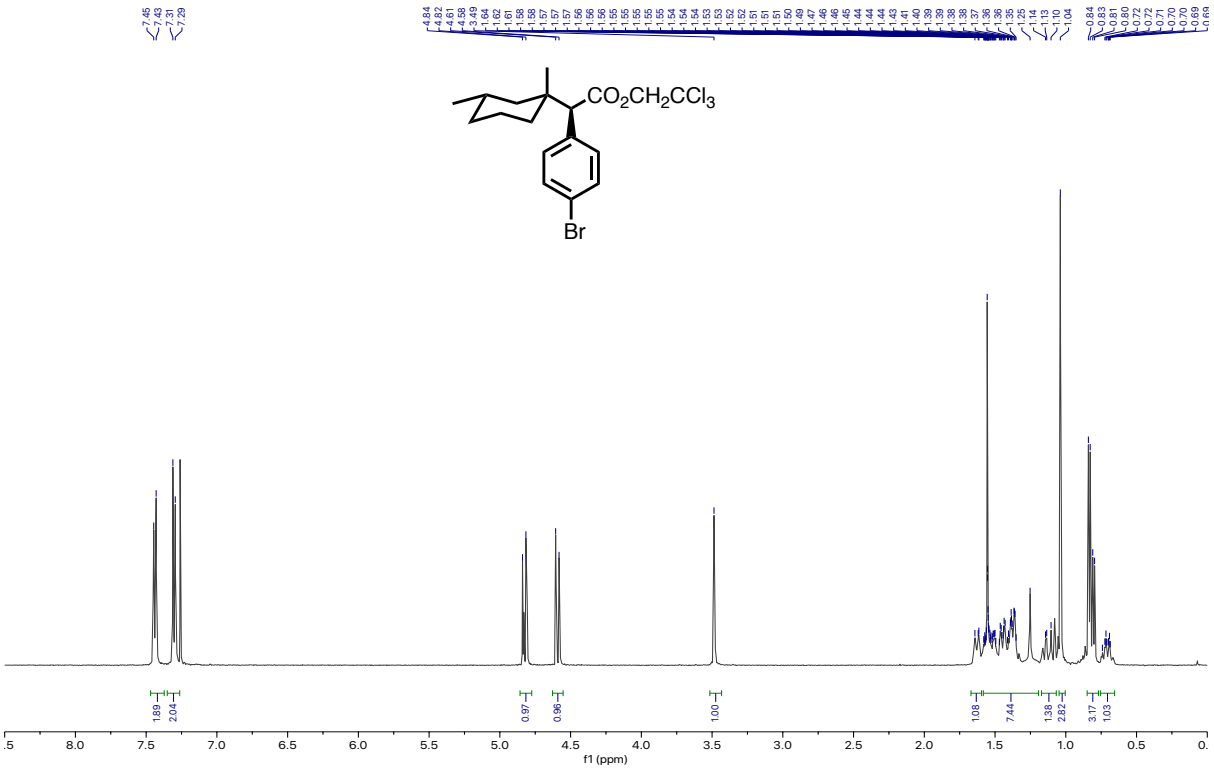
CO2CH2CCl3
Br
f1 (ppm)

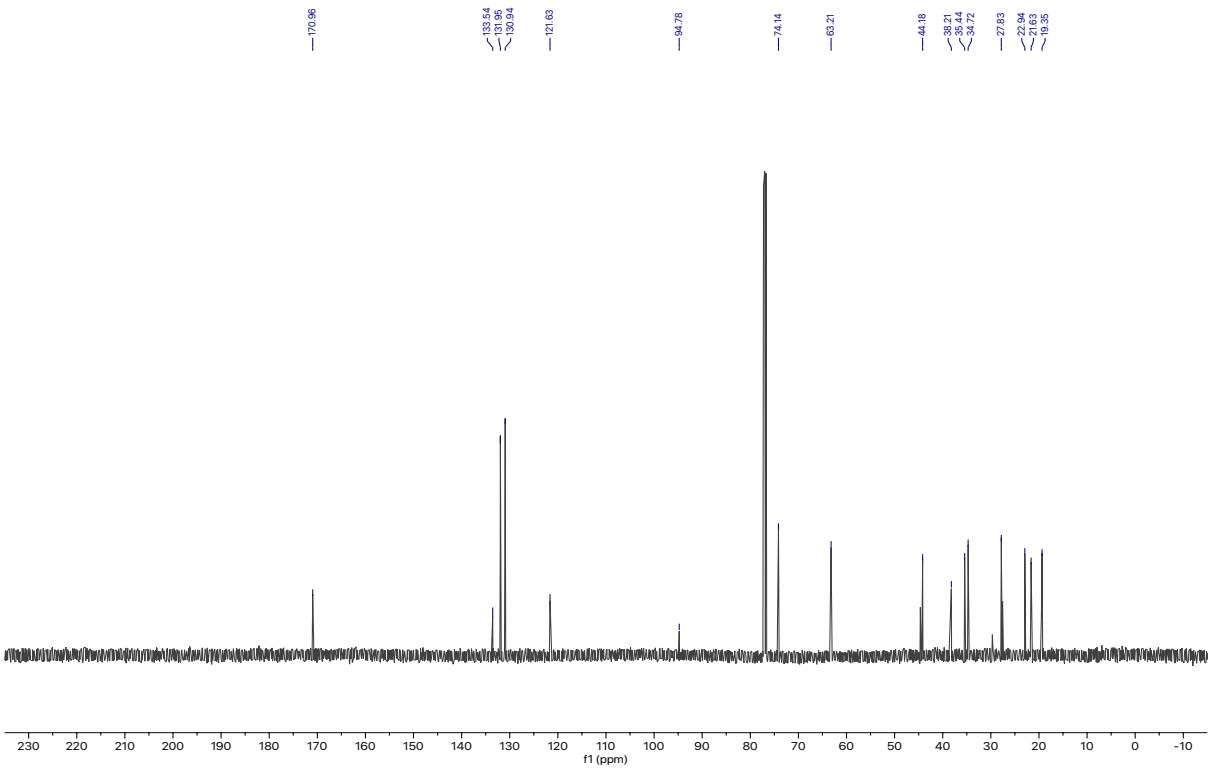
f1 (ppm)

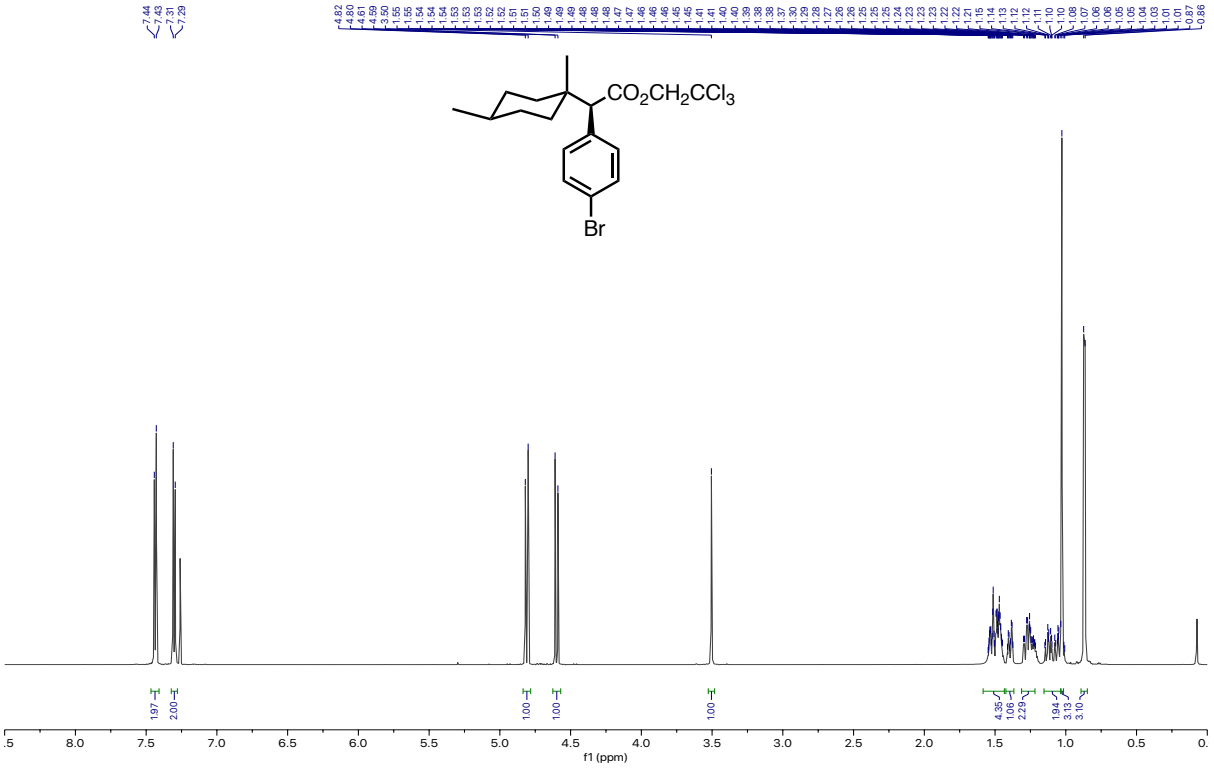
7.44
7.43
7.31
7.29
4.82
4.80
4.61
4.59
3.60
3.55
1.55
1.54
1.54
1.54
1.53
1.53
1.53
1.52
1.52
1.51
1.51
1.50
1.50
1.49
1.49
1.49
1.48
1.48
1.48
1.47
1.47
1.46
1.46
1.46
1.45
1.45
1.41
1.41
1.40
1.40
1.39
1.38
1.38
1.37
1.30
1.29
1.28
1.27
1.26
1.26
1.25
1.25
1.25
1.24
1.24
1.23
1.23
1.22
1.22
1.21
1.15
1.14
1.13
1.12
1.12
1.11
1.10
1.10
1.08
1.07
1.06
1.06
1.05
1.05
1.04
1.03
1.01
1.01
0.87
0.86
CO2CH2CCl3
Br
1.97
2.00
1.00
1.00
1.00
4.35
1.06
2.29
1.94
3.13
3.10
f1 (ppm)

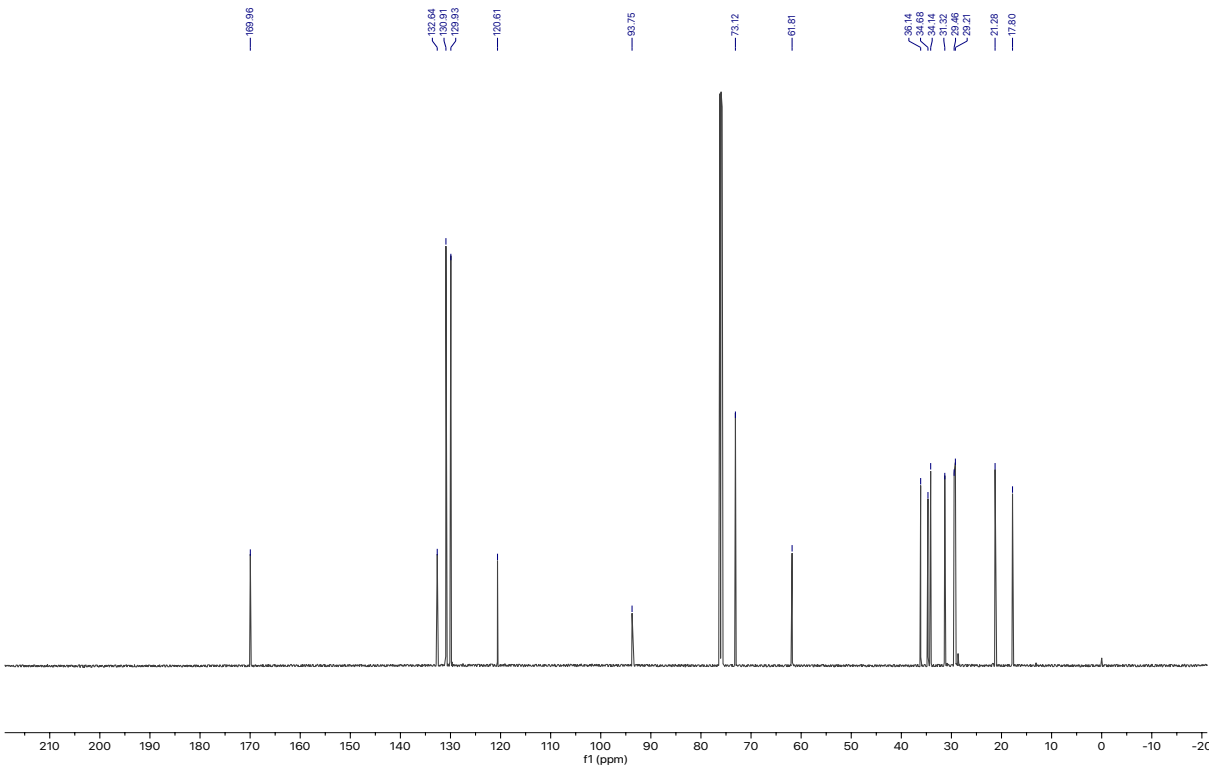
169.96
132.64
130.91
129.93
120.61
93.75
73.12
61.81
36.14
34.68
34.14
31.32
29.46
29.21
21.28
17.80
f1 (ppm)

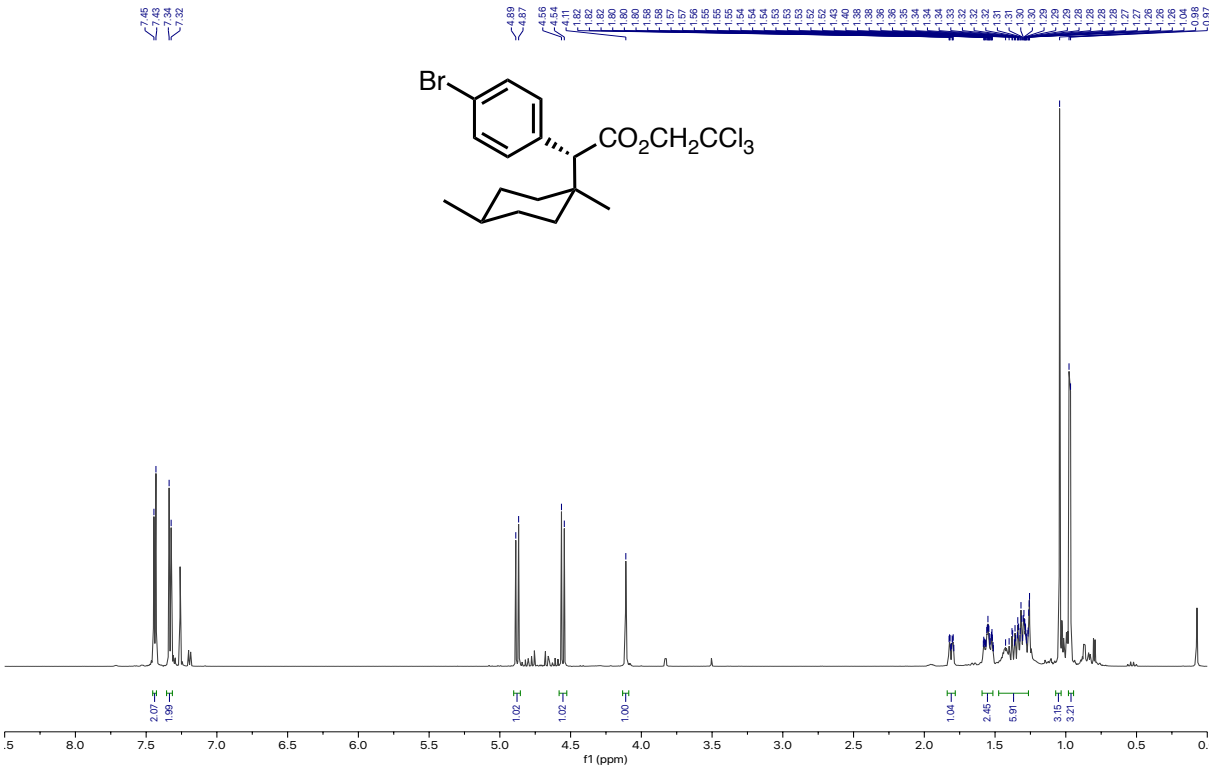
Br
CO2CH2CCl3
f1 (ppm)

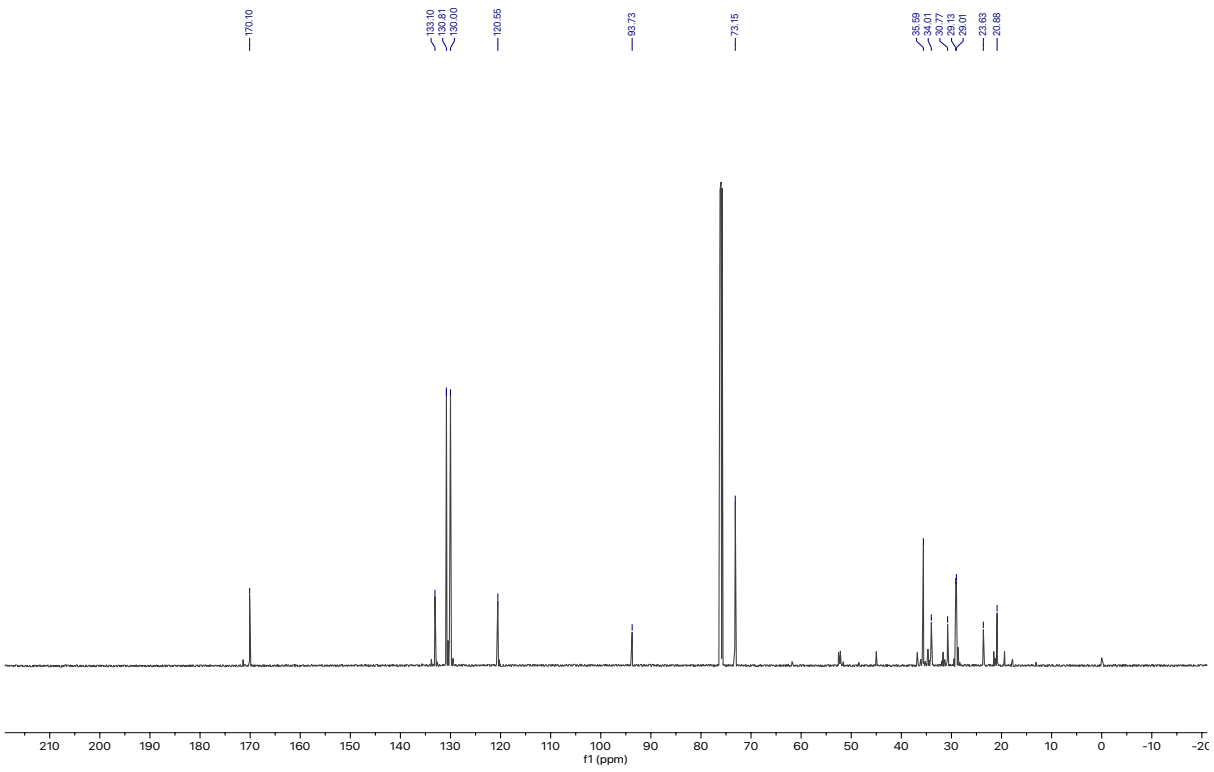
f1 (ppm)

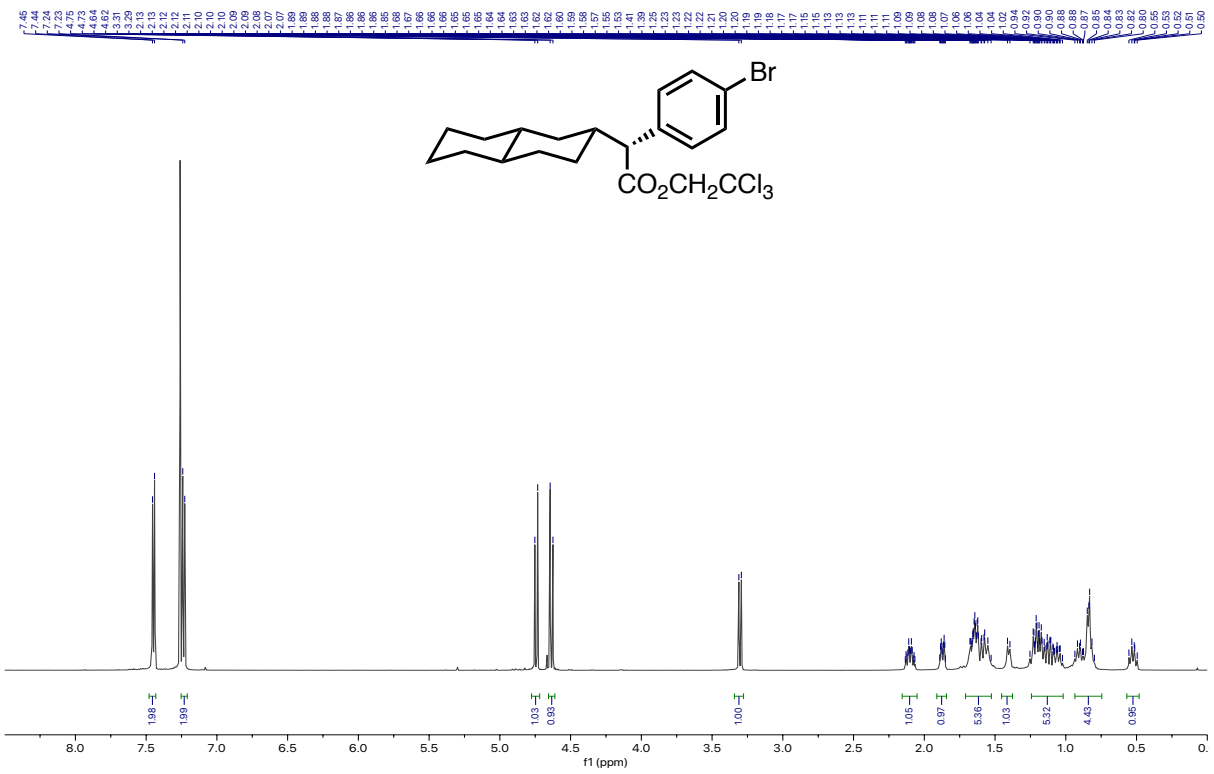
Br
CO2CH2CCl3
f1 (ppm)

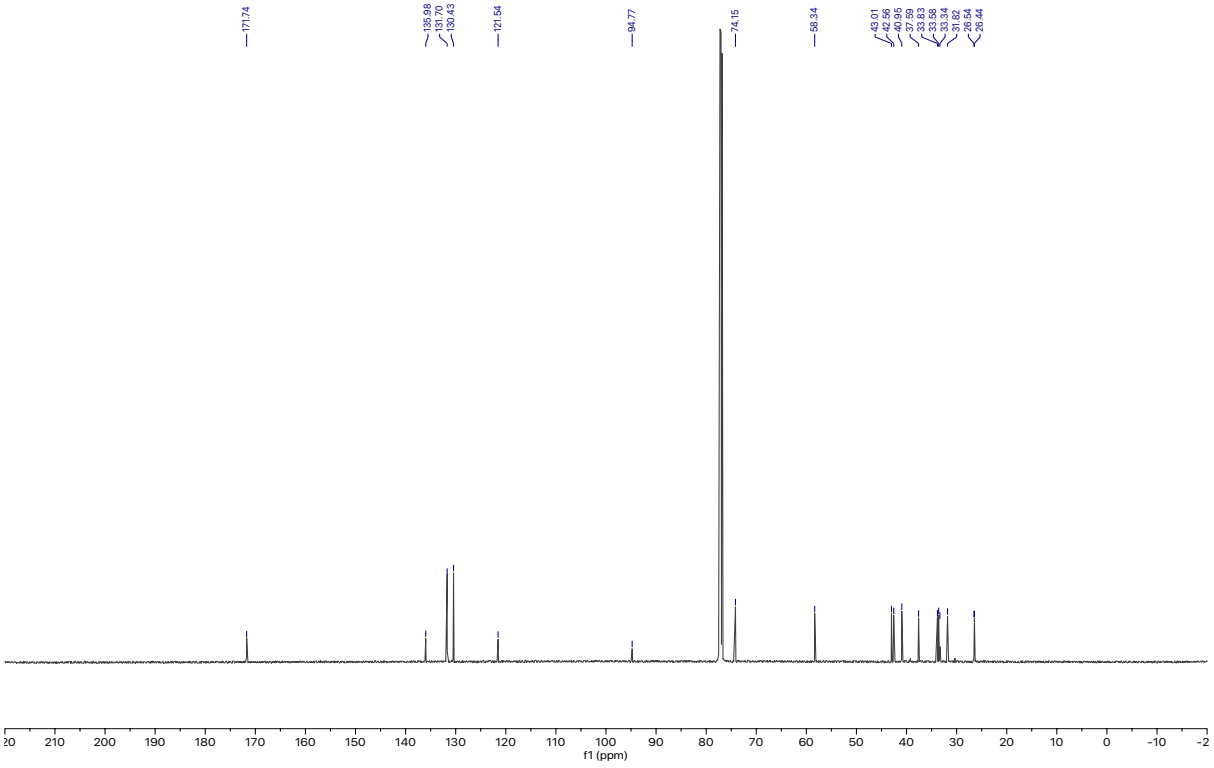
171.74
135.98
133.70
130.43
121.54
94.77
74.15
58.34
43.01
42.56
40.95
37.59
33.83
33.58
33.34
31.82
26.54
26.44
f1 (ppm)

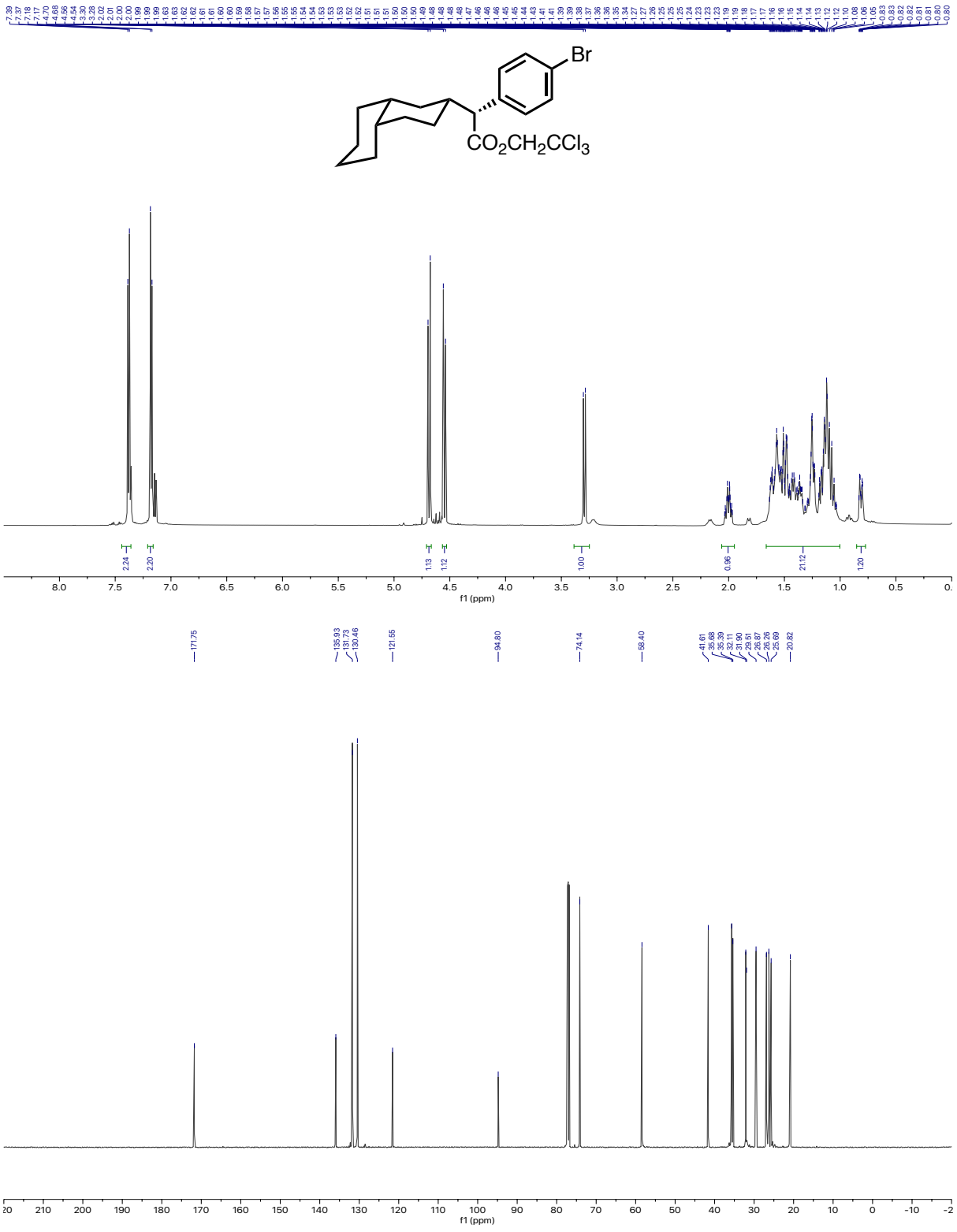
Br
CO2CH2CCl3
f1 (ppm)
f1 (ppm)

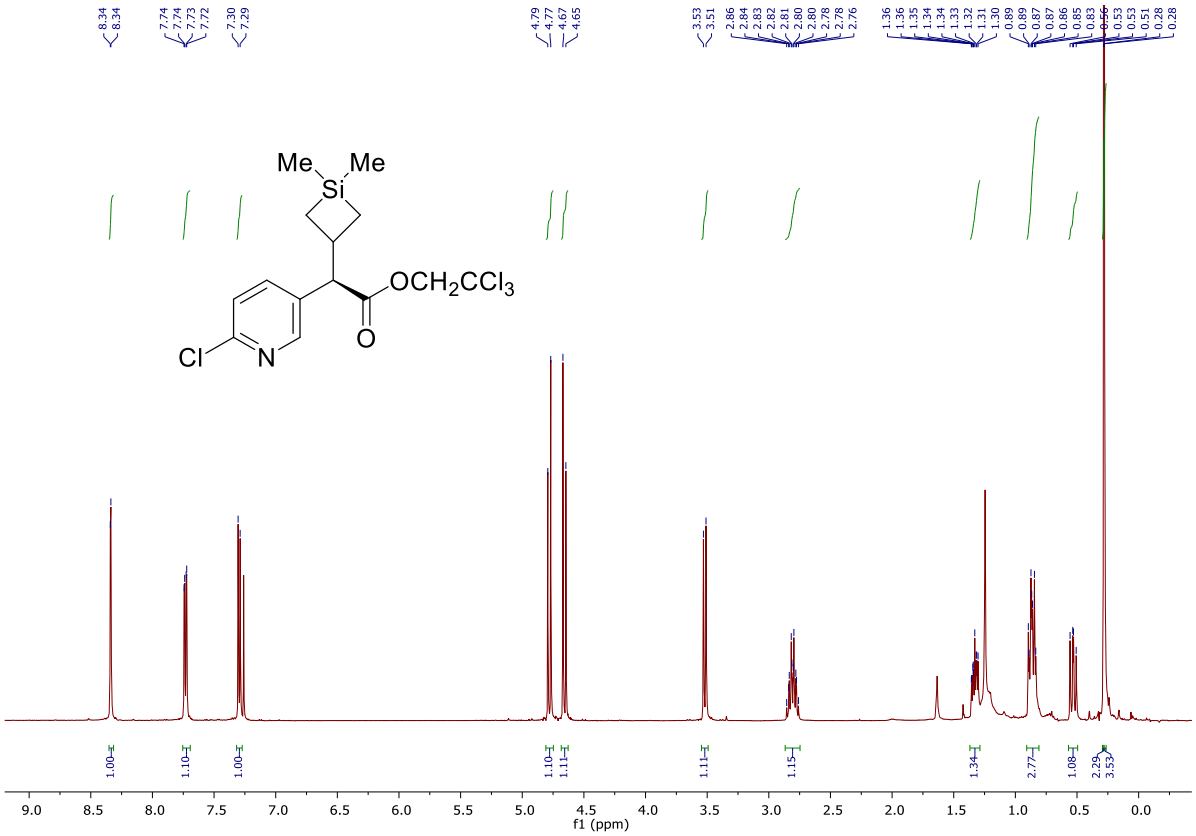
8.34
8.34
7.74
7.74
7.73
7.72
7.30
7.29
4.79
4.77
4.67
4.65
3.53
3.51
2.86
2.84
2.83
2.82
2.81
2.80
2.80
2.78
2.78
2.76
1.36
1.36
1.35
1.34
1.34
1.33
1.32
1.31
1.30
0.89
0.89
0.87
0.87
0.86
0.85
0.83
0.56
0.53
0.53
0.51
0.28
0.28
Me
Si
Me
OCH2CCl3
O
Cl
N
1.00
1.10
1.00
1.10
1.11
1.11
1.15
1.34
2.77
1.08
2.29
3.53
9.0
8.5
8.0
7.5
7.0
6.5
6.0
5.5
5.0
4.5
4.0
3.5
3.0
2.5
2.0
1.5
1.0
0.5
0.0
f1 (ppm)

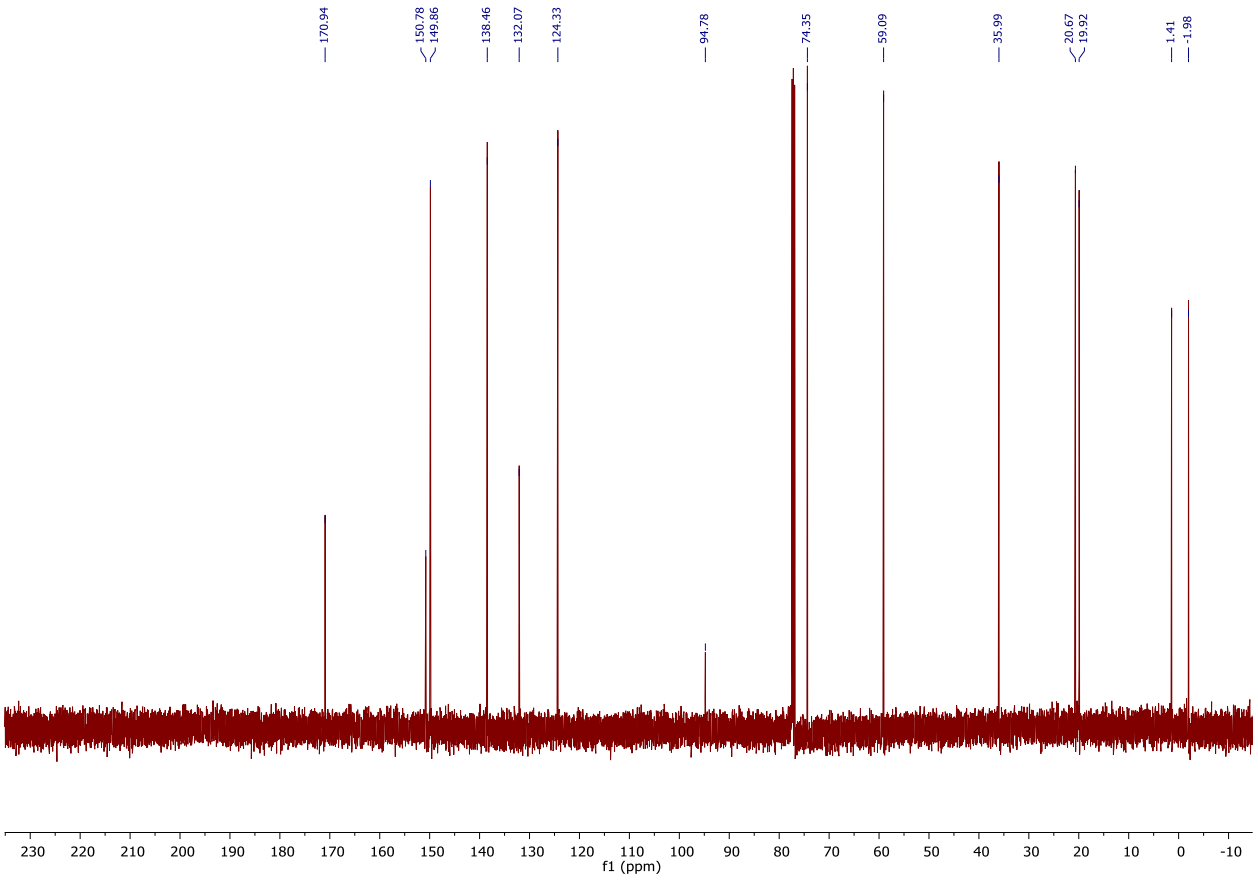
170.94
150.78
149.86
138.46
132.07
124.33
94.78
74.35
59.09
35.99
20.67
19.92
1.41
-1.98
230
220
210
200
190
180
170
160
150
140
130
120
110
100
90
80
70
60
50
40
30
20
10
0
-10
f1 (ppm)

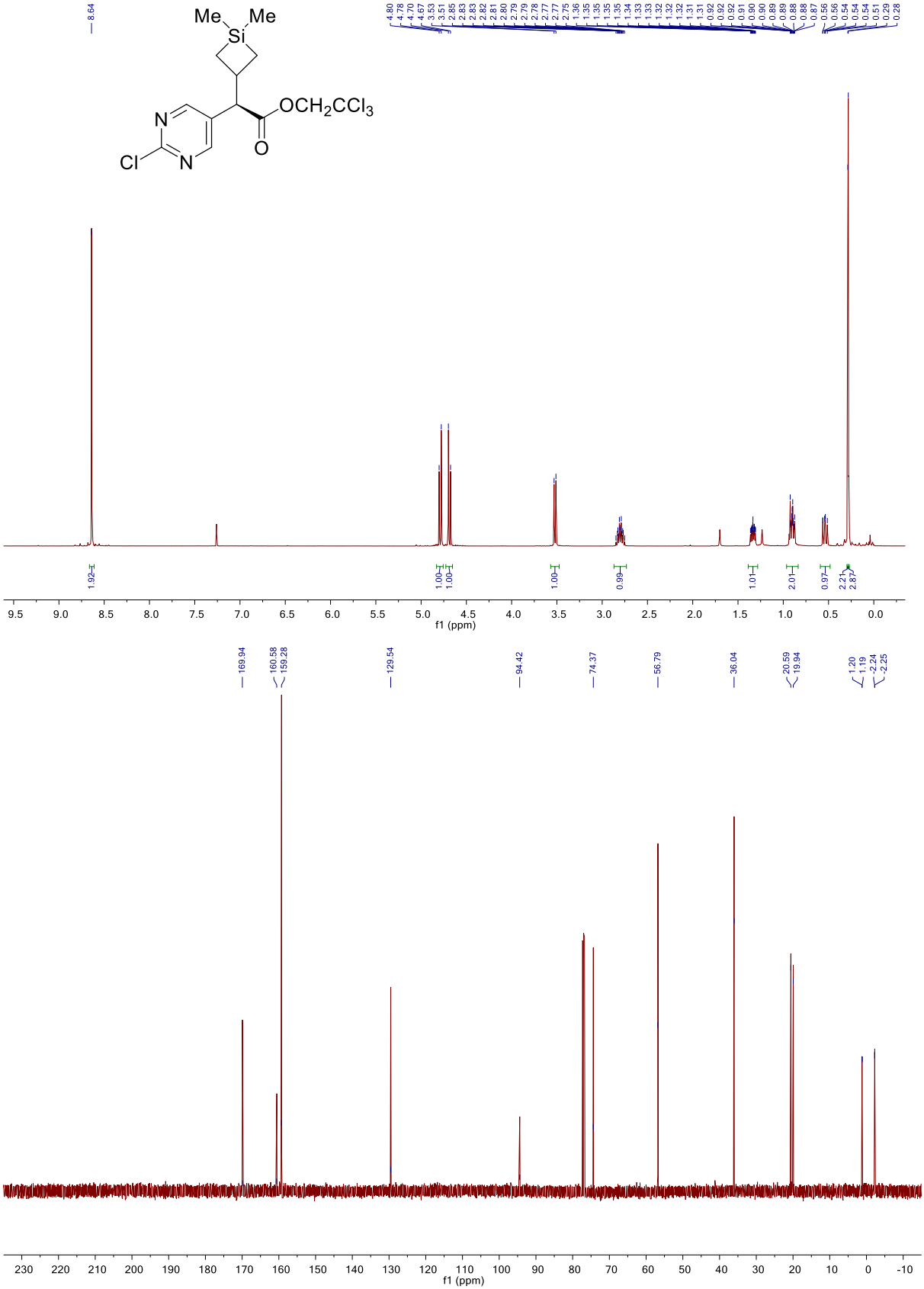
Me
Si
Me
N
Cl
N
OCH2CCl3
O
f1 (ppm)
f1 (ppm)

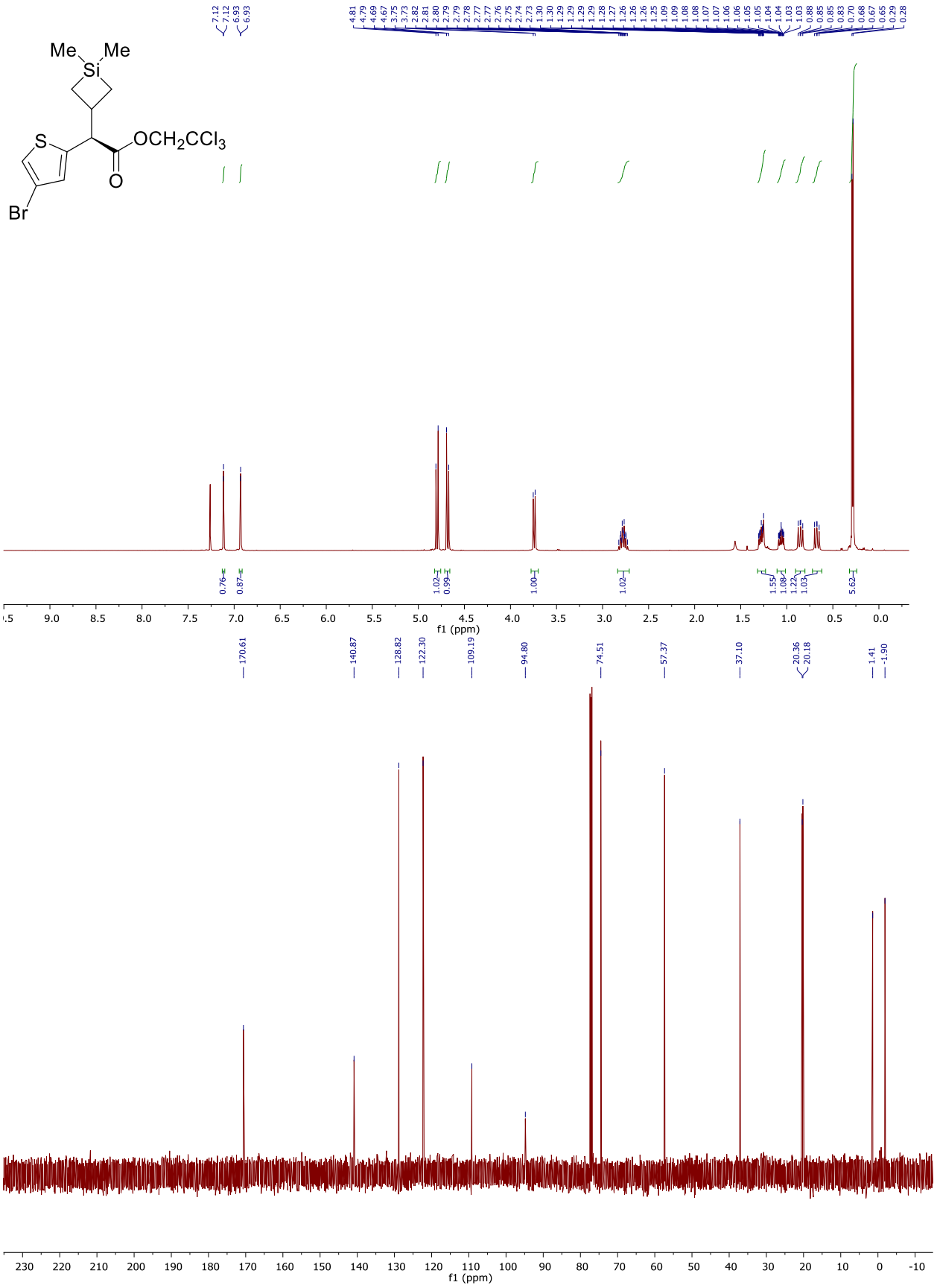
Me
Me
Si
S
OCH2CCl3
O
Br
f1 (ppm)
f1 (ppm)

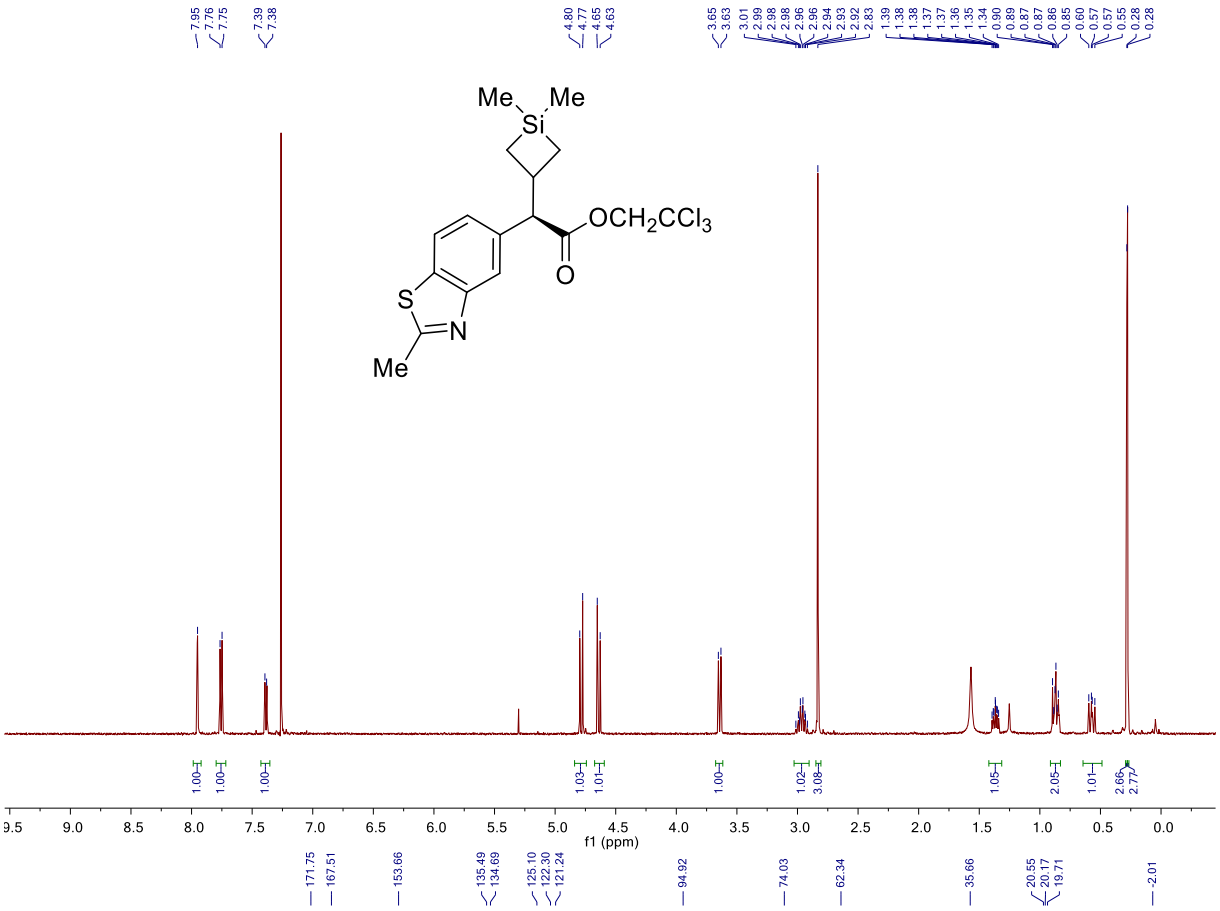
7.95
7.76
7.75
7.39
7.38
4.80
4.77
4.65
4.63
3.65
3.63
3.01
2.99
2.98
2.98
2.96
2.96
2.94
2.93
2.92
2.83
1.39
1.38
1.38
1.37
1.37
1.36
1.35
1.34
0.90
0.89
0.87
0.87
0.86
0.85
0.60
0.57
0.57
0.55
0.28
0.28
Me
Me
Si
OCH2CCl3
O
S
N
Me
1.00
1.00
1.00
1.03
1.01
1.00
1.02
3.08
1.05
2.05
1.01
2.66
2.77
f1 (ppm)
171.75
167.51
153.66
135.49
134.69
125.10
122.30
121.24
94.92
74.03
62.34
35.66
20.55
20.17
19.71
-2.01
f1 (ppm)

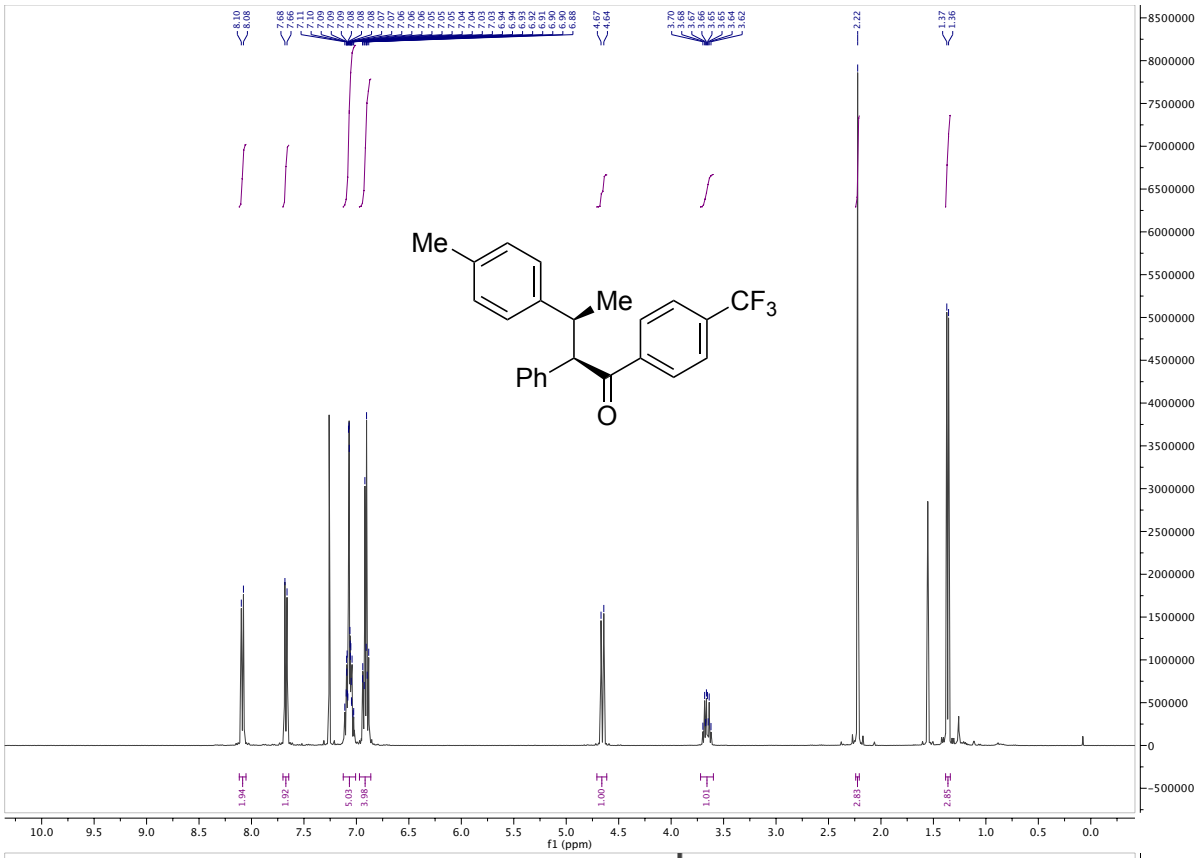
Me
Me
CF3
Ph
O
f1 (ppm)

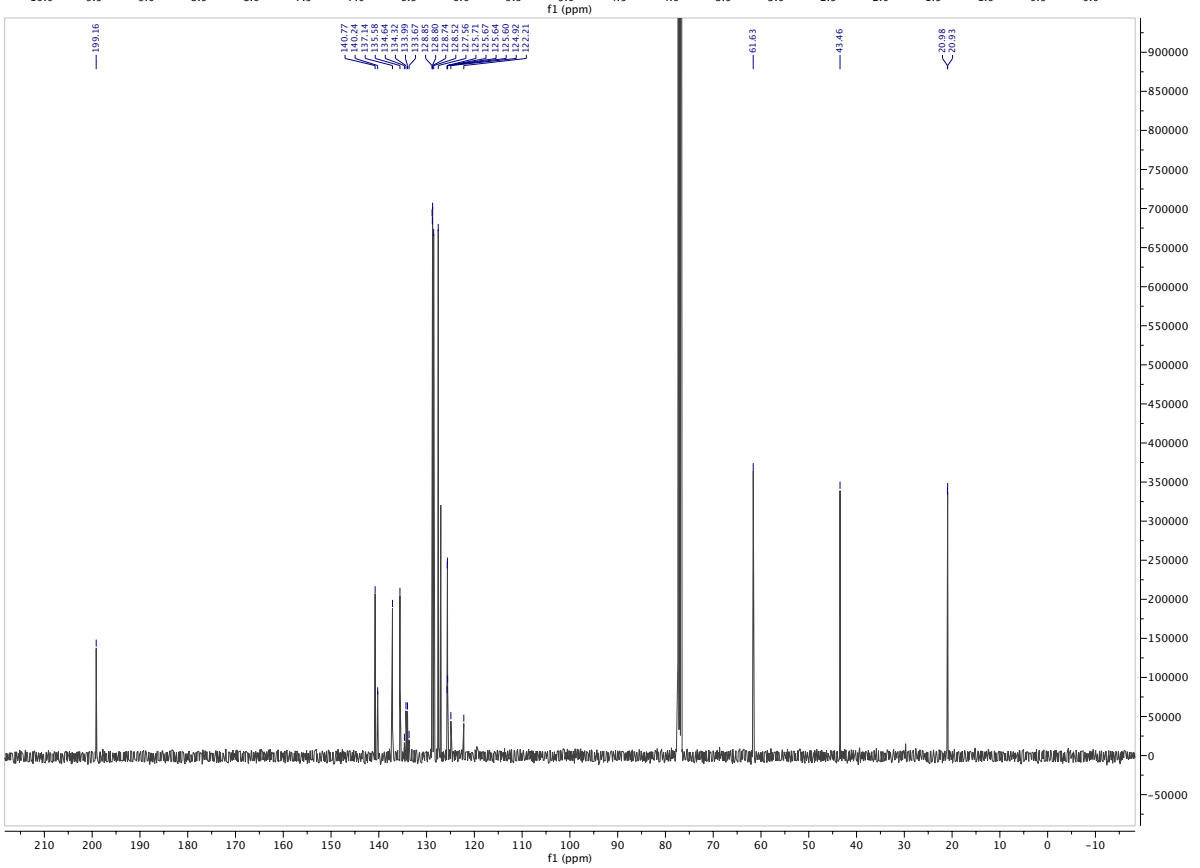
f1 (ppm)

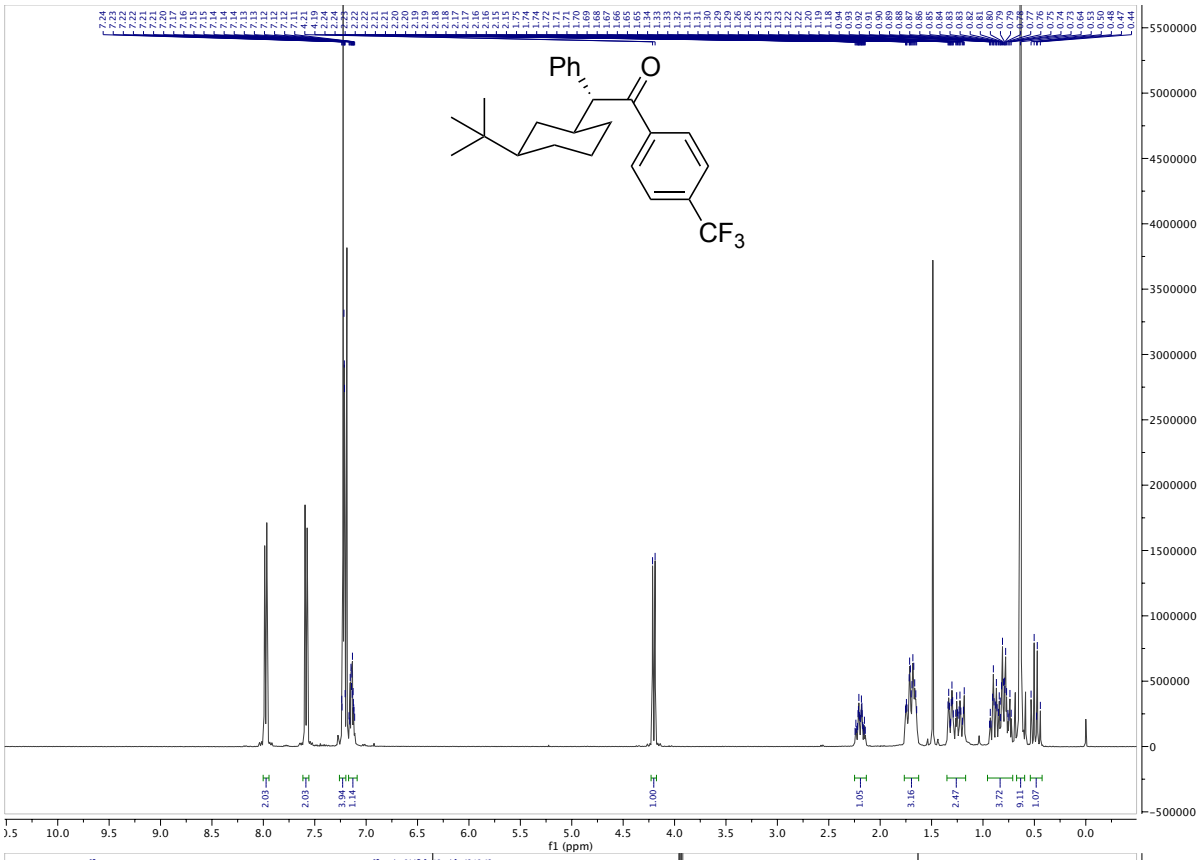
Ph
O
CF3
f1 (ppm)

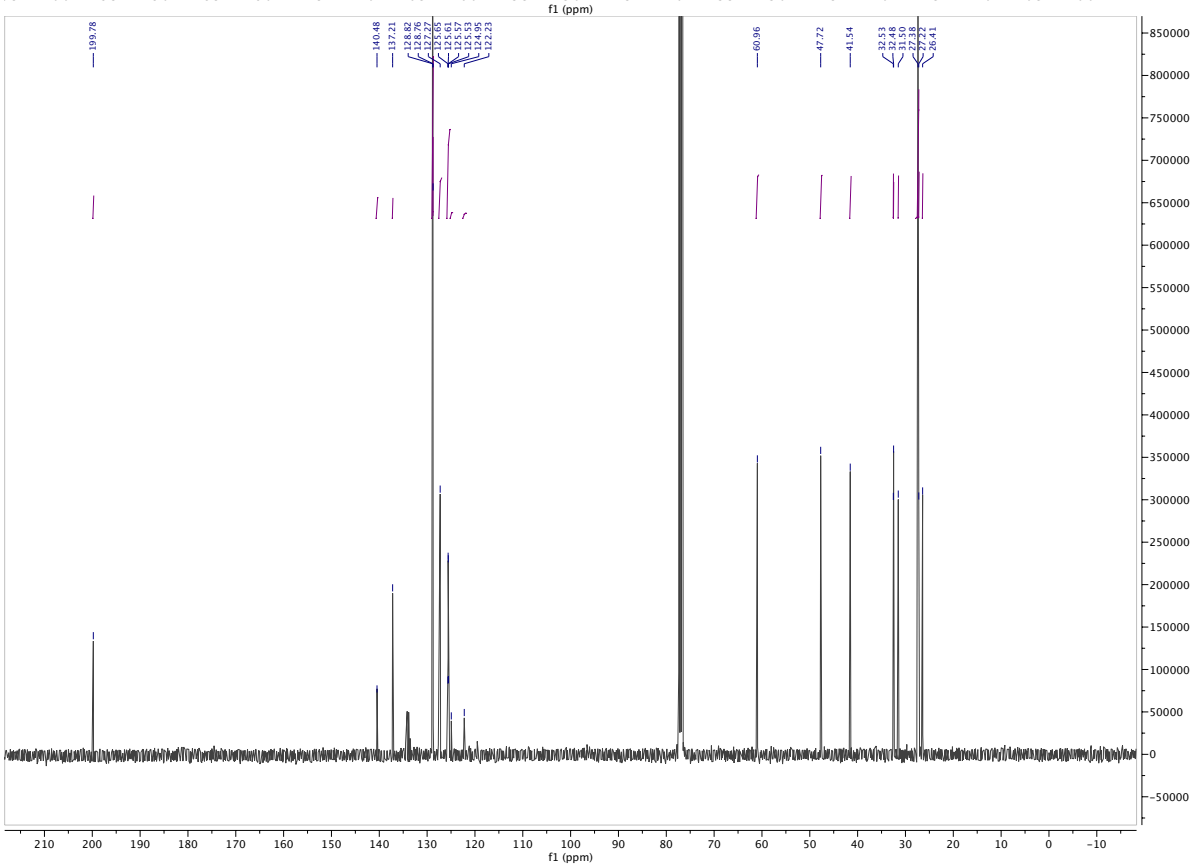
199.78
140.48
137.21
128.82
128.76
125.61
125.57
125.53
124.95
122.23
60.96
47.72
41.54
32.53
32.48
31.65
27.38
27.22
26.41
f1 (ppm)

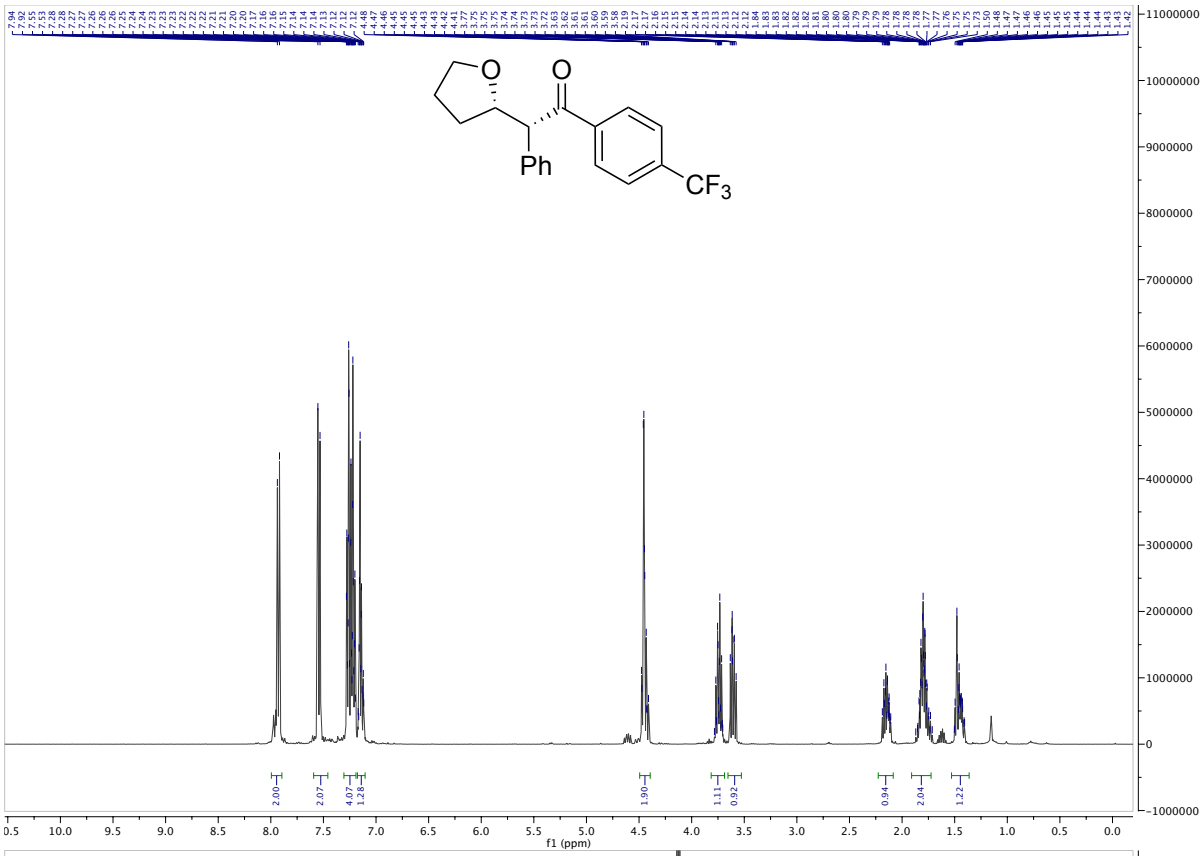
O
O
Ph
CF3
f1 (ppm)

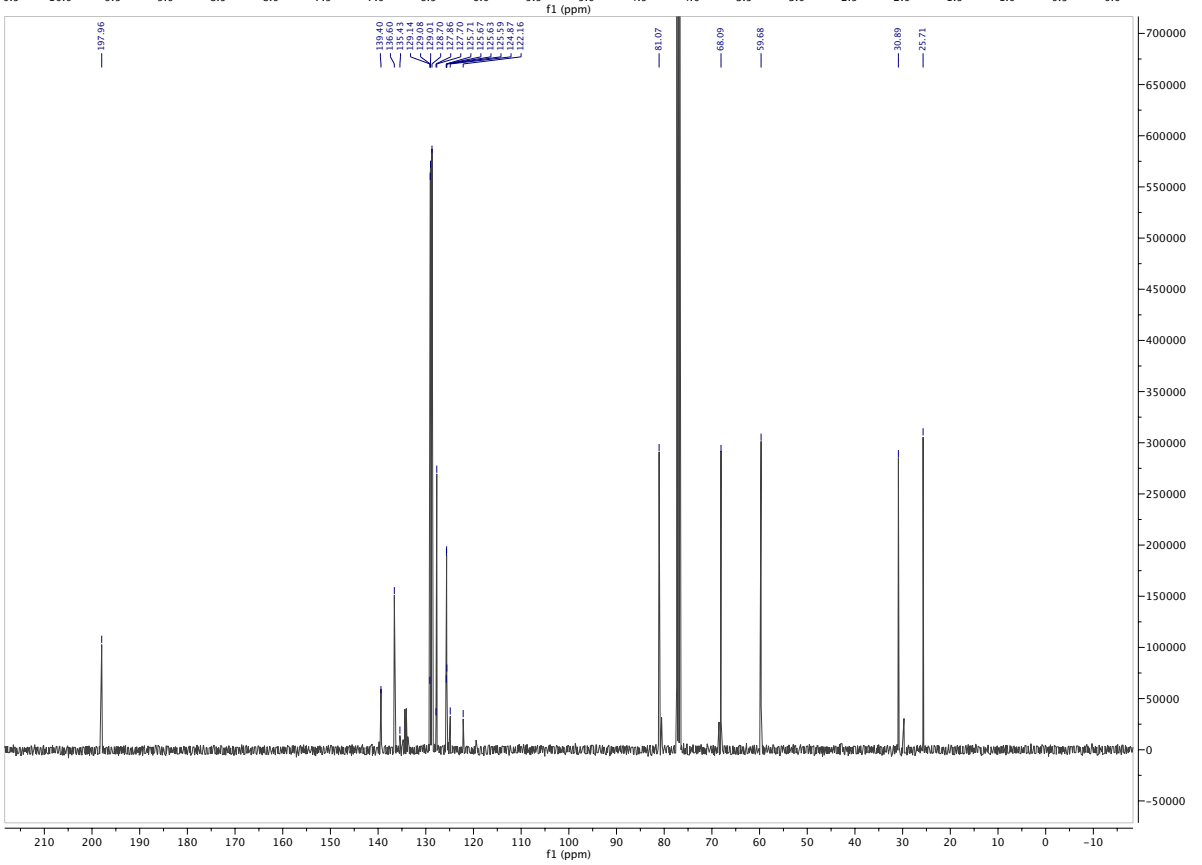
197.96
139.40
136.60
135.43
133.44
129.08
129.01
128.70
127.86
127.70
125.71
125.67
125.63
125.59
124.87
122.16
81.07
68.09
59.68
30.89
25.71
f1 (ppm)

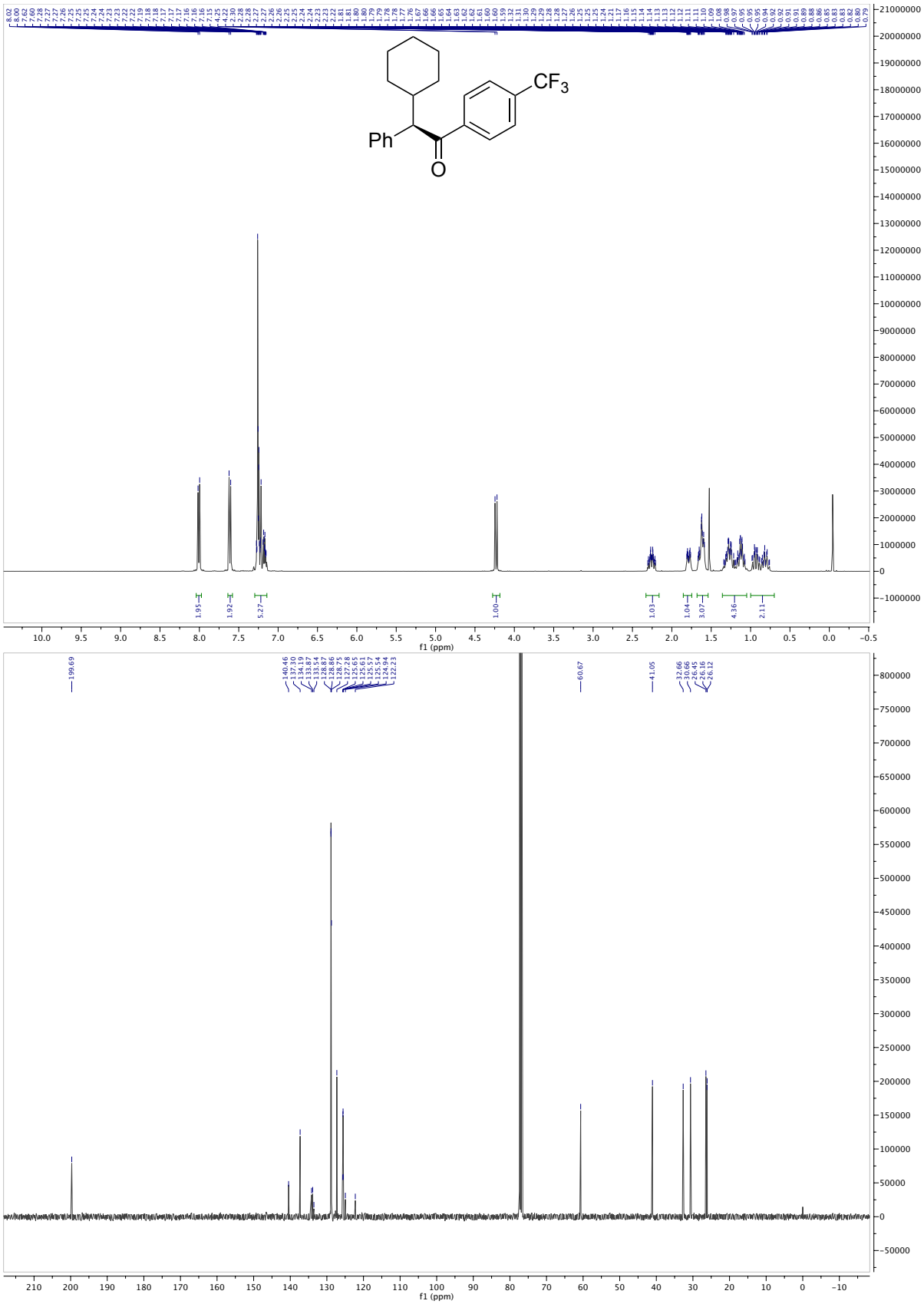
CF3
Ph
O
f1 (ppm)
199.69
140.46
137.10
134.19
133.87
131.54
128.87
128.86
128.75
128.28
125.61
125.57
125.54
124.94
122.23
60.67
41.05
32.66
30.66
26.45
26.16
26.12

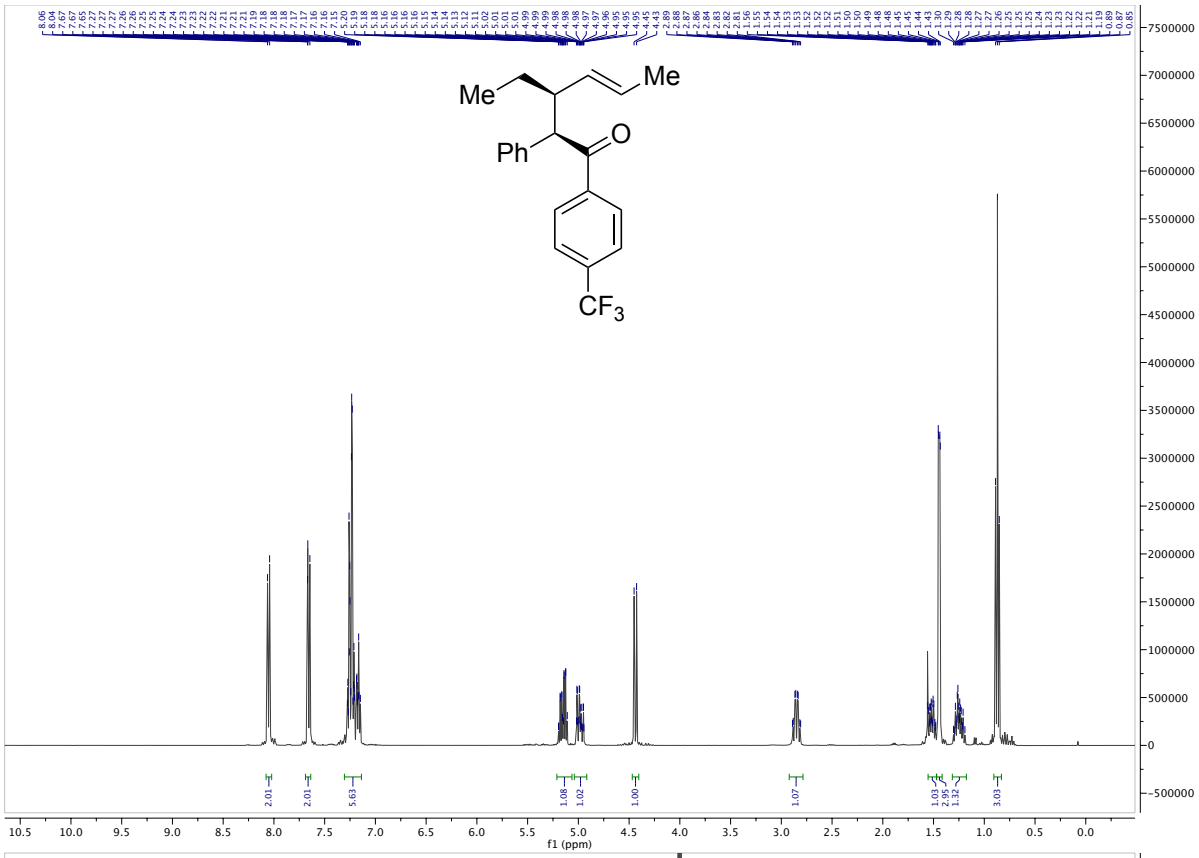
Me
Me
Ph
O
CF3
f1 (ppm)

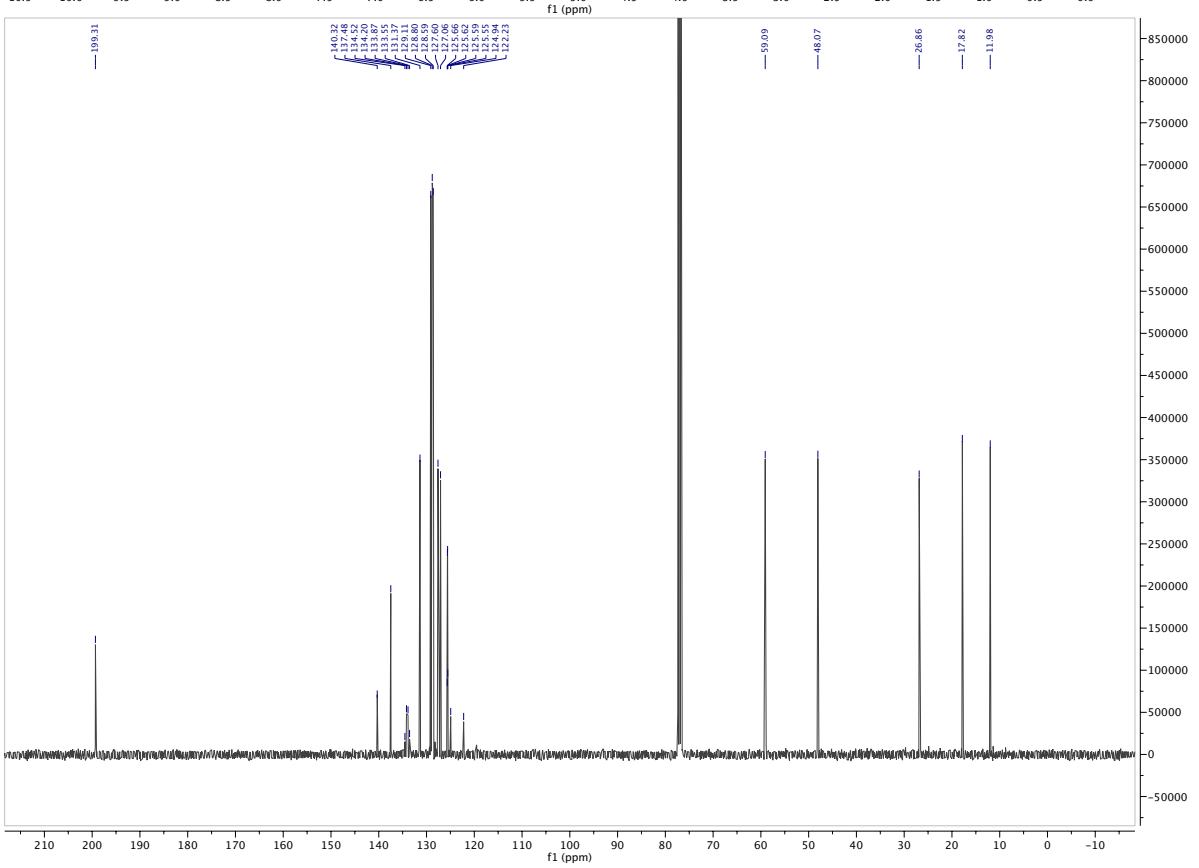
199.31
140.32
137.48
134.52
134.20
133.87
131.75
131.37
129.11
128.80
128.50
127.60
127.06
125.66
125.62
125.59
125.55
125.49
122.23
59.09
48.07
26.86
17.82
11.98
f1 (ppm)

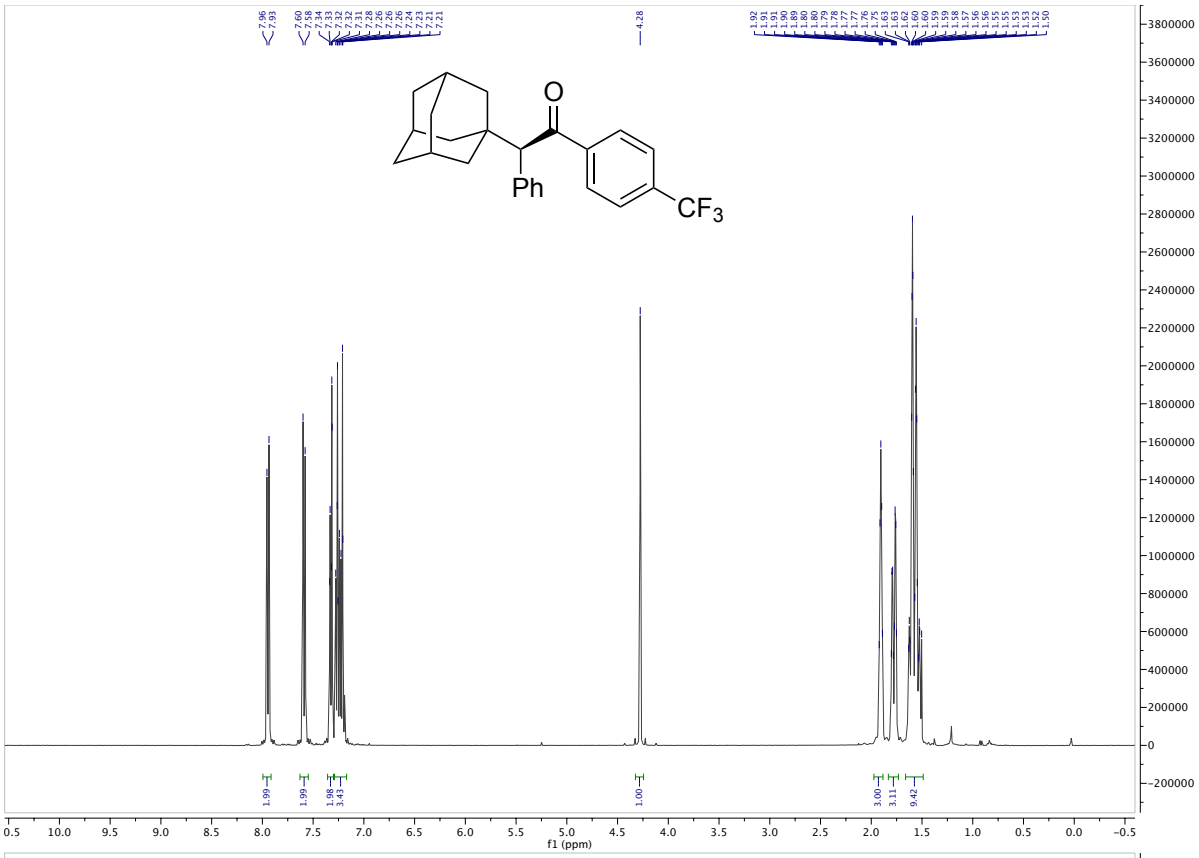
O
Ph
CF3
f1 (ppm)

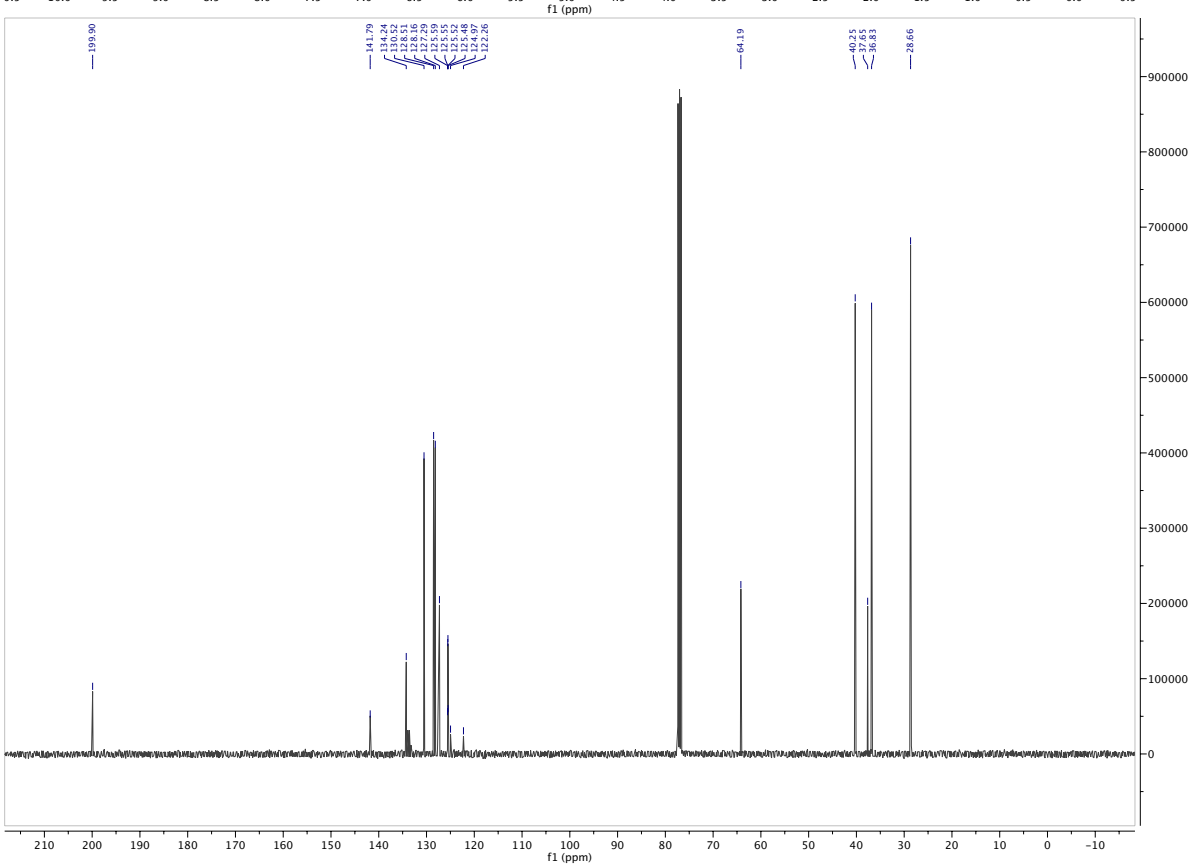
f1 (ppm)

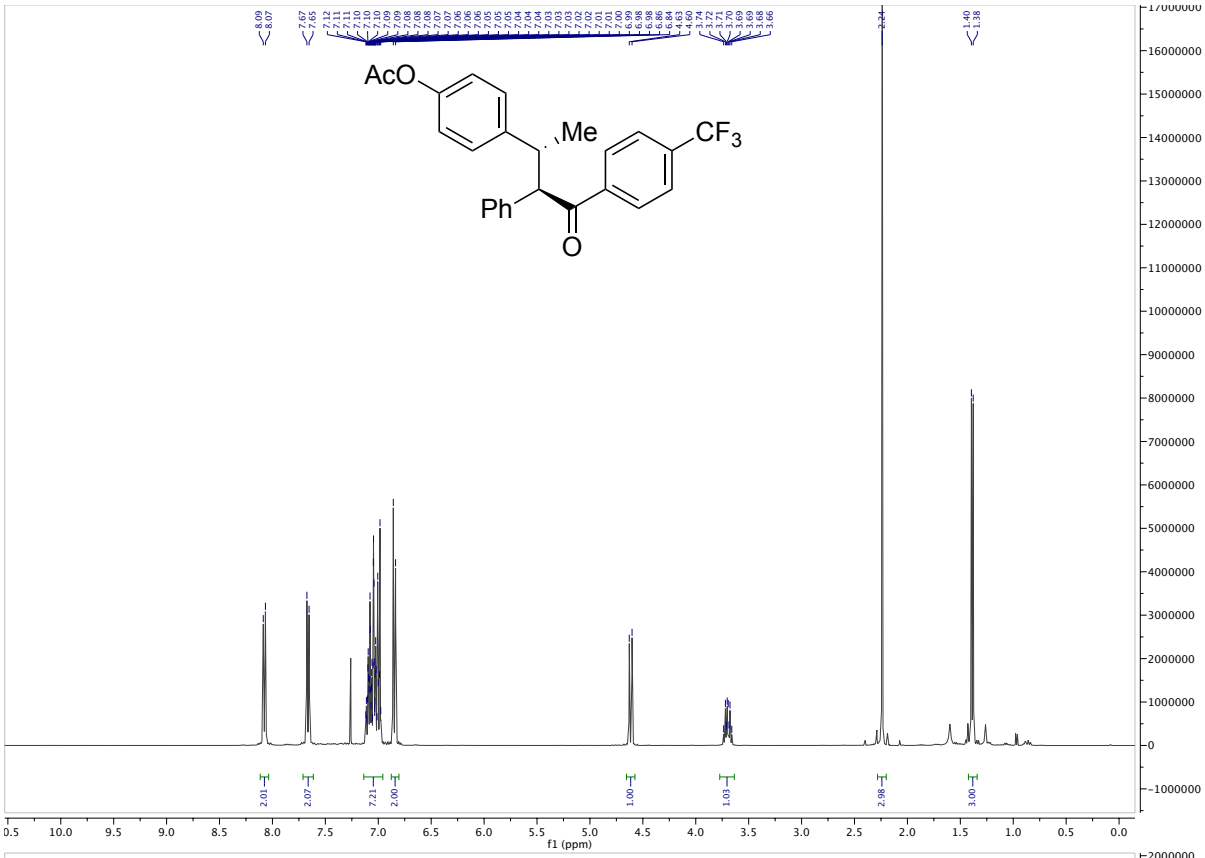
AcO
Me
CF3
Ph
O
f1 (ppm)

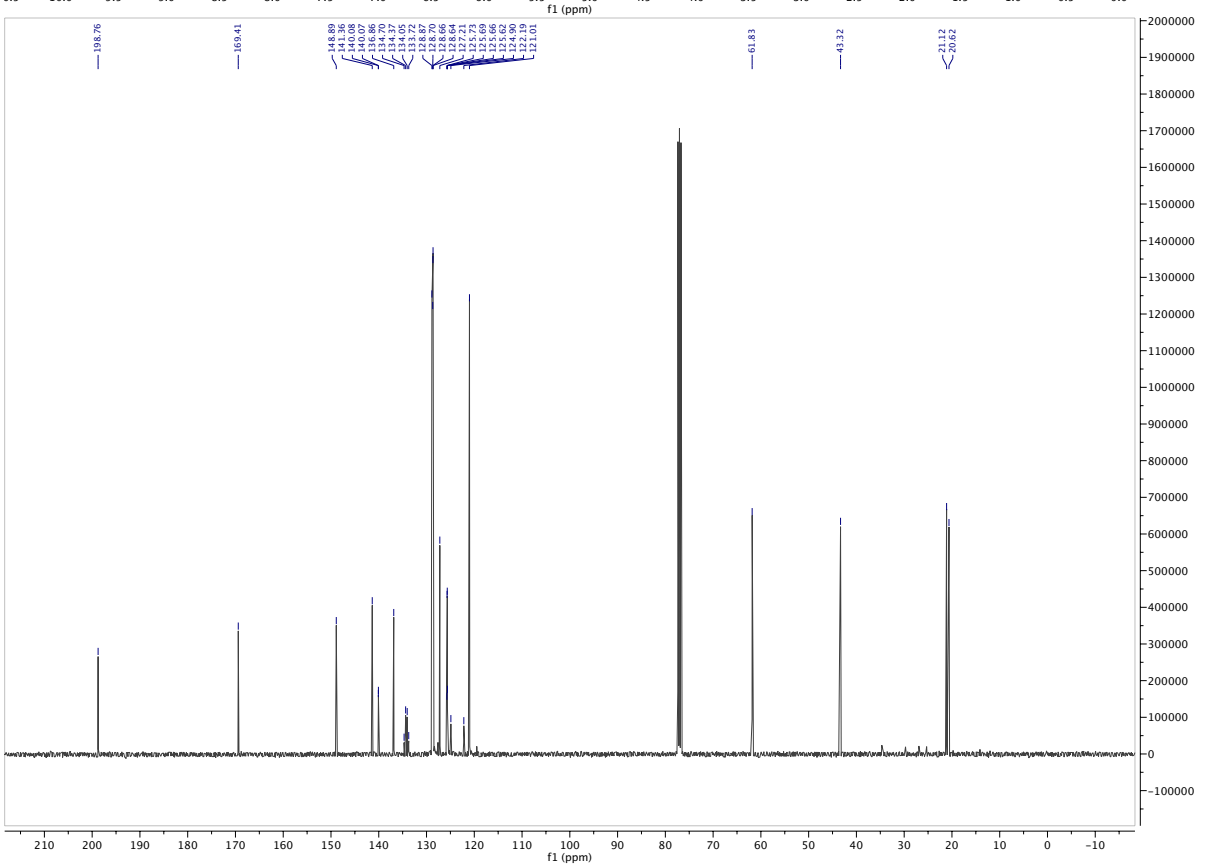
198.76
169.41
61.83
43.32
21.12
20.62
f1 (ppm)

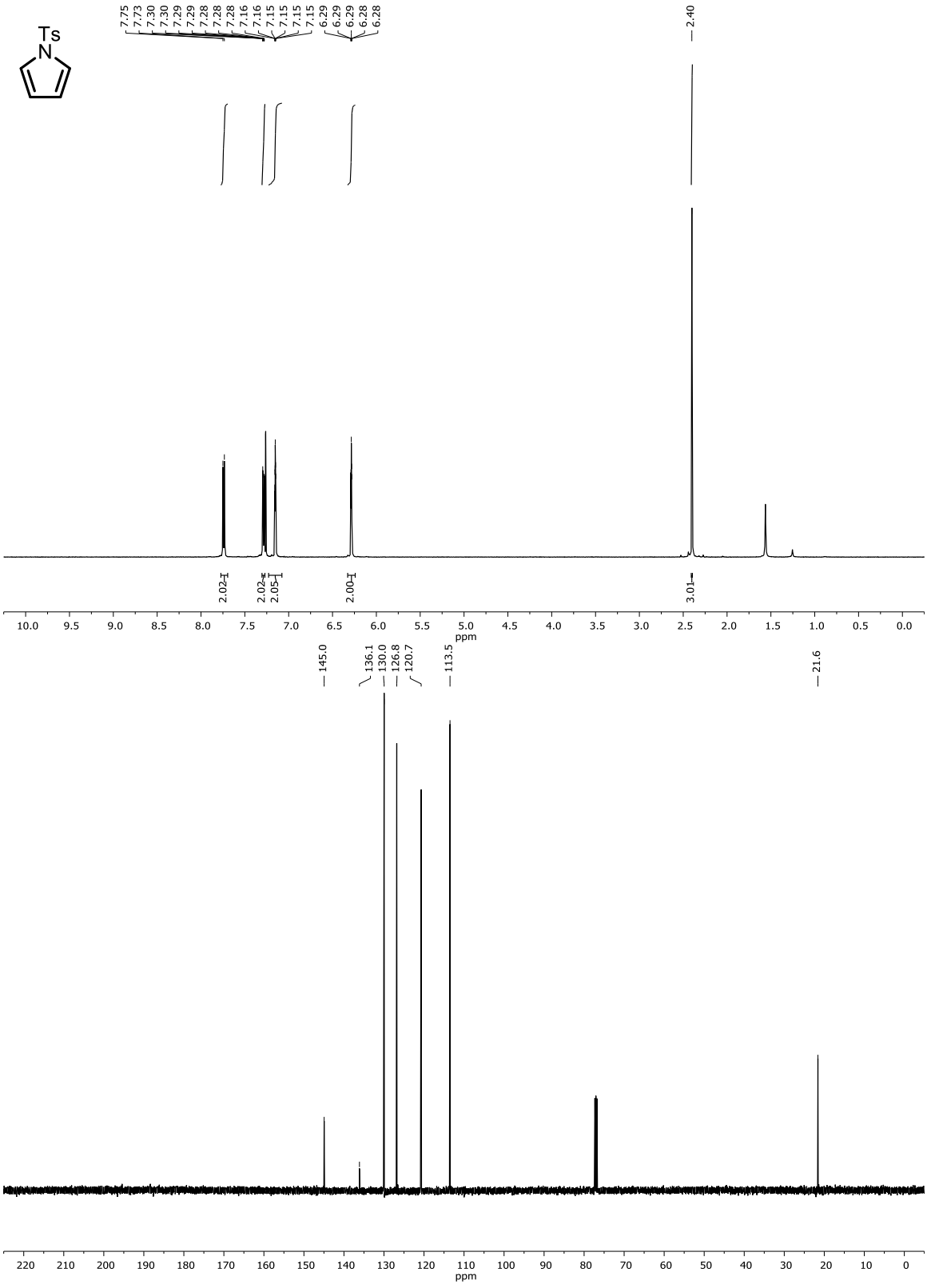
Ts
N
7.75
7.73
7.30
7.30
7.29
7.29
7.28
7.28
7.28
7.16
7.16
7.15
7.15
7.15
7.15
6.29
6.29
6.29
6.28
6.28
2.40
2.02
2.02
2.05
2.00
3.01
ppm
145.0
136.1
130.0
126.8
120.7
113.5
21.6
ppm

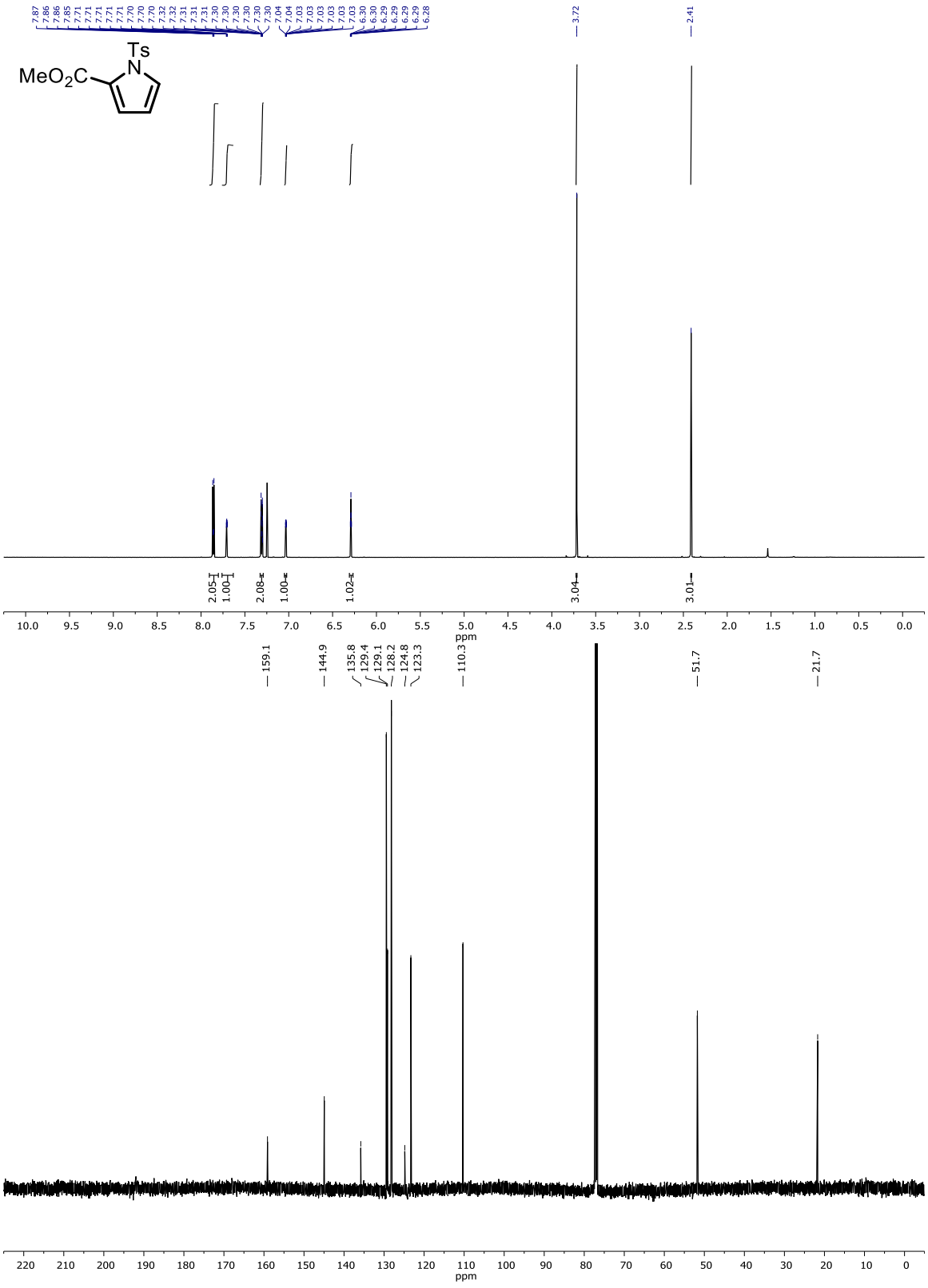
Ts
N
MeO2C
7.87
7.86
7.86
7.85
7.71
7.71
7.71
7.71
7.71
7.70
7.70
7.70
7.32
7.31
7.31
7.31
7.30
7.30
7.30
7.30
7.30
7.04
7.04
7.03
7.03
7.03
7.03
7.03
6.30
6.29
6.29
6.29
6.28
3.72
2.41
2.05
1.00
2.08
1.00
1.02
3.04
3.01
ppm
159.1
144.9
135.8
129.4
129.1
128.2
124.8
123.3
110.3
51.7
21.7
ppm

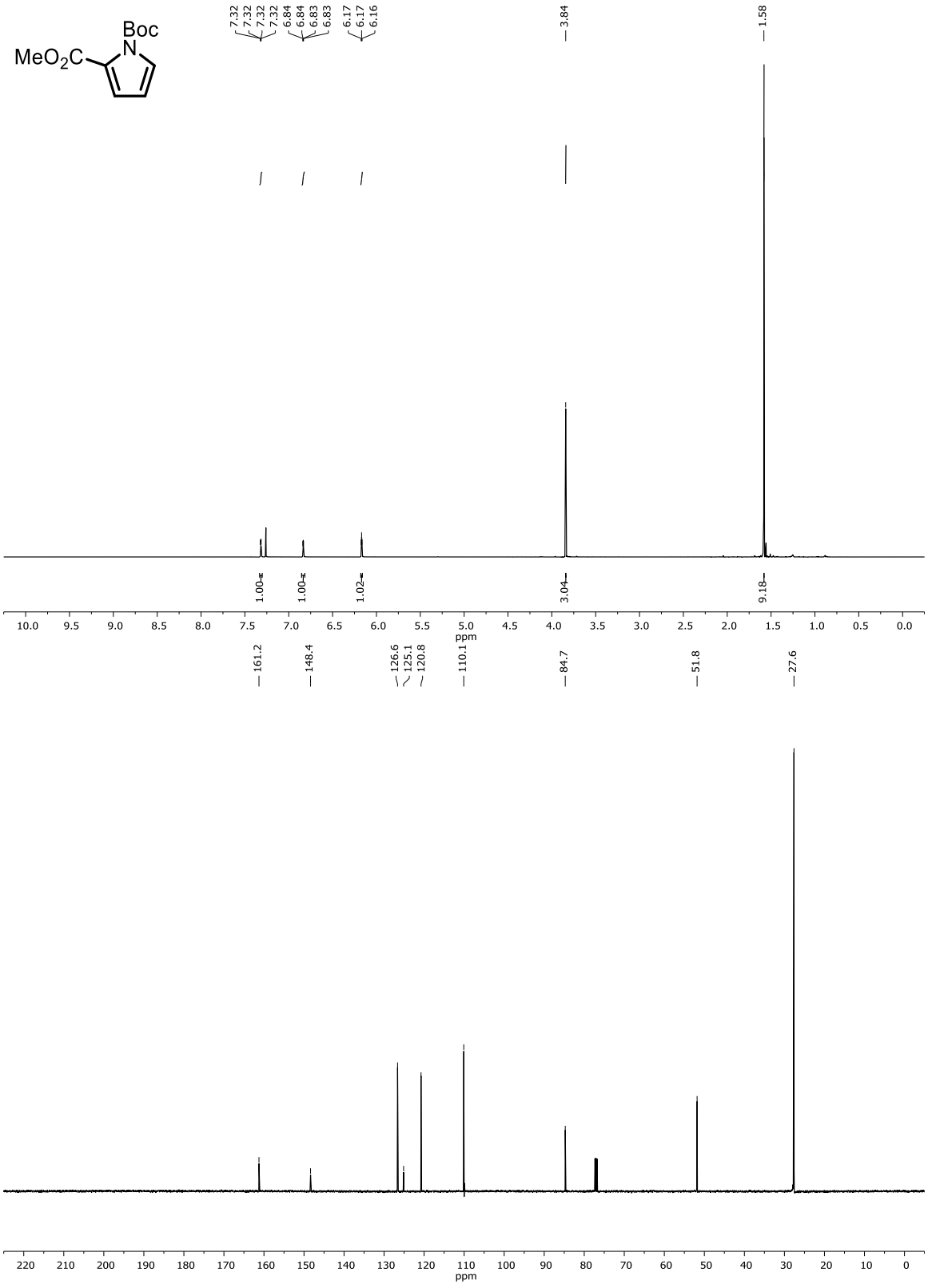
Boc
N
MeO2C
7.32
7.32
7.32
7.32
6.84
6.84
6.83
6.83
6.17
6.17
6.16
3.84
1.58
1.00
1.00
1.02
3.04
9.18
ppm
161.2
148.4
126.6
125.1
120.8
110.1
84.7
51.8
27.6
ppm

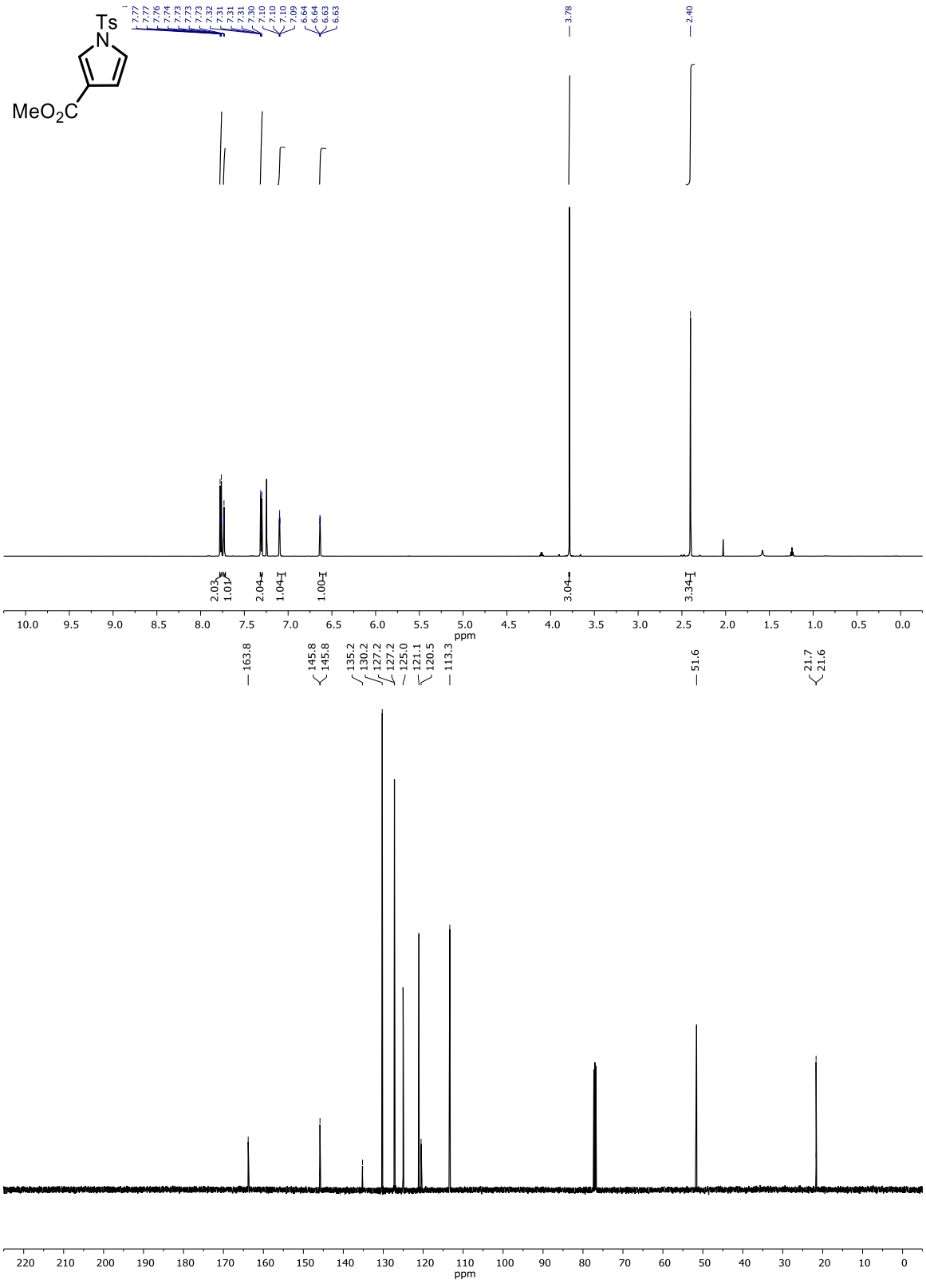
Ts
N
MeO2C
7.77
7.77
7.76
7.74
7.73
7.73
7.73
7.32
7.31
7.31
7.30
7.10
7.10
7.09
6.64
6.64
6.63
6.63
3.78
2.40
2.03
1.01
2.04
1.04
1.00
3.04
3.34
ppm
163.8
145.8
145.8
135.2
130.2
127.2
127.2
125.0
121.1
120.5
113.3
51.6
21.7
21.6
ppm

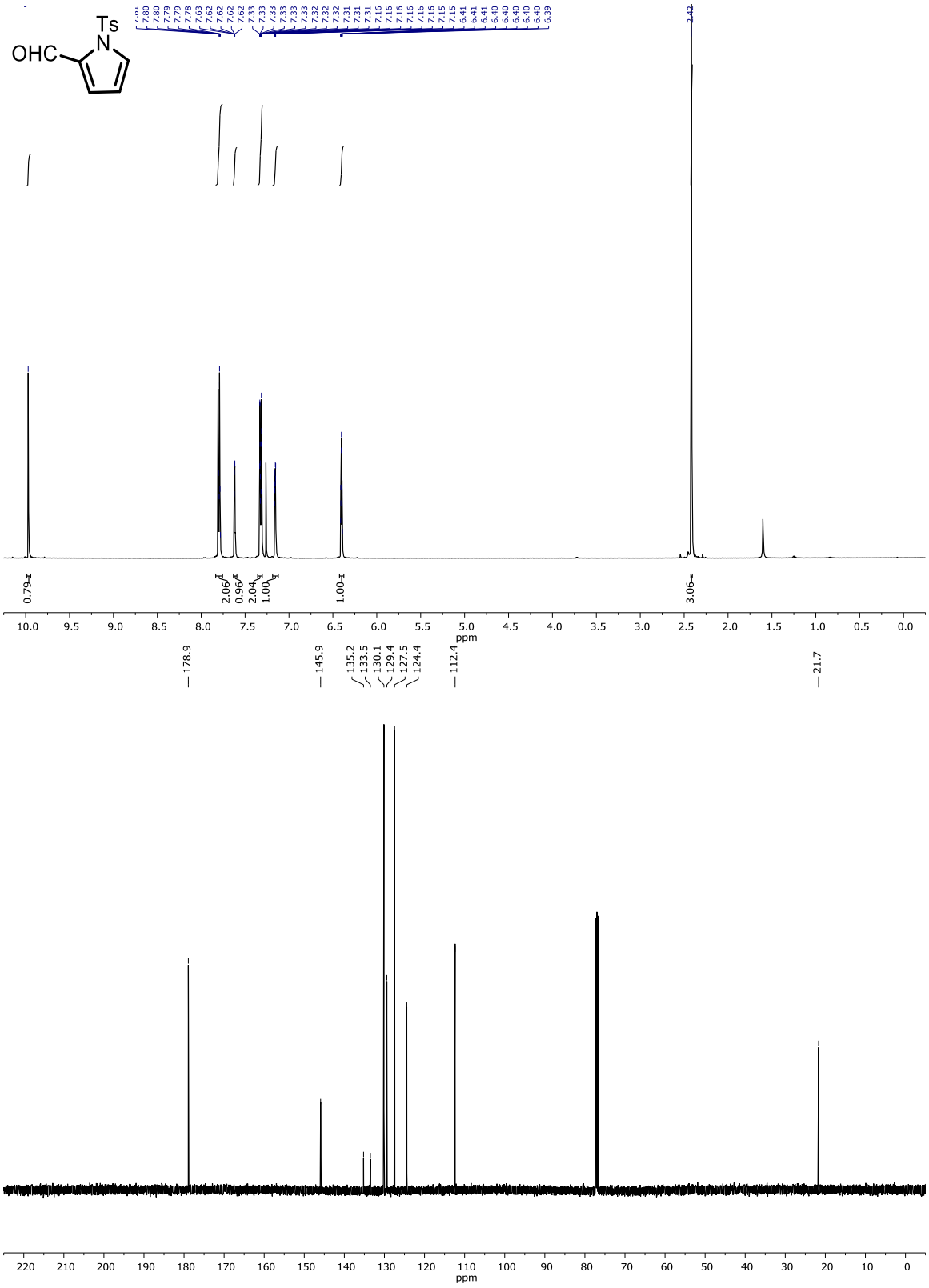
Ts
N
OHC
7.80
7.79
7.78
7.63
7.62
7.33
7.32
7.31
7.16
7.15
6.41
6.40
6.39
3.42
0.79
2.06
0.96
2.04
1.00
1.00
3.06
10.0
9.5
9.0
8.5
8.0
7.5
7.0
6.5
6.0
5.5
5.0
4.5
4.0
3.5
3.0
2.5
2.0
1.5
1.0
0.5
0.0
ppm
178.9
145.9
135.2
133.5
130.1
129.4
127.5
124.4
112.4
21.7
220
210
200
190
180
170
160
150
140
130
120
110
100
90
80
70
60
50
40
30
20
10
0
ppm

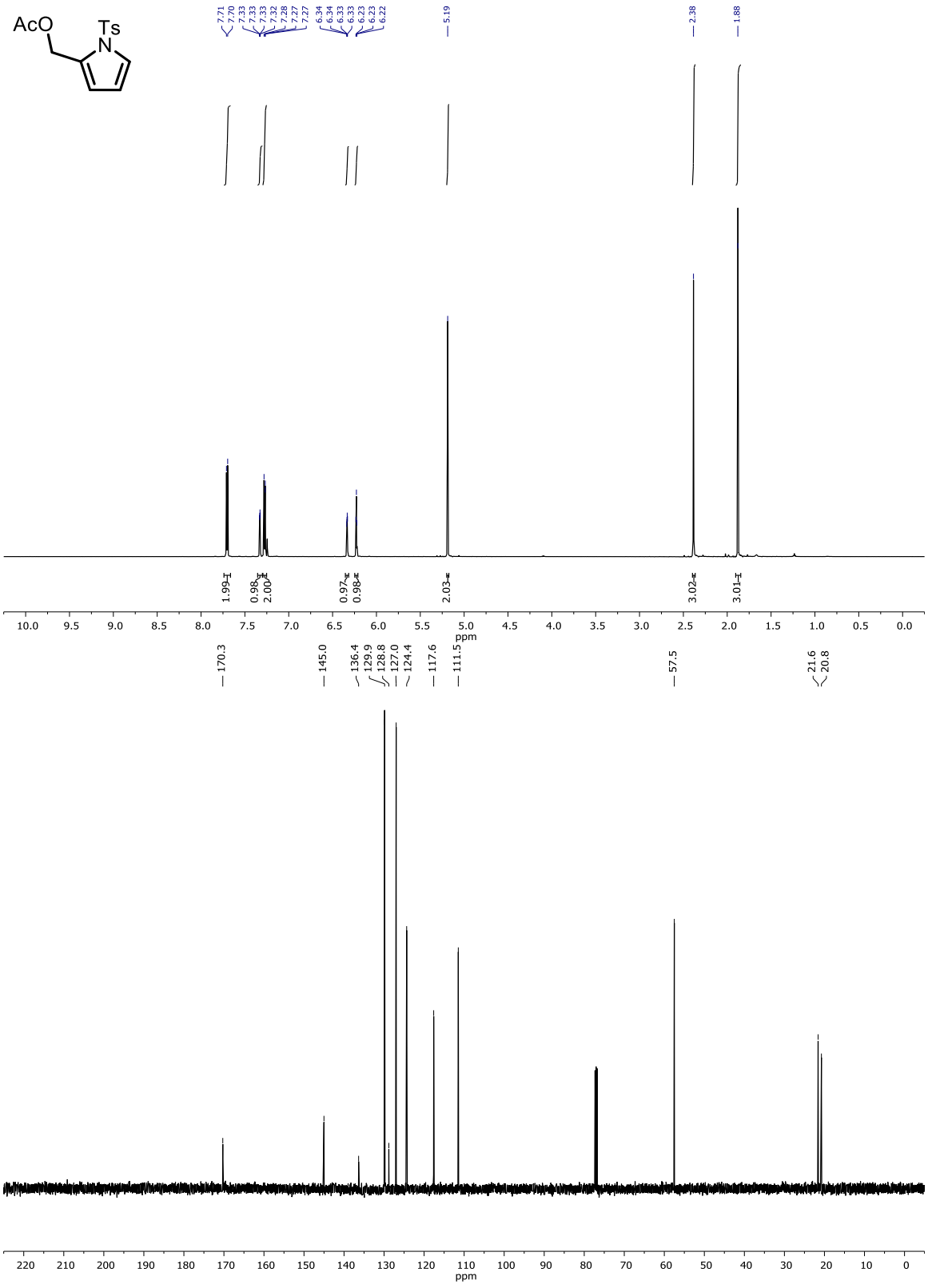
AcO
Ts
N
7.71
7.70
7.33
7.33
7.33
7.32
7.28
7.27
7.27
6.34
6.34
6.33
6.33
6.23
6.23
6.22
5.19
2.38
1.88
1.99
0.98
2.00
0.97
0.98
2.03
3.02
3.01
ppm
170.3
145.0
136.4
129.9
128.8
127.0
124.4
117.6
111.5
57.5
21.6
20.8
ppm

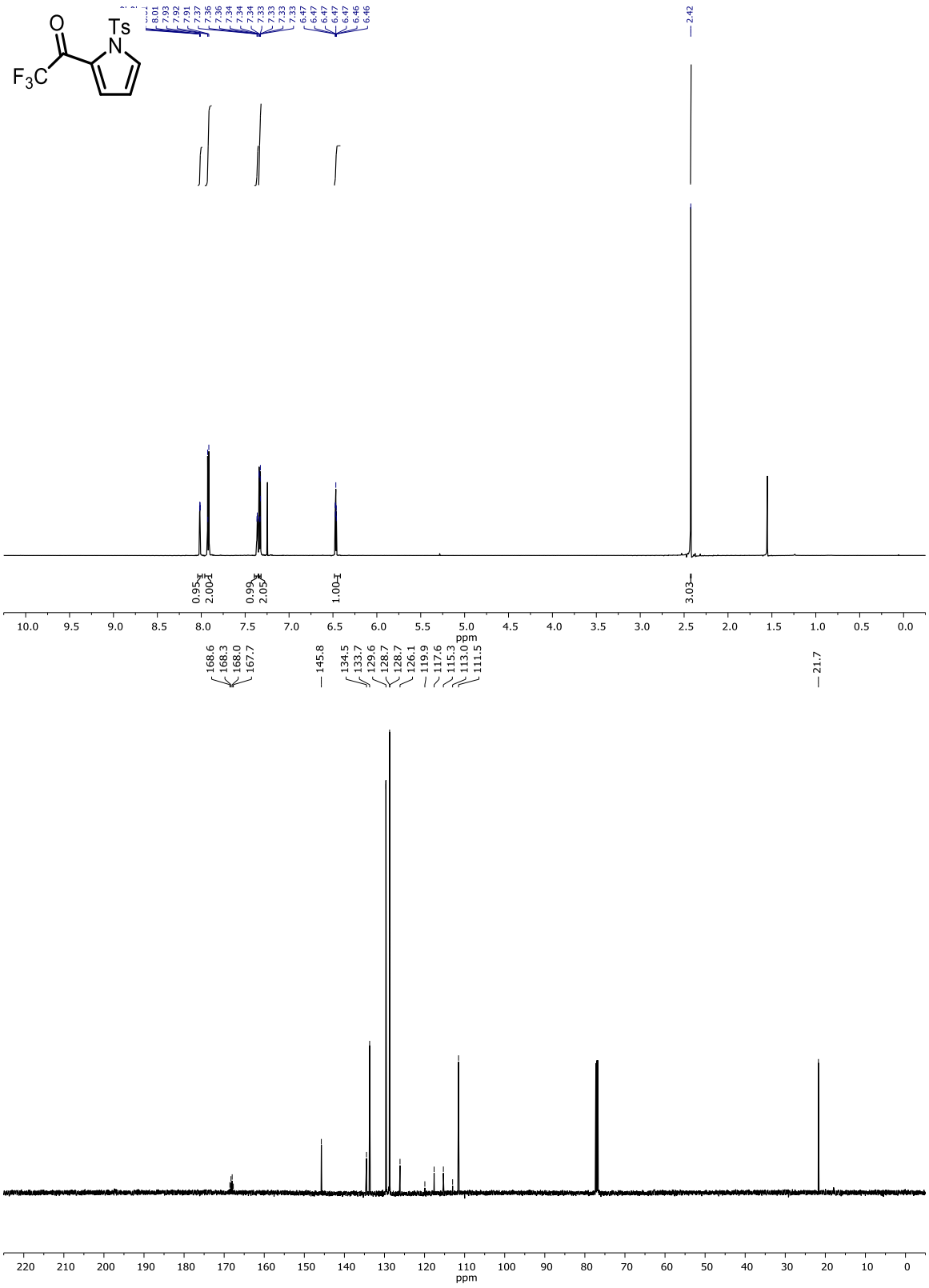

^{19}F-NMR (282 MHz, $CDCl_3$)

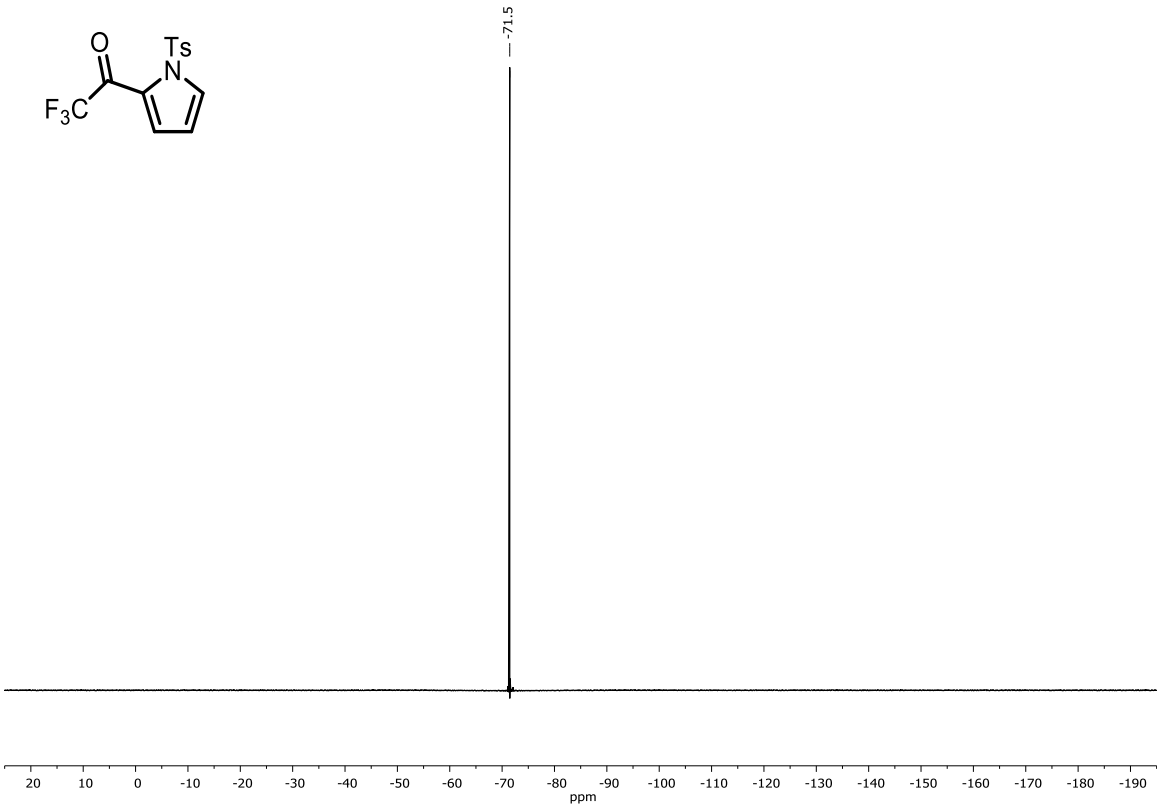
O
Ts
N
F3C
-71.5
20
10
0
-10
-20
-30
-40
-50
-60
-70
-80
-90
-100
-110
-120
-130
-140
-150
-160
-170
-180
-190
ppm

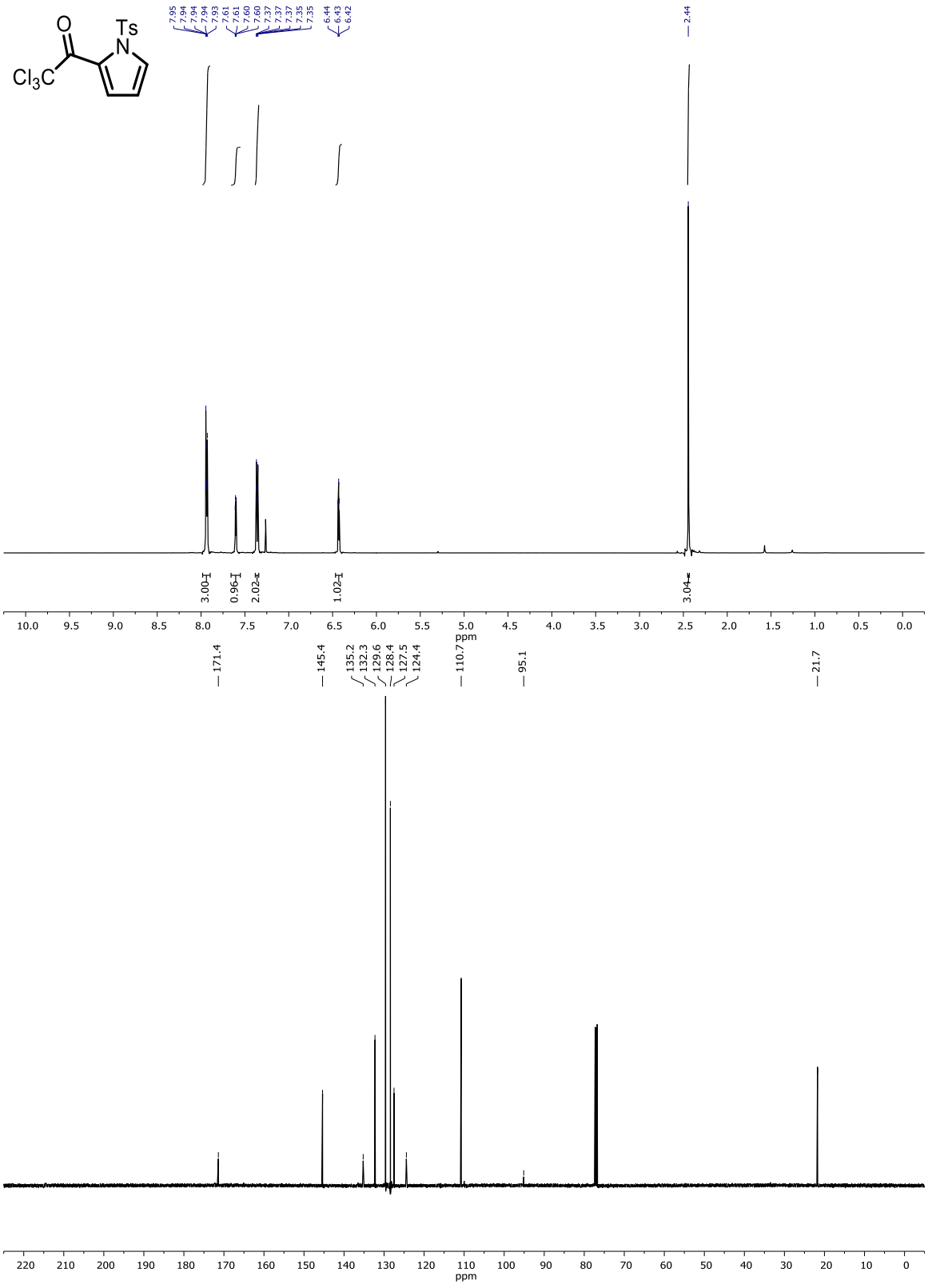
O
Ts
N
Cl3C
7.95
7.94
7.94
7.94
7.93
7.61
7.61
7.60
7.60
7.37
7.37
7.37
7.35
7.35
6.44
6.43
6.42
2.44
3.00
0.96
2.02
1.02
3.04
10.0
9.5
9.0
8.5
8.0
7.5
7.0
6.5
6.0
5.5
5.0
4.5
4.0
3.5
3.0
2.5
2.0
1.5
1.0
0.5
0.0
ppm
171.4
145.4
135.2
132.3
129.6
128.4
127.5
124.4
110.7
95.1
21.7
220
210
200
190
180
170
160
150
140
130
120
110
100
90
80
70
60
50
40
30
20
10
0
ppm

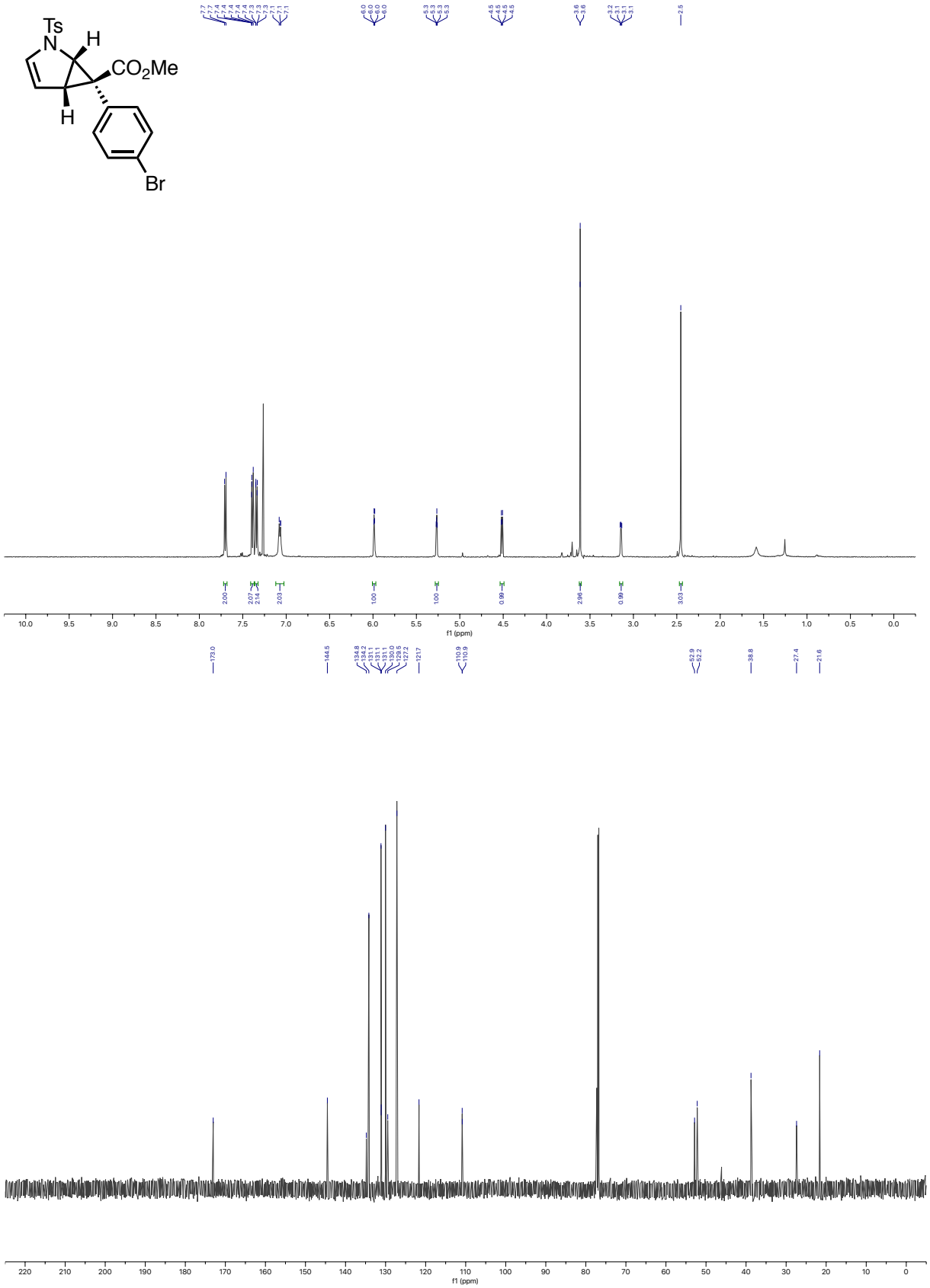
Ts
N
H
CO2Me
H
Br
f1 (ppm)
f1 (ppm)

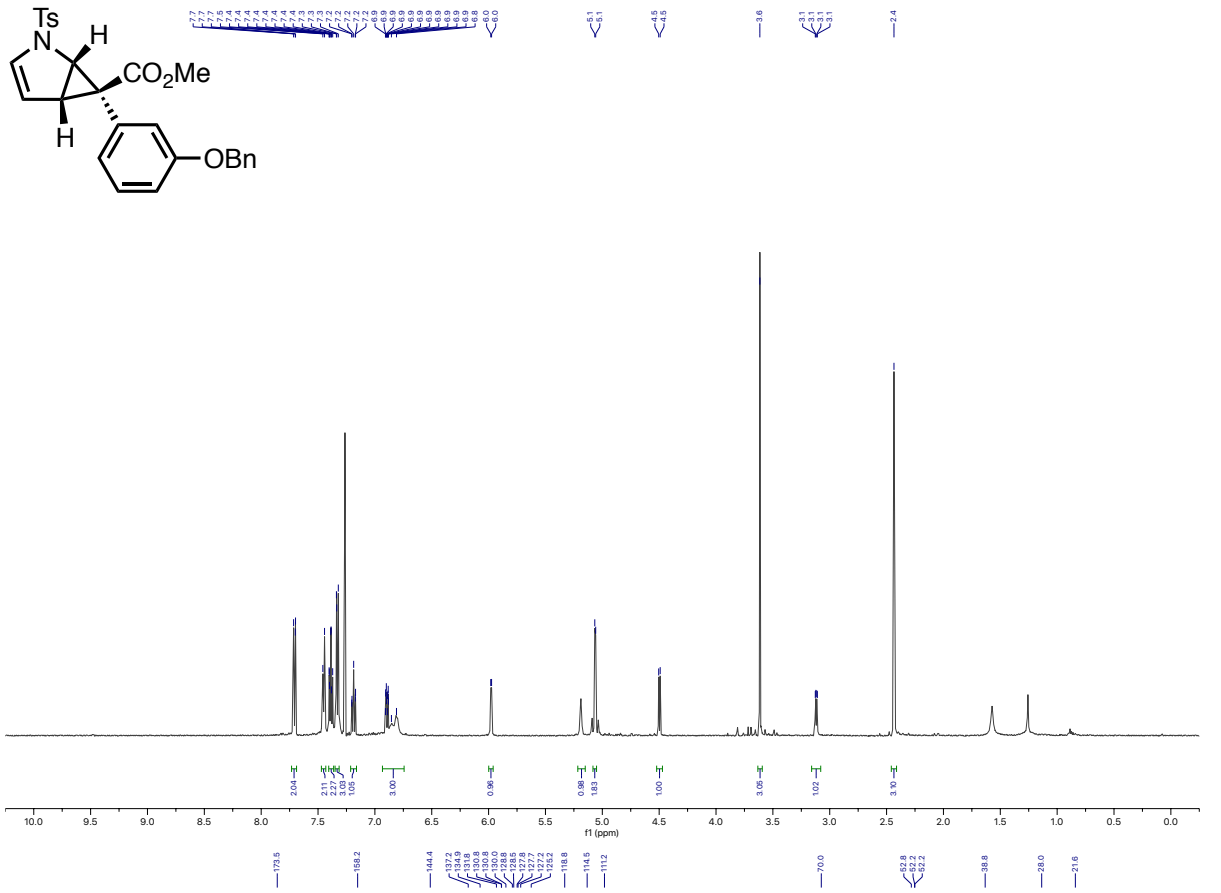
Ts
N
H
CO2Me
H
OBn
f1 (ppm)

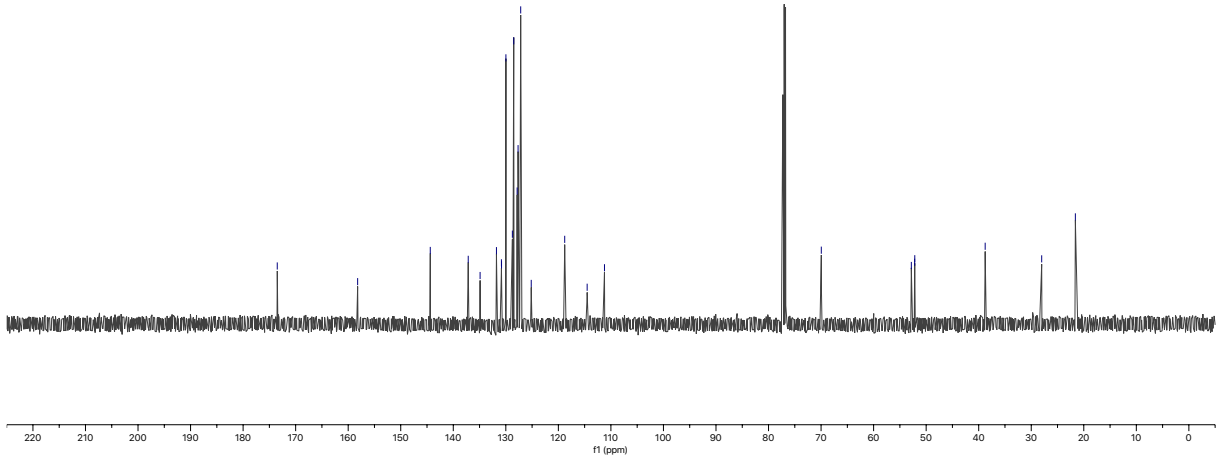
f1 (ppm)

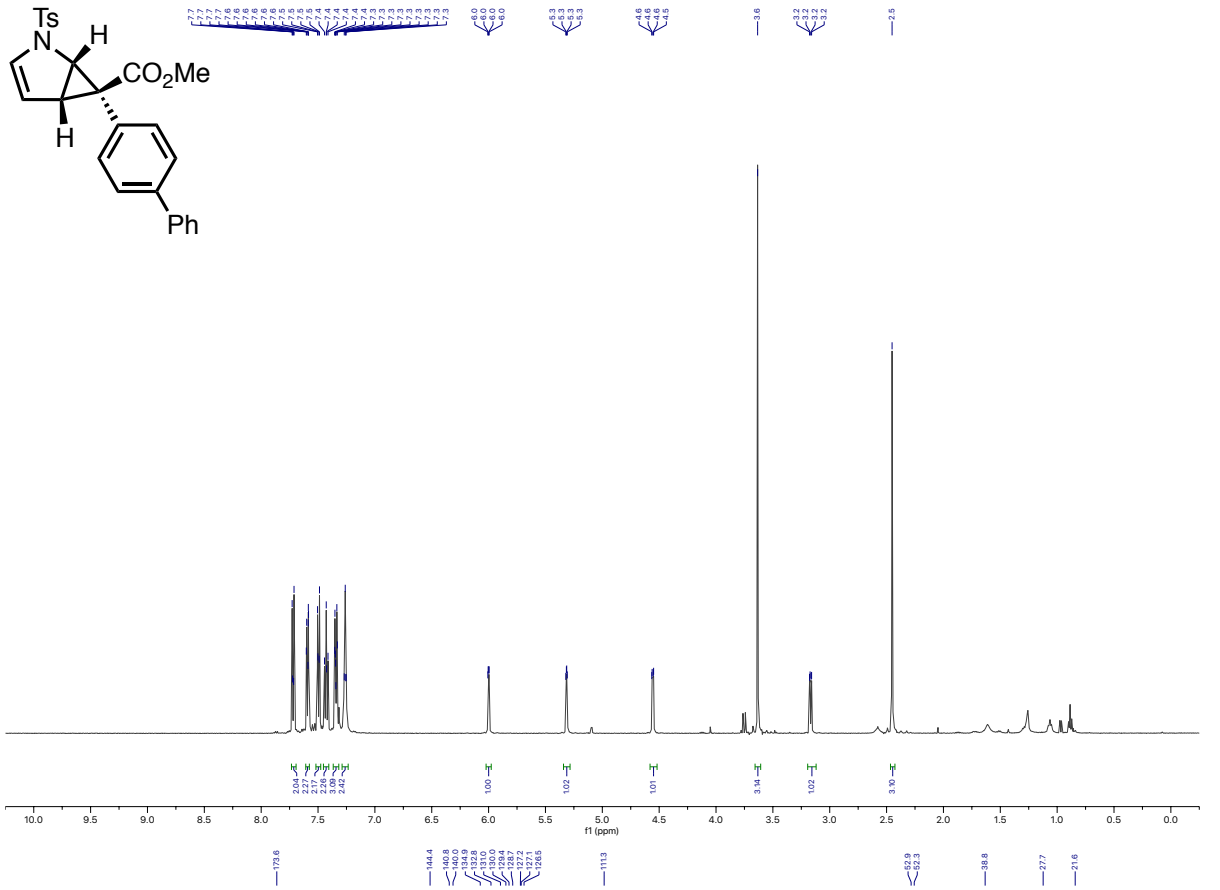
Ts
N
H
CO2Me
H
Ph
f1 (ppm)

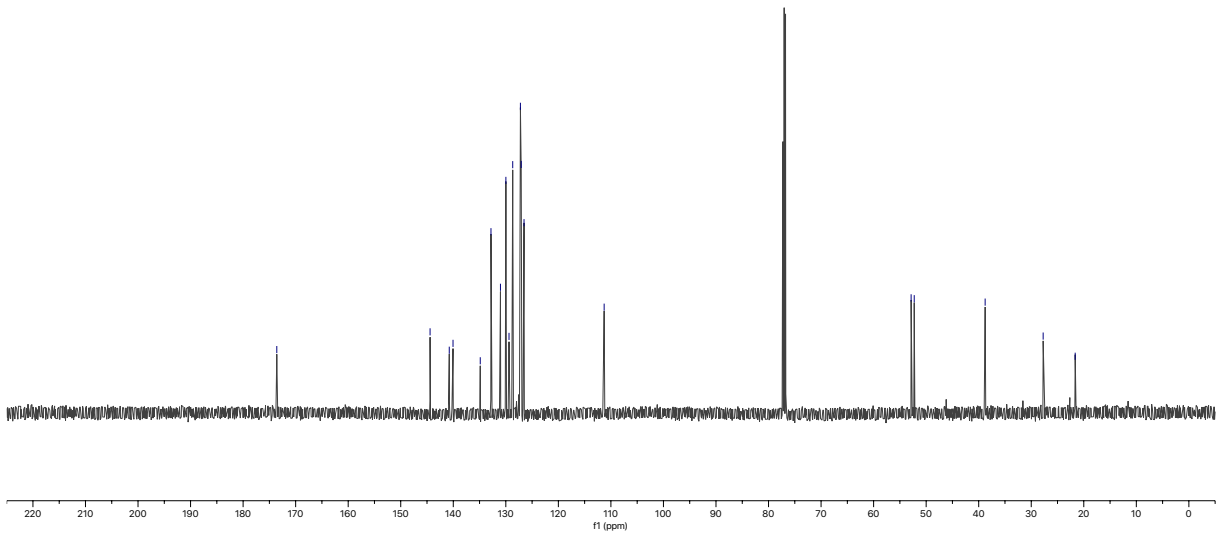
f1 (ppm)

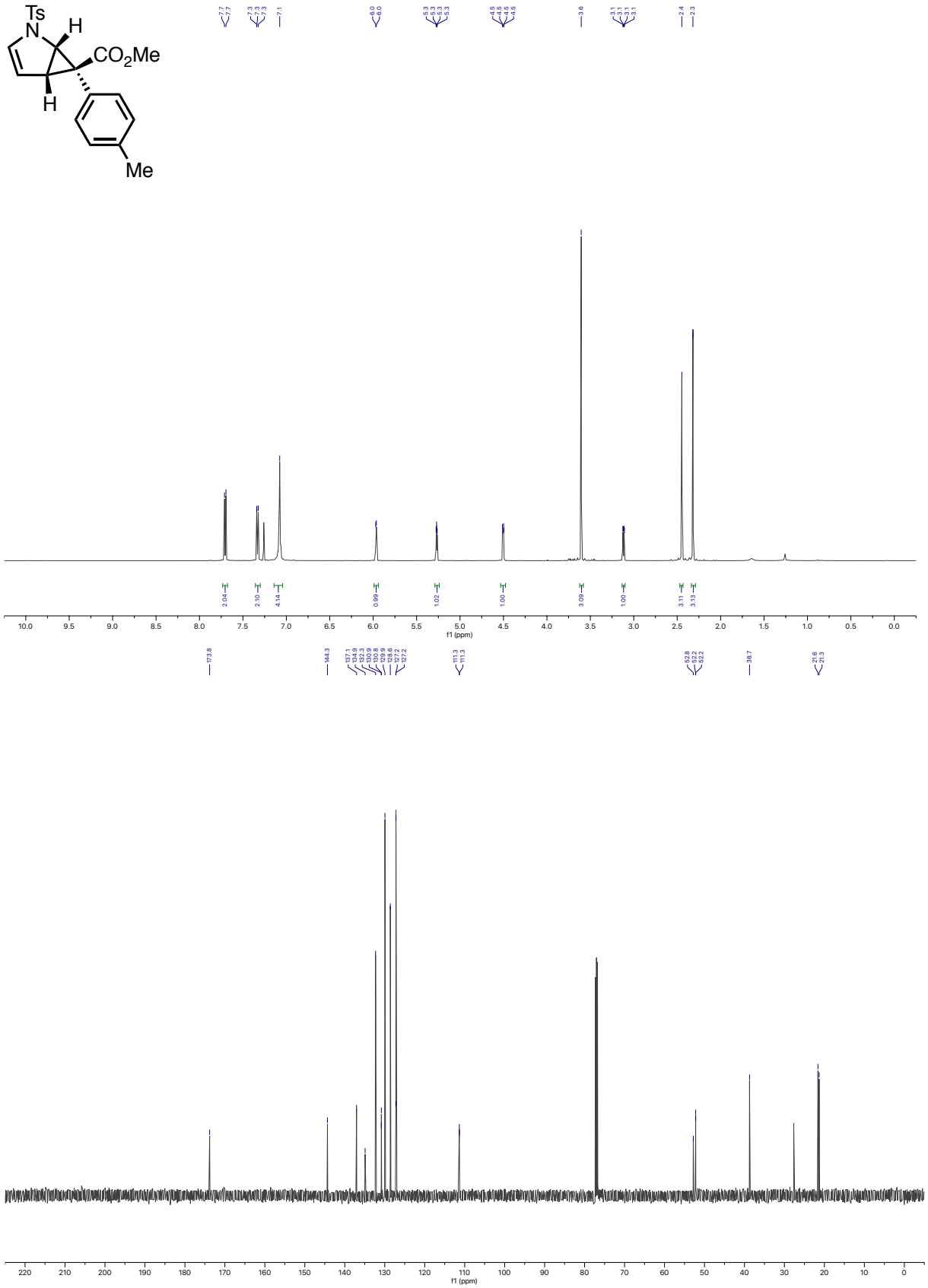
Ts
N
H
CO2Me
H
Me
f1 (ppm)
f1 (ppm)

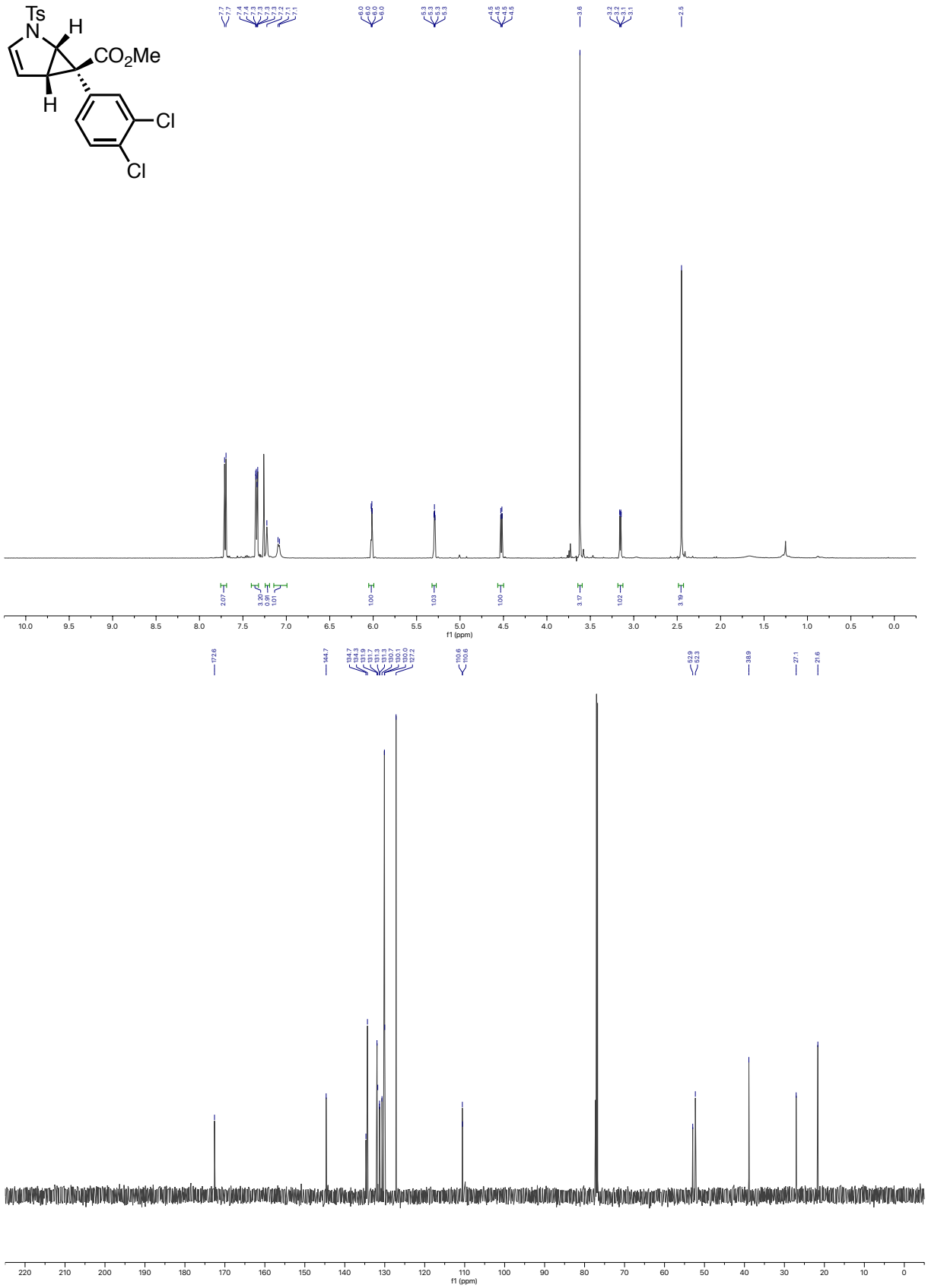
Ts
N
H
CO2Me
H
Cl
Cl
f1 (ppm)
f1 (ppm)

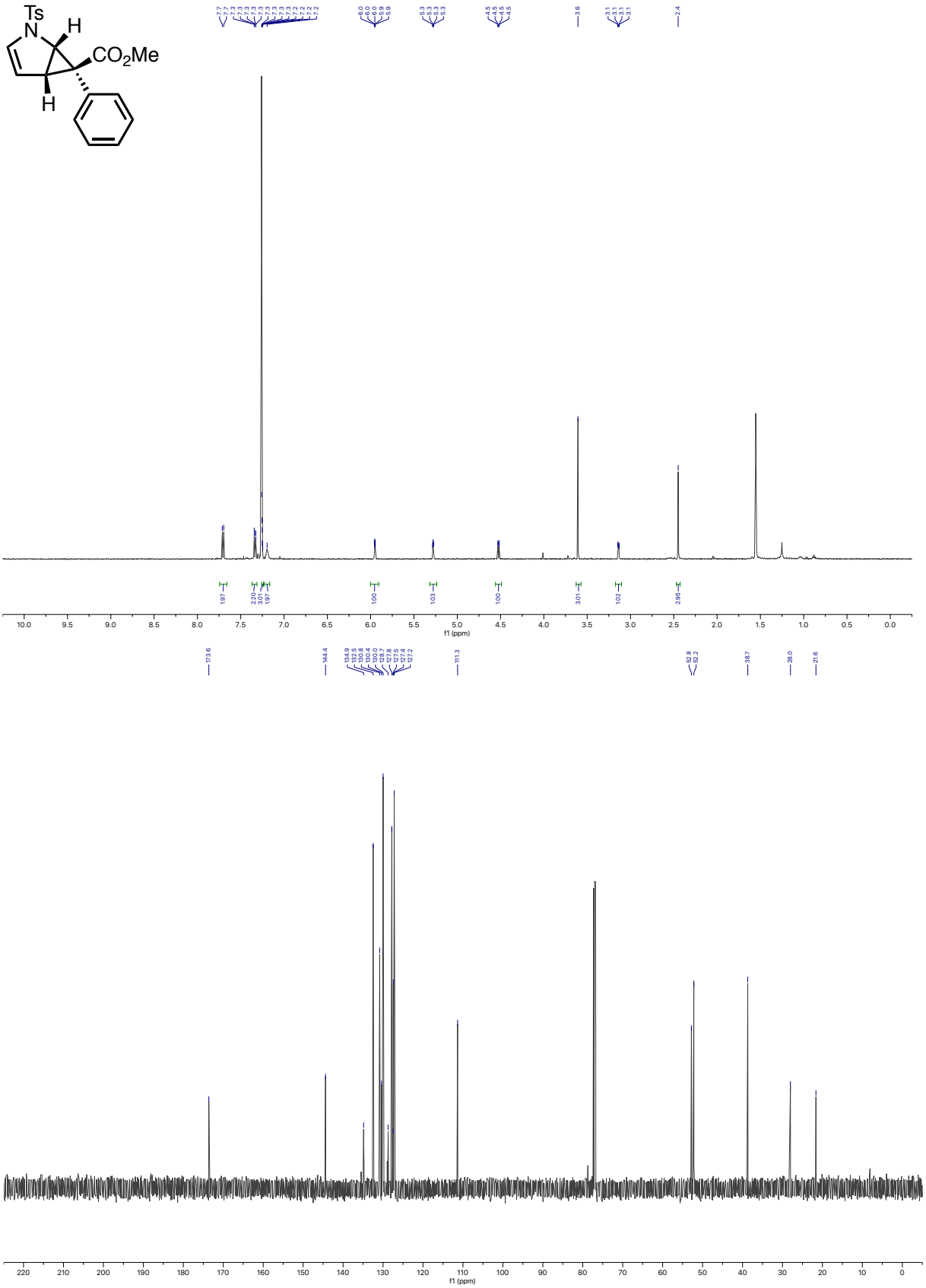
Ts
N
H
CO2Me
H
f1 (ppm)
f1 (ppm)

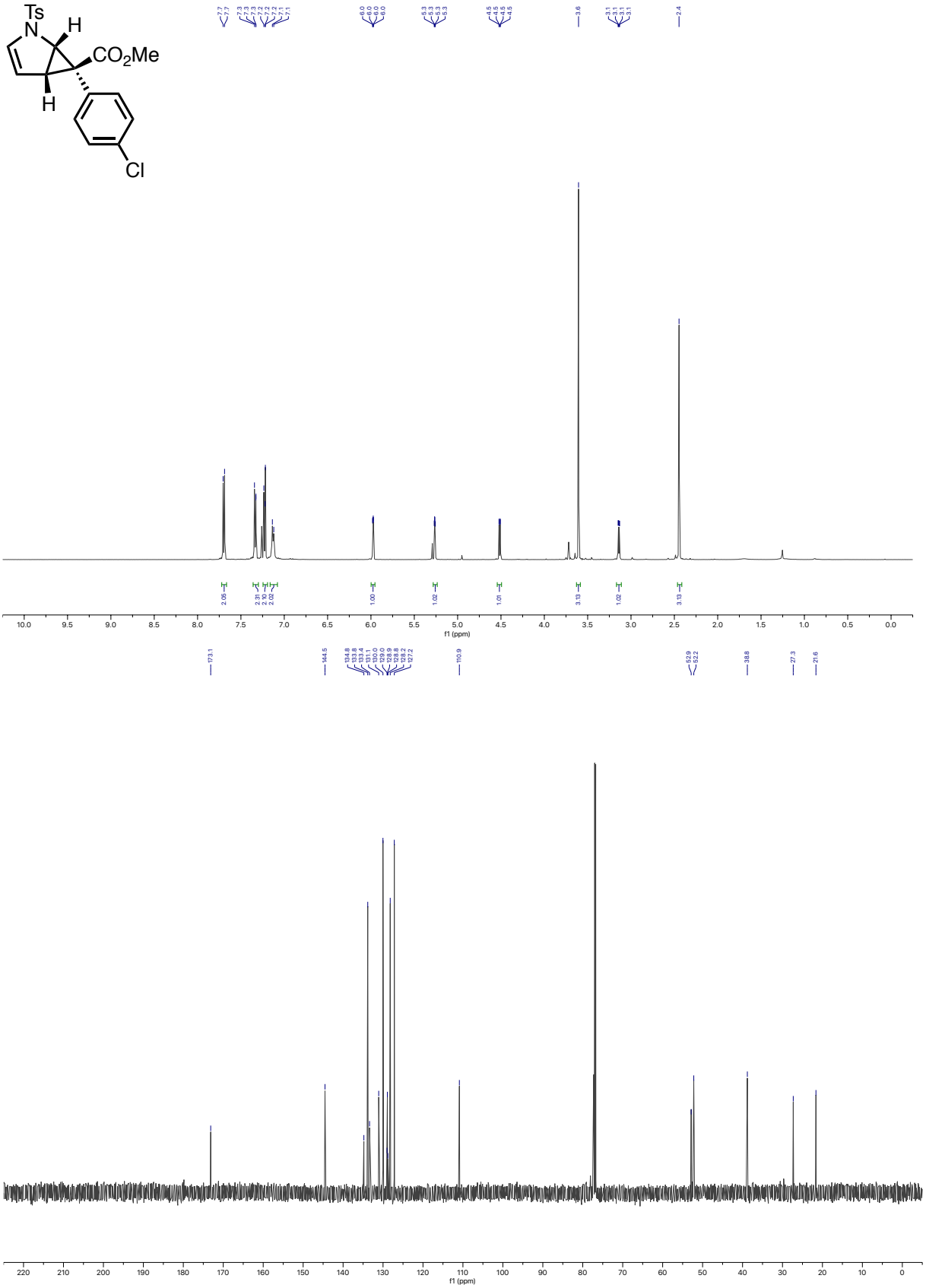
Ts
N
H
CO2Me
H
Cl
f1 (ppm)
f1 (ppm)

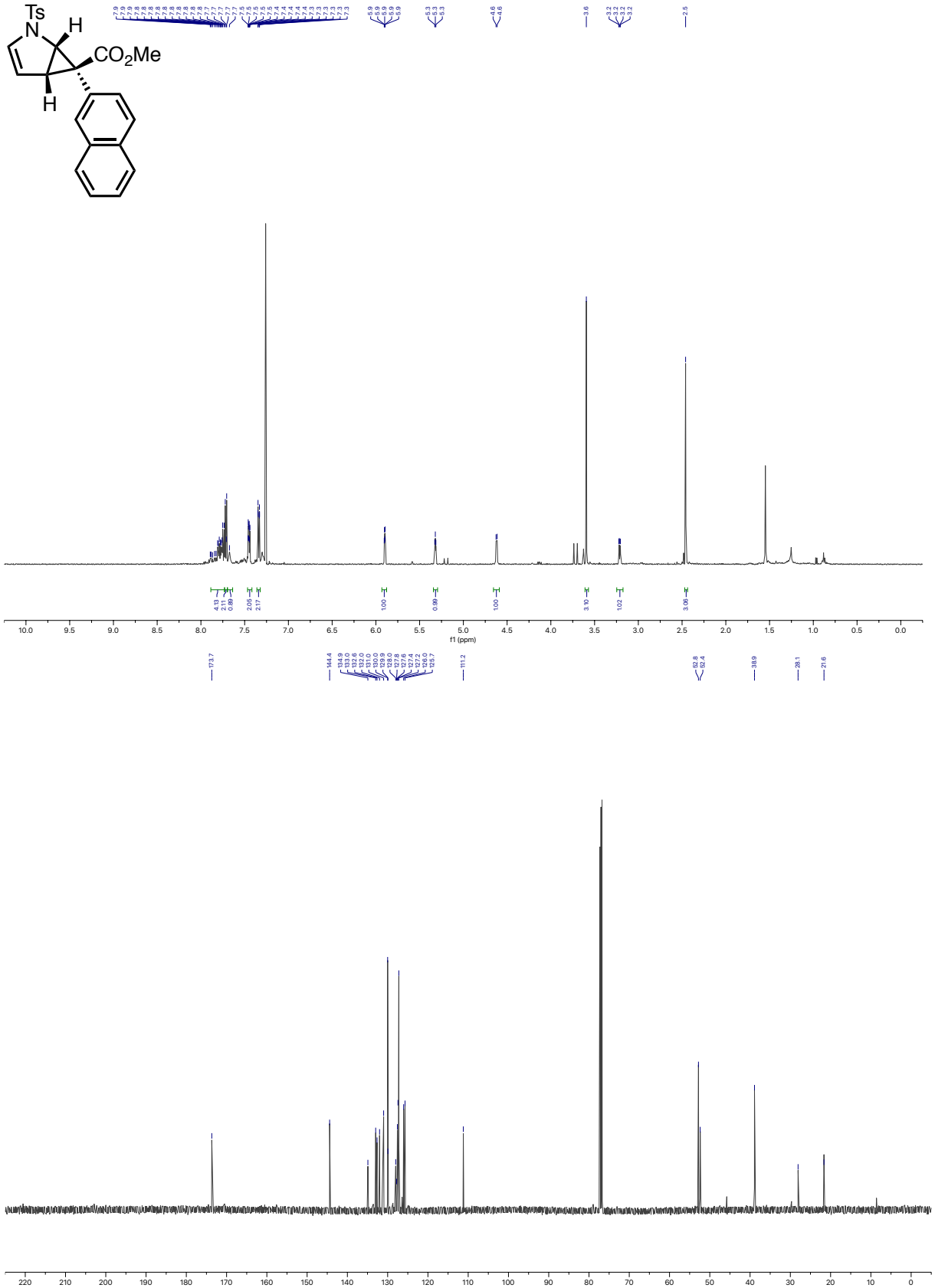
Ts
N
H
CO2Me
H
f1 (ppm)
f1 (ppm)

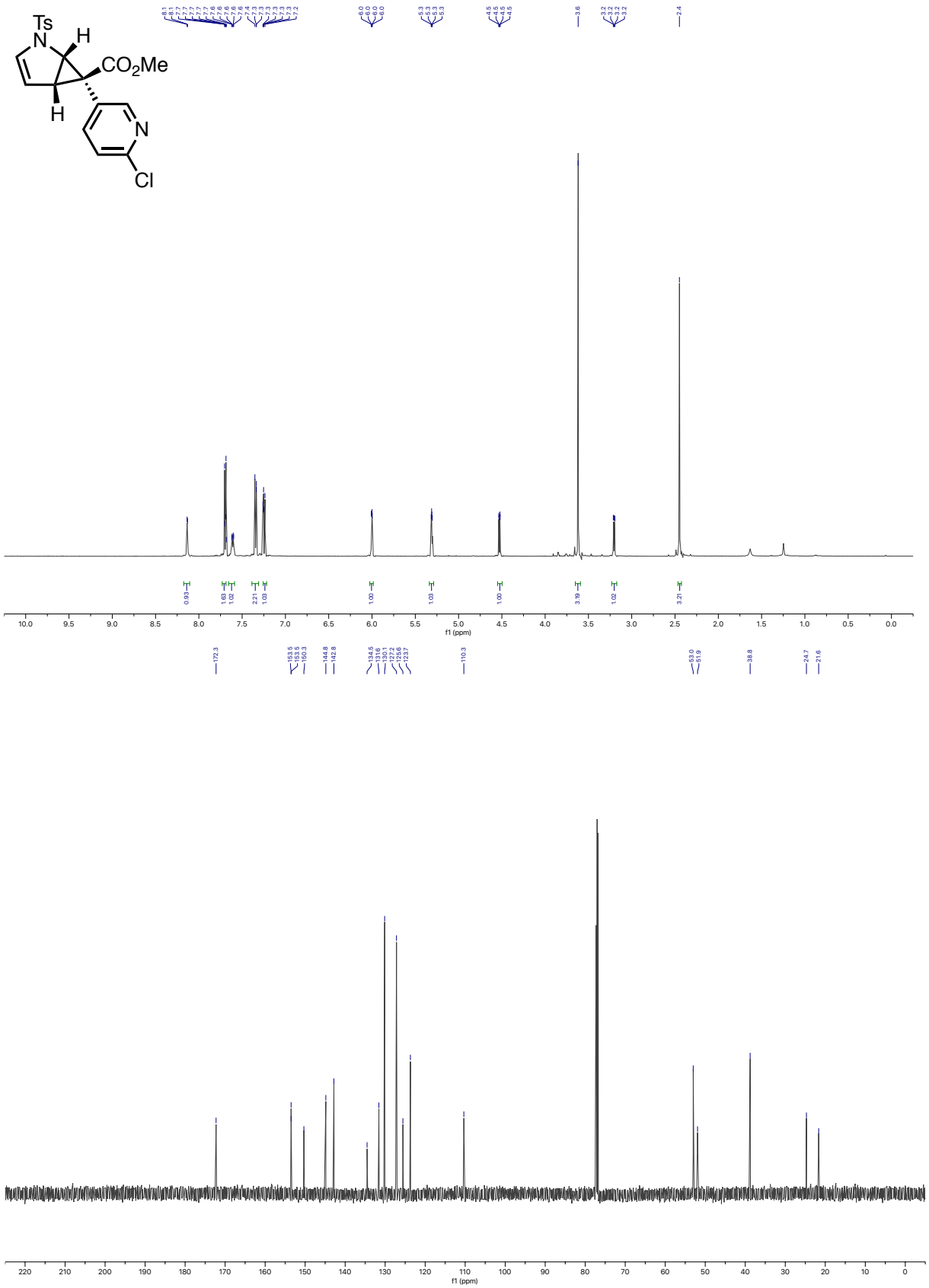
Ts
N
H
CO2Me
H
N
Cl
f1 (ppm)
f1 (ppm)

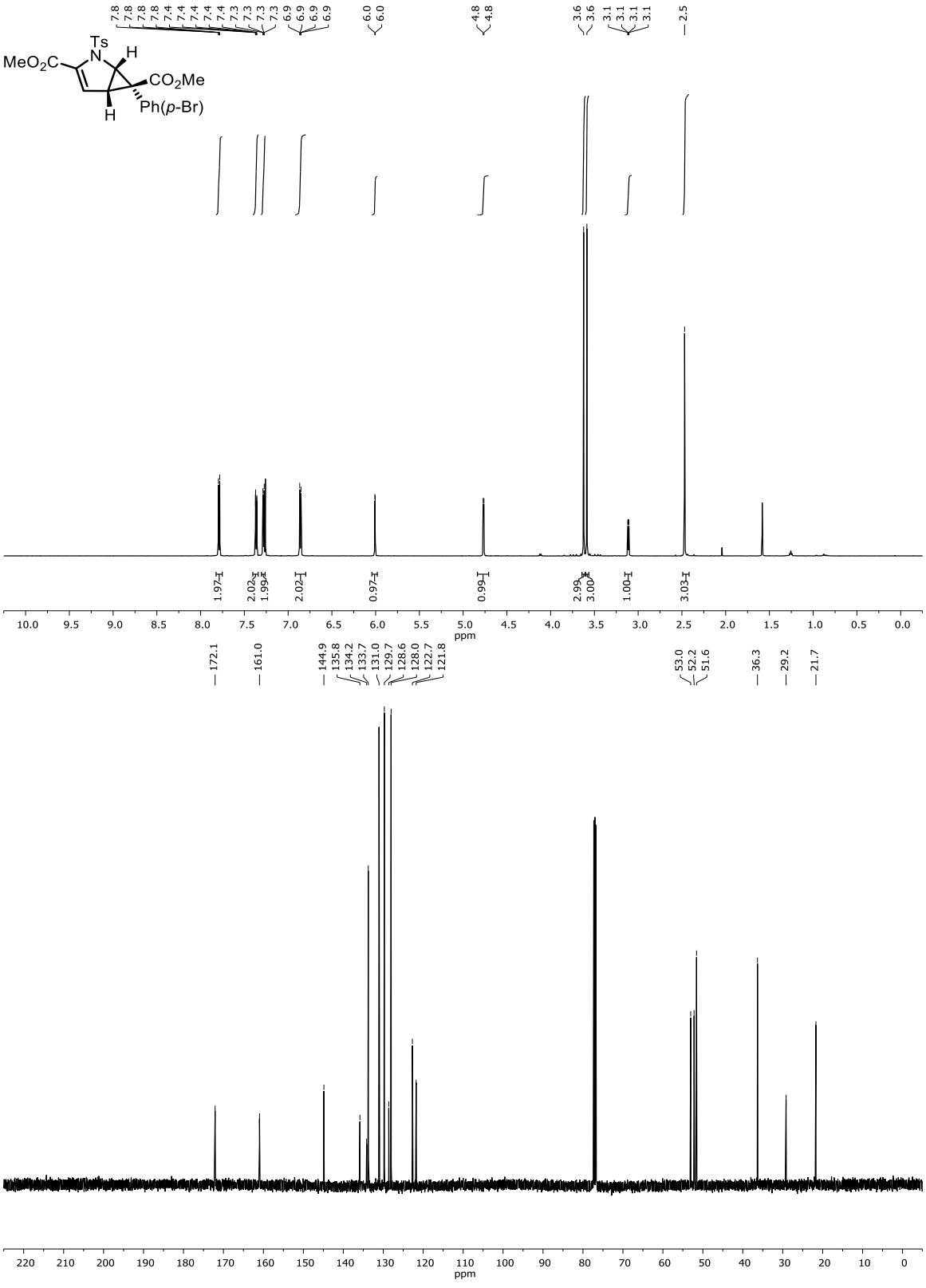
Ts
N
H
MeO2C
CO2Me
Ph(p-Br)
H
7.8 7.8 7.8 7.4 7.4 7.4 7.4 7.3 7.3 7.3 6.9 6.9 6.9
6.0 6.0
4.8 4.8
3.6 3.6 3.1 3.1 3.1 3.1
2.5
1.97 2.02 1.99 2.02 0.97 0.99 2.99 3.00 1.00 3.03
ppm
172.1 161.0 144.9 135.8 134.2 133.7 131.0 129.7 128.6 128.0 122.7 121.8
53.0 52.2 51.6 36.3 29.2 21.7
ppm

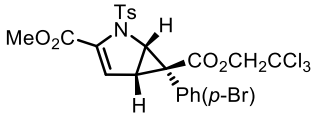
Ts
N
H
MeO2C
CO2CH2CCl3
Ph(p-Br)
H

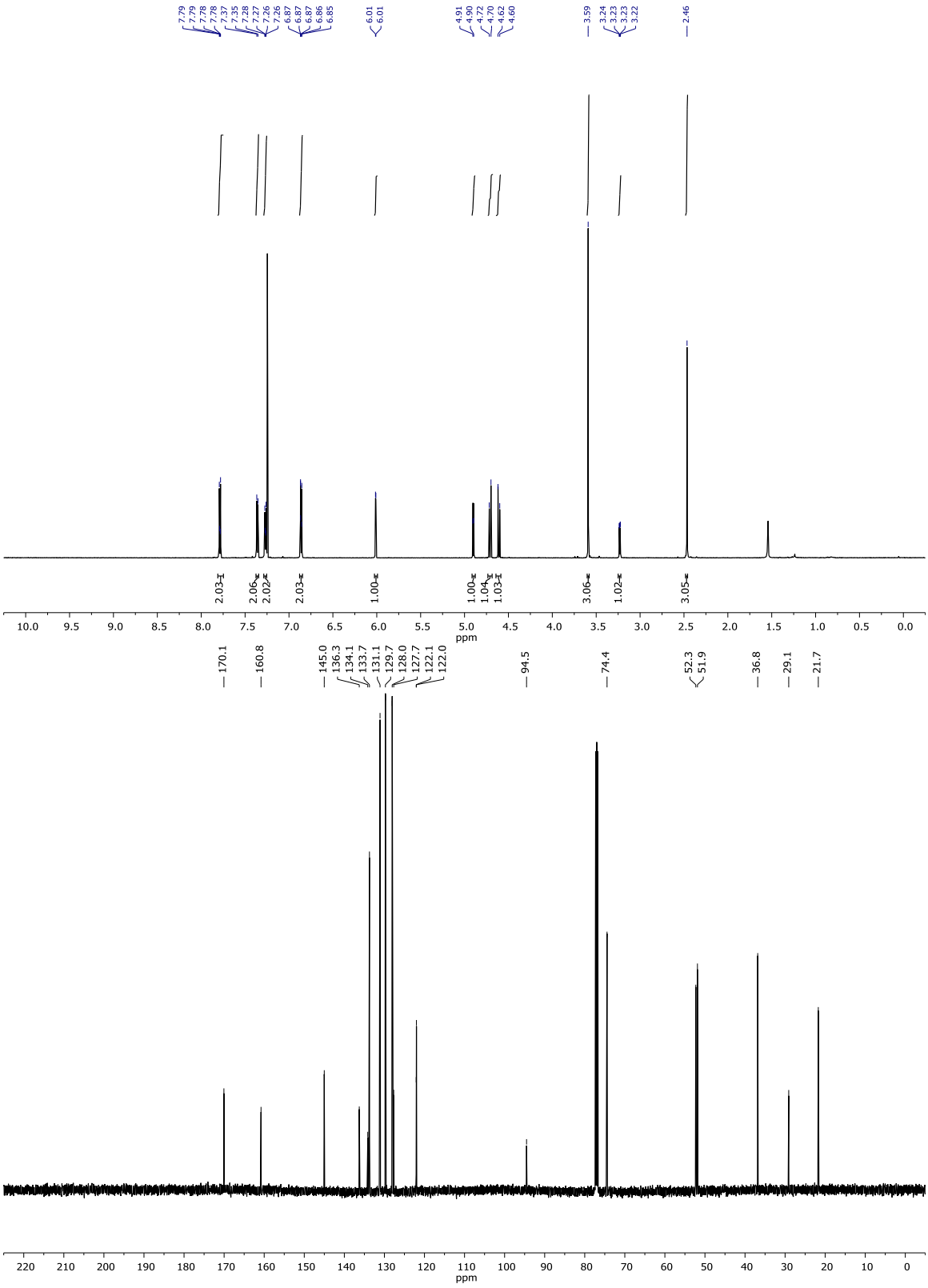
7.79
7.75
7.78
7.78
7.37
7.35
7.28
7.27
7.26
7.26
6.87
6.87
6.87
6.86
6.85
6.01
6.01
4.91
4.90
4.72
4.70
4.62
4.60
3.59
3.24
3.23
3.23
3.22
2.46
2.03
2.06
2.02
2.03
1.00
1.00
1.04
1.03
3.06
1.02
3.05
ppm
170.1
160.8
145.0
136.3
134.1
133.7
131.1
129.7
128.0
127.7
122.1
122.0
94.5
74.4
52.3
51.9
36.8
29.1
21.7
ppm

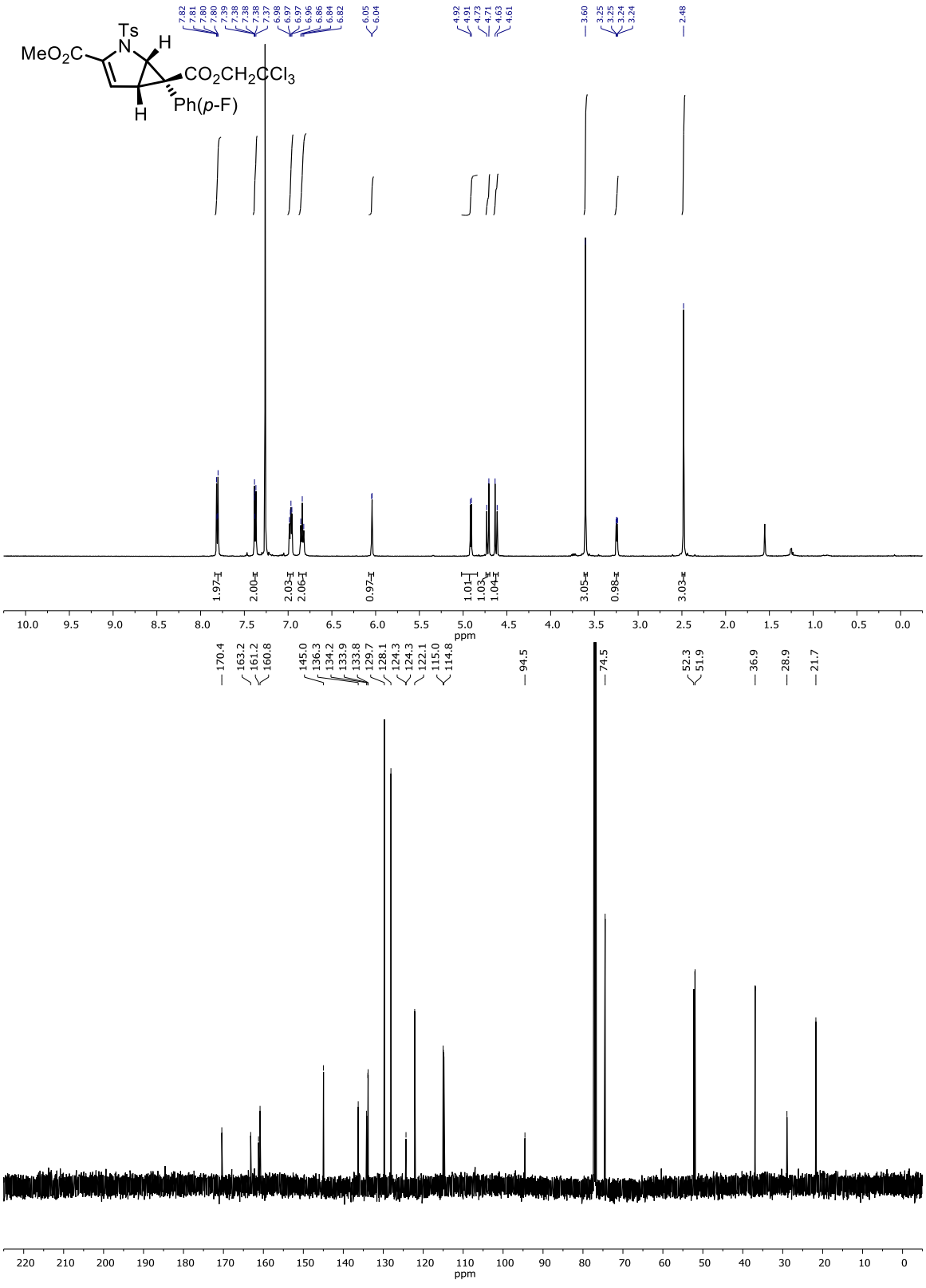
Ts
N
H
MeO2C
CO2CH2CCl3
Ph(p-F)
H
7.82
7.81
7.80
7.80
7.39
7.38
7.38
7.38
7.37
6.98
6.97
6.97
6.96
6.86
6.84
6.82
6.05
6.04
4.92
4.91
4.73
4.71
4.63
4.61
3.60
3.25
3.25
3.24
3.24
2.48
1.97
2.00
2.03
2.06
0.97
1.01
1.03
1.04
3.05
0.98
3.03
ppm
170.4
163.2
161.2
160.8
145.0
136.3
134.2
133.9
133.8
129.7
128.1
124.3
124.3
122.1
115.0
114.8
94.5
74.5
52.3
51.9
36.9
28.9
21.7
ppm

^{19}F-NMR (282 MHz, $CDCl_3$)

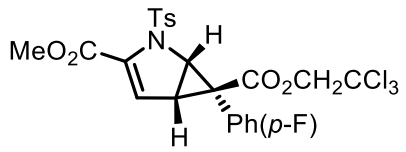

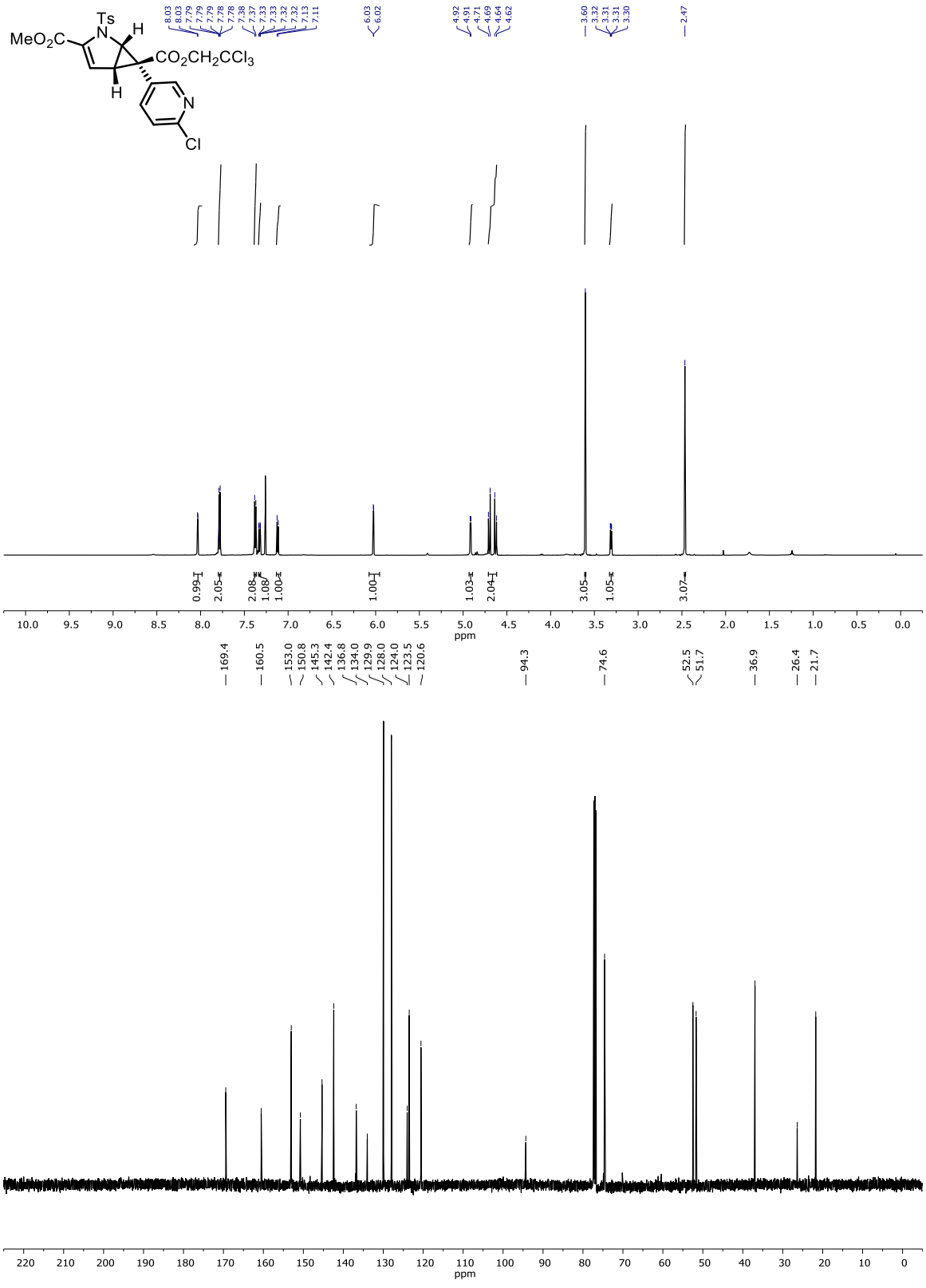
Ts
N
H
MeO2C
CO2CH2CCl3
H
N
Cl
8.03
8.03
7.79
7.79
7.79
7.78
7.78
7.38
7.37
7.33
7.33
7.32
7.32
7.13
7.11
6.03
6.02
4.92
4.91
4.71
4.69
4.64
4.62
3.60
3.32
3.31
3.31
3.30
2.47
0.99
2.05
2.08
1.08
1.00
1.00
1.03
2.04
3.05
1.05
3.07
ppm
169.4
160.5
153.0
150.8
145.3
142.4
136.8
134.0
129.9
128.0
124.0
123.5
120.6
94.3
74.6
52.5
51.7
36.9
26.4
21.7
ppm

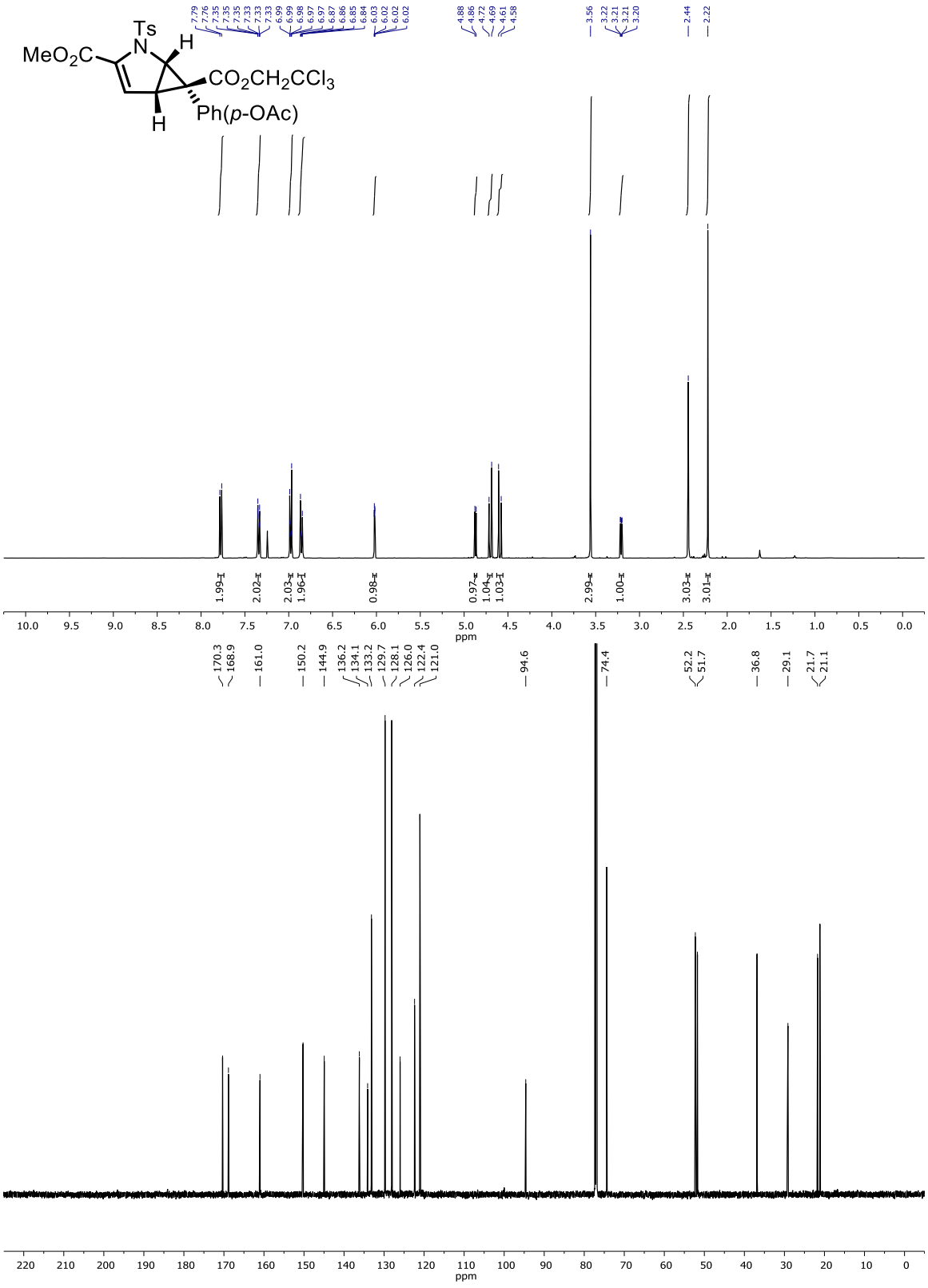
Ts
N
H
MeO2C
CO2CH2CCl3
Ph(p-OAc)
H
7.79
7.76
7.35
7.35
7.35
7.33
7.33
7.33
6.99
6.99
6.98
6.97
6.97
6.87
6.86
6.85
6.84
6.03
6.02
6.02
6.02
4.88
4.86
4.72
4.69
4.61
4.58
3.56
3.22
3.21
3.21
3.20
2.44
2.22
1.99
2.02
2.03
1.96
0.98
0.97
1.04
1.03
2.99
1.00
3.03
3.01
ppm
170.3
168.9
161.0
150.2
144.9
136.2
134.1
133.2
129.7
128.1
126.0
122.4
121.0
94.6
74.4
52.2
51.7
36.8
29.1
21.7
21.1
ppm

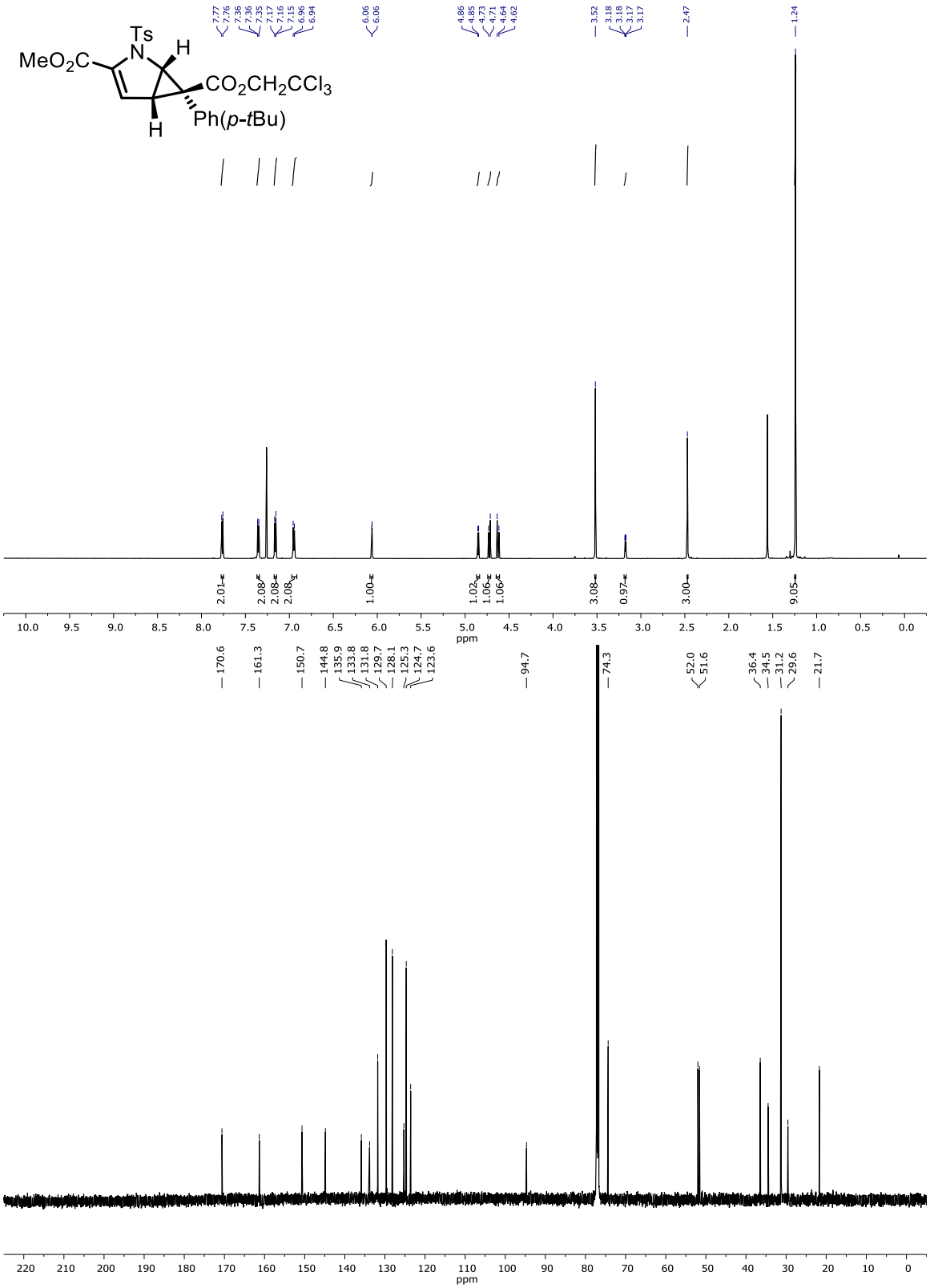
Ts
N
H
MeO2C
CO2CH2CCl3
Ph(p-tBu)
H
7.77
7.76
7.36
7.36
7.35
7.17
7.16
7.15
6.96
6.94
6.06
6.06
4.86
4.85
4.73
4.71
4.64
4.62
3.52
3.18
3.18
3.17
3.17
2.47
1.24
2.01
2.08
2.08
2.08
1.00
1.02
1.06
1.06
3.08
0.97
3.00
9.05
ppm
170.6
161.3
150.7
144.8
135.9
133.8
131.8
129.7
128.1
125.3
124.7
123.6
94.7
74.3
52.0
51.6
36.4
34.5
31.2
29.6
21.7
ppm

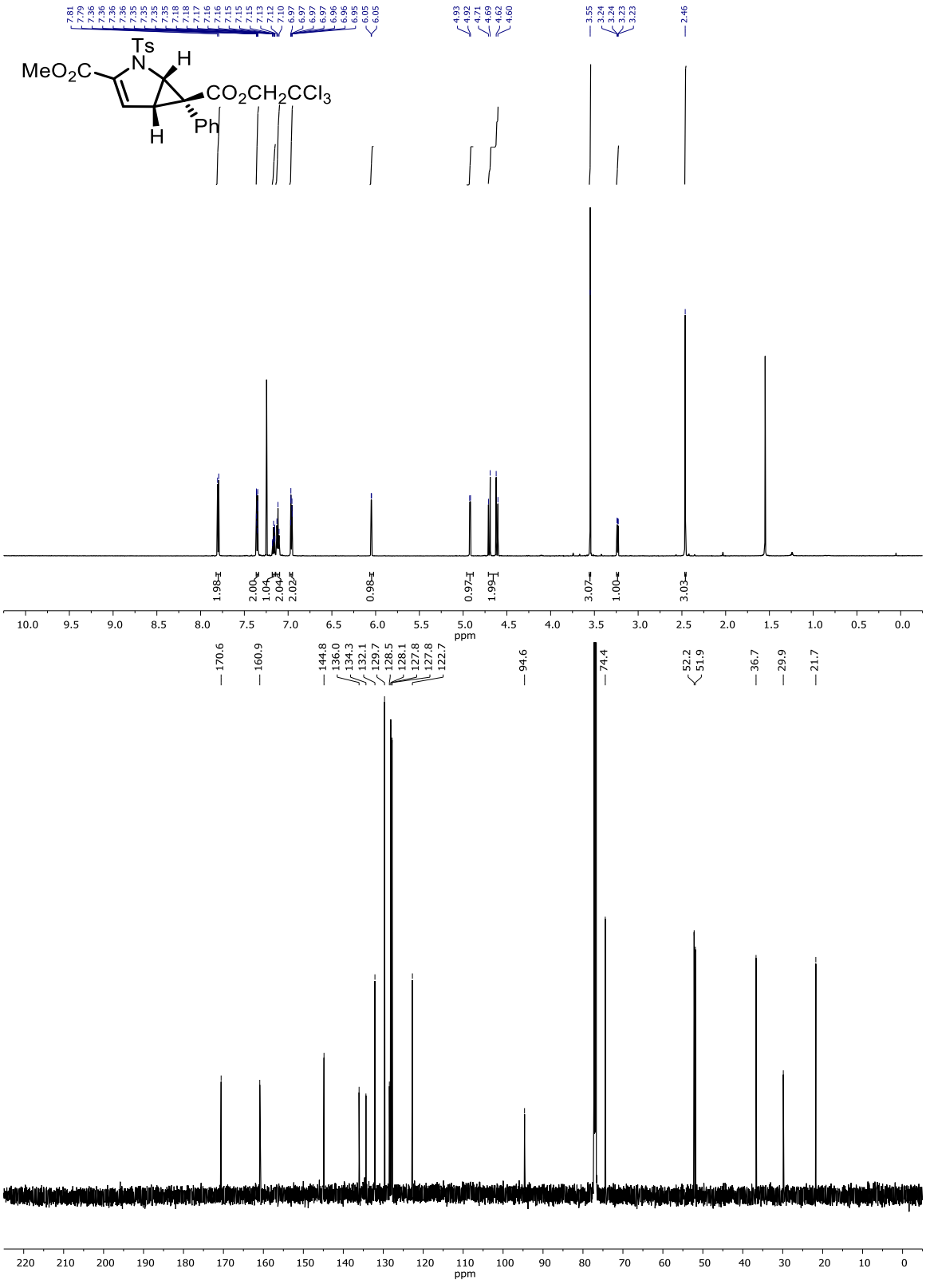
Ts
N
H
MeO2C
CO2CH2CCl3
Ph
H
7.81 7.79 7.36 7.36 7.36 7.36 7.35 7.35 7.35 7.35 7.18 7.18 7.17 7.16 7.16 7.15 7.15 7.13 7.12 7.10 6.97 6.97 6.97 6.96 6.96 6.95 6.05 6.05
4.93 4.92 4.71 4.69 4.62 4.60
3.55 3.24 3.24 3.23 3.23
2.46
1.98 2.00 1.04 2.04 2.02 0.98 0.97 1.99 3.07 1.00 3.03
ppm
170.6 160.9 144.8 136.0 134.3 132.1 129.7 128.5 128.1 127.8 127.8 122.7 94.6 74.4 52.2 51.9 36.7 29.9 21.7
ppm

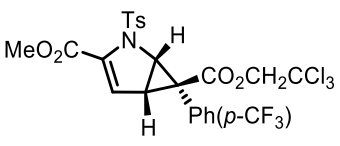
Ts
N
H
MeO2C
CO2CH2CCl3
Ph(p-CF3)
H

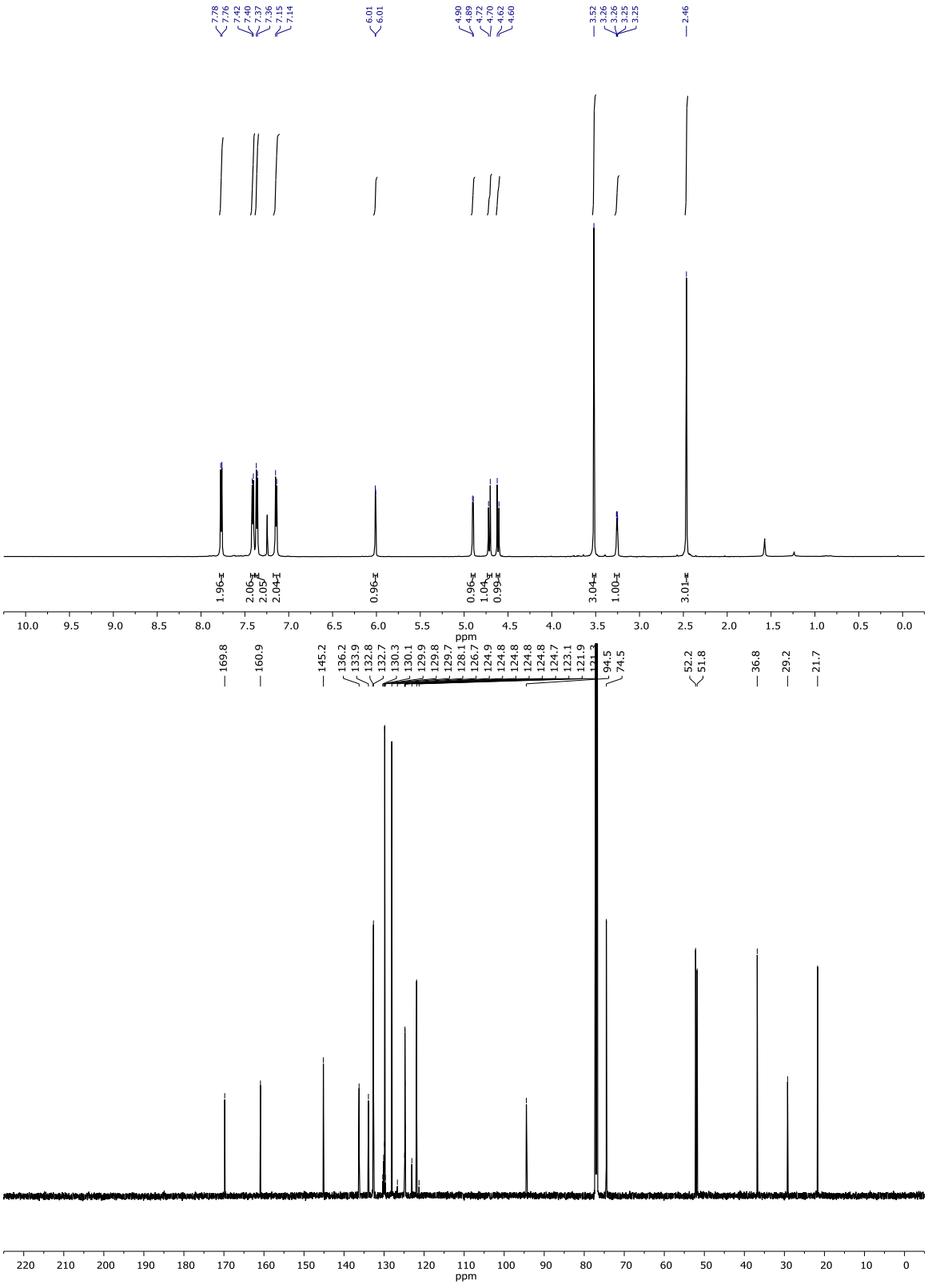
7.78
7.76
7.42
7.40
7.37
7.36
7.15
7.14
6.01
6.01
4.90
4.89
4.72
4.70
4.62
4.60
3.52
3.26
3.26
3.25
3.25
2.46
1.96
2.06
2.05
2.04
0.96
0.96
1.04
0.99
3.04
1.00
3.01
ppm
169.8
160.9
145.2
136.2
133.9
132.8
132.7
130.3
130.1
129.9
129.8
129.7
128.1
126.7
124.9
124.8
124.8
124.8
124.7
123.1
121.9
121.3
94.5
74.5
52.2
51.8
36.8
29.2
21.7
ppm

^{19}F-NMR (282 MHz, $CDCl_3$)

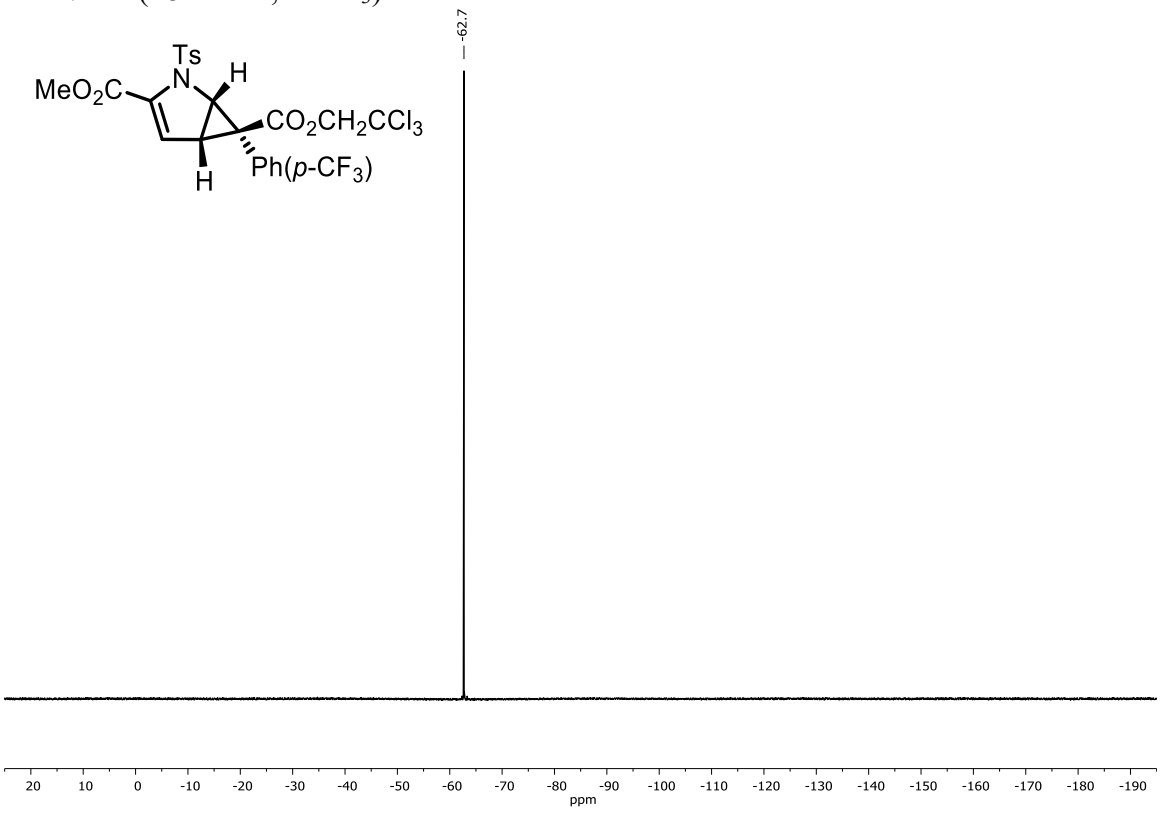

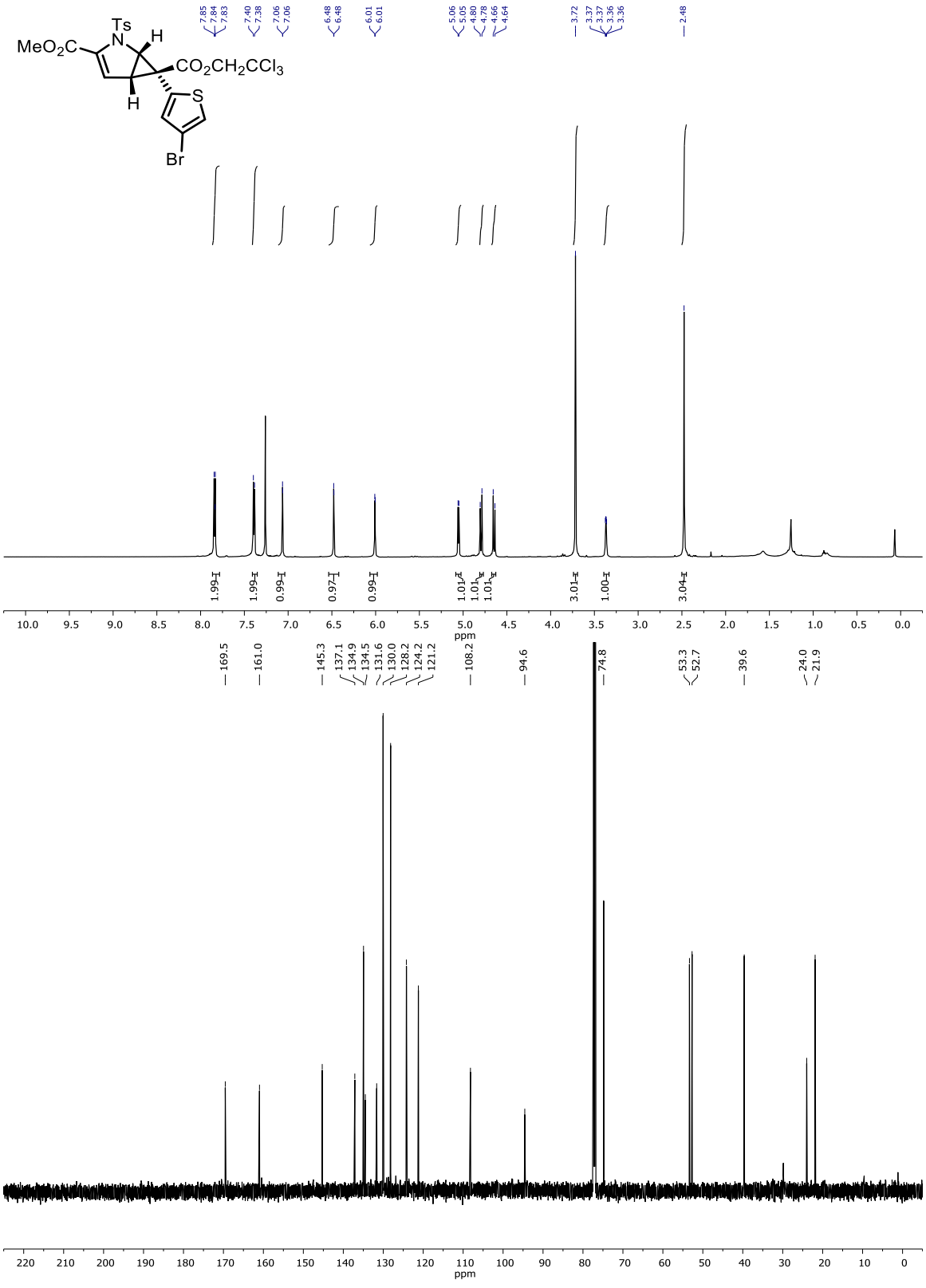
Ts
N
H
MeO2C
CO2CH2CCl3
H
S
Br
7.85
7.84
7.83
7.40
7.38
7.06
7.06
6.48
6.48
6.01
6.01
5.06
5.05
4.80
4.78
4.66
4.64
3.72
3.37
3.37
3.36
3.36
2.48
1.99
1.99
0.99
0.97
0.99
1.01
1.01
1.01
3.01
1.00
3.04
ppm
169.5
161.0
145.3
137.1
134.9
134.5
131.6
130.0
128.2
124.2
121.2
108.2
94.6
74.8
53.3
52.7
39.6
24.0
21.9
ppm

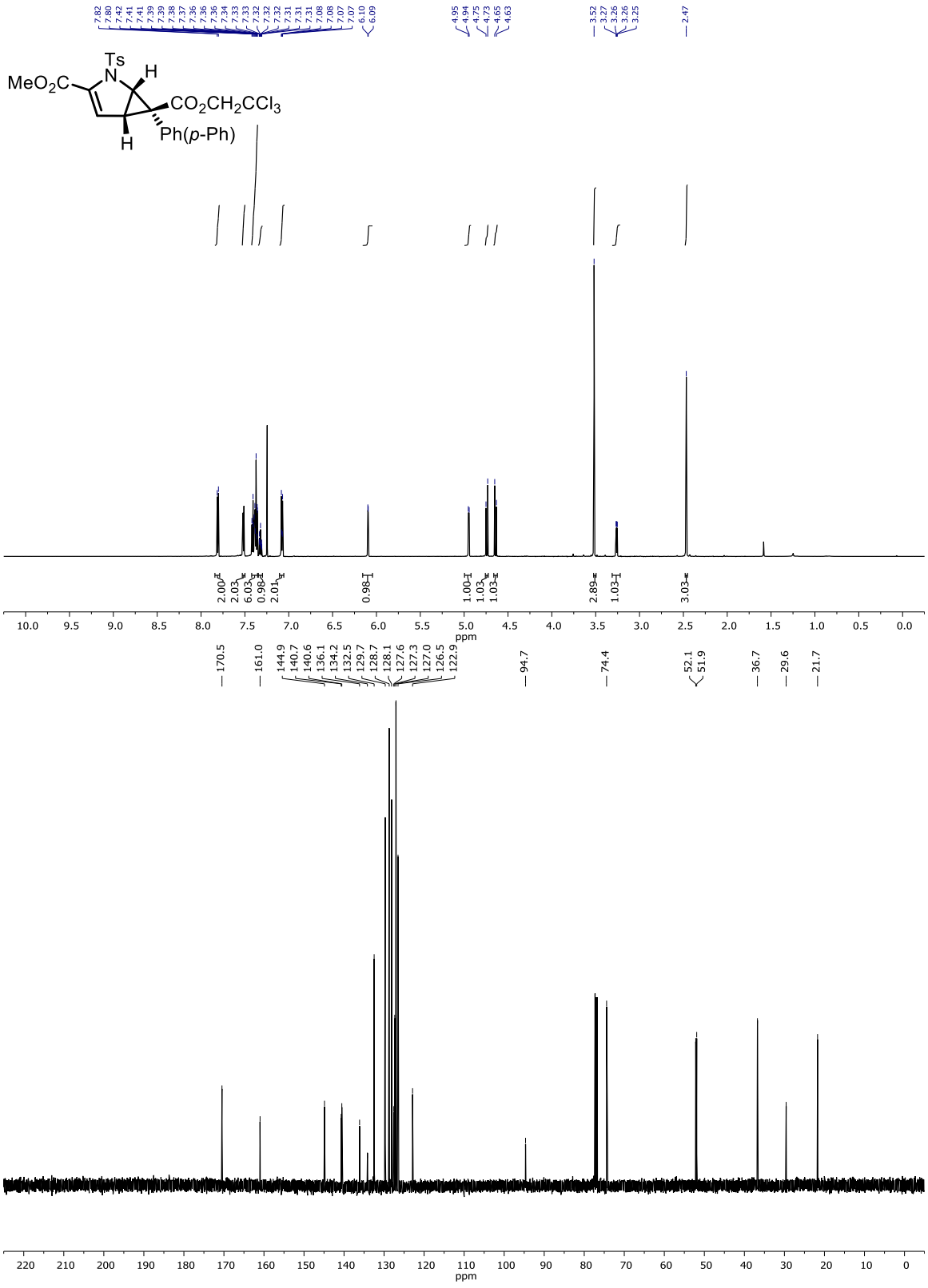
Ts
N
H
MeO2C
CO2CH2CCl3
Ph(p-Ph)
H
ppm
ppm

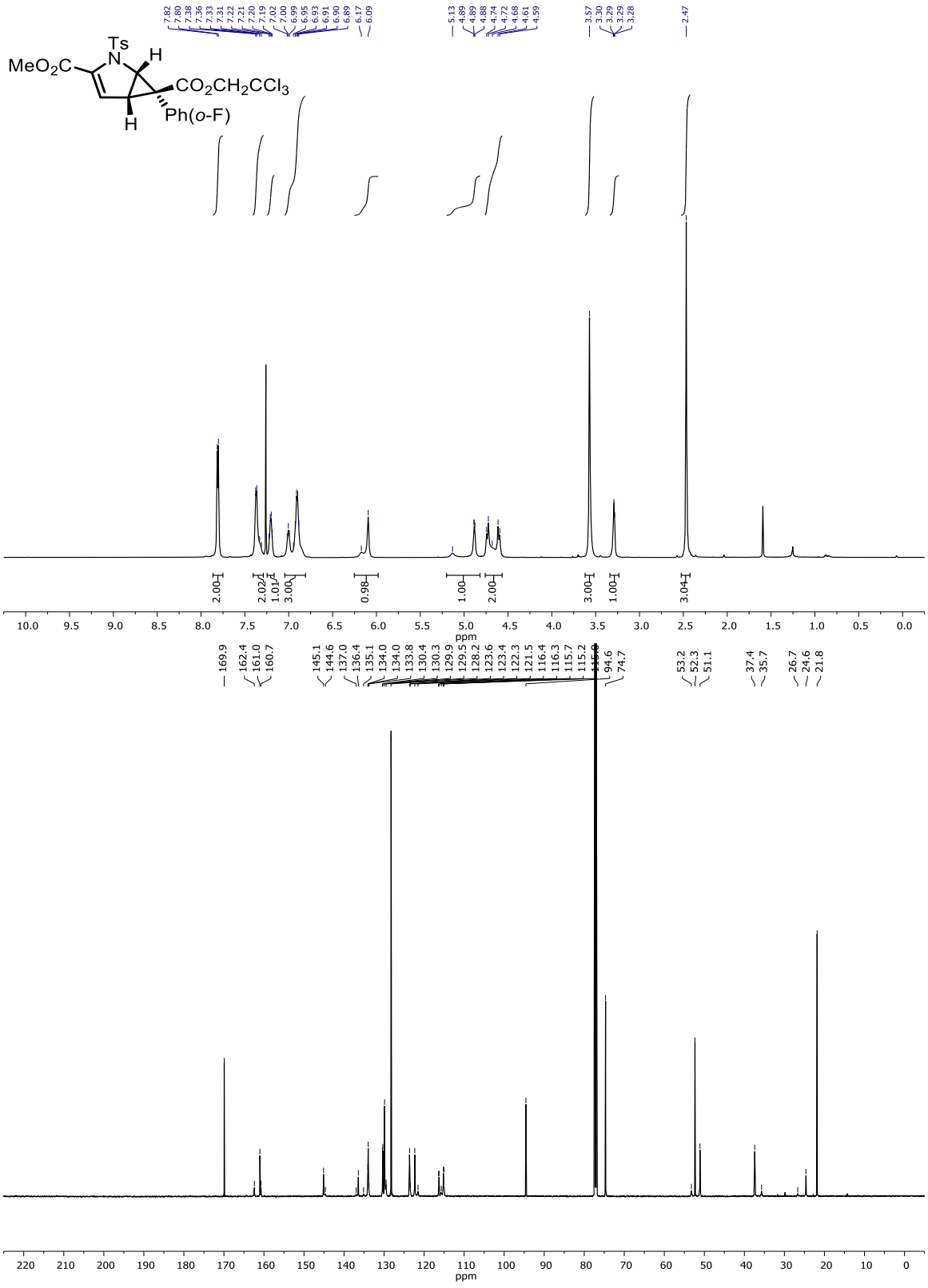
Ts
N
H
MeO2C
CO2CH2CCl3
Ph(o-F)
H
7.82
7.80
7.38
7.36
7.33
7.31
7.22
7.21
7.20
7.19
7.02
7.00
6.99
6.95
6.93
6.91
6.90
6.89
6.17
6.09
5.13
4.89
4.89
4.88
4.74
4.72
4.68
4.61
4.59
3.57
3.30
3.29
3.29
3.28
2.47
2.00
2.02
1.01
3.00
0.98
1.00
2.00
3.00
1.00
3.04
ppm
169.9
162.4
161.0
160.7
145.1
144.6
137.0
136.4
135.1
134.0
134.0
133.8
130.4
130.3
129.9
129.5
128.2
123.6
123.4
122.3
121.5
116.4
116.3
115.7
115.2
94.6
74.7
53.2
52.3
51.1
37.4
35.7
26.7
24.6
21.8
ppm

^{19}F-NMR (282 MHz, $CDCl_3$)

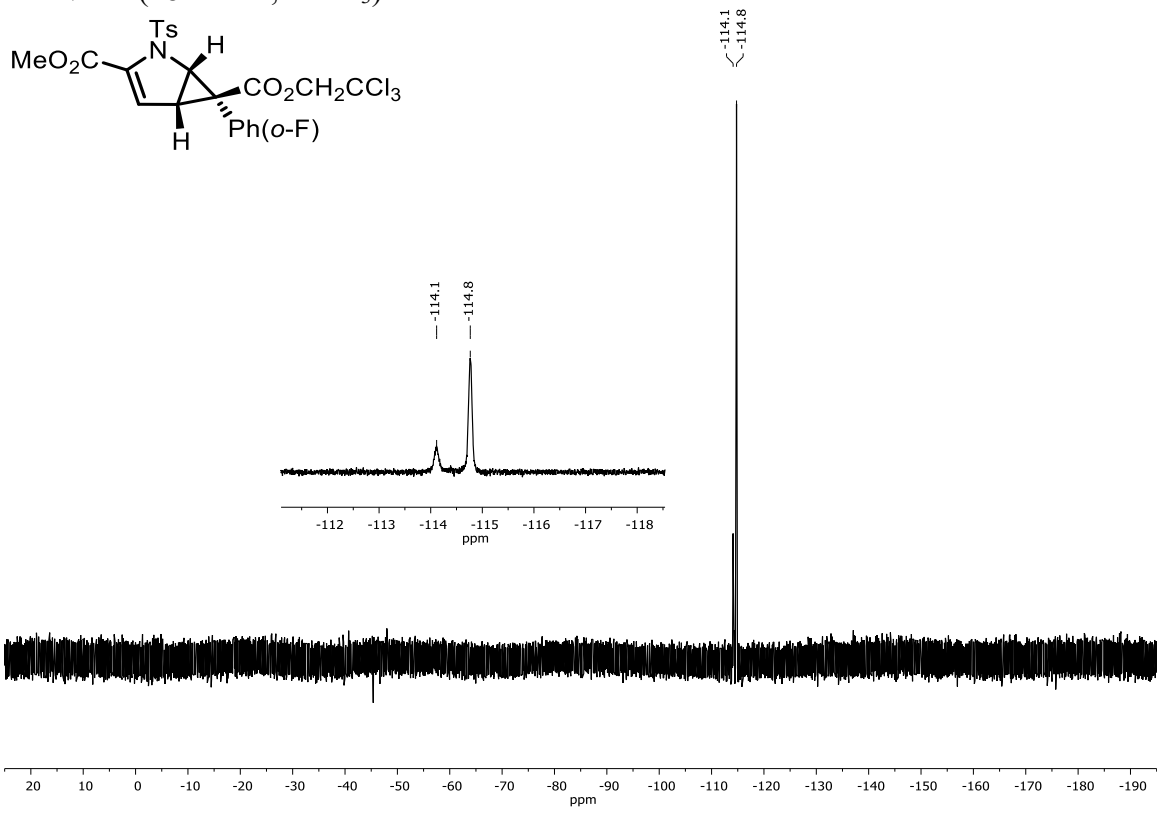

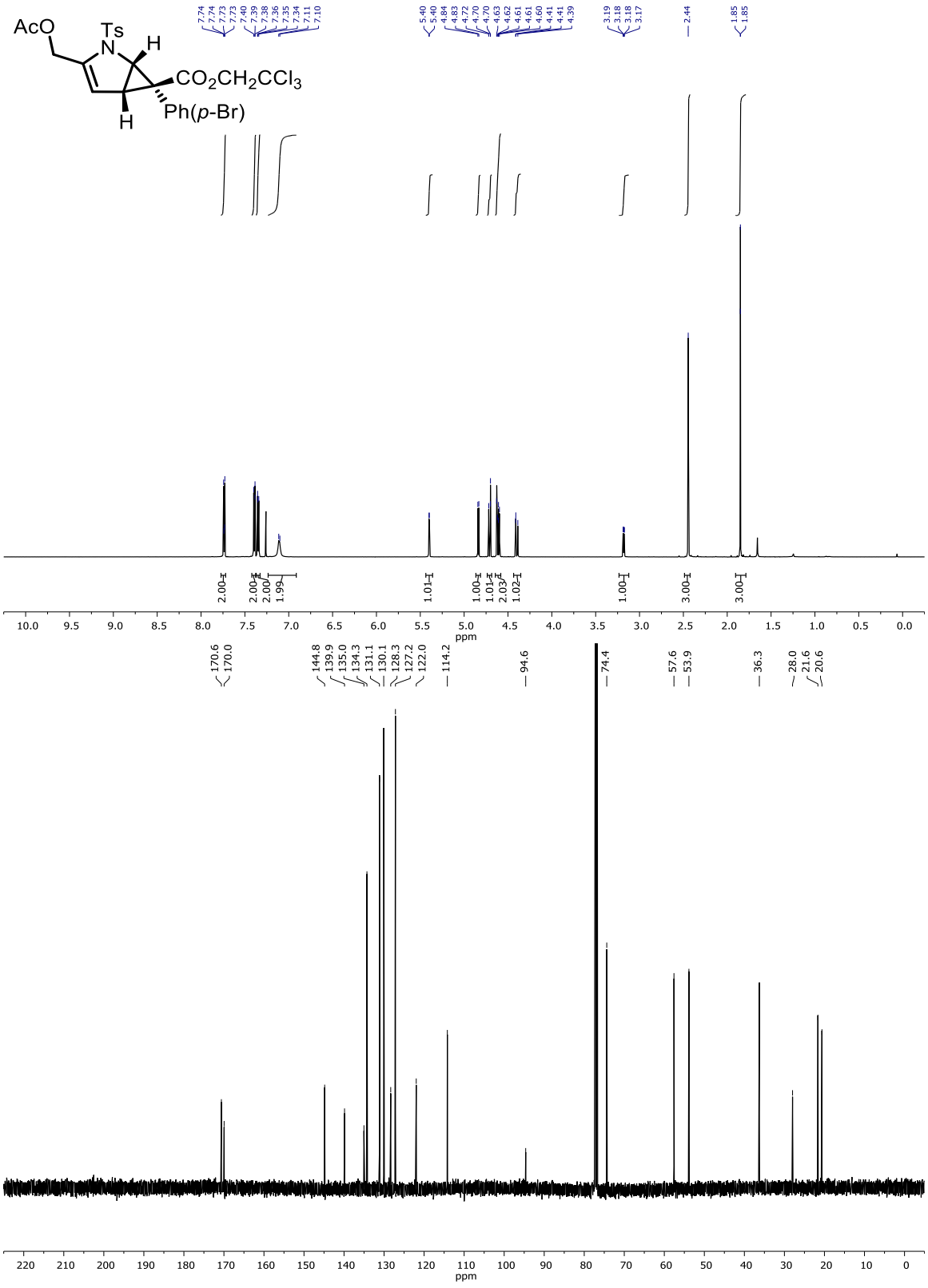
AcO
Ts
N
H
H
CO2CH2CCl3
Ph(p-Br)
7.74
7.74
7.73
7.73
7.40
7.39
7.38
7.36
7.35
7.34
7.11
7.10
5.40
5.40
4.84
4.83
4.72
4.70
4.70
4.65
4.62
4.61
4.61
4.60
4.41
4.41
4.39
3.19
3.18
3.18
3.17
2.44
1.85
1.85
2.00
2.00
2.00
1.99
1.01
1.00
1.01
2.03
1.02
1.00
3.00
3.00
ppm
170.6
170.0
144.8
139.9
135.0
134.3
131.1
130.1
128.3
127.2
122.0
114.2
94.6
74.4
57.6
53.9
36.3
28.0
21.6
20.6
ppm

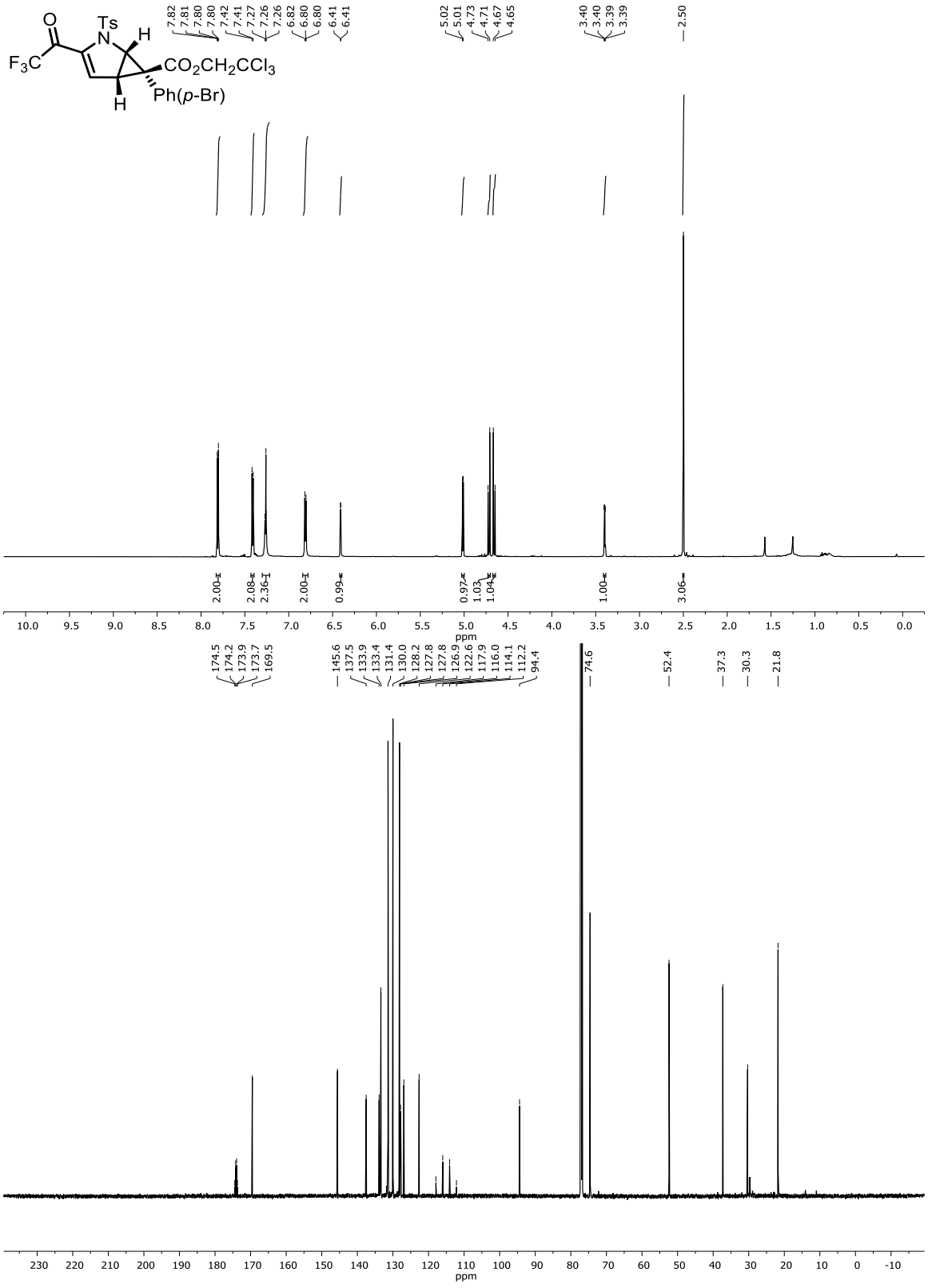
O
Ts
N
H
F3C
CO2CH2CCl3
Ph(p-Br)
H
7.82
7.81
7.80
7.80
7.42
7.41
7.27
7.26
7.26
6.82
6.80
6.80
6.41
6.41
5.02
5.01
4.73
4.71
4.67
4.65
3.40
3.40
3.39
3.39
2.50
2.00
2.08
2.36
2.00
0.99
0.97
1.03
1.04
1.00
3.06
ppm
174.5
174.2
173.9
173.7
169.5
145.6
137.5
133.9
133.4
131.4
130.0
128.2
127.8
127.8
126.9
122.6
117.9
116.0
114.1
112.2
94.4
74.6
52.4
37.3
30.3
21.8
ppm

^{19}F-NMR (282 MHz, $CDCl_3$)

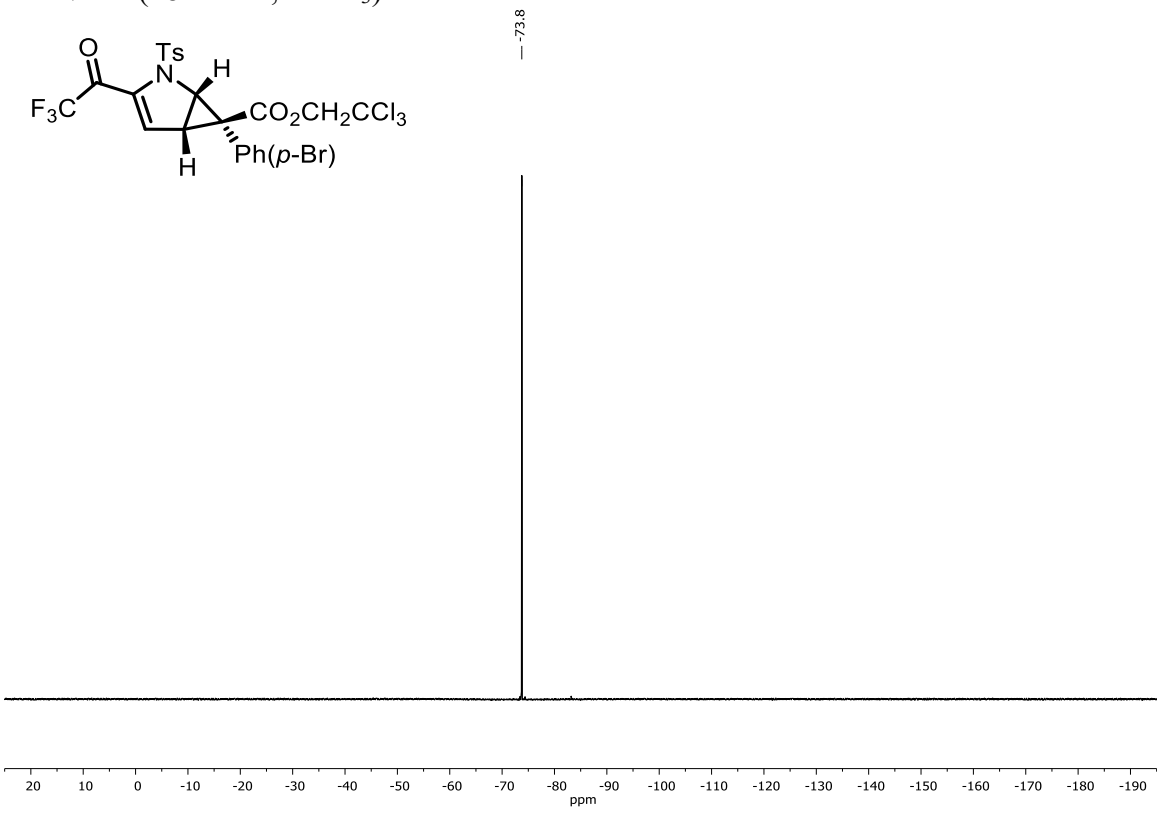

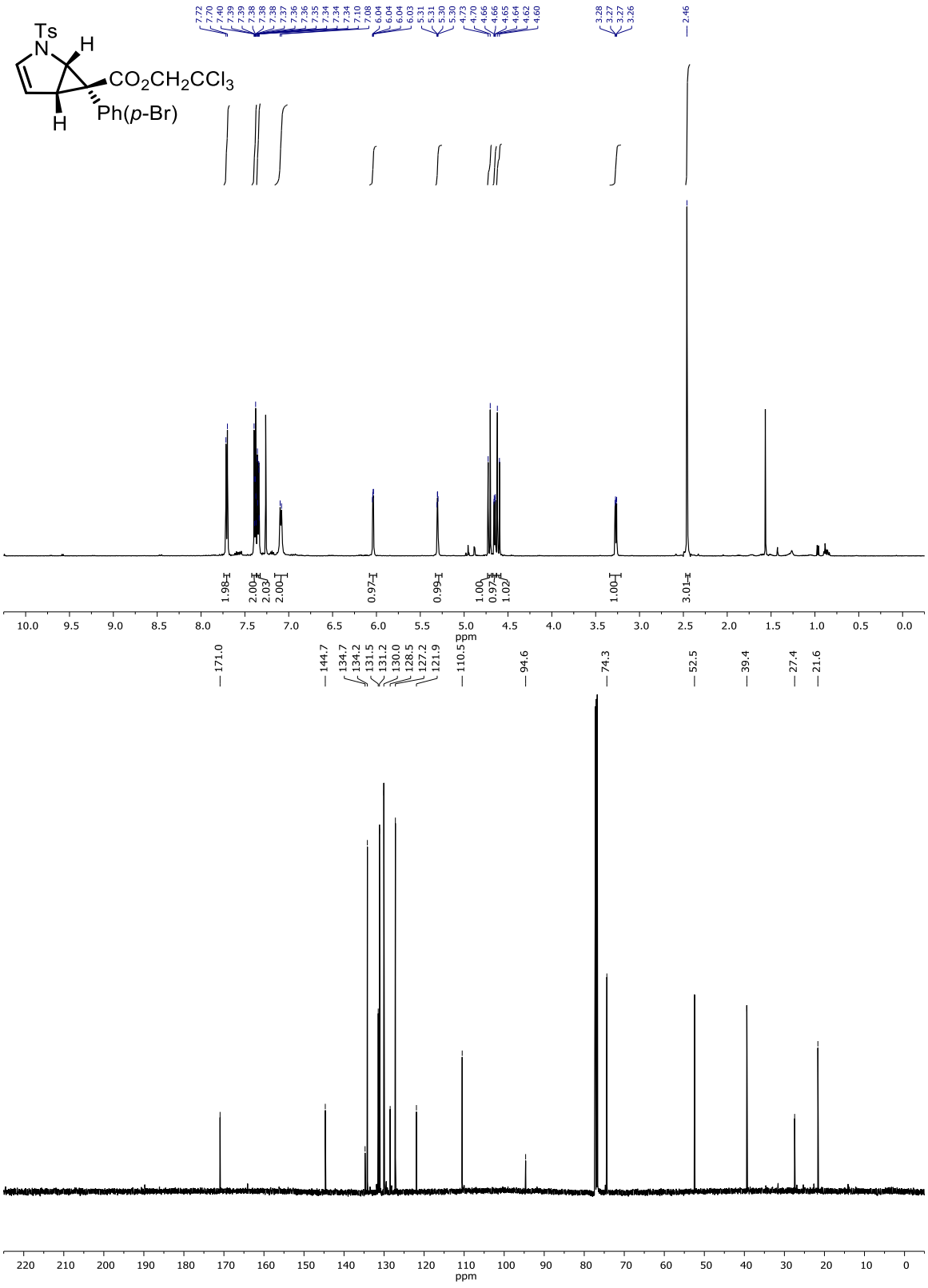
Ts
N
H
CO2CH2CCl3
Ph(p-Br)
H
7.72
7.70
7.40
7.39
7.39
7.38
7.38
7.38
7.37
7.36
7.36
7.35
7.34
7.34
7.34
7.10
7.08
6.04
6.04
6.04
6.03
5.31
5.31
5.30
5.30
5.73
4.70
4.66
4.66
4.65
4.64
4.62
4.60
3.28
3.27
3.27
3.27
3.26
2.46
1.98
2.00
2.03
2.00
0.97
0.99
1.00
0.97
1.02
1.00
3.01
ppm
171.0
144.7
134.7
134.2
131.5
131.2
130.0
128.5
127.2
121.9
110.5
94.6
74.3
52.5
39.4
27.4
21.6
ppm

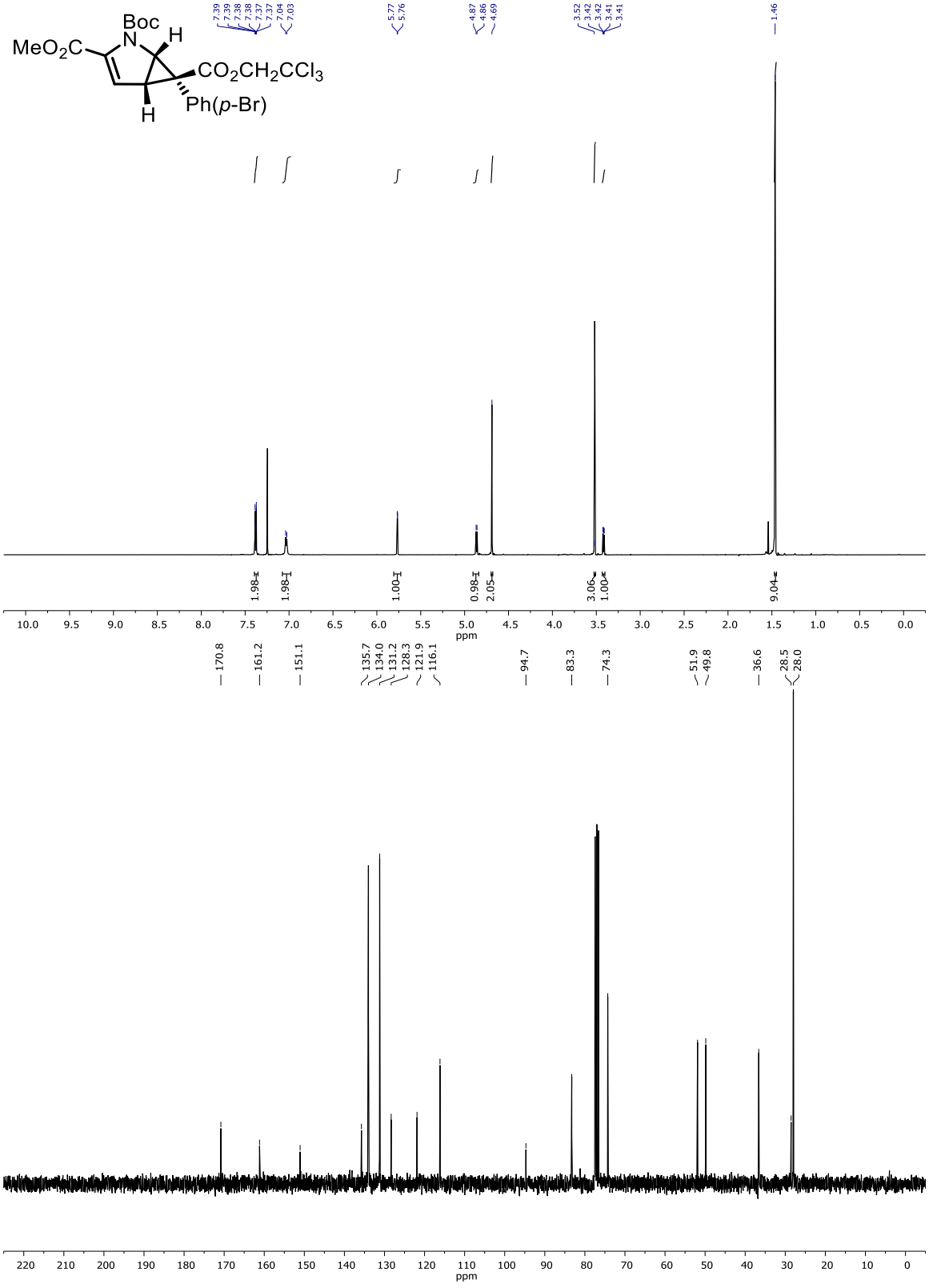
Boc
N
H
MeO2C
CO2CH2CCl3
Ph(p-Br)
H
7.39
7.39
7.38
7.38
7.37
7.37
7.04
7.03
5.77
5.76
4.87
4.86
4.69
3.52
3.42
3.42
3.41
3.41
1.46
1.98
1.98
1.00
0.98
2.05
3.06
1.00
9.04
ppm
170.8
161.2
151.1
135.7
134.0
131.2
128.3
121.9
116.1
94.7
83.3
74.3
51.9
49.8
36.6
28.5
28.0
ppm

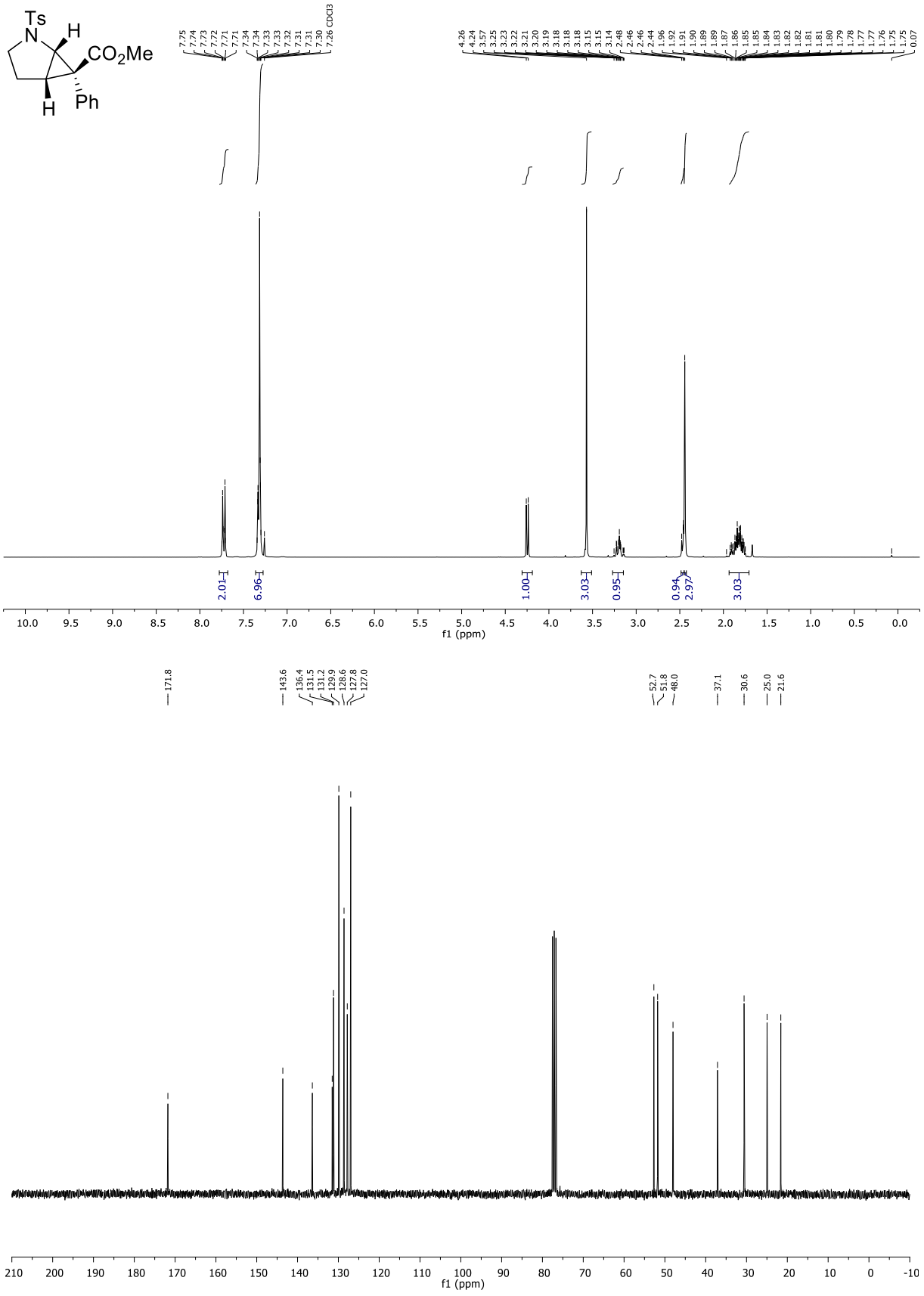
Ts
N
H
CO2Me
H
Ph
7.75 7.74 7.73 7.72 7.71 7.71 7.34 7.34 7.33 7.33 7.32 7.31 7.31 7.30 7.26 CDCl3
4.26 4.24 3.57 3.25 3.23 3.22 3.21 3.20 3.19 3.18 3.18 3.18 3.15 3.15 3.14 2.48 2.46 2.46 2.44 1.96 1.92 1.91 1.90 1.89 1.89 1.89 1.87 1.86 1.85 1.85 1.84 1.83 1.82 1.81 1.81 1.80 1.79 1.78 1.77 1.77 1.76 1.75 1.75 0.07
2.01 6.96 1.00 3.03 0.95 0.94 2.97 3.03
f1 (ppm)
171.8 143.6 136.4 131.5 131.2 129.9 128.6 127.8 127.0 52.7 51.8 48.0 37.1 30.6 25.0 21.6
f1 (ppm)

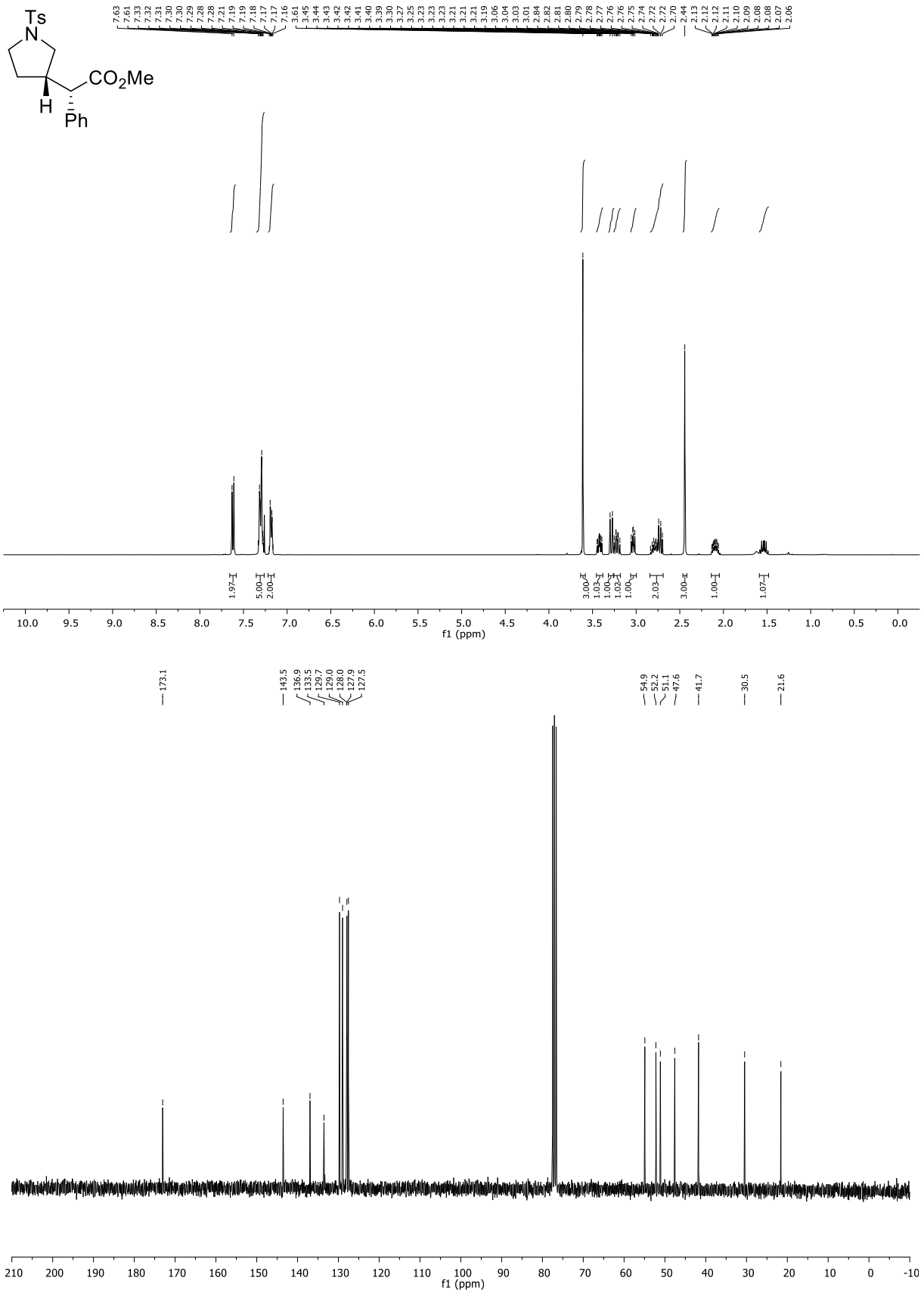
Ts
N
CO2Me
H
Ph
f1 (ppm)
f1 (ppm)

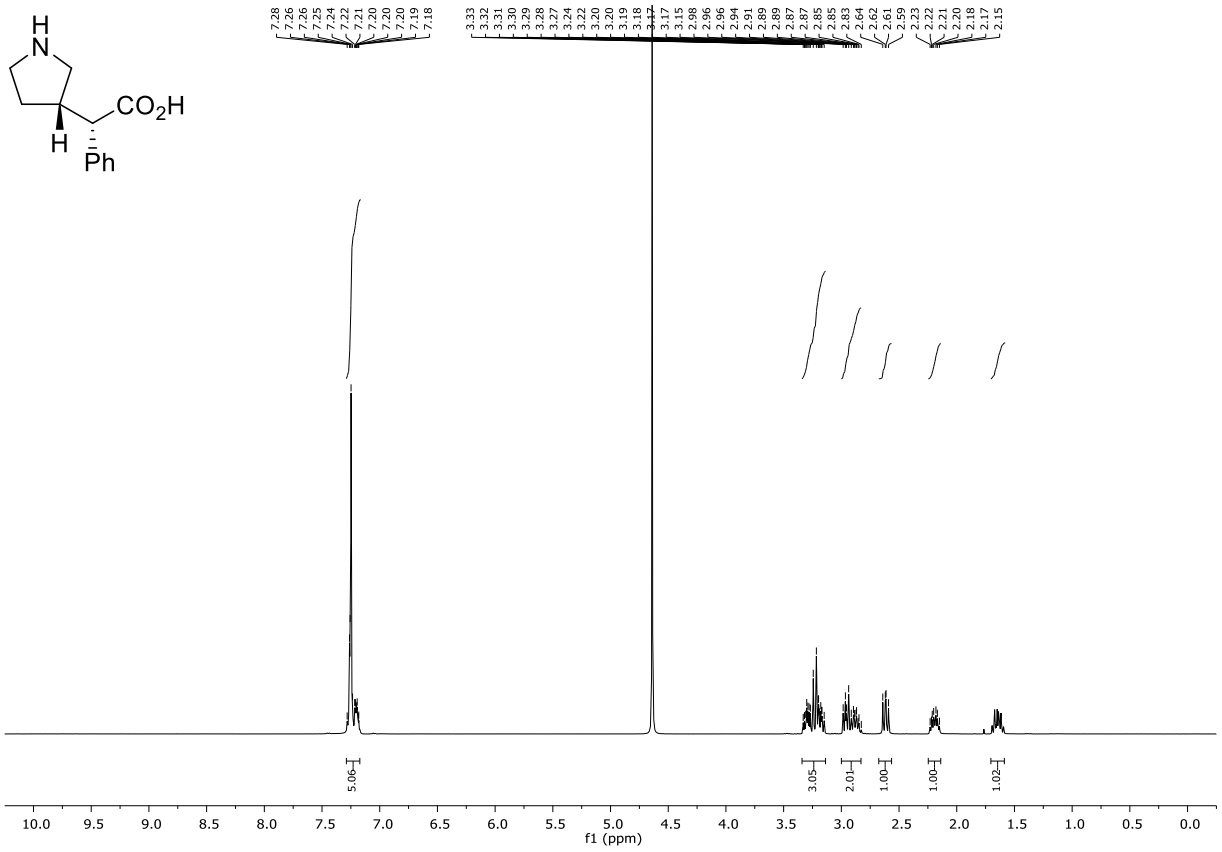
7.28
7.26
7.26
7.26
7.25
7.24
7.22
7.21
7.20
7.20
7.20
7.19
7.18
3.33
3.32
3.31
3.30
3.29
3.28
3.27
3.24
3.22
3.20
3.20
3.19
3.18
3.17
3.17
3.15
2.98
2.96
2.96
2.94
2.91
2.89
2.89
2.87
2.87
2.85
2.83
2.64
2.62
2.61
2.59
2.23
2.22
2.21
2.20
2.18
2.17
2.15
5.06
3.05
2.01
1.00
1.00
1.02
f1 (ppm)

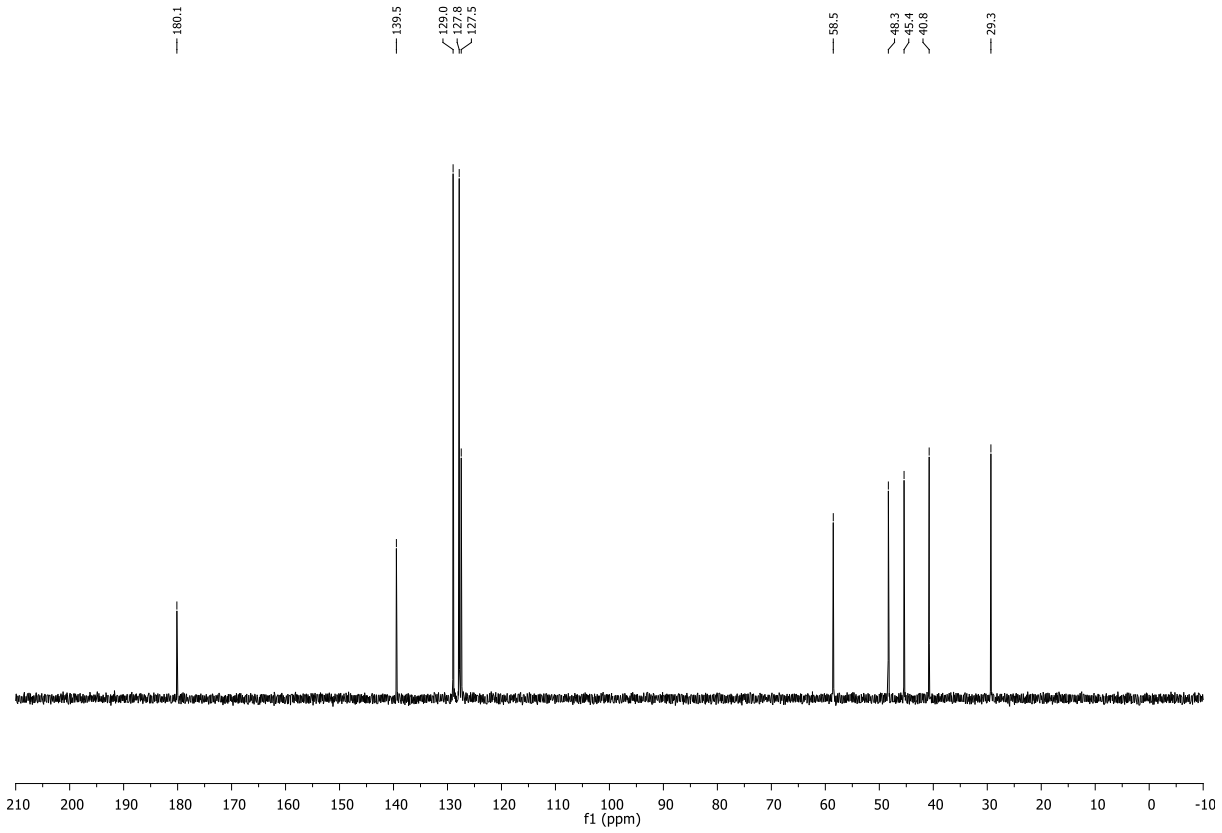
180.1
139.5
129.0
127.8
127.5
58.5
48.3
45.4
40.8
29.3
f1 (ppm)

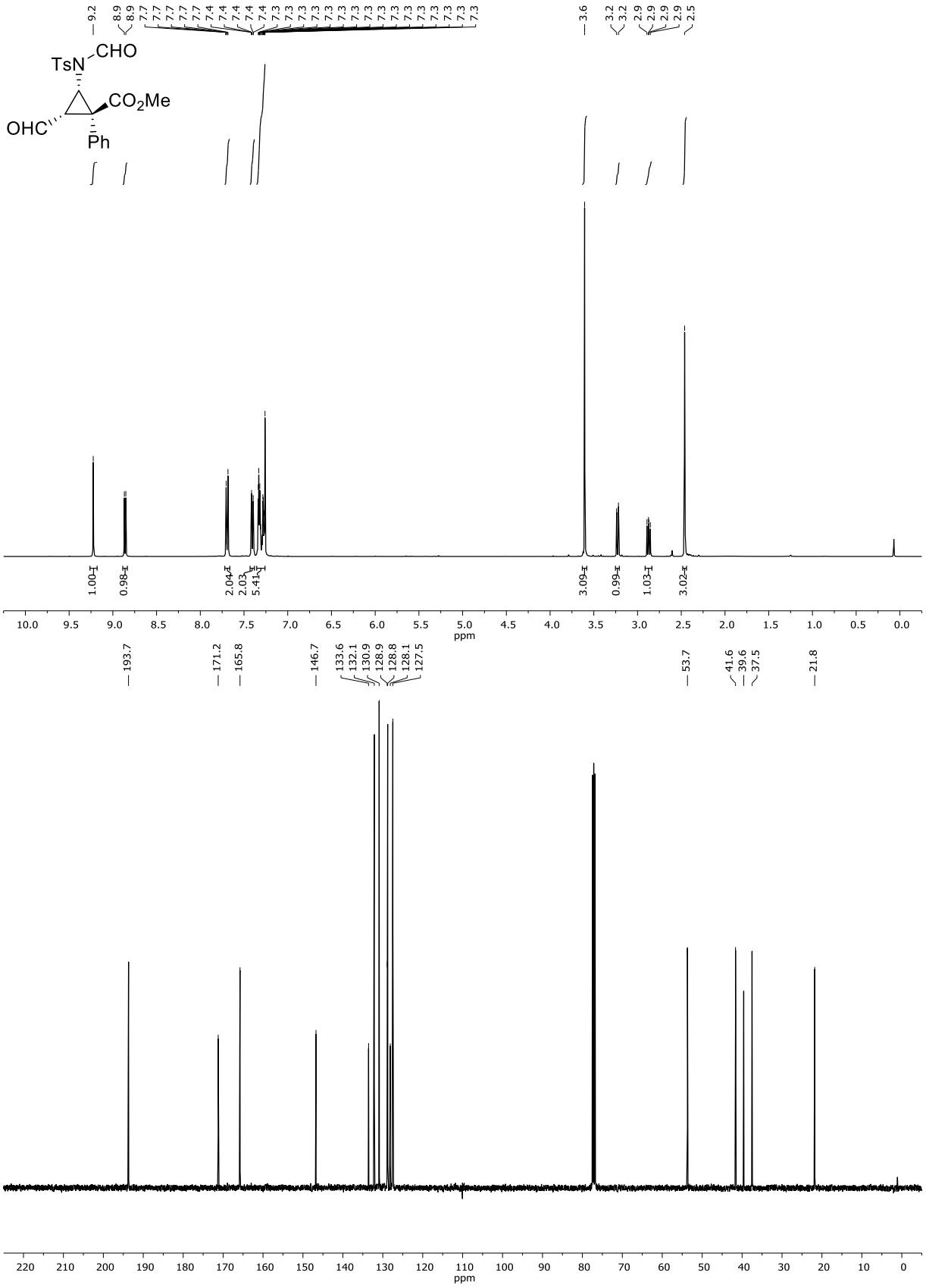
TsN
CHO
CO2Me
OHC
Ph
ppm

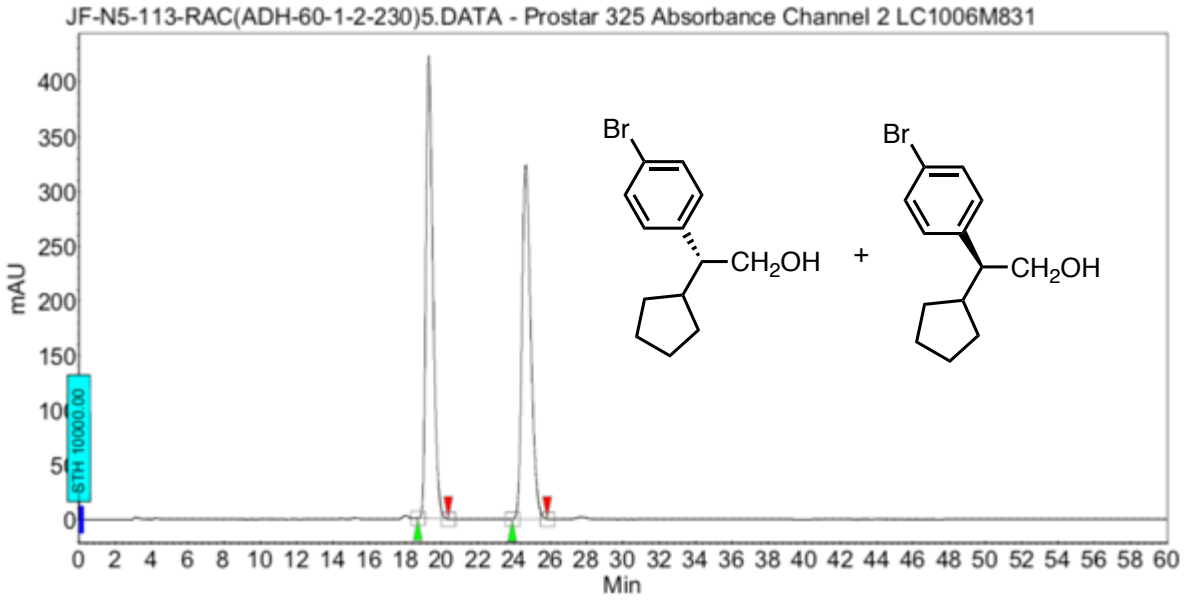

Peak results :

Index	Name	Time [Min]	Quantity [% Area]	Height [mAU]	Area [mAU.Min]	Area % [%]
1	UNKNOWN	19.29	50.95	422.4	190.3	50.953
2	UNKNOWN	24.64	49.05	323.5	183.2	49.047
Total			100.00	745.9	373.5	100.000

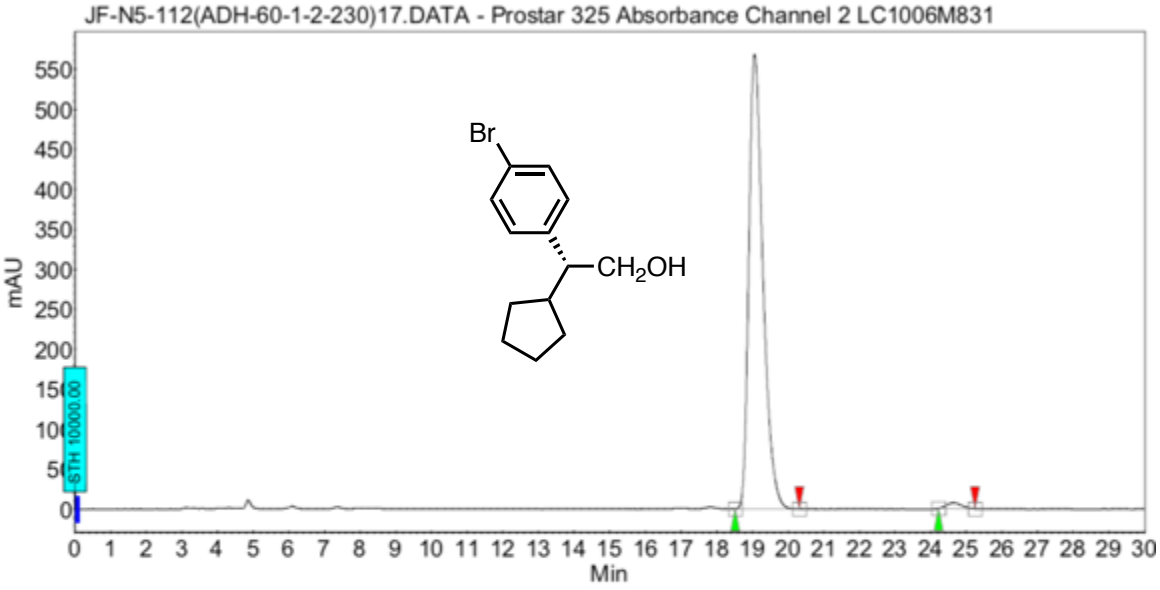

Peak results :

Index	Name	Time [Min]	Quantity [% Area]	Height [mAU]	Area [mAU.Min]	Area % [%]
2	UNKNOWN	19.06	98.66	568.5	260.9	98.663
1	UNKNOWN	24.64	1.34	7.2	3.5	1.337
Total			100.00	575.7	264.4	100.000

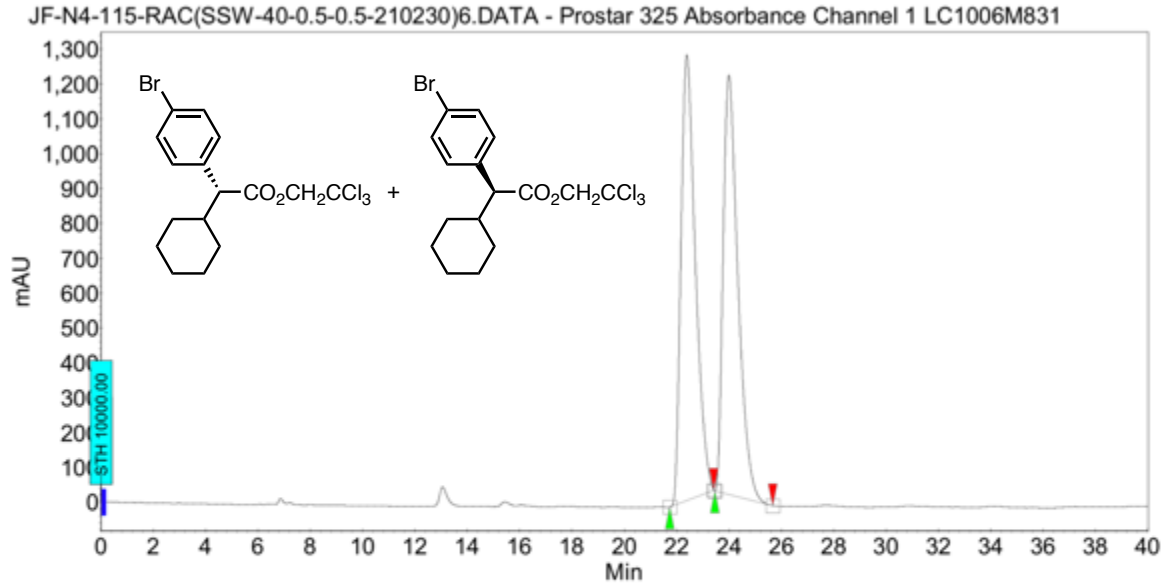

Peak results :

Index	Name	Time [Min]	Quantity [% Area]	Height [mAU]	Area [mAU.Min]	Area % [%]
1	UNKNOWN	22.39	50.88	1280.4	816.4	50.876
2	UNKNOWN	24.00	49.12	1204.7	788.3	49.124
Total			100.00	2485.1	1604.6	100.000

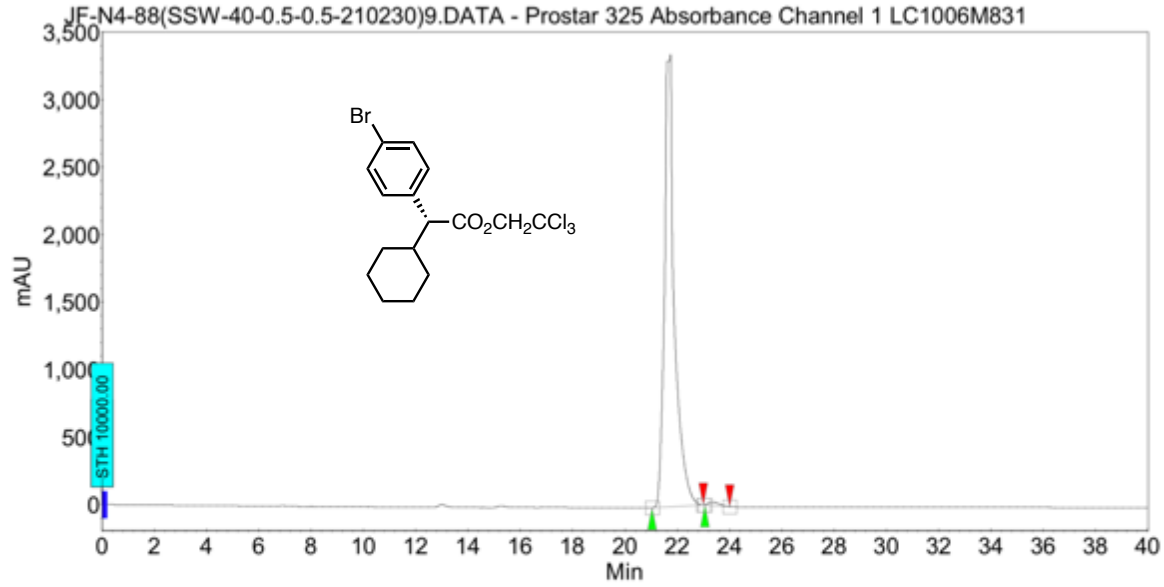

Peak results :

Index	Name	Time [Min]	Quantity [% Area]	Height [mAU]	Area [mAU.Min]	Area % [%]
1	UNKNOWN	21.74	99.26	3348.2	1500.0	99.256
2	UNKNOWN	23.38	0.74	24.0	11.2	0.744
Total			100.00	3372.2	1511.3	100.000

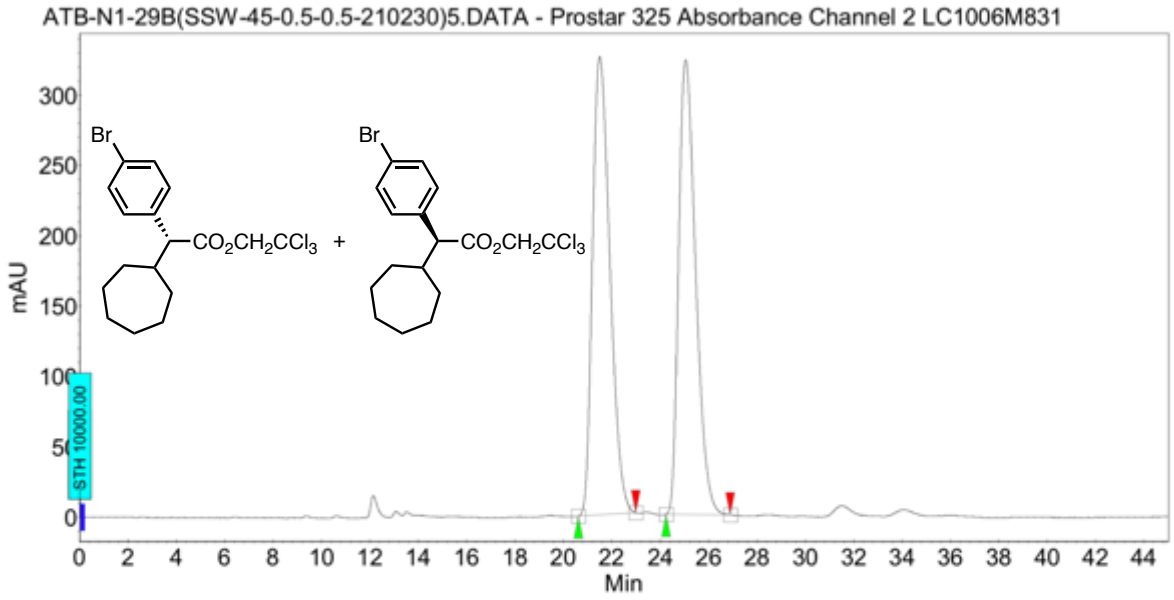

Peak results :

Index	Name	Time [Min]	Quantity [% Area]	Height [mAU]	Area [mAU.Min]	Area % [%]
1	UNKNOWN	21.50	50.84	325.9	272.5	50.837
2	UNKNOWN	25.05	49.16	323.5	263.5	49.163
Total			100.00	649.3	536.0	100.000

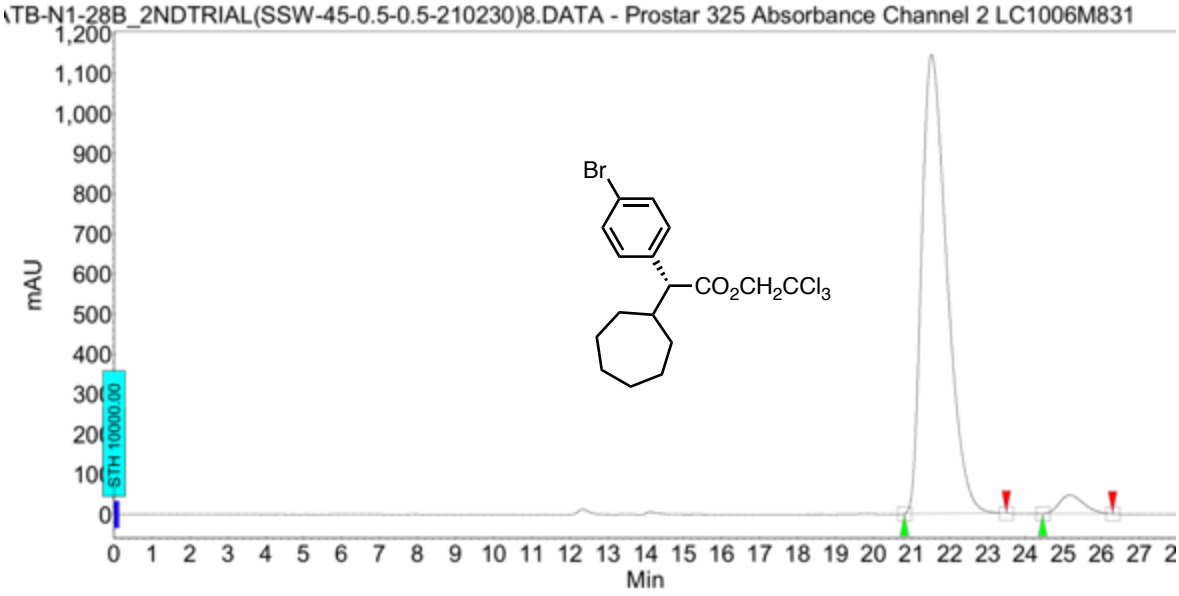

Peak results :

Index	Name	Time [Min]	Quantity [% Area]	Height [mAU]	Area [mAU.Min]	Area % [%]
1	UNKNOWN	21.53	96.23	1145.9	881.8	96.226
2	UNKNOWN	25.17	3.77	46.7	34.6	3.774
Total			100.00	1192.6	916.4	100.000

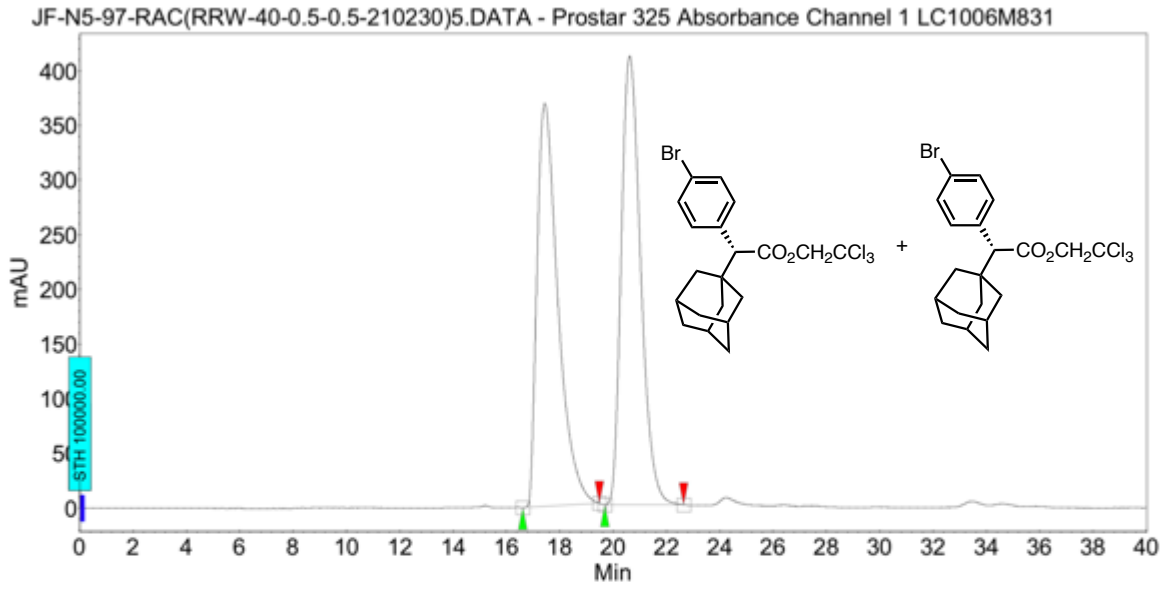

Peak results :

Index	Name	Time [Min]	Quantity [% Area]	Height [mAU]	Area [mAU.Min]	Area % [%]
1	UNKNOWN	17.44	49.33	368.6	336.2	49.326
2	UNKNOWN	20.63	50.67	410.3	345.4	50.674
Total			100.00	778.8	681.7	100.000

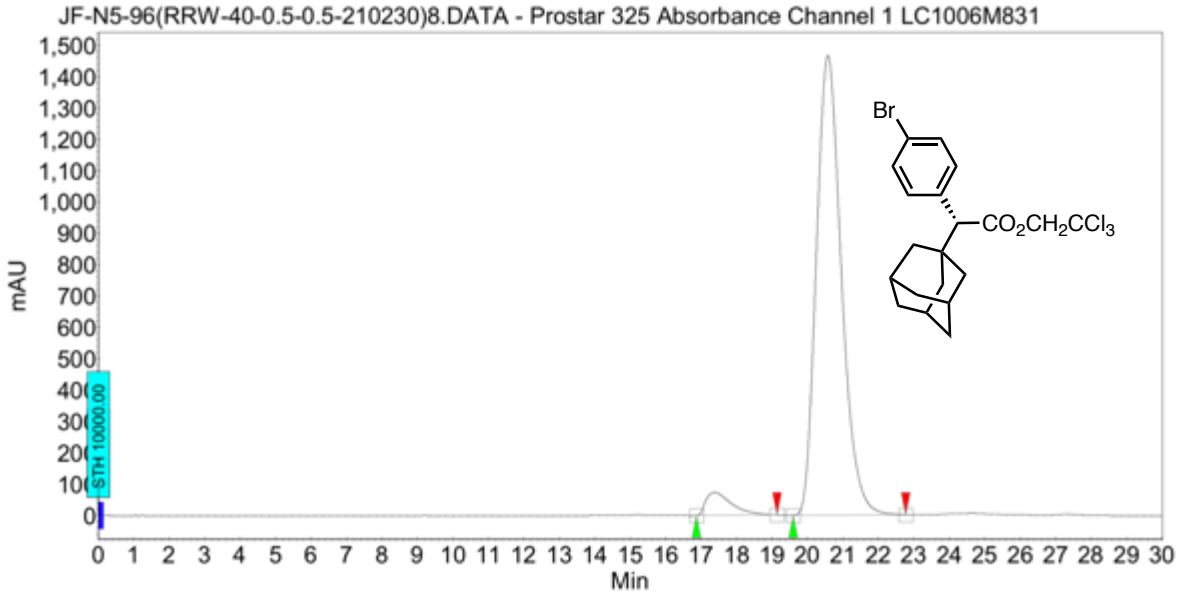

Peak results :

Index	Name	Time [Min]	Quantity [% Area]	Height [mAU]	Area [mAU.Min]	Area % [%]
1	UNKNOWN	17.38	4.91	72.9	61.9	4.911
2	UNKNOWN	20.58	95.09	1465.8	1197.6	95.089
Total			100.00	1538.6	1259.4	100.000

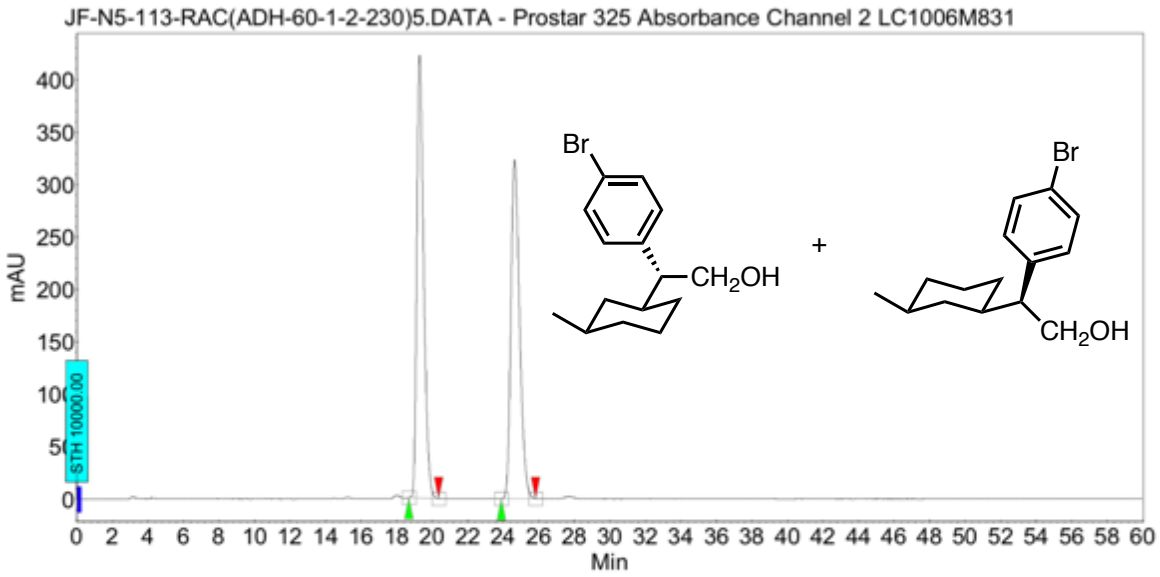

Peak results :

Index	Name	Time [Min]	Quantity [% Area]	Height [mAU]	Area [mAU.Min]	Area % [%]
1	UNKNOWN	19.29	50.95	422.4	190.3	50.953
2	UNKNOWN	24.64	49.05	323.5	183.2	49.047
Total			100.00	745.9	373.5	100.000

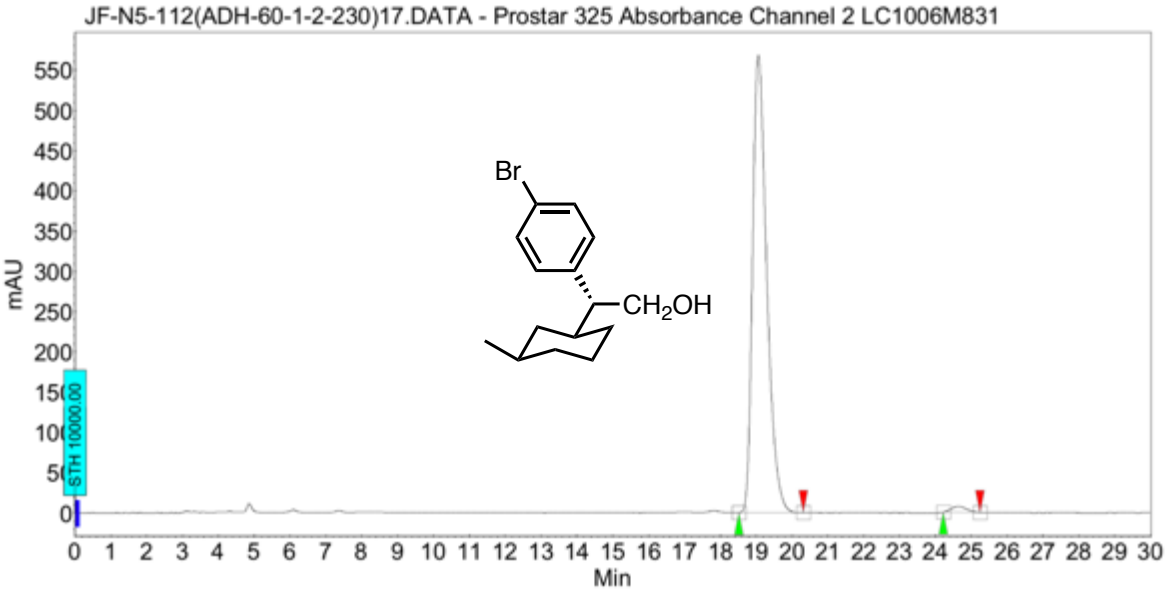

Peak results :

Index	Name	Time [Min]	Quantity [% Area]	Height [mAU]	Area [mAU.Min]	Area % [%]
2	UNKNOWN	19.06	98.66	568.5	260.9	98.663
1	UNKNOWN	24.64	1.34	7.2	3.5	1.337
Total			100.00	575.7	264.4	100.000

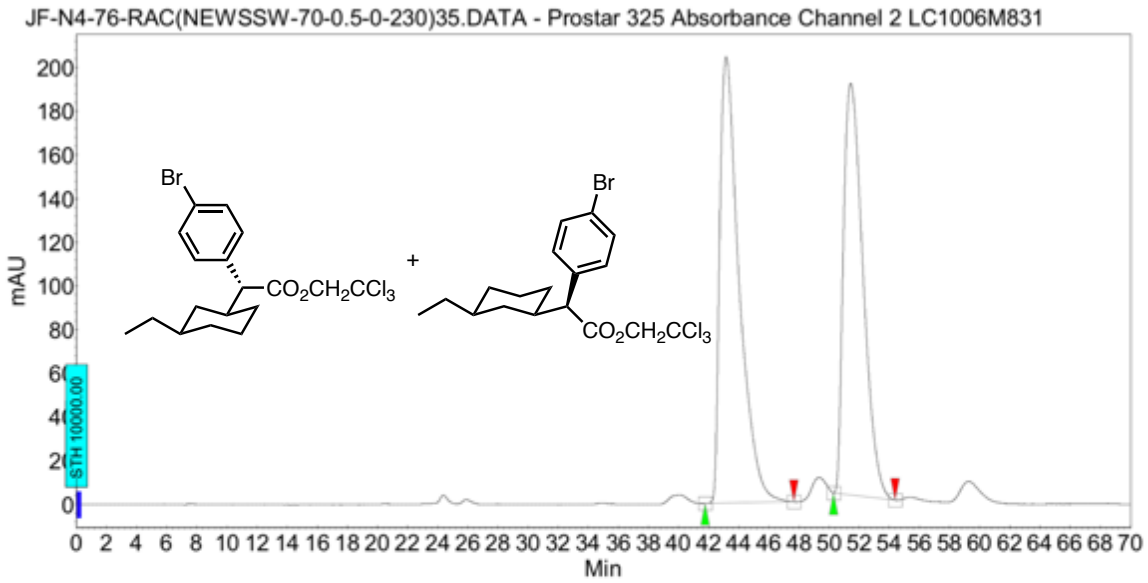

Peak results :

Index	Name	Time [Min]	Quantity [% Area]	Height [mAU]	Area [mAU.Min]	Area % [%]
1	UNKNOWN	43.16	51.86	204.5	306.2	51.858
2	UNKNOWN	51.44	48.14	188.7	284.3	48.142
Total			100.00	393.2	590.5	100.000

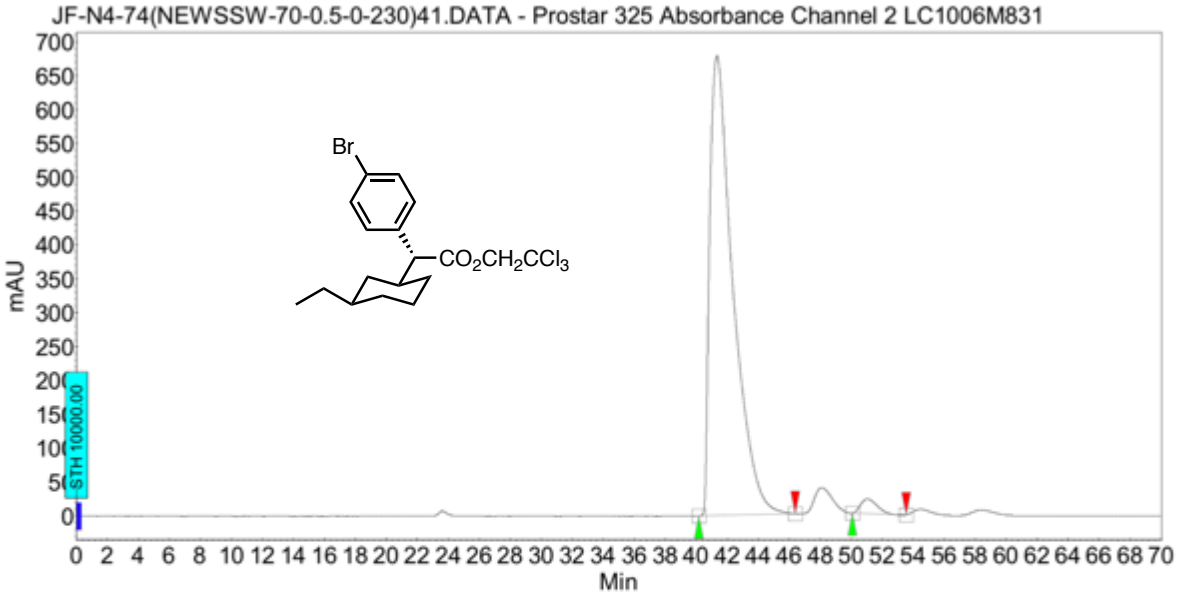

Peak results :

Index	Name	Time [Min]	Quantity [% Area]	Height [mAU]	Area [mAU.Min]	Area % [%]
1	UNKNOWN	41.34	97.80	678.9	1179.0	97.804
2	UNKNOWN	51.07	2.20	21.9	26.5	2.196
Total			100.00	700.8	1205.4	100.000

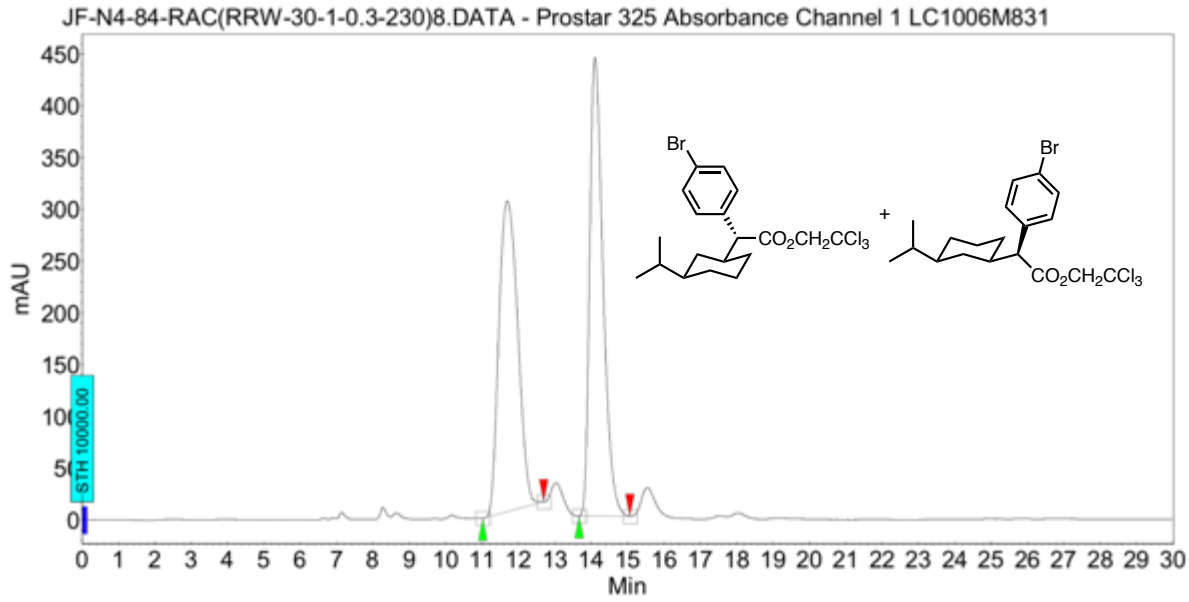

Peak results :

Index	Name	Time [Min]	Quantity [% Area]	Height [mAU]	Area [mAU.Min]	Area % [%]
2	UNKNOWN	11.69	49.12	299.9	180.6	49.119
1	UNKNOWN	14.10	50.88	442.6	187.1	50.881
Total			100.00	742.5	367.6	100.000

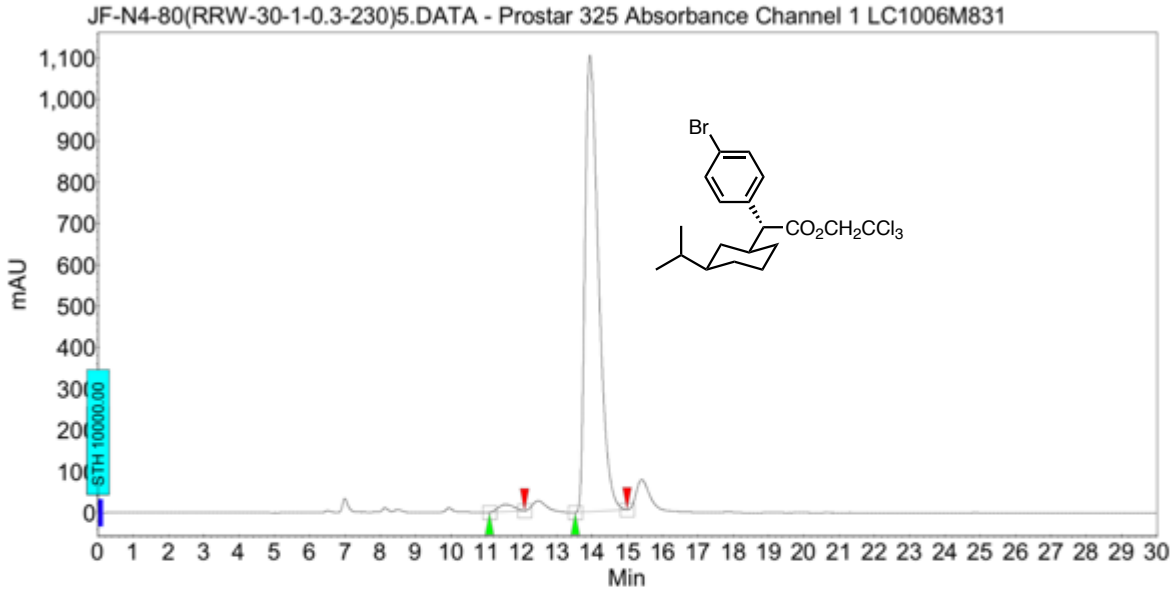

Peak results :

Index	Name	Time [Min]	Quantity [% Area]	Height [mAU]	Area [mAU.Min]	Area % [%]
2	UNKNOWN	11.54	1.72	16.8	8.6	1.718
1	UNKNOWN	13.94	98.28	1103.9	493.1	98.282
Total			100.00	1120.7	501.7	100.000

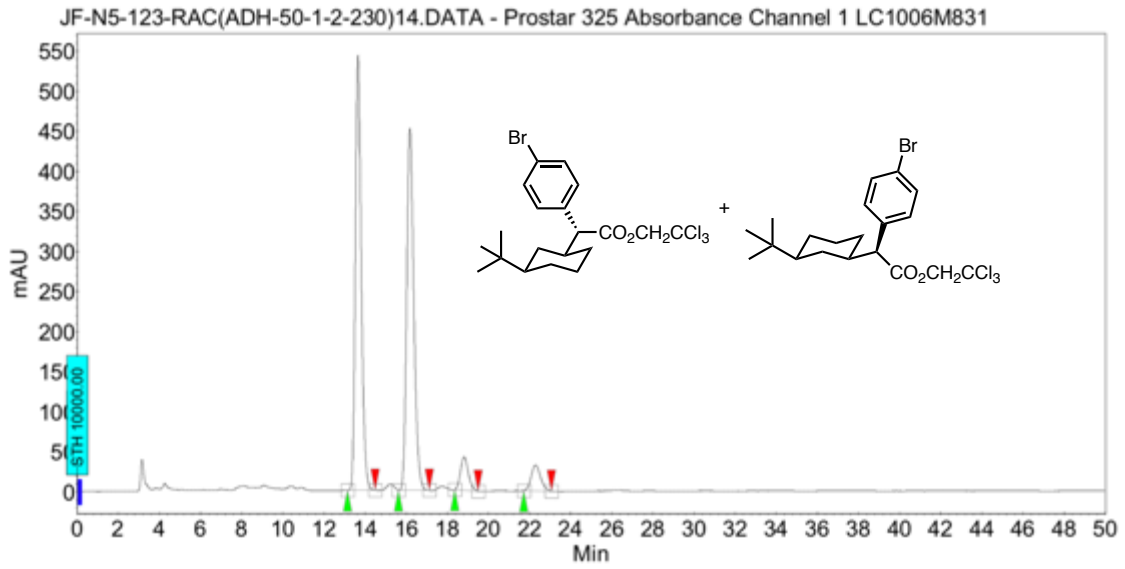

Peak results :

Index	Name	Time [Min]	Quantity [% Area]	Height [mAU]	Area [mAU.Min]	Area % [%]
1	UNKNOWN	13.65	45.52	543.1	180.9	45.521
2	UNKNOWN	16.18	45.59	451.8	181.2	45.590
3	UNKNOWN	18.82	4.61	41.6	18.3	4.610
4	UNKNOWN	22.29	4.28	32.1	17.0	4.278
Total			100.00	1068.6	397.4	100.000

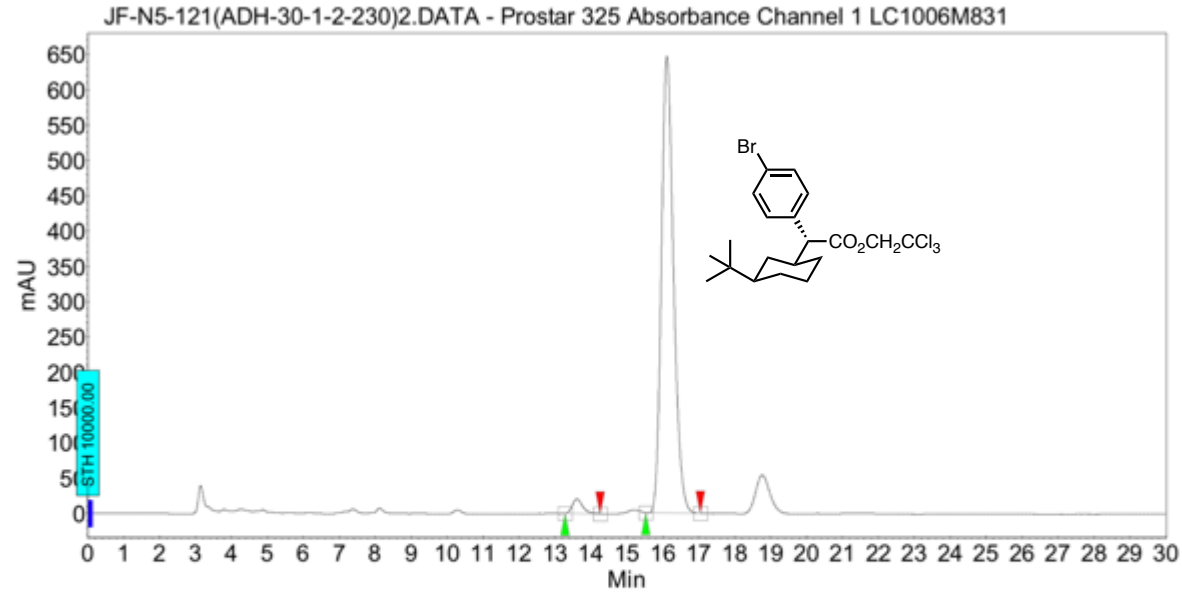

Peak results :

Index	Name	Time [Min]	Quantity [% Area]	Height [mAU]	Area [mAU.Min]	Area % [%]
1	UNKNOWN	13.61	2.63	20.6	6.8	2.628
2	UNKNOWN	16.11	97.37	647.1	253.5	97.372
Total			100.00	667.6	260.3	100.000

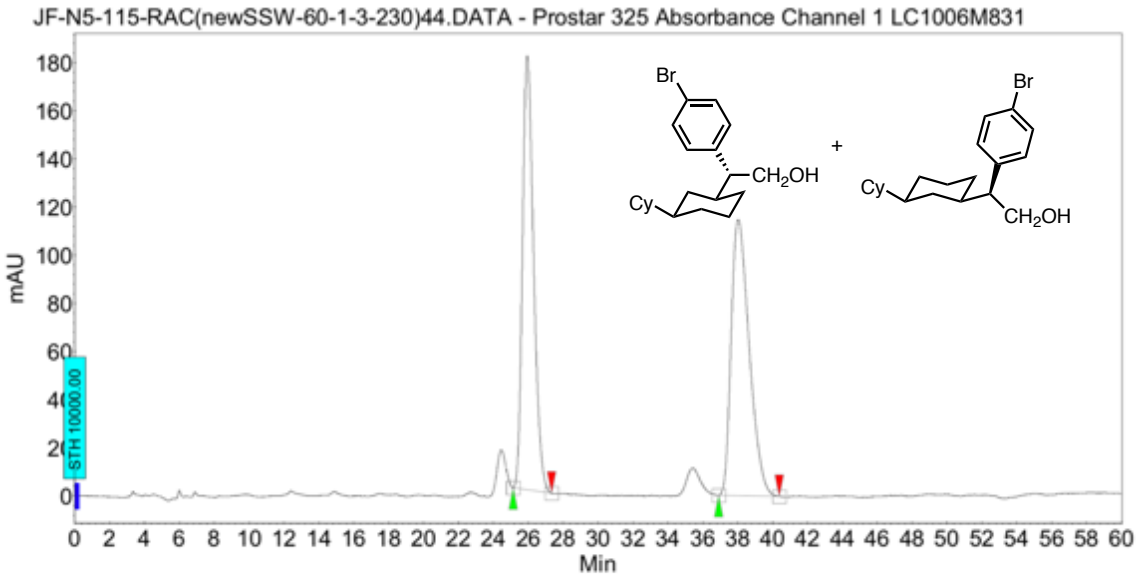

Peak results :

Index	Name	Time [Min]	Quantity [% Area]	Height [mAU]	Area [mAU.Min]	Area % [%]
1	UNKNOWN	25.94	49.18	180.5	133.1	49.177
2	UNKNOWN	38.04	50.82	114.8	137.6	50.823
Total			100.00	295.3	270.7	100.000

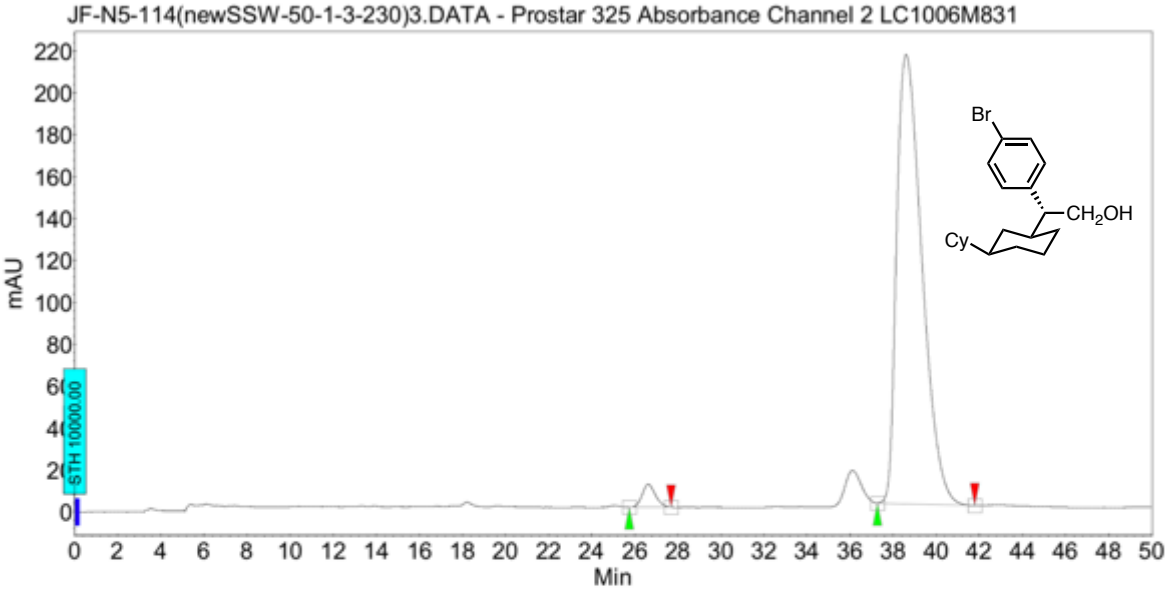

Peak results :

Index	Name	Time [Min]	Quantity [% Area]	Height [mAU]	Area [mAU.Min]	Area % [%]
1	UNKNOWN	26.62	2.59	10.9	7.8	2.590
2	UNKNOWN	38.60	97.41	214.5	292.0	97.410
Total			100.00	225.5	299.7	100.000

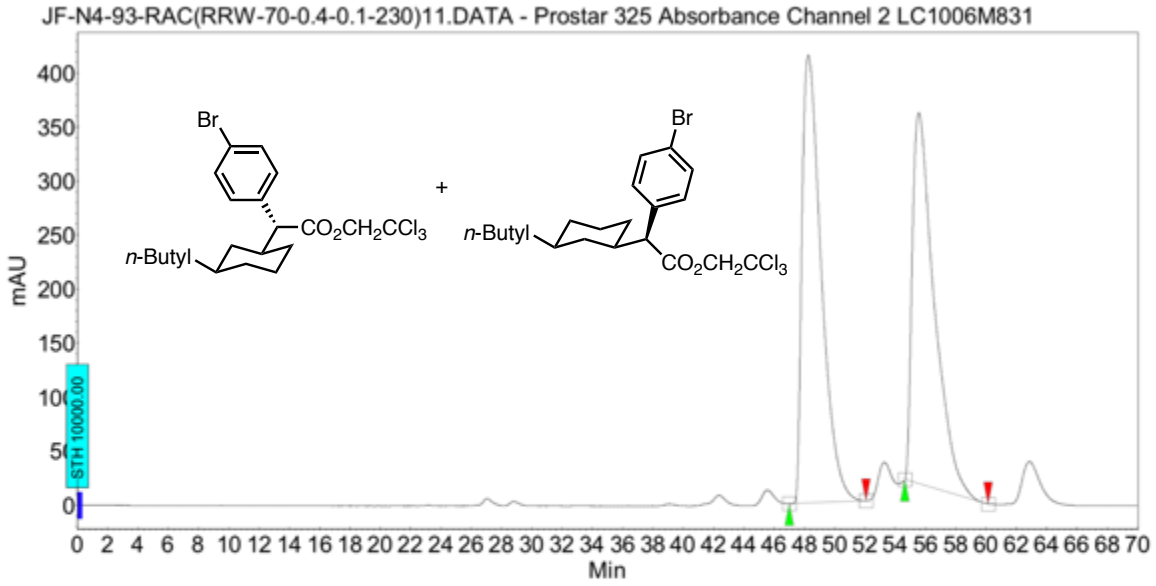

Peak results :

Index	Name	Time [Min]	Quantity [% Area]	Height [mAU]	Area [mAU.Min]	Area % [%]
1	UNKNOWN	48.26	51.53	414.6	612.1	51.530
2	UNKNOWN	55.56	48.47	343.1	575.8	48.470
Total			100.00	757.6	1187.9	100.000

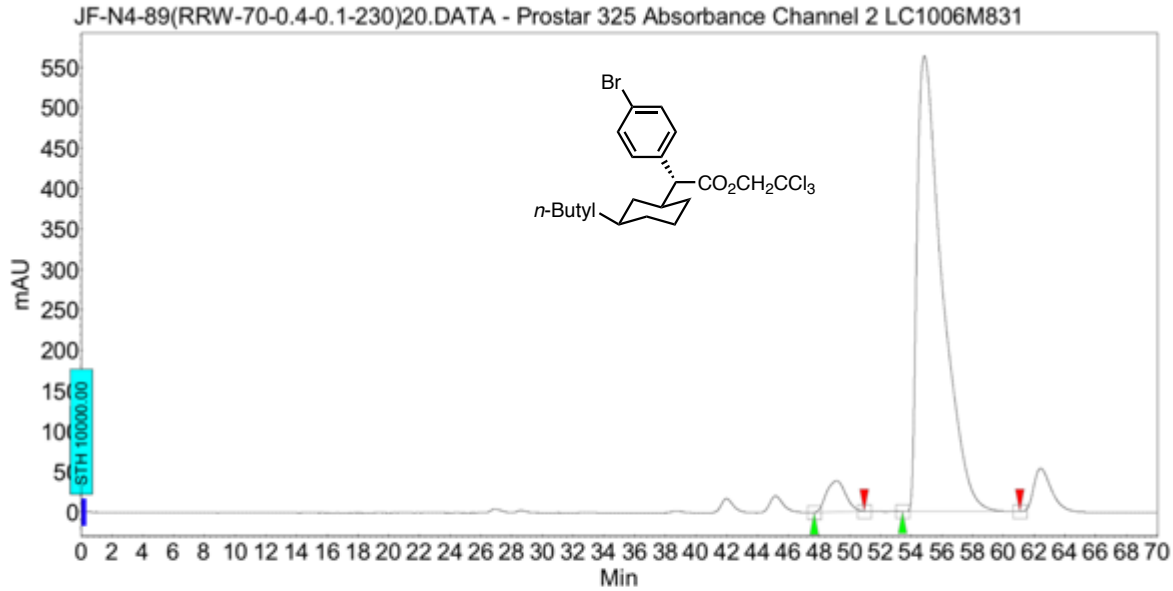

Peak results :

Index	Name	Time [Min]	Quantity [% Area]	Height [mAU]	Area [mAU.Min]	Area % [%]
1	UNKNOWN	49.14	4.93	38.4	55.4	4.927
2	UNKNOWN	54.86	95.07	563.5	1068.4	95.073
Total			100.00	601.9	1123.8	100.000

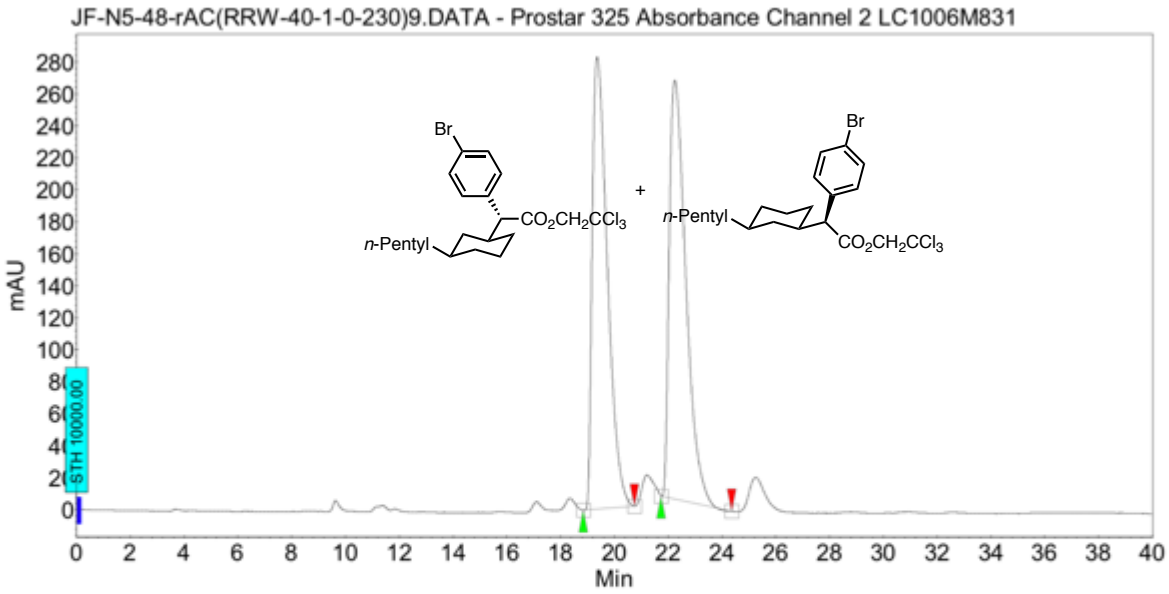

Peak results :

Index	Name	Time [Min]	Quantity [% Area]	Height [mAU]	Area [mAU.Min]	Area % [%]
1	UNKNOWN	19.36	49.63	282.8	185.1	49.634
2	UNKNOWN	22.25	50.37	262.0	187.8	50.366
Total			100.00	544.7	372.9	100.000

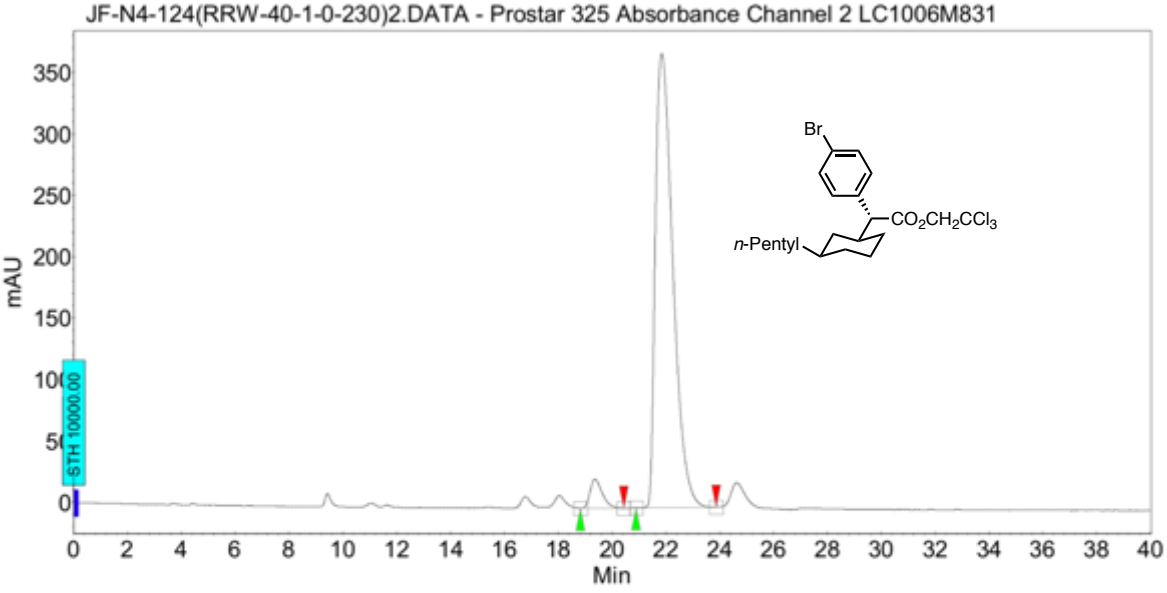

Peak results :

Index	Name	Time [Min]	Quantity [% Area]	Height [mAU]	Area [mAU.Min]	Area % [%]
1	UNKNOWN	19.36	4.36	23.8	12.7	4.357
2	UNKNOWN	21.84	95.64	369.6	278.3	95.643
Total			100.00	393.4	290.9	100.000

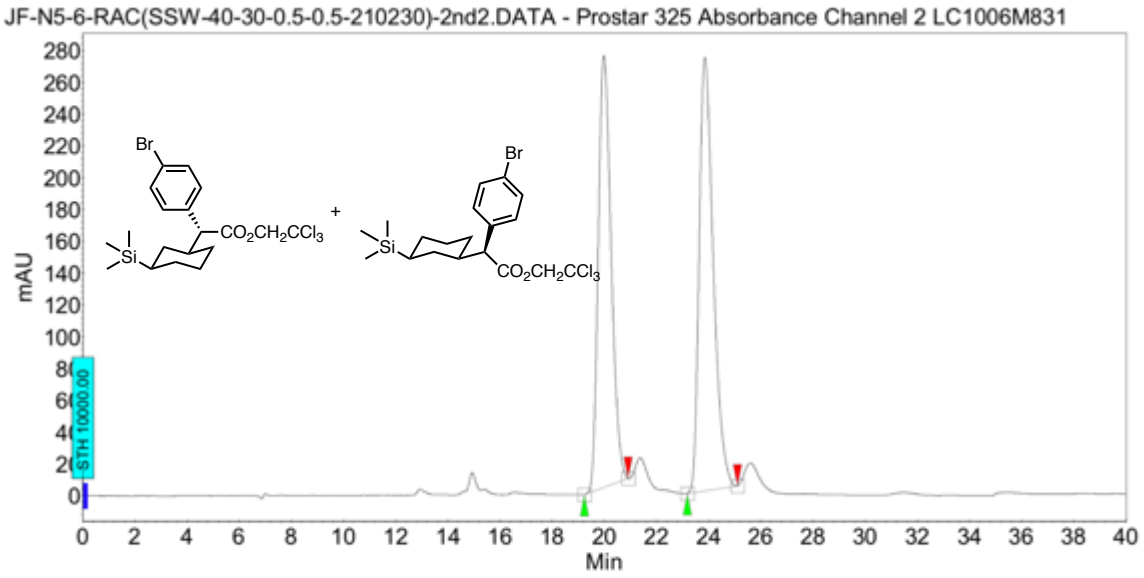

Peak results :

Index	Name	Time [Min]	Quantity [% Area]	Height [mAU]	Area [mAU.Min]	Area % [%]
1	UNKNOWN	19.98	47.75	271.7	155.6	47.752
2	UNKNOWN	23.85	52.25	272.4	170.2	52.248
Total			100.00	544.1	325.8	100.000

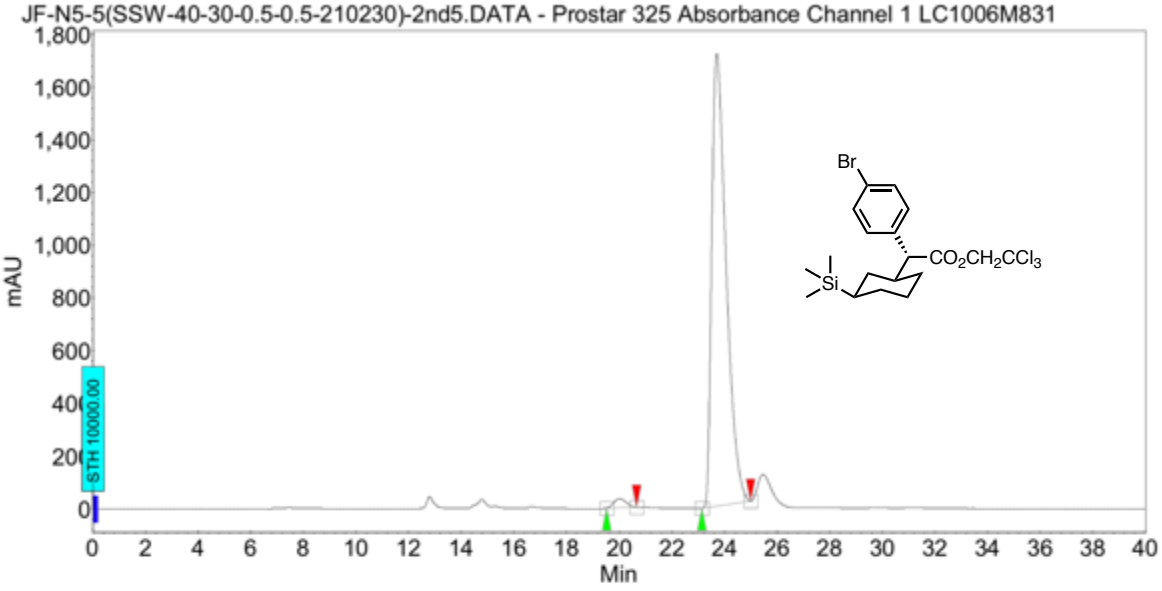

Peak results :

Index	Name	Time [Min]	Quantity [% Area]	Height [mAU]	Area [mAU.Min]	Area % [%]
1	UNKNOWN	20.01	1.70	34.8	18.9	1.705
2	UNKNOWN	23.71	98.30	1717.9	1090.6	98.295
Total			100.00	1752.8	1109.5	100.000

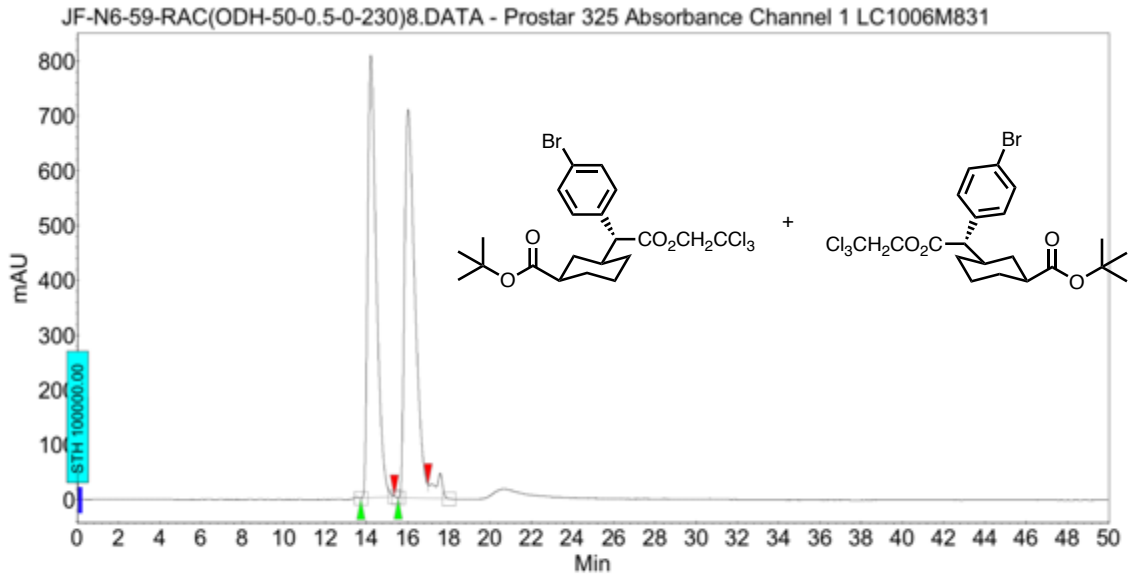

Peak results :

Index	Name	Time [Min]	Quantity [% Area]	Height [mAU]	Area [mAU.Min]	Area % [%]
1	UNKNOWN	14.22	48.61	807.0	391.8	48.605
2	UNKNOWN	16.03	51.39	708.6	414.3	51.395
Total			100.00	1515.7	806.0	100.000

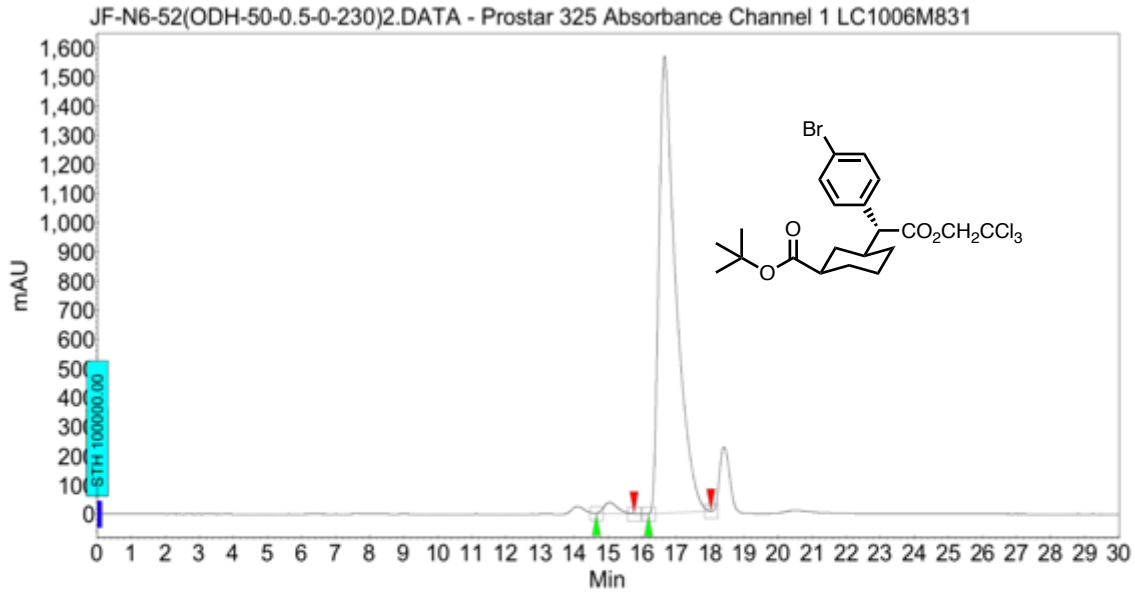

Peak results :

Index	Name	Time [Min]	Quantity [% Area]	Height [mAU]	Area [mAU.Min]	Area % [%]
1	UNKNOWN	15.05	1.85	37.4	17.1	1.852
2	UNKNOWN	16.66	98.15	1568.2	907.4	98.148
Total			100.00	1605.7	924.5	100.000

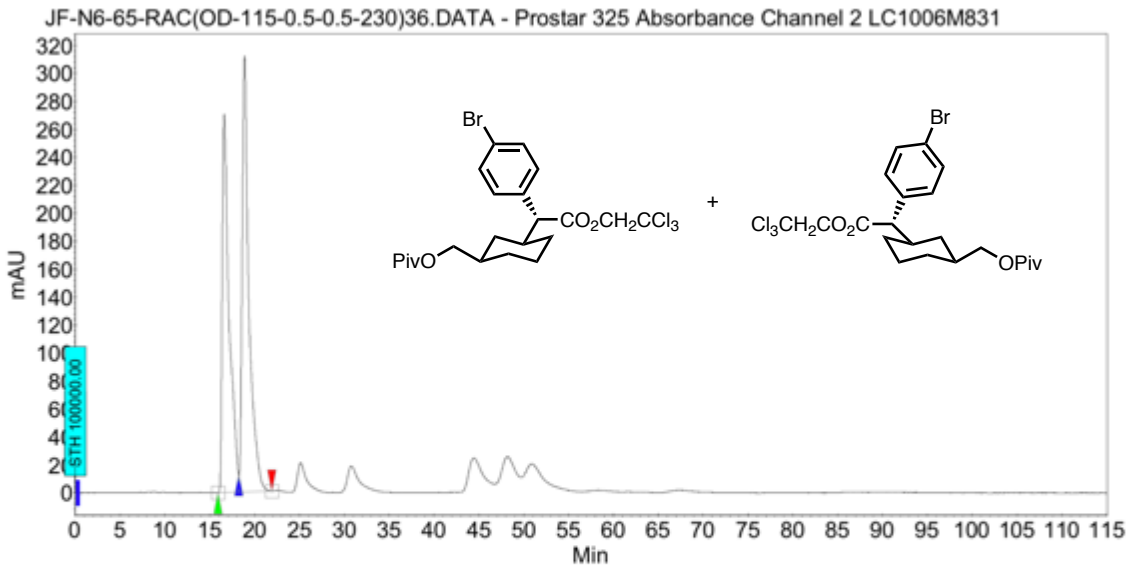

Peak results :

Index	Name	Time [Min]	Quantity [% Area]	Height [mAU]	Area [mAU.Min]	Area % [%]
1	UNKNOWN	16.61	46.93	270.4	242.5	46.933
2	UNKNOWN	18.89	53.07	312.0	274.2	53.067
Total			100.00	582.4	516.7	100.000

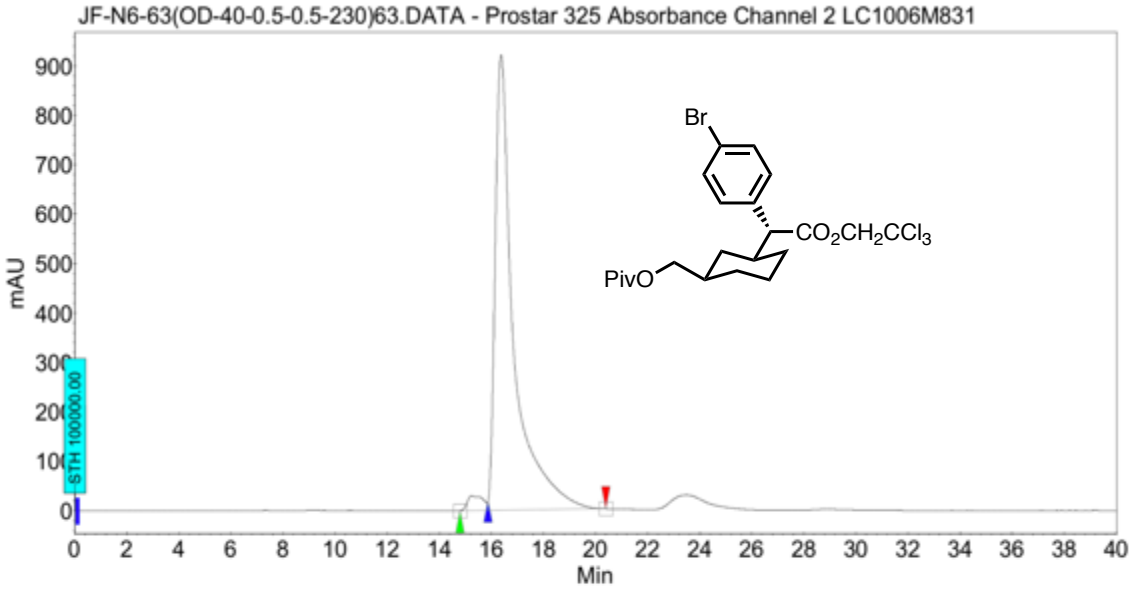

Peak results :

Index	Name	Time [Min]	Quantity [% Area]	Height [mAU]	Area [mAU.Min]	Area % [%]
1	UNKNOWN	15.24	2.64	29.6	20.6	2.636
2	UNKNOWN	16.37	97.36	920.9	762.2	97.364
Total			100.00	950.5	782.8	100.000

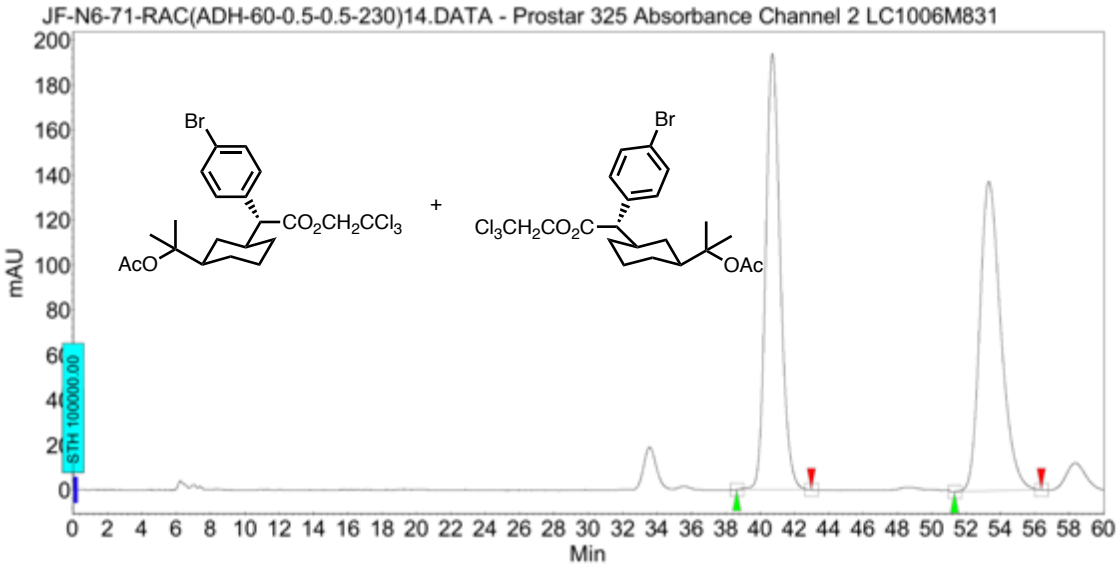

Peak results :

Index	Name	Time [Min]	Quantity [% Area]	Height [mAU]	Area [mAU.Min]	Area % [%]
1	UNKNOWN	40.72	49.38	193.8	191.2	49.380
2	UNKNOWN	53.32	50.62	137.5	196.0	50.620
Total			100.00	331.4	387.2	100.000

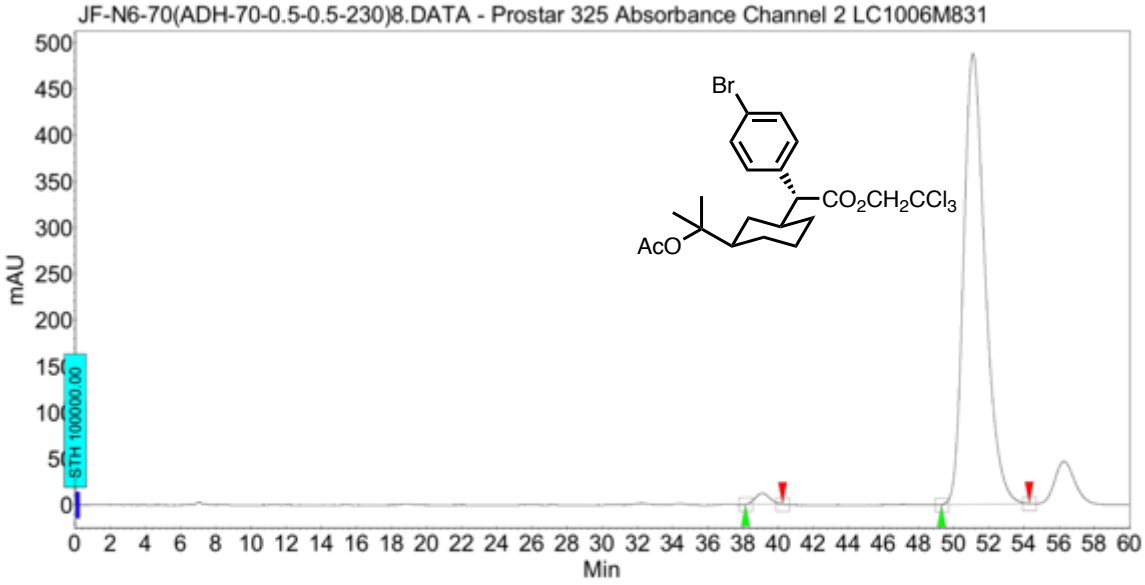

Peak results :

Index	Name	Time [Min]	Quantity [% Area]	Height [mAU]	Area [mAU.Min]	Area % [%]
1	UNKNOWN	39.12	1.62	12.0	11.3	1.620
2	UNKNOWN	51.09	98.38	487.2	688.9	98.380
Total			100.00	499.2	700.2	100.000

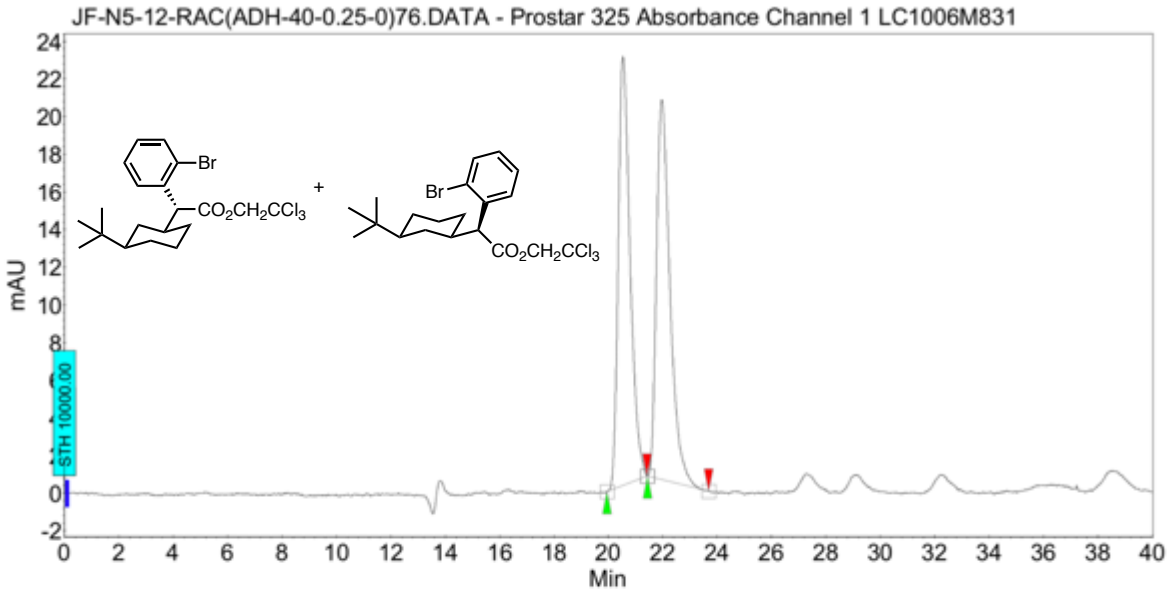

Peak results :

Index	Name	Time [Min]	Quantity [% Area]	Height [mAU]	Area [mAU.Min]	Area % [%]
1	UNKNOWN	20.53	49.94	22.8	11.6	49.941
2	UNKNOWN	21.97	50.06	20.2	11.6	50.059
Total			100.00	43.0	23.2	100.000

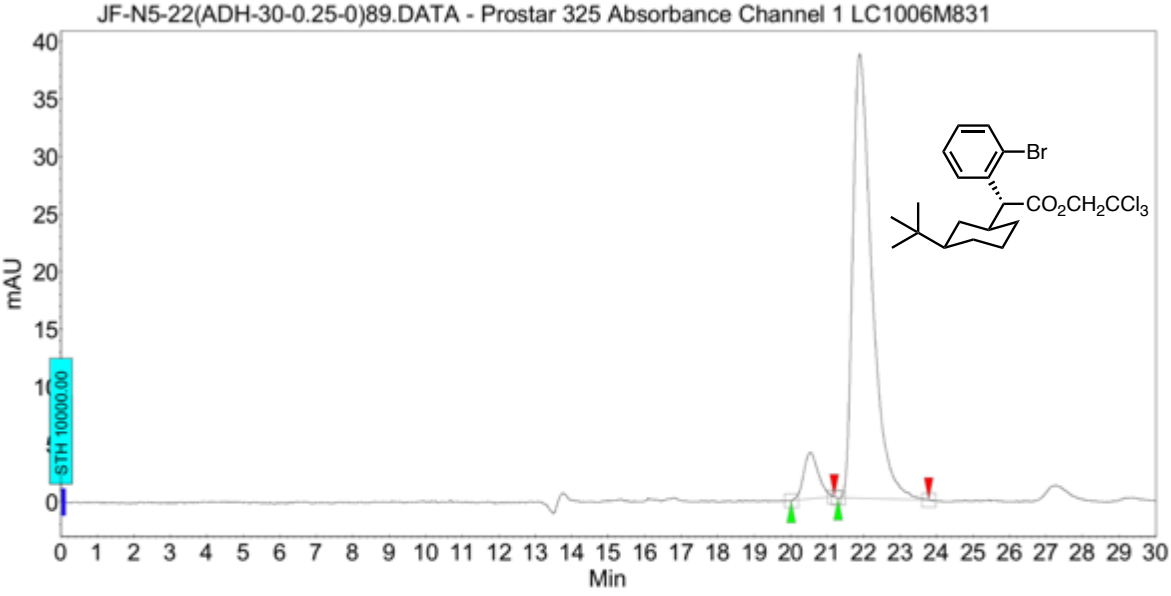

Peak results :

Index	Name	Time [Min]	Quantity [% Area]	Height [mAU]	Area [mAU.Min]	Area % [%]
1	UNKNOWN	20.54	7.46	4.1	1.9	7.458
2	UNKNOWN	21.89	92.54	38.6	23.5	92.542
Total			100.00	42.7	25.4	100.000

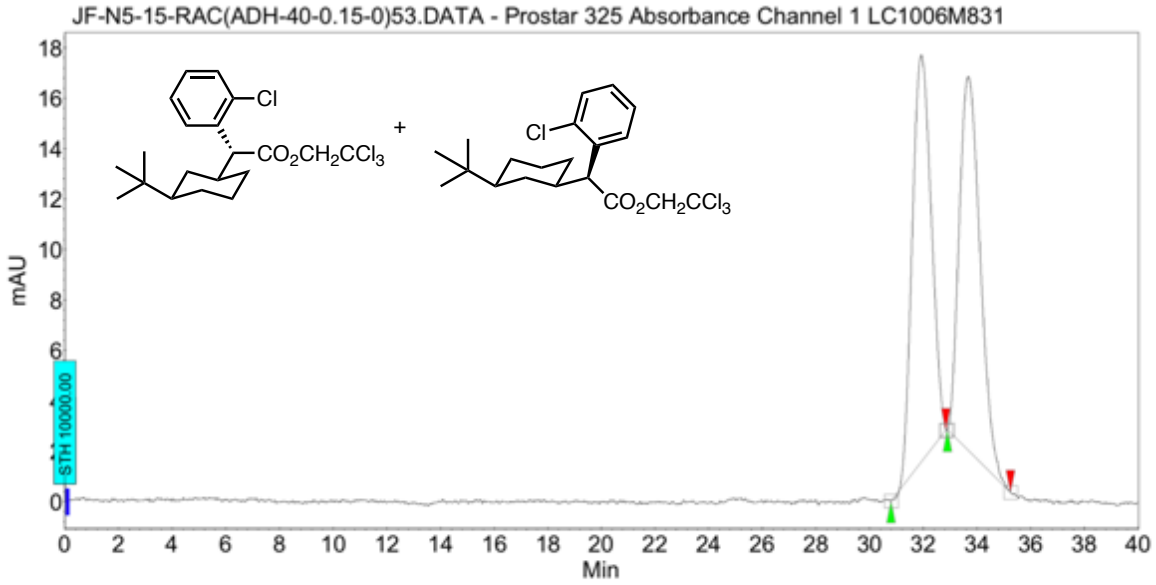

Peak results :

Index	Name	Time [Min]	Quantity [% Area]	Height [mAU]	Area [mAU.Min]	Area % [%]
1	UNKNOWN	31.92	49.69	16.1	13.2	49.692
2	UNKNOWN	33.68	50.31	14.8	13.4	50.308
Total			100.00	31.0	26.6	100.000

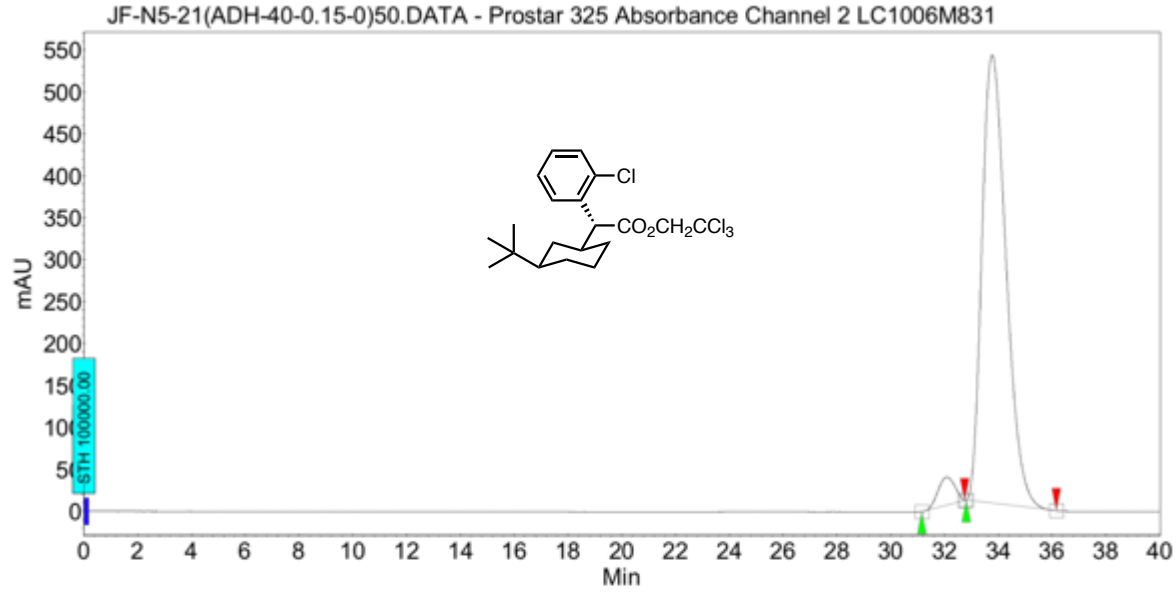

Peak results :

Index	Name	Time [Min]	Quantity [% Area]	Height [mAU]	Area [mAU.Min]	Area % [%]
1	UNKNOWN	32.06	4.20	33.6	24.3	4.200
2	UNKNOWN	33.77	95.80	534.4	554.4	95.800
Total			100.00	568.0	578.7	100.000

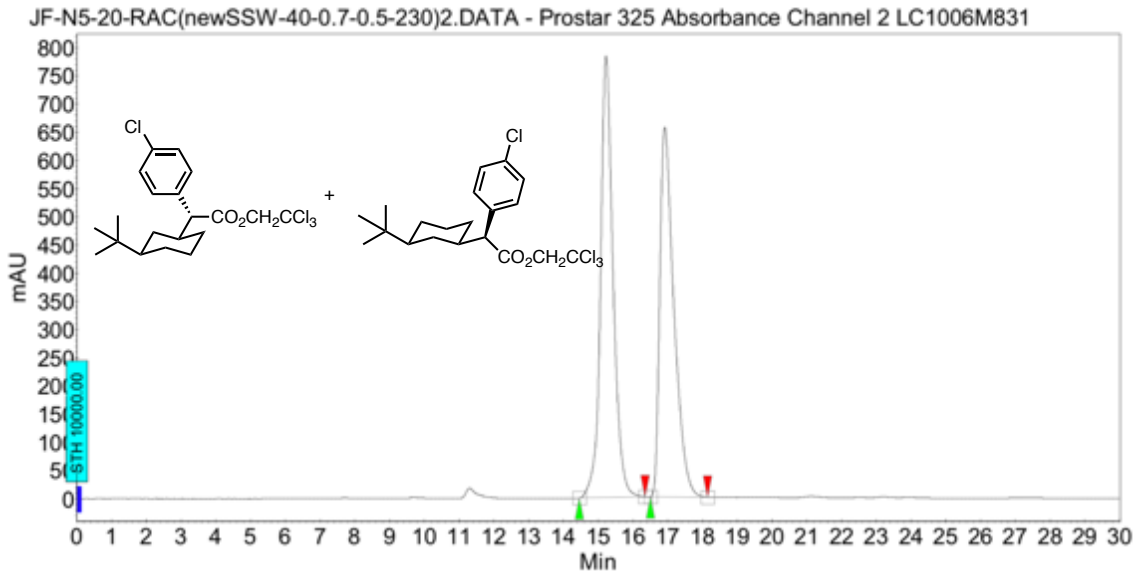

Peak results :

Index	Name	Time [Min]	Quantity [% Area]	Height [mAU]	Area [mAU.Min]	Area % [%]
1	UNKNOWN	15.22	51.59	783.4	329.1	51.594
2	UNKNOWN	16.92	48.41	655.7	308.8	48.406
Total			100.00	1439.1	637.9	100.000

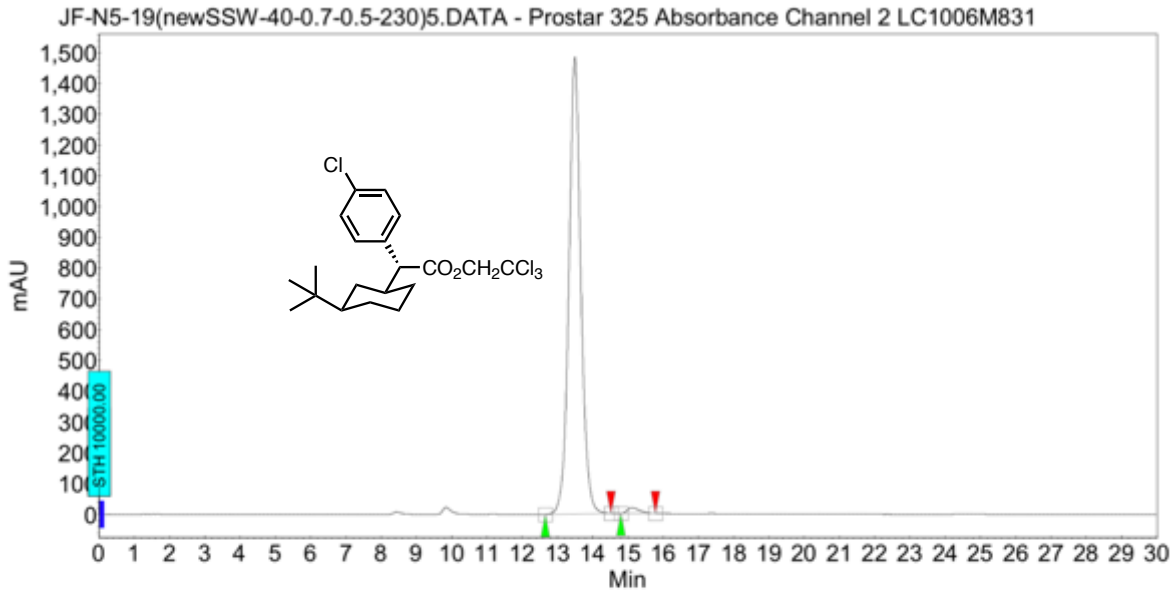

Peak results :

Index	Name	Time [Min]	Quantity [% Area]	Height [mAU]	Area [mAU.Min]	Area % [%]
1	UNKNOWN	13.50	98.70	1485.5	584.9	98.697
2	UNKNOWN	15.12	1.30	19.2	7.7	1.303
Total			100.00	1504.7	592.6	100.000

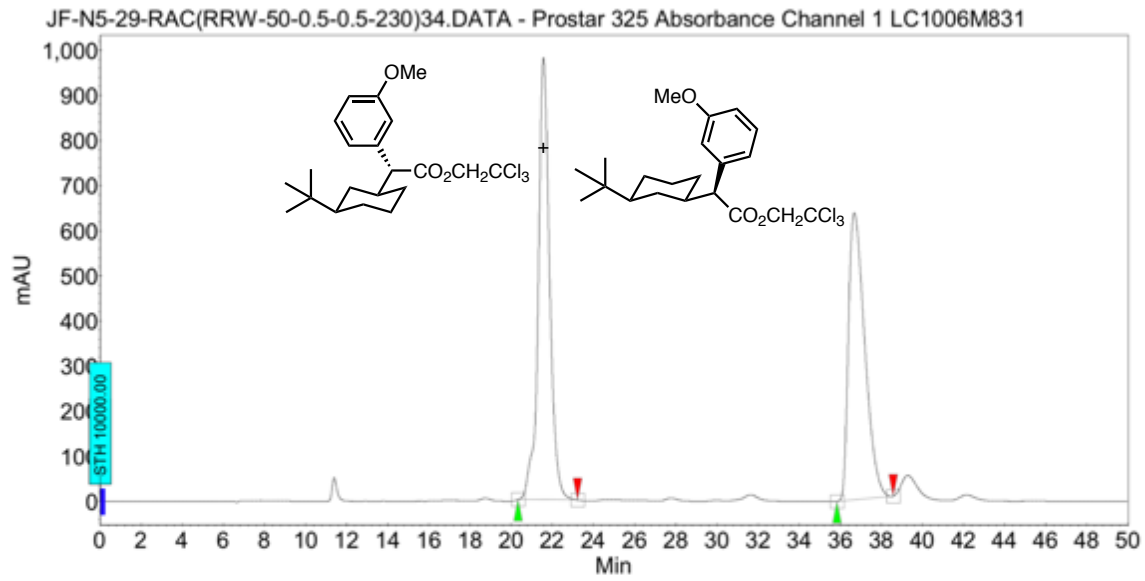

Peak results :

Index	Name	Time [Min]	Quantity [% Area]	Height [mAU]	Area [mAU.Min]	Area % [%]
1	UNKNOWN	21.57	51.94	979.7	630.2	51.943
2	UNKNOWN	36.69	48.06	635.6	583.0	48.057
Total			100.00	1615.2	1213.2	100.000

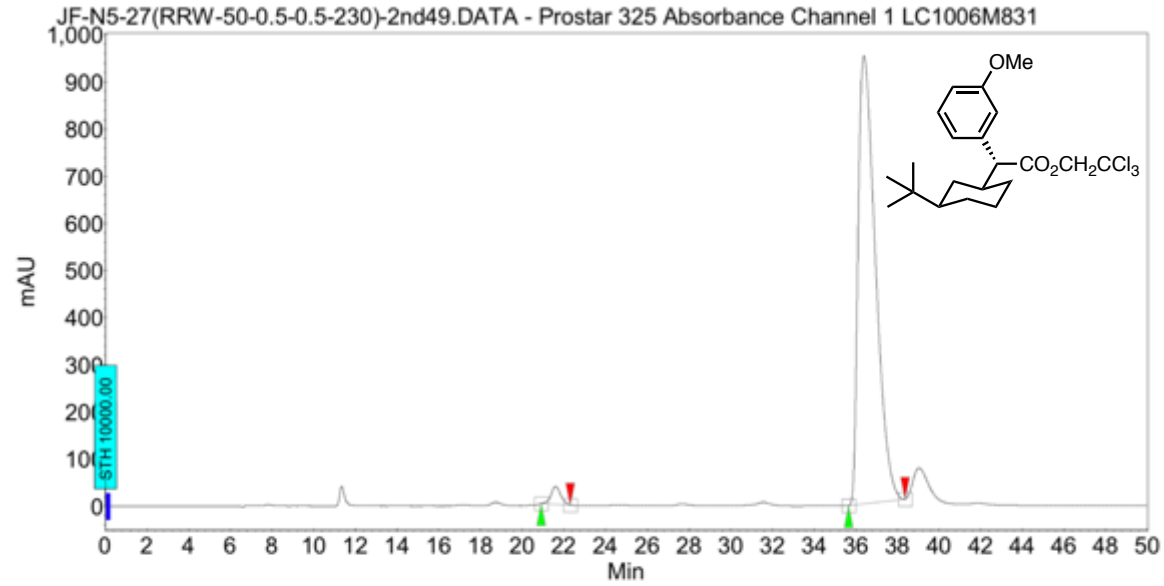

Peak results :

Index	Name	Time [Min]	Quantity [% Area]	Height [mAU]	Area [mAU.Min]	Area % [%]
2	UNKNOWN	21.60	2.17	37.9	20.2	2.165
1	UNKNOWN	36.40	97.83	949.8	913.9	97.835
Total			100.00	987.7	934.1	100.000

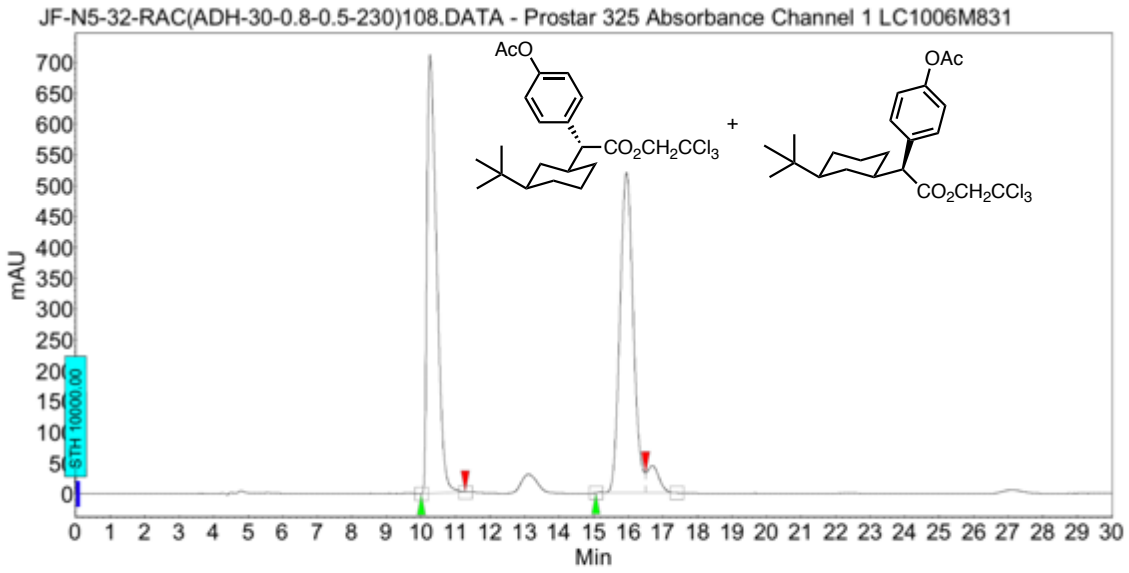

Peak results :

Index	Name	Time [Min]	Quantity [% Area]	Height [mAU]	Area [mAU.Min]	Area % [%]
1	UNKNOWN	10.26	49.62	711.0	230.2	49.618
2	UNKNOWN	15.95	50.38	520.0	233.7	50.382
Total			100.00	1230.9	463.9	100.000

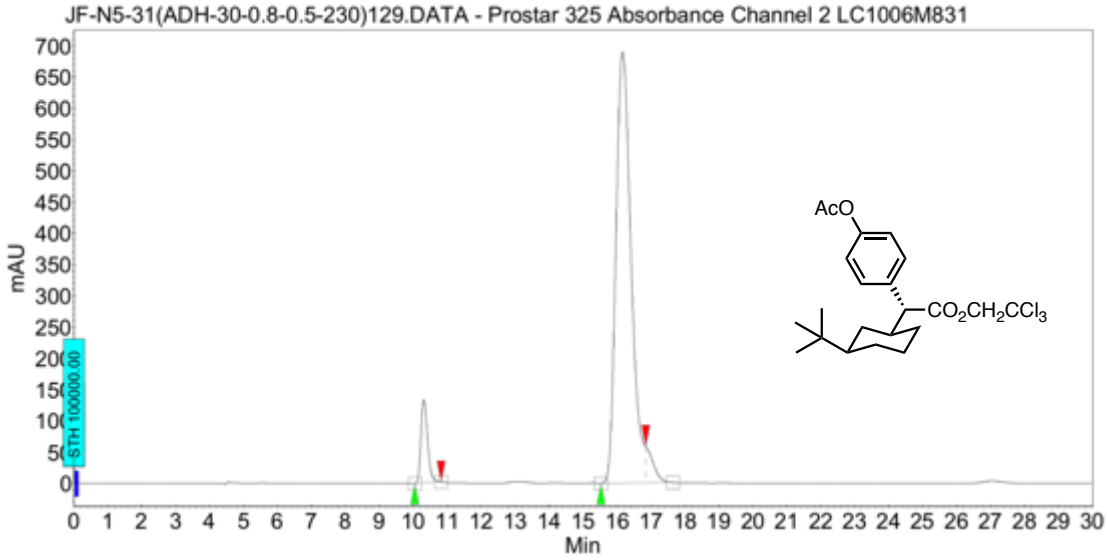

Peak results :

Index	Name	Time [Min]	Quantity [% Area]	Height [mAU]	Area [mAU.Min]	Area % [%]
1	UNKNOWN	10.30	7.80	132.9	30.0	7.802
2	UNKNOWN	16.16	92.20	689.6	355.0	92.198
Total			100.00	822.5	385.0	100.000

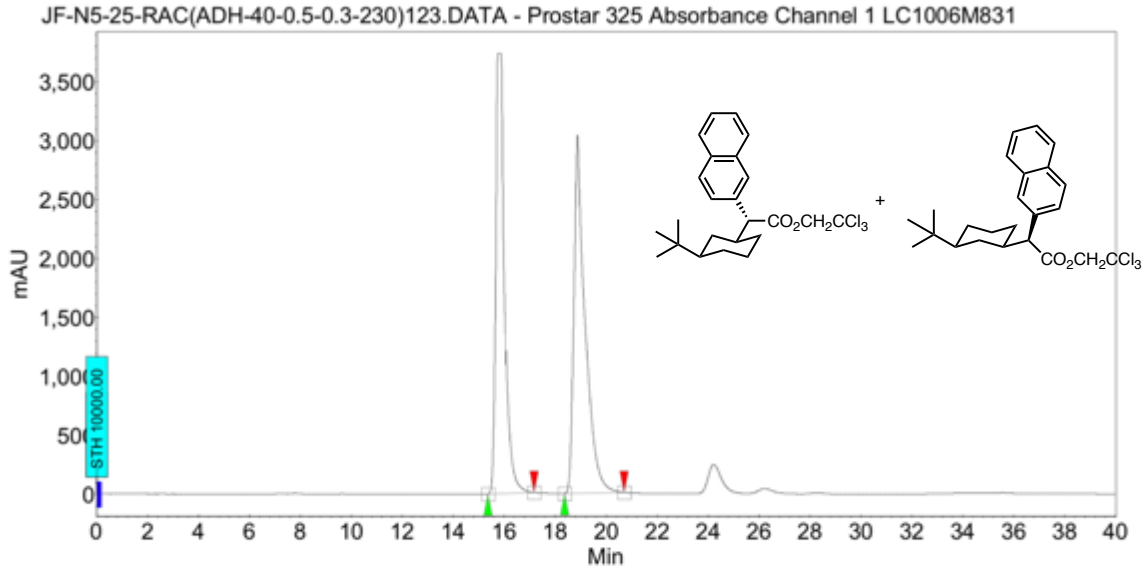

Peak results :

Index	Name	Time [Min]	Quantity [% Area]	Height [mAU]	Area [mAU.Min]	Area % [%]
1	UNKNOWN	15.76	49.22	3736.9	1495.8	49.225
2	UNKNOWN	18.87	50.78	3044.0	1542.9	50.775
Total			100.00	6780.9	3038.7	100.000

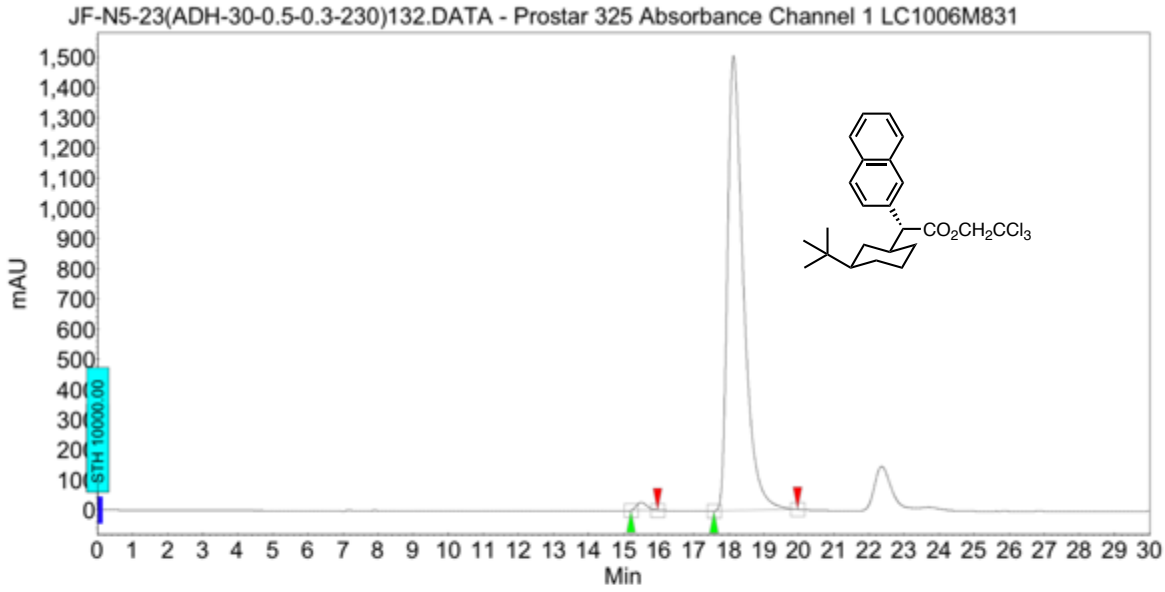

Peak results :

Index	Name	Time [Min]	Quantity [% Area]	Height [mAU]	Area [mAU.Min]	Area % [%]
1	UNKNOWN	15.50	1.12	26.5	9.1	1.124
2	UNKNOWN	18.14	98.88	1507.9	798.5	98.876
Total			100.00	1534.4	807.6	100.000

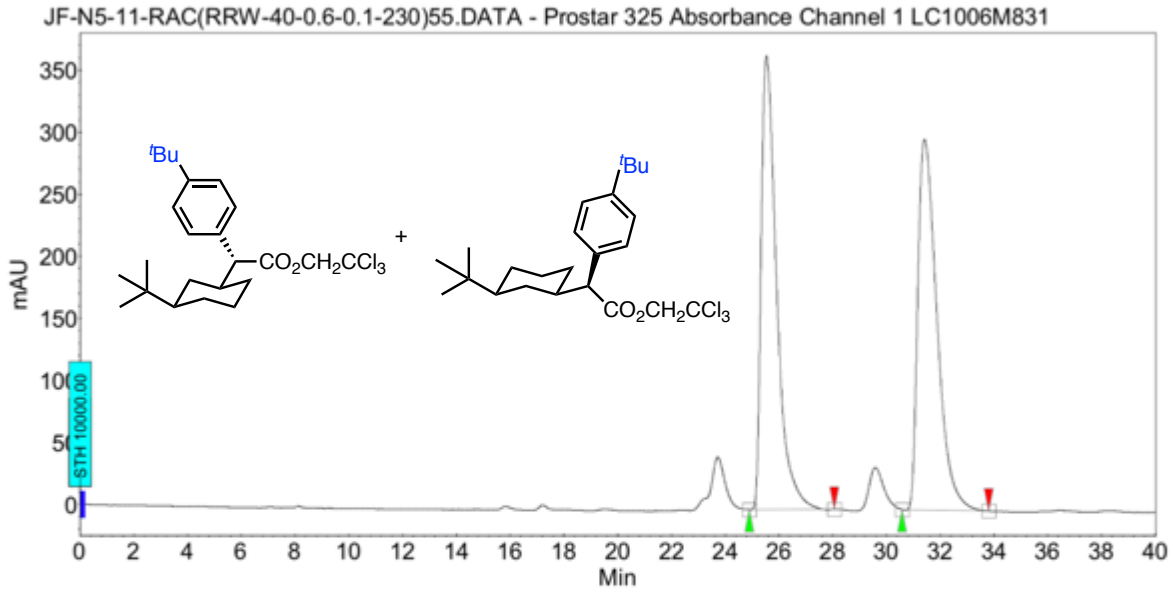

Peak results :

Index	Name	Time [Min]	Quantity [% Area]	Height [mAU]	Area [mAU.Min]	Area % [%]
1	UNKNOWN	25.54	49.76	365.8	243.6	49.760
2	UNKNOWN	31.42	50.24	298.9	245.9	50.240
Total			100.00	664.7	489.5	100.000

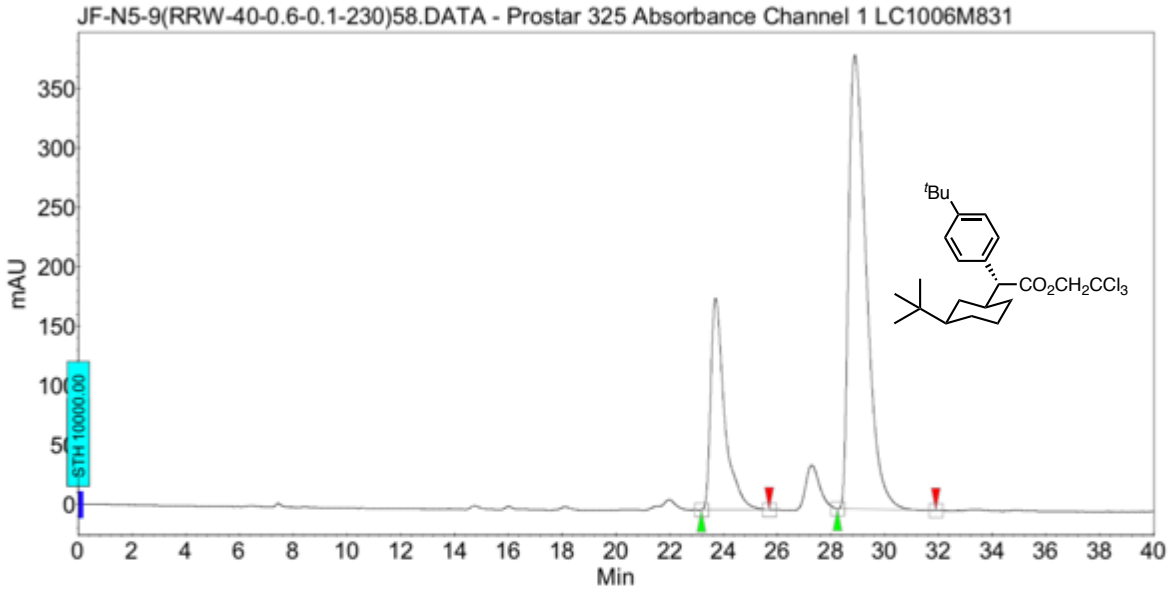

Peak results :

Index	Name	Time [Min]	Quantity [% Area]	Height [mAU]	Area [mAU.Min]	Area % [%]
1	UNKNOWN	23.71	26.74	178.3	106.5	26.737
2	UNKNOWN	28.89	73.26	382.4	291.9	73.263
Total			100.00	560.8	398.5	100.000

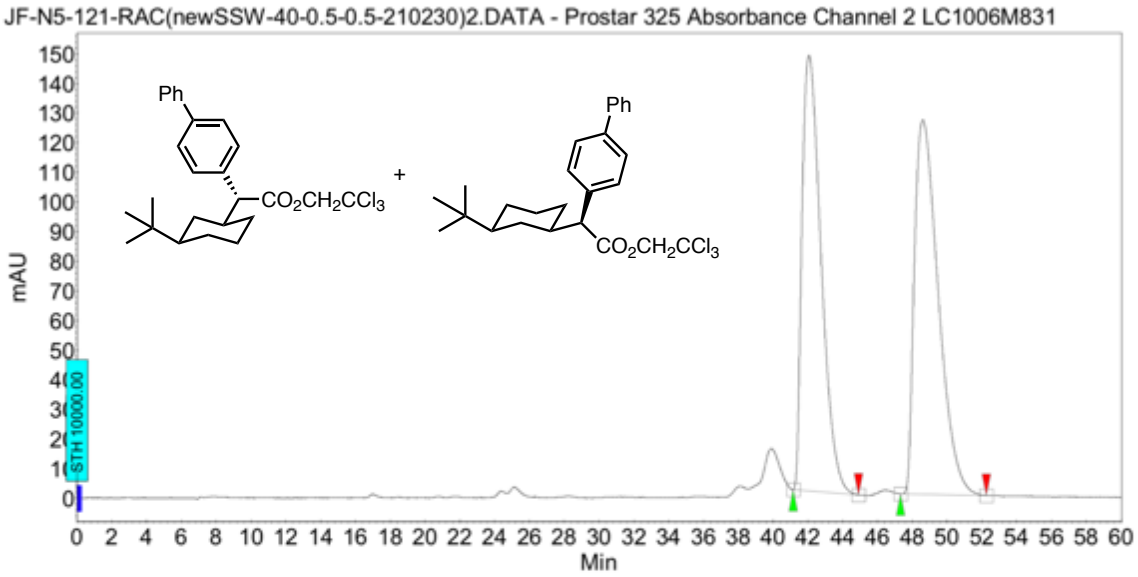

Peak results :

Index	Name	Time [Min]	Quantity [% Area]	Height [mAU]	Area [mAU.Min]	Area % [%]
1	UNKNOWN	42.07	48.30	147.1	187.5	48.302
2	UNKNOWN	48.60	51.70	126.4	200.7	51.698
Total			100.00	273.5	388.2	100.000

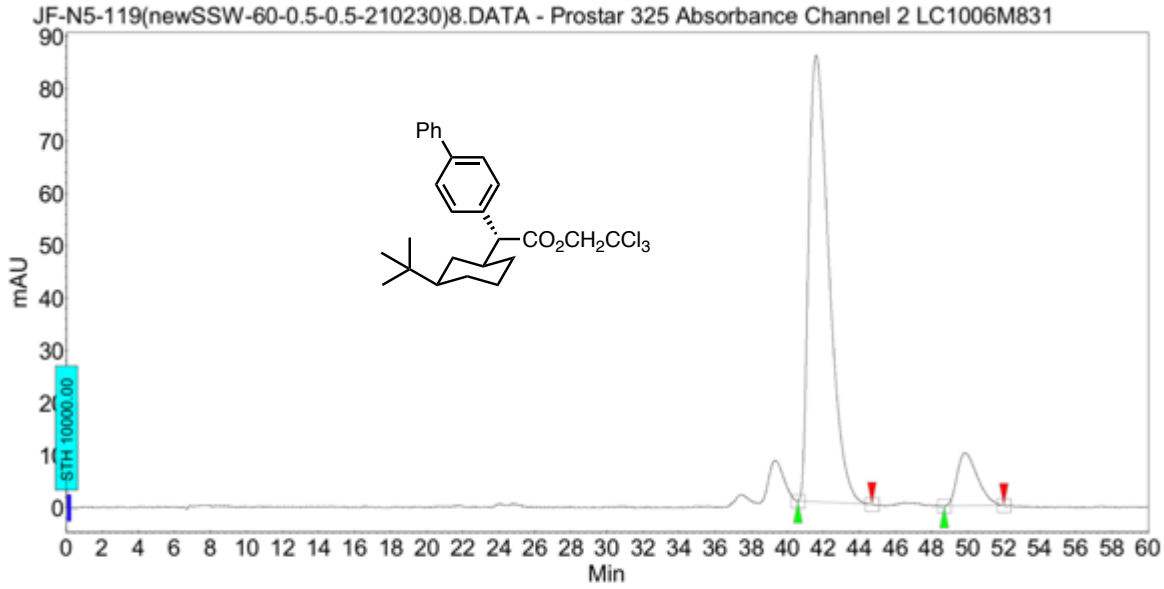

Peak results :

Index	Name	Time [Min]	Quantity [% Area]	Height [mAU]	Area [mAU.Min]	Area % [%]
1	UNKNOWN	41.59	89.37	85.2	111.4	89.371
2	UNKNOWN	49.89	10.63	10.1	13.2	10.629
Total			100.00	95.3	124.6	100.000

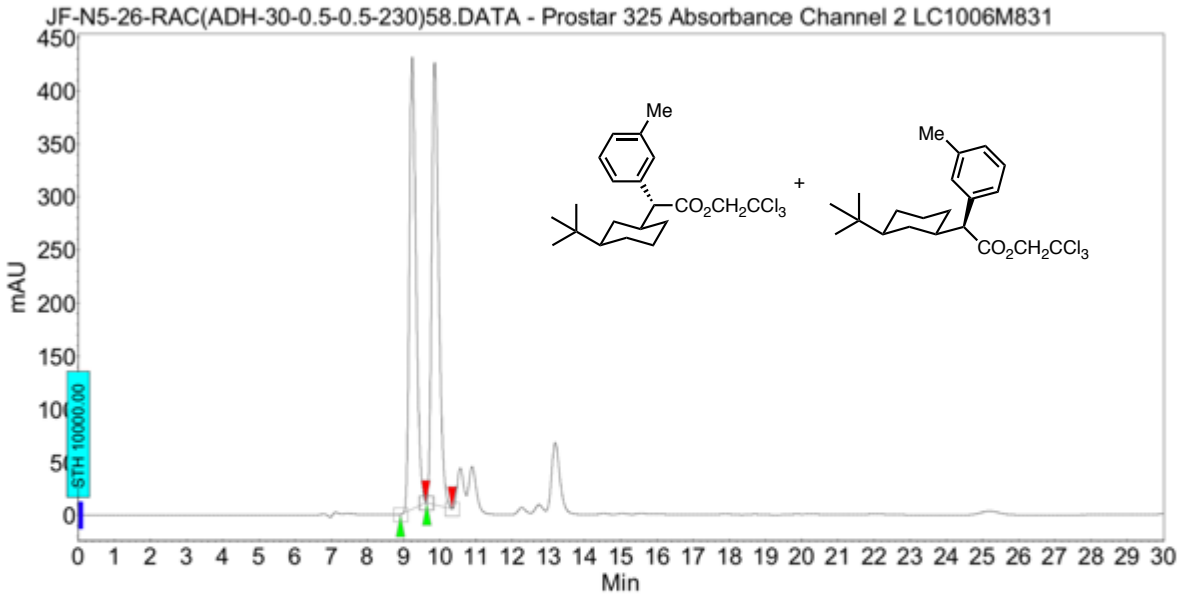

Peak results :

Index	Name	Time [Min]	Quantity [% Area]	Height [mAU]	Area [mAU.Min]	Area % [%]
1	UNKNOWN	9.24	49.10	425.8	91.0	49.101
2	UNKNOWN	9.86	50.90	416.6	94.4	50.899
Total			100.00	842.4	185.4	100.000

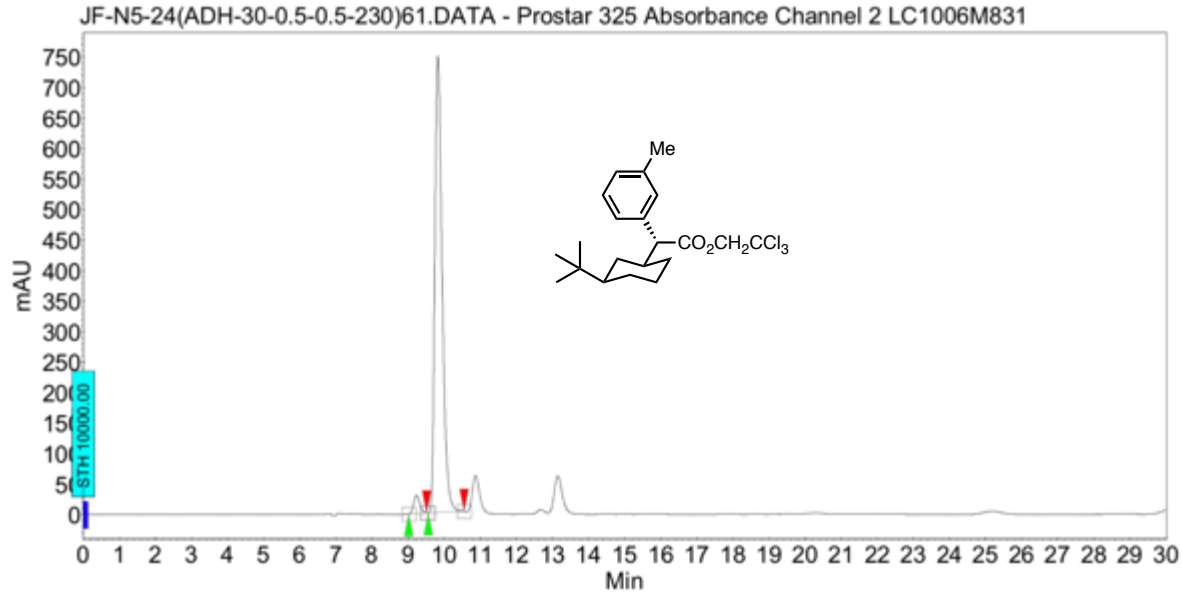

Peak results :

Index	Name	Time [Min]	Quantity [% Area]	Height [mAU]	Area [mAU.Min]	Area % [%]
1	UNKNOWN	9.23	3.23	30.0	5.9	3.234
2	UNKNOWN	9.82	96.77	748.5	176.6	96.766
Total			100.00	778.5	182.5	100.000

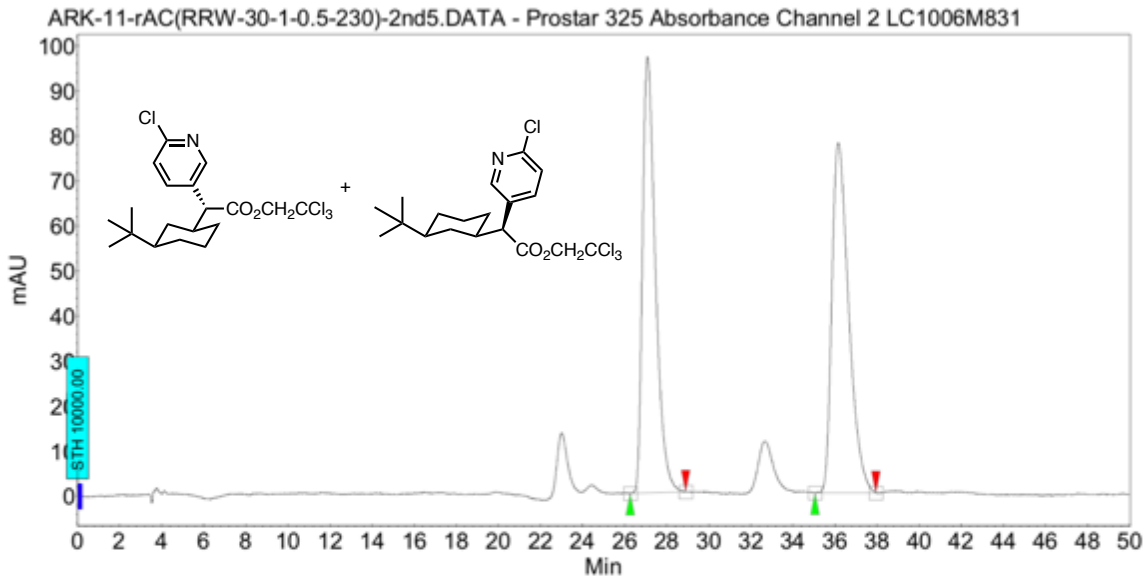

Peak results :

Index	Name	Time [Min]	Quantity [% Area]	Height [mAU]	Area [mAU.Min]	Area % [%]
1	UNKNOWN	27.08	48.85	96.7	68.7	48.853
2	UNKNOWN	36.15	51.15	77.6	72.0	51.147
Total			100.00	174.3	140.7	100.000

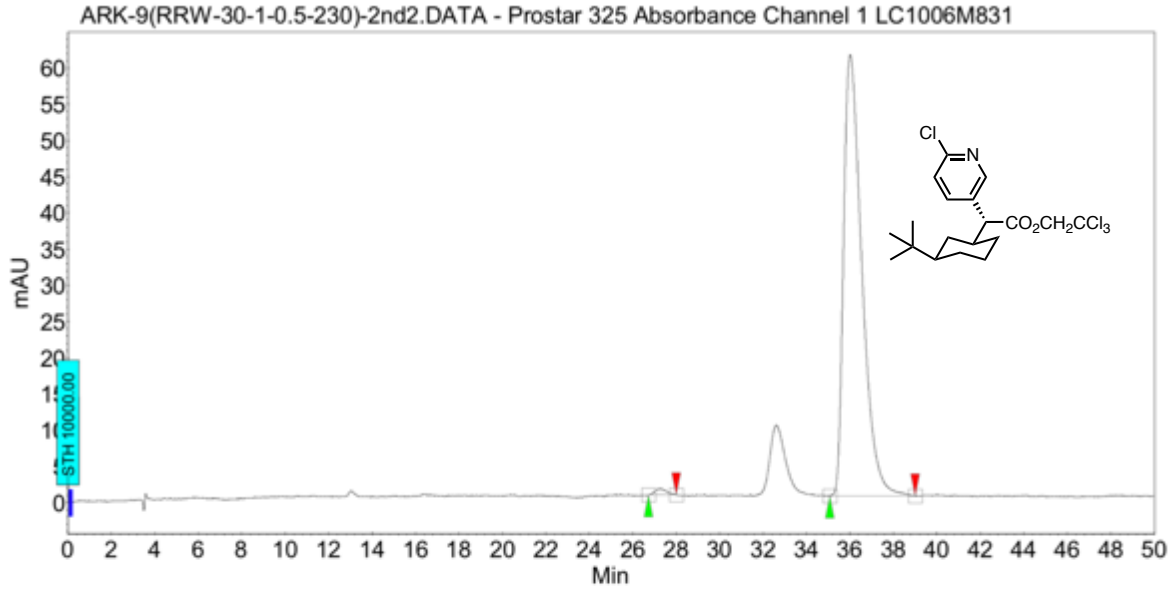

Peak results :

Index	Name	Time [Min]	Quantity [% Area]	Height [mAU]	Area [mAU.Min]	Area % [%]
1	UNKNOWN	27.23	0.91	0.8	0.5	0.909
2	UNKNOWN	36.01	99.09	60.9	59.4	99.091
Total			100.00	61.7	60.0	100.000

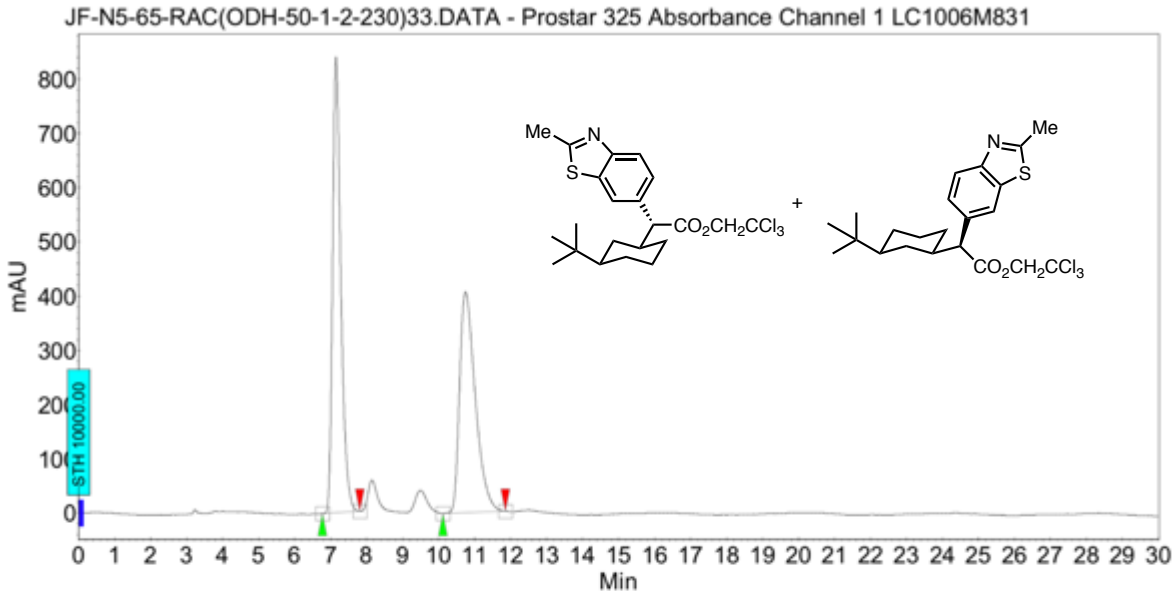

Peak results :

Index	Name	Time [Min]	Quantity [% Area]	Height [mAU]	Area [mAU.Min]	Area % [%]
1	UNKNOWN	7.15	51.97	840.7	223.3	51.965
2	UNKNOWN	10.75	48.03	407.3	206.4	48.035
Total			100.00	1248.0	429.7	100.000

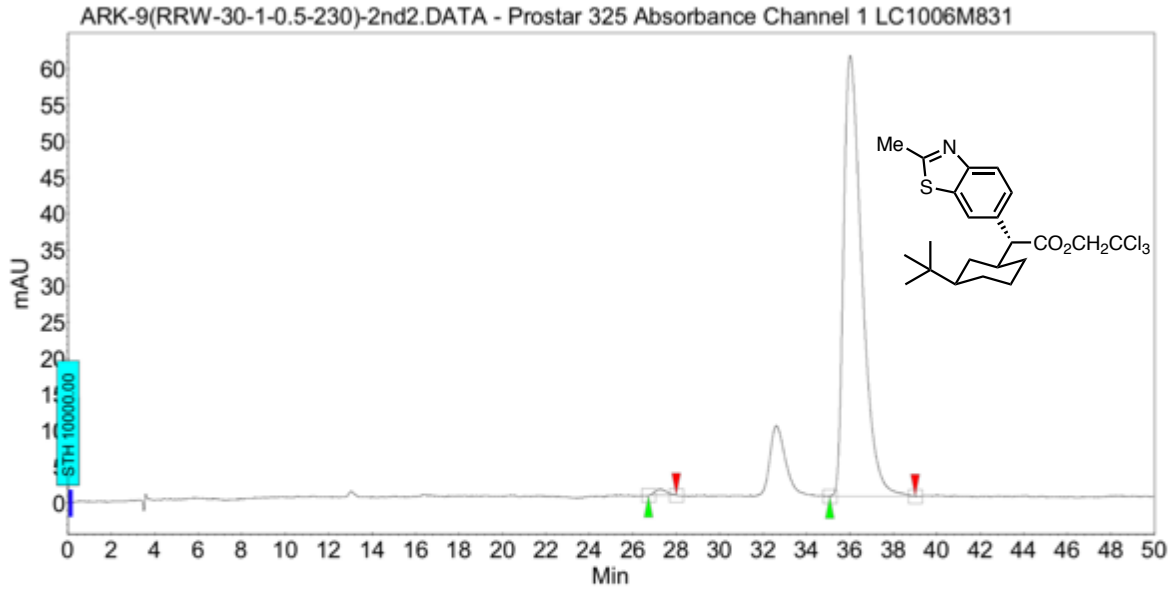

Peak results :

Index	Name	Time [Min]	Quantity [% Area]	Height [mAU]	Area [mAU.Min]	Area % [%]
1	UNKNOWN	27.23	0.91	0.8	0.5	0.909
2	UNKNOWN	36.01	99.09	60.9	59.4	99.091
Total			100.00	61.7	60.0	100.000

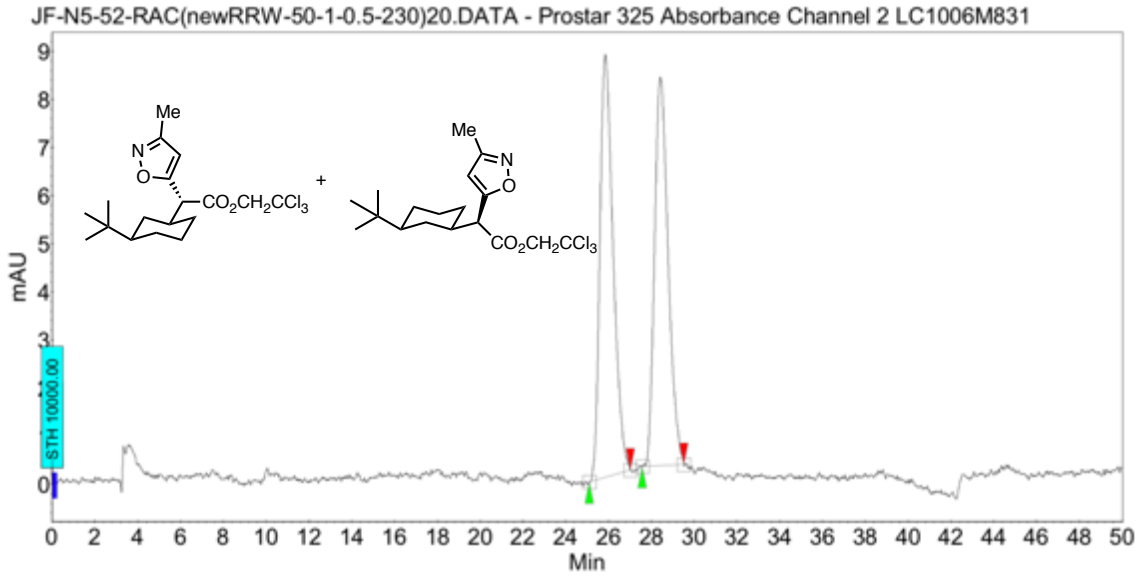

Peak results :

Index	Name	Time [Min]	Quantity [% Area]	Height [mAU]	Area [mAU.Min]	Area % [%]
1	UNKNOWN	25.85	51.33	8.8	6.3	51.333
2	UNKNOWN	28.42	48.67	8.1	6.0	48.667
Total			100.00	16.9	12.2	100.000

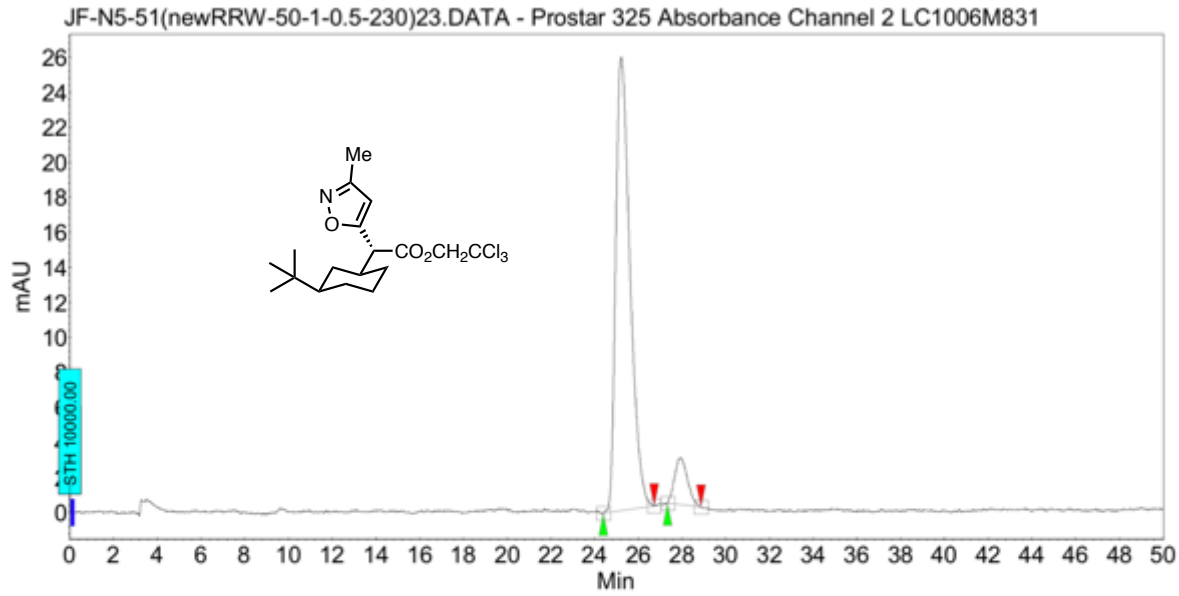

Peak results :

Index	Name	Time [Min]	Quantity [% Area]	Height [mAU]	Area [mAU.Min]	Area % [%]
1	UNKNOWN	25.22	91.47	25.9	19.6	91.469
2	UNKNOWN	27.94	8.53	2.7	1.8	8.531
Total			100.00	28.6	21.4	100.000

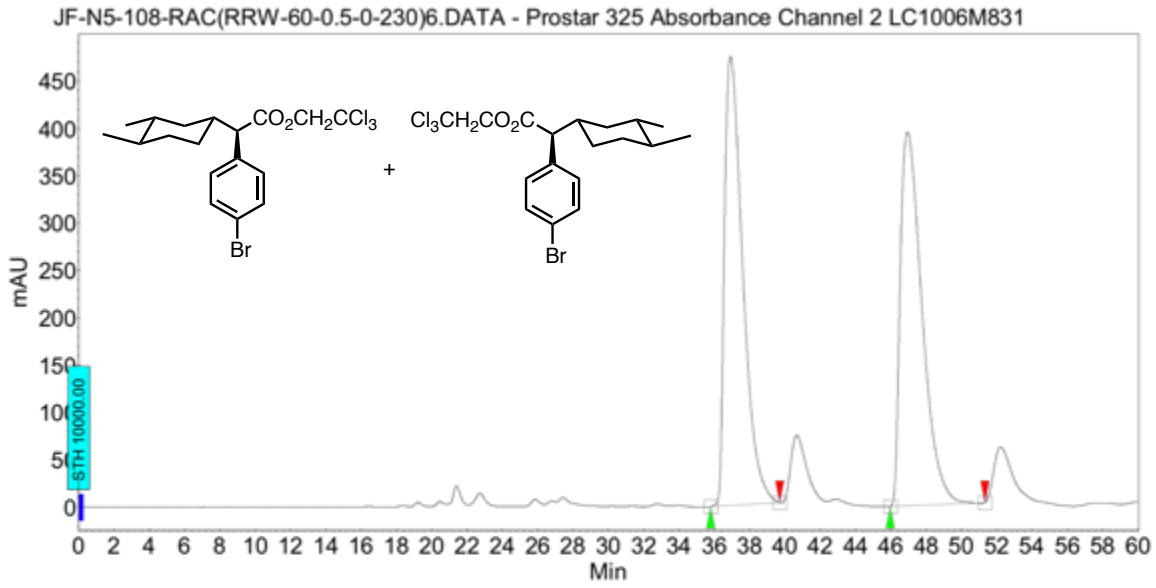

Peak results :

Index	Name	Time [Min]	Quantity [% Area]	Height [mAU]	Area [mAU.Min]	Area % [%]
1	UNKNOWN	36.92	50.27	474.4	570.5	50.275
2	UNKNOWN	46.94	49.73	394.9	564.3	49.725
Total			100.00	869.3	1134.8	100.000

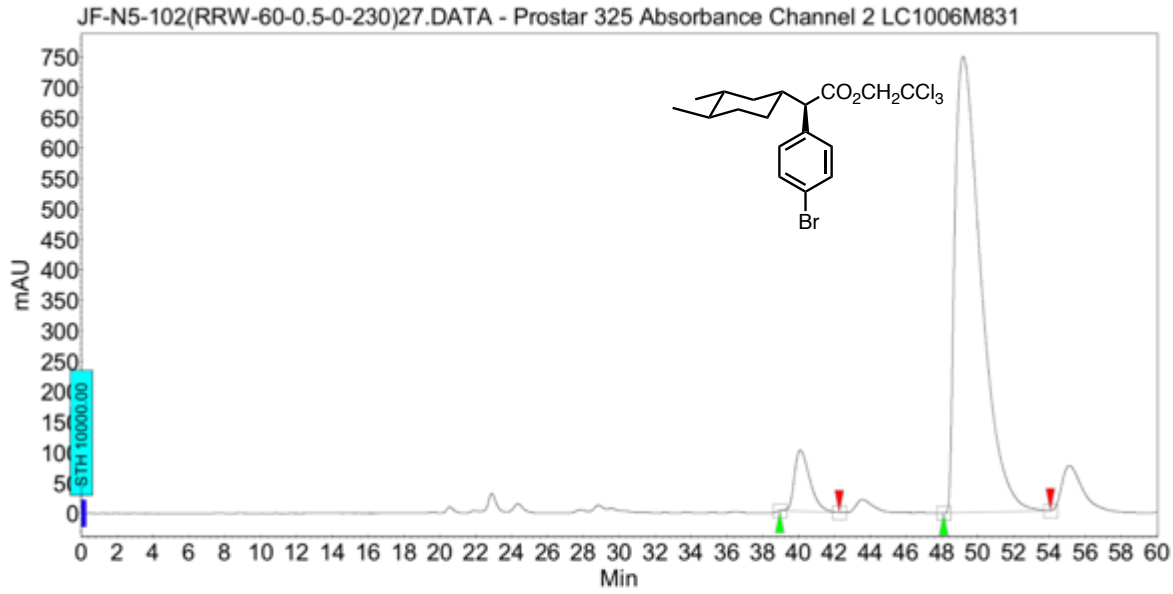

Peak results :

Index	Name	Time [Min]	Quantity [% Area]	Height [mAU]	Area [mAU.Min]	Area % [%]
1	UNKNOWN	40.10	7.34	100.3	100.2	7.342
2	UNKNOWN	49.19	92.66	750.1	1264.3	92.658
Total			100.00	850.4	1364.5	100.000

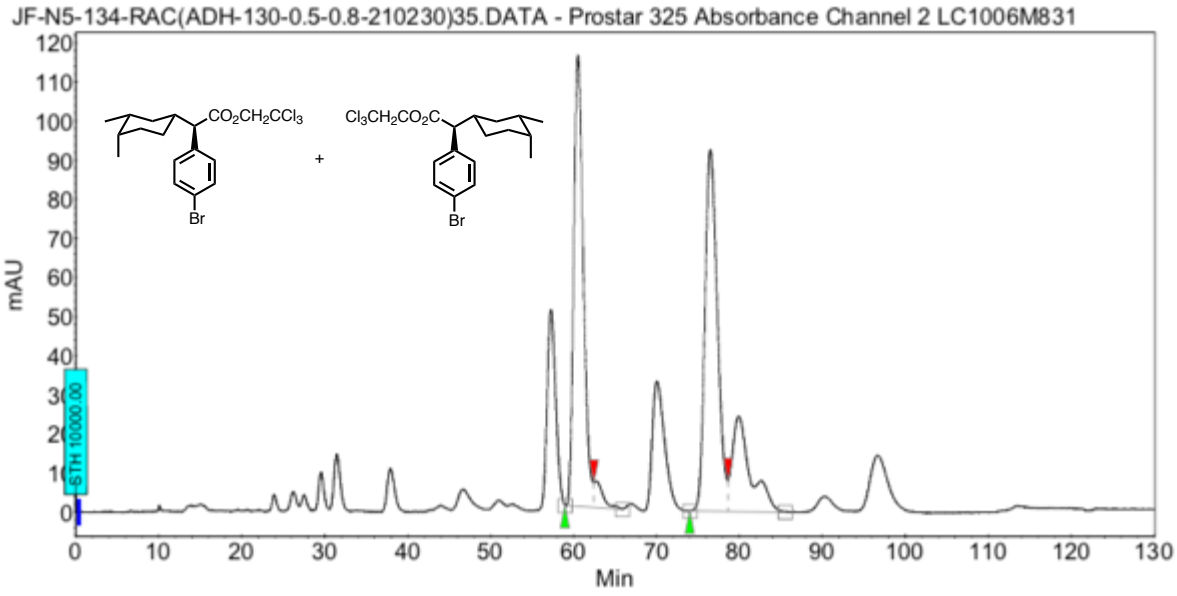

Peak results :

Index	Name	Time [Min]	Quantity [% Area]	Height [mAU]	Area [mAU.Min]	Area % [%]
2	UNKNOWN	60.52	49.12	115.4	155.1	49.116
1	UNKNOWN	76.49	50.88	92.4	160.7	50.884

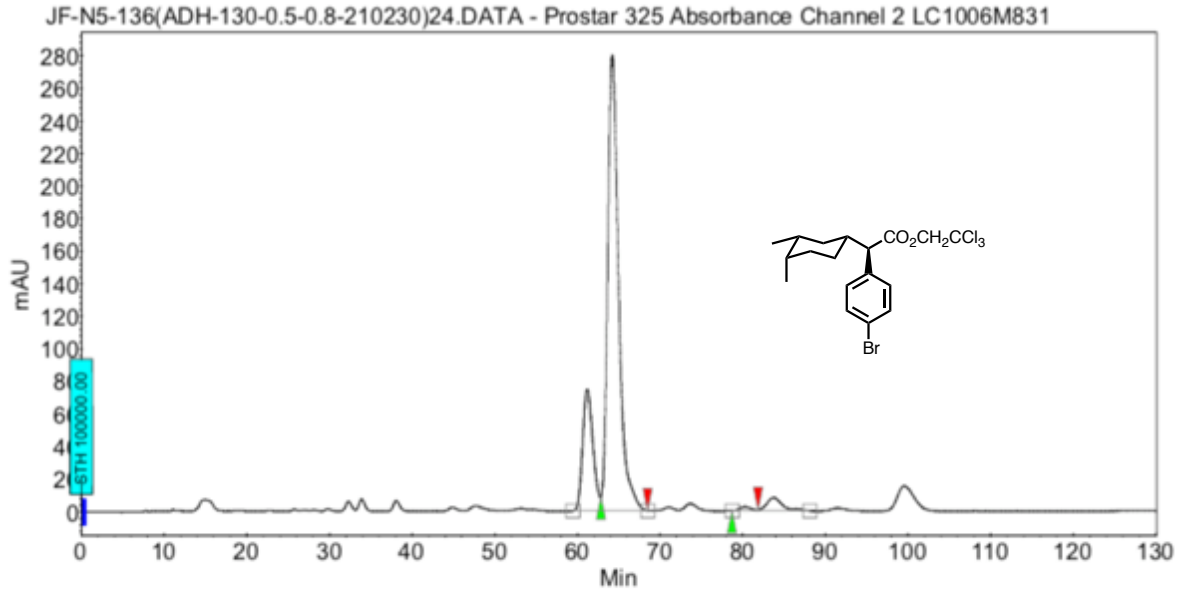

Peak results :

Index	Name	Time [Min]	Quantity [% Area]	Height [mAU]	Area [mAU.Min]	Area % [%]
2	UNKNOWN	64.22	99.09	279.8	431.2	99.092
1	UNKNOWN	80.26	0.91	2.6	4.0	0.908
Total			100.00	282.4	435.1	100.000

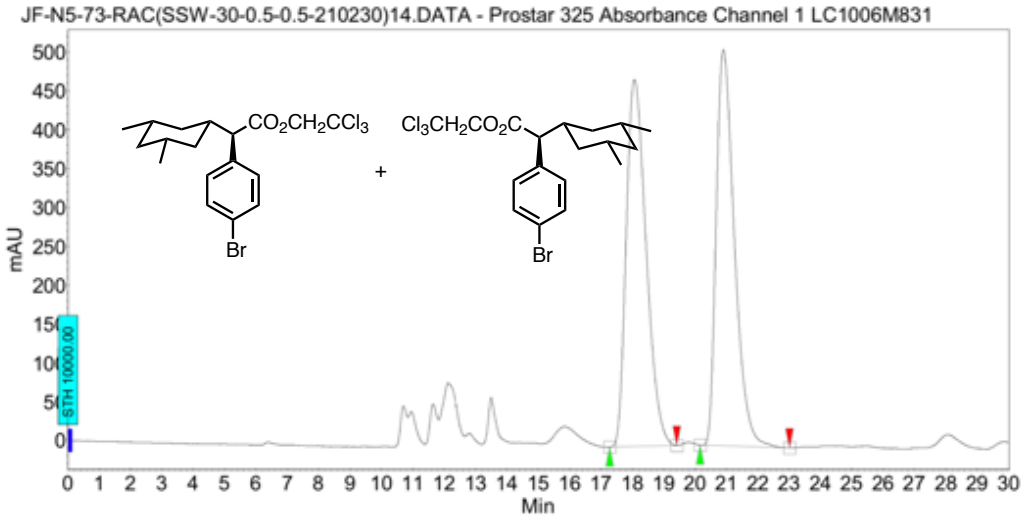

Peak results :

Index	Name	Time [Min]	Quantity [% Area]	Height [mAU]	Area [mAU.Min]	Area % [%]
1	UNKNOWN	18.07	50.32	472.3	347.4	50.321
2	UNKNOWN	20.91	49.68	510.1	343.0	49.679
Total			100.00	982.4	690.4	100.000

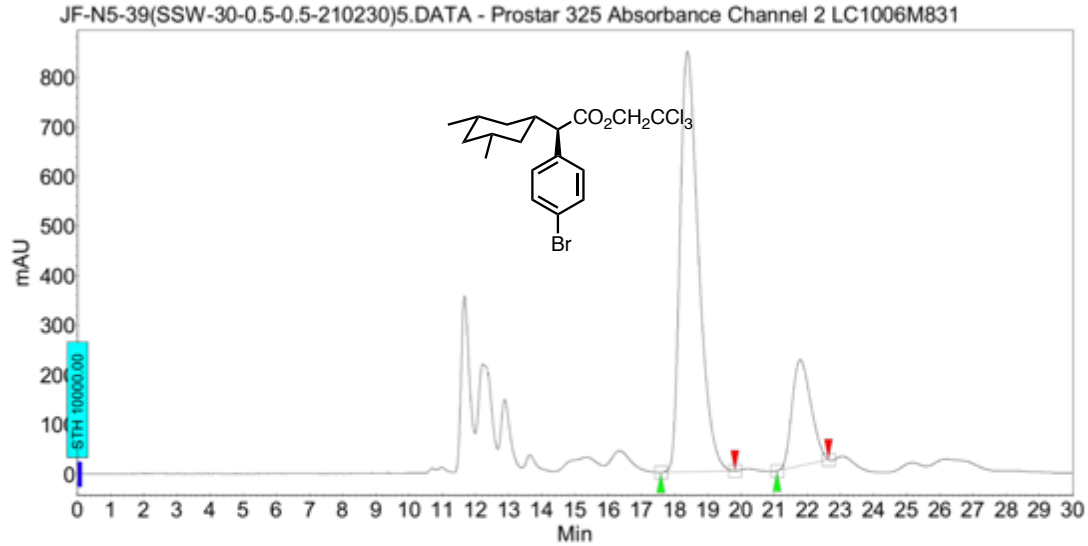

Peak results :

Index	Name	Time [Min]	Quantity [% Area]	Height [mAU]	Area [mAU.Min]	Area % [%]
1	UNKNOWN	18.39	79.61	848.8	548.5	79.607
2	UNKNOWN	21.78	20.39	214.2	140.5	20.393
Total			100.00	1063.0	689.0	100.000

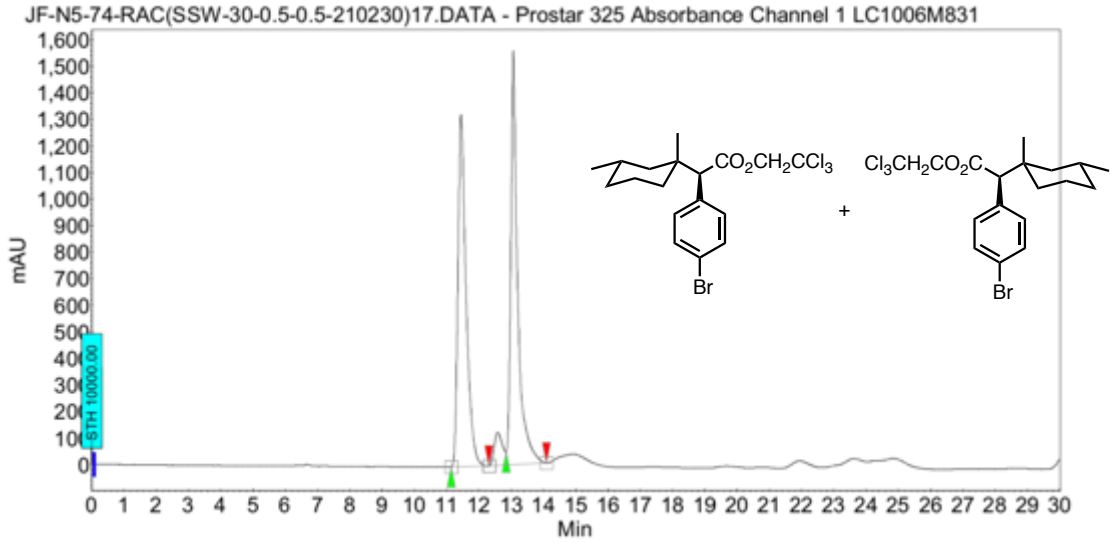

Peak results :

Index	Name	Time [Min]	Quantity [% Area]	Height [mAU]	Area [mAU.Min]	Area % [%]
1	UNKNOWN	11.45	50.25	1326.5	387.0	50.250
2	UNKNOWN	13.07	49.75	1560.5	383.2	49.750
Total			100.00	2887.0	770.2	100.000

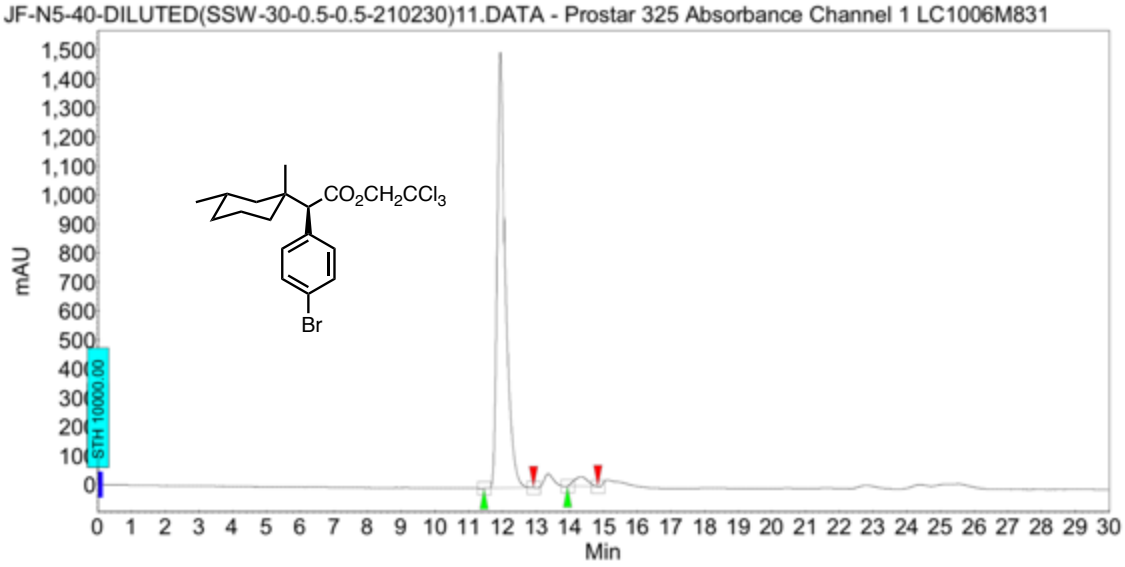

Peak results :

Index	Name	Time [Min]	Quantity [% Area]	Height [mAU]	Area [mAU.Min]	Area % [%]
1	UNKNOWN	11.94	96.52	1503.8	432.8	96.516
2	UNKNOWN	14.35	3.48	33.0	15.6	3.484
Total			100.00	1536.8	448.4	100.000

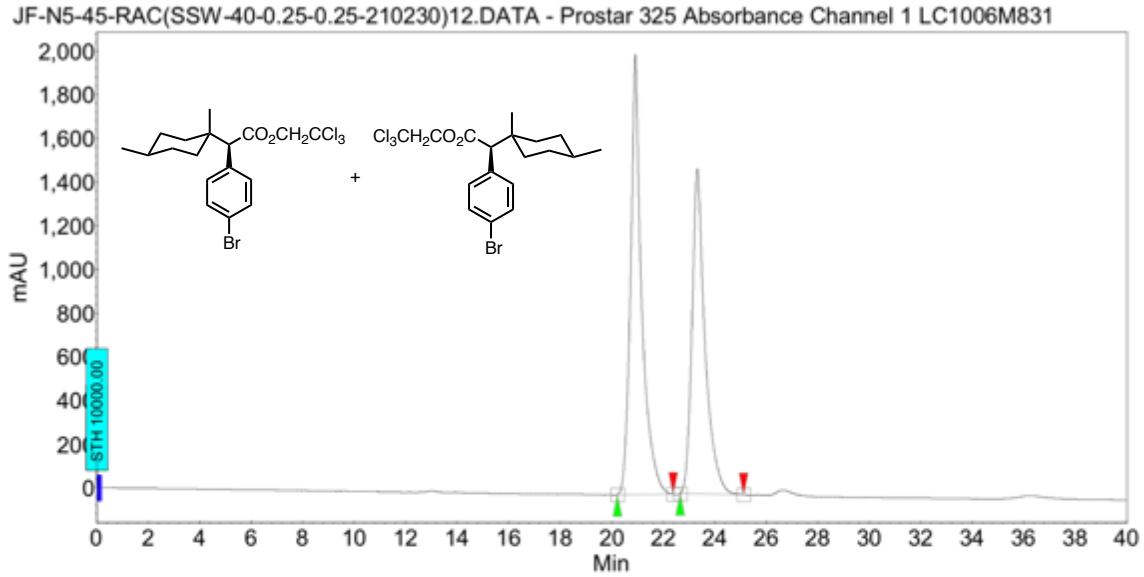

Peak results :

Index	Name	Time [Min]	Quantity [% Area]	Height [mAU]	Area [mAU.Min]	Area % [%]
2	UNKNOWN	20.92	53.72	2014.6	1005.6	53.723
1	UNKNOWN	23.33	46.28	1487.6	866.2	46.277
Total			100.00	3502.2	1871.8	100.000

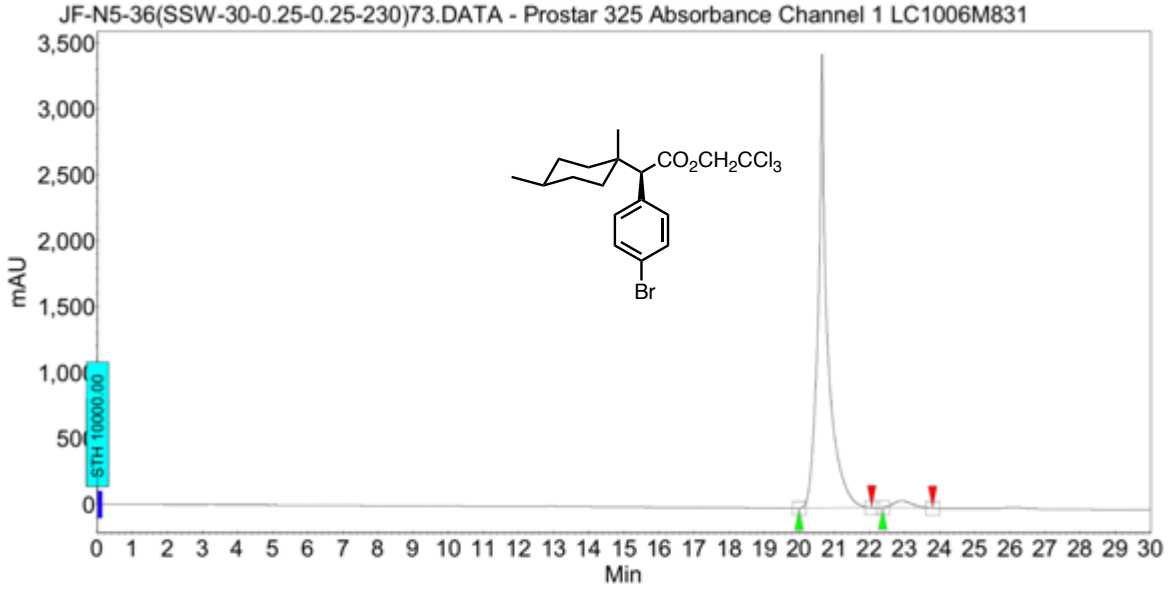

Peak results :

Index	Name	Time [Min]	Quantity [% Area]	Height [mAU]	Area [mAU.Min]	Area % [%]
1	UNKNOWN	20.65	96.94	3445.4	1065.7	96.935
2	UNKNOWN	22.92	3.06	54.2	33.7	3.065
Total			100.00	3499.6	1099.4	100.000

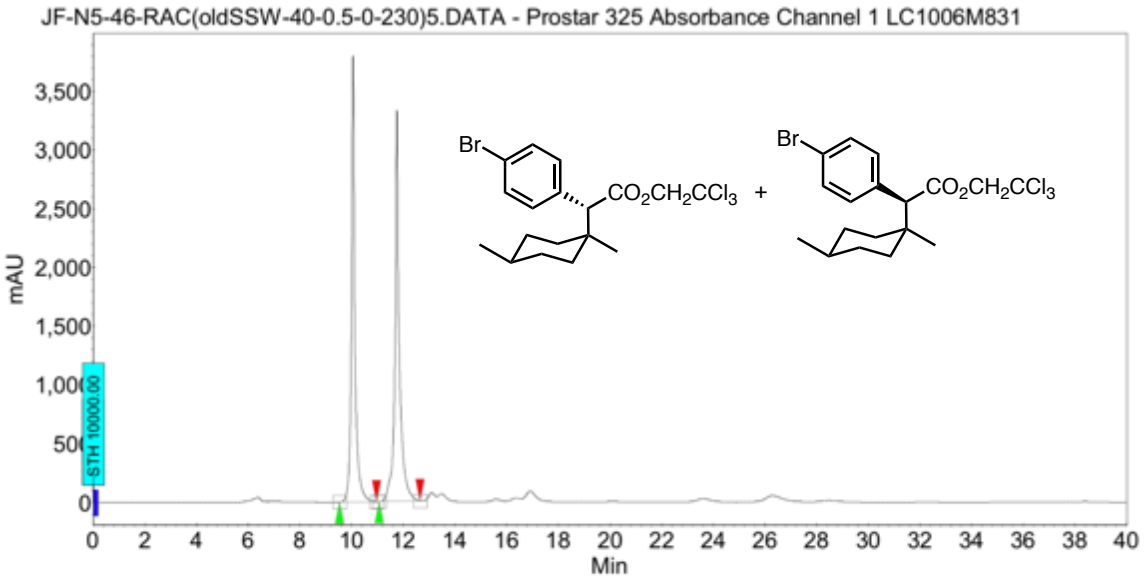

Peak results :

Index	Name	Time [Min]	Quantity [% Area]	Height [mAU]	Area [mAU.Min]	Area % [%]
1	UNKNOWN	10.05	48.05	3800.1	600.9	48.050
2	UNKNOWN	11.75	51.95	3330.9	649.7	51.950
Total			100.00	7130.9	1250.6	100.000

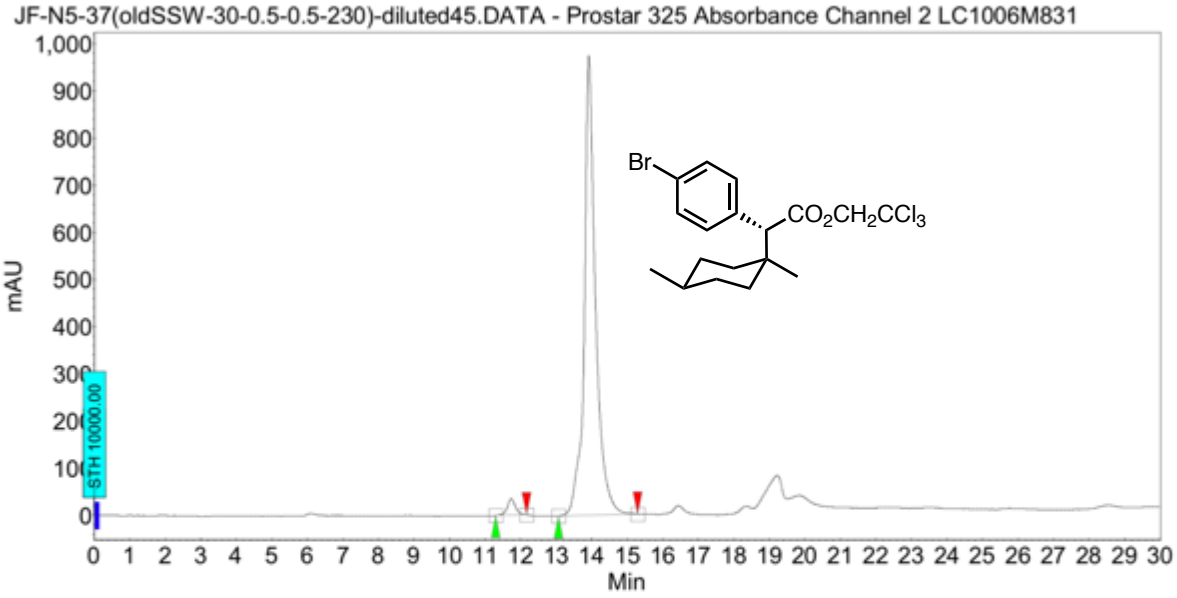

Peak results :

Index	Name	Time [Min]	Quantity [% Area]	Height [mAU]	Area [mAU.Min]	Area % [%]
1	UNKNOWN	11.74	2.54	34.9	9.3	2.536
2	UNKNOWN	13.92	97.46	974.7	358.6	97.464
Total			100.00	1009.6	368.0	100.000

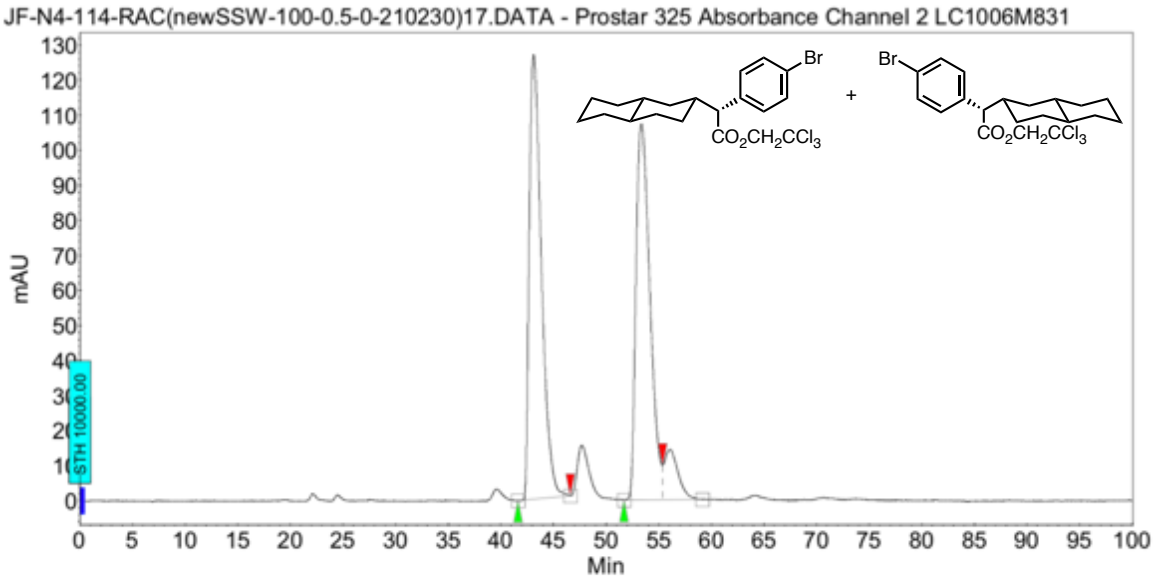

Peak results :

Index	Name	Time [Min]	Quantity [% Area]	Height [mAU]	Area [mAU.Min]	Area % [%]
1	UNKNOWN	43.12	50.75	126.8	170.1	50.751
2	UNKNOWN	53.36	49.25	107.2	165.0	49.249
Total			100.00	233.9	335.1	100.000

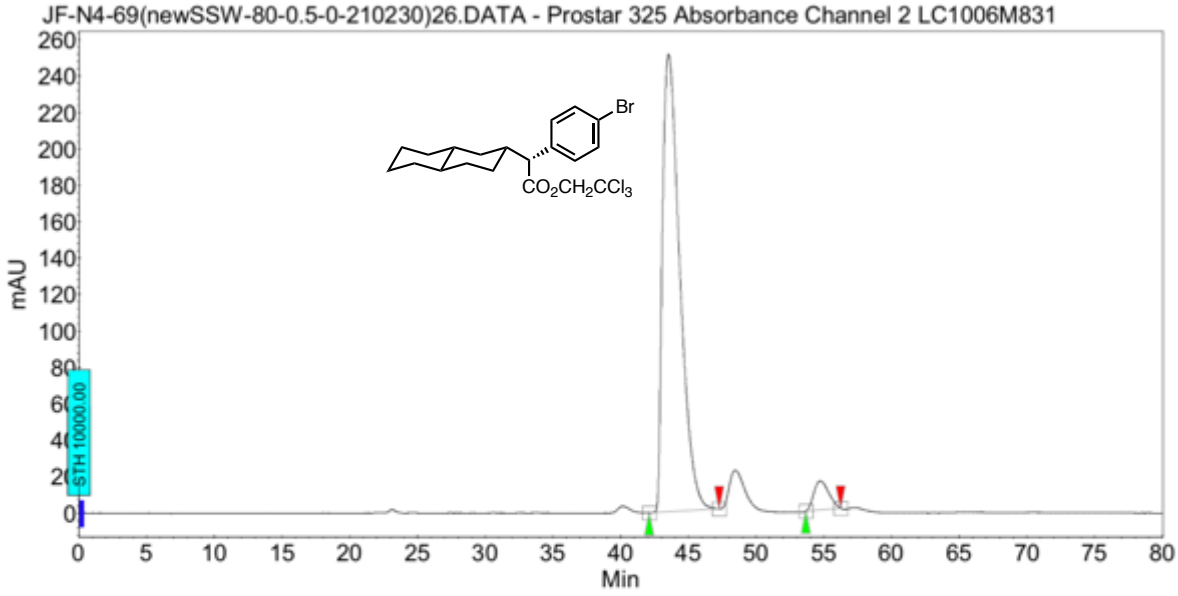

Peak results :

Index	Name	Time [Min]	Quantity [% Area]	Height [mAU]	Area [mAU.Min]	Area % [%]
1	UNKNOWN	43.54	94.84	251.2	371.8	94.840
2	UNKNOWN	54.74	5.16	15.9	20.2	5.160
Total			100.00	267.2	392.0	100.000

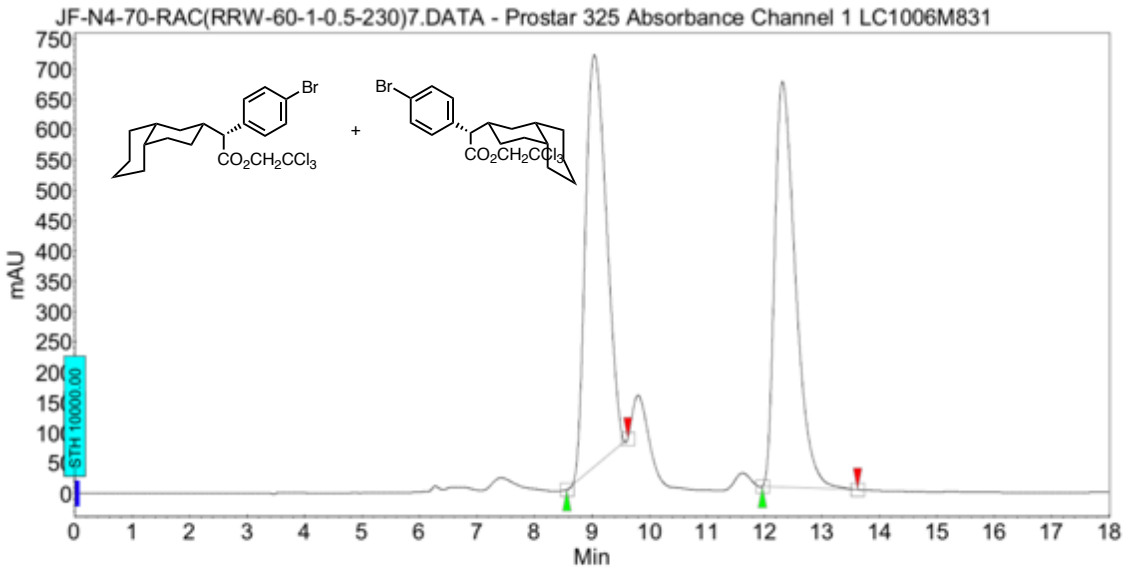

Peak results :

Index	Name	Time [Min]	Quantity [% Area]	Height [mAU]	Area [mAU.Min]	Area % [%]
1	UNKNOWN	9.04	50.50	679.9	286.5	50.501
2	UNKNOWN	12.32	49.50	669.0	280.8	49.499
Total			100.00	1348.9	567.3	100.000

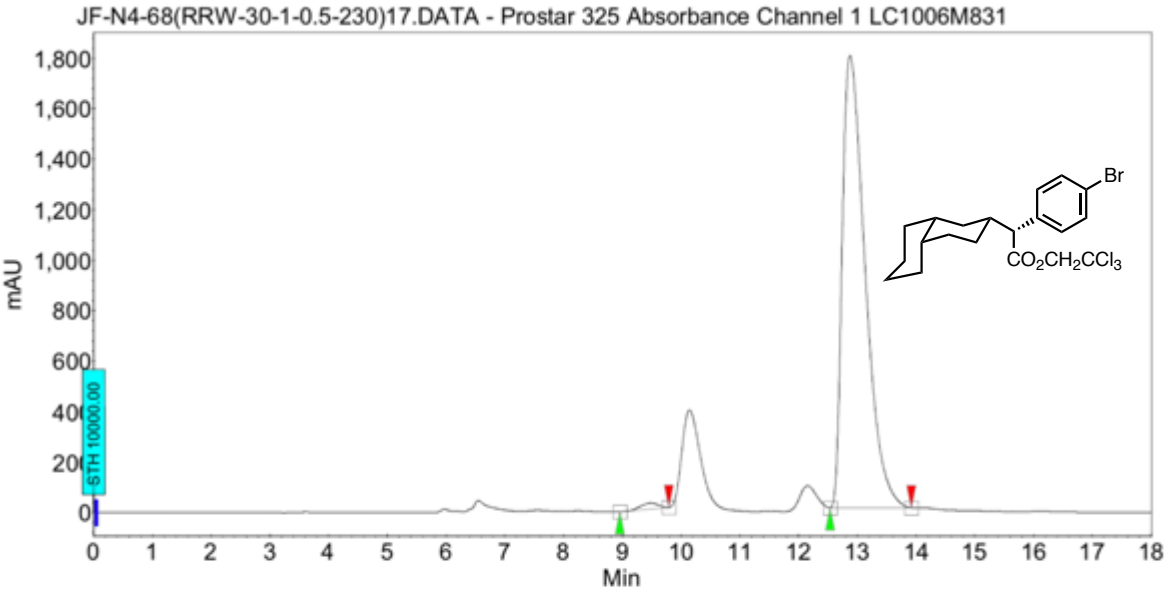

Peak results :

Index	Name	Time [Min]	Quantity [% Area]	Height [mAU]	Area [mAU.Min]	Area % [%]
1	UNKNOWN	9.46	1.01	23.8	8.3	1.012
2	UNKNOWN	12.88	98.99	1793.4	808.6	98.988
Total			100.00	1817.1	816.9	100.000

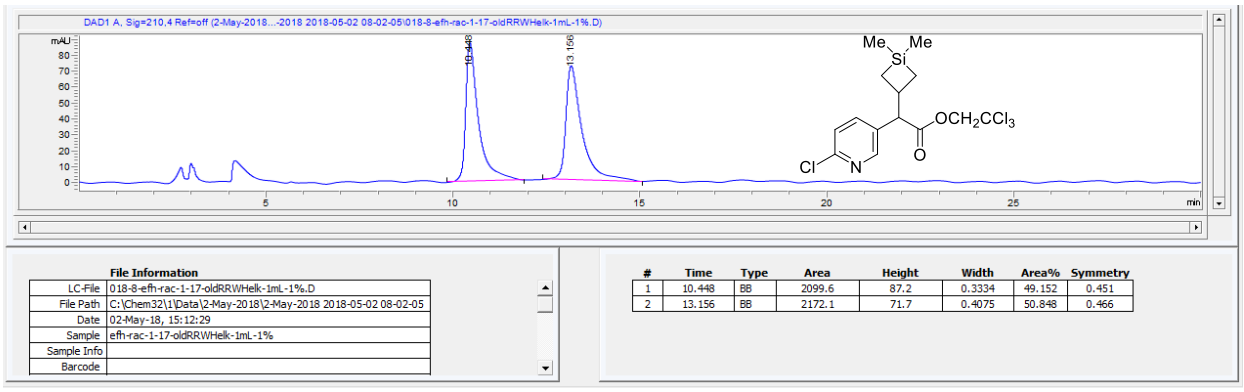

File Information

LC-File	018-8-efh-rac-1-17-oldRRWHelk-1mL-1%.D
File Path	C:\Chem32\1\Data\2-May-2018\2-May-2018 2018-05-02 08-02-05
Date	02-May-18, 15:12:29
Sample	efh-rac-1-17-oldRRWHelk-1mL-1%
Sample Info	
Barcode	

#	Time	Type	Area	Height	Width	Area%	Symmetry
1	10.448	BB	2099.6	87.2	0.3334	49.152	0.451
2	13.156	BB	2172.1	71.7	0.4075	50.848	0.466

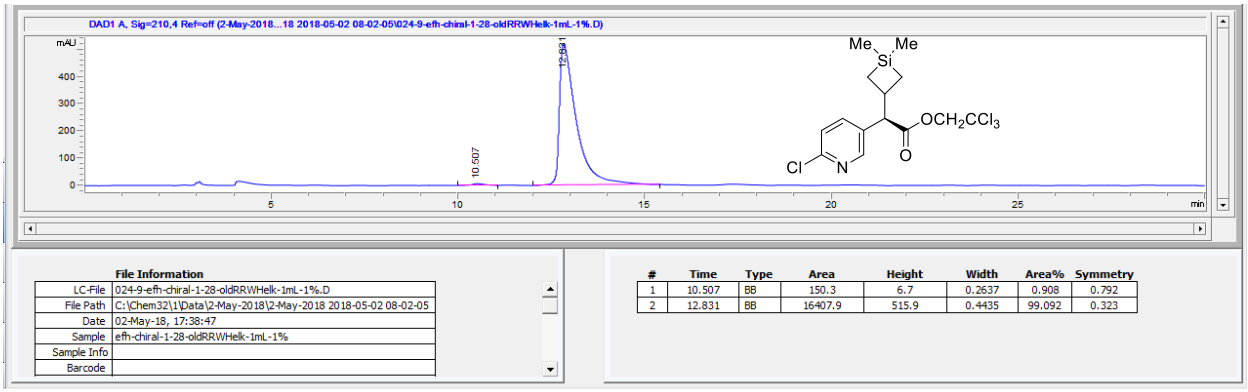

File Information

LC-File	024-9-efh-chiral-1-28-oldRRWHelk-1mL-1%.D
File Path	C:\Chem32\1\Data\2-May-2018\2-May-2018 2018-05-02 08-02-05
Date	02-May-18, 17:38:47
Sample	efh-chiral-1-28-oldRRWHelk-1mL-1%
Sample Info	
Barcode	

#	Time	Type	Area	Height	Width	Area%	Symmetry
1	10.507	BB	150.3	6.7	0.2637	0.908	0.792
2	12.831	BB	16407.9	515.9	0.4435	99.092	0.323

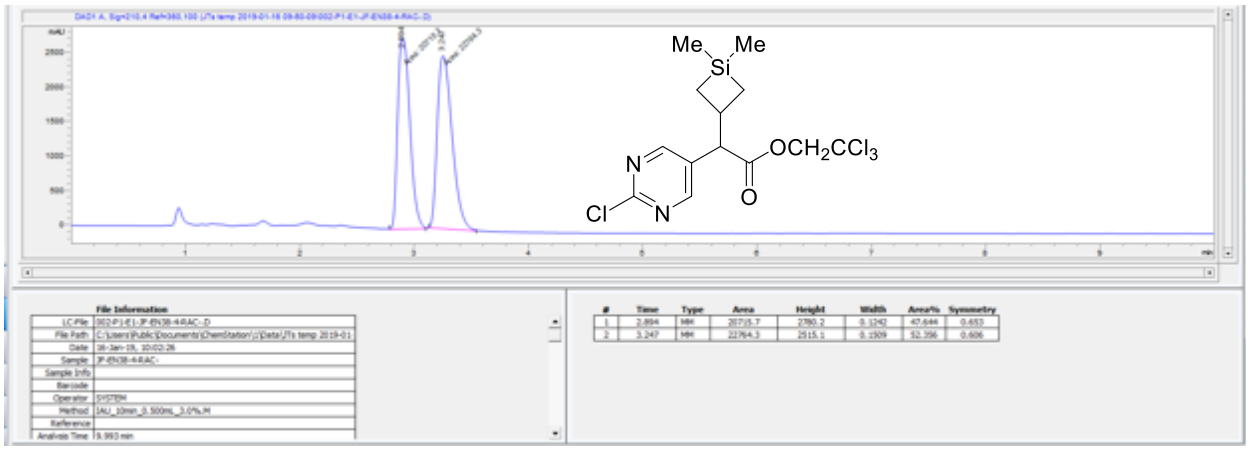
Me
Si
Me
N
Cl
N
O
OCH2CCl3

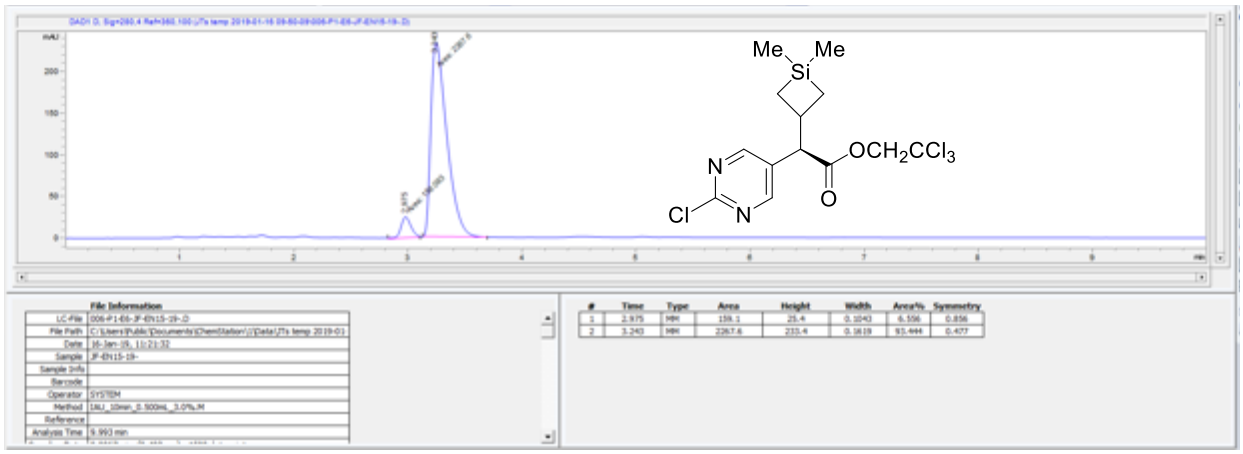
Me
Si
Me
N
Cl
N
O
OCH2CCl3

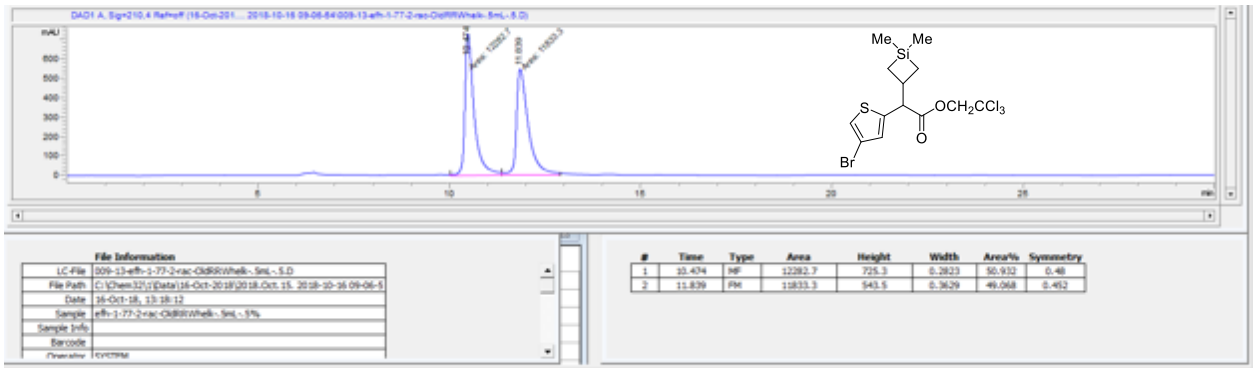

#	Time	Type	Area	Height	Width	Area%	Symmetry
1	10.474	MF	12282.7	725.3	0.2823	50.932	0.48
2	11.839	FM	11833.3	543.5	0.3629	49.068	0.452

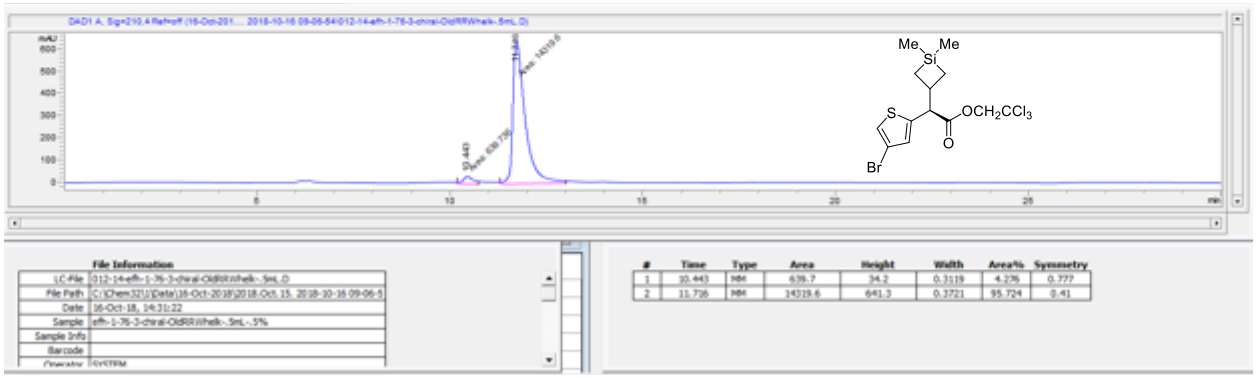

#	Time	Type	Area	Height	Width	Area%	Symmetry
1	10.443	MM	639.7	34.2	0.3119	4.276	0.777
2	11.736	MM	14319.6	641.3	0.3721	95.724	0.41

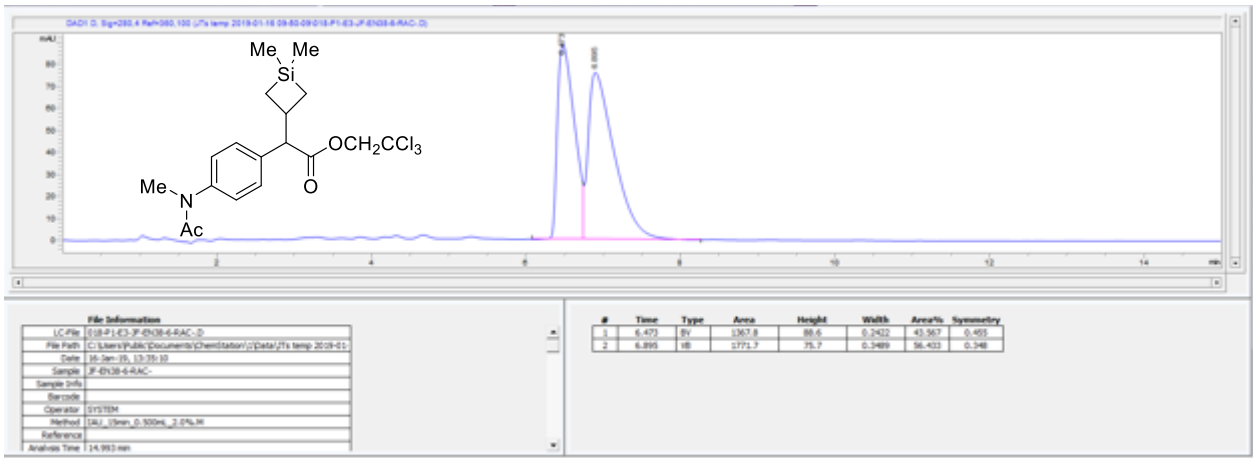
Me
Me
Si
OCH2CCl3
O
Me
N
Ac

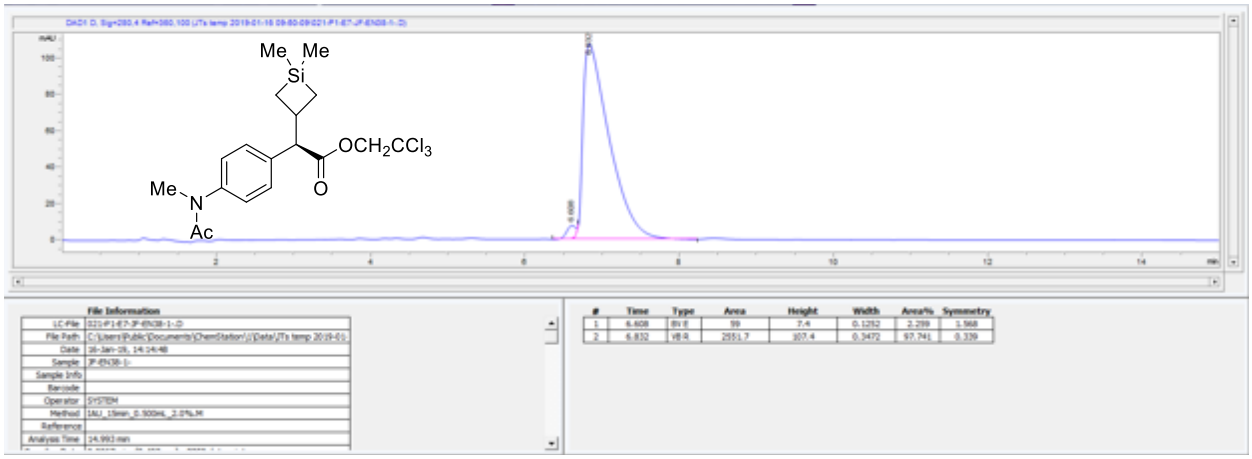
Me
Me
Si
OCH2CCl3
O
Me
N
Ac

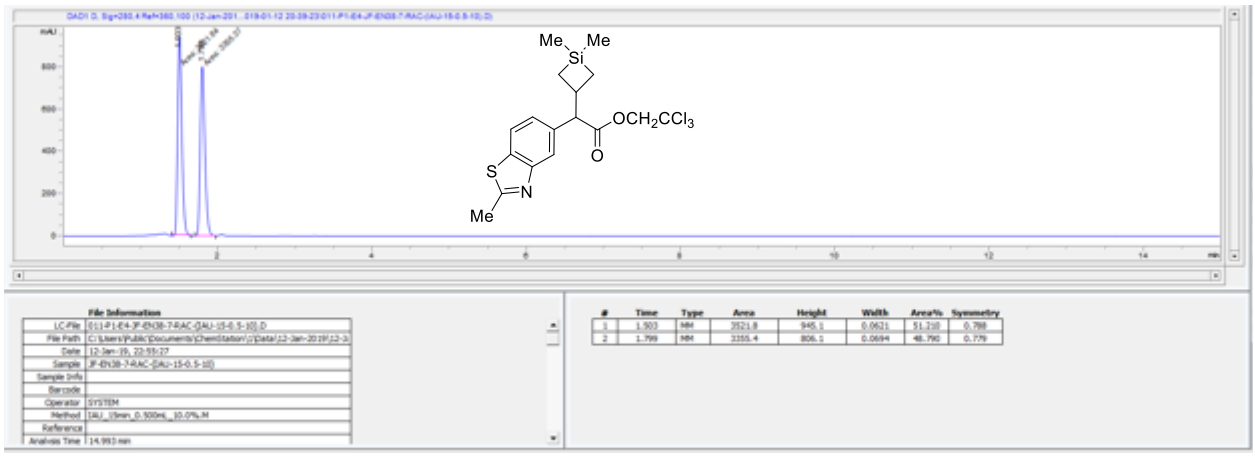
Me
Me
Si
OCH2CCl3
O
S
N
Me

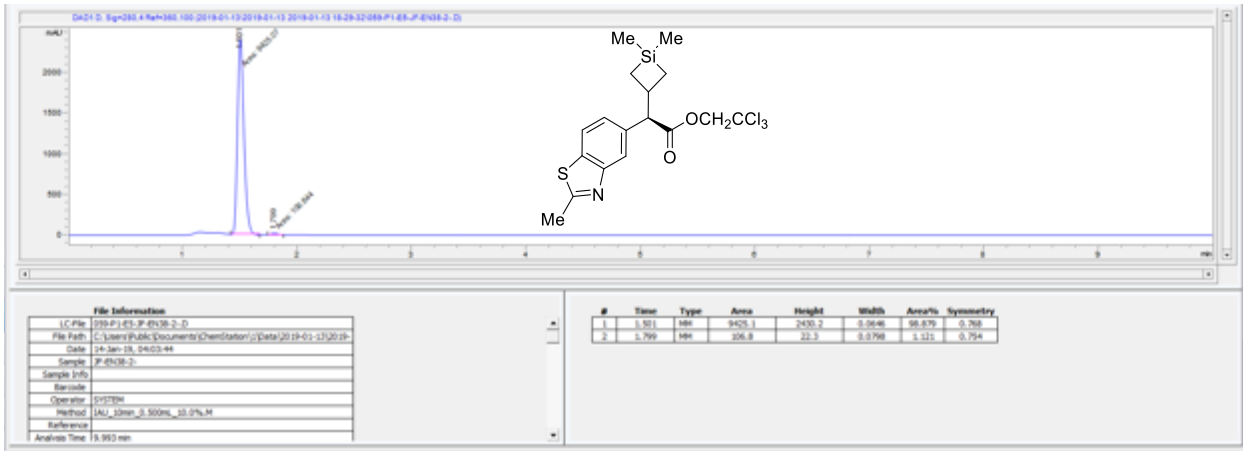
Me
Me
Si
OCH2CCl3
O
S
N
Me

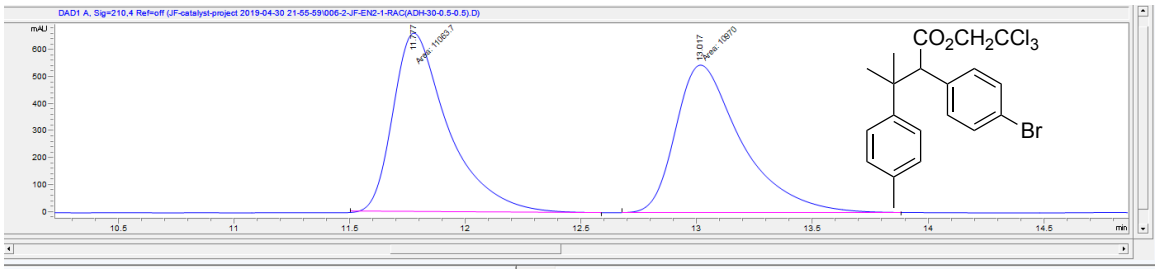

File Information	
LC-File	006-2-JF-EN2-1-RAC(ADH-30-0.5-0.5).D
File Path	C:\Chem32\1\Data\JF-catalyst-project 2019-04-30 21-55-59
Date	30-Apr-19, 23:52:07
Sample	JF-EN2-1-RAC(ADH-30-0.5-0.5)
Sample Info	
Barcode	
Operator	SYSTEM
Method	ADH_30min_0.5OML_0.5%.M

#	Time	Type	Area	Height	Width	Area%	Symmetry
1	11.777	MM	11063.7	661.3	0.2788	50.213	0.582
2	13.017	MM	10970	547.4	0.334	49.787	0.592

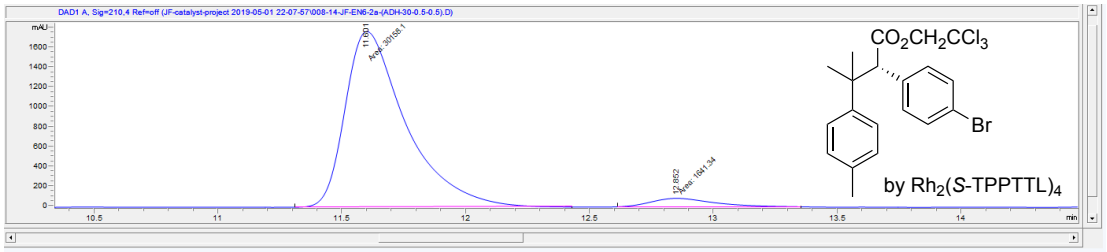

File Information

LC-File	008-14-JF-EN6-2a-(ADH-30-0.5-0.5).D
File Path	C:\Chem32\1\Data\JF-catalyst-project 2019-05-01 22-07-57
Date	02-May-19, 01:06:25
Sample	JF-EN6-2a-(ADH-30-0.5-0.5)
Sample Info	
Barcode	
Operator	SYSTEM
Method	ADH_30min_0.50ML_0.5%.M

#	Time	Type	Area	Height	Width	Area%	Symmetry
1	11.601	MM	30158.1	1770.3	0.2839	94.838	0.545
2	12.852	MM	1641.3	88.4	0.3094	5.162	0.651

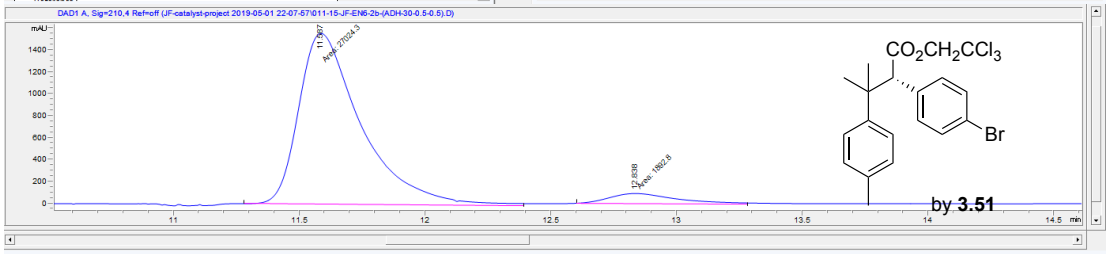

File Information

LC-File	011-15-JF-EN6-2b-(ADH-30-0.5-0.5).D
File Path	C:\Chem32\1\Data\JF-catalyst-project 2019-05-01 22-07-57
Date	02-May-19, 02:19:45
Sample	JF-EN6-2b-(ADH-30-0.5-0.5)
Sample Info	
Barcode	
Operator	SYSTEM
Method	ADH_30min_0.50ML_0.5%.M

#	Time	Type	Area	Height	Width	Area%	Symmetry
1	11.587	MM	27024.3	1563.2	0.2881	93.454	0.533
2	12.838	MM	1892.8	96	0.3286	6.546	0.576

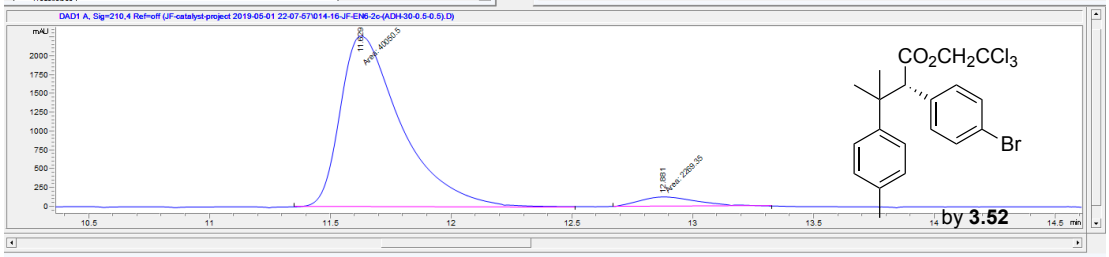

File Information

LC-File	014-16-JF-EN6-2c-(ADH-30-0.5-0.5).D
File Path	C:\Chem32\1\Data\JF-catalyst-project 2019-05-01 22-07-57
Date	02-May-19, 03:33:01
Sample	JF-EN6-2c-(ADH-30-0.5-0.5)
Sample Info	
Barcode	
Operator	SYSTEM
Method	ADH_30min_0.50ML_0.5%.M

#	Time	Type	Area	Height	Width	Area%	Symmetry
1	11.629	MM	40050.5	2272.2	0.2938	94.638	0.517
2	12.881	MM	2269.4	130.5	0.2898	5.362	0.715

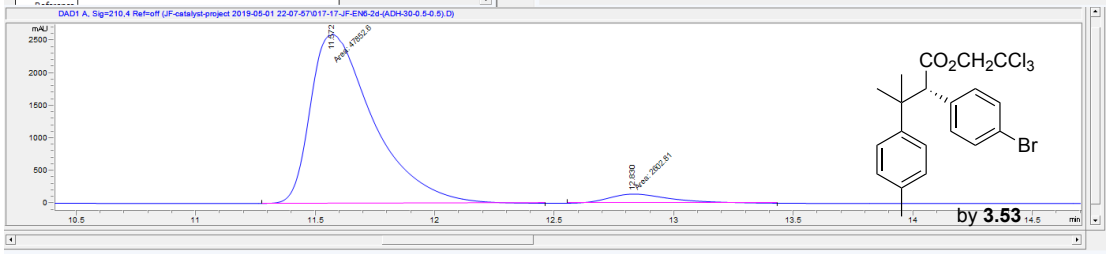

File Information

LC-File	017-17-JF-EN6-2d-(ADH-30-0.5-0.5).D
File Path	C:\Chem32\1\Data\JF-catalyst-project 2019-05-01 22-07-57
Date	02-May-19, 04:46:15
Sample	JF-EN6-2d-(ADH-30-0.5-0.5)
Sample Info	
Barcode	
Operator	SYSTEM
Method	ADH_30min_0.50ML_0.5%.M

#	Time	Type	Area	Height	Width	Area%	Symmetry
1	11.572	MM	47852.6	2615.3	0.3049	94.841	0.532
2	12.83	MM	2602.8	140.6	0.3086	5.159	0.623

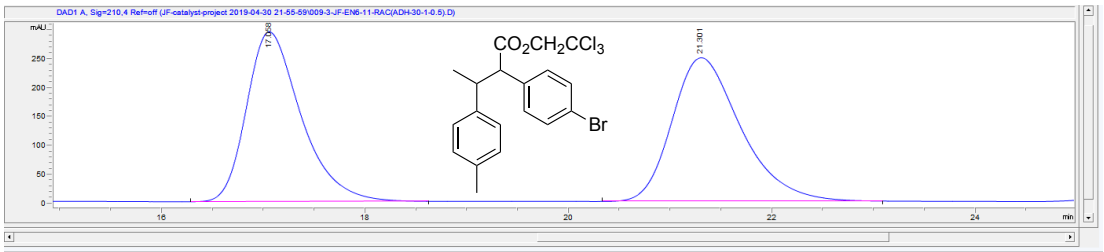

File Information	
LC-File	009-3-JF-EN6-11-RAC(ADH-30-1-0.5).D
File Path	C:\Chem32\1\Data\JF-catalyst-project 2019-04-30 21-55-59
Date	01-May-19, 01:05:11
Sample	JF-EN6-11-RAC(ADH-30-1-0.5)
Sample Info	
Barcode	
Operator	SYSTEM
Method	ADH_30min_1.0ML_0.5%.M

#	Time	Type	Area	Height	Width	Area%	Symmetry
1	17.058	BB	10939.8	293.5	0.5058	48.339	0.683
2	21.301	BB	11691.6	248.3	0.5608	51.661	0.713

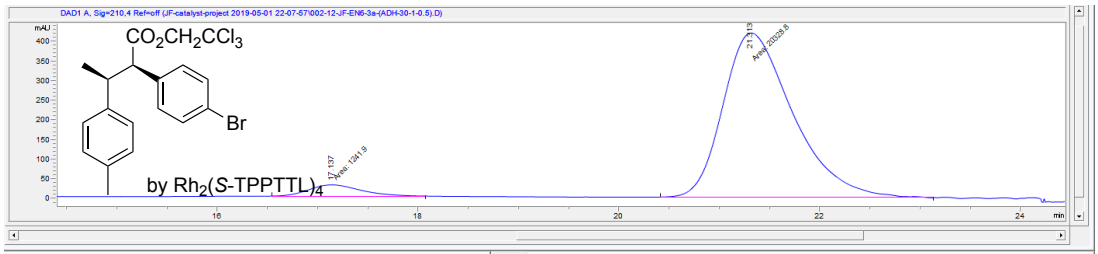

File Information

LC-File	002-12-JF-EN6-3a-(ADH-30-1-0.5).D
File Path	C:\Chem32\1\Data\JF-catalyst-project 2019-05-01 22-07-57
Date	01-May-19, 22:39:51
Sample	JF-EN6-3a-(ADH-30-1-0.5)
Sample Info	
Barcode	
Operator	SYSTEM
Method	ADH_30min_1.0ML_0.5%.M

#	Time	Type	Area	Height	Width	Area%	Symmetry
1	17.137	MM	1241.9	31	0.6687	5.757	0.761
2	21.313	MM	20328.8	420	0.8067	94.243	0.66

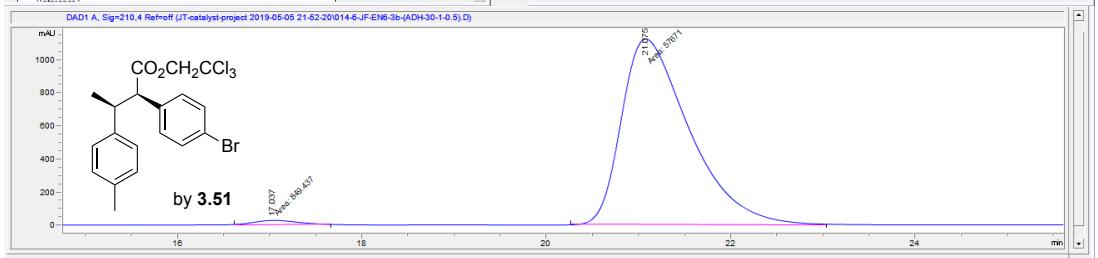

File Information

LC-File	014-6-JF-EN6-3b-(ADH-30-1-0.5).D
File Path	C:\Chem32\1\Data\JT-catalyst-project 2019-05-05 21-52-20
Date	06-May-19, 03:16:49
Sample	JF-EN6-3b-(ADH-30-1-0.5)
Sample Info	
Barcode	
Operator	SYSTEM
Method	ADH_30min_1.0ML_0.5%.M
Reference	

#	Time	Type	Area	Height	Width	Area%	Symmetry
1	17.037	MM	849.4	26.3	0.5384	1.452	0.871
2	21.075	MM	57671	1124.8	0.8545	98.548	0.547

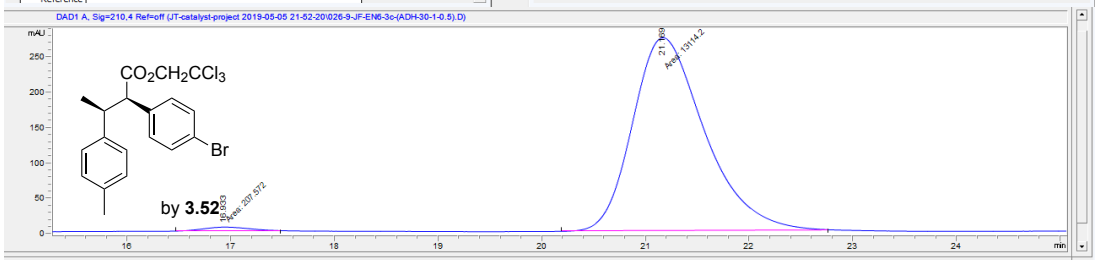

File Information

LC-File	026-9-JF-EN6-3c-(ADH-30-1-0.5).D
File Path	C:\Chem32\1\Data\JT-catalyst-project 2019-05-05 21-52-20
Date	06-May-19, 08:09:34
Sample	JF-EN6-3c-(ADH-30-1-0.5)
Sample Info	
Barcode	
Operator	SYSTEM
Method	ADH_30min_1.0ML_0.5%.M
Reference	

#	Time	Type	Area	Height	Width	Area%	Symmetry
1	16.933	MM	207.6	6.1	0.5678	1.558	0.834
2	21.169	MM	13114.2	271.7	0.8045	98.442	0.711

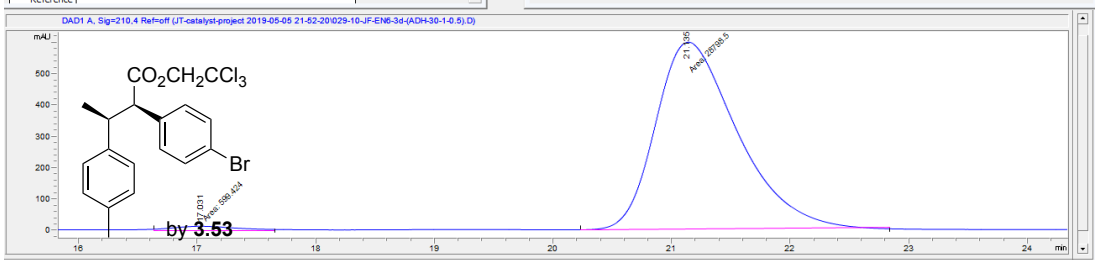

File Information

LC-File	029-10-JF-EN6-3d-(ADH-30-1-0.5).D
File Path	C:\Chem32\1\Data\JT-catalyst-project 2019-05-05 21-52-20
Date	06-May-19, 09:22:50
Sample	JF-EN6-3d-(ADH-30-1-0.5)
Sample Info	
Barcode	
Operator	SYSTEM
Method	ADH_30min_1.0ML_0.5%.M
Reference	

#	Time	Type	Area	Height	Width	Area%	Symmetry
1	17.031	MM	599.4	14.9	0.6699	2.039	0.743
2	21.135	MM	28798.5	599.6	0.8005	97.961	0.643

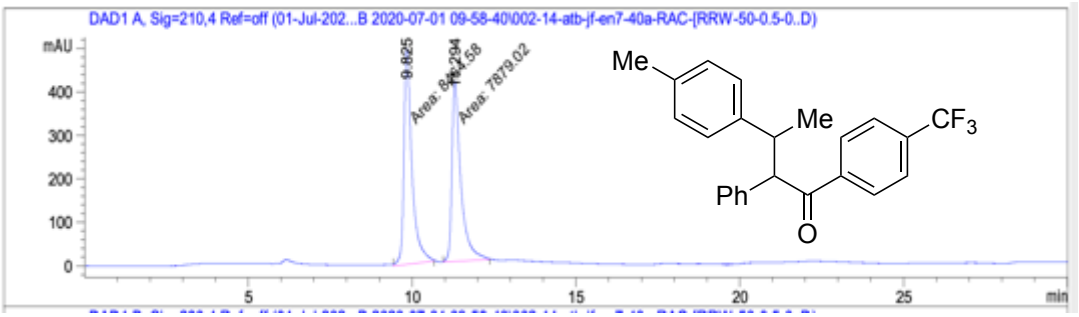

Signal 1: DAD1 A, Sig=210,4 Ref=off

Peak #	RetTime [min]	Type	Width [min]	Area [mAU*s]	Height [mAU]	Area %
1	9.825	MM	0.2833	8464.57617	497.93561	51.7914
2	11.294	MM	0.3168	7879.01904	414.51773	48.2086
Totals :				1.63436e4	912.45334	

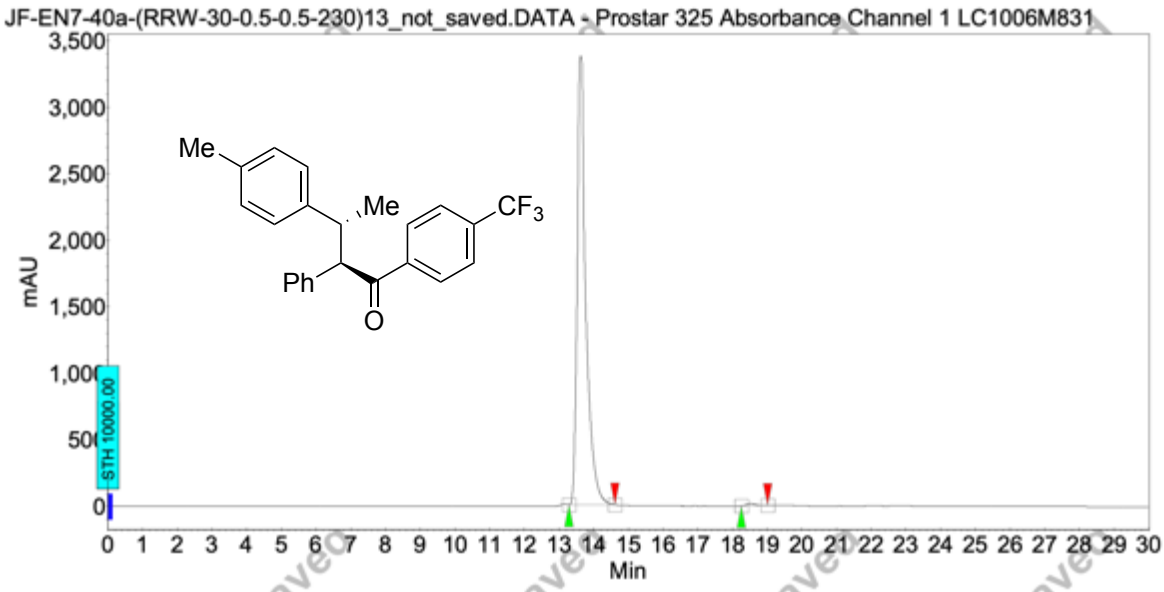

Peak results :

Index	Name	Time [Min]	Quantity [% Area]	Height [mAU]	Area [mAU.Min]	Area % [%]
1	UNKNOWN	13.64	99.50	3367.8	982.5	99.504
2	UNKNOWN	18.53	0.50	15.1	4.9	0.496
Total			100.00	3382.9	987.4	100.000

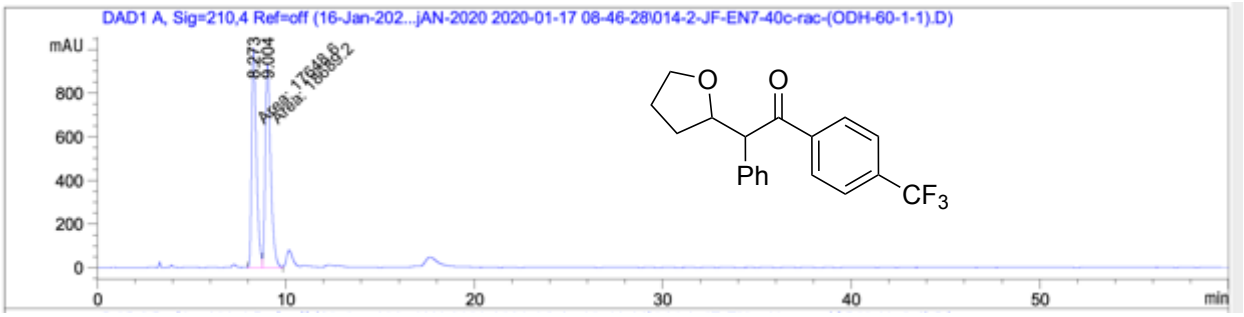

Signal 1: DAD1 A, Sig=210,4 Ref=off

Peak #	RetTime [min]	Type	Width [min]	Area [mAU*s]	Height [mAU]	Area %
1	8.273	MF	0.2915	1.76486e4	1009.18073	48.5682
2	9.004	FM	0.3341	1.86892e4	932.24548	51.4318
Totals :				3.63379e4	1941.42621	

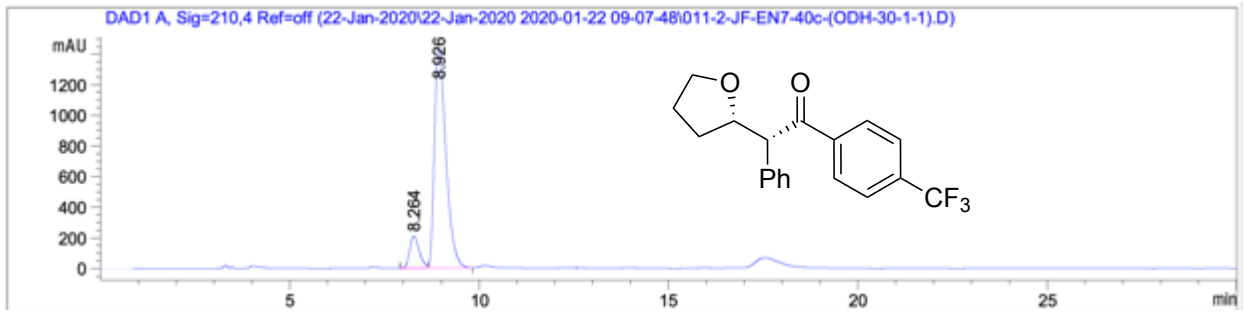

Signal 1: DAD1 A, Sig=210,4 Ref=off

Peak #	RetTime [min]	Type	Width [min]	Area [mAU*s]	Height [mAU]	Area %
1	8.264	BV E	0.2671	3717.57568	209.89127	10.9328
2	8.926	VB R	0.2980	3.02862e4	1439.06470	89.0672
Totals :				3.40038e4	1648.95596	

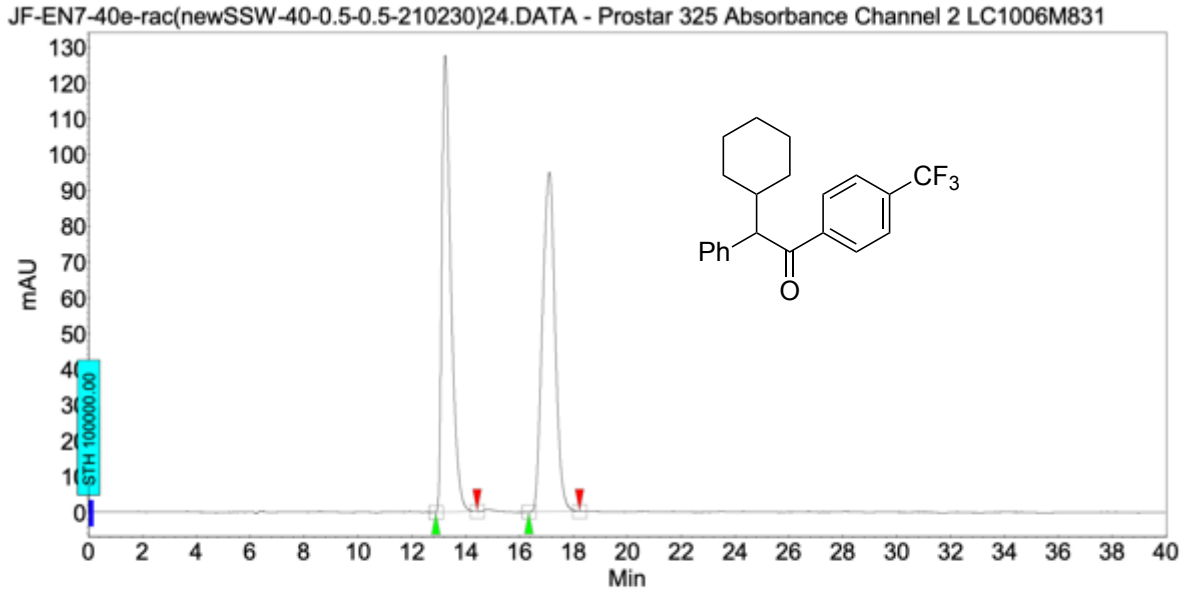

Peak results :

Index	Name	Time [Min]	Quantity [% Area]	Height [mAU]	Area [mAU.Min]	Area % [%]
1	UNKNOWN	13.24	48.93	127.6	49.7	48.929
2	UNKNOWN	17.10	51.07	94.8	51.9	51.071
Total			100.00	222.5	101.6	100.000

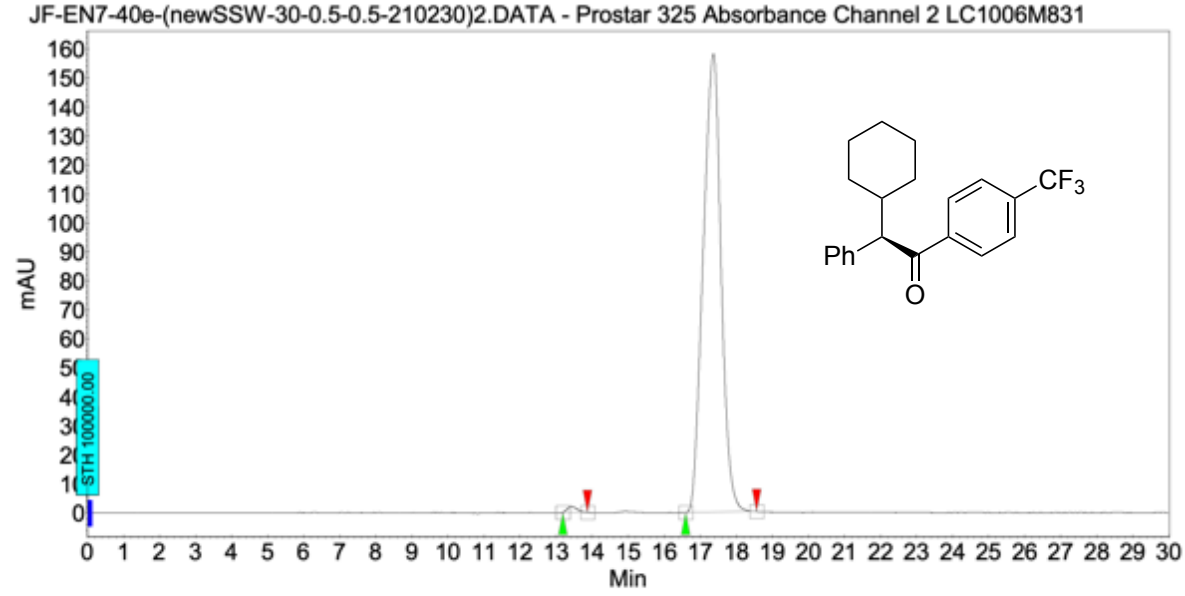

Peak results :

Index	Name	Time [Min]	Quantity [% Area]	Height [mAU]	Area [mAU.Min]	Area % [%]
1	UNKNOWN	13.43	0.69	2.0	0.6	0.688
2	UNKNOWN	17.37	99.31	157.8	90.9	99.312
Total			100.00	159.9	91.5	100.000

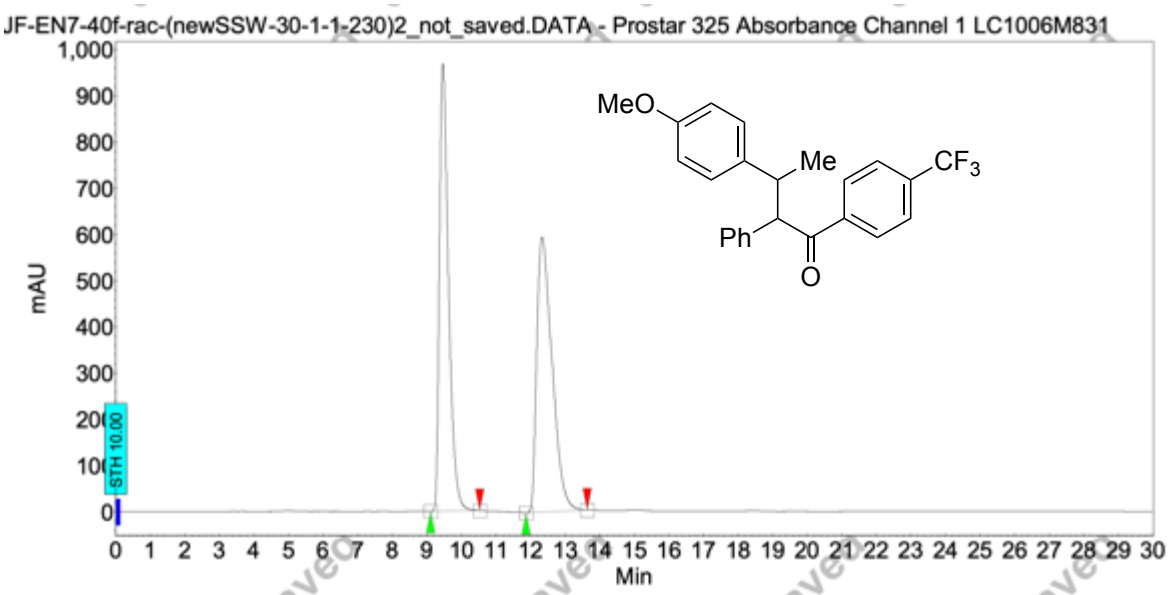

Peak results :

Index	Name	Time [Min]	Quantity [% Area]	Height [mAU]	Area [mAU.Min]	Area % [%]
1	UNKNOWN	9.46	49.28	968.3	297.0	49.282
2	UNKNOWN	12.33	50.72	595.3	305.6	50.718
Total			100.00	1563.6	602.6	100.000

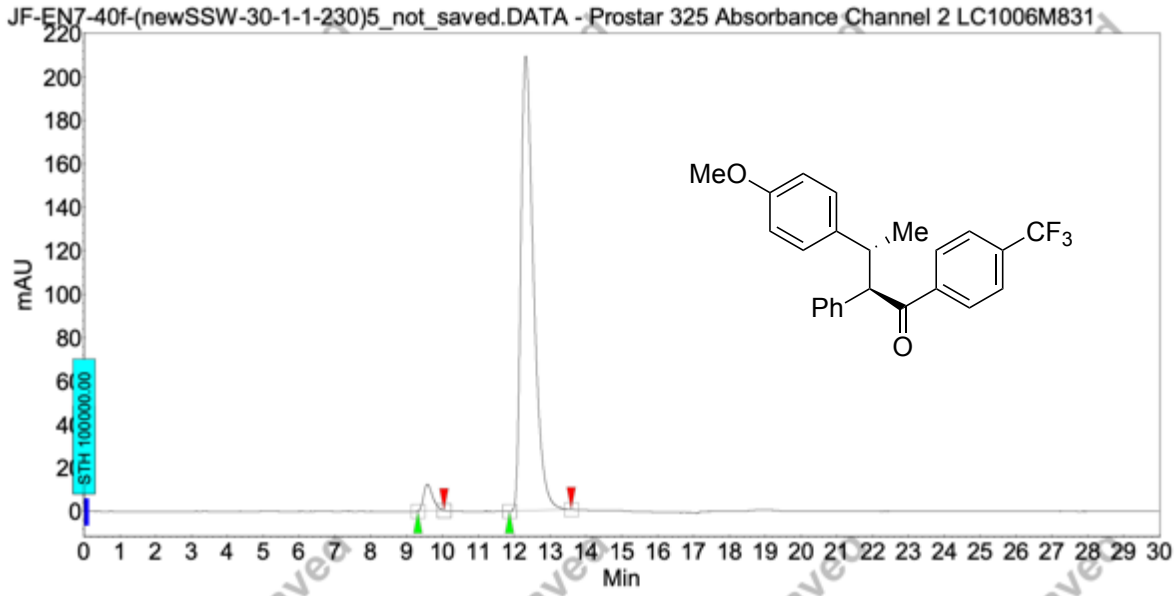

Peak results :

Index	Name	Time [Min]	Quantity [% Area]	Height [mAU]	Area [mAU.Min]	Area % [%]
1	UNKNOWN	9.58	4.03	12.3	3.6	4.034
2	UNKNOWN	12.32	95.97	209.3	86.1	95.966
Total			100.00	221.6	89.7	100.000

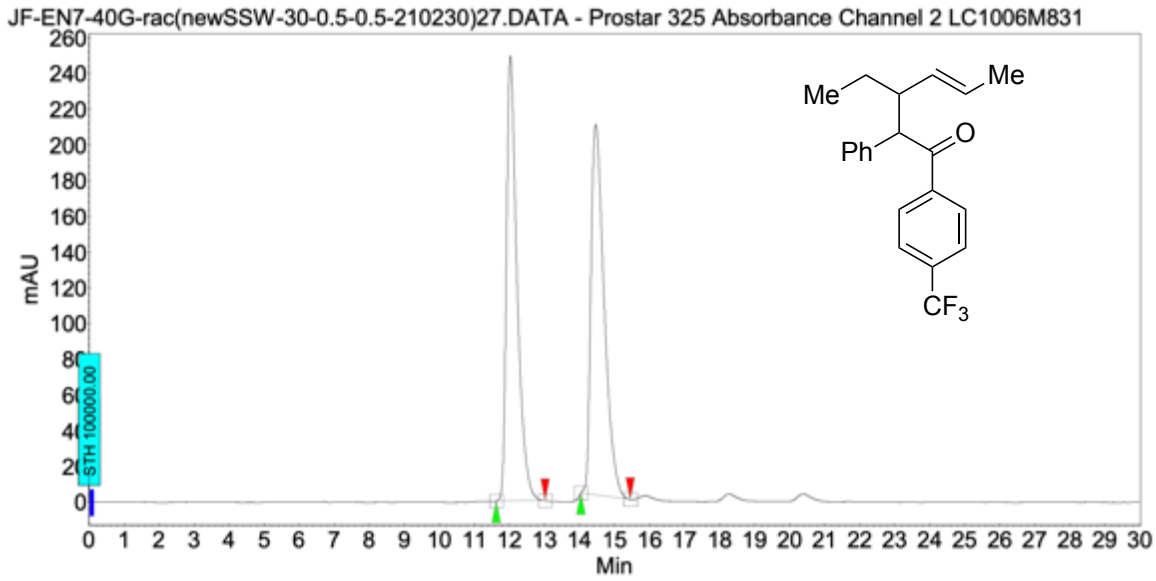

Peak results :

Index	Name	Time [Min]	Quantity [% Area]	Height [mAU]	Area [mAU.Min]	Area % [%]
1	UNKNOWN	12.03	48.88	249.2	87.2	48.876
2	UNKNOWN	14.46	51.12	207.5	91.2	51.124
Total			100.00	456.7	178.3	100.000

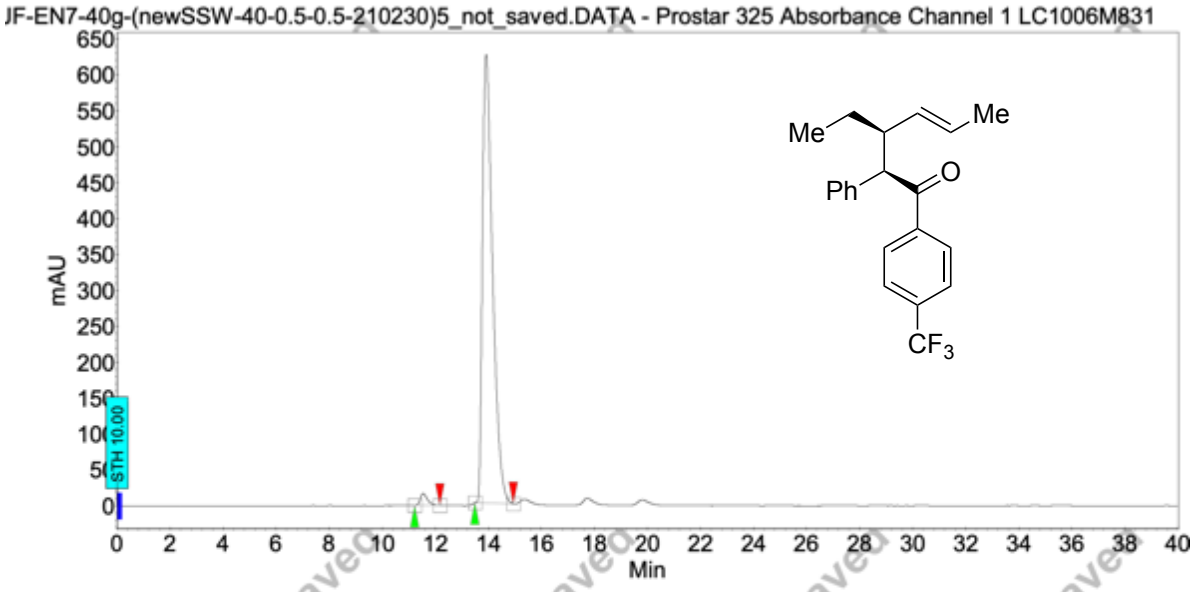

Peak results :

Index	Name	Time [Min]	Quantity [% Area]	Height [mAU]	Area [mAU.Min]	Area % [%]
1	UNKNOWN	11.54	1.86	16.7	5.2	1.862
2	UNKNOWN	13.91	98.14	623.8	276.7	98.138
Total			100.00	640.5	281.9	100.000

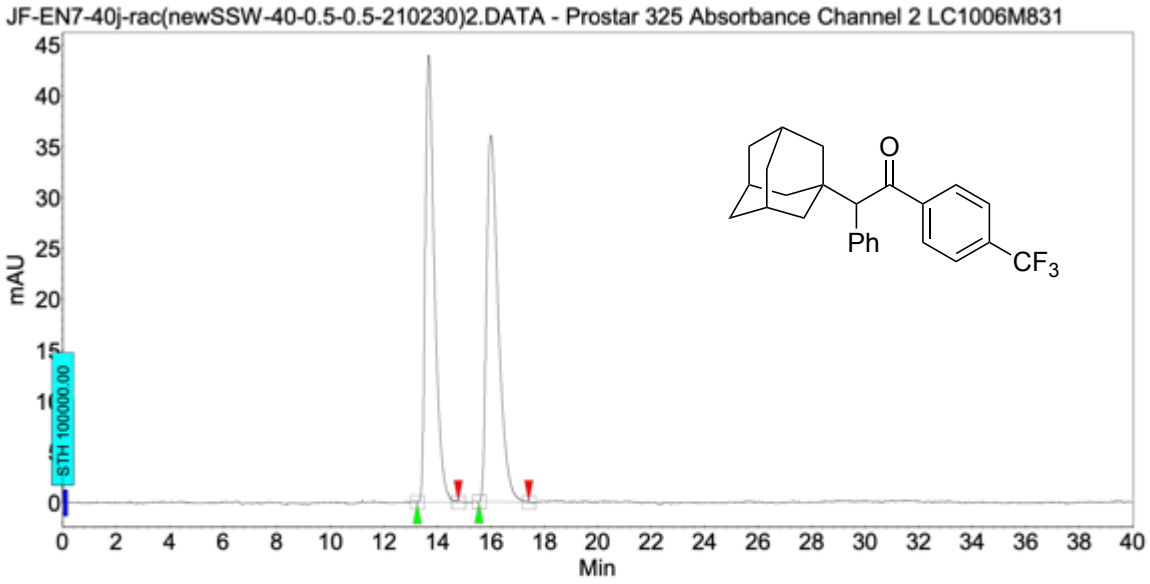

Peak results :

Index	Name	Time [Min]	Quantity [% Area]	Height [mAU]	Area [mAU.Min]	Area % [%]
1	UNKNOWN	13.68	48.76	44.0	17.6	48.761
2	UNKNOWN	16.00	51.24	36.1	18.5	51.239
Total			100.00	80.0	36.1	100.000

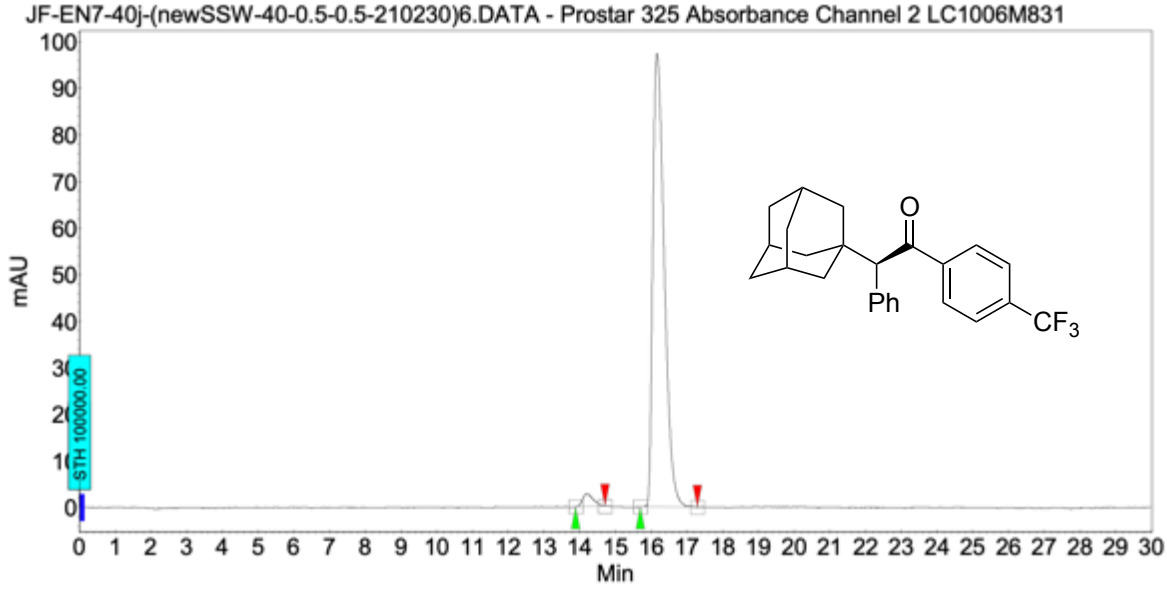

Peak results :

Index	Name	Time [Min]	Quantity [% Area]	Height [mAU]	Area [mAU.Min]	Area % [%]
1	UNKNOWN	14.20	2.62	2.8	1.0	2.622
2	UNKNOWN	16.16	97.38	97.4	36.2	97.378
Total			100.00	100.2	37.2	100.000

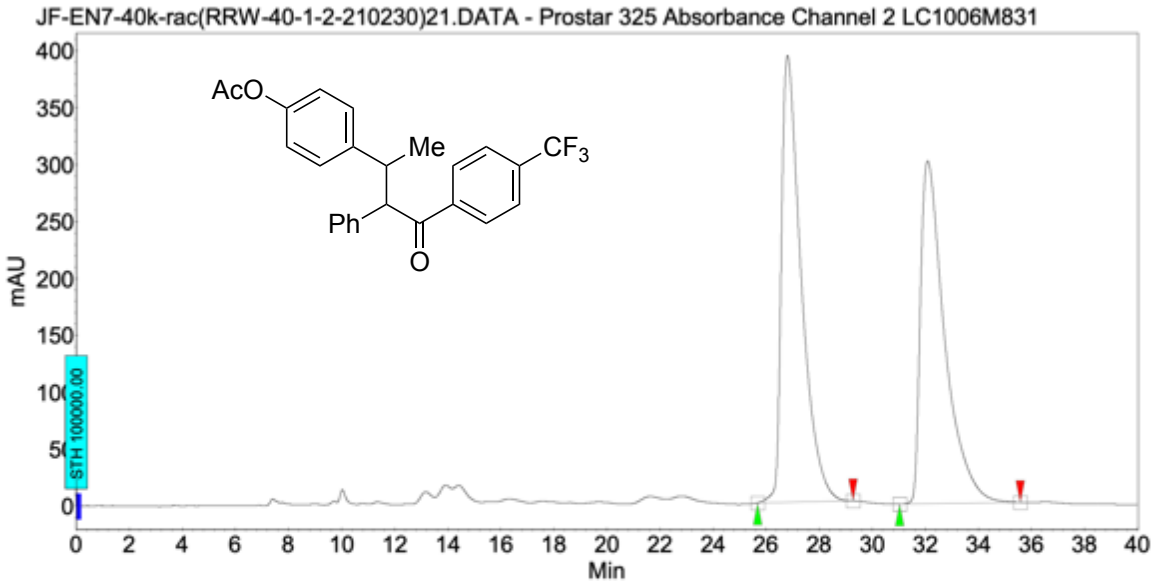

Peak results :

Index	Name	Time [Min]	Quantity [% Area]	Height [mAU]	Area [mAU.Min]	Area % [%]
1	UNKNOWN	26.81	51.59	392.4	340.2	51.591
2	UNKNOWN	32.09	48.41	301.2	319.2	48.409
Total			100.00	693.7	659.5	100.000

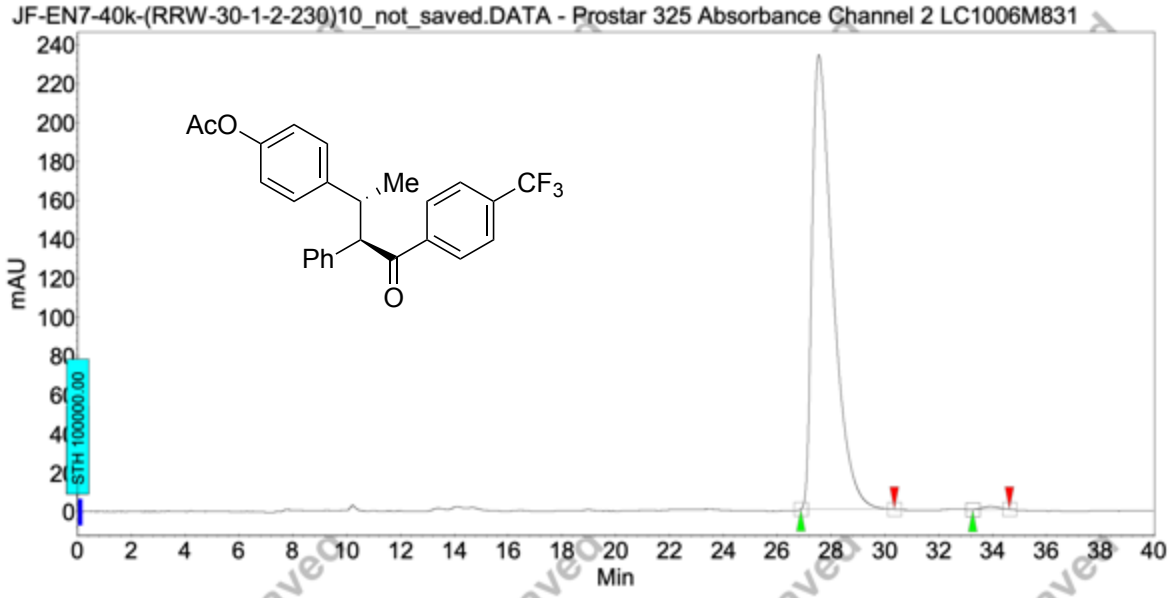

Peak results :

Index	Name	Time [Min]	Quantity [% Area]	Height [mAU]	Area [mAU.Min]	Area % [%]
1	UNKNOWN	27.55	99.50	233.8	209.8	99.498
2	UNKNOWN	33.89	0.50	1.5	1.1	0.502
Total			100.00	235.3	210.9	100.000

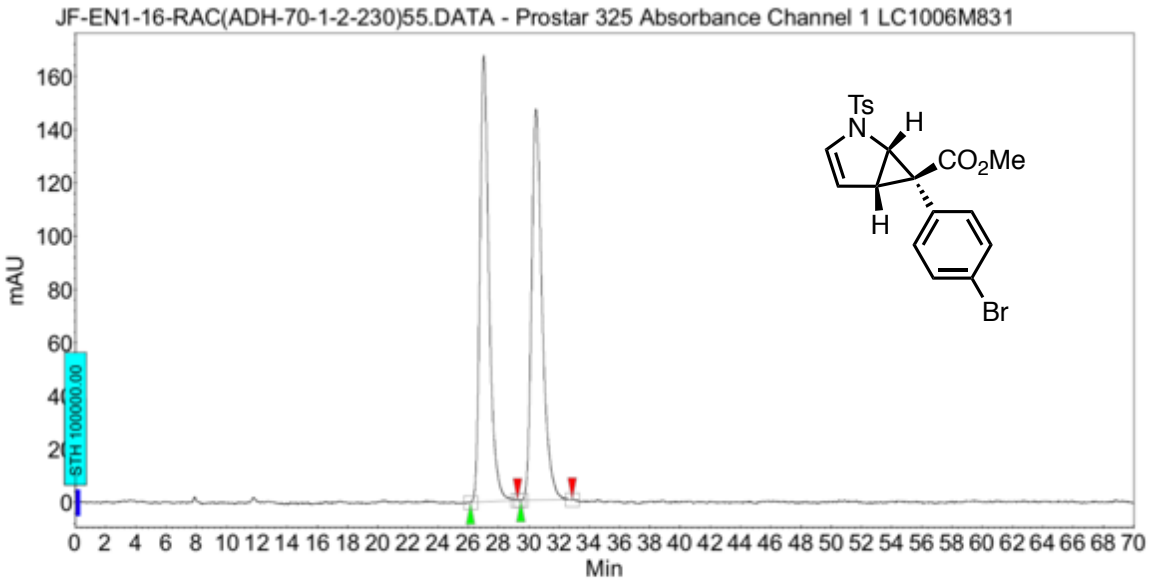

Peak results :

Index	Name	Time [Min]	Quantity [% Area]	Height [mAU]	Area [mAU.Min]	Area % [%]
1	UNKNOWN	27.02	49.61	167.7	117.5	49.614
2	UNKNOWN	30.47	50.39	147.0	119.3	50.386
Total			100.00	314.7	236.8	100.000

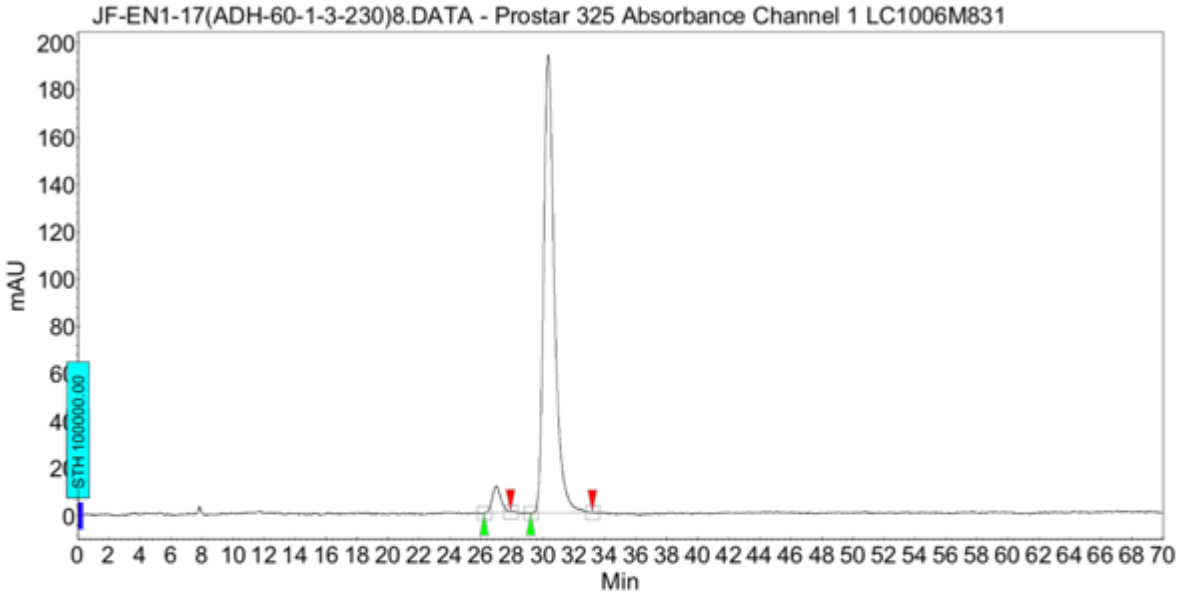

Peak results :

Index	Name	Time [Min]	Quantity [% Area]	Height [mAU]	Area [mAU.Min]	Area % [%]
1	UNKNOWN	27.01	4.42	11.2	7.2	4.418
2	UNKNOWN	30.34	95.58	193.6	156.6	95.582
Total			100.00	204.8	163.9	100.000

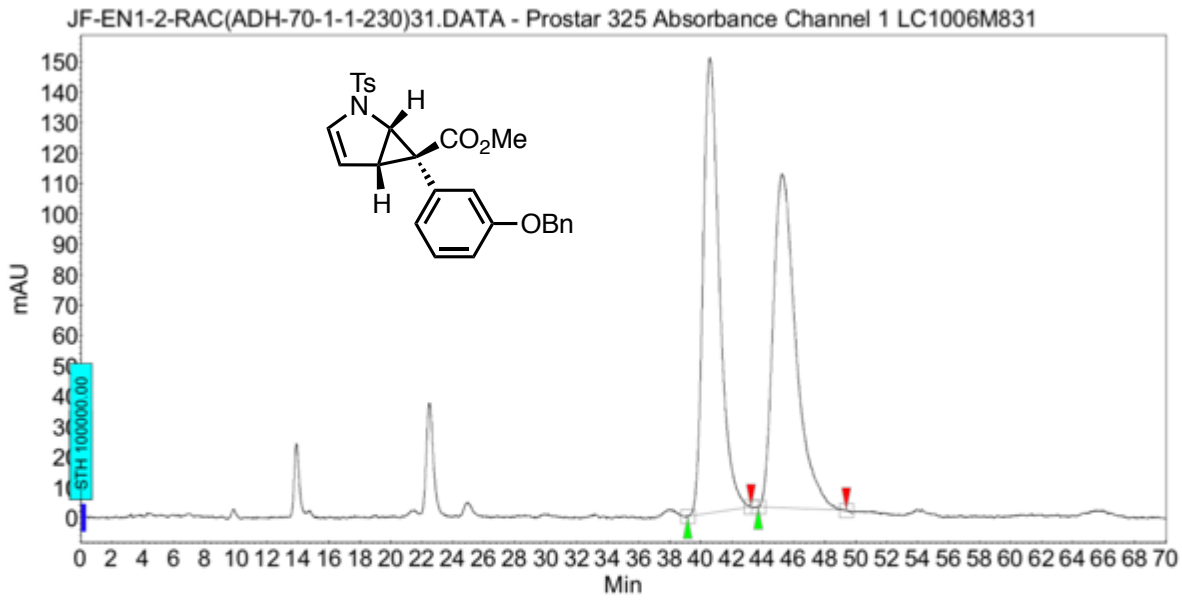

Peak results :

Index	Name	Time [Min]	Quantity [% Area]	Height [mAU]	Area [mAU.Min]	Area % [%]
1	UNKNOWN	40.58	49.52	149.7	183.2	49.517
2	UNKNOWN	45.25	50.48	109.8	186.7	50.483
Total			100.00	259.5	369.9	100.000

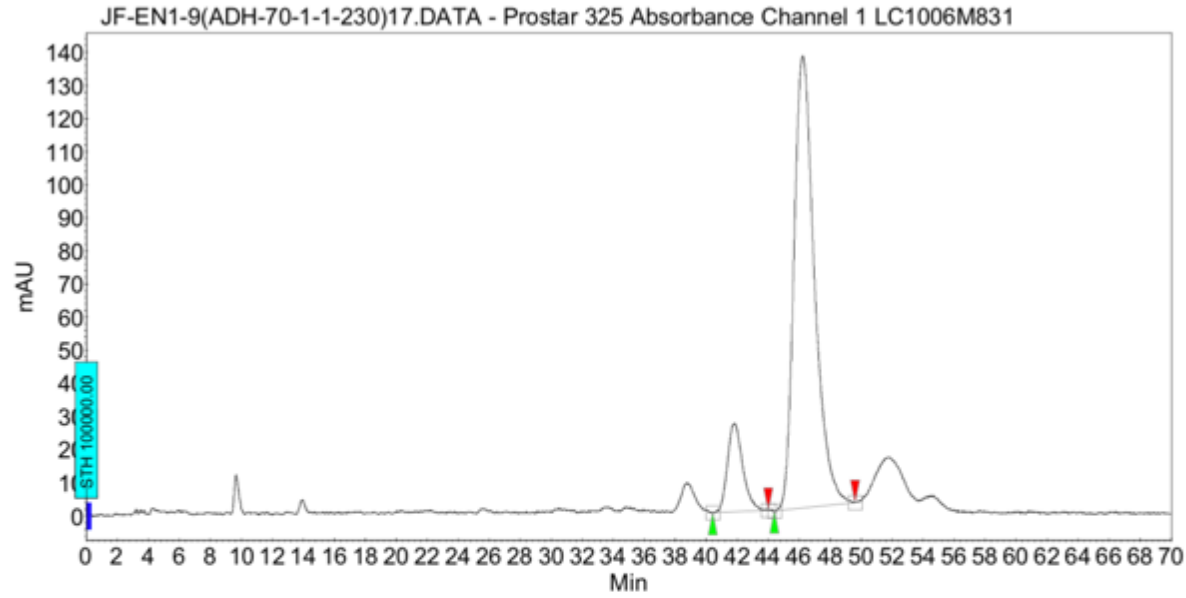

Peak results :

Index	Name	Time [Min]	Quantity [% Area]	Height [mAU]	Area [mAU.Min]	Area % [%]
1	UNKNOWN	41.85	12.65	26.7	30.4	12.646
2	UNKNOWN	46.23	87.35	136.5	209.8	87.354
Total			100.00	163.2	240.2	100.000

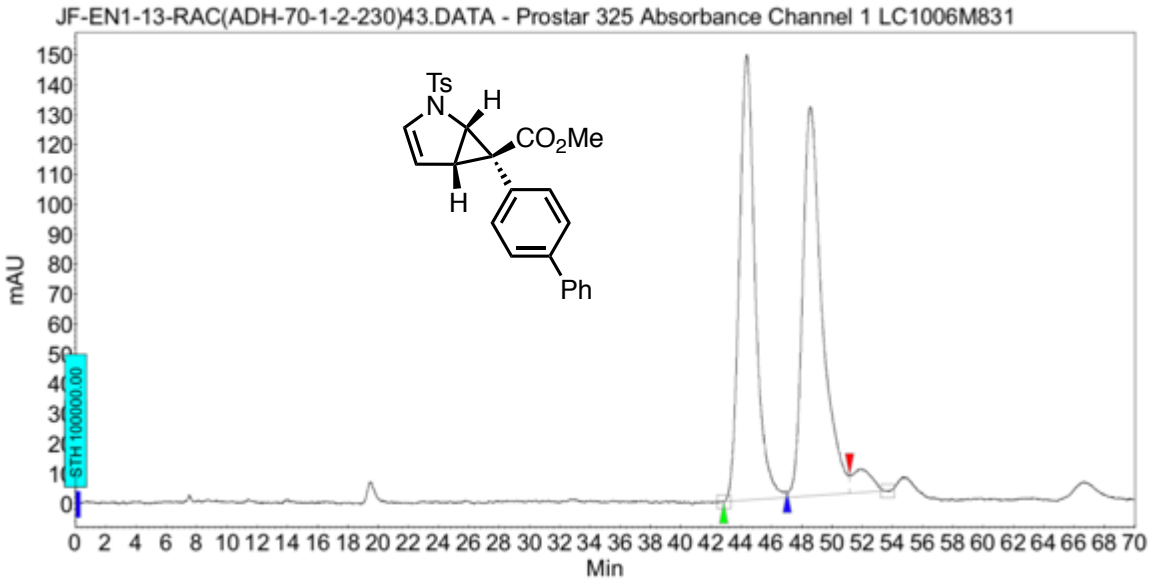

Peak results :

Index	Name	Time [Min]	Quantity [% Area]	Height [mAU]	Area [mAU.Min]	Area % [%]
1	UNKNOWN	44.37	48.20	148.8	181.1	48.200
2	UNKNOWN	48.56	51.80	130.1	194.7	51.800
Total			100.00	278.9	375.8	100.000

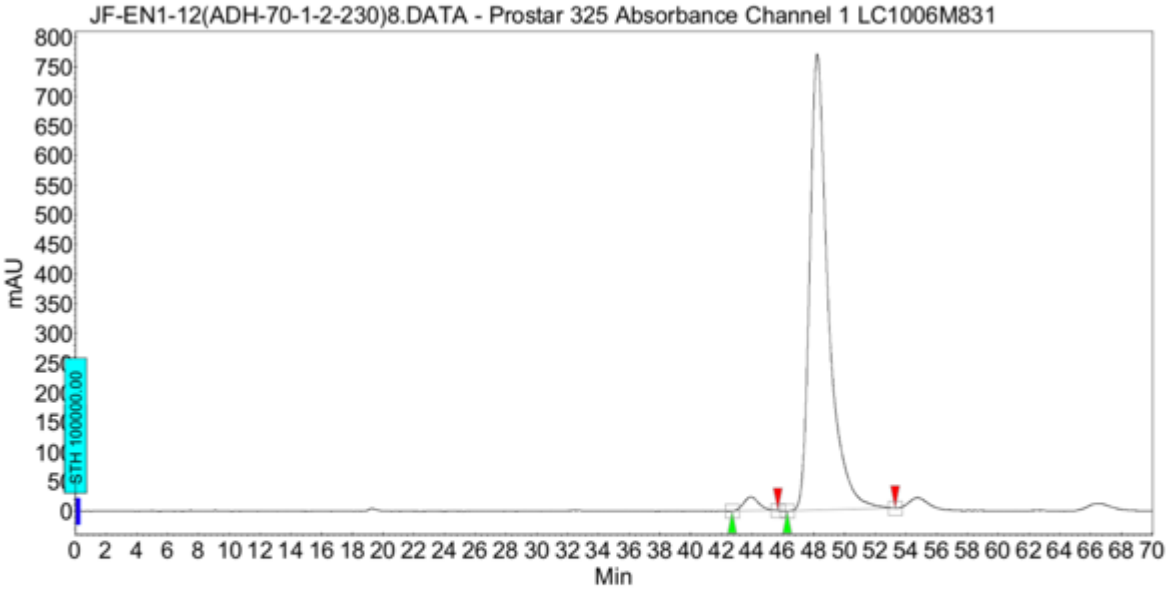

Peak results :

Index	Name	Time [Min]	Quantity [% Area]	Height [mAU]	Area [mAU.Min]	Area % [%]
1	UNKNOWN	43.91	2.44	23.2	27.0	2.439
2	UNKNOWN	48.22	97.56	769.4	1078.5	97.561
Total			100.00	792.7	1105.4	100.000

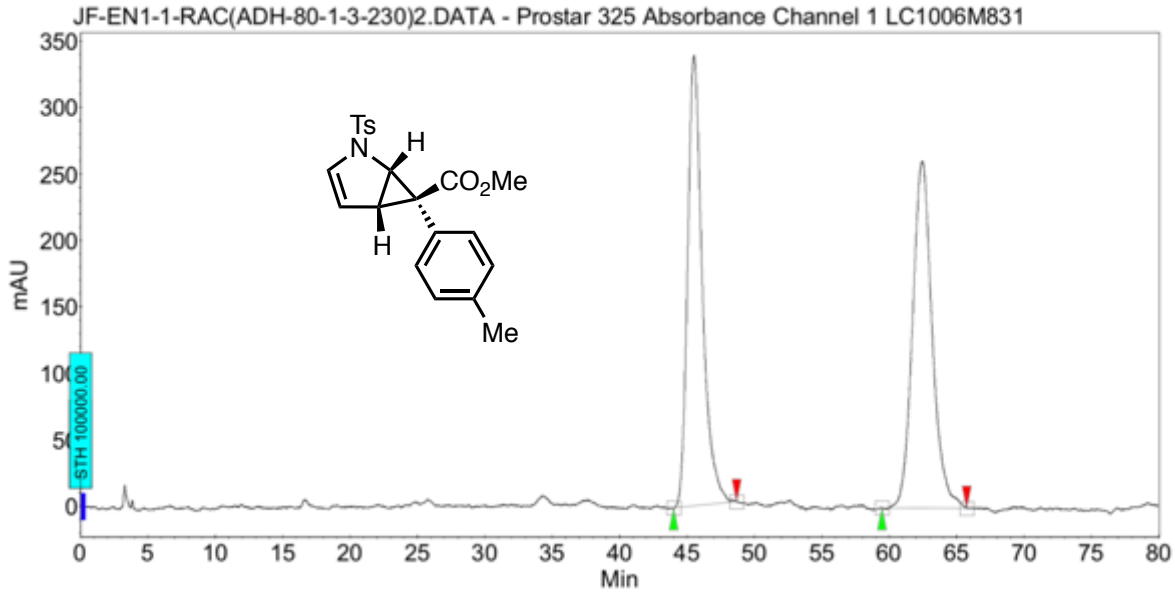

Peak results :

Index	Name	Time [Min]	Quantity [% Area]	Height [mAU]	Area [mAU.Min]	Area % [%]
1	UNKNOWN	45.51	49.30	338.7	429.6	49.298
2	UNKNOWN	62.46	50.70	260.7	441.8	50.702
Total			100.00	599.3	871.4	100.000

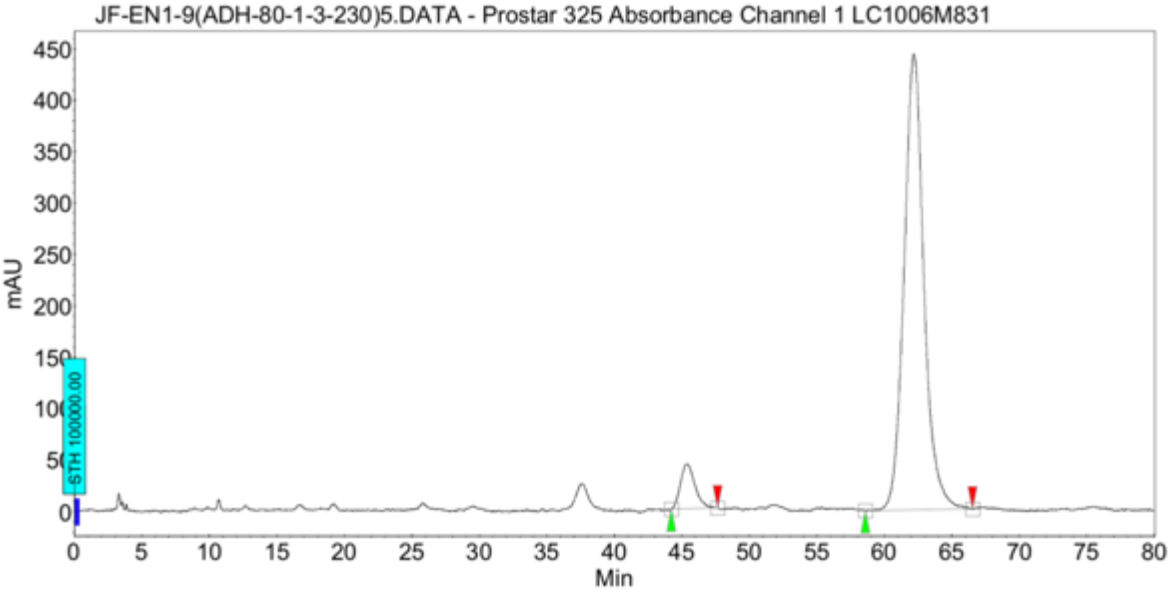

Peak results :

Index	Name	Time [Min]	Quantity [% Area]	Height [mAU]	Area [mAU.Min]	Area % [%]
1	UNKNOWN	45.34	6.71	43.7	54.5	6.711
2	UNKNOWN	62.18	93.29	443.3	757.8	93.289
Total			100.00	487.0	812.3	100.000

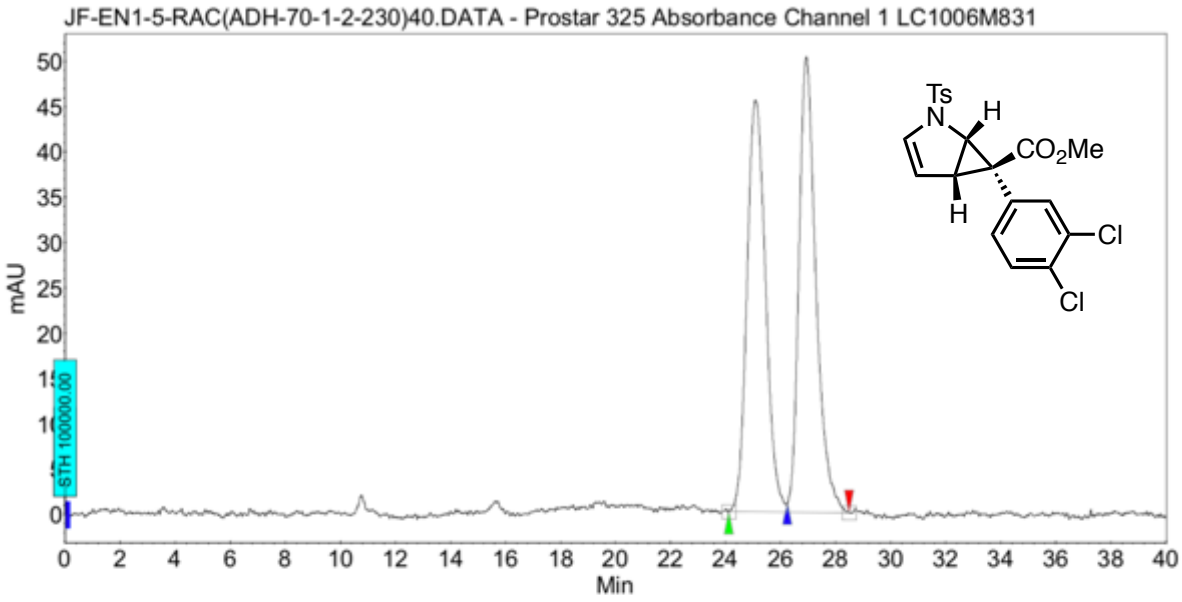

Peak results :

Index	Name	Time [Min]	Quantity [% Area]	Height [mAU]	Area [mAU.Min]	Area % [%]
1	UNKNOWN	25.08	49.61	45.5	35.5	49.607
2	UNKNOWN	26.93	50.39	50.2	36.1	50.393
Total			100.00	95.7	71.6	100.000

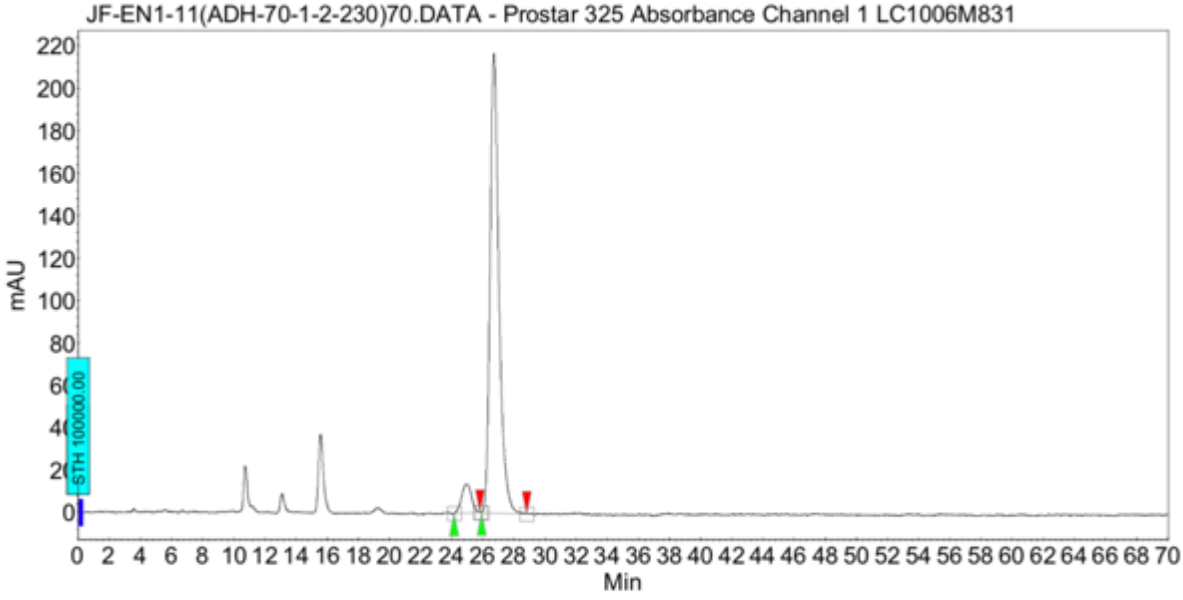

Peak results :

Index	Name	Time [Min]	Quantity [% Area]	Height [mAU]	Area [mAU.Min]	Area % [%]
1	UNKNOWN	25.01	6.40	13.5	9.8	6.400
2	UNKNOWN	26.72	93.60	216.7	144.0	93.600
Total			100.00	230.2	153.9	100.000

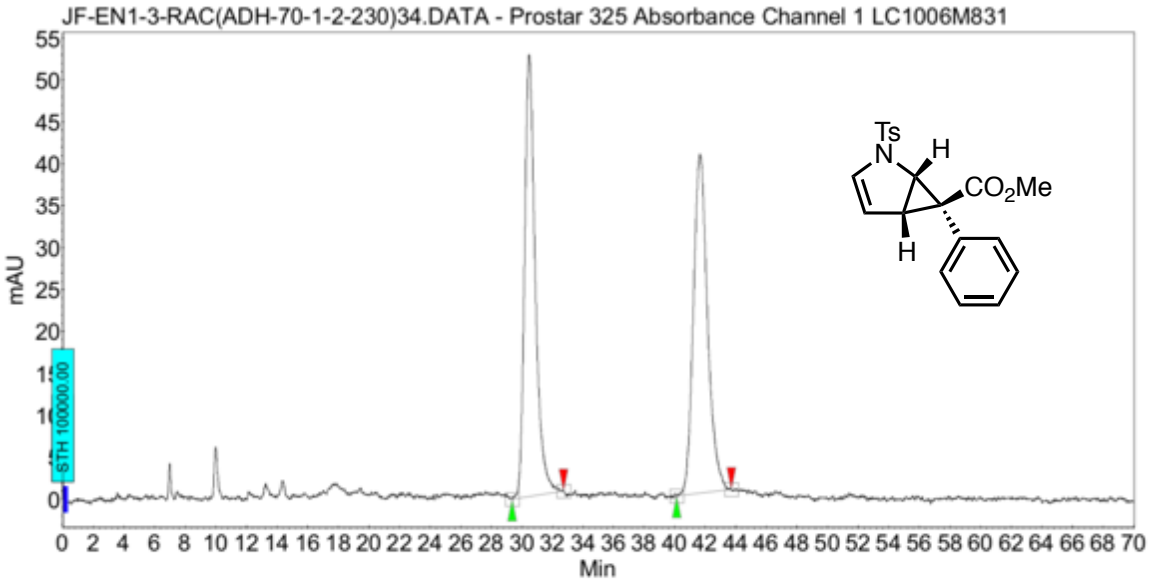

Peak results :

Index	Name	Time [Min]	Quantity [% Area]	Height [mAU]	Area [mAU.Min]	Area % [%]
1	UNKNOWN	30.48	49.55	52.7	42.7	49.546
2	UNKNOWN	41.65	50.45	40.5	43.5	50.454
Total			100.00	93.1	86.3	100.000

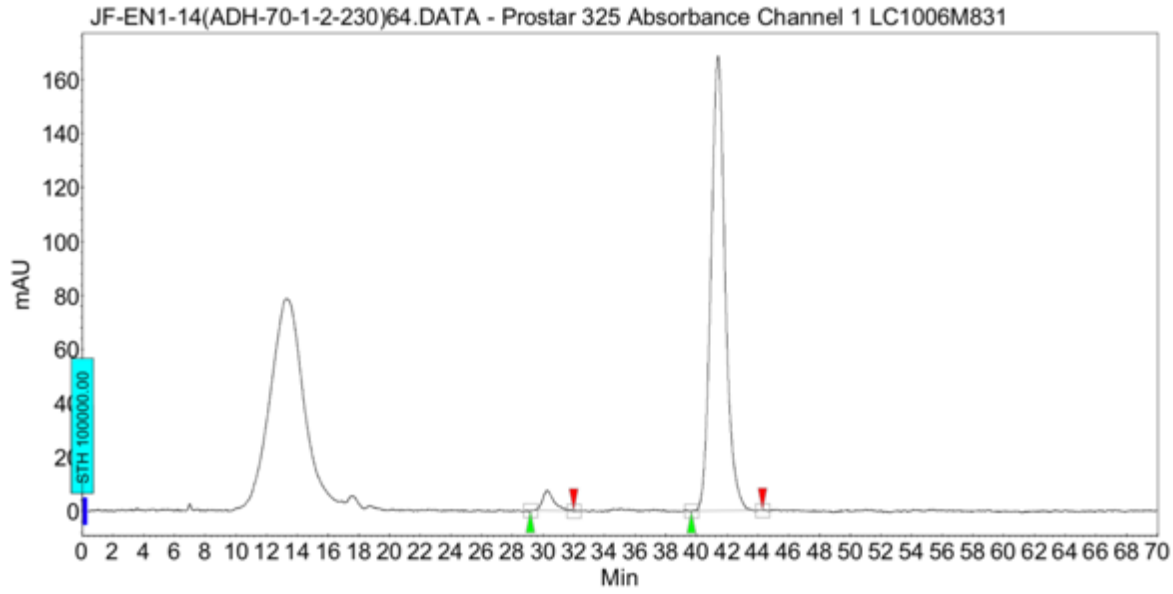

Peak results :

Index	Name	Time [Min]	Quantity [% Area]	Height [mAU]	Area [mAU.Min]	Area % [%]
1	UNKNOWN	30.27	3.48	7.5	6.5	3.478
2	UNKNOWN	41.40	96.52	168.6	181.4	96.522
Total			100.00	176.1	187.9	100.000

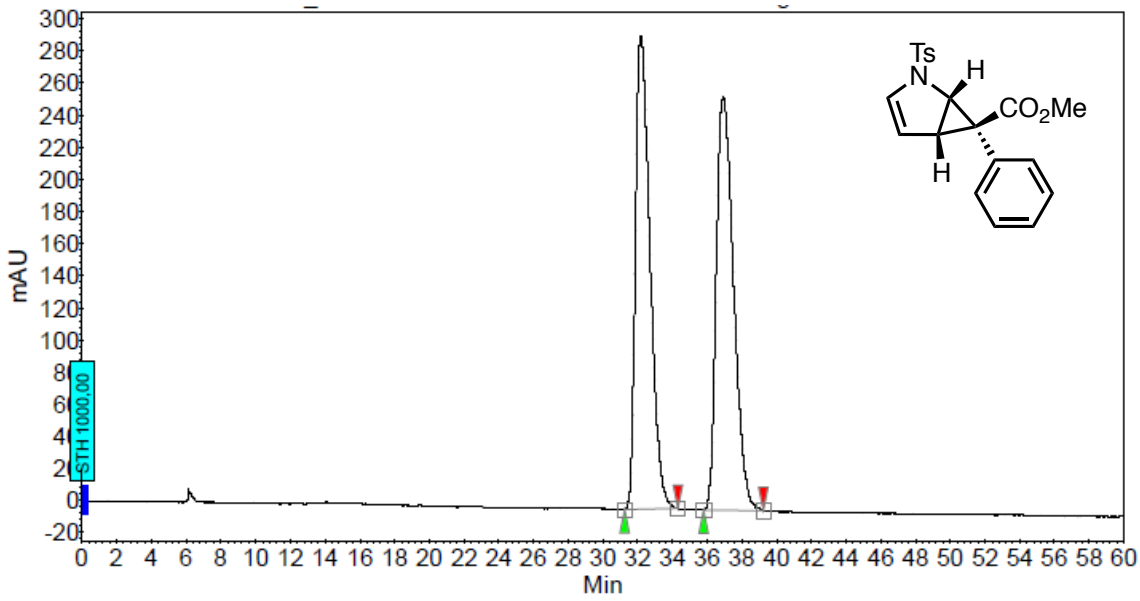

Peak Results :

Index	Name	Time [Min]	Quantity [% Area]	Height [mAU]	Area [mAU.Min]	Area % [%]
2	UNKNOWN	32,19	49,13	294,5	286,5	49,128
1	UNKNOWN	36,92	50,87	257,7	296,7	50,872
Total			100,00	552,2	583,2	100,000

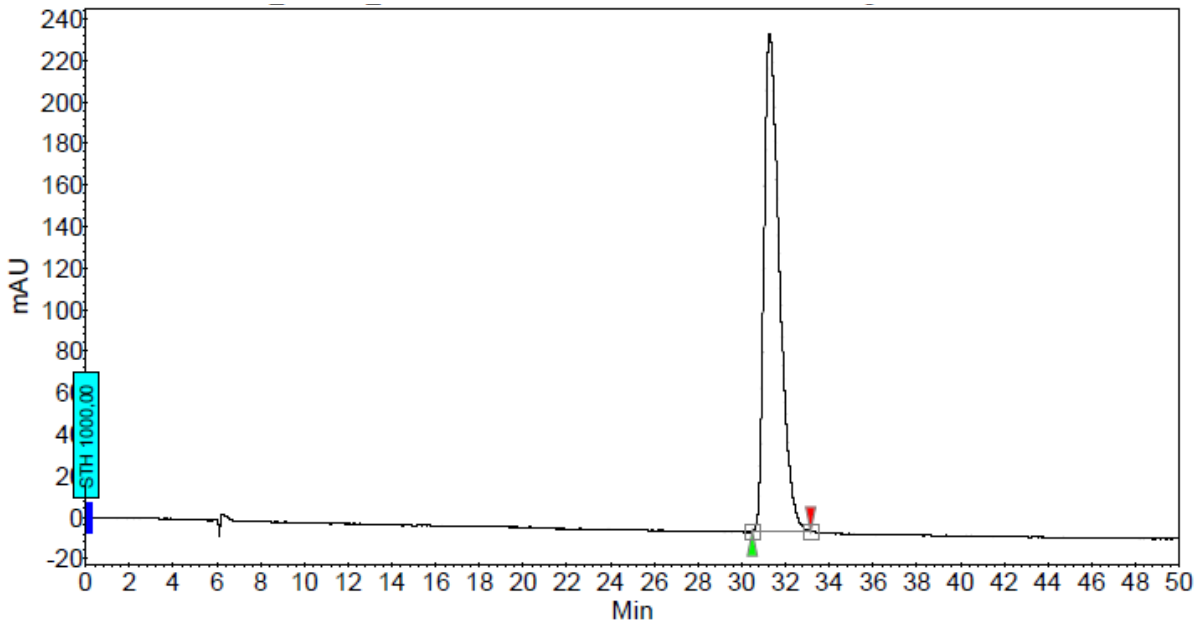

Peak Results :

Index	Name	Time [Min]	Quantity [% Area]	Height [mAU]	Area [mAU.Min]	Area % [%]
1	UNKNOWN	31,27	100,00	239,7	197,3	100,000
Total			100,00	239,7	197,3	100,000

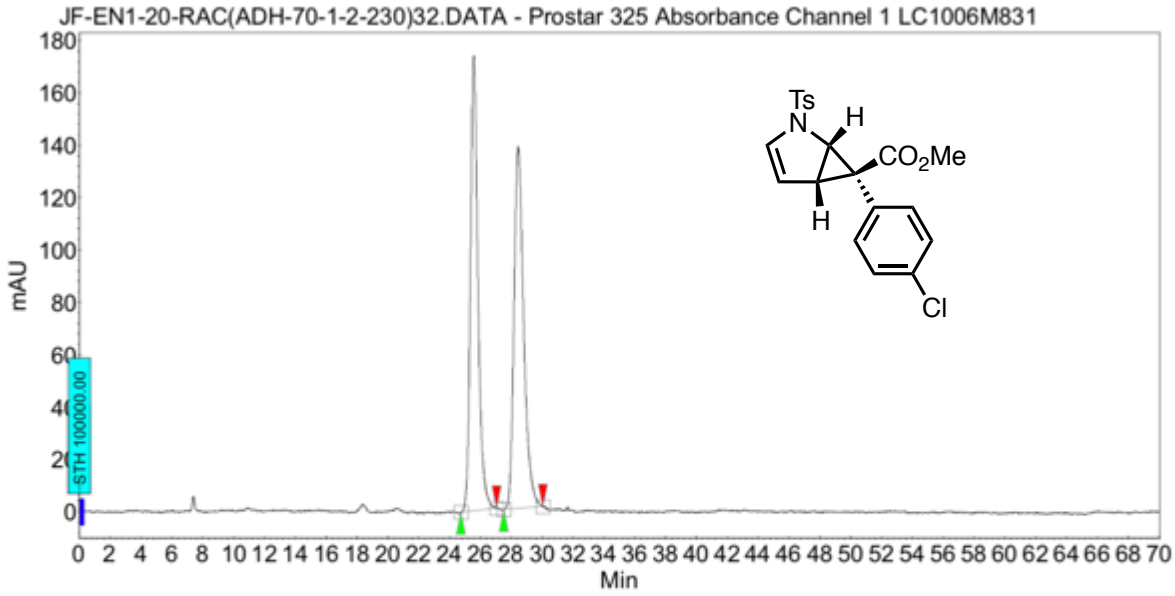

Peak results :

Index	Name	Time [Min]	Quantity [% Area]	Height [mAU]	Area [mAU.Min]	Area % [%]
1	UNKNOWN	25.57	49.49	173.9	98.8	49.491
2	UNKNOWN	28.44	50.51	138.3	100.8	50.509
Total			100.00	312.2	199.5	100.000

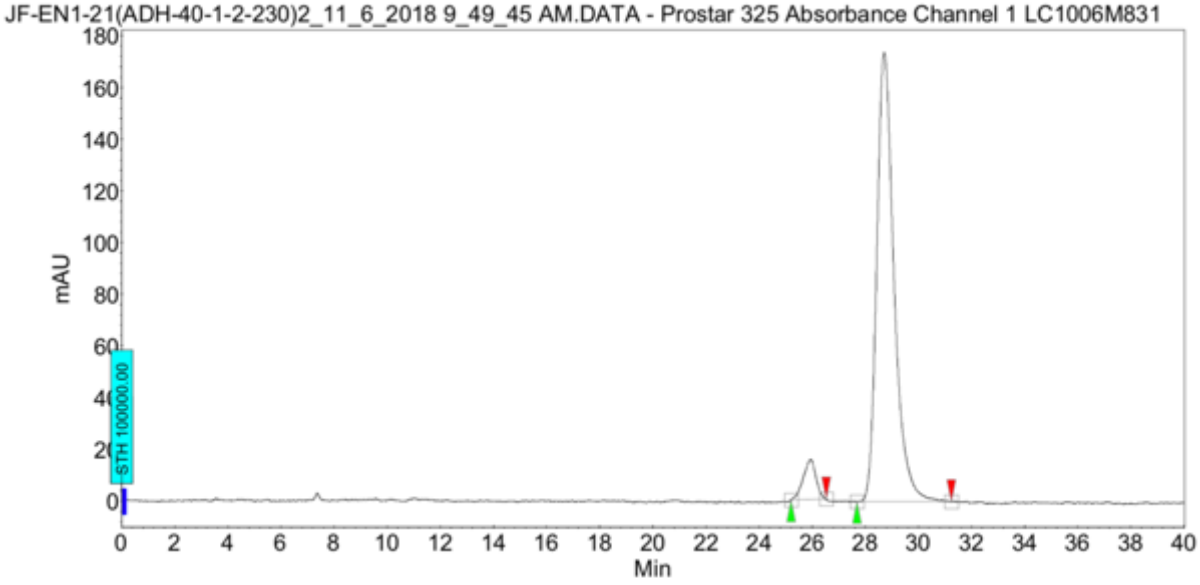

Peak results :

Index	Name	Time [Min]	Quantity [% Area]	Height [mAU]	Area [mAU.Min]	Area % [%]
1	UNKNOWN	25.94	6.15	15.5	8.6	6.147
2	UNKNOWN	28.71	93.85	173.7	130.6	93.853
Total			100.00	189.2	139.2	100.000

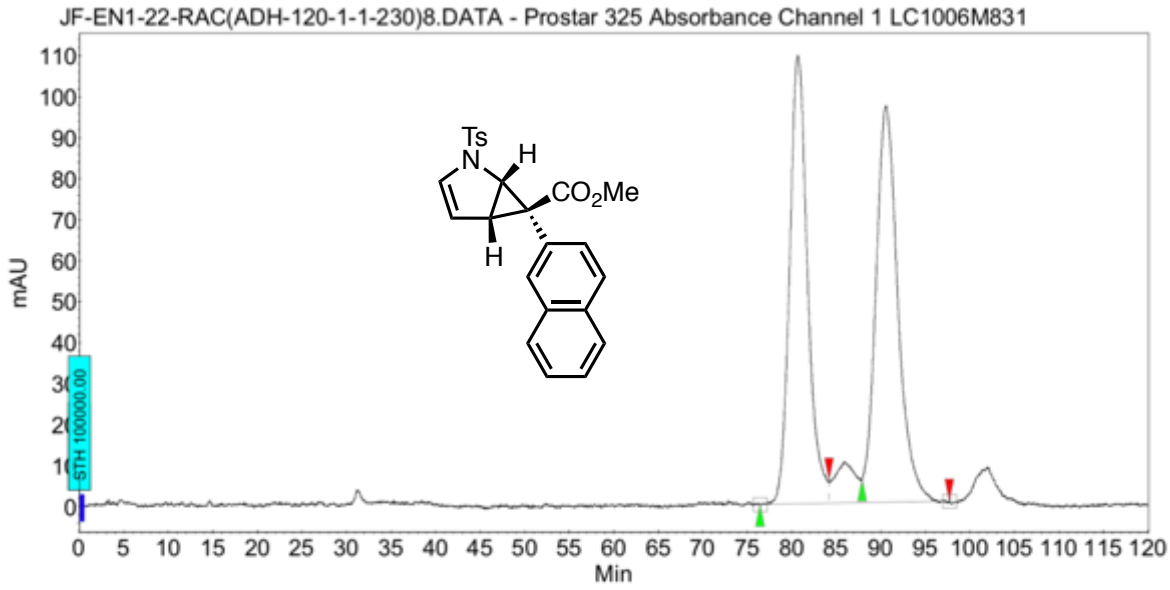

Peak results :

Index	Name	Time [Min]	Quantity [% Area]	Height [mAU]	Area [mAU.Min]	Area % [%]
1	UNKNOWN	80.71	48.07	109.3	256.7	48.069
2	UNKNOWN	90.59	51.93	96.7	277.3	51.931
Total			100.00	206.0	534.0	100.000

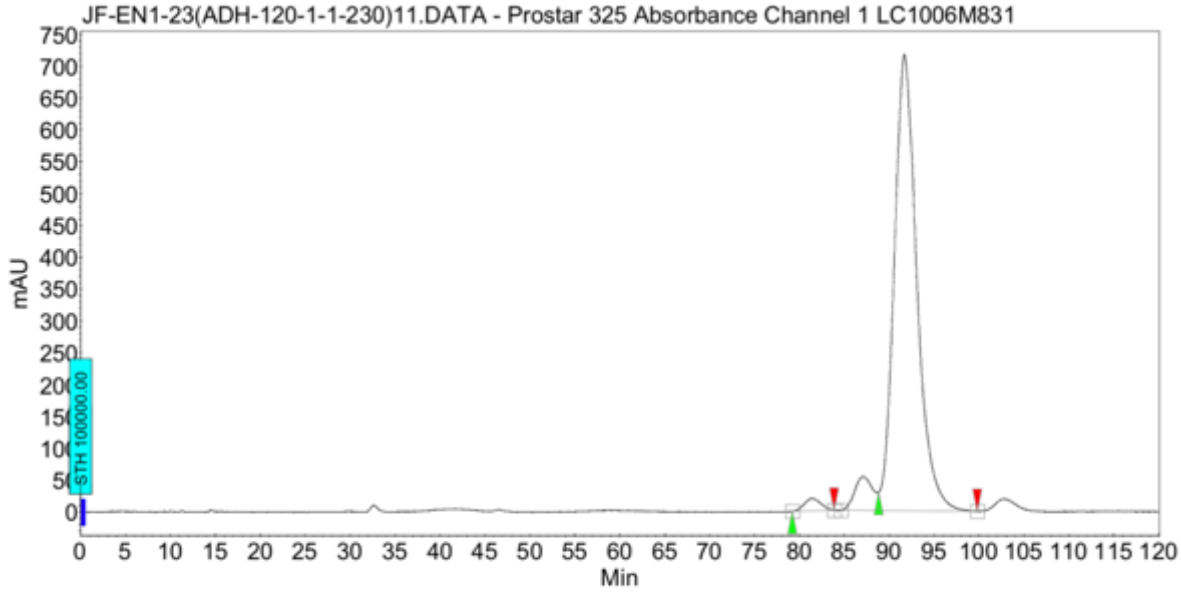

Peak results :

Index	Name	Time [Min]	Quantity [% Area]	Height [mAU]	Area [mAU.Min]	Area % [%]
1	UNKNOWN	81.36	1.94	19.5	41.3	1.941
2	UNKNOWN	91.69	98.06	716.7	2089.1	98.059
Total			100.00	736.1	2130.5	100.000

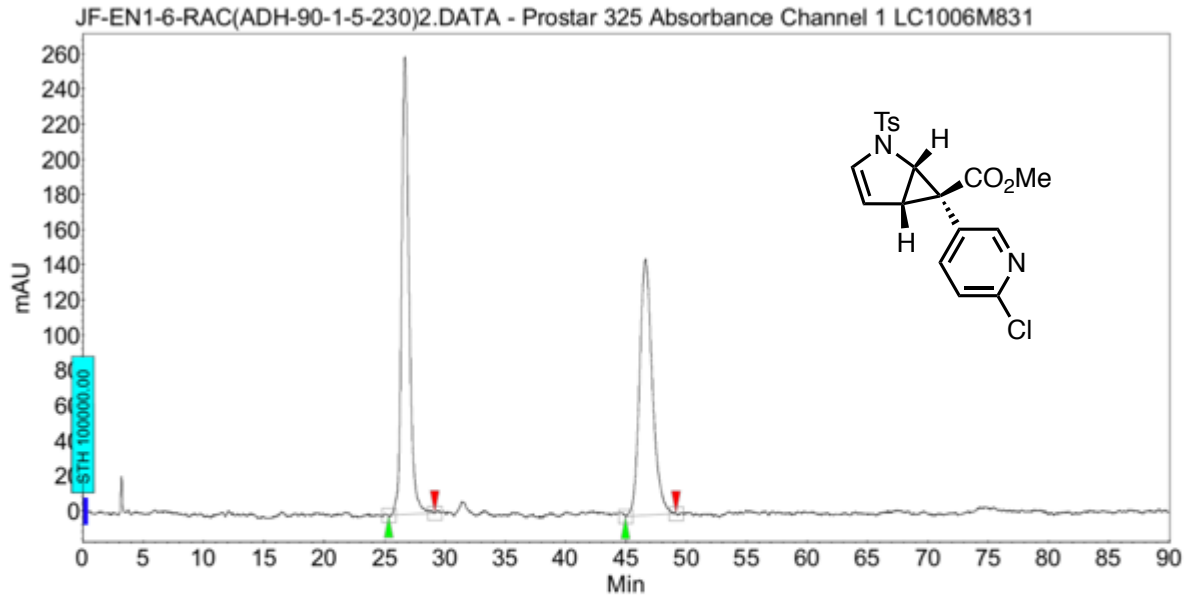

Peak results :

Index	Name	Time [Min]	Quantity [% Area]	Height [mAU]	Area [mAU.Min]	Area % [%]
1	UNKNOWN	26.68	51.22	260.5	187.8	51.218
2	UNKNOWN	46.63	48.78	145.7	178.8	48.782
Total			100.00	406.2	366.6	100.000

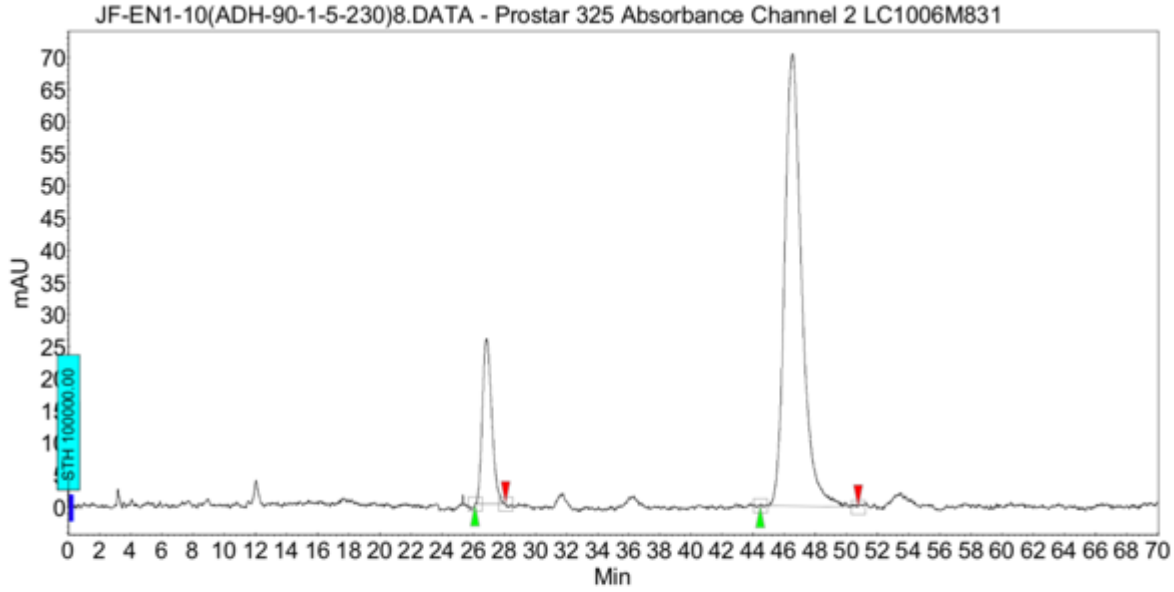

Peak results :

Index	Name	Time [Min]	Quantity [% Area]	Height [mAU]	Area [mAU.Min]	Area % [%]
1	UNKNOWN	26.87	16.66	25.7	18.0	16.660
2	UNKNOWN	46.54	83.34	70.3	89.9	83.340
Total			100.00	96.0	107.9	100.000

DAD1 B, Sig=230,4 Ref=off (09-Aug-201...ug-2018 2018-08-09 10-32-29\091-12-NW-US-105-RAC-ADH-0.5mL-10%.D)

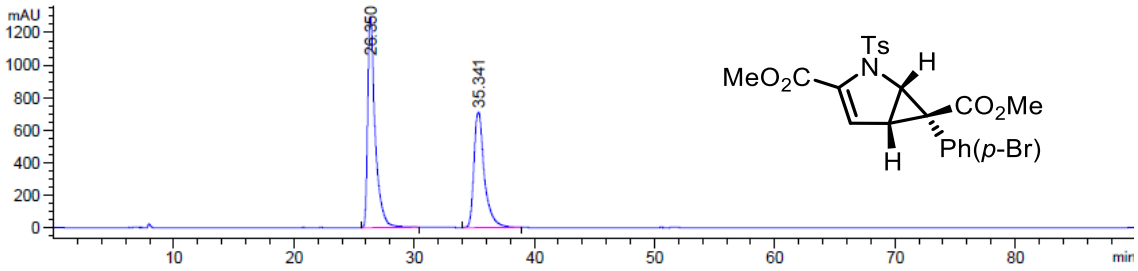

Peak #	RetTime [min]	Type	Width [min]	Area [mAU*s]	Height [mAU]	Area %
1	26.350	BB	0.5561	5.58265e4	1297.23413	56.5822
2	35.341	BB	0.7183	4.28380e4	710.13232	43.4178

DAD1 B, Sig=230,4 Ref=off (13-Aug-201...g-2018 2018-08-13 09-11-38\010-11-NW-US-99-ADH-60min-0.5mL-10%.D)

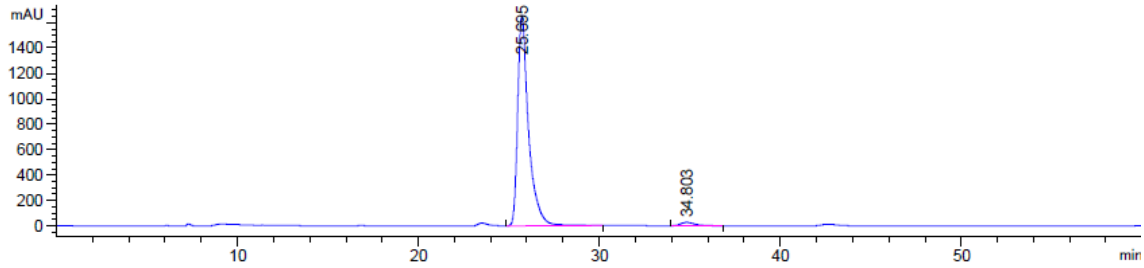

Peak #	RetTime [min]	Type	Width [min]	Area [mAU*s]	Height [mAU]	Area %
1	25.695	BB	0.5135	6.91148e4	1652.20984	97.8606
2	34.803	BB	0.6299	1510.99731	28.20802	2.1394

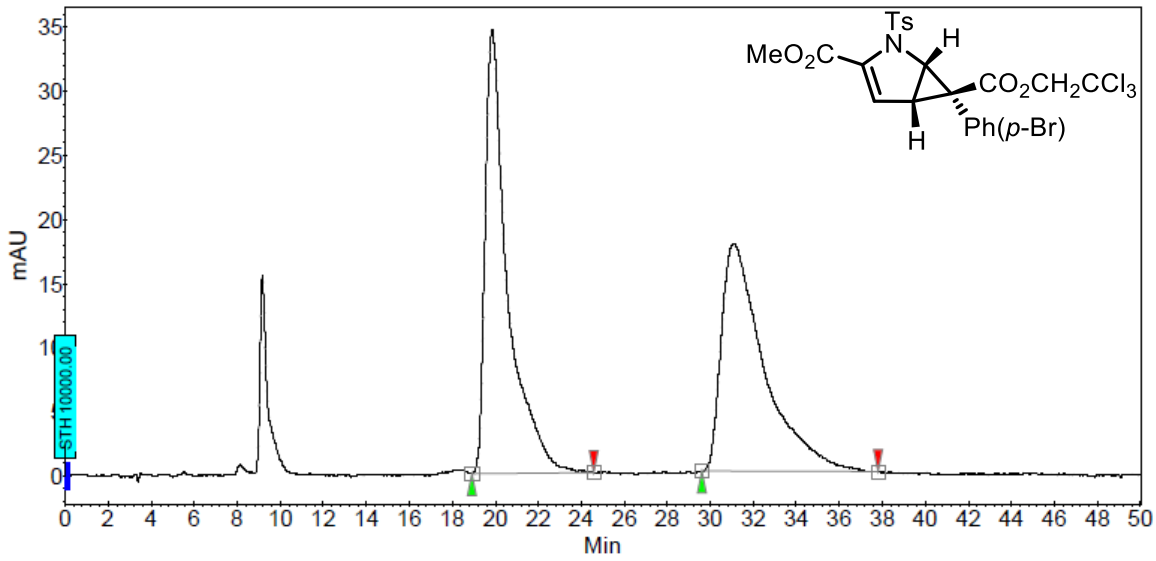

Peak results :

Index	Name	Time [Min]	Quantity [% Area]	Height [mAU]	Area [mAU.Min]	Area % [%]
1	UNKNOWN	19.85	50.57	34.6	41.8	50.567
2	UNKNOWN	31.10	49.43	17.8	40.9	49.433
Total			100.00	52.4	82.7	100.000

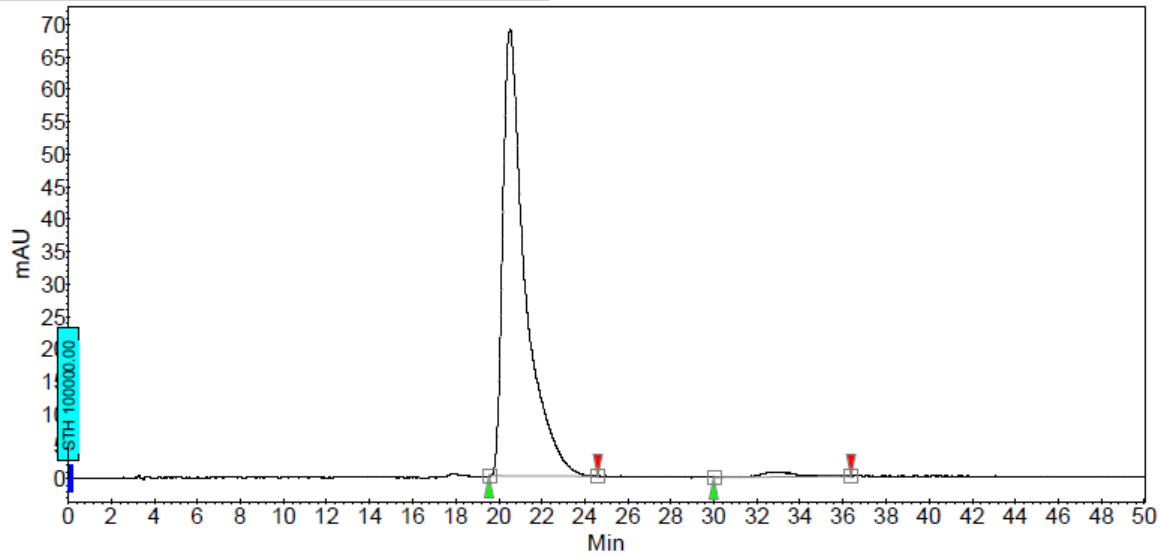

Peak results :

Index	Name	Time [Min]	Quantity [% Area]	Height [mAU]	Area [mAU.Min]	Area % [%]
1	UNKNOWN	20.53	98.32	69.0	82.6	98.322
2	UNKNOWN	32.62	1.68	0.6	1.4	1.678
Total			100.00	69.7	84.0	100.000

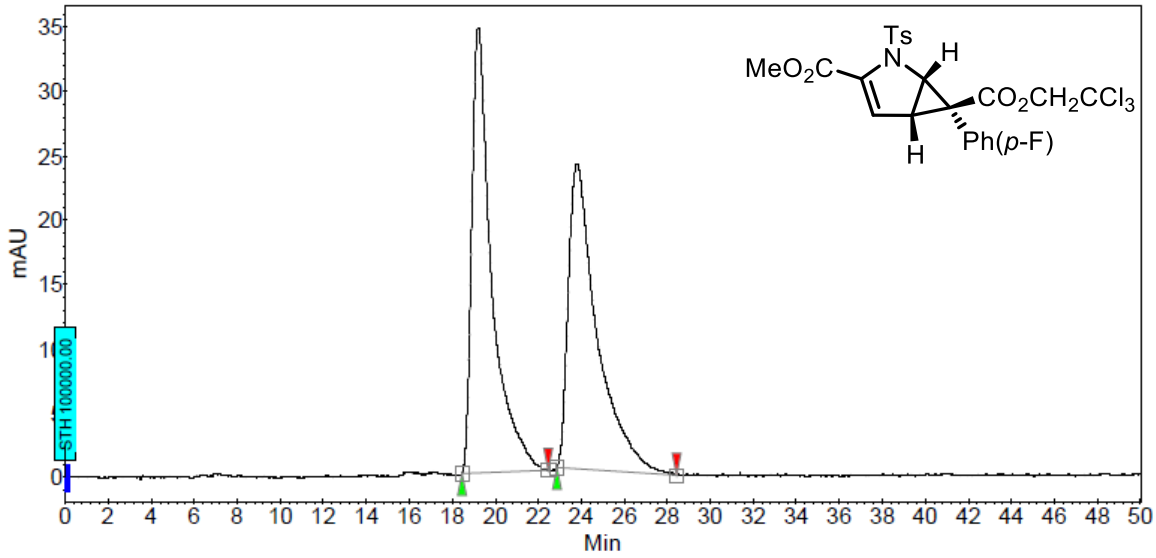

Peak results :

Index	Name	Time [Min]	Quantity [% Area]	Height [mAU]	Area [mAU.Min]	Area % [%]
1	UNKNOWN	19.21	50.52	34.6	37.3	50.524
2	UNKNOWN	23.81	49.48	23.7	36.5	49.476
Total			100.00	58.3	73.8	100.000

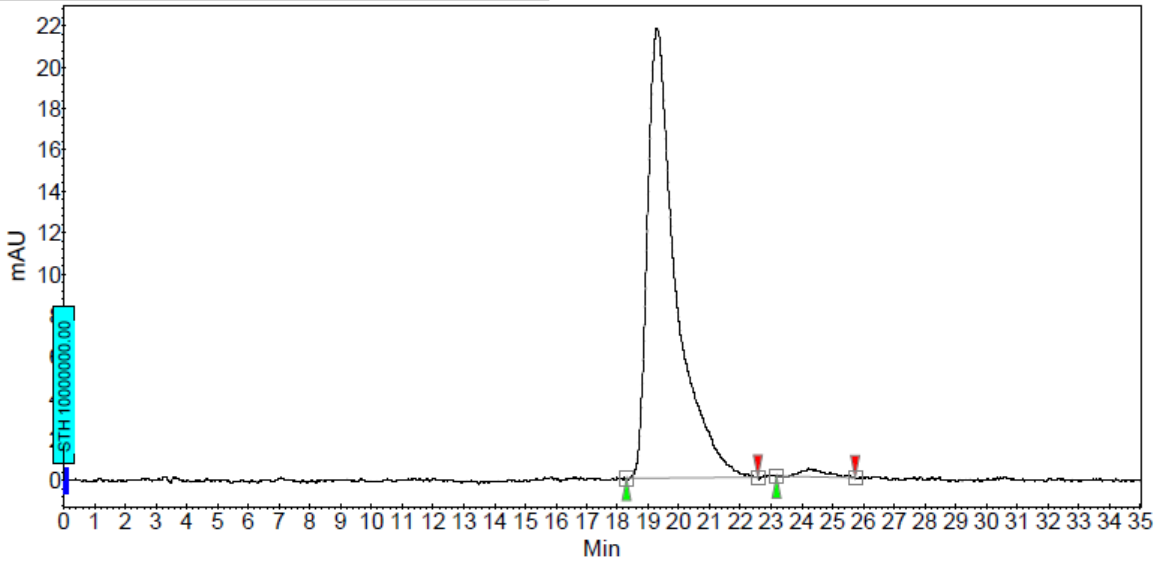

Peak results :

Index	Name	Time [Min]	Quantity [% Area]	Height [mAU]	Area [mAU.Min]	Area % [%]
1	UNKNOWN	19.29	98.31	21.8	23.3	98.309
2	UNKNOWN	24.20	1.69	0.4	0.4	1.691
Total			100.00	22.2	23.7	100.000

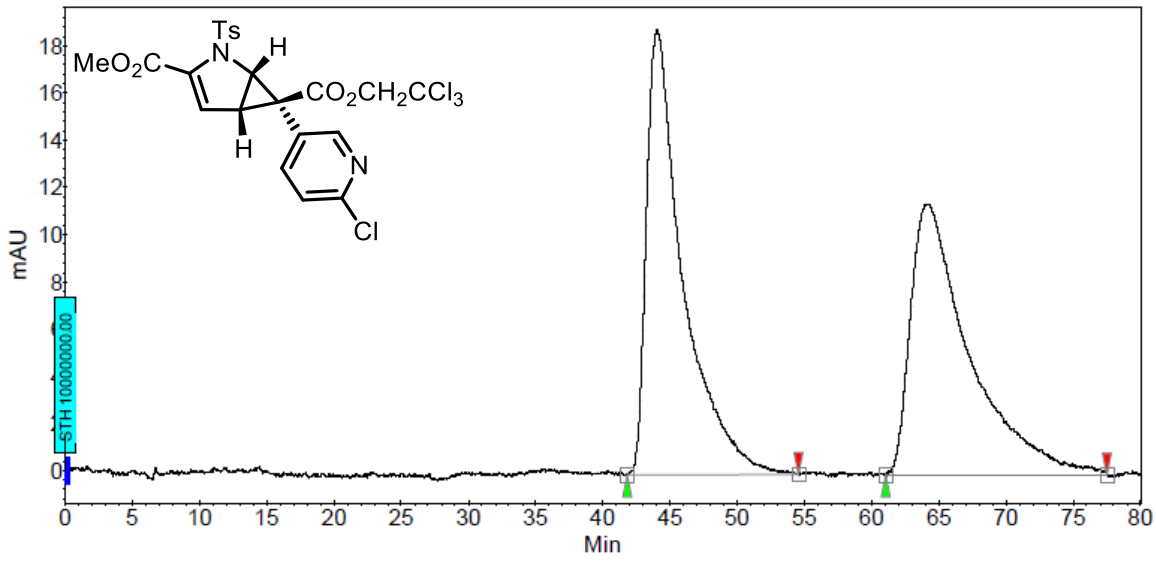

Peak results :

Index	Name	Time [Min]	Quantity [% Area]	Height [mAU]	Area [mAU.Min]	Area % [%]
1	UNKNOWN	44.07	50.57	18.9	59.4	50.567
2	UNKNOWN	64.18	49.43	11.5	58.1	49.433
Total			100.00	30.4	117.5	100.000

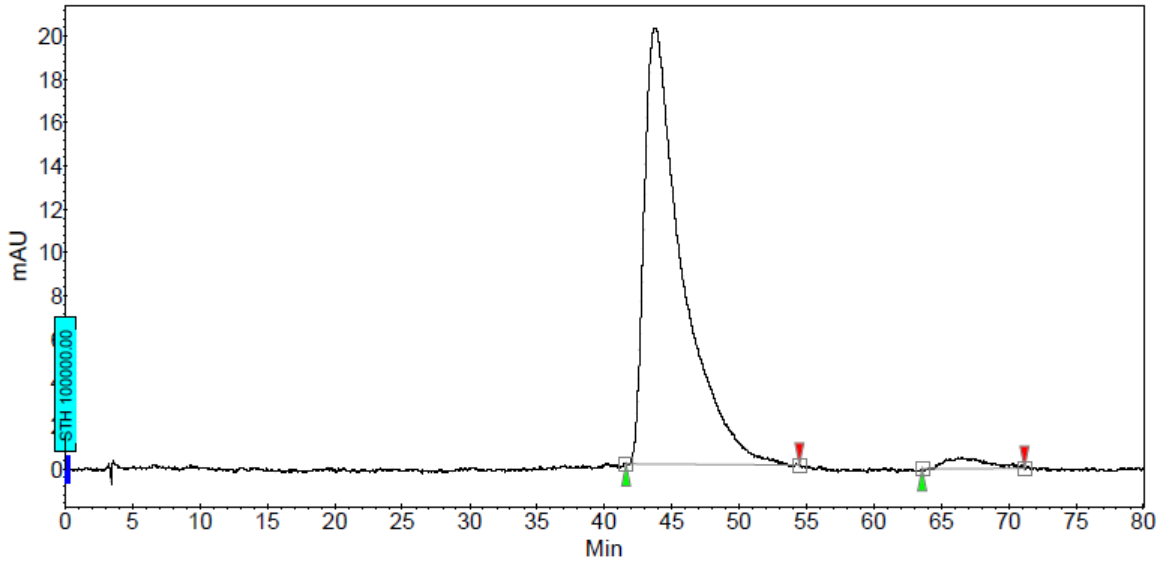

Peak results :

Index	Name	Time [Min]	Quantity [% Area]	Height [mAU]	Area [mAU.Min]	Area % [%]
1	UNKNOWN	43.78	97.30	20.1	65.4	97.302
2	UNKNOWN	66.51	2.70	0.6	1.8	2.698
Total			100.00	20.7	67.2	100.000

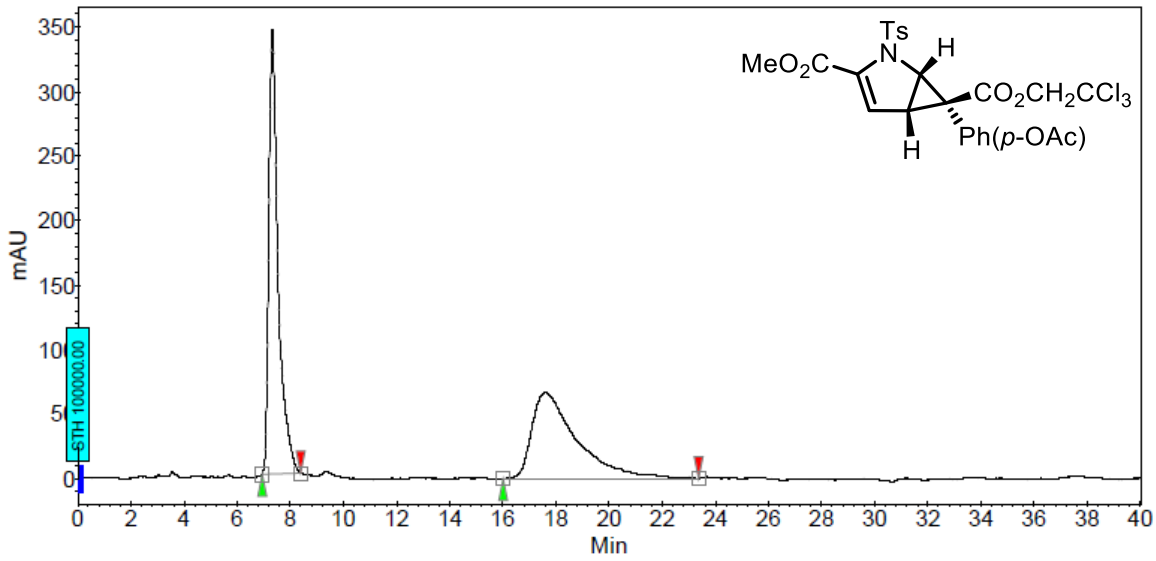

Peak results :

Index	Name	Time [Min]	Quantity [% Area]	Height [mAU]	Area [mAU.Min]	Area % [%]
2	UNKNOWN	7.32	51.66	344.9	140.1	51.662
1	UNKNOWN	17.60	48.34	66.9	131.1	48.338
Total			100.00	411.9	271.3	100.000

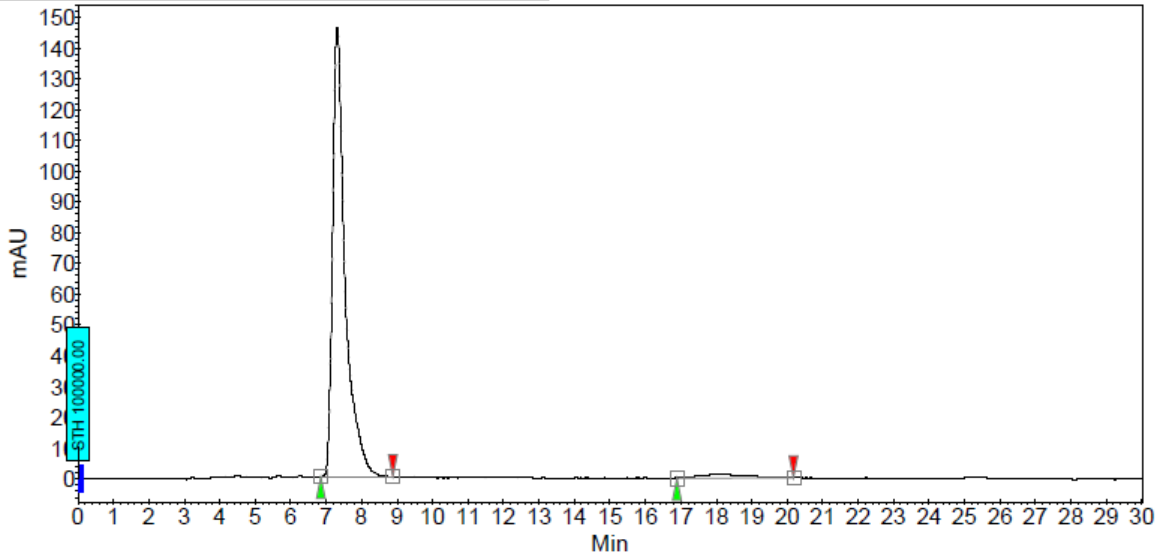

Peak results :

Index	Name	Time [Min]	Quantity [% Area]	Height [mAU]	Area [mAU.Min]	Area % [%]
1	UNKNOWN	7.31	96.89	146.1	60.0	96.888
2	UNKNOWN	18.20	3.11	1.2	1.9	3.112
Total			100.00	147.3	61.9	100.000

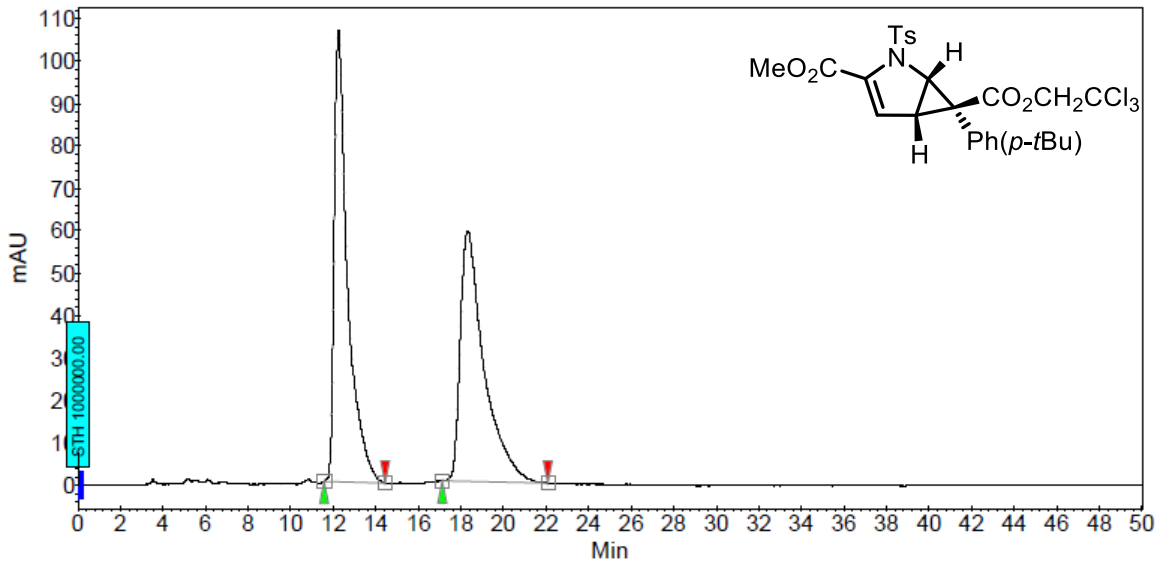

Peak results :

Index	Name	Time [Min]	Quantity [% Area]	Height [mAU]	Area [mAU.Min]	Area % [%]
1	UNKNOWN	12.24	50.36	106.6	77.6	50.365
2	UNKNOWN	18.32	49.64	59.1	76.5	49.635
Total			100.00	165.7	154.1	100.000

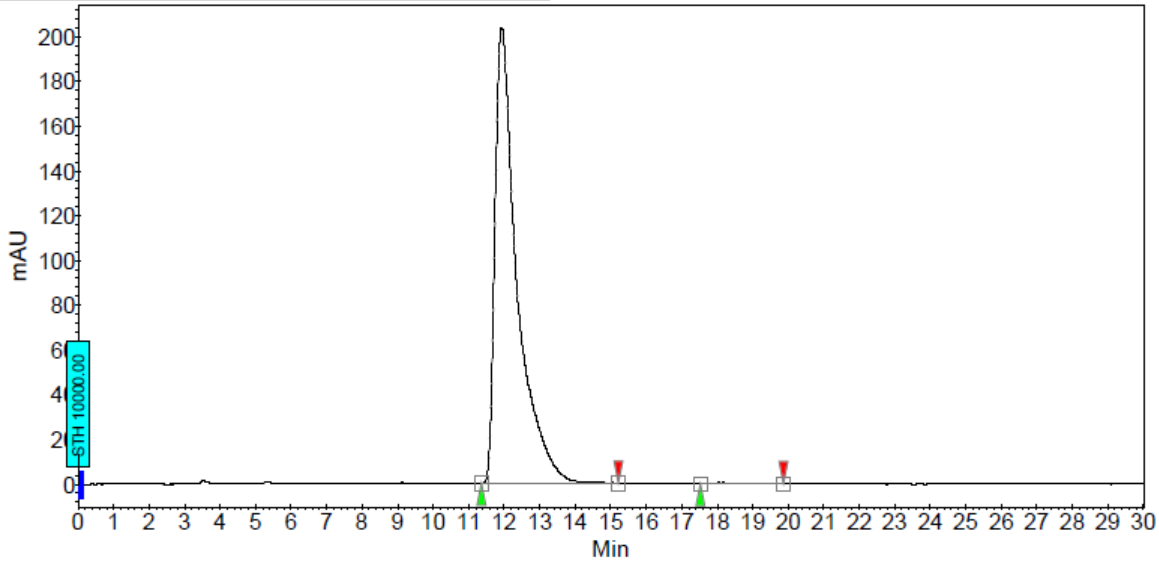

Peak results :

Index	Name	Time [Min]	Quantity [% Area]	Height [mAU]	Area [mAU.Min]	Area % [%]
2	UNKNOWN	11.93	99.75	203.8	146.4	99.746
1	UNKNOWN	18.18	0.25	0.3	0.4	0.254
Total			100.00	204.1	146.8	100.000

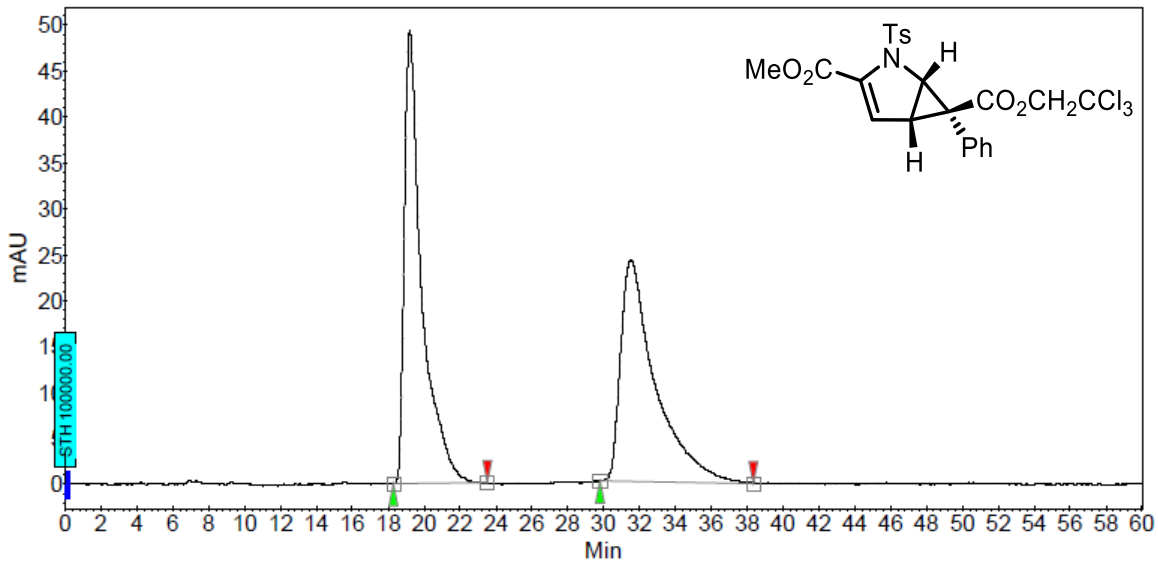

Peak results :

Index	Name	Time [Min]	Quantity [% Area]	Height [mAU]	Area [mAU.Min]	Area % [%]
1	UNKNOWN	19.20	50.89	49.4	55.7	50.895
2	UNKNOWN	31.53	49.11	24.1	53.7	49.105
Total			100.00	73.5	109.4	100.000

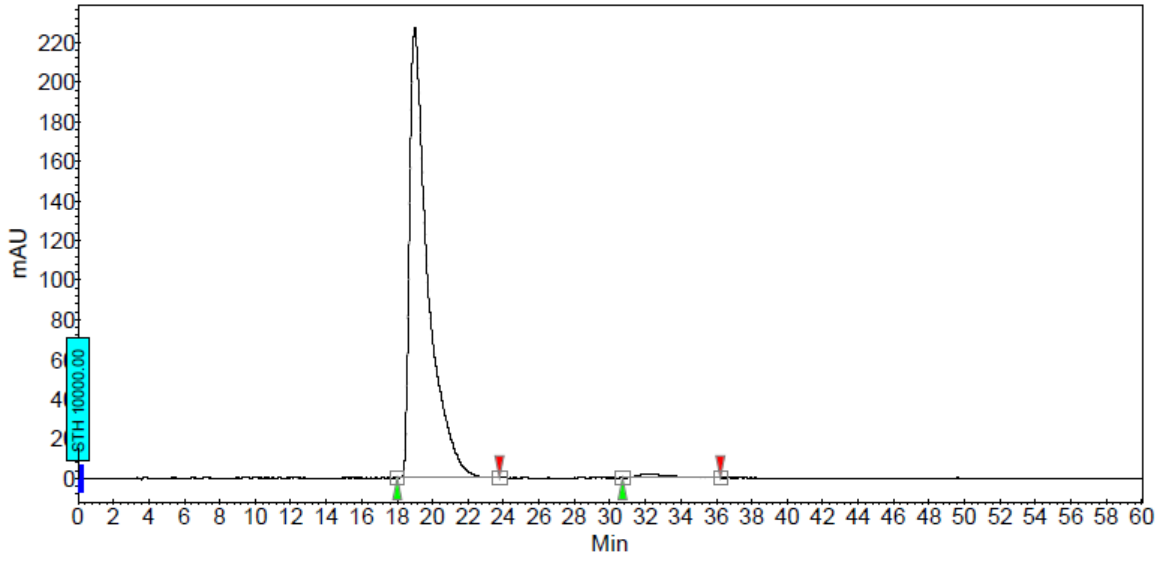

Peak results :

Index	Name	Time [Min]	Quantity [% Area]	Height [mAU]	Area [mAU.Min]	Area % [%]
1	UNKNOWN	18.99	98.45	227.4	273.3	98.446
2	UNKNOWN	32.17	1.55	2.1	4.3	1.554
Total			100.00	229.6	277.6	100.000

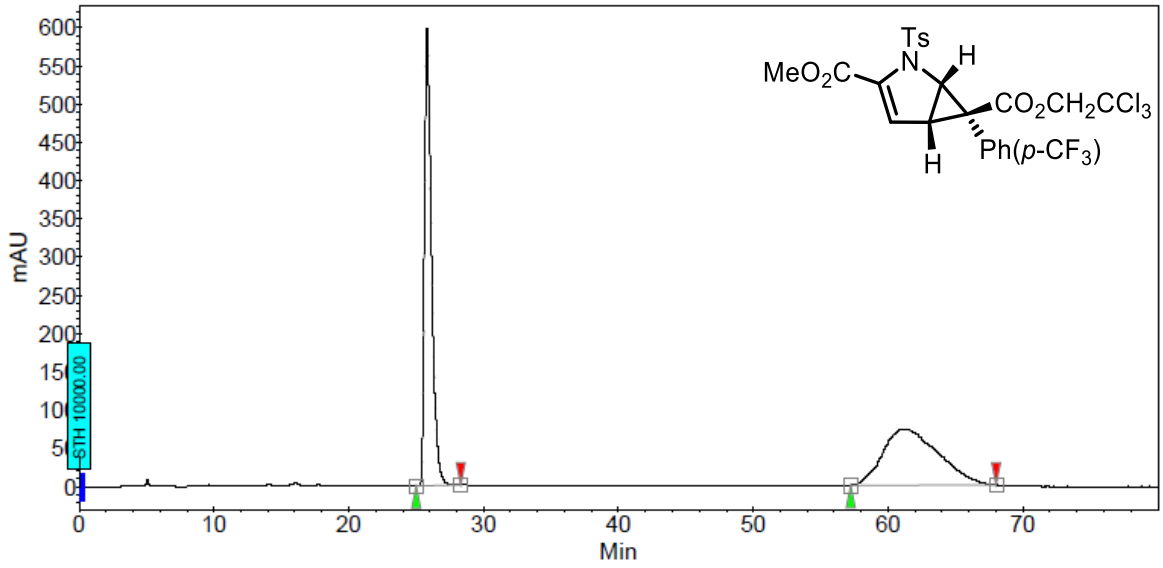

Peak results :

Index	Name	Time [Min]	Quantity [% Area]	Height [mAU]	Area [mAU.Min]	Area % [%]
1	UNKNOWN	25.80	50.70	598.5	360.4	50.703
2	UNKNOWN	61.16	49.30	72.9	350.4	49.297
Total			100.00	671.5	710.8	100.000

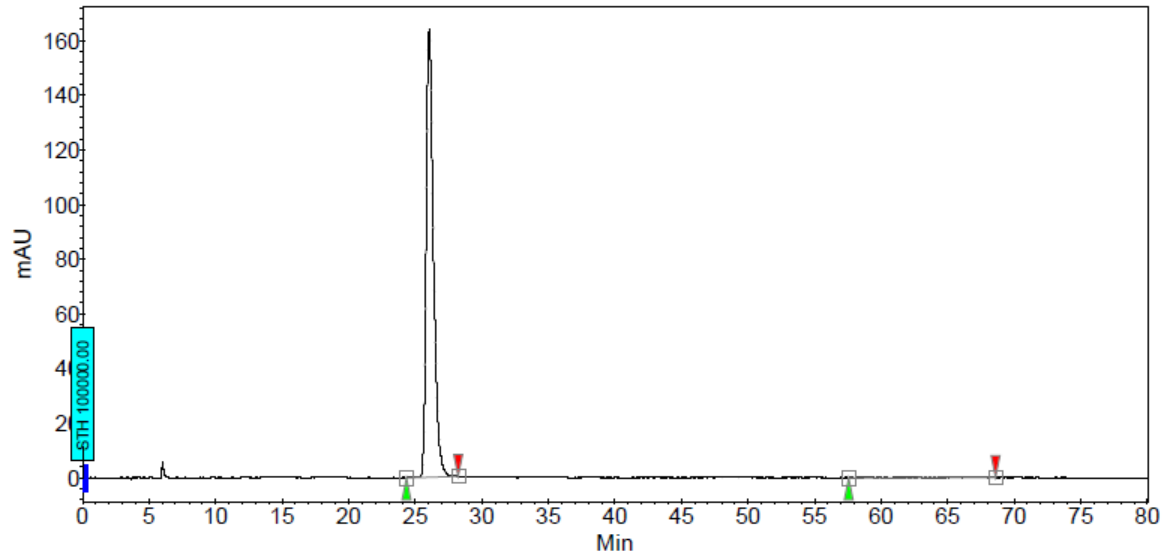

Peak results :

Index	Name	Time [Min]	Quantity [% Area]	Height [mAU]	Area [mAU.Min]	Area % [%]
1	UNKNOWN	26.04	99.94	164.2	103.6	99.943
2	UNKNOWN	66.23	0.06	0.1	0.1	0.057
Total			100.00	164.3	103.6	100.000

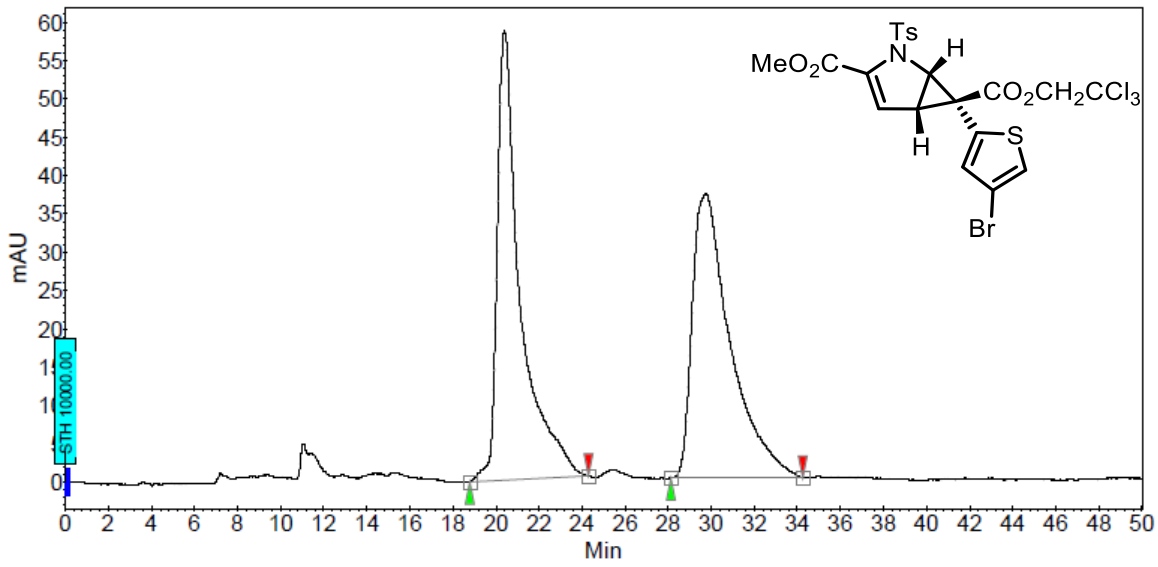

Peak results :

Index	Name	Time [Min]	Quantity [% Area]	Height [mAU]	Area [mAU.Min]	Area % [%]
1	UNKNOWN	20.40	49.04	58.7	73.0	49.039
2	UNKNOWN	29.73	50.96	37.1	75.8	50.961
Total			100.00	95.8	148.8	100.000

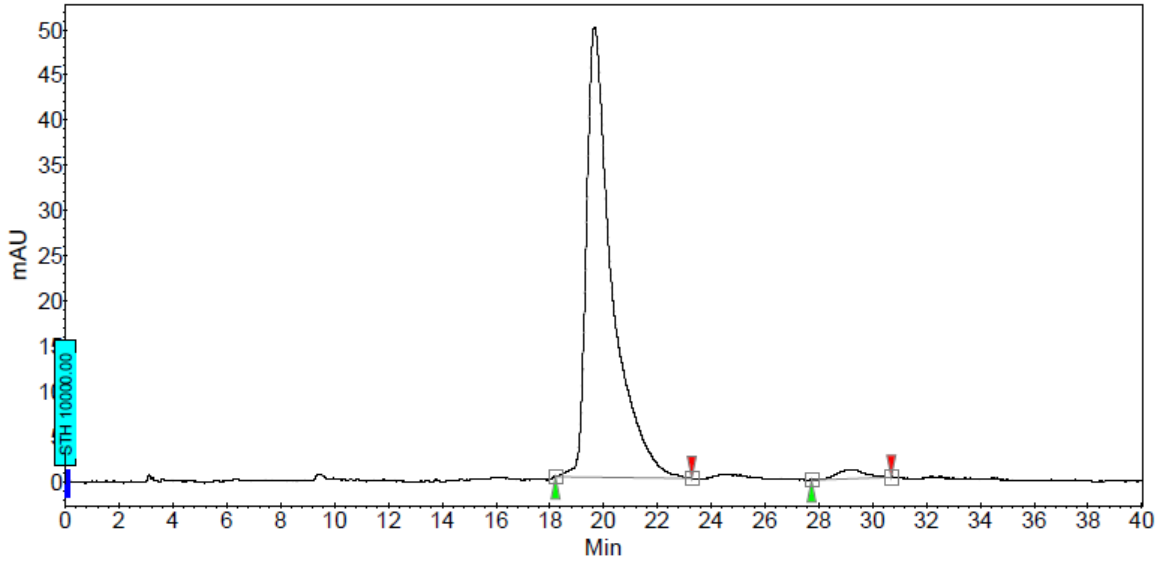

Peak results :

Index	Name	Time [Min]	Quantity [% Area]	Height [mAU]	Area [mAU.Min]	Area % [%]
1	UNKNOWN	19.66	97.80	49.7	54.5	97.797
2	UNKNOWN	29.18	2.20	1.0	1.2	2.203
Total			100.00	50.8	55.7	100.000

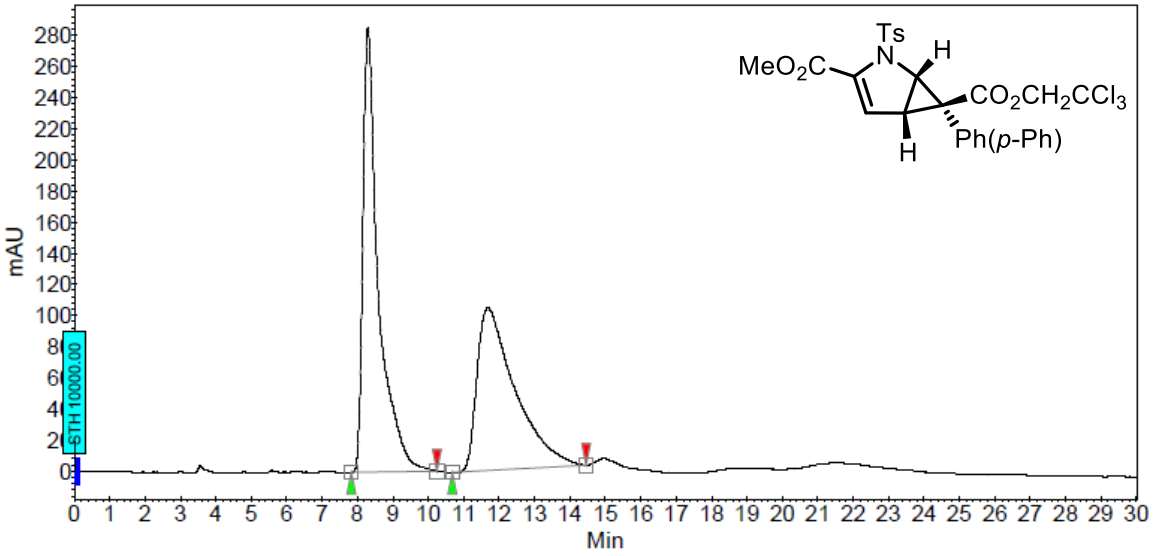

Peak results :

Index	Name	Time [Min]	Quantity [% Area]	Height [mAU]	Area [mAU.Min]	Area % [%]
1	UNKNOWN	8.29	52.81	285.9	145.4	52.809
2	UNKNOWN	11.68	47.19	104.5	129.9	47.191
Total			100.00	390.4	275.2	100.000

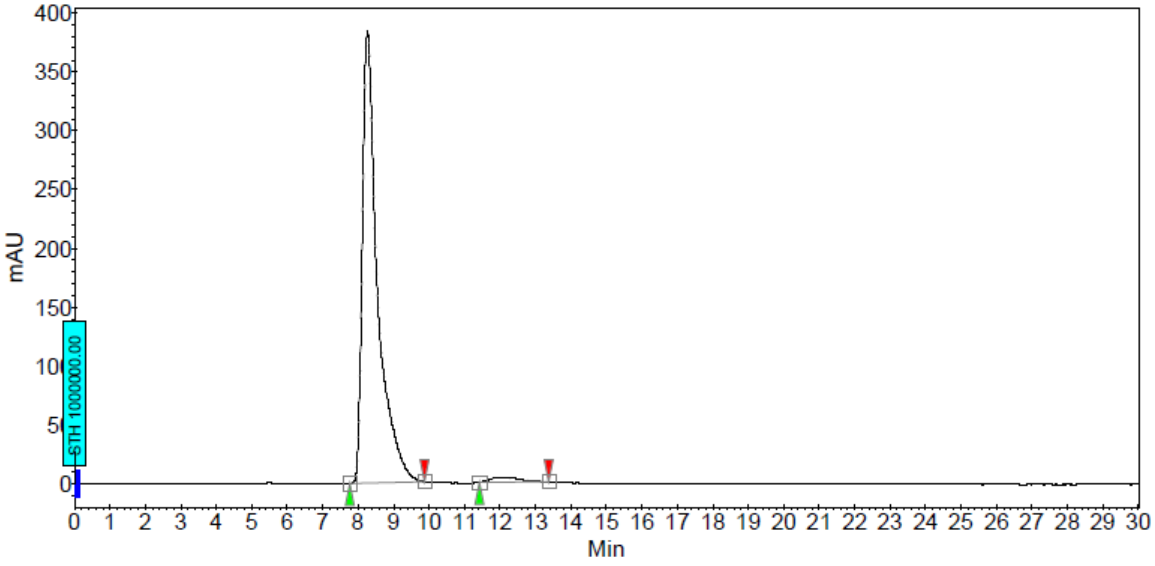

Peak results :

Index	Name	Time [Min]	Quantity [% Area]	Height [mAU]	Area [mAU.Min]	Area % [%]
1	UNKNOWN	8.26	97.94	384.4	190.4	97.944
2	UNKNOWN	12.11	2.06	3.9	4.0	2.056
Total			100.00	388.3	194.4	100.000

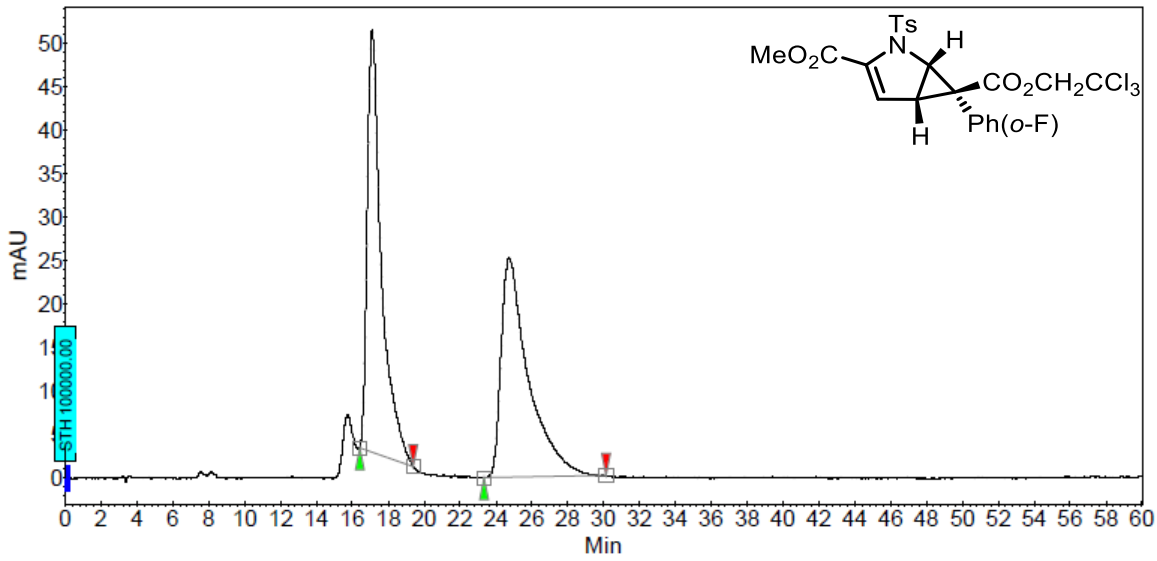

Peak results :

Index	Name	Time [Min]	Quantity [% Area]	Height [mAU]	Area [mAU.Min]	Area % [%]
2	UNKNOWN	17.10	50.15	48.6	44.6	50.147
1	UNKNOWN	24.73	49.85	25.2	44.4	49.853
Total			100.00	73.9	89.0	100.000

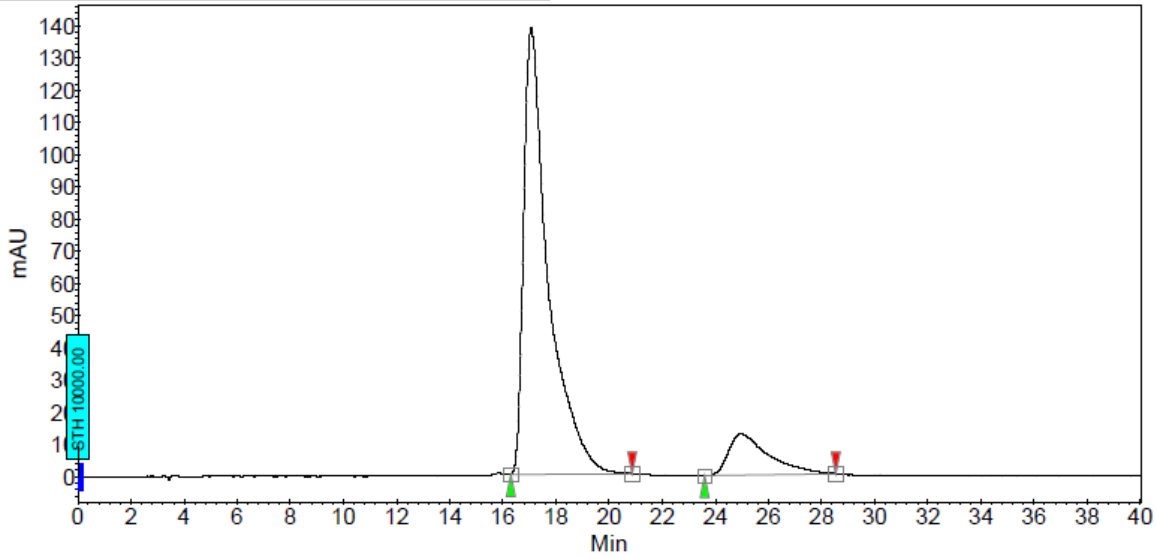

Peak results :

Index	Name	Time [Min]	Quantity [% Area]	Height [mAU]	Area [mAU.Min]	Area % [%]
2	UNKNOWN	17.07	86.98	138.7	148.7	86.980
1	UNKNOWN	24.96	13.02	12.7	22.3	13.020
Total			100.00	151.4	171.0	100.000

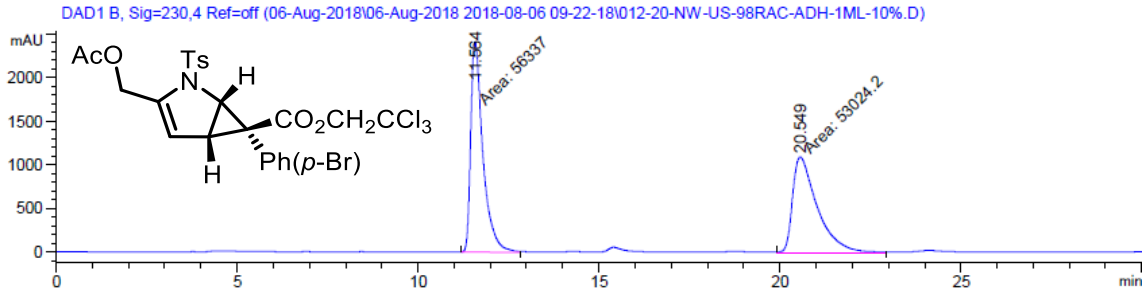

Signal 2: DAD1 B, Sig=230,4 Ref=off

Peak #	RetTime [min]	Type	Width [min]	Area [mAU*s]	Height [mAU]	Area %
1	11.564	MM	0.3898	5.63370e4	2409.02661	51.5146
2	20.549	MM	0.8016	5.30242e4	1102.52490	48.4854

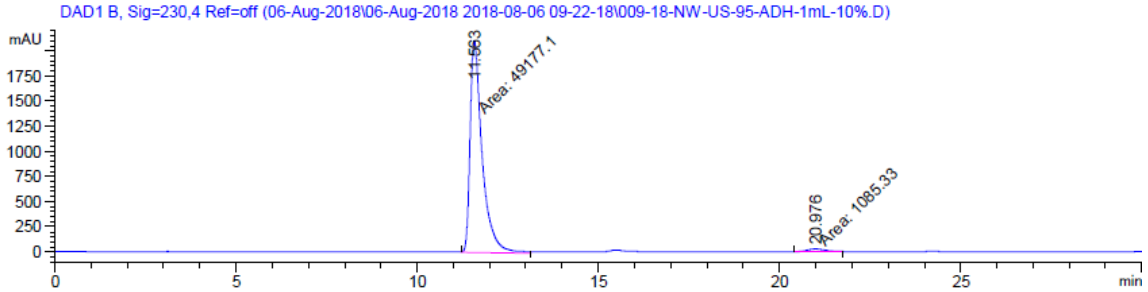

Signal 2: DAD1 B, Sig=230,4 Ref=off

Peak #	RetTime [min]	Type	Width [min]	Area [mAU*s]	Height [mAU]	Area %
1	11.563	MM	0.3881	4.91771e4	2111.66064	97.8407
2	20.976	MM	0.6277	1085.32715	28.81922	2.1593
Totals :				5.02625e4	2140.47987	

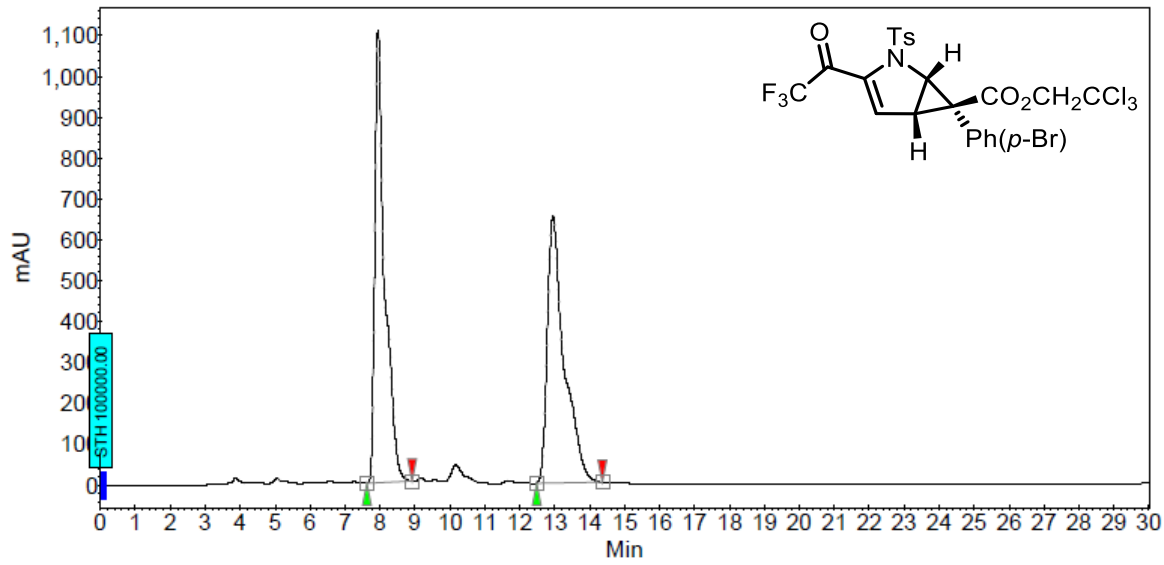

Peak results :

Index	Name	Time [Min]	Quantity [% Area]	Height [mAU]	Area [mAU.Min]	Area % [%]
1	UNKNOWN	7.94	49.78	1108.3	363.2	49.777
2	UNKNOWN	12.95	50.22	655.4	366.4	50.223
Total			100.00	1763.7	729.6	100.000

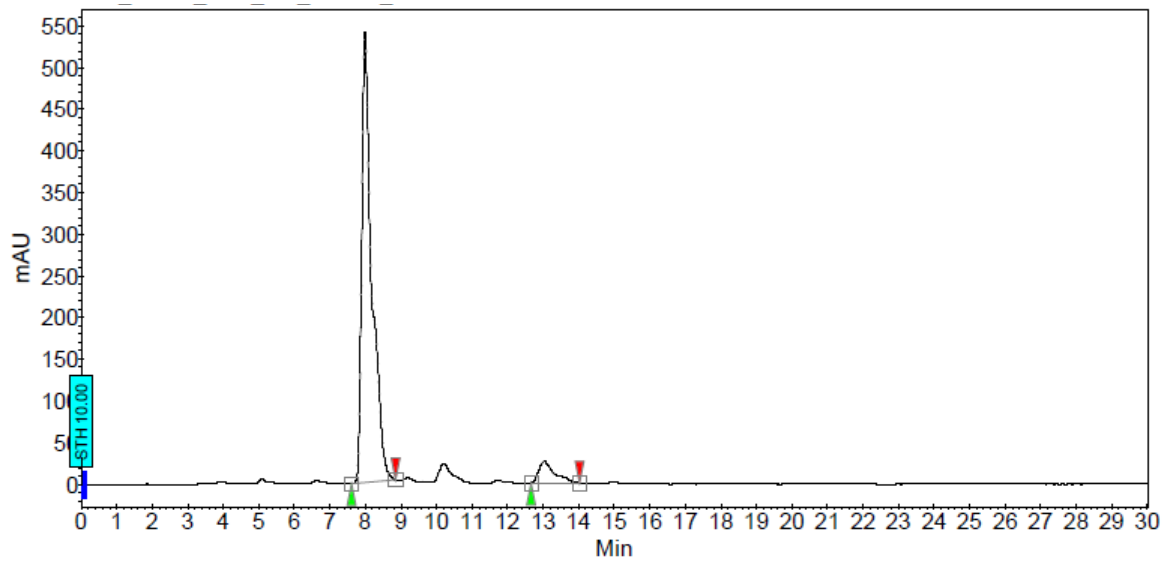

Peak results :

Index	Name	Time [Min]	Quantity [% Area]	Height [mAU]	Area [mAU.Min]	Area % [%]
1	UNKNOWN	7.99	92.92	540.7	176.8	92.923
2	UNKNOWN	13.04	7.08	25.7	13.5	7.077
Total			100.00	566.4	190.3	100.000

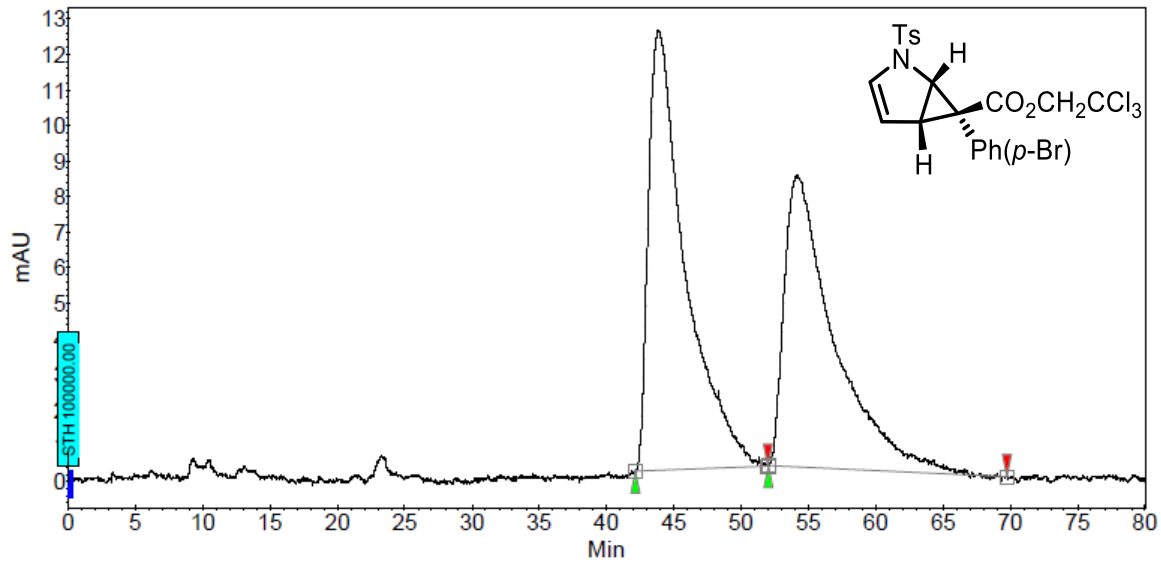

Peak results :

Index	Name	Time [Min]	Quantity [% Area]	Height [mAU]	Area [mAU.Min]	Area % [%]
1	UNKNOWN	43.89	52.79	12.4	39.2	52.793
2	UNKNOWN	54.21	47.21	8.2	35.1	47.207
Total			100.00	20.6	74.3	100.000

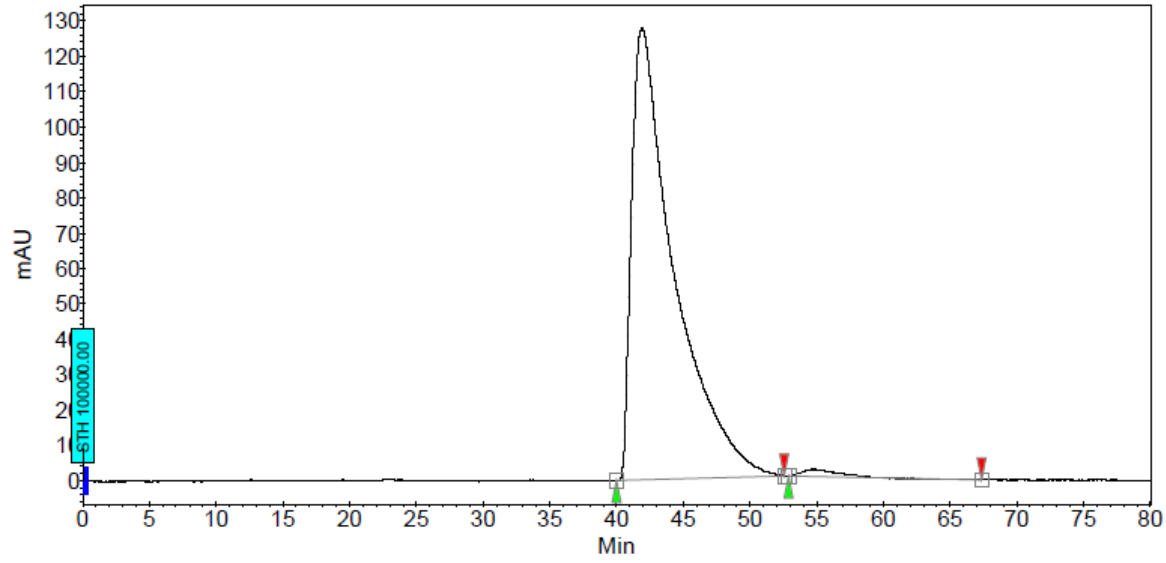

Peak results :

Index	Name	Time [Min]	Quantity [% Area]	Height [mAU]	Area [mAU.Min]	Area % [%]
1	UNKNOWN	41.91	98.75	127.9	470.9	98.753
2	UNKNOWN	54.62	1.25	2.0	5.9	1.247
Total			100.00	129.9	476.8	100.000

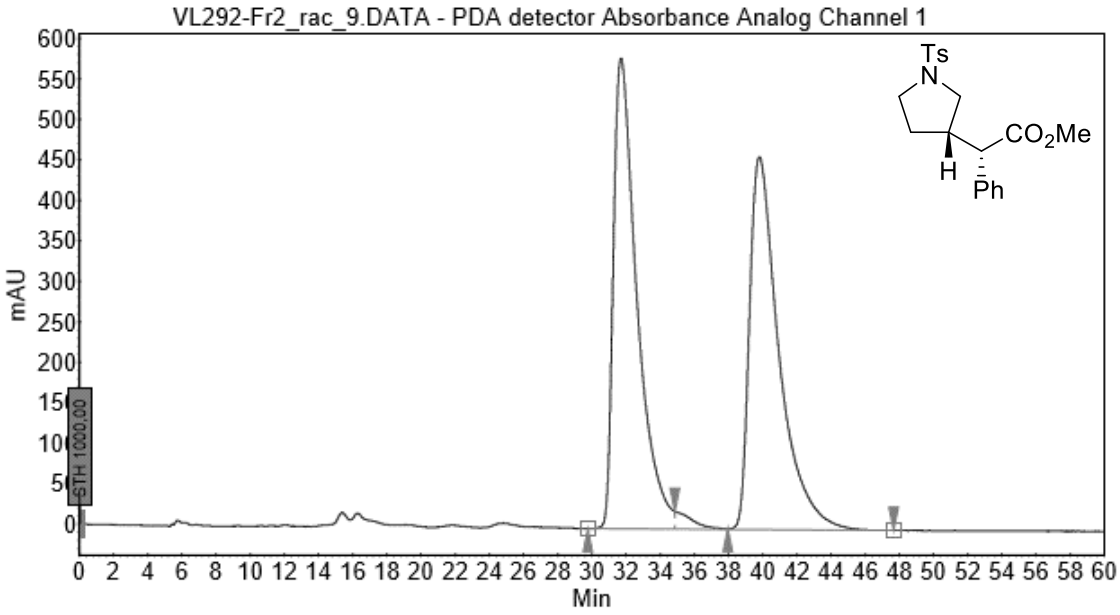

Peak Results :

Index	Name	Time [Min]	Quantity [% Area]	Height [mAU]	Area [mAU.Min]	Area % [%]
1	UNKNOWN	31,72	50,23	582,0	931,7	50,229
2	UNKNOWN	39,80	49,77	461,0	923,2	49,771
Total			100,00	1043,0	1854,8	100,000

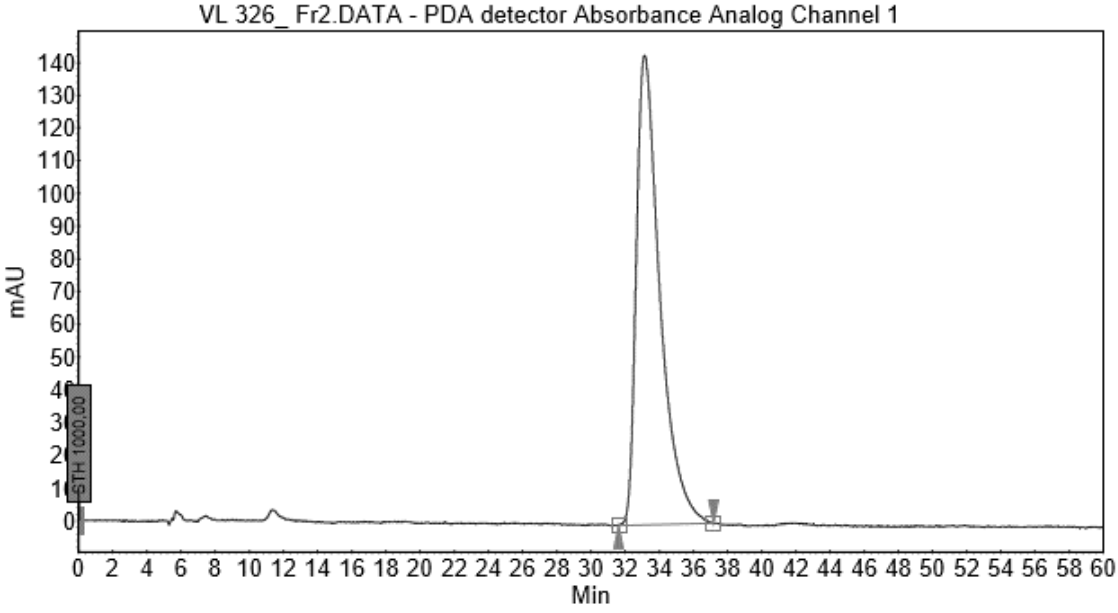

Peak Results :

Index	Name	Time [Min]	Quantity [% Area]	Height [mAU]	Area [mAU.Min]	Area % [%]
1	UNKNOWN	33,14	100,00	143,4	229,7	100,000
Total			100,00	143,4	229,7	100,000